University of Southampton

Faculty of Environmental and Life Sciences

School of Biological Sciences

Physiology of rest/activity cycles in *Drosophila melanogaster*

by

Jonathan Charles Anns

ORCID ID: 0009-0005-8349-4986

Thesis for the degree of Doctor of Philosophy

January 2024

University of Southampton

Abstract

Faculty of Environmental and Life Sciences

School of Biological Sciences

Doctor of Philosophy

Physiology of rest/activity cycles in *Drosophila melanogaster*

by

Jonathan Charles Anns

Sleep is a vital behavioural state present across the whole animal kingdom. In small organisms, a behavioural definition of sleep is typically used to define sleep. *Drosophila melanogaster*, the common fruit fly, is an important model organism whose rest is considered sleep-like. A key behavioural feature of sleep is a species-specific posture and place preference; however, this aspect of sleep has not been well characterised in *Drosophila*. In this thesis, I demonstrate a novel assay, Trumelan, which uses side-on video tracking to monitor fly location, pose, and behaviour.

I first find that behavioural classification in Trumelan is highly accurate and can yield expected patterns of daily fly behaviour in both wild-type and circadian mutants. In addition, I compare the behaviour of Trumelan to the commonly used *Drosophila* Activity Monitor (DAM) assay for studying rest in flies and show that DAM assays overestimate rest. By analysing rest posture, I find that flies adopt a supported upright position at the beginning of rest but show negligible changes during a rest bout. In addition, resting flies prefer to be near, but facing away from, the food source. This preference remains in all stationary behaviours that occur away from the food port, suggesting stationary flies have a general place preference. Finally, I discovered a novel daily rhythm in y-position place preference. Wild-type flies typically rest on the ground during the day but shift to more rest on the ceiling at night. This place preference rhythm remains in constant-dark conditions but is lost in circadian mutants. These findings are the first quantitative analysis of typical rest posture, place preference, and the discovery of a novel place preference under circadian control.

To supplement the behavioural approach for studying sleep, I explored the efficacy of using in vivo luciferase assays for discovering molecular correlates of sleep. I performed a preliminary luciferase screen of a collection of neuronal populations implicated in sleep-wake regulation by utilising calcium signalling as a proxy for neuronal activity. I show luciferase activity rhythms associated with expression in various neuronal populations. Due to low signal strength with firefly Luciferase, I also created new luciferase-expressing flies based on NanoLuc to improve the signal-to-noise ratio. I found that these generate much stronger signals at the expense of a rapid decline in signal.

Table of Contents

Table of Tables

Table of Figures

Table of Figures

Research Thesis: Declaration of Authorship

Print name: Jonathan Charles Anns

Title of thesis: Physiology of rest/activity cycles in *Drosophila melanogaster*

I declare that this thesis and the work presented in it are my own and has been generated by me as the result of my own original research.

I confirm that:

1. This work was done wholly or mainly while in candidature for a research degree at this University;
2. Where any part of this thesis has previously been submitted for a degree or any other qualification at this University or any other institution, this has been clearly stated;
3. Where I have consulted the published work of others, this is always clearly attributed;
4. Where I have quoted from the work of others, the source is always given. With the exception of such quotations, this thesis is entirely my own work;
5. I have acknowledged all main sources of help;
6. Where the thesis is based on work done by myself jointly with others, I have made clear exactly what was done by others and what I have contributed myself;
7. None of this work has been published before submission

Signature: ..... Date: 17/01/2024

Acknowledgements

First and foremost, I wish to thank my exceptional supervisors, Herman Wijnen and Adam Claridge-Chang. I have never been made to feel inadequate, and I never felt unable to ask for help if required. I also greatly appreciate that both supervisors allowed me to do my work relatively independently without micromanaging. The guidance and feedback I received during informal chats and lab meetings have been invaluable in shaping my scientific journey. In addition, I would like to thank my thesis progression examiners, Prof. Vincent O'connor and Prof. John Chad. While I look back and feel embarrassed at the quality of the submitted progression reports, I thank both examiners for their helpful comments and advice.

I am incredibly grateful to have been given the opportunity to do a PhD split between two supervisors, one in the UK and one in Singapore. I want to thank the School of Biological Sciences at the University of Southampton, alongside A*STAR, for funding my studies. Before receiving the offer, I never had the opportunity or the means to travel beyond central Europe. I hardly knew where Singapore was or what living so far from home would be like. While initially daunting, I quickly discovered how amazing Singapore is to live and work. It now feels like a second home.

I would also like to thank all the lab members and PhD colleagues I had the pleasure of interacting with during my studies. While it can sometimes feel overwhelming to interact with such brilliant individuals, these last four years have been an invaluable learning experience. I am constantly amazed and humbled by how quickly other lab members and supervisors can recall a million different research papers and generate new hypotheses and creative solutions to problems. I hope to have gleaned some of these skills during my studies, and I hope to continue honing these research skills. I am also grateful to have begun my PhD at the same time as other lab members. We have had a lot of fun times together, and it has been a pleasure to watch all of us grow over these past few years.

I want to dedicate this final section to those closest to me. I am eternally thankful for my family and how supportive they have been throughout my life and during my studies. My parents instilled in me (whether learned or due to genetics) a strong work ethic and discipline, which has been instrumental in staying sane while completing my studies and this thesis. The best discovery of my PhD was my partner, Esther. I was not expecting to find someone so kind, caring, funny, and supportive. I greatly appreciate her support during my studies and especially during the final few months before submission. Lastly, I would like to thank Esther's family and friends for taking me in and making me feel at home while so far from home.

Regardless of the outcome, this PhD has been an incredible experience, and I do not regret undertaking this journey.

Definitions and Abbreviations

BA ..... Body angle

BDSC ..... Bloomington *Drosophila* Stock Centre

BK ..... Berlin-K

CS ..... Canton-S

CI ..... 95% confidence interval

CT ..... Circadian time

Cyc ..... Cycle (circadian gene/protein)

DAM ..... *Drosophila* Activity Monitor (TriKinetics)

DD ..... Dark Dark / Constant darkness

dFB ..... Dorsal fan-shaped body

EB ..... Ellipsoid body

F ..... Female

FFz ..... Fluorofurimazine

FLP.DD ..... Flippase (recombinase) with an added destabilising domain

FLuc ..... Firefly Luciferase

Fps ..... Frames per second

GEI ..... Genetic element of interest

LD ..... Light Dark

LO ..... Locomotive

LUC ..... Luciferase

M ..... Male

MB ..... Mushroom body

MESA ..... Maximum Entropy Spectral Analysis

nBA ..... Normalised body angle

NLuc ..... NanoLuc

OMD ..... overweight misclassified data

Per..... Period (circadian gene/protein)

PI ..... Pars Intercerebralis

PSD..... Power spectral density

RI ..... Rhythmic Index

SA ..... Stationary Active

snBA ..... Starting normalised body angle

SS ..... Stationary Static

SSB ..... Stationary Static Brief (short rest)

SSL..... Stationary Static Long (long rest)

sY-Pos..... Starting y-position

TTFL..... Transcription-translation feedback loop

UAS ..... Upstream Activating Sequence

VNC ..... Ventral nerve cord

X-Pos ..... X-position

Y-Pos ..... Y-position

ZT ..... Zeitgeber time

Chapter 1 Introduction

1.1 Introduction to circadian rhythms and sleep

The circadian (Latin: 'circa diem', which translates to 'about a day') clock refers to the autonomous internal timekeeping system that most organisms, from simple unicellular algae to complex multicellular humans, possess within their cells (Mittag and Wagner, 2003; Mohawk, Green and Takahashi, 2012). Environmental conditions, such as light and ambient temperature, oscillate over 24 hours due to the rotation of the Earth. A timekeeping mechanism allows organisms to predict these daily environmental changes, enabling them to organise their physiological and behavioural processes, such as sleep-wake rhythms, to occur at an optimal time over this 24-hour cycle (Curtis and Fitzgerald, 2006; Levi and Schibler, 2007; Patke, Young and Axelrod, 2020). These rhythms of physiology and behaviour are termed 'circadian rhythms'. A circadian clock has three main characteristics:

1. External environmental cues, termed zeitgebers ('time givers' in German), can entrain an organism's circadian clock, such that the phase of their clock can be either advanced or delayed, thus synchronising their internal clock, and downstream physiology and behaviour, with the daily environmental cycle (Roenneberg, Daan and Merrow, 2003). For example, exposing individuals to bright light early in the morning leads to a phase advance (the clock advances its cycle to match the new environment), accompanied by an earlier rise in melatonin levels at night, an advanced body temperature rise during sleep, and an advance in waking time (Dijk *et al.*, 1987).
2. The circadian clock is endogenously driven such that it continues functioning in free-running conditions, like constant darkness and constant temperature, with near 24-hour periodicity. An organism, when placed into constant conditions, will continue to show behavioural and physiological rhythms with a period of around 24 hours.
3. The clock is temperature compensated, meaning that while temperature cycles act as a zeitgeber, the period of the clock, and therefore the downstream physiological and behavioural rhythms, is not altered by changes in temperature (Kidd, Young and Siggia, 2015; Narasimamurthy and Virshup, 2017).

The most prominent example of circadian rhythms is sleep-wake behaviour. Sleep is a reversible behavioural state thought to be conserved across the whole animal kingdom, yet its function remains relatively unclear (Campbell and Tobler, 1984; Cirelli and Tononi, 2008; Krueger *et al.*, 2016). Sleep can be considered as an animal sacrificing responsiveness to the outside world for

the benefit of internal restorative processes (Zepelin and Rechtschaffen, 1974; Campbell and Tobler, 1984; Rechtschaffen, 1998; Cirelli and Tononi, 2008; Keene and Duboue, 2018).

Sleep is widely thought to be regulated via two processes (Figure 1.1.1), a model initially described by two papers in the 1980s (Borbély, 1982; Daan, Beersma and Borbély, 1984). The first process is the circadian clock. Individuals have a biological clock entrained to the 24-hour fluctuations in environmental conditions and adapt their behaviour, including sleep timing, to occur at an optimal time of day (E.g., night-time sleep for diurnal species). The circadian process therefore is illustrated as a periodic function which is not altered by whether the organism has slept or not. The second process is a homeostatic mechanism. It represents the sleep debt, which increases during waking experience and decreases during sleep. Depriving an individual of sleep will increase this sleep debt, and subsequent sleep (rebound) will be longer and of greater quality (a deeper state) (Patrick and Gilbert, 1896; Webb and Agnew, 1975; Dijk and Beersma, 1989).

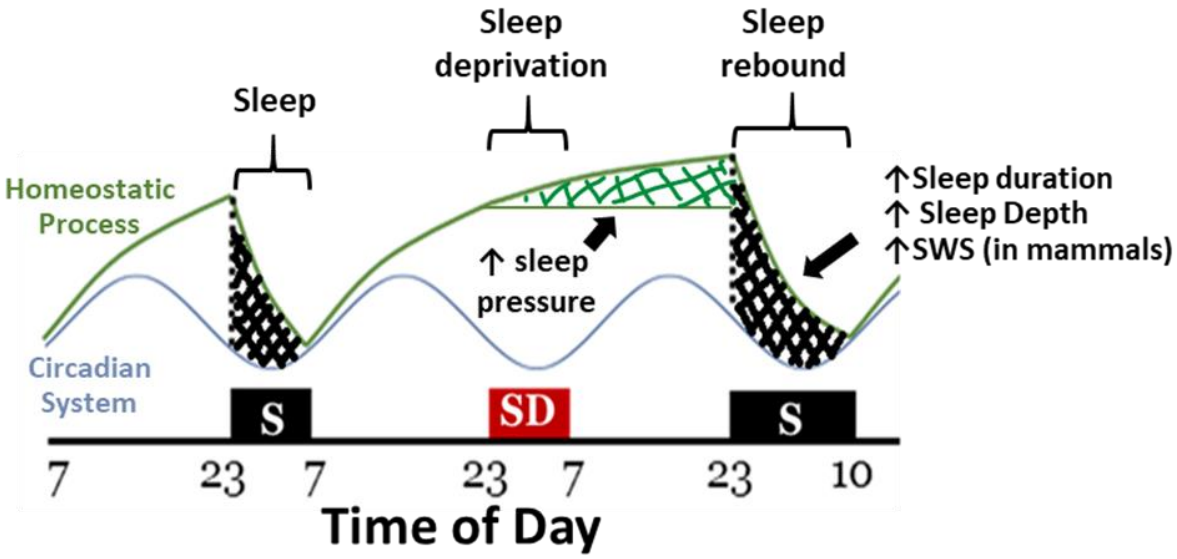

Figure 1.1.1 The two-process model of sleep regulation

Circadian and homeostatic mechanisms result in consolidated periods of sleep. Under baseline conditions, sleep occurs when sleep debt is high and the circadian wakefulness drive is low. During sleep deprivation, sleep pressure increases, resulting in a stronger homeostatic sleep rebound of increased sleep duration, depth, and slow wave sleep (SWS) in mammals. Figure modified significantly from (Borbély, 1982; Daan, Beersma and Borbély, 1984).

The two-process model posits that the likelihood of sleep (sleep pressure) corresponds to the difference between the homeostatic and circadian processes (Borbély, 1982). In most common cases, sleep occurs when sleep debt is high, while the circadian waking drive is low. Certain situations, such as jetlag and shift work, lead to the phenomena where the circadian and

homeostatic processes are misaligned (Sack *et al.*, 2007). In such cases, sleep quality and neurobehavioural function is greatly reduced. While the original model suggested that the circadian and homeostatic processes are separate, subsequent studies have demonstrated that these two processes can interact and influence each other (Borbély *et al.*, 2016).

While the typical human spends ~8 hours per day sleeping, large proportions of the population suffer from insufficient sleep and daytime hypersomnolence (Ford and Kamerow, 1989; Simon and VonKorff, 1997; Strine and Chapman, 2005; Institute of Medicine, Board on Health Sciences Policy and Committee on Sleep Medicine and Research, 2006; Olesen *et al.*, 2012). Insufficient sleep and disrupted circadian rhythms are associated with many negative health consequences and can occur due to a myriad of reasons (Brainard *et al.*, 2015; Medic, Wille and Hemels, 2017). These can be generally grouped into:

1. Personal lifestyle choices such as the use of caffeine or alcohol (Thakkar, Sharma and Sahota, 2015; Clark and Landolt, 2017; Gardiner *et al.*, 2023), performing shift work (Boivin and Boudreau, 2014; Costa, 2015), or travel associated 'jet lag' (Cingi, Emre and Muluk, 2018).
2. Environmental factors, such as noise and light (Basner, Müller and Griefahn, 2010; Smolensky, Sackett-Lundeen and Portaluppi, 2015; Touitou, 2015; Touitou, Reinberg and Touitou, 2017).
3. Psychosocial and medical conditions. High stress levels are associated with difficulty falling asleep and maintaining sleep (Y. Liu *et al.*, 2014; Kalmbach, Anderson and Drake, 2018). Furthermore, chronic stress is a significant risk factor for insomnia, a sleep disorder characterised by issues with beginning and maintaining sleep, alongside disruption to daytime performance (Basta *et al.*, 2007). Experiencing pain also disrupts sleep. For example, a study of children's experience post tonsillectomy found that those with more heightened pain experienced worse sleep disruption (Sutters and Miaskowski, 1997).
4. Sleep disorders such as obstructive sleep apnoea, restless leg syndrome, and insomnia (Institute of Medicine, Board on Health Sciences Policy and Committee on Sleep Medicine and Research, 2006; Medic, Wille and Hemels, 2017). While sleep loss is a typical result of sleep disorders, hypersomnolence is present in a small subset of sleep disorders such as narcolepsy and Klein-Levin syndrome (Scammell, 2015; Arnulf, Groos and Dodet, 2018).

The personal and societal costs associated with poor sleep are of worldwide concern. Sleep-loss has both short- and long-term consequences. In the short-term, general performance, such as reaction time, ability to focus, and cognitive processing, is significantly reduced (Durmer and Dinges, 2005). Notably, performance loss is a dose-dependent effect that accumulates over time

(Belenky *et al.*, 2003; Van Dongen *et al.*, 2003). Given that many jobs rely on the ability to focus and make correct judgements, short-term consequences of sleep loss can be severe. Take intensive care unit (ICU) workers as an example. In the early 2000s, ICUs had exceedingly long work hours, which correlates to less sleep and a high rate of medical errors. A study found that reducing the working hours of interns led to increased sleep and lower numbers of serious medical errors made (Landrigan *et al.*, 2004). In addition to medical errors, around 20% of serious crashes are associated with driver tiredness from lack of sleep (Connor *et al.*, 2002). Many significant disasters, such as the nuclear meltdowns at Three Mile Island and Chornobyl, have also been linked to sleep loss and fatigue-related incompetence (Mitler *et al.*, 1988). These major disasters cost millions of dollars, caused far-reaching environmental damage, and negatively shifted the general public's view of nuclear power.

Sleep disruption also has a significant impact on mental and physical health. Sleep disruption and sleep disorders are associated with a poor quality of life (Kuppermann *et al.*, 1995; Baldwin *et al.*, 2001; Reimer and Flemons, 2003; Hasler *et al.*, 2005; Strine and Chapman, 2005). Individuals whose partners suffered from sleeping issues reported worse mental health and lower marital satisfaction (Strawbridge, Shema and Roberts, 2004). Long-term sleep disruption is associated with many severe health conditions, including obesity (Hasler *et al.*, 2004; Taheri *et al.*, 2004), diabetes (Gottlieb *et al.*, 2005), cardiovascular disease (Qureshi *et al.*, 1997; Newman *et al.*, 2000; Ayas *et al.*, 2003), depression and anxiety (Fredriksen *et al.*, 2004; Hasler *et al.*, 2005; Strine and Chapman, 2005), suicidal behaviour (Liu, 2004), and increased age-specific mortality (Patel *et al.*, 2004; Tamakoshi, Ohno and JACC Study Group, 2004).

Given the high prevalence of sleep disruption, billions of dollars a year are spent on doctor appointments, hospital visits, and medication in the US alone (Walsh and Engelhardt, 1999). For example, individuals with insomnia, sleepiness, fatigue, or sleep apnoea are associated with increased healthcare system use (Weissman *et al.*, 1997; Kapur *et al.*, 2002; Léger *et al.*, 2002). In 2004, it was estimated to cost over 20 billion dollars to test and treat every case of sleep apnoea in the US (Sassani *et al.*, 2004). There are also indirect healthcare costs that result from situations where sleep disruption is a significant risk factor (e.g., car crashes) (Institute of Medicine, Board on Health Sciences Policy and Committee on Sleep Medicine and Research, 2006). Aside from healthcare costs, there are substantial indirect costs to businesses via absenteeism and reduced productivity of their workers (Institute of Medicine, Board on Health Sciences Policy and Committee on Sleep Medicine and Research, 2006).

In conclusion, the prevalence of poor sleep and its impact on many aspects of daily life should greatly concern all societal strata. Research into the mechanisms by which sleep arises, the

functions occurring during sleep, and how these mechanisms are dysregulated during disease are of great importance.

1.2 *Drosophila* as a model to study circadian rhythms and sleep

Studying the underlying mechanisms of circadian rhythms and sleep directly in humans is challenging due to cost, time constraints, and, most importantly, ethical issues. To overcome these barriers, model organisms have provided a way to study the fundamental mechanisms of how and why organisms sleep. A model organism is a non-human species used in biological research, with the expectation that understanding how processes occur in these simpler organisms will elucidate conserved or similar mechanisms in more complex systems, such as humans (Leonelli and Ankeny, 2013).

Mammalian models, such as rats and mice, are often used due to their relative similarities to humans with regards to behaviour and physiology; however, they also have drawbacks. Mammalian models have relatively long gestational and developmental periods before experiments can be performed. This is a major stumbling block for generating fast, high throughput results with sufficient sample size. Mammalian models also have ethical limitations, are expensive, and produce relatively few offspring. In addition, mammalian models suffer from the issue of complexity. While mammalian models have significantly fewer neurons than humans, they are often too complex to probe the fundamental logic or mechanisms underlying biological processes.

Drosophila melanogaster, commonly known as the fruit fly, has risen to prominence as a (relatively) simple model organism for many aspects of biological research. Fruit flies have short developmental periods, high fecundity, and are incredibly cheap and easy to maintain. Given its lower complexity, and the multitude of genetic tools created, biological processes can be studied down to the single neuron level. For example, researchers at the Howard Hughes Medical Institute have recently produced a single-cell level connectome of a large portion of the fly brain (Scheffer *et al.*, 2020). Although fruit flies are considered simple, they exhibit a wide range of complex behaviours, such as learning and memory (Takemura *et al.*, 2017), navigation (Su *et al.*, 2017), courtship (Pavlou and Goodwin, 2013; Yamamoto and Koganezawa, 2013), sleep and circadian rhythms (Beckwith and French, 2019; Patke, Young and Axelrod, 2020), and even addiction (Kaun, Devineni and Heberlein, 2012).

1.2.1 Model for circadian rhythms

Drosophila melanogaster is a key model organism in the field of chronobiology, and studies in the fly pioneered the identification of many circadian genes and their interaction pathways (Patke, Young and Axelrod, 2020). Much circadian research has been conducted following the discovery of the first clock gene *'period'* in 1971 (Konopka and Benzer, 1971), with the 2017 Nobel Prize in Physiology and Medicine being awarded to the key researchers Hall, Rosbash, and Young for their contribution to elucidating the molecular mechanisms underlying the circadian clock in flies. Notably, the core features and many of the molecular clock genes are conserved between *D.melanogaster* and mammals (Young and Kay, 2001; Patke, Young and Axelrod, 2020).

Three major assays have been used to study circadian rhythms in *Drosophila*. In the initial stages of circadian research in flies, researchers began by recording the number of flies eclosing (pupal to adult transition) at various times of day. Eclosion is a circadian-controlled process that tends to occur in the early morning after dawn (Patke, Young and Axelrod, 2020). This was used successfully to discover the first circadian clock mutant, *period (per)* (Konopka and Benzer, 1971).

Following the use of eclosion rhythms, locomotor behaviour assays were created which were found to be a robust measure of the circadian clock and have been used successfully to discover many circadian clock genes (Figure 1.2.1A,(Axelrod, Saez and Young, 2015)). Locomotor assays (such as *Drosophila* Activity Monitor, 'DAM'; TriKinetics), involve placing individual flies within glass tubes (~65mm long) and recording flies within a 24-hour cycle of 12 hours of light and 12 hours of dark (12:12 Light:Dark; LD cycle). Their activity is measured by an infrared beam passing through the chamber's vertical midpoint. When a fly crosses the midpoint, the beam is broken, and the computer records a count. The number of counts per 5 minutes is used as a robust measure of locomotor activity and a correlate of circadian clock function.

Within a DAM assay, wild-type behaviour is described as crepuscular, whereby flies have high levels of locomotor activity at dawn and dusk (Figure 1.2.1B). Locomotor activity gradually increases prior to the lights turning on at dawn and off at dusk. This phenomenon is called anticipation and is thought of as the fly adjusting its behaviour and physiology in anticipation of the changes in environmental conditions that occur over a 24-hour day. In contrast, flies lacking a functional circadian clock have altered locomotor behaviour which can be easily detected with DAM. Flies also demonstrate a direct response to light changes, whereby they have a burst of locomotion at the occurrence of a light change. This phenomenon is called the startle response, which masks the underlying circadian behaviour. For example, circadian mutants that lack a functional circadian clock have a startle response and may appear 'rhythmic' in a light-dark cycle. As a result, experiments are also performed in constant darkness (DD) to ensure that rhythmic behaviour seen is due to the circadian clock.

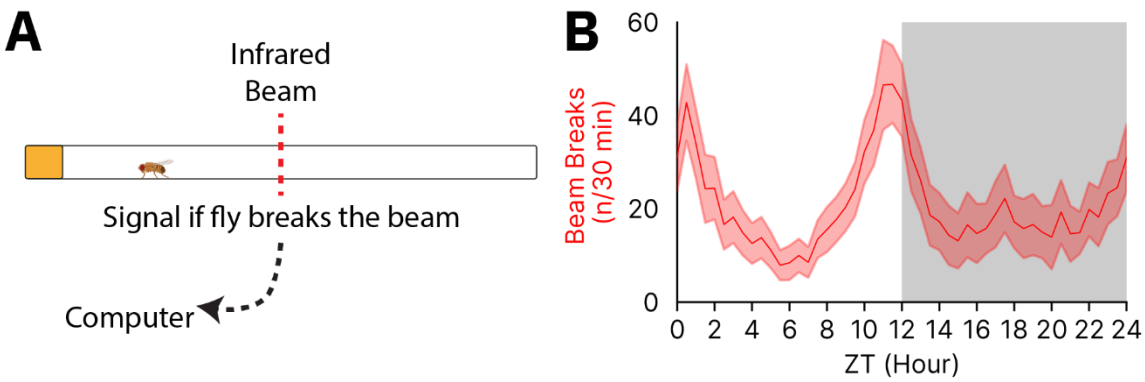

Figure 1.2.1 Schematic of the *Drosophila* Activity Monitor assay

(A) Flies are loaded into individual glass tubes, each with an infrared beam passing through the middle. When a fly crosses the midpoint of the tube, the infrared beam is broken and a count is recorded by the DAM computer. Counts are usually summed for every 5-minutes of recording. **(B)** Example plot of the number of beam breaks (Activity) recorded for each 30-minute time point in a 12:12 LD cycle (ZT 0 lights come on, ZT12 the lights turn off) averaged across each fly. Peaks of locomotor activity are noticeable around dawn and dusk in wild-type flies.

In addition to behaviour, Luciferase assays are frequently used to study circadian gene expression rhythms to better understand the circadian clock (Figure 1.2.1(Tataroglu and Emery, 2014)). Luciferases are a category of enzymes found within many species. Firefly (*Photinus pyralis*) Luciferase is used for circadian research and functions by converting its substrate D-luciferin to oxyluciferin via a two-step ATP-dependent process resulting in the release of a photon of light. Expressing firefly Luciferase as a transgene controlled by a sequence from a circadian promoter of interest (e.g., *period*) allows experimenters to record bioluminescence generated over time (by providing flies with D-luciferin in the food) as a result of the expression of Luciferase. A sensitive light detector, such as a plate reader with photomultiplier tubes can then be used to detect the released photons of light. As a chosen promoter controls Luciferase expression, the bioluminescence pattern represents that chosen promoter's expression pattern. Luciferase has a half-life of around 3 hours in mammalian cells (Thompson, Hayes and Lloyd, 1991), making it suitable for detecting rhythmic expression. For example, flies expressing *per-luciferase* show strong 24-hour bioluminescence rhythms, demonstrating that the *period* gene is rhythmically transcribed (Brandes *et al.*, 1996).

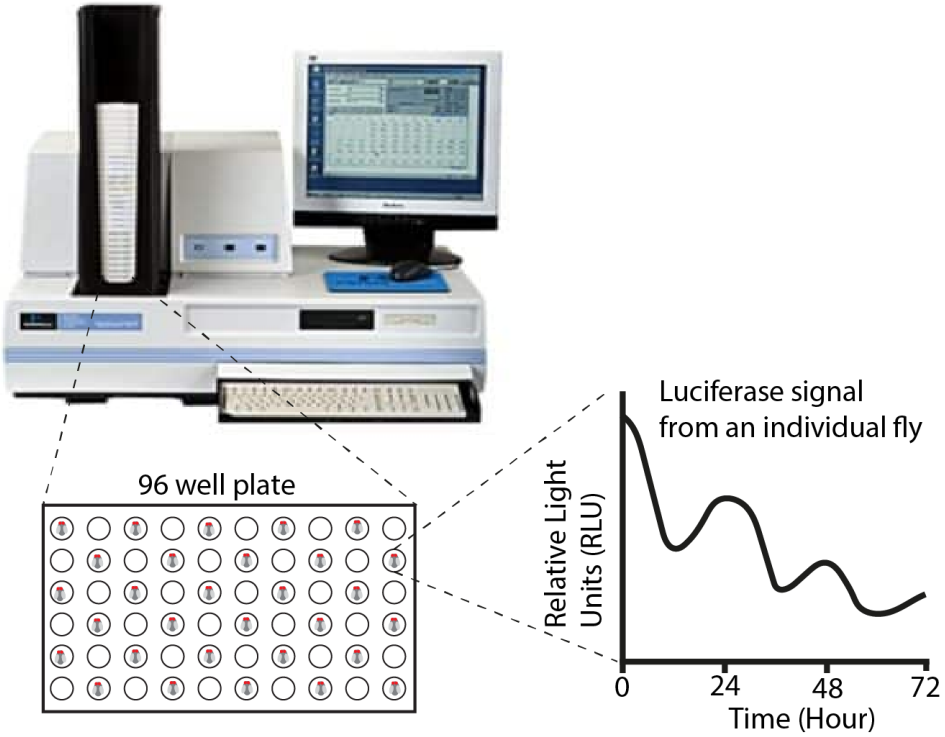

Figure 1.2.2 Basic schematic of a Luciferase Assay

Individual flies are placed within each well (or every other well) of a 96-well plate. Each fly will generate a Luciferase signal over time via the expression of Luciferase whose expression is rhythmically controlled by a circadian promoter of interest. The Luciferase activity is detected by a machine such as the Topcount NXT scintillation counter (*Packard Topcount NXT scintillation counter: GMI - Trusted Laboratory Solutions*, 2022), which contains photomultiplier tubes to detect incoming photons of light from each well of the plate. Images of the 96-well plate and luciferase signal trace are recreated and modified from Figure 4 of (Tataroglu and Emery, 2014).

1.2.2 *Drosophila* rest as a sleep-like state

While *Drosophila* has been used for many years to study the circadian clock, it was not known until the end of the 20th century whether fruit flies sleep. This was also despite the fact that sleep-wake rhythms are one of the most prominent circadian outputs observable in mammals. The delay in defining sleep in flies can be partially attributed to the fact that a sleep state was commonly defined by recording cortical activity in mammals and avian species (see Chapter 1.6.1 for more information), a process unsuitable for use in smaller, less complex organisms. To define sleep in a way that is also applicable to less complex organisms, a behavioural definition of sleep was suggested (Campbell and Tobler, 1984; Hendricks, Sehgal and Pack, 2000). There was precedent for this, given that historically, behavioural criteria were utilised to facilitate the

discovery of electrophysiological changes occurring during mammalian sleep (Campbell and Tobler, 1984). The behavioural criteria are:

1. Sleep is associated with a species-specific pose (or set of) and preferred resting location.
2. The circadian system influences the timing of sleep. An organism will display consolidated periods of sleep at specific times of the day with a circadian rhythm. This rhythm should remain in free-running conditions (e.g., DD).
3. Sleep is homeostatically regulated. As waking time increases, the need for sleep increases (considered a 'sleep debt'). Sleep deprivation leads to a subsequent increase in sleep, termed 'Sleep Rebound'.
4. Sleep is associated with an increased arousal threshold. An organism becomes less responsive to a given stimulus (e.g., a noise) during sleep.
5. Sleep is reversible, given a strong enough stimulus. This is a fundamental difference from a comatose or seizure state in which the individual will not awaken/move regardless of the strength of the stimuli.

Drosophila melanogaster rest as a sleep-like state was first posited by two independent research groups at the end of the 20th century (Hendricks *et al.*, 2000; Shaw *et al.*, 2000). Both laboratories utilised the DAM assay commonly used in circadian fly research (Figure 1.2.1).

(Hendricks *et al.*, 2000) first suggested that flies typically rest close to but facing away from the food source (96% of the time) (criteria 1). Flies were also described as initiating rest bouts in a supported upright position, subsequently lowering the body to a prone position during rest (criteria 1). By visually annotating fly behaviour in DAM assays, (Hendricks *et al.*, 2000) found that inactive periods (≥ 1 minute) were inversely correlated with activity counts and that flies rested for ~11 hours a day, with the majority of this being consolidated during subjective night (criteria 2). Shaw *et al.*, 2000 also found that most rest (≥ 5 minutes of no beam breaks in a DAM assay) occurred during the night (criteria 2). Consolidated rest was ablated in circadian mutants (Shaw *et al.*, 2000; Hendricks *et al.*, 2003; Dubowy and Sehgal, 2017)). Flies with mutations in their clock genes (See Chapter 1.3.1), rendering them arrhythmic, showed a lack of a consolidated rest period. Instead, these arrhythmic flies had fragmented sleep throughout the day while displaying a typical amount of total rest (Hendricks *et al.*, 2003).

By testing the responsiveness of flies in group-housed interactions, inactive flies (≥ 5 minutes) were found to have an increased arousal threshold (criteria 4; (Hendricks *et al.*, 2000)). (Hendricks *et al.*, 2000) also found that resting flies were less responsive to mechanical stimuli than active flies, and that previously rest deprived flies were even less responsive while resting. As expected, all flies responded to a strong enough mechanical stimulus. They, therefore, conclude that resting flies have a heightened arousal threshold during rest (criteria 4), which is reversible given a strong

enough stimulus (criteria 5). Similarly, Shaw *et al.*, 2000 found that, by using a vibrational stimulus, active flies responded to low vibration levels, whereas fewer resting flies responded (90% vs. <20%; criteria 4). Significantly, all flies responded with a strong enough stimulus, regardless of rest duration (criteria 5).

Finally, both (Hendricks *et al.*, 2000) and Shaw *et al.*, 2000 demonstrated that rest-deprived flies (via mechanical stimulus) showed a significant increase in rest compared to controls (criteria 3). To rule out stress as a confounding variable in mechanical sleep deprivation protocols, they performed a follow-up experiment using the same protocol, but with rest deprivation occurring during a 6-hour period when flies are most active. No difference in rest rebound compared to controls was seen, suggesting that the prior results were not due to a stress response to the deprivation stimulation. In addition, Shaw *et al.*, 2000 analysed the rest rebound process in the per^{01} circadian mutant. These flies lack a functional circadian clock, and they show that under baseline free-running (constant darkness) conditions, per^{01} flies rest the same overall amount as wild-type flies but without any consolidated period (criteria 2). In addition, 12-hour dark phase rest deprived per^{01} mutants still experienced a rest rebound following deprivation, providing evidence that the homeostatic rest process can be uncoupled from the circadian system.

Beyond the behavioural tenets, both studies demonstrated aspects of rest in *Drosophila* that correlate with mammalian sleep. Both studies demonstrated that the mammalian wake-promoting compound caffeine, which is a non-selective A1/A2A adenosine receptor agonist (Ferre *et al.*, 2008), reduces rest in *Drosophila* (Hendricks *et al.*, 2000; Shaw *et al.*, 2000). As with mammalian sleep, total rest duration in *Drosophila* was increased with the application of an anti-histamine (hydroxyzine) in a dose-dependent manner (Shaw *et al.*, 2000).

Shaw *et al.*, 2000 also demonstrated that age impacts the duration of *Drosophila* rest like in mammalian sleep. In humans, new-borns sleep around 16 hours daily (Chokroverty, 2010). This sleep requirement decreases with age until stabilising to around 8 hours during adulthood. In later (elderly) life, humans experience reduced and more fragmented sleep. Similarly, *Drosophila* rest is highest on the first day post-eclosion and reduced until stabilising at day 3 (adulthood) (Shaw *et al.*, 2000). Old-aged flies also had lower levels of rest.

Finally, Shaw *et al.*, 2000 found gene transcripts that were upregulated specifically during wake or rest in both mammals and *Drosophila*. Multiple transcripts, such as Cytochrome oxidase C (subunit I), were found to be upregulated in both *Drosophila* and rats, suggesting conserved processes are being upregulated during wake/rest.

In conclusion, Hendricks *et al.*, 2000 and Shaw *et al.*, 2000 provide a case in which all five behavioural tenets of sleep are met by *Drosophila* rest. In addition, both studies provide evidence for correlates between mammalian sleep and *Drosophila* rest, with similar responses to the

application of known wake/sleep-promoting compounds and upregulation of specific gene transcript levels during wake/sleep.

1.3 Circadian clock in *Drosophila*

1.3.1 The molecular clock

The *Drosophila* core clock mechanism is a transcription-translation feedback loop (TTFL). The first clock gene *period* was discovered via forward genetic screening of eclosion mutants (Konopka and Benzer, 1971). The first circadian mutant discovered was arrhythmic (per^{01}), and the subsequently named *period* (*per*) gene was found to be the site of mutation. Subsequent experiments found two more mutants of the same gene, one of which leads to a longer than 24-hour period (per^{L}) and one which has a shorter period (per^{S}).

After the discovery of *period*, additional circadian proteins were discovered, which form the core transcription-translation feedback loop (Figure 1.3.1). The TTFL begins with transcription factors Clock (CLK) and Cycle (CYC) (Allada *et al.*, 1998; Rutila *et al.*, 1998), which are expressed in the nucleus, heterodimerise, and bind to E-box enhancer domains (typically a CACGTG sequence) within the promoters of their target genes (Dubowy and Sehgal, 2017). Many genes contain E-box domains, and these clock-controlled genes are rhythmically expressed via CLK:CYC transcriptional activation (Patke, Young and Axelrod, 2020). Alongside *period*, *timeless* was discovered to encode the binding partner to Period (Timeless or TIM), which together form the inhibitory (negative arm) of the feedback loop (Sehgal *et al.*, 1994). Both *period* and *timeless* have E-box domains within their promoters, and CLK:CYC activity leads to their transcription during the day (Hao, Allen and Hardin, 1997; Allada *et al.*, 1998; Darlington *et al.*, 1998; Rutila *et al.*, 1998).
Period and *timeless* RNA levels accumulate during the day and peak in the early evening. PER and TIM levels, however, are delayed such that they peak during the middle of the night (Zheng and Sehgal, 2012; Patke, Young and Axelrod, 2020).

PER and TIM accumulation leads to their heterodimerisation, entering the nucleus with the help of importins (Jang *et al.*, 2015) and repressing CLK:CYC activity during the late night-early morning period. This repression of CLK:CYC is not fully understood, but the data suggest that it involves PER binding to CLK and acting as a scaffold for the recruitment of the casein kinase 1ε homolog 'Doubletime' (DBT) and potentially other kinases, which subsequently phosphorylates CLK (Lee, Bae and Edery, 1999; Kim and Edery, 2006; Kim *et al.*, 2007; Nawathean, Stoleru and Rosbash, 2007). An additional CLK:CYC transcriptional target is *clockwork orange* (*cwo*). In addition to PER:TIM repressing CLK:CYC activity, Clockwork orange (CWO) also functions to bind to CLK:CYC

and inhibit their transcriptional activity (Kadener *et al.*, 2007; Lim *et al.*, 2007). MicroRNAs (miRNAs) are thought to be involved in delaying the TTFL. One example of this comes from data that overexpression of the miRNA *let-7* leads to an increased period length, and *let-7* was shown to repress CWO translation (Chen *et al.*, 2014). PER:TIM repressing CLK:CYC activity leads to repressing their own transcription. Both PER and TIM are degraded during the early-to-mid day such that CLK:CYC complexes are no longer repressed and can initiate a new cycle of the TTFL (Patke, Young and Axelrod, 2020).

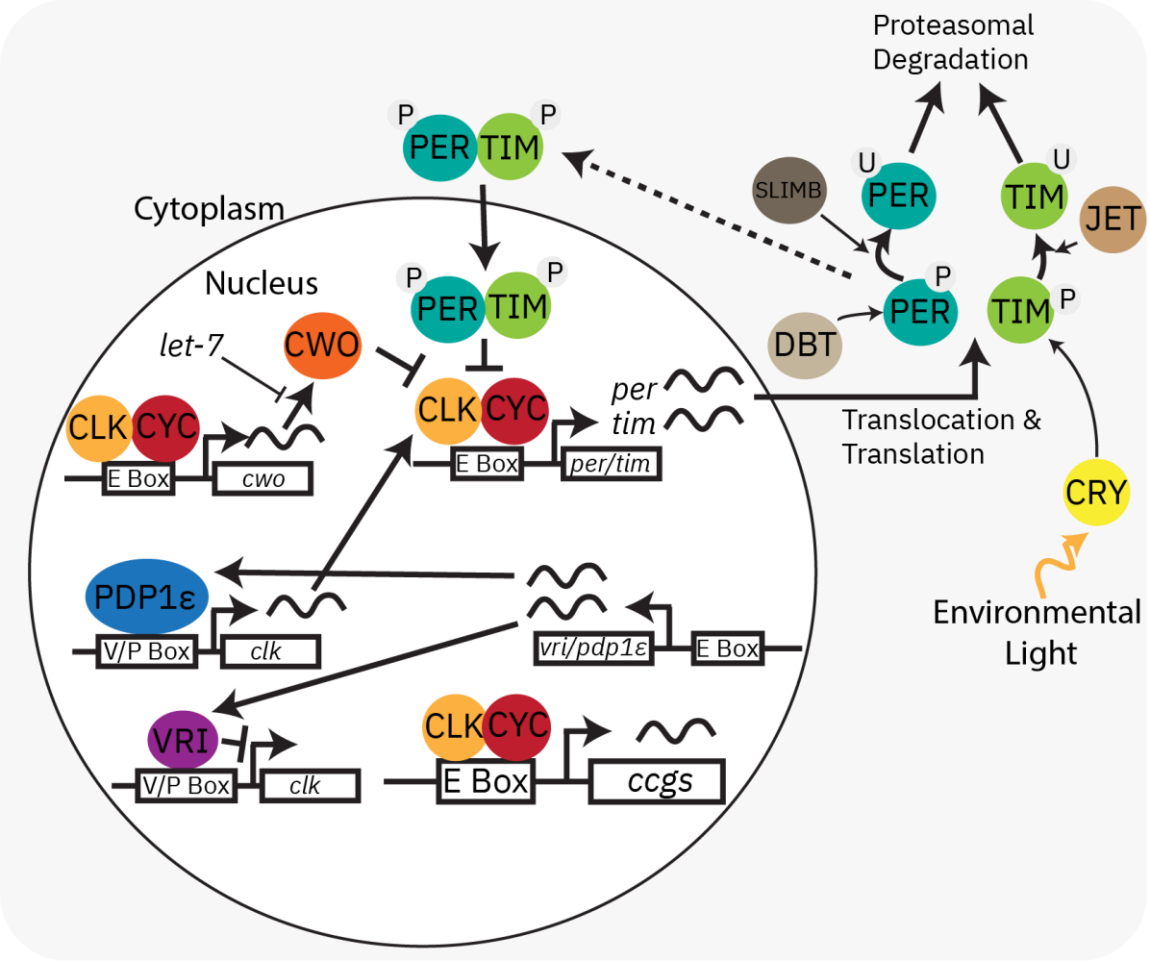

Figure 1.3.1 The *Drosophila* molecular clock

At a simplistic level, the molecular clock is a transcription-translation feedback loop whereby the core clock proteins CLK and CYC are transcriptional activators of genes contain E-box domains within their promoters. The core clock genes *period* and timeless are two such genes and are expressed downstream of CLK:CYC activity. The role of PER and TIM is in inhibiting the transcriptional activity of CLK:CYC, thereby inhibiting their own transcription and eventually starting the transcriptional cycle again once PER and TIM are degraded. This cycle takes around

24-hours due to a variety of regulatory mechanisms. Figure created with inspiration and modifications from Figure 1 of (Patke, Young and Axelrod, 2020).

Light is a potent zeitgeber for the circadian clock. In flies, the molecular clock can be entrained and reset by light information received from the rhodopsin 1-7 photoreceptors in the visual system (Senthilan *et al.*, 2019). In addition, environmental light can be detected in a cell-autonomous manner via the blue-light photoreceptor Cryptochrome (CRY) (Stanewsky *et al.*, 1998). When flies are in a light-dark (LD) cycle, TIM degradation is mediated by CRY. While mammalian CRY is a core clock protein (functioning like TIM in flies), *Drosophila* CRY has an essential role in light-mediated entrainment and resetting of the clock (Ceriani *et al.*, 1999; Koh, Zheng and Sehgal, 2006; Peschel *et al.*, 2009). Light leads to a conformational change in CRY, allowing it to bind to TIM (Ceriani *et al.*, 1999). TIM is subsequently phosphorylated (Naidoo *et al.*, 1999), which allows Jetlag (JET) to bind and lead to its degradation. Interestingly, CRY is also a target of JET and is therefore degraded in response to light as well. TIM, however, stabilises CRY, protecting it from JET-mediated degradation (Peschel *et al.*, 2009). This results in a temporal difference in light-dependent TIM and CRY degradation, whereby JET preferentially targets TIM for degradation first and CRY afterwards (Yoshii *et al.*, 2008; Peschel *et al.*, 2009). During free-running conditions (constant darkness), TIM degradation is thought to involve Supernumerary Limbs (SLIMB) (Grima *et al.*, 2002). Both SLIMB and JET are F-box proteins which are part of the E3 ubiquitin ligase complex and target TIM for degradation by ubiquitination and subsequent sequestering to the proteasome. In the absence of TIM, PER is targeted by DBT for phosphorylation. For example, a critical phosphorylation site on PER is the serine at position 47, although other phosphorylation sites are likely also involved (Chiu *et al.*, 2008; Dubowy and Sehgal, 2017). Hyperphosphorylated PER is targeted by SLIMB for ubiquitination and subsequent proteasomal degradation (Grima *et al.*, 2002; Ko, Jiang and Edery, 2002; Chiu *et al.*, 2008).

A secondary loop regulates *clock* (*clk*). CLK:CYC bind to the E-boxes in the promoters of *vrille* (*vri*) and *PAR domain protein 1ε* (*Pdp1ε*). These genes encode the transcriptional repressor Vrille (VRI) and the transcriptional activator PAR domain protein 1ε (PDP1ε) (Cyran *et al.*, 2003). These transcriptional regulators regulate *clock* transcription (Cyran *et al.*, 2003). Within the *clock* promoter are VRI/PDP1ε binding motifs, which these two transcriptional regulators can bind to (Cyran *et al.*, 2003). Expression of *vri* occurs prior to *Pdp1ε* such that transcriptional repression of *clk* is followed by transcriptional activation, resulting in a robust cycling of *clock* expression (Zheng and Sehgal, 2012). Interestingly, while *clk* RNA is cyclical, protein levels of CLK do not cycle (Houl *et al.*, 2006). The purpose of *clk* mRNA cycling is currently unclear, and changing the phase of *clk* mRNA does not impact behavioural rhythms (Kim *et al.*, 2002).

Given that unregulated transcription-translation occurs rapidly, delays are required within the TTFL to generate a ~24-hour rhythm. Mechanisms were described above, such as delaying the build-up of protein translation (e.g., with miRNAs), nuclear entry of PER:TIM, and controlling PER:TIM stability via post-translational modifications. However, many more mechanisms of regulation at the post-transcriptional and post-translational have also been discovered (Zheng and Sehgal, 2012; Patke, Young and Axelrod, 2020).

1.3.2 Clock neurons

Within the fly, the central circadian clock is comprised of 150 neurons within the brain, which contain a functional molecular clock and drive downstream circadian behaviour and physiology (75 in each hemisphere) (Figure 1.3.2(Allada and Chung, 2010)). The central clock neurons within wild-type flies all exhibit a synchronised molecular clock (Yoshii, Vanin, *et al.*, 2009; Roberts *et al.*, 2015). These neurons are subdivided into five major clusters and named based on their morphology and location within the brain. There are the small ventrolateral neurons (s-LNvs), the large ventrolateral neurons (l-LNvs), the dorsolateral neurons (LNds), the lateral posterior neurons (LPNs), and the dorsal neurons (DNs). The dorsal neurons (DNs) are further subdivided into the DN1, DN2, and DN3.

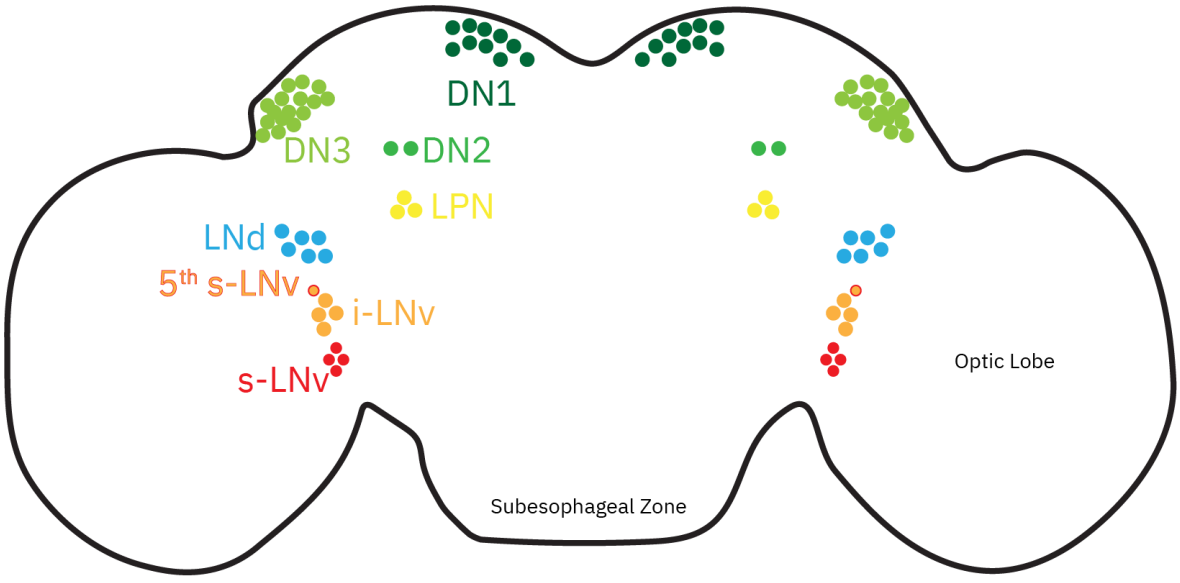

Figure 1.3.2 The core circadian clock neurons in *Drosophila*

The core circadian clock is comprised of 75 pairs of neurons within the fly brain and named based on their location within the brain.

Locomotor behaviour is biphasic and is *Drosophila's* primary circadian output measure. The clock neuron regulation of locomotor behaviour is, in a simplistic model, considered to be controlled by

two central populations in light-dark cycles. Pigment dispersing factor (PDF) is a neuropeptide expressed in all ventrolateral neurons except one, commonly described as the 5th s-LNv (Helfrich-Förster, 1995; Rieger *et al.*, 2006). The *pdf* expressing (*pdf*+) s-LNvs are typically described as 'morning cells' as they are thought to promote the morning peak in locomotor activity, while the *pdfr*+ LNds and a singular *pdf*- s-LNV (5th s-LNv) are considered the 'evening cells' as they are important for the timing of the evening peak in locomotion (Grima *et al.*, 2004; Stoleru *et al.*, 2004; Liang, Holy and Taghert, 2016). The morning cells are also considered a key population for synchronising the clock circuit and the pacemaker in constant darkness (Stoleru *et al.*, 2005; Guo *et al.*, 2014; Yao and Shafer, 2014).

To manipulate specific populations of circadian neurons, a binary expression system such as GAL4/UAS or LexA/LexAop is used (Figure 1.3.3; (Brand and Dormand, 1995; Lai and Lee, 2006)). This functions by expressing a transgene (called the 'responder') containing a gene of interest (e.g., the thermosensitive cation channel TrpA1) downstream of an upstream activating sequence (UAS). A second transgene (termed a 'driver') is used which contains the sequence for a GAL4 transcription factor. The GAL4 is targeted to specific cells of interest by expressing it downstream of a promoter with a desired expression pattern. In cells where the GAL4 is expressed, it will bind to UAS sequences in the genome and activate the expression of the gene of interest downstream. For example, the *pdf*+ neurons can be activated by expressing UAS-TrpA1 and the pdf-GAL4 driver within flies. The LexA/LexAop system works the same way as for GAL4/UAS.

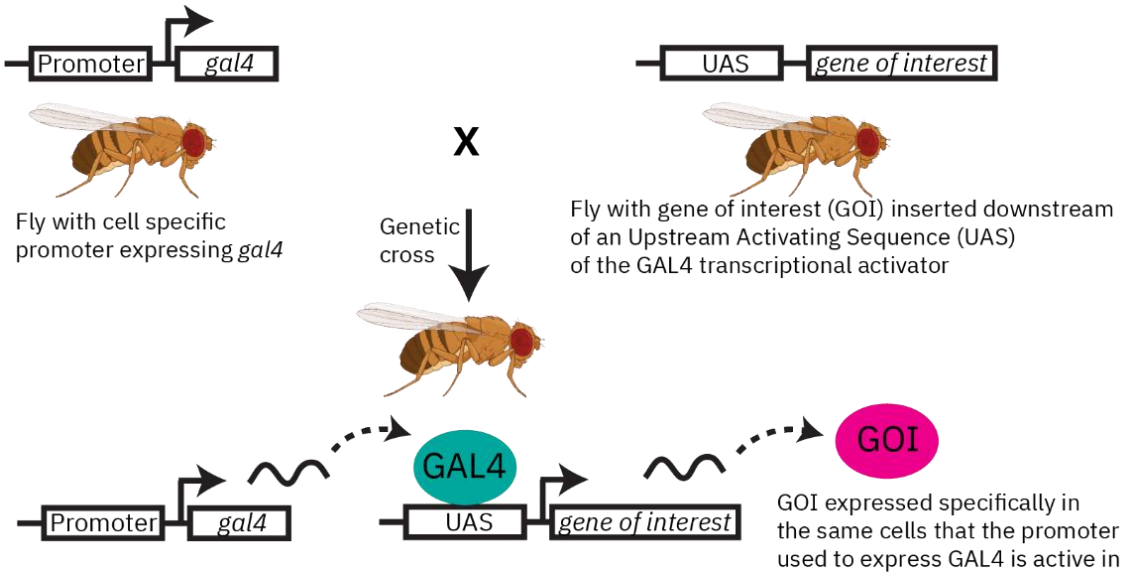

Figure 1.3.3 GAL4/UAS binary expression system

The GAL4 protein binds to upstream activating sequence (UAS) leading to the gene downstream to be expressed. A GAL4 transcription factor can be expressed downstream of a tissue-specific promoter such that the gene downstream of a UAS sequence is only activated in those cells.

Silencing or ablating the s-LNvs leads to arrhythmicity in constant darkness (Renn *et al.*, 1999; Nitabach, Blau and Holmes, 2002; Depetris-Chauvin *et al.*, 2011). In addition, restoring *per* expression to the s-LNvs within otherwise per^{01} flies rescues typical locomotor behavioural rhythms in constant darkness (Grima *et al.*, 2004). The *pdf+* s-LNvs project to a region of the brain termed the dorsal protocerebrum and release PDF. The PDF receptor (PDFR) is a GPCR expressed in half of the LNds, the 5th s-LNv, and a subset of the DN1s (Im and Taghert, 2010). A major role of PDF is in synchronising the phase of the molecular clocks across the clock neuron populations (Lin, Stormo and Taghert, 2004). pdf^{01} flies lack a morning locomotor peak with an early evening peak in light-dark cycles and gradually become arrhythmic in constant darkness (Renn *et al.*, 1999). In pdf^{01} flies, the molecular clocks of the s-LNvs become desynchronised, the molecular clocks in the *pdfr*+ LNds phase advance, and the cyclic expression of clock components (e.g. PER) reduces in amplitude (Lin, Stormo and Taghert, 2004). The impact of PDF signalling differs between populations, however. In the s-LNvs, PDF signalling back onto the s-LNvs is required to maintain synchronicity between the s-LNvs. Meanwhile, the LNds and the 5th s-LNv are not synchronised, as such, by PDF, but PDF is important for maintaining their period length as well as for maintaining robust high amplitude rhythms (Lin, Stormo and Taghert, 2004; Yoshii, Wülbeck, *et al.*, 2009). Interestingly, while the *cry*+ LNds have a shortened period in flies lacking *pdf*, the 5th s-LNv and *cry*- LNds have a lengthened period (Yoshii, Wülbeck, *et al.*, 2009). One mechanism of PDF action is that PDF release from the s-LNvs can induce phase shifts in the evening cells via CRY-independent TIM degradation (Guo *et al.*, 2014).

In addition to synchronised molecular clocks, the core clock neurons also have rhythmic calcium levels (a correlate of neuronal activity) (Yoshii, Vanin, *et al.*, 2009; Roberts *et al.*, 2015; Liang, Holy and Taghert, 2016). Interestingly, however, the calcium levels of the various core clock populations are not synchronised, with some having a delayed phase compared to others (Liang, Holy and Taghert, 2016). The s-LNvs peaked during the night, while the LNd population peaked during the day, with around a 10-hour difference in phase. The s-LNvs are considered necessary for the morning peak, while the LNds are important for timing the evening peak. The calcium data nicely aligns with the behavioural output such that there is a ~4-hour gap between the peak calcium signal and the behavioural output associated with that neuronal population (Liang, Holy and Taghert, 2016). PDF appears to be essential for mediating this phase difference, as loss of the PDF receptor (*pdfr*) leads to the LNd population having a similar phase to the s-LNvs (Liang, Holy and Taghert, 2016).

The regulation of behaviour is much more complicated than the morning and evening cell oscillator model. For example, the evening cells were shown to be important for both the morning

and evening peaks in locomotor activity during light-dark cycles and disrupting their activity can also reduce activity rhythms in constant darkness (Guo *et al.*, 2014). Furthermore, in a light-dim light cycle, *period* rescue, specifically within the evening cells (3 *pdfr*+ LNds and the 5th s-LNv), re-establishes both morning and evening peaks of locomotor behaviour (Rieger *et al.*, 2009). In addition, much of circadian research in *Drosophila* focuses on locomotor behaviour in standard light-dark, dark-dark, or light-light conditions. There are many behavioural and physiological changes downstream of a circadian clock, and the regulation of these may preferentially require different clock neurons. For example, temperature is also a potent zeitgeber. Flies in constant light or dark conditions with a temperature cycle (temperature is a zeitgeber) have rhythmic locomotor activity, and the DN2s and LPNs are considered important for mediating this (Yoshii *et al.*, 2005; Miyasako, Umezaki and Tomioka, 2007; Dubowy and Sehgal, 2017). The DN1s are also crucial for circadian control of locomotor behaviour. A functional molecular clock within a subset of the DN1s is sufficient to rescue the morning peak of locomotor activity in light-dark cycles (L. Zhang *et al.*, 2010; Y. Zhang *et al.*, 2010; Cavanaugh *et al.*, 2014; Seluzicki *et al.*, 2014). Interestingly, these neurons are also sufficient for the evening locomotor activity peak when flies are in constant darkness and a temperature cycle (Y. Zhang *et al.*, 2010).

Peripheral clocks are also present within the fly. The fly excretory system is one example of peripheral clocks (Hege *et al.*, 1997). The malpighian tubules (MTs) are considered the equivalent structure to the kidneys in mammals and have a functional molecular clock even in decapitated flies (Giebultowicz and Hege, 1997). Core clock neurons do not innervate the MTs and yet are robustly rhythmic and light-sensitive (Giebultowicz *et al.*, 2000). Transplanting MTs which are entrained to a light-dark cycle into a fly entrained with an anti-phase light-dark cycle (12-hour difference) leads to maintenance of the different phased oscillations between the molecular clock in the fly brain versus the transplanted MTs in constant darkness (Giebultowicz *et al.*, 2000). The work from (Myers, Yu and Sehgal, 2003) and Giebultowicz *et al.*, 2000 demonstrates that some peripheral clocks within the fly are connected downstream of the central clock in the brain, while other peripheral clocks function completely autonomously.

1.3.3 Clock output circuits in sleep-wake regulation

The circadian clock is involved in timing a vast array of behaviour and physiology in flies. Research often focuses on locomotor activity rhythms; however, many other behaviours, such as eclosion, feeding, and courtship, are also rhythmic (Franco, Frenkel and Ceriani, 2018). For this thesis, regulating sleep/locomotion via the circadian clock is the most relevant output pathway of interest. A functional molecular clock within circadian neurons is required for proper timing of *Drosophila* sleep. Core clock mutants such as per^{01} have similar amounts of total sleep but do

not have any rhythmicity in when this sleep occurs over the 24-hour day. Typical wild-type flies, on the other hand, have two major peaks of activity, one during the middle of the day (termed 'siesta') and a large, consolidated period during the whole night. Interestingly, cyc^{01} is a core clock mutant with a nocturnality phenotype in a light-dark cycle (Lee *et al.*, 2013). These cyc^{01} flies have increased rest during the day and less at night, suggesting that *cyc* has an additional role beyond the core molecular clock.

Various output pathways/circuits have been implicated in the circadian control of sleep/locomotion. The l-LNvs are not typically described as having a role in circadian locomotor behaviour; however, they are key in promoting wakefulness. These neurons are important for circadian phase resetting in response to light at dawn, a process which likely utilises PDF signalling to the s-LNvs (Shang, Griffith and Rosbash, 2008). In addition, the l-LNvs respond to light with increased firing and are involved in promoting wakefulness at dawn (Shang, Griffith and Rosbash, 2008; Sheeba, Fogle, *et al.*, 2008; Sheeba, Gu, *et al.*, 2008). Part of this mechanism is via PDF signalling from the l-LNvs to the s-LNvs (Parisky *et al.*, 2008); however, there are likely additional targets of the l-LNvs (Sheeba, Fogle, *et al.*, 2008). GABAergic transmission via the $GABA_A$ receptor Resistant to dieldrin (RDL) is important for regulating the total amount of sleep and sleep initiation (Agosto *et al.*, 2008). The l-LNvs were discovered to be important Rdl-expressing neurons for this process and are inhibited by GABA (Parisky *et al.*, 2008; Chung *et al.*, 2009).

wide awake (*wake*) was a mutant discovered during a forward genetic screen that has dramatically reduced sleep during all points of the day and increased sleep latency at dawn and dusk (S. Liu *et al.*, 2014). Overexpressing *wake* leads to increased sleep and reduced sleep latency at dusk, suggesting that *wake* is important for promoting sleep (S. Liu *et al.*, 2014). Interestingly, while *wake* is expressed in multiple clock neuron subsets (LNvs, LNds, DN1s, and DN2s), the l-LNvs are the neurons found to mediate the sleep initiation effect of *wake* (S. Liu *et al.*, 2014). The role of *wake* in the l-LNvs to promote sleep initiation requires PDF-PDFR signalling (S. Liu *et al.*, 2014). In addition, *wake* expression in l-LNvs is rhythmic (peaks around dusk/early night) and requires CLK/CYC for this rhythmic expression (S. Liu *et al.*, 2014). WAKE functions in the l-LNvs to promote sleep at dusk by forming a complex with the $GABA_A$ receptor RDL, which upregulates the levels of RDL within the cell (S. Liu *et al.*, 2014). RDL functions in the l-LNvs by receiving GABAergic input and inhibiting the neuron, and thus, part of the role of WAKE occurs via reducing l-LNv excitability at dusk (S. Liu *et al.*, 2014).

A recent study suggested that an output pathway mediating the l-LNv wakefulness signal during the day involves the inhibition of a specific sleep-promoting PPM3 neuron via PDF signalling from the s-LNvs (Potdar and Sheeba, 2018). (Potdar and Sheeba, 2018) suggest a mechanism whereby at night, GABAergic neurons inhibit the l-LNv which therefore results in reduced signalling to the

s-LNvs and reduced inhibitory PDF signalling to the PPM3s, which results in sleep promotion. This is a surprising finding, as dopamine signalling is considered purely wake-promoting (Andretic, van Swinderen and Greenspan, 2005; Kume *et al.*, 2005). In contrast, another laboratory found that PPM3 neurons are wake-promoting and connect downstream to the ellipsoid body ring neurons, a key population implicated in sleep/wake regulation (Liang *et al.*, 2019).

Broadly activating Neuropeptide Y-like short neuropeptide F (sNPF) expressing neurons via TrpA1 increases sleep and induces a negative sleep rebound (less sleep than baseline) after removal of the activation (Shang *et al.*, 2013). sNPF is expressed in many brain regions; however, the relevant neurons for nighttime sleep increase by release of sNPF were found to the s-LNvs (Shang *et al.*, 2013). sNPF signalling from the s-LNvs to the sNPF receptor (sNPFR) on l-LNvs is inhibitory and mediates the sNPF sleep promotion (Shang *et al.*, 2013).

Leucokinin (LK) and Leucokinin receptor (LKR) RNAi knockdown or mutation both lead to reduced circadian sleep/locomotor rhythms (Cavey *et al.*, 2016). The locomotor defects were narrowed down to two LK neurons within the lateral horn (termed LHLK neurons). The LHLK neurons form close connections with central clock neuron populations (e.g., LNvs, LNds, and DN1s) and are inhibited by LNv activity (Cavey *et al.*, 2016). LHLK neurons are known to form direct inhibitory connections to LKR+ neurons, which project to regions of the brain implicated in sleep and locomotor control, such as the central complex and pars intercerebralis (Al-Anzi *et al.*, 2010; Cavey *et al.*, 2016). Activation of LKR neurons or inhibiting LHLK neurons leads to increased locomotion/reduced sleep, while inhibiting LKR neurons or activating LHLK neurons has the opposite effect, confirming that this output pathway from the clock regulates rest and locomotion (Al-Anzi *et al.*, 2010; Cavey *et al.*, 2016).

The neuropeptide Diuretic hormone 31 (DH31) was discovered to be wake-promoting during the late night to dawn transition. Loss of DH31 leads to flies sleeping more, and sleep was more consolidated (fewer bouts of longer durations). Interestingly, the increased and more consolidated sleep was only seen during the night, although there were some minor changes during the latter half of the day (Kunst *et al.*, 2014). In addition, the increase in sleep was most profound during the late night, when wild-type flies begin to be more active, and the sleep duration reduces. Similarly, overexpressing DH31 leads to reduced, less consolidated sleep, specifically during the late night, suggesting the role of DH31 is in promoting wakefulness in anticipation of dawn (Kunst *et al.*, 2014). The role of DH31 was narrowed down to DH31 expressing DN1 clock neurons, which also promote wakefulness prior to dawn when activated by the thermosensitive cation channel TrpA1 or by activation of the PDF receptor (Kunst *et al.*, 2014). DH31+ DN1s are electrically active late at night due to PDF signalling and appear to promote wakefulness via DH31 secretion. GABA is an important neurotransmitter for promoting sleep, and

part of this GABAergic sleep-promoting mechanism likely involves reducing DH31 secretion (Kunst *et al.*, 2014).

The DN1 neurons are not only wake-promoting during late night but also have a sleep-promoting role during the day (Guo *et al.*, 2016). Blocking DN1 neurotransmission reduces sleep levels, and optogenetic activation of the DN1s increases the duration of siesta sleep (Guo *et al.*, 2016). DN1 efferents project to both the LNvs and the LNds, and activation of DN1s leads to reduced activity in these populations via glutamate (Guo *et al.*, 2016).

The pars intercerebralis has a crucial role as a circadian output pathway. Most clock neurons project to the PI (Helfrich-Förster, 1995; Kaneko and Hall, 2000; Helfrich-Förster *et al.*, 2007), suggesting an essential role in outputting circadian timed behaviour. A critical pathway in the timing of locomotor output from the clock was shown to be via the DN1s which form synaptic connections with the s-LNvs and project to the pars intercerebralis (PI) (Cavanaugh *et al.*, 2014). The PI is considered the *Drosophila* equivalent of the mammalian hypothalamus and is a heterogeneous population expressing various neuropeptides (de Velasco *et al.*, 2007). Activation or ablation of the Diuretic Hormone 44 (DH44) positive PI neurons leads to arrhythmicity of locomotor behaviour in constant darkness (Cavanaugh *et al.*, 2014). In addition, the Drosophila insulin-like peptide 2 expressing neurons (Dilp2+ neurons) are wake-promoting and receive octopaminergic input via ASM neurons. These neurons also receive projections from the DN1s, a source of circadian timing input (Barber *et al.*, 2016). SIFa+ PI neurons are also involved in regulating the circadian timing of sleep/locomotion, likely via connection from the DN1s (Cavanaugh *et al.*, 2014).

The DH44+ neurons regulate sleep/locomotion via DH44 signalling to neurons in the subesophageal zone (SEZ) that express *hugin.* These *hugin*+ neurons have some projections back to the PI, suggesting an ability for reciprocal feedback, as well as descending projections to the ventral nerve cord, where they likely target motor circuits (King *et al.*, 2017). Subsequent work from the same laboratory found that the *hugin*+ neurons are also regulated by homeostatic sleep circuits (Schwarz *et al.*, 2021). *Hugin*+ neurons have reduced activity during sleep deprivation and form synaptic connections to neurons captured by the R23E10 driver (typically considered dFB, but caveats are described later) (Schwarz *et al.*, 2021). The R23E10 neurons, when activated, increase sleep, which is further exacerbated by the ablation of *hugin*+ neurons (Schwarz *et al.*, 2021). These results suggest that R23E10 neurons likely inhibit *hugin+* neurons. Mutation of *hugin* leads to increased homeostatic sleep rebound following sleep deprivation and enhances the sleep-promoting effect of R23E10 activation (Schwarz *et al.*, 2021). Schwarz et al. discovered that *hugin*+ neurons also project to the LNvs (Schwarz *et al.*, 2021). The s-LNVs also have reduced activity during sleep deprivation, which was lost in *hugin* mutant flies (Schwarz *et al.*, 2021).

Altogether, the data suggest circadian timing from the s-LNvs to DN1s signals to the PI. A critical pathway discovered is the connection from the DN1s to the DH44+ neurons of the PI, which activate *hugin*+ neurons in the SEZ. These *hugin*+ neurons project to, and likely activate, downstream motor circuits in the VNC to promote locomotion. Prolonged wakefulness/sleep deprivation leads to decreased activity within *hugin*+ neurons. This process is mediated at least in part by inhibitory signalling from the R23E10 neurons and also results in reduced *hugin*+ neuron signalling to the s-LNVs. The *hugin*+ neurons are, therefore, considered a key population of signal integrators from circadian and sleep centres.

DN1 outputs to the PI have been described in detail. Another output from a subset of DN1s is projections to the TuBu neurons in the anterior optic tubercle ((Guo *et al.*, 2018; Lamaze *et al.*, 2018). These TuBu neurons connect to the ellipsoid body neurons, which are implicated in sleep homeostasis. While two separate laboratories discovered this output pathway, they suggest opposite effects on rest/wake. (Lamaze *et al.*, 2018) found that TuBu neurons promote sleep and are inhibited by DN1s. (Guo *et al.*, 2018) on the other hand, found that the DN1s targeting TuBu neurons are sleep-promoting. This pathway requires more work; it could be that the DN1s have a sleep/wake-promoting role onto the TuBu at different times of day or in different contexts.

1.4 Sleep-wake promoting circuits in *Drosophila*

1.4.1 Is there a central sleep homeostat?

In mammals, no specific region of the brain has been discovered which encompasses ‘the sleep homeostat’. While it was initially posited that the homeostatic process was a global phenomenon, more recent hypotheses include the concept of a local, use-dependent component (Krueger and Tononi, 2011). The homeostatic process is thought to involve molecules that build up during wake and promote sleep via paracrine signalling. Such sleep-promoting molecules are termed somnogens (Krueger *et al.*, 2011).

In *Drosophila*, the central complex is widely considered the main sleep homeostat. The central complex is a symmetrical neuropil located on the midline of the protocerebrum. It is a highly conserved region in insects and has been demonstrated to be vital for many behaviours, such as navigation and locomotion (Young and Armstrong, 2010). Within the central complex, two critical components implicated in sleep regulation are the fan-shaped body (FB) and the ellipsoid body (EB).

Over a decade ago, (Donlea *et al.*, 2011) found that activating a broadly expressing driver (104y-GAL4) with a heat sensitive cation channel led to inactivity in a DAM assay. While 104y is broadly expressing, the authors suggest the dFB is heavily targeted by this driver and is the relevant sleep promoting region. This finding led to a collection of research studies on the dFB (using a more specific driver termed R23E10) as the main homeostatic sleep centre in the fly brain (Figure 1.4.1A, (Donlea *et al.*, 2011, 2018; Donlea, Pimentel and Miesenböck, 2014; Pimentel *et al.*, 2016)).

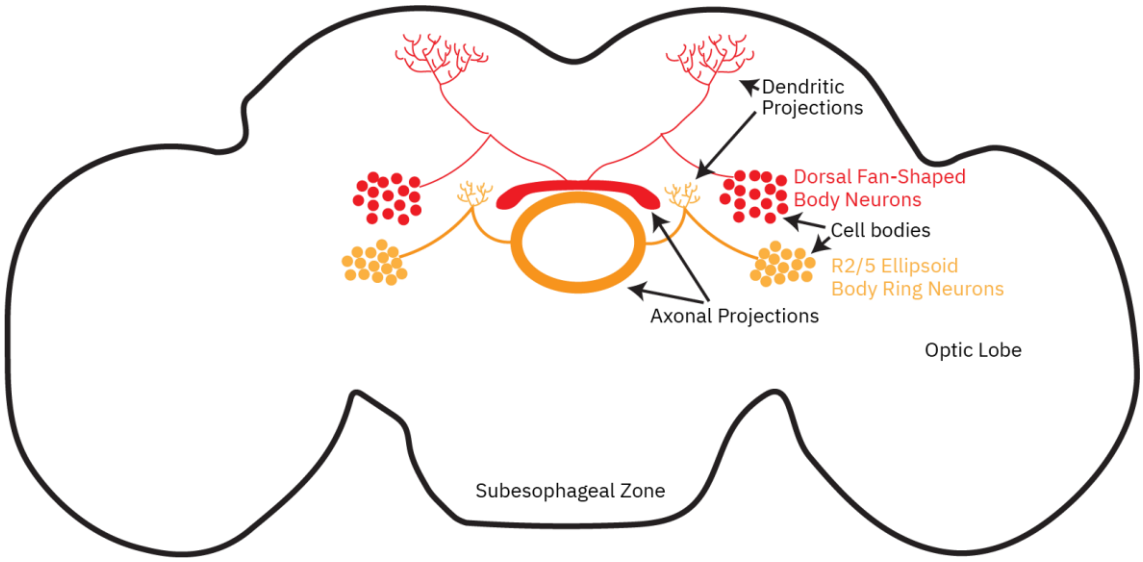

Figure 1.4.1 The role of the central complex in sleep

The dFB is thought to be the central sleep homeostat due to a strong sleep promoting phenotype when activated. Within the Central Complex it is thought to form a circuit with R2 ellipsoid body ring neurons, which receive waking experience information various regions including visual information from Helicon cells.

This was proposed due to the findings that the dFB neurons form a homeostatically regulated circuit within the central complex, whereby the circuit shows higher activity when sleep pressure rises above a certain level, associated with changes in membrane channels and increased excitability of the dFB. The change in excitability due to increased sleep pressure is thought to occur due to reduced dopaminergic signalling to the dFB (Pimentel *et al.*, 2016). The described circuit is composed of:

- The dorsal fan-shaped body neurons (by using the driver R23E10) are implicated as the homeostatic sleep switch.

- The Ellipsoid body ring neurons (EB RNs) are implicated as a sleep-need sensor and signal this to the dFB neurons. Like with the dFB neurons, inhibiting the EB RNs impairs homeostatic sleep rebound (Liu *et al.*, 2016). The R2 neurons of the EB fire in a synchronised manner correlating to sleep need (Raccuglia *et al.*, 2019). These neurons are also targeted and synchronised by tubercular-bulbar neurons (TuBu); part of the circadian output pathway involved in sleep/wake regulation.
- Helicon cells – Visually responsive cells which are thought to be inhibited by the dFB neurons via allatostatin A (AstA) and which signal to the EB RNs (Donlea *et al.*, 2018).

While the dFB is widely cited to be the homeostatic sleep centre, recent studies call this narrative into question. Firstly, a recent study showed that the original driver used to implicate the dFB as a sleep promoting centre (104y-GAL4), widely expresses in the fly brain (De *et al.*, 2023). Upon activation of 104y expressing cells with a heat sensitive cation channel, De *et al.*, 2023 found that flies exhibited prolonged irreversible inactivity even once the stimulation was removed. Furthermore, upon visual inspection, these flies were found to be experiencing a seizure-like phenotype. This illustrates an issue with utilising DAM assays and inactivity as a correlate of sleep, as seizure-like phenotypes are not noticeable.

For the purposes of studying the dFB, a more restricted driver called 'R23E10' is used as it expresses strongly in 31 dFB neurons (Hulse *et al.*, 2021). This Gal4 driver, however, expresses in 50 cells within the brain and 18 cells within the ventral nerve cord (VNC; equivalent to the spinal mammalian cord) (Jones *et al.*, 2023). Two separate studies utilised the R23E10 driver and found that the sleep promoting role when activating this driver is not related to the dFB neurons, but due to neurons within the ventral nerve cord of the fly (equivalent to the mammalian spinal cord) which are also captured by the R23E10 driver (De *et al.*, 2023; Jones *et al.*, 2023). Within dFB neurons, (De *et al.*, 2023) were also unable to find expression of AstA, or of the ion channel Sandman which was described to mediate the change in dFB excitability in response to sleep pressure (Pimentel *et al.*, 2016; De *et al.*, 2023). One contrasting results between (De *et al.*, 2023; Jones *et al.*, 2023) was whether the dFB projecting neurons may still play a role in sleep homeostasis. Both studies tested inhibition of R23E10 with an inwardly rectifying potassium channel (kir2.1) and tested the sleep rebound after a sleep deprivation protocol. (De *et al.*, 2023) found no difference between the control and the experimental flies with inhibited R23E10 neurons, suggesting that these neurons are not involved in promoting sleep homeostasis. In contrast, (Jones *et al.*, 2023)found that the experimental flies had reduced sleep rebound following deprivation. One difference between the two studies is that Jones *et al.*, 2023 utilised a much longer deprivation protocol compared to De *et al.*, 2023 (12 vs. 4 hours). Further work is required to clear up these differences with regards to sleep homeostasis. In addition, the role of

the other regions of the central complex and circuits described to be involved with the dFB and sleep homeostasis will likely need to be revisited, as to what the mechanism of action is.

1.4.2 The mushroom body

The mushroom body (MB) is an important region of the fly brain implicated in sleep/wake regulation (Figure 1.4.2A-B). The MB is crucial for olfactory learning; however, the MB also receives other stimuli such as temperature and humidity (Heisenberg, 2003; Frank *et al.*, 2015; Liu, Mazor and Wilson, 2015; Marin *et al.*, 2020). Olfactory stimuli are sensed by olfactory receptor neurons (ORNs), which bind to projection neurons (PNs) in the antennal lobe (Figure 1.4.2A; (Bates *et al.*, 2020). PNs project to the calyx of the mushroom bodies where the dendrites of the Kenyon cells are. The Kenyon cells (KCs) are the primary integrator neurons in olfactory processing. Each KC receives multiple PN inputs and requires simultaneous signalling inputs to fire (Gruntman and Turner, 2013). While there is more complexity than described here, the result is that each odour sensed by the ORNs will end up activating a sparse array of KCs (Li *et al.*, 2020). The KC axons project to various lobes of the mushroom bodies (α/β, α'/β', or γ lobes) (Tanaka, Tanimoto and Ito, 2008) and are thus named according to their projection location. The KC axons synapse to mushroom body output neurons (MBONS), which then project to various brain regions and elicit downstream effects, such as approaching an arousing stimulus or avoiding an aversive stimulus. KCs receive dopaminergic signalling via multiple dopaminergic neurons (DANs) populations. The KC projecting DANs encode either positive or negative valence, and their activity is required for aversive or appetitive olfactory conditioning (Cognigni, Felsenberg and Waddell, 2018).

Inhibiting the KCs reduces sleep (Pitman *et al.*, 2006). By using split-Gal4s and the heat sensitive cation channel TrpA1, Sitaraman and colleagues screened for KCs split-Gal4s, which respond to the temperature-induced neuron activation with increased or decreased sleep (Sitaraman, Aso, Jin, *et al.*, 2015). Briefly, a split Gal4 is where the Gal4 is split into two separate constructs, one half with the DNA binding domain (DBD) and the other half with the activation domain (AD). Each half is expressed downstream of a cell specific promoter such that only cells expressing both promoters will allow the split Gal4 to combine and form a functional transcription factor. Activation of α'/β' KCs leads to increased wake and a subsequent homeostatic sleep rebound (Sitaraman, Aso, Jin, *et al.*, 2015). In addition, a pair of inhibitory interneurons, called dorsal paired medial (DPM) neurons, inhibit the α'/β' KCs via GABA and serotonin, and are therefore sleep-promoting (Haynes, Christmann and Griffith, 2015). Thermogenetic activation of the γmain KCs also leads to increased wake, while activation of the γdorsal KCs increases sleep (Sitaraman, Aso, Jin, *et al.*, 2015). Increasing both the γmain and γdorsal KCs simultaneously

has no major impact on sleep, which would be expected if these cells integrate opposite sleep/wake signals. Unlike the other lobes, α/β KCs appear to have no significant impact on sleep/wake (Sitaraman, Aso, Jin, *et al.*, 2015).

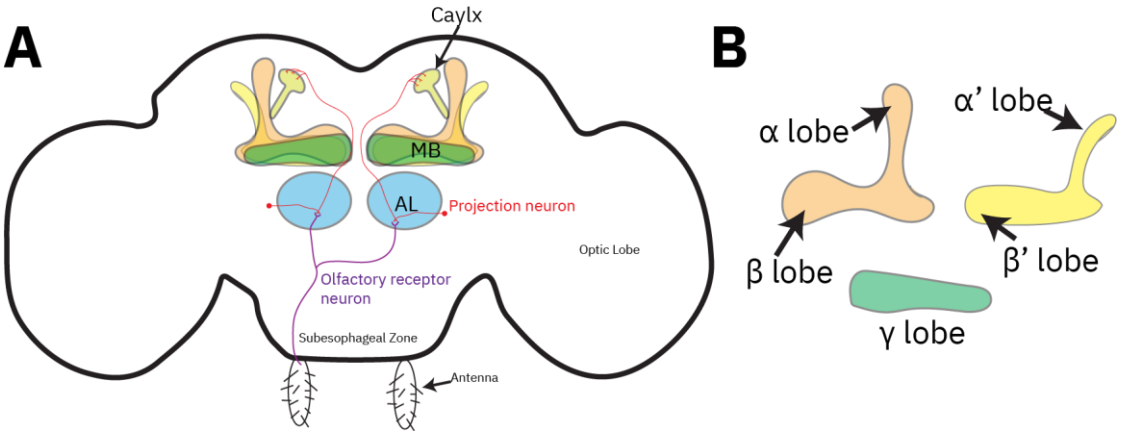

Figure 1.4.2 The Mushroom body

(A) The mushroom body (MB) is a large structure in the brain which receives olfactory input from olfactory receptor neurons indirectly via antennal lobe (AL) projection neurons. **(B)** The MB has various subregions which have been split apart from their usual positions (which can be seen in A).

The same laboratory also performed a thermogenetic screen for MBONs involved in sleep (Aso, Sitaraman, *et al.*, 2014). From this screen, a subset of glutamatergic MBONs (MBON-γ5β′2a, MBON-β′2mp, MBON-β′2a_bilateral and MBON-γ4>γ1γ2) were discovered to be wake-promoting, while a subset of both GABAergic (MBON-γ3β′1 and MBON-γ3) and cholinergic MBONs (MBON-γ2α′1) were sleep-promoting. The MBON-γ5β′2a, MBON-β′2mp, and MBON-β′2a_bilateral are commonly described as one population (MBON-γ5β′2a/β′2mp/β′2a_bilateral) due to all three neurons being present in any split-Gal4 that expresses in any of these neurons. Interestingly, the wake-promoting MBON-γ5β′2a/β′2mp/β′2a_bilateral and the sleep-promoting MBON-γ2α′1 project to the superior medial protocerebrum (SMP) (Aso, Hattori, *et al.*, 2014). Both these MBON populations also have dendritic processes within the α'/β' and γ lobes of the MB (Aso, Hattori, *et al.*, 2014). The sleep and wake-promoting KC and MBON populations were described to form segregated circuits (Sitaraman, Aso, Jin, *et al.*, 2015). The wake-promoting α'/β' KCs form strong connections to the wake-promoting MBON-γ5β′2a/β′2mp/β′2a_bilateral population while having a much weaker connection to the sleep-promoting MBON-γ2α′1. Similarly, thermogenetic experiments suggest that the wake-promoting γmain KCs function by activating the MBON-

γ5β′2a/β′2mp/β′2a_bilateral neurons, while the sleep-promoting γdorsal KCs promote sleep via activating MBON-γ2α'1 (Sitaraman, Aso, Jin, *et al.*, 2015).

The MB is also implicated in sleep homeostasis. The wake-promoting α'/β' KCs are less electrically active (as measured by explanted tissue electrophysiology) in sleep-deprived flies. In contrast, the sleep-promoting γdorsal KCs were more active (Sitaraman, Aso, Jin, *et al.*, 2015). As with the KCs, sleep-promoting MBON-γ2α′1 dendrites are more electrically active (as measured by electrophysiology in explanted tissue) in sleep-deprived flies while the dendrites of the wake-promoting MBON-γ5β′2a/β′2mp/β′2a_bilateral neurons were less active (Sitaraman, Aso, Jin, *et al.*, 2015).

1.4.3 Wake promoting biogenic amines

In mammals, biogenic amines such as dopamine, noradrenaline, and histamine are considered potent wake-promoting neurotransmitters (Scammell, Arrigoni and Lipton, 2017). Similarly, in flies, dopamine is a strongly wake promoting. A dopamine transporter mutant, *fumin*, was first discovered, which increases dopaminergic signalling (by reducing reuptake), and these flies have reduced rest and significantly increased locomotor activity compared to wild-type flies (Kume *et al.*, 2005). In addition, thermogenetic activation of dopaminergic neurons significantly reduces sleep (Liu *et al.*, 2012). Similarly, mutating *Drosophila* tyrosine hydroxylase 1 (DTH1), an enzyme involved in generating dopamine in the brain, leads to increased sleep (Riemensperger *et al.*, 2011). Clusters of dopaminergic neurons are found within various fly brain regions and labelled according to the cluster location (White, Humphrey and Hirth, 2010).

As mentioned earlier, one site of dopaminergic wake-promotion is thought to be inhibitory projections to the R23E10 neurons. Both the paired posterior medial 3 (PPM3s) and the paired posterior lateral 1 (PPL1s) are implicated in promoting wakefulness via projections to the R23E10 neurons (Liu *et al.*, 2012; Ueno *et al.*, 2012). Given the recent findings of R23E10, further work could better elucidate whether the wake-promoting role of dopaminergic neurons on R23E10 occurs specifically due to the VNC neurons captured by the R23E10 driver. Many dopaminergic neurons from the PPL1 and the paired anterior medial (PAM) clusters also project to the MB and were found to be wake-promoting when thermogenetically activated, increasing activity in the wake-promoting MBONs (Sitaraman, Aso, Rubin, *et al.*, 2015). Furthermore, the effect of caffeine, a wake-promoting adenosine receptor antagonist, in flies appears to be mediated by caffeine-induced activation of wake-promoting PAM neurons (Nall *et al.*, 2016).

Histamine is strongly wake-promoting in both mammals and flies (Parmentier *et al.*, 2002; Thakkar, 2011). As described earlier, a histamine receptor antagonist hydroxyzine promotes sleep initiation (Shaw *et al.*, 2000). In addition, a null mutation of the histamine receptor histamine-

gated chloride channel subunit 1 (HisCl1) leads to increased sleep (Oh *et al.*, 2013). Furthermore reducing histamine synthesis via a hypomorphic mutation of histidine decarboxylase (HDC) leads to increased sleep during the day (Oh *et al.*, 2013).

In mammals, noradrenergic neurons in the locus coeruleus have been shown to be strongly wake promoting (Aston-Jones and Bloom, 1981). Octopamine is the fly equivalent of noradrenaline and is also considered wake-promoting (Crocker and Sehgal, 2008). Mutating an essential enzyme in octopamine synthesis, tyrosine decarboxylase (Tdc2), leads to reduced octopamine levels and significantly increased sleep (Crocker and Sehgal, 2008). Similarly, activating (via expressing a bacterial sodium channel 'NaChBac') or inhibiting (via expressing a potassium channel 'kir2.1') octopaminergic neurons leads to reduced and increased sleep, respectively (Crocker and Sehgal, 2008). Interestingly, thermogenetic activation of octopaminergic neurons does not elicit a homeostatic sleep rebound (whereas dopaminergic activation does), suggesting that octopaminergic wake-promotion may also inhibit or bypass sleep homeostasis (Seidner *et al.*, 2015). A key octopaminergic population (termed 'ASM') were found to be wake-promoting (Crocker *et al.*, 2010). The ASM neurons were found to project to a group of neurons in the pars intercerebralis that express *Drosophila* insulin-like peptide (Dilp2) (Crocker *et al.*, 2010). As with octopamine neurons, activating the Dilp2 neurons reduces rest and inhibiting them increases rest (Crocker *et al.*, 2010). ASM octopaminergic signalling to the Dilp2 neurons increases excitability by inhibiting a potassium channel called 'Slowpoke'.

1.4.4 Sleep promoting role of serotonin and GABA

In mammals, the role of serotonin in sleep/wake has been an area of much research, with our current understanding suggesting that serotonin plays a role as both a wake- and sleep-promoting neurotransmitter in different contexts (see (Ursin, 2002) for a specific review). In *Drosophila*, serotonergic neurons are widely distributed across the brain with widespread projections (Monastirioti, 1999). Increasing serotonin levels in the brain, via addition of a serotonin precursor (5-hydroxytryptophan), increases sleep (Yuan, Joiner and Sehgal, 2006). Mutation of a serotonin receptor (d5-HT1A), leads to reduced baseline sleep with more fragmentation and reduced rebound sleep post deprivation (Yuan, Joiner and Sehgal, 2006). The sleep promoting role of d5-HT1A was found to be within the mushroom bodies (Yuan, Joiner and Sehgal, 2006). As mentioned in Chapter 1.4.2, the DPM neurons are considered sleep promoting by inhibiting wake-promoting α'/β' KCs with serotonin and GABA (Haynes, Christmann and Griffith, 2015). (Qian *et al.*, 2017) also demonstrate a role for the d5-HT2b receptor within a pair of dFB neurons for sleep homeostasis.

γ-Aminobutyric acid (GABA) is an important inhibitory neurotransmitter with a vital role for mammalian sleep. GABAergic neurons within the ventrolateral preoptic nucleus (VLPO) and the median preotic nucleus (MnPO), which are considered key sleep promoting regions, are active during sleep (Sherin *et al.*, 1996, 1998; Gaus *et al.*, 2002; Alam *et al.*, 2014). Lesions of the MnPO or VLPO lead to strong reductions in total sleep durations in rodents (John and Kumar, 1998; Lu *et al.*, 2000; Vetrivelan *et al.*, 2012; Vetrivelan, Saper and Fuller, 2014). Chemogenetic and optogenetic activation experiments of the VLPO in mice lead to strong sleep increases (Kroeger *et al.*, 2018). Both the VLPO and MnPO form reciprocally inhibitory connections (some indirectly) with arousal-promoting brain regions (Sherin *et al.*, 1998; Gallopin *et al.*, 2000, 2004; Chou *et al.*, 2002; Uschakov *et al.*, 2007; Williams *et al.*, 2014). For example, Optogenetic activation of the GABAergic neurons in the preoptic area resulted in the inhibition of orexinergic neurons (Saito *et al.*, 2013). Alongside promoting baseline NREM sleep, the VLPO and MnPO are implicated in homeostatic sleep regulation (Reviewed in (Szymusiak, Gvilia and McGinty, 2007)). Both neuronal populations are more active during a sleep deprivation protocol and the recovery sleep afterwards (Alam *et al.*, 2014). As mentioned in the previously subchapters (Chapter 1.3.3 and 1.4.2), GABA is also considered an important inhibitory neurotransmitter in *Drosophila* which promotes sleep (Agosto *et al.*, 2008; Parisky *et al.*, 2008; Chung *et al.*, 2009; Aso, Sitaraman, *et al.*, 2014; Haynes, Christmann and Griffith, 2015).

1.4.5 The pars intercerebralis and pars lateralis

The pars intercerebralis (PI) and pars lateralis (PL) are heterogeneous neuroendocrine structures equivalent to the hypothalamus-pituitary axis (de Velasco *et al.*, 2007), and have been implicated in sleep-wake regulation. The Dilp2 PI neurons are implicated in promoting wakefulness, as described earlier. In addition, neuropeptide SIFamide (SIFa) expressing PI neurons are implicated in sleep promotion (Park *et al.*, 2014). Ablating SIFa PI neurons (via inducing apoptosis) decreases rest (Park *et al.*, 2014). Depleting SIFa or the SIFa receptor (SIFR) in the fly brain via RNAi also leads to decreased rest, suggesting that SIFa to SIFR signalling is important for the rest-promoting property of SIFa PI neurons (Park *et al.*, 2014). Interestingly, the SIFR population responsible for this rest promotion was narrowed down to another PI population (SIFR+ Dilp2-). Within the same PI neurons, epidermal growth factor receptor (EGFR) signalling was found to be sleep-promoting (Foltenyi, Greenspan and Newport, 2007).

Some evidence also points to the PL as having a sleep-promoting role. For example, *taranis* (*tara*) was discovered via a forward genetic screen (Afonso *et al.*, 2015). *tara* encodes a cell cycle regulatory molecule, and the mutated gene leads to reduced rest (Afonso *et al.*, 2015). In addition, Tara was found to function by binding to CycA, which has previously been implicated in

promoting sleep (Rogulja and Young, 2012). Tara appears to stabilise CycA, as flies with mutated *tara* have lower levels of CycA protein but unaffected mRNA levels (Afonso *et al.*, 2015). A population of CycA-expressing neurons were found in the PL and knocking down *tara* within these neurons reduces sleep equivalent to the broad *tara* mutant (Afonso *et al.*, 2015).

1.4.6 The role of glia in sleep-wake behaviour

Alongside neurons, glial cells are also present within the *Drosophila* brain (Awasaki *et al.*, 2008). Compared to neurons, less is understood about glia and their role in behaviour. Astrocyte-like glia are typical stellate non-electrically active cells in *Drosophila* that form close connections with neuronal synapses (Awasaki *et al.*, 2008). Notch-delta cell-cell signalling from astrocytic glia to neurons is implicated in sleep homeostasis (Seugnet *et al.*, 2011). A transcription factor, '*bunched*', that regulates Notch expression is upregulated by sleep deprivation or physiological stress, such as reactive oxygen species in flies (Dobens *et al.*, 2005; Seugnet *et al.*, 2011). The mouse homolog *bunched* was also upregulated by sleep deprivation (Maret *et al.*, 2007). Bunched expression negatively regulates Notch-Delta signalling, such that loss of *bunched* results in upregulation of the Notch-Delta pathway (Dobens *et al.*, 2005). *bunched* mutant flies have impaired homeostatic sleep rebound following sleep deprivation and expressing a dominant negative *bunched* specifically within the MB phenocopies the impaired homeostasis (Seugnet *et al.*, 2011). In addition, Delta is found in the Kenyon cells, and overexpressing *delta* within the MB also blocks homeostatic sleep rebound (Seugnet *et al.*, 2011). On the other hand, Notch is expressed in astrocyte-like glia, and overexpressing *notch* also leads to impaired homeostatic sleep rebound (Seugnet *et al.*, 2011).

The tumour necrosis factor-alpha (TNFα) *Drosophila* homolog, Eiger, is also involved in astrocytic sleep regulation (Vanderheyden *et al.*, 2018). Flies with mutated *eiger* have reduced total sleep, and sleep is more fragmented than in wild-type flies. Targeted *eiger* knockdown via RNAi in the astrocytes, but not neurons, phenocopied the mutant *eiger* results (Vanderheyden *et al.*, 2018). RNAi knockdown of Wengen (fly TNFα receptor) leads to impaired homeostatic sleep rebound after sleep deprivation and blocks the increases in sleep seen when injecting human TNFα into flies. This suggests that an astrocytic to neuronal signal via Eiger (TNFα) and Wengen is important for sleep homeostasis and potentially baseline sleep (Vanderheyden *et al.*, 2018).

Another neuron-glia interaction involves GABAergic regulation. A forward genetic screen found a mutant of the gene *sleepless* (*sss*), which has greatly reduced sleep (Koh *et al.*, 2008). *sss* encodes a small glycophosphatidylinositol-anchored protein, which regulates the voltage-gated potassium channel, 'Shaker' (Wu *et al.*, 2010; Dean *et al.*, 2011). SSS can modulate Shaker channel activity via accelerating Shakers activation, and thus, loss of SSS leads to increased neuronal excitability (Wu

et al., 2010; Dean *et al.*, 2011). Loss of Shaker leads to reduced sleep; however, the SSS phenotype is much stronger, suggesting SSS functions through additional mechanisms to impact sleep (Chen *et al.*, 2015). Restoring expression of *sss* within GABAergic neurons (in otherwise *sss* mutant flies) recovers sleep back to almost wild-type levels (Chen *et al.*, 2015). γ-aminobutyric acid transaminase (GABAT) is an enzyme upregulated in *sss* mutants (Chen *et al.*, 2015). GABAT functions in mitochondria to break down GABA. As expected, GABAT mutant flies have increased GABAergic signalling and increased sleep (Chen *et al.*, 2015). *GABAT* mutation within the *sss* mutant flies recovers the sleep deficits that the *sss* flies have (Chen *et al.*, 2015). In addition, expressing *GABAT* within glia is sufficient to recapitulate the *sss* mutant sleep deficits (Chen *et al.*, 2015).

Both ensheathing glia and surface glia are also implicated in sleep regulation. Ensheathing glia have a phagocytic function like mammalian microglia (MacDonald *et al.*, 2006). The taurine transporter, Excitatory amino acid transporter 2 (Eaat2), was discovered to promote wakefulness, and its loss from ensheathing glia specifically leads to increased sleep (Stahl *et al.*, 2018). This process is likely taurine-dependent as administering taurine to flies (via the food) increases sleep (Lin *et al.*, 2010), and the sleep-promoting effect of taurine is abolished in *Eaat2* mutants (Stahl *et al.*, 2018). Barrier/surface glia form part of the hemolymph-brain barrier, and blocking endocytosis (via a dominant negative *dynamin*) within these cells leads to increased sleep under baseline conditions and increased sleep during a sleep deprivation protocol (Artiushin *et al.*, 2018). Overexpression of Rab11 within surface glia was found to increase sleep (Artiushin *et al.*, 2018). Rab11 plays a key role in endocytic recycling (Jing and Prekeris, 2009), and endocytic processes are increased in surface glia during sleep, suggesting a role of surface glia in sleep function (Artiushin *et al.*, 2018).

1.5 Sleep functions

As humans, we all understand that we need sleep – we become irritable, lack focus, feel tired, and perform poorly at a given task without sleep. As a result, proper sleep appears to provide a restorative function. Studying sleep function is an area of active research, however, there has yet to be a clear consensus and sleep likely serves multiple functions. As described below, multiple hypotheses for how sleep acts to restore function have arisen. In addition to the functions described below, sleep is also thought to be important in modulating immune function (reviewed in (Imeri and Opp, 2009)).

1.5.1 Energy balance

One common theory is that sleep is required for energy restoration/conservation. The brain comprises only 2% of total body mass but utilises around 20% of the available glucose during waking (Erbsloh, Bernsmeier and Hillesheim, 1958; Mergenthaler *et al.*, 2013). This demonstrates the substantial energetic demand that neural tissue requires to function. During sleep, the energetic demand of the brain is greatly reduced, which suggests a role for sleep in energy restoration (Madsen *et al.*, 1991; Maquet, 1995). However, it was found that ATP levels, a cell's primary energy currency, increase during the first few hours of sleep in wake-active but not in sleep-active rat neural tissue (Dworak *et al.*, 2010). This ATP increase was delayed in sleep-deprived rats whereas inducing sleep during a rat's typical active phase increased ATP. In addition, phosphorylated AMP-activated protein kinase (P-AMPK) levels were lower during the ATP surge period of sleep. AMPK acts as an energy sensor within a cell whereby the AMP/ATP levels dictate the level of AMPK phosphorylation. During waking, neuronal activity is high; therefore, the use of ATP is high, resulting in a large AMP/ATP ratio, leading to increased levels of P-AMPK. P-AMPK is the active form that suppresses anabolic processes and promotes catabolic processes such as fatty acid oxidation, glucose uptake and glycolysis. During the initial hours of sleep, when slow-wave sleep is dominant, the use of ATP is low as neuronal activity is reduced and the ATP levels surge, leading to a low AMP/ATP ratio and, therefore, a decreased level of P-AMPK. The reduction of P-AMPK allows an anabolic state of increased fatty acid, glycogen, and protein synthesis. The findings of Dworak *et al.*, 2010 suggest that instead of sleep being an energy restoration mechanism, it is a time for a surge in energy, allowing anabolic processes to occur. An essential sleep function may, therefore, be an increase in restorative biosynthetic processes.

1.5.2 Synaptic homeostasis function

A key sleep function hypothesis came from work by Giulio Tononi and Chiara Cirelli with the synaptic homeostasis hypothesis (SHY) (Tononi and Cirelli, 2003, 2006, 2012, 2014). The concept for SHY comes from two main biological problems that neurons face: (1) Neuronal firing is energetically costly, especially when burst firing (Attwell and Gibb, 2005), and (2) Neurons have an informational issue, whereby a neuron receives a wide range of inputs and signals to only a few outputs. Therefore, a neuron must only strongly respond to a few selective inputs and not the rest (Balduzzi and Tononi, 2013). This idea is backed up by data showing low firing rates and sparse responses of neurons to stimuli in rodents (Barth and Poulet, 2012; Haider, Häusser and Carandini, 2013).

Situations where multiple inputs often coincide with a likelihood greater than chance are when a neuron should recognise the pattern and fire accordingly (Barlow, 1985). An example of such a

situation at the macro behavioural level could be fear conditioning, whereby an animal can be trained to associate an otherwise inoffensive stimulus, such as a specific odour, with an electric shock. A random event whereby an electric shock coincides with a specific odour should not elicit any learning as it could have just been a coincidence. Multiple simultaneous inputs, however, represent a pattern occurring in the environment. As such, the organism must be able to associate the two stimuli and learn to avoid the odour. At the cellular level, a neuron should burst fire in response to strongly associated inputs and show reduced/no firing to weakly associated inputs. This pattern recognition functions by strengthening the synapses that are transmitting the simultaneous inputs.

During active waking, synaptic strengthening occurs as organisms explore the environment, react to stimuli, and perform specific motor actions. Many learning mechanisms, such as fear conditioning and cue-reward learning, have been shown to cause synaptic potentiation during wake (Matsuo, Reijmers and Mayford, 2008; Tye *et al.*, 2008). While synaptic plasticity is required for our ability to learn, these processes result in a situation where net synaptic strength increases with time awake, which comes at a cost. Increasing synaptic strength has cellular costs for the neurons and supporting glia, increasing the need for energy, and increasing cellular stress. At the system level, increasing net synaptic strength impairs one's ability to learn as synapses become saturated. Alongside these issues, the broad increase of synaptic strength during wake reduces signal-to-noise ratio (SNR) and neuronal response selectivity (Tononi and Cirelli, 2014).

SHY proposes restoring synaptic homeostasis via synaptic downscaling as a key sleep function. This would lower cellular energy costs, allow synaptic plasticity desaturation, and allow memory consolidation to occur (Nere *et al.*, 2013). SHY suggests this synaptic downscaling must occur during sleep rather than wake, as organisms experience a limited sample of the environment during a typical waking day. Synaptic downscaling occurring during wake would be biased towards the current day's sensory input. In contrast, synaptic downscaling during sleep would allow neurons to broadly sample the whole brain's knowledge of the environment without sensory input bias.

SHY proposes that slow wave activity (SWA) during sleep mediates the synaptic downscaling, whereby the waves of spontaneous activity allow for neuronal knowledge sampling. The intensity of cortical slow wave activity during NREM sleep correlates with sleep need and has been shown to be modulated in local, use-dependent contexts (Achermann *et al.*, 1993; Kattler, Dijk and Borbély, 1994; Franken, Chollet and Tafti, 2001). Synaptic strengthening in specific regions of the cortex leads to increased slow wave activity during subsequent sleep, a theory supported by computational models and direct evidence (Huber, Ghilardi, *et al.*, 2004; Esser, Hill and Tononi, 2007). The slope and amplitude of SWA, a correlate of synaptic strength, reduces over the

duration of sleep, suggesting synaptic downscaling is occurring (Riedner *et al.*, 2007; Vyazovskiy, Achermann and Tobler, 2007). Proteins involved in long-term potentiation increased during prolonged wake, whereas proteins involved in long-term depression increased during sleep (Cirelli and Tononi, 2000b, 2000a). More direct evidence for this theory came from *Drosophila,* whereby it was shown that synapse size or number increased during waking and sleep was required to decrease these (Bushey, Tononi and Cirelli, 2011). Proteins required for synaptic depression are upregulated during sleep, and sleep was required to decrease synaptic size/number following the wake-specific increase of synaptic size/number in *Drosophila* (Bushey, Tononi and Cirelli, 2011).

Neuromodulators such as dopamine, acetylcholine, and noradrenaline are considered wake-promoting in both mammals and *Drosophila* (Nall and Sehgal, 2014; Zielinski, McKenna and McCarley, 2016; Ly, Pack and Naidoo, 2018) and are also involved in synaptic potentiation (Pawlak *et al.*, 2010). The switch from synaptic potentiation during wake to synaptic depression/protection during sleep could, therefore, be due to the decrease in the levels of these neuromodulators that occur during sleep (Tononi and Cirelli, 2014). The way downscaling occurs is still unclear. All synapses may be downscaled equally, and only those above a threshold are still effectively functional (Hill, Tononi and Ghilardi, 2008). Alternatively, stronger synapses may receive less downscaling than weaker synapses (Olcese, Esser and Tononi, 2010), or those neurons which constantly detect simultaneous inputs during sleep are protected from being downscaled (Hashmi, Nere and Tononi, 2013; Nere *et al.*, 2013).

At the cellular level, there are a few potential mechanisms by which the synapses activated strongly during sleep could receive less downscaling than those not. Calcineurin is a phosphatase that is upregulated during sleep and is known to promote synaptic depression (Cirelli, Gutierrez and Tononi, 2004). Calcineurin can be inhibited by high calcium levels, which would be present in the strongly activated synapses (Cirelli, Gutierrez and Tononi, 2004; Tononi and Cirelli, 2014).

Another mechanism may be via inhibiting the reversal of long-term potentiation (LTP). CaMKII is implicated in LTP, both in the induction and maintenance of LTP (Lisman, Yasuda and Raghavachari, 2012). Regarding the maintenance of LTP, it is thought that CaMKII binding to the NMDA receptor acts as an LTP tag, allowing proteins involved in late LTP to bind and potentiate the synapse. The CaMKII inhibitor (CaMKIIN) disrupts CaMKII binding to the NMDAR and thus prevents synapse strengthening (Sanhueza and Lisman, 2013). The alpha isoform of CaMKIIN is upregulated during sleep and is inhibited by high calcium levels like calcineurin, which suggests a potential mechanism for how strongly activated synapses can be protected (Cirelli, Gutierrez and Tononi, 2004; Gouet *et al.*, 2012).

Lastly, the action of Arc may contribute. Arc, or Arg3.1, is an immediate early gene upregulated by strong synaptic activity (Link *et al.*, 1995; Lyford *et al.*, 1995). Arc is present at the postsynaptic

density (PSD) of activated neurons, where it is thought to promote synaptic depression by the internalisation of AMPA receptors (Moga *et al.*, 2004; Chowdhury *et al.*, 2006). Notably, while Arc requires activity at a synapse, it is only maintained at synapses via the interaction with the inactive form of CaMKIIβ, which is present in less active synapses but not in strongly active synapses (Okuno *et al.*, 2012). This suggests that Arc and inactive CaMKIIβ act as an "inverse tag" whereby the weakly activated synapses are tagged. Therefore, synaptic potentiation is blocked at the weakly activated synapses via AMPA-R endocytosis, while strongly activated synapses are spared.

1.5.3 Glymphatic waste clearance

Neuronal activity is energetically costly, and the brain generates toxic by-products which build up in the interstitial fluid. Amyloidogenic proteins which underlie neurodegenerative disorders, such as β-amyloid (Alzheimer's disease) and α-synuclein (Parkinson's disease), are secreted into the brain interstitial fluid (Cirrito *et al.*, 2005; Larson *et al.*, 2012). These interstitial solutes are subsequently cleared from the brain via the glymphatic system, whereby cerebrospinal fluid (CSF) acts to remove waste from the interstitial fluid of the brain and drains via the paravenous pathway (Iliff *et al.*, 2012; Iliff, Lee, *et al.*, 2013; Iliff, Wang, *et al.*, 2013). It has been hypothesised that sleep increases the clearance of these waste products.

Interstitial Aβ concentration is higher during the awake phase than during sleep (Kang *et al.*, 2009). This could be due to increased Aβ production during wakefulness or increased clearance during sleep. The latter hypothesis was tested by injecting fluorescent tracers into the subarachnoid CSF of mice (Xie *et al.*, 2013). Sleep, natural or induced, was associated with significantly increased tracer influx compared to during wake. This result was found in naturally sleeping mice and mice anesthetised during their active period, suggesting that this finding is a sleep/wake state-specific process rather than a circadian rhythm. The increased influx was found to correlate to an increased interstitial fluid volume rather than increased arterial pulsation. Induced sleep increased interstitial fluid volume by >60%, suggesting that the sleep state is associated with an increased interstitial fluid volume, allowing for increased CSF flow and waste removal. To provide further evidence for this claim, Xie and colleagues found that Aβ was cleared at a much greater rate during sleep (Xie *et al.*, 2013).

1.5.4 Oxidative stress and is lack of sleep lethal?

In addition to the ascribed restorative functions, sleep is often viewed as necessary for survival, which stems from two concepts. The first is that sleep is an evolutionarily conserved process throughout the animal kingdom (Cirelli and Tononi, 2008). This evidence suggests that sleep

provides a competitive advantage; however, it does not justify the assumption that sleep is essential for survival. The second piece of evidence is that chronic sleep deprivation is linked to poor health and often death.

In brief, a sleep deprivation experiment is where test animals are forced to remain awake during their natural sleeping periods, whereas the control animals can typically sleep naturally. Specific deprivation protocols vary; however, the most frequently used types are:

- Mechanical stimulation, such as shaking or moving the test chamber. This method is the easiest but has the most chance of causing stress to the animal, which is a confounding variable.
- Genetic manipulations can be performed to activate arousal-promoting neurons (For example, in *Drosophila*: (Seidner *et al.*, 2015)).
- Air puffs. This is considered less stressful than mechanical methods (Gross *et al.*, 2015).

An issue with sleep deprivation protocols is the potentially stressful nature of the deprivation method. The deprivation method can be enacted constitutively during a given period. Alternatively, a more sophisticated protocol involves enacting the deprivation method only when the animal transitions into a sleep state. This second method requires more complex technology to track the sleep state and to enact the deprivation protocol automatically but benefits from reducing the impact of the deprivation method. To further minimise this confounding variable, it is common to perform an additional control experiment whereby the control organisms experience the same deprivation protocol while awake.

Experimentation with chronic sleep deprivation dates back to a paper in 1894 by Marie de Manacéine (de Manaceine, 1894; Bentivoglio and Grassi-Zucconi, 1997). In this original study, ten puppies were sleep-deprived by being kept in constant activity. Sadly, all the puppies could not be rescued after sleep deprivation of 4 to 5 days. de Manacéine also described how older dogs were impacted less by the sleep deprivation and how the sleep deprivation led to a decrease in body temperature. Upon examination of the deceased dogs' bodies, de Manacéine noted that their brains suffered the most severely, with damage to blood vessels, haemorrhaging, and widespread degeneration. This led De Manacéine to the now commonplace notion that sleep deprivation is lethal because of its effects on the brain.

Another sleep deprivation study using dogs corroborated these findings while utilising a less stressful sleep deprivation protocol (Agostini, 1898; Bentivoglio and Grassi-Zucconi, 1997). Subsequent work on sleep deprivation in rats also demonstrated severe consequences of sleep deprivation (Rechtschaffen *et al.*, 1983; Rechtschaffen and Bergmann, 1995, 2002). Chronically sleep deprived rats showed various pathologies, including skin lesions, damaged paws, altered appearance, loss of balance, muscle weakness, and weight loss. Death, or imminent death, was

recorded in all the rats. Rechtschaffen concluded that, although no specific cause of death was noticeable across all the rats, sleep must be a vital process.

Due to ethical reasons, It is still unknown whether chronic sleep deprivation causes death in humans, although lack of sleep has been linked to poor health (Medic, Wille and Hemels, 2017; Chattu *et al.*, 2018). Sleep deprivation experiments have been utilised in a few additional model systems, like in cockroaches (Stephenson, Chu and Lee, 2007), pigeons (Newman *et al.*, 2008), and fruit flies (Shaw *et al.*, 2002), without any clear conclusions on how sleep deprivation causes death or if sleep deprivation is genuinely vital.

One study calls into question the notion that lack of sleep deprivation is lethal, at least for *Drosophila* (Geissmann, Beckwith and Gilestro, 2019). Using video tracking and machine learning techniques, they showed that extremely short-sleeping flies are present within a wild-type population, with some showing less than 30 minutes a day of sleep. They also showed that chronic sleep deprivation had only a small, if any, impact on longevity.

In contrast, a recent study aimed to explain why sleep deprivation may lead to death (Vaccaro *et al.*, 2020). Using mouse and fly models, Vaccaro *et al.*, 2020 demonstrated that chronic sleep deprivation accumulates reactive oxygen species (ROS) in the gut, leading to oxidative damage, including DNA damage, stress granule formation, and eventual cell death. When these organisms were engineered to prevent ROS accumulation in the gut via two differing antioxidant methods, they exhibited an average lifespan while still lacking sleep. Alongside sleep deprivation protocols, Vaccaro *et al.*, 2020 also tested classical sleep mutants, such as the knockdown of Cyclin A (Rogulja and Young, 2012; Afonso *et al.*, 2015) or mutation of *redeye* (Shi *et al.*, 2014). Each of these manipulations resulted in reduced sleep and longevity and accumulation of ROS in the gut (Vaccaro *et al.*, 2020). Interestingly, this was not true for the dopamine transporter mutant *fumin* (*fmn*) (Kume *et al.*, 2005). *fmn* mutant flies had significantly reduced sleep; however, they do not have a reduced lifespan nor show ROS accumulation in the gut. Why the *fmn* mutant differs from all other forms of sleep deprivation used is unclear. However, it provides further evidence for the possibility that sleep deprivation is not lethal if you can prevent ROS accumulation in the gut. The data suggests that ROS accumulation in the gut is the underlying cause of death when sleep deprived. The gut being the primary site of action heavily suggests a feeding cause. It is unknown, however, how ROS accumulates and what events occur downstream to cause death.

Interestingly, while both studies looked at the effect of chronic sleep deprivation in fruit flies, they seem to reach opposing conclusions. The questions they answer, however, are subtly different. (Geissmann, Beckwith and Gilestro, 2019) aimed to determine whether it is possible for *Drosophila* to survive without sleep. In contrast, (Vaccaro *et al.*, 2020) look at the underlying

reason why animals often die due to chronic sleep deprivation. Even with this distinction, they have differing results for the effect of chronic sleep deprivation on longevity.

This difference may be explained by the sleep deprivation protocols used in each study. (Geissmann, Beckwith and Gilestro, 2019) used a custom-made sleep deprivation protocol involving a small rotation in the tube, but only when the fly seems to fall asleep. (Vaccaro *et al.*, 2020), on the other hand, used multiple methods. The primary method utilised was thermogenetically activating a population of wake-promoting neurons that do not induce a subsequent homeostatic response (Seidner *et al.*, 2015), depriving the flies of sleep throughout the experiment. (Vaccaro *et al.*, 2020) also used a mechanical sleep deprivation protocol; however, this was less specific and more intrusive than in (Geissmann, Beckwith and Gilestro, 2019). Perhaps these contrasting sleep deprivation methods have differing capacities to induce ROS in the gut, or perhaps, as mentioned in (Geissmann, Beckwith and Gilestro, 2019), their custom method for sleep deprivation may still allow for microsleep periods, which are sufficient for survival.

Another potential explanation is that survival and ROS generation depends on how you lose sleep, not the act of losing sleep itself. The methods utilised in (Vaccaro *et al.*, 2020) lead to either constant stimulation (thermogenetic approach) or exhaustion (intense mechanical stimulation). These methods may lead to differences in ROS production and feeding compared to the less exhaustion-inducing sleep deprivation protocol used by (Geissmann, Beckwith and Gilestro, 2019). Finally, both papers differ in the food composition that the flies were kept on. (Vaccaro *et al.*, 2020) used a standard yeast cornmeal sugar agar diet, while (Geissmann, Beckwith and Gilestro, 2019) use a homemade recipe. Different food substrates may provide different levels of antioxidants.

1.6 Defining and measuring sleep

1.6.1 The mammalian gold standard

Mammalian models, such as mice and rats, are often used for sleep research due to their high genetic similarity to humans, the availability of genetic tools, and the ability to record sleep states via electrophysiology. The electrophysiological criteria for mammalian sleep, which is considered the gold standard, come from three recordings which make up the 'polysomnogram' (Hori *et al.*, 2001; Brown *et al.*, 2012; Miyazaki, Liu and Hayashi, 2017). The polysomnogram mainly consists of an electroencephalogram (EEG) to record cortical brain activity, an electromyogram (EMG) to record electrical field potentials of skeletal muscle, and electro-oculogram (EOG) to record

electrical field potentials of the muscles controlling eye movement (Loomis, Harvey and Hobart, 1937; Dement and Kleitman, 1957). Altogether, the polysomnogram allows the different stages of sleep and wakefulness to be tracked (Brown *et al.*, 2012).

In mammals and birds, sleep can be separated into rapid eye movement (REM) and non-rapid eye movement (NREM), which cycle throughout the night. NREM sleep can be further divided into three distinct states: N1, N2, and N3. While EEG activity during quiet wake shows low amplitude and high-frequency alpha waves (Carskadon, Dement and Others, 2005), NREM sleep is generally characterised by lower frequency and higher amplitude activity (Brown *et al.*, 2012). Sleep onset occurs through NREM stage 1, the healthy transition between wake and sleep. This contrasts with the sleep disorder 'narcolepsy', where patients can transition from waking directly into the REM state (Carskadon and Rechtschaffen, 2005; Saper *et al.*, 2010). N1 is a brief sleep stage characterised by low amplitude waves of mixed frequency in the EEG. It is also the stage with the lowest arousal threshold, as very little sensory stimulation is required to reverse this sleep state (Institute of Medicine, Board on Health Sciences Policy and Committee on Sleep Medicine and Research, 2006). The N2 stage is characterised by sleep spindles and K-complexes present in the EEG and a higher arousal threshold. These sleep spindles are thought to be involved in memory consolidation as human subjects who underwent a learning paradigm before sleep showed increased sleep spindle density during the N2 state (Gais *et al.*, 2002). Sleep spindles are not present in animals whose thalamus has been lesioned, and it is thought that the sleep spindles emerge from the interactions of the reticular nucleus of the thalamus and the thalamocortical neurons (Buzsaki *et al.*, 1988; Huguenard and McCormick, 2007; Fuller *et al.*, 2011). The N3 stage (which can be further divided into stages 3 and 4) is described as deep or slow-wave sleep with high amplitude delta waves and the highest arousal threshold. These delta waves arise from the synchronised activity of cortical neurons, whereby they show synchronised switching between hyperpolarised ('DOWN' state) and depolarised ('UP' state) membrane potentials, with a frequency of <4Hz (Steriade, Nuñez and Amzica, 1993; Compte *et al.*, 2003; Brown *et al.*, 2012).

REM sleep, on the other hand, is characterised by rapid eye movements, muscle atonia, variable arousal thresholds, and similar EEG patterns to the waking state with low amplitude high-frequency activity (Institute of Medicine, Board on Health Sciences Policy and Committee on Sleep Medicine and Research, 2006). Brain activity during human REM sleep is associated with dreaming, with subjects able to vividly recall their dream almost 80% of the time when woken up during REM sleep (Dement and Kleitman, 1957). The reason we dream is still unclear; however, REM sleep may be involved in memory consolidation (Smith and Lapp, 1991; Landmann *et al.*, 2015).

Mammalian sleep is considered cyclic, whereby NREM and REM sleep cycle alternately. One sleep cycle in humans lasts for 70-120 minutes (typically ~90 minutes), and individuals usually go through 3-5 cycles during a consolidated nighttime sleep period. A healthy individual will transition from wake to NREM N1, where the cycle begins. They will then pass through each NREM stage and finish the cycle with REM sleep before the cycle repeats. The initial sleep cycle is dominated by slow wave (N3) sleep with only a short amount of REM at the end of the cycle. Subsequent cycles have little to no time spent in N3, with N2 dominating the NREM portion of the cycle (Institute of Medicine, Board on Health Sciences Policy and Committee on Sleep Medicine and Research, 2006). REM sleep increases in duration during each subsequent cycle (Carskadon and Rechtschaffen, 2011).

1.6.2 The *Drosophila* Activity Monitor

The seminal studies demonstrating *Drosophila* rest as a sleep-like state utilised a variety of protocols, ranging from visual inspection to ultrasound recordings, to demonstrate that rest is a sleep-like state. Both studies, however, end up focusing on the *Drosophila* Activity Monitor (DAM) assay for studying sleep. As mentioned in Chapter 1.2.1, the DAM assay is commonly used in circadian research (Figure 1.2.1). These were quickly adopted by sleep researchers due to being high throughput, cost-effective, community supported (many users!), and produce simple to analyse results. Notably, the main difference in experimental setup for sleep studies is that the number of activity counts are recorded per minute instead of every five minutes.

A major drawback of DAM is the low spatial, temporal, and informational resolution. DAM assays use one beam through the centre of the fly tubes (Figure 1.2.1). Flies performing small movements, or even lots of movement, but only in one half of the locomotor tube, would be classed as sleeping due to not crossing the centre of the tube. A potential issue is sleep overrepresentation when performing genetic manipulations or screening for sleep-promoting genes. For example, an increased feeding or grooming mutant would be measured as sleeping more. In addition, activating a neuronal population may seem to induce 'sleep' when it may induce other behaviours, such as feeding. One method used to mitigate this potential effect is to record the number of beam crosses during the active period. If a potential fly sleep mutant shows a similar value to controls, the difference in sleep seen is likely not due to overall reduced locomotion. While this is likely to be generally effective, there is still the potential for flies to show time-of-day effects, such as increased feeding at night or differences in locomotor behaviour.

Newer DAM assays, with multiple infrared beams, were created to improve spatial resolution. For example, the TriKinetics DAM5M monitors have four beams, while the MB5 multibeam activity monitors have 17 (DAMsystem – TriKinetics Inc, Waltham, MA USA). These provide a higher

spatial resolution recording of locomotor activity and minimise the effect of locomotion being misrepresented as sleep (Garbe *et al.*, 2015). These improved DAM monitors have not been widely taken up by laboratories using DAM assays for sleep purposes, likely due to increased costs and lower throughput. In addition, a multi-beam DAM assay is unable to detect stationary active behaviours such as grooming and feeding.

1.6.3 Video-tracking

Concerns about the DAM has led a handful of laboratories to create video-tracking assays for sleep research (Zimmerman *et al.*, 2008; Donelson *et al.*, 2012; Gilestro, 2012; Faville *et al.*, 2015; Garbe *et al.*, 2015; Geissmann *et al.*, 2017). Video-tracking typically functions by recording flies from a top-down or bottom-up perspective with a video camera and typically use the same glass tubes as in a DAM assay (Figure 1.6.1). An algorithm (typically background subtraction) is then used to track the fly's position throughout the course of the experiment. The published video-tracking systems vary significantly in terms of resolution. Older video-tracking studies, such as Zimmerman *et al.*, 2008 and (Donelson *et al.*, 2012) utilise a relatively low-resolution video-tracker, whereby the fly position is tracked (the centroid of the body) and used to inform whether the fly has moved over a period of time. Zimmerman *et al.*, 2008 demonstrate that DAM overestimates sleep as compared to video-tracking. Interestingly, the level of sleep was shown to differ significantly based on a variety of factors such as sex, age, genotype, and time-of-day (Zimmerman *et al.*, 2008).

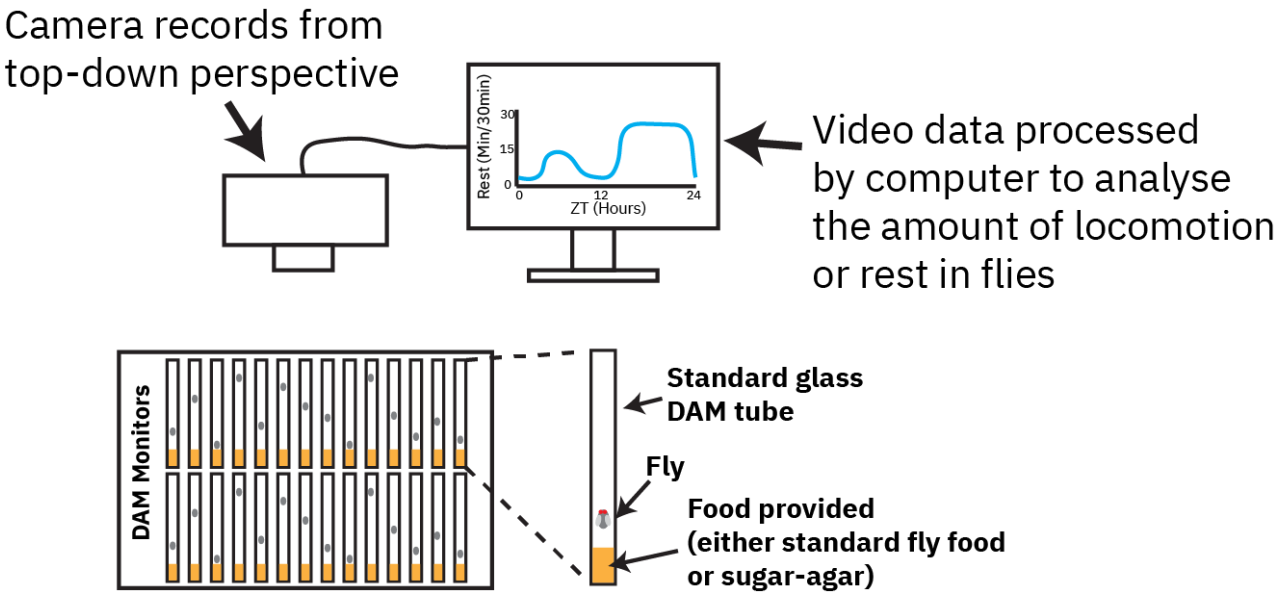

Figure 1.6.1 Video-tracking assays in *Drosophila*

An illustration of video-tracking assays, whereby DAM tubes (or equivalent) are used to house individual flies, while a video camera is placed above these tubes to record flies from a top-down perspective. Image analysis algorithms can then be used to track individual flies.

However, an issue with low-resolution video-tracking assays is that they focus solely on locomotion versus inactivity. In reality, flies exhibit a wide variety of behaviours which could be missed when testing for a sleep phenotype in a low resolution assay (Branson *et al.*, 2009). Higher resolution video-tracking assays have been demonstrated in the past few years (for example, Geissman(Geissmann *et al.*, 2017; B. Qiao *et al.*, 2018). Both of these studies demonstrated an ability to accurately measure more complex behaviours that occur when flies are stationary active. (B. Qiao *et al.*, 2018) showed that stationary active behaviours such as feeding and grooming make up a significant portion of a fly's daily behaviour, further justifying the value of high-resolution video-tracking.

As with the multi-DAM assay, video-tracking assays have not been widely adopted by the *Drosophila* sleep field. This could be due to the increased technical requirements to set up a video-tracking assay, as well as increased costs, lower throughput, and less technical and analytical support compared to DAM assays.

1.6.4 Brain imaging

In a similar vein to the mammalian approach to measuring sleep, multiple laboratories have utilised electrophysiological and calcium imaging assays to study sleep in *Drosophila* (Nitz *et al.*, 2002; van Alphen *et al.*, 2013; Bushey, Tononi and Cirelli, 2015; Tainton-Heap *et al.*, 2021). These assays typically function by tethering an individual fly and placing it on an air-supported ball to allow it to perform behaviours such as locomotion without physically moving. Brain activity, whether local field potentials using electrodes inserted into the fly brain or calcium imaging (calcium sensitive fluorescent proteins and two-photon imaging), can be recorded from broad or restricted regions of the brain. Video recording is then used to score fly behaviour and correlate it to the brain recordings.

Such a setup allows for probing brain activity during behavioural states and behavioural state transitions. For example, the work of van Swinderen's lab has provided strong evidence that various sleep states are present in *Drosophila* (van Alphen *et al.*, 2013; Tainton-Heap *et al.*, 2021). However, there are drawbacks to this experimental protocol. Creating such a setup involves significant costs and technical difficulties, and most laboratories cannot afford this. In addition, these experiments have limited throughput as only one fly can be recorded, and the experiment

can only be performed for a short amount of time. Furthermore, there is concern about how naturalistic a fly's behaviour is when tethered.

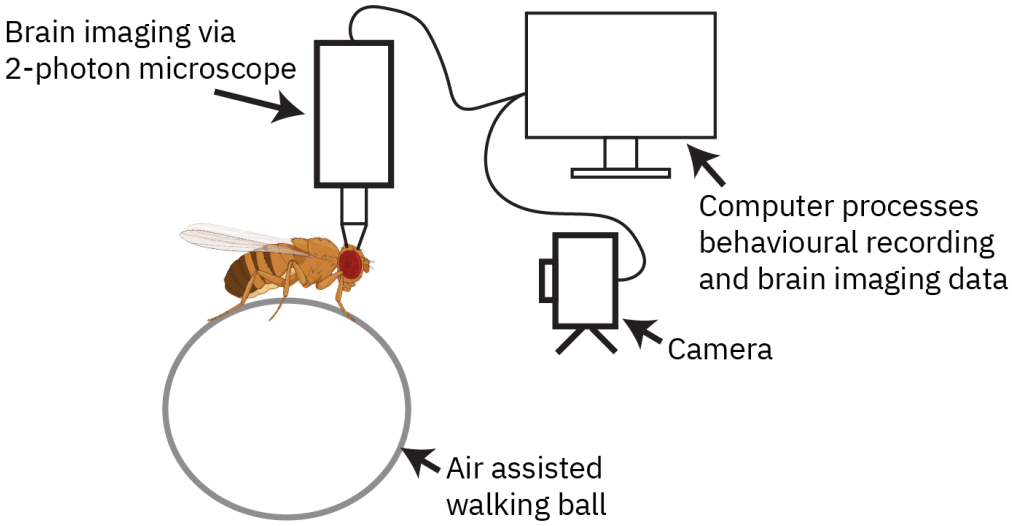

Figure 1.6.2 Recording the brain activity of tethered flies

Schematic of a two-photon calcium imaging setup, whereby a fly is head tethered and placed on an air suspended ball to simulate walking. Calcium fluorescence imaging can then be performed with a two-photon microscope and the activity of brain regions can be correlated with the fly behaviour.

1.6.5 When does inactivity become sleep?

With the variety of assays used to study sleep in *Drosophila*, the one consistent factor is the need to define when inactivity becomes sleep. In the seminal papers, how sleep-like rest was defined varied significantly with no expressed logic. To begin with, (Hendricks *et al.*, 2000) utilised a definition of ≥1 minute of inactivity as measured by visual inspection. With group housed flies, they then utilised a ≥5 minutes of inactivity. With DAM, they utilised ≥30 minutes of inactivity (no beam breaks). In comparison, Shaw *et al.*, 2000 used a definition of ≥5 minutes of inactivity within an ultrasound assay to measure rest. They also used DAM; however, it is unclear whether the equivalent of ≥5 minutes threshold was used.

Later research by Huber *et al.*, 2004 provided evidence for a 5-minute threshold. They found that the responsiveness of flies to a mechanical stimulus reduced for each minute that flies had been inactive within a DAM assay (as defined by no beam breaks), until the five-minute time point. They also saw a significant difference in the frequency of response between the light and dark phases, suggesting that sleep during the dark period is a deeper sleep state than during the light period. While the average frequency of response decreased until 5 minutes of prior immobility, the error bars were large and no statistical analysis was performed. In addition, the sample size

was relatively small and biased, with only females of the Canton-S (CS) wild-type genotype being used.

More recent research utilising a similar vibration stimulus assay shows a response rate drop after only 2 minutes, suggesting sleep relevant processes may occur much earlier than 5 minutes (Tainton-Heap *et al.*, 2021). (Tainton-Heap *et al.*, 2021) further suggest that the 1-5 minutes of immobility may be an active or light sleep phase. Such a suggestion echoes the findings of (van Alphen *et al.*, 2013) where they describe differences in local field potentials when comparing active flies to those that have been inactive for 1-5 minutes.

Within the *Drosophila* sleep field, 5 minutes of inactivity, measured in a DAM assay, has remained the industry standard for recording sleep-like rest. As illustrated above, this was the first estimate of sleep in flies and has allowed for research into sleep function and neural circuitry. There are, however, some apparent concerns with the current way of measuring a sleep-like state. The use of 5 minutes as a threshold is based on a correlation of a relatively small group of flies from preliminary research. It is therefore somewhat arbitrary as flies may take different times to transition to a sleep state. It also follows that both sexes and other genotypes may show different patterns of sleep transition timing and arousal thresholds (van Alphen *et al.*, 2013; Faville *et al.*, 2015), which this generic sleep definition would miss. In addition, the original definition, where sleep is essentially a binary on/off switch, also precludes the potential for various sleep states, a concept which is seen in mammals and has been described in flies (van Alphen *et al.*, 2013; Faville *et al.*, 2015; Tainton-Heap *et al.*, 2021).

1.7 Sleep posture and place preference

The behavioural criteria of sleep, which Drosophila are considered to fulfil, include the concept of a sleep pose and place preference. The idea of a sleep pose is relatively intuitive, given that we as humans adopt a set of stereotypical postures while sleeping (Spörrle and Stich, 2010; Skarpsno *et al.*, 2017). Beyond humans, researchers have described this concept in organisms across the animal kingdom. The Sunda slow loris (*Nycticebus coucang*) is a mammalian example, whereby they typically rest in the corners of the cage (which can be considered a place preference) in either an upright or lying down position (Tenaza *et al.*, 1969). Sleep posture has also been described for reptiles such as *Caiman sclerops* (Flanigan, Wilcox and Rechtschaffen, 1973), two species of Iguanid Lizards (Flanigan, 1973), as well as birds (Hediger, 1980) and fish (Weber, 1961). Within the field of invertebrates, cockroaches were described to have specific postures associated with rest (Tobler and Neuner-Jehle, 1992). Mosquitos were also shown to have a posture

associated with rest (Ajayi *et al.*, 2022). Finally, bees were shown to have a lowered position prone on the ground and have changes in antennal position due to reduced muscle tone (Kaiser, 1988, 1995). Like the honeybee, *Drosophila melanogaster* was initially described as initiating a rest bout in a supported upright position and subsequently lowering the body to a prone position during rest (Hendricks *et al.*, 2000). However, later studies disputed the existence of a stereotypic rest pose in *Drosophila* (Cirelli and Bushey, 2008), and whether a stereotypic rest pose is present in flies remains unclear to date (Helfrich-Förster, 2018; Beckwith and French, 2019).

While posture has been more widely studied, sleep is also considered to be associated with a species-specific place preference. As humans, we carefully select our sleeping location (Spörrle and Stich, 2010; Skarpsno *et al.*, 2017). In the wild, a safe location, such as a cave or canopy, provides animals vital shelter from poor weather. In addition, the choice of sleeping location is often a feature of predator-prey dynamics. For example, lions are widely known to sleep out in the open, with the security that, as a large predator, they do not need to hide. For other animals, however, finding a protected/sheltered location could be considered an important survival mechanism (Shukla, Kilpatrick and Beltran, 2021). One published example is the buffy-headed marmoset, which was found to use trees as a protected resting location away from predators (Ferrari and Ferrari, 1990). Similarly, diurnal birds are commonly found resting perched in trees and elevated places to protect them from land predators (Tisdale *et al.*, 2018). A safe location, such as a cave or canopy, also provides animals with vital shelter from poor weather.

In the insect world, many species have been described to rest in a specific protected location (Rau and Rau, 1916; Rau, 1938). Very little literature on *Drosophila* place preference exists, whether that is in a laboratory setting or in nature. In nature, flies will typically be found feeding, courting, laying offspring, and resting directly on top of, or inside of, ripe and rotting fruit (Soto-Yéber *et al.*, 2018). Within a laboratory setting, flies are separated and recorded individually in glass tubes (~65mm in length) with food provided on one end. This limits the context of a place preference to the chamber size. Within the original paper describing rest as a sleep-like state, the authors describe flies as displaying a strong place preference during rest (Hendricks *et al.*, 2000). They describe that flies almost always will rest near, but slightly away from the food while also facing away from the food. A preference for being near the food within a laboratory setting could be due to flies prioritising food availability. It could also be due to humidity, as the fly food being on one end of the chamber results in a humidity gradient within the chamber. However, no data was provided to justify the description of a place preference in this paper. Two subsequent studies using video-tracking assays subsequently suggested that flies prefer to rest near a food source, although the results are low resolution and it was not shown whether flies also perform other behaviours near food (Zimmerman *et al.*, 2008; Donelson *et al.*, 2012). In addition, these studies did not show whether flies have a facing direction preference.

To my knowledge, a systematic quantitative analysis of *Drosophila* place preference and rest posture has not yet been shown. As mentioned, video tracking assays are becoming increasingly popular for studying fly behaviour. Published video tracking assays all record from top-down and are thus unsuitable for analysing rest posture. Whether flies adopt a specific place and posture during rest remains unknown. If flies adopt a specific posture, an assay that tracks fly behaviour and posture could become an attractive method for improving how sleep is behaviourally defined. Similarly, if flies were to adopt a specific place preference during long rest, that would be of interest and an additional metric, alongside any specific postures, that could indicate the fly is sleeping.

1.8 Study aims

Since demonstrating that *Drosophila* rest is a sleep-like state, many molecules and cellular populations have been implicated in sleep-wake regulation (Ly, Pack and Naidoo, 2018). The most common method for analysing sleep involves using a DAM assay to record gross fly locomotor patterns. Five minutes or more of gross inactivity (as measured via beam breaks) is utilised as a correlate of sleep, and changes in inactivity due to genetic manipulation indicate these cells may be involved in sleep/wake regulation. As previously mentioned, DAM and low-resolution video-tracking assays have drawbacks and may misclassify phenotypes of grooming, feeding, or mild seizures as sleep.

For my thesis, I am interested in furthering the research fields' understanding of *Drosophila* rest/activity behaviour using two separate but complementary assays. Firstly, I will demonstrate a new behavioural video-tracking assay, named 'Trumelan', which has a high spatial and temporal resolution. In addition, Trumelan can record fly posture and position in both the x- and y-dimension by recording flies from a side-on perspective. A behavioural definition of a sleep-like state includes the concept of a pose and place preference. Sleeping flies were described as having a place preference and adopting a specific pose, but this has not yet been well established. It would be an important discovery if posture and place preference could be used within video tracking assays to help define a sleeping fly. Similarly, if posture and place preference are not specific to sleep or cannot help identify sleeping flies, this would also be valuable to know.

Here, I set out to quantitatively describe the characteristics of rest posture and place preference in *Drosophila* by utilising Trumelan. As Trumelan cannot justify that a fly is sleeping, I aimed to quantify typical fly positioning and posture within this behavioural assay and study whether any posture/place preference can be found that is specific to rest.

- Demonstrate a newly created video tracking assay, 'Trumelan', which tracks flies from a side-on perspective.
- Create a behavioural state classifier using simple machine learning algorithms and explore the accuracy of these against visually selected definitions of behaviour.
- Analyse wild-type fly behaviour within Trumelan and compare the outputs to typical beam-breaking style analysis (DAM).
- Quantify wild-type flies' rest posture, including their starting position and postural changes during the rest bout.
- Quantify wild-type flies' resting place preference, including the x- and y-position within the chamber and the direction the fly faces.

During my place preference experiments, I discovered that flies have preference for being on the ground or the ceiling of the Trumelan chamber (y-position preference). The discovery of a y-position preference was a novel aspect of rest place analysis. From the results, I adjusted my aims to investigate y-position further.

- Analyse y-position place preference for wild-type and circadian mutants in various light conditions.

Alongside behavioural correlates of sleep, recording patterns of brain activity measured by an EEG is the current gold-standard for recording sleep in mammals. In *Drosophila*, recent advances in brain imaging have demonstrated neural correlates of sleep and suggested that distinct sleep states can be identified (van Alphen *et al.*, 2013; Yap *et al.*, 2017; Tainton-Heap *et al.*, 2021). These assays involve an individual fly being head tethered and placed on an air-suspended ball to allow the fly to simulate walking. The fly head tethered such that brain activity can be recorded with the use of either electrodes (to record local field potentials) or with two-photon calcium fluorescence imaging from regions or cells of interest. Brain activity is recorded in regions of interest and correlated to the behaviour the fly is performing (analysed via video-tracking). This current setup should be considered the current gold-standard for recording brain activity and neural correlates of sleep in *Drosophila*.

A major drawback of the current approach to recording neural correlates of sleep in *Drosophila* is that the assay is expensive to setup and requires extensive technical expertise to create, use, and maintain. In addition, the throughput is low as only a single fly can be recorded, and experiments can only be performed for short periods. Furthermore, it is unclear whether tethered flies behave naturally and if the brain activity recorded in this manner is consistent in freely moving flies.

For the second part of my thesis, I aimed to study the efficacy of utilising in vivo luciferase assays for recording cellular activity in specific populations of cells in freely moving flies over long periods. It would be of interest to the *Drosophila* sleep field if neural correlates of sleep can be discovered using Luciferase reporter assays. This technique is not meant to directly compete with tethered fly brain recordings, which function on a different timescale to Luciferase assays, but instead represents a method to study whether rhythmic patterns of brain activity can be found as correlates of sleep.

- Screen GAL4 drivers which have been implicated in sleep-wake regulation, as well as broadly expressing drivers, with calcium sensitive Luciferase reporters (CaLexA-LUC and TRIC-LUC) to find populations of cells with rhythmic Luciferase activity

Following the discovery of low signal strength in restricted cell populations using firefly luciferase (FLuc), I expanded my study aims to test whether an alternative luciferase, based on NanoLuc (England, Ehlerding and Cai, 2016), could produce stronger bioluminescence signals in *Drosophila*. NLuc-based reporters have yet to be tested within flies, and whether the substrate for NanoLuc can reach the brain is currently unknown.

- Create flies with new luciferase constructs based on NanoLuc and test their functionality.

Chapter 2 Materials and Methods

2.1 Fly husbandry and Genetic Crosses

Flies were cultured in plastic vials containing ~10 ml of standard fly diet containing 1.25% w/v agar, 10.5% w/v dextrose, 10.5% w/v maise and 2.1% w/v yeast at 25˚C, ~60% humidity, and in a 12:12 Light:Dark (LD) cycle. Fly handling was performed per standard fly pushing protocols, with flies being anaesthetised with CO_2 before being manipulated on a pad using a soft brush.

Within this thesis and across fly research, a genotype is represented as a string of three pairs of chromosomes (Figure 2.1.1). While there are technically four pairs, the fourth pair contains very little information and is therefore excluded from the genetic schema. Chromosomal pairs are shown together, one above the other, separated by a horizontal line. Each pair is separated from the next pair via a semicolon. A genotype with a pair of wild-type chromosomes is usually skipped such that two semicolons are used instead. In the case of Figure 2.1.1, we have a male fly with a mutant white allele (*w**) on the X Chromosome, which leads to a white-eyed phenotype (Genes are commonly named after the mutant phenotype). As with the fourth chromosome, the Y chromosome is typically left out of written genotypes due to its lack of important features. The second pair of chromosomes is comprised of one wild-type chromosome (represented as a '+') and one chromosome containing a genetic element of interest (GEI, represented as {locus mw+}). This specific GEI contains a miniwhite+ construct, which provides a functional white allele, thus generating orange/red-eyed flies if present. Most genetic elements generated will contain such a construct to allow simple tracking of this GEI via eye colour.

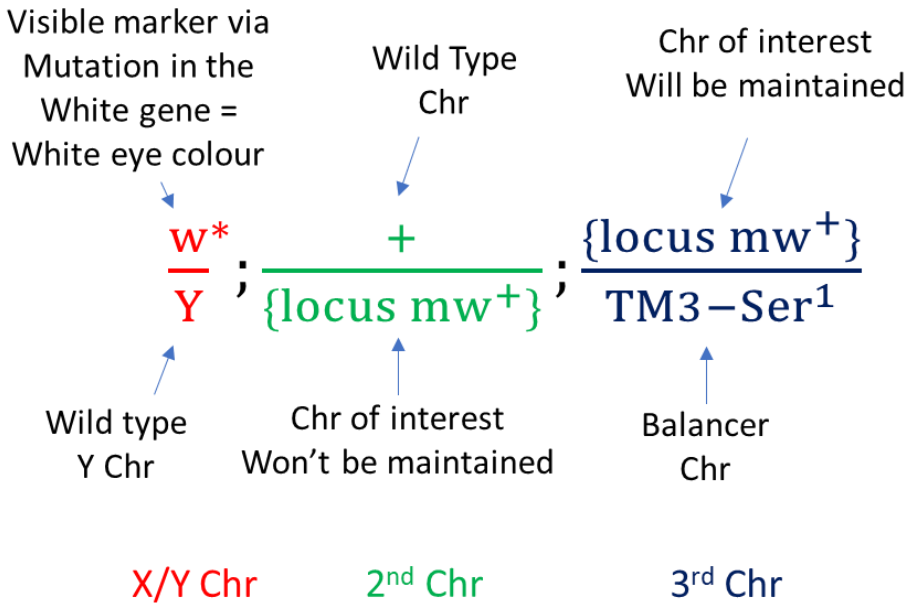

Figure 2.1.1 A standard fly genotype example

In this case, our GEI will not be guaranteed to be maintained throughout the generations, especially if the GEI lowers fitness or is deleterious. On the other hand, the third chromosome has a GEI, which will be maintained throughout the generations due to being 'balanced'. An essential process in fly genetics is using balancer chromosomes to maintain GEIs. Balancer chromosomes allow you to maintain a stable stock with a deleterious mutation and allow you to keep track of a specific chromosome of interest during genetic mating schemes by preventing recombination from occurring. Balancer chromosomes are chromosomes which have been purposely modified to have three key features:

1. A recessive lethal mutation prevents the other chromosome from being lost over the generations, e.g. The TM3-Sb[1] balancer chromosome has the recessive lethal Sb[1] mutation, which causes thicker, stubble-like hairs.
2. Multiple inversions prevent recombination from occurring.
3. A visible marker allows easy tracking of which chromosomes are present during a genetic cross. e.g., The TM3-Ser[1] balancer has the Ser[1] allele, a visible marker whereby the fly has serrated wings.

Therefore, a third chromosomal GEI can be maintained by using a balancer chromosome for the paired chromosome. A TM3-Ser[1] balancer created a balanced third chromosome in this example.

2.2 Fly strains

Table 2.2.1 Fly Strains.

Flies were received from either the Bloomington *Drosophila* stock centre (BDSC), or from current stocks within my laboratories.

Name	Chapter (s) used	Function of fly strain	Received from
Canton-S (CS)	3,4	Wild-type strain	Received from Adam Claridge-Chang lab members
Berlin-K (BK)	3,4	Wild-type strain	BDSC:8522

Name	Chapter (s) used	Function of fly strain	Received from
w^{*}	3,4	Considered 'wild-type' although has mutated *white* gene (white eyes)	Received from Adam Claridge-Chang lab members
per^{01}	4	Circadian mutant, mutated *per* gene	BDSC:80928
cyc^{01}	4	Circadian mutant, mutated *cyc* gene	BDSC:80929
w*;;UAS-mLexA-VP16-NFAT/TM3-Sb[1]	5	Calcium sensitive LexA transcription factor (CaLexA)	BDSC: 66543
w*;LexAop-Luciferase	5	The expression of firefly luciferase is controlled by a LexAop promoter	Received from Herman Wijnen Lab
w*;UAS-MKII:nlsLexA.DBD,UAS-p65.AD::CaM/CyO;Pri[1]/TM6B-Tb[1]	5	Calcium sensitive LexA transcription factor (TRIC)	BDSC: 62830
y[1] w[*];tim$_{62}$-Gal4	5	GAL4 driver expresses widely in circadian clocks	BDSC: 7126
w[1118];UAS-tim-GAL4 (tim(UAS)-GAL4)	5	GAL4 driver expresses in circadian neurons.	BDSC: 80941
w[*];clk$_{856}$-Gal4	5	GAL4 driver expresses in circadian neurons.	BDSC: 93198
elav[c155]::GAL4;;	5	GAL4 driver expresses pan-neuronally.	BDSC: 458
w[1118];;repo-GAL4/TM3-Sb[1]	5	GAL4 driver expresses pan-glial.	BDSC: 7415
w[1118];;R54G12-GAL4	5	GAL4 driver expresses in GABAergic neurons.	BDSC: 41280
w[1118];;R92E10-GAL4	5	GAL4 driver expressed broadly in fly brain.	BDSC: 40623
w[1118];;R23E10-GAL4	5	GAL4 driver expresses in dFB neurons and some VNC neurons.	BDSC: 49032

Name	Chapter (s) used	Function of fly strain	Received from
w[*];Ilp2-GAL4/CyO	5	GAL4 driver expresses in Ilp2 expressing PI neurons.	BDSC: 37516
w[1118];;R56H10-GAL4/TM3-Ser[1]	5	GAL4 driver expresses in R1-4 EB ring neuron subgroups.	BDSC: 61644
w[1118];OK371-GAL4 (vglut-GAL4)	5	GAL4 driver expresses in glutamatergic neurons in fly brain and VNC.	BDSC: 26160
w[1118];;R70F10-GAL4	5	GAL4 driver expresses widely in the fly brain.	BDSC: 39545
w1118;R52H03-p65.AD;ple.GAL4.DBD (MB504B)	5	Split GAL4 expresses in 4 PPL1 dopamine neurons in the fly brain.	BDSC: 68329
w1118;R26E07.GAL4.DBD; R35B12.p65.AD (MB461B)	5	Split GAL4 expresses in α'/β' lobes of the MB.	BDSC: 68327
w[1118];;R75H04-GAL4	5	GAL4 driver expresses mostly in the EB.	BDSC: 39909
w[1118];;R65C07-GAL4 (LKR-GAL4)	5	GAL4 driver expressing in LKR expressing neurons.	BDSC: 39344
w[1118];;ple-GAL4 (TH-GAL4)	5	GAL4 driver expresses in dopaminergic neurons.	BDSC: 8848
w[1118];kurs58-GAL4/CyO	5	GAL4 driver expresses strongly in the PI (the non-Ilp2 expressing PI neurons).	Received from Herman Wijnen Lab, from BDSC:80985
w[*];ChAT-GAL4 UAS-GFP.S65T	5	GAL4 driver expresses in cholinergic neurons.	BDSC: 6793
w[1118];;R92G05/TM3-Ser[1]	5	GAL4 driver expresses in Dopaminergic PPM3-EB neurons	BDSC: 48416
w[*];;UAS-FLPD5.DD (FLP.DD)	5	FLP recombinase (D5 variant) with added destabilising domains is expressed under the control of UAS promoter sequences.	BDSC: 79026

Name	Chapter (s) used	Function of fly strain	Received from
w[*];;5Xcre(FRT.Stop.FRT)-LUC	5	Luciferase expressed under the control of CRE promoter sequences once the FRT.STOP.FRT cassette is removed by FLP.	BDSC: 79022
w[*];;*tim*(FRT.Stop.FRT)-LUC	5	Luciferase expressed under the control of *tim* promoter sequences once the FRT.STOP.FRT cassette is removed by FLP.	Received from Herman Wijnen Lab
y[1],w[*];; nSyb-GAL4	5	Expresses GAL4 pan neuronally via a synaptobrevin promoter fragment	Received from Herman Wijnen Lab

2.3 Trumelan and video tracking

Trumelan is a simple video-tracking assay consisting of a camera, infrared LEDs to image flies, and a recording chamber which contains flies (Figure 2.3.1A-C). The video-tracking assay records flies from a side-on perspective (sagittal plane); the camera can see flies in the x- and y-dimension. While a third dimension (Z) is possible, the assay is designed so that flies can only turn in the Z-dimension. The Trumelan assay consists of a ~3mm thick acrylic plate, with compartments cut out of the centre using carbide create/motion (Figure 2.3.1C). The Trumelan chamber has two configurations. One consists of 13 full-length (65x3mm) compartments. In contrast, the second consists of 26 half-length (32x3mm) compartments. Each compartment houses an individual fly. A clear piece of acrylic covers either side of the chamber to prevent flies from escaping while being recorded. A matte black card paper covers the acrylic backplate to provide contrast for video tracking. Fly diet (~45mm^3) was provided at the left end of each chamber. The chamber was placed vertically within a 25˚C incubator, so flies were viewed side-on. The flies were recorded at either 10 or 45 frames per second with a FLIR Grasshopper3 near-infrared video camera (GS3-U3-41C6NIR-C) equipped with a 50mm Fixed Focus Lens (VS-C5024-10M) and 850nm filter (Green.L, 58-850). Two sets of Infrared LED boards (850nm) illuminated the arena.

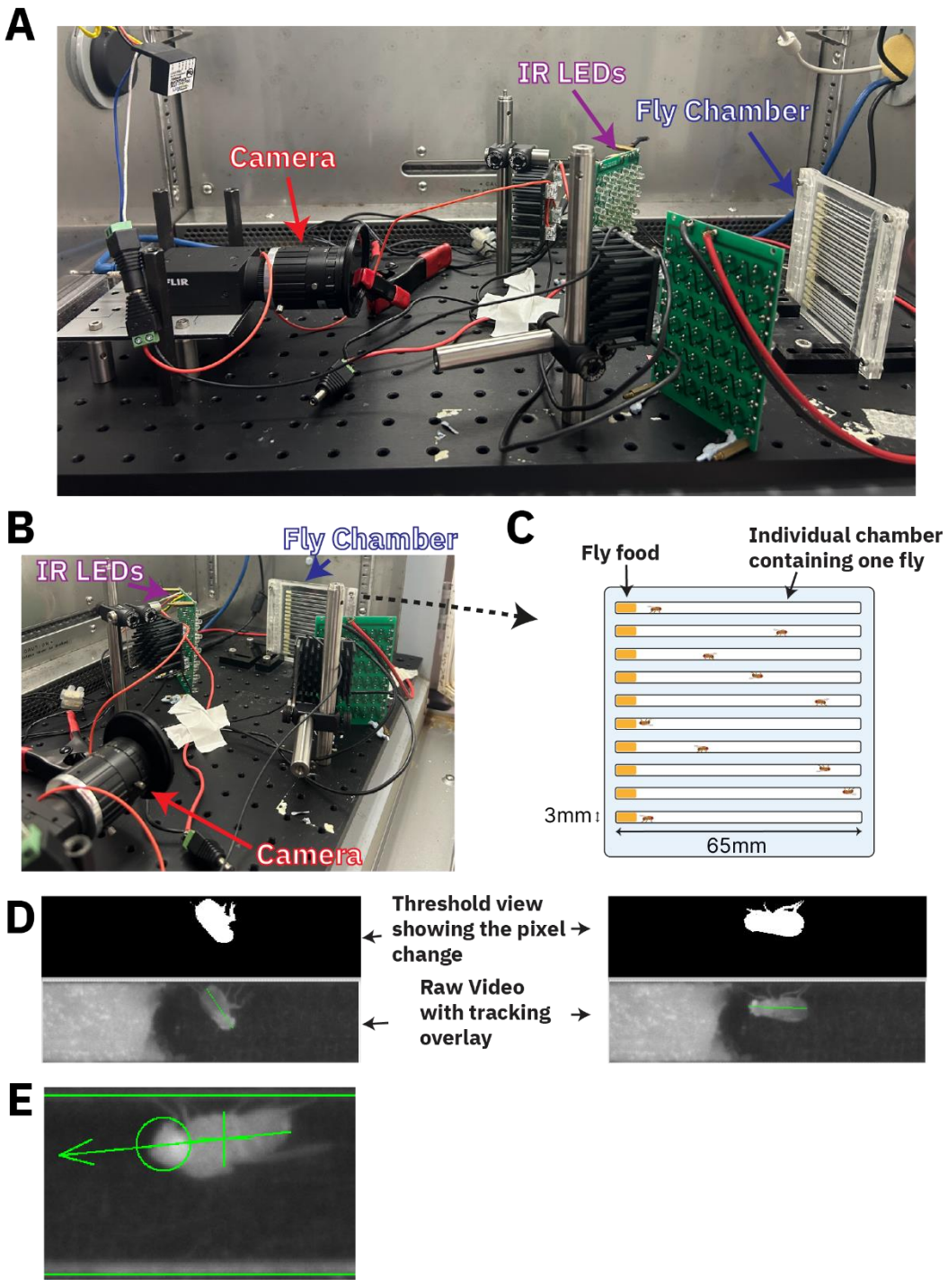

Figure 2.3.1 Trumelan and behavioural tracking

(A-B) Images of the Trumelan layout consisting of a high-quality video camera, infrared LEDs and a fly chamber, housed within an environmentally controlled incubator. **(C)** Illustration of the fly chamber design. **(D)** Raw tracking images with body angle (green line) overlaid, and the tracking threshold (white fly above). **(E)** An example raw image with behavioural tracking overlaid. The head is located and represented as a green circle, while the body angle and direction the fly is facing is represented as the green line and arrowhead. The Y-Position is also shown as the distance between the floor of the chamber and the centroid (middle of the green plus/red dot) of the fly.

Each recorded video frame is processed in real-time with Control and Real-Time Imaging Tool for Tracking Animals (CRITTA), an in-house custom software created in National Instruments LabView (Krishnan *et al.*, 2014). CRITTA tracks each fly using image subtraction as previous studies have done (Zimmerman *et al.*, 2008; Donelson *et al.*, 2012; Faville *et al.*, 2015; B. Qiao *et al.*, 2018). In brief, flies appear as bright objects against the dark background with images converted to grayscale. The change in corresponding pixel value from frame to frame are calculated and computed for each pixel. Grayscale values for each pixel range from 0 (completely black) to 255 (completely white). From each pixel change, a threshold is employed such that the pixel value must change by a sufficient amount (20 in this case) to consider a change having occurred. From the pixel change values, specific pixels will be considered to have changed from frame to frame and are represented as white (e.g., grayscale value of 255) in the threshold image (Figure 2.3.1D). The video tracking then utilises a minimum object size of 400 pixels as a threshold for detecting a fly. This means that if a contiguous area of 400 or more pixels change value from frame to frame, it considers this a fly and will track this object. The video tracking can also detect the fly head location by utilising the understanding that flies almost always walk forwards, and then by detecting the circular collection of pixels at the front of the tracked object that corresponds to the head (Figure 2.3.1E; green circle). Similarly, by knowing the head location and the fly body, the tracking also outputs a body angle of the fly Figure 2.3.1E; green arrow).

The video tracking records behavioural metrics and generates an image of each fly. I used a few key behavioural metrics for my analyses:

- *Centroid X and Centroid Y Position*. The x- and y-position of the fly's centre (centroid). Measured as millimetres from the bottom left of the chamber.
- *Speed (mm/sec)*. Raw velocity values in pixel/s are converted into mm/s values. Speed is adjusted via a weighted moving average function by averaging the current value with the four previous values (equal biases). Finally, a rebound filter was applied to smooth any spiking due to tracking loss by taking the mean of the last two values.
- *Activity Level*. The change in pixels from the current frame compared to the previous.
- *Body Angle*. The angle at which the fly body is positioned. The body angle is measured perpendicular to the side-on view or sagittal plane. Flies angled parallel to the ground will have a body angle of 180° (facing left) or 360° (facing right).

Many *Drosophila* tracking methods have come about over the last 20 years with varying designs and features. I tabulate these below, illustrating how they function and then how Trumelan compares (Table 2.3.1). The key difference with Trumelan is the side-on recording which provides an alternative view of the fly (the side of the fly rather than the top) and the ability to record the fly's angle of the body, as well as the Y-Position of the fly.

Table 2.3.1 Tabulating published *Drosophila* video-tracking methods alongside Trumelan

Assay	**DAM / TriKinetics**	(Zimmerman *et al.*, 2008)	**Tracker /** (Donelson *et al.*, 2012)	**DART /** (Faville *et al.*, 2015)	(B. Qiao *et al.*, 2018)	**Ethoscope /** (Geissmann *et al.*, 2017)	**Trumelan / This thesis**
Tracking Method	IR beam through centre. Fly crossing = count	Image subtraction	Image subtraction	Image subtraction	Image subtraction	Image subtraction or haar-cascades tracking (multi animal)	Image subtraction
Recording Rate	Counts per 1min or 5min	0.2 fps	1 fps (but can go up to 30 fps)	5 fps video; 1 fps analysis	10 fps video 5 fps analysis	1-4 fps (depending on load)	Up to 45 fps
Camera View	N/A	Camera above / Top-Down view	Camera above / Top-Down view	Camera above / Top-Down view	Camera above / Top-Down view	Camera above / Top-Down view	Camera to side / Side-on view
Chamber Size	65mm length glass tubes	65mm length glass tubes	65mm length glass tubes	65mm length glass tubes	65mm length glass tubes	Various designs available	Various designs available. Commonly use 65mm length acrylic cuboid shape
Metrics	Count data	Centroid X-Position, Speed	Centroid X-Position, Speed	Centroid X-Position, Speed	Centroid X-Position, Speed, Activity level of core and periphery	Centroid X-Position, Speed	Centroid X- & Y-Pos, Speed, Activity level, Body angle
Detected Behaviours	Locomotion / Stationary derived from count data	Locomotion / Stationary	Locomotion / Stationary	Locomotion / Stationary	Locomotion, Stationary Static, Feeding, Grooming	Locomotion, Stationary static, Stationary active	Locomotion, Stationary static, Stationary active
Arousal Testing?	No	No	No	Yes (Vibration)	No	Yes (spins individual fly chambers)	No (Hopefully in the future!)

2.4 Trumelan behavioural classifier

The behavioural state classifier was trained on flies' speed and activity level. Five standard classification algorithms were tested: Multinomial Logistic Regression, Decision Tree, Random Forest, Multilayer Perceptron, and Gradient Boosting. The dataset for training/test/validation was created by selecting multiple 1-second clips (45 frames) from around four different time points (ZT0, ZT6, ZT12, ZT18) for both male and female flies from the three wild-type genotypes (Berlin-K, Canton-S, and w*). To create a more balanced dataset, I evenly sampled 1-second clips which fell within three average activity level thresholds (0-10, 10-400, 400+). The end dataset consisted of >400000 frames, which were manually annotated for the behavioural state that I considered the fly to be performing. The three considered states were locomotive (LO), stationary active (SA), and stationary static (SS). Additional metrics supplied each frame with the speed and activity level for the prior five frames. Finally, the dataset was trimmed to remove tracking errors and the first five frames of each 1-second clip. The resulting dataset (>380000 frames) was split into training (60%), test (20%), and validation (20%) subsets. For each algorithm tested, I performed hyperparameter tuning via GridSearchCV (Scikit-learn; (Pedregosa *et al.*, 2012), whereby the training set was used to train each model with varying hyperparameters, and the test set was used to test and calculate the accuracy of each model. I subsequently selected the best model generated for each algorithm and stored these for validation. Each model generated was tested against the validation set, and confusion matrices were generated.

During validation, I noticed the model struggles mainly with classifying SA. This could be due to a high frame rate leading to more ambiguity with fly behaviour at the frame-by-frame level. I subsequently tested a 10 fps model in the same manner as for 45 fps, but with a smaller dataset of 27000 frames.

2.5 Trumelan experiments

2–3-day old flies were collected, anaesthetised on ice, and placed into individual compartments of the Trumelan chamber. For the female experiments, virgin females were selected post-eclosion and allowed to mature until 2-3 days old. The chamber was subsequently placed within the recording incubator, and flies were allowed to wake up and move. Once all flies had begun moving and I had verified that each fly was successfully being tracked, they were allowed at least 30 minutes to acclimate to their new living space before the recording began. Recordings began on the hour and lasted 26-50 hours (typically 48 hours). Following the end of an experiment, each

chamber was observed, and any fly stuck in the food, looked sickly, or died, was removed from subsequent analyses.

2.6 Data analysis & DABEST

All data analyses were performed in Visual Studio Code (VS Code, Microsoft Corporation) running on the latest version of Python. Data cleaning and manipulation were performed using the Pandas and NumPy modules (McKinney, 2010; Harris *et al.*, 2020). Data were plotted using Plotly (Plotly Technologies Inc. Collaborative data science. Montréal, QC, 2015. https://plot.ly.) or Matplotlib and Seaborn modules (Hunter, 2007; Waskom, 2021). For time series plots, the raw data was averaged over a 24-hour day with 30- or 60-minute bins.

Data analysis and interpretation were performed using estimation statistical methods (Cumming, 2014). The experiment's effect size, as measured by mean difference, is the primary output within estimation statistics. Effect size plots were generated in Python, using the DABEST module for effect sizes (Ho *et al.*, 2019) and matplotlib, seaborn, and pandas for data manipulation and plotting.

Most of my thesis uses DABEST plots as an estimation statistical analysis method (Ho *et al.*, 2019). The code and plotting tools can be found both via the website (https://www.estimationstats.com) and on GitHub (Python: https://github.com/ACCLAB/DABEST-python, R: https://github.com/ACCLAB/dabestr, and Matlab: https://github.com/ACCLAB/DABEST-Matlab). The main concepts for DABEST plots are to display all the raw data and to focus on the magnitude of the effect (effect size) being measured (e.g., mean difference) and the confidence around that effect size measurement. A typical DABEST plot contains two sections (Figure 2.6.1). One section, typically at the top, comprises the raw data points, paired or unpaired (as shown in the example; Figure 2.6.1) as required. If applicable, alongside the raw data, there may be a summary statistic in the form of two lines (the standard deviation) with a small gap in the middle (the mean). The second section, typically below the raw data, comprises the effect size plots which examine the mean difference between two or multiple groups. The difference between the two means is shown as a dot, and the 95% confidence interval around the mean difference estimate, generated by bootstrapping (2000 resamples), is shown as a line on either side of the dot. The half-violin curve demonstrates the distribution of the bootstrapped resamples of the mean difference. Bootstrapping is bias-corrected and accelerated to account for skewed distributions. In some cases (as shown in the example; Figure 2.6.1), a final curve indicates the weighted delta across all the comparisons. In the summary tables for DABEST plots (typically in the appendix), a p-value

may be shown. This is generated via a two-sided permutation t-test and illustrates the probability of observing the effect size (or a greater effect size) if the null hypothesis of no mean difference is true. The p-value is shown only for legacy purposes only, as estimation statistics is an alternative approach to null hypothesis significance testing. For each comparison, the mean difference will be shown as well as the 95%CI lower and upper bound of that mean difference.

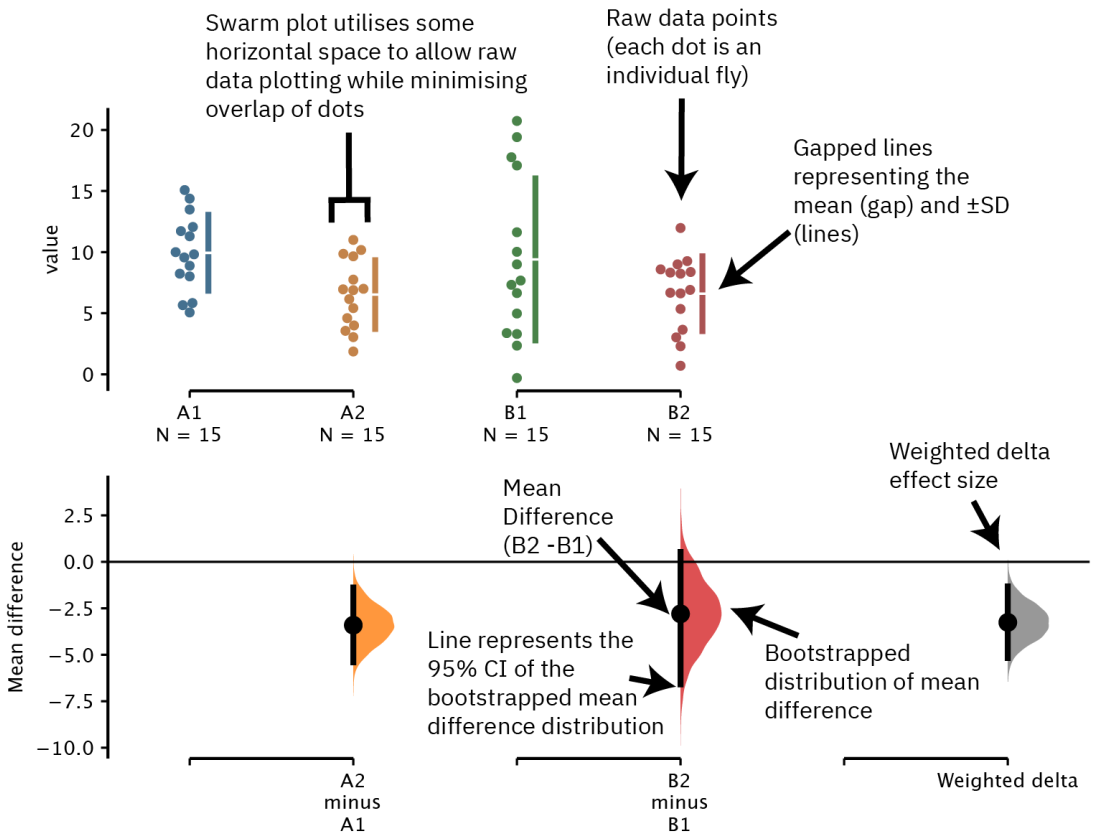

Figure 2.6.1 A typical DABEST plot

2.7 Virtual DAM analysis

I created a virtual vertical beam within Trumelan, which splits the chamber in half (at 32.5mm). A fly crossing this point was recorded as a beam break. To filter out periods when a fly hovers across the boundary (and thus causes many incorrect beam breaks), I required the fly to not recross the boundary within the next second. Beam break data is binned for each minute as per typical DAM assays. I recorded a virtual DAM rest period as 5 minutes or more of no beam breaks.

2.8 Rest posture

I utilised two key features of the Trumelan behavioural tracking assay, the Y-Position and the normalised body angle, to measure posture. The first metric is the y-position of a fly which is utilised to measure how close to the chamber floor the fly is (Figure 2.8.1A-B). It is recorded as the height (in mm) of the fly's centroid above the chamber's floor. The second metric is termed the 'body angle' of the fly. To recap the info in Chapter 2.3, the tracking finds the fly blob via background image subtraction (to discover large enough objects which move from frame to frame) and then finds the head by using the logic that flies typically walk forward (See green circle in Figure 2.8.1B for head location). The raw body angle is measured as the angle perpendicular to the side-on view (sagittal plane; Figure 2.8.1C). The tracking uses the central portion of the rear of the fly blob and the position of the fly head to measure the body angle (imagine drawing a line from the centre of the fly blob through the head; Figure 2.8.1B-C). A fly facing to the left would have a body angle of ~180°, while a fly facing to the right would have a body angle of ~360/0°. For posture analysis, the raw body angle itself is problematic as a fly is typically facing either left (~180°) or right (360/0°). For example, a fly with the same posture but facing the opposite direction would have a completely different body angle. To account for this, I converted the raw body angle into a 'normalised body angle' metric, which is measured as the body angle of the fly relative to the horizontal plane, where the parallel is 0° (Figure 2.8.1D). This allows flies facing opposite directions to be analysed together. When flies are on the ground, a negative normalised body angle indicates a fly's rear is lower than its front (the fly is in a supported, upright position). A positive normalised body angle would be the opposite, whereby the fly's body is less upright with a raised rear and lowered head. For flies on the ceiling, the normalised body angle interpretations are opposite (as flies are flipped upside down).

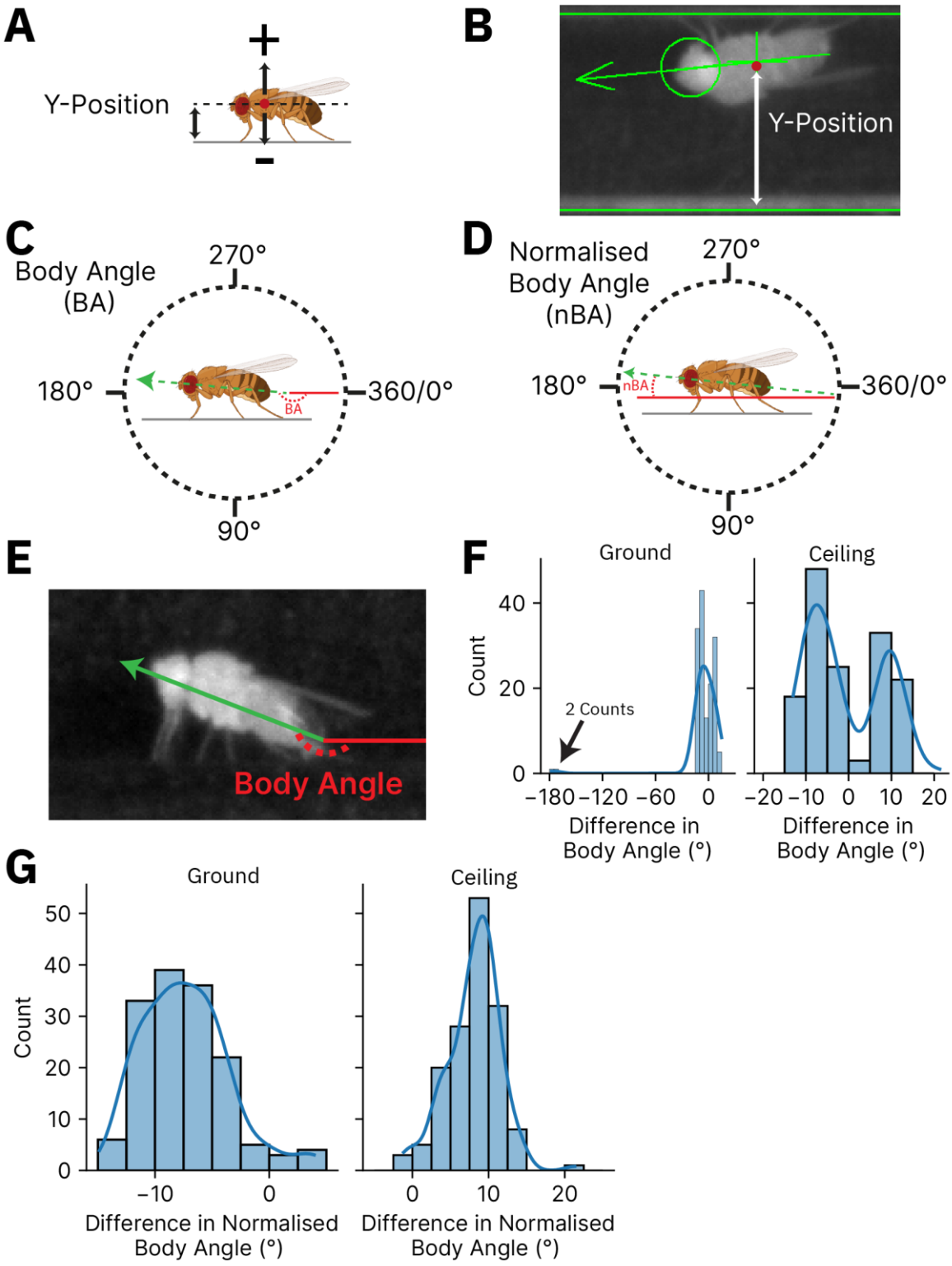

Figure 2.8.1 Measuring rest posture with Trumelan

(A) Illustration of how Y-Position is measured. **(B)** An example raw image with behavioural tracking overlaid. The head is located and represented as a green circle, while the body angle and direction the fly is facing is represented as the green line and arrowhead. The Y-Position is also shown as the distance between the floor of the chamber and the centroid (middle of the green plus/red dot) of the fly. **(C-D)** Illustration of how body angle **(C)** and normalised body angle **(D)** are

measured. **(E)** Example raw image with overlaid example of how body angle is measured. **(F)** The difference between human validated vs. Trumelan body angle for 150 ground and 150 ceiling examples of rest posture extracted from three Berlin-K male flies. **(G)** Same as for (F) but excluding the two counts of tracking errors, and now comparing normalised body angle.

Start/End posture data is collected as a given bout's first/last frame. Rest-posture time series plots were created by grouping long rest bouts (Stationary Static for ≥60 seconds) and recording the posture at each frame relative to the first frame. Three Berlin-K male fly recordings were used to collect the start and end posture image examples. Eleven ground and ceiling bouts were randomly selected. One bout of each was chosen to represent the starting posture shown in Figure 4.1.1B; the rest are shown in Appendix B Figure 1-2. The images were extracted (in Python) from the raw pixel values in the video file. The end posture from the same rest bouts as shown in Appendix B Figure 1-2 were taken and shown in Appendix B Figure 8-9. The same three Berlin-K Male flies were used for the fly outlines (Figure 4.1.2E-F) as for the prior images. Four example bouts were selected from ground and ceiling-based rest. The postural images were chosen by filtering for stationary static bouts longer than 60 seconds. Python code extracted the associated start and end image frames for a given bout. Pixel thresholding, in Python, was used to adjust images such that the fly appears black against a transparent background. Photoshop (Adobe Inc. (2019), *Adobe Photoshop*) was used to trim images further, and the 'find edges' command was used to create the final image consisting of a black outline of the fly.

A significant aspect for both the postural and place preference analyses was the body angle (or normalised body angle) metric. As described, this makes use of the video tracking's ability to locate the fly, the direction the fly is facing, and the angle of the body. To validate the accuracy of this parameter, I randomly selected 150 frames from 3 ground resting Berlin-K males (50 from each), and 150 frames from the same 3 Berlin-K males while resting on the ceiling. I measured the body angle of the fly in each image frame using a protractor. For the hand measurements, I drew a straight line from the centre of the fly's rear through the fly head and measured the angle (Figure 2.8.1E). Importantly, I was blinded to the body angle that the video tracking generated for each frame, such that the hand measured body angle could be compared to the video tracking. To begin with, I plotted the difference in raw body angle for ground and ceiling-based examples (Figure 2.8.1F; Hand drawn - Video tracking). The first thing that stood out is the small bump in counts of extremely large differences between the hand drawn and video tracking for ground-based examples (Figure 2.8.1F; black arrow). These constituted two examples of where the fly's body angle was not even close to the hand drawn measurement (13.96° and 20.72° for video tracking versus 202° and 203.2° for hand drawn, respectively). Further analysis showed that these

were two bouts from the same fly at a very close timepoint and the fly has a similar posture, suggesting that these were not two distinct instances of major body angle tracking errors. In contrast, none of the ceiling examples had major tracking errors (Figure 2.8.1F). Given there were only two major incorrect body angle errors, the data provide strong evidence for the effective use of the body angle metric for place preference (facing direction) in Chapter 4.3. To further analyse the minor BA differences, I subsequently excluded the two major errors. As flies facing left or right have a different body angle associated with the same posture, I converted the body angle data to normalised body angle data. By plotting the normalised body angle difference (Hand drawn - Video tracking), I found that the video tracking body angle was almost always considering the fly to be in a less extreme posture than the hand drawn posture (Figure 2.8.1G). In ground resting flies, this means that the video tracking will consider flies to be in a slightly more parallel posture (less negative normalised body angle and therefore a more negative difference in Figure 2.8.1G) compared to hand drawn. Similarly, ceiling resting flies are also considered to be in a slightly more parallel posture by the video tracking (positive difference in Figure 2.8.1G). The average difference (Mean±SD) between hand drawn and video tracking was -7.35±3.75° and 8.09±3.41° for ground and ceiling-based examples, respectively.

2.9 Place preference

The x-position, y-position, and raw body angle metrics were analysed for the first frame of each bout of behaviour. Long Rest (SSL) was defined as Stationary Static behaviour lasting longer than 60 seconds. Short Rest (SSB) was defined as Stationary Static behaviour lasting less than 60 seconds. Bouts of behaviour shorter than 1 second were removed from the analysis.

2.10 Rhythmicity analysis of Trumelan behaviour and ceiling occupancy

Raw fly behaviour, as measured by the Trumelan behavioural classifier, was averaged into 30-minute bins for each fly in Python. The data was subsequently imported into BioDare2 (biodare2.ed.ac.uk, (Zielinski *et al.*, 2014), which functions as both a data repository and a circadian period analysis software. Here I performed rhythmicity analysis on the data using the empirical JTK-CYCLE with asymmetry search method (Hutchison *et al.*, 2015). JTK Cycle is a non-parametric algorithm which works well on short time series data (Hughes, Hogenesch and Kornacker, 2010). This method was further improved upon by Hutchinson et al., whereby they can better detect rhythms by empirically calculating p-values (Hutchison *et al.*, 2015). In addition, this

method allows for a variety of waveforms, whereas the original only tests against a cosine waveform. (Hutchison *et al.*, 2015). eJTK_Cycle functions by correlating the times series provided against a set of rhythmic curves. The highest correlation for each fly is provided as the Tau metric, and an empirical p-value is calculated alongside Tau to provide an indication of how likely a correlation of tau magnitude or greater is expected to be seen if the time series is not rhythmic.

2.11 Luciferase reporters

2.11.1 CaLexA-LUC

The first is named CaLexA (calcium-dependent nuclear import of LexA) and is based on the nuclear factor of activated T cells (NFAT) protein (Figure 2.11.1, (Masuyama *et al.*, 2012)). NFAT is a transcription factor that rapidly enters the nucleus upon depolarisation and requires prolonged calcium levels within the cell for NFAT-mediated transcription to occur (Dolmetsch *et al.*, 1997; Graef *et al.*, 1999). NFAT is highly conserved between humans, mice, and flies (Gwack *et al.*, 2006), providing further evidence for using an NFAT-based system.

CaLexA is a fusion protein composed of three domains:

- A LexA DNA binding domain. LexA is part of the LexA/LexAop system, which functions in the same manner as GAL4/UAS. As with a split GAL4, the LexA can be split into DNA binding and activation domains. The LexA DNA binding domain binds to a LexA operator (LexAop) DNA sequence.
- A VP16 activation domain which promotes the transcription of the genetic element downstream of a LexAop sequence.
- A modified NFAT domain contains a nuclear localisation sequence (NLS) controlled by the level of intracellular calcium.

High neuronal activity leads to high intracellular calcium, which activates calcineurin. Calcineurin dephosphorylates the modified NFAT domain of CaLexA, leading to the nuclear import of CaLexA. Once in the nucleus, CaLexA binds to a LexAop domain and activates the transcription of *luciferase*. CaLexA is under the transcriptional control of the GAL4/UAS system to allow for cell-specific targeting of the calcium reporter (Brand and Dormand, 1995).

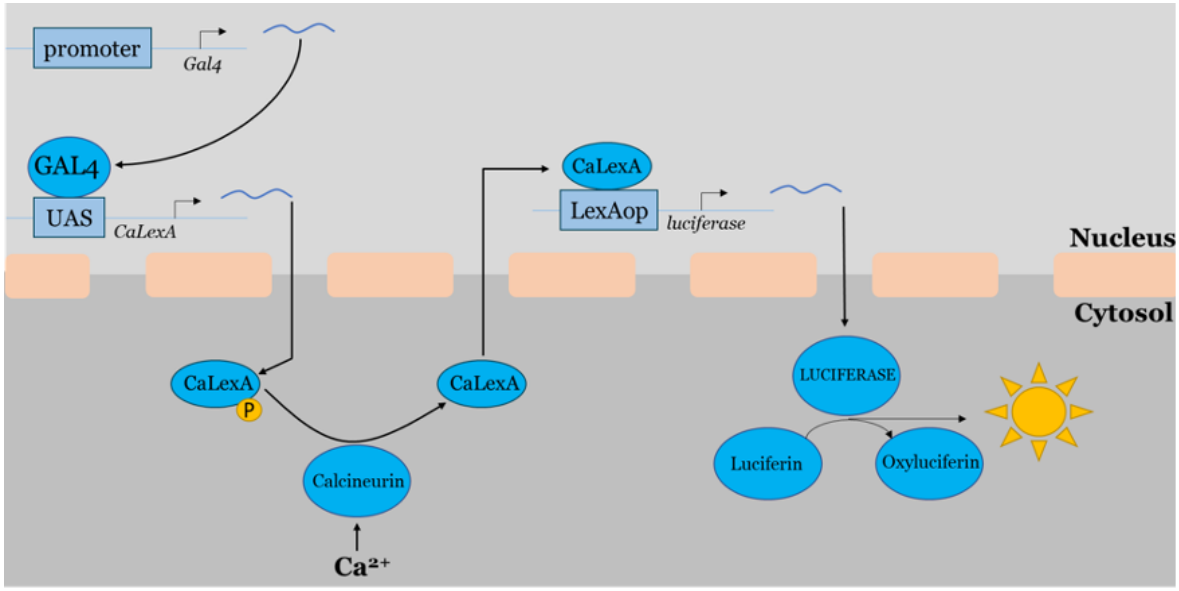

Figure 2.11.1 CaLexA-LUC, calcium-dependent nuclear import of LexA

2.11.2 TRIC-LUC

The second calcium reporter is a calmodulin-based system named 'transcriptional reporter of intracellular Ca2+', or TRIC (Figure 2.11.2; (Gao *et al.*, 2015)). TRIC functions as a calcium-dependent split transcription factor whereby a LexA DNA binding domain (DBD) is fused with the calmodulin target peptide from CaMKII (MKII), and a LexA activation domain (AD) is fused to calmodulin (CaM). Calmodulin binds to its target peptide in a calcium-dependent manner. Therefore, neuronal activity will lead to the binding of CaM-AD to MKII-DBD, thereby forming a functional transcription factor which activates the transcription of luciferase. As with CaLexA, both components of TRIC are under the transcriptional control of the GAL4/UAS system so that TRIC can be targeted to specific cell populations (Brand and Dormand, 1995).

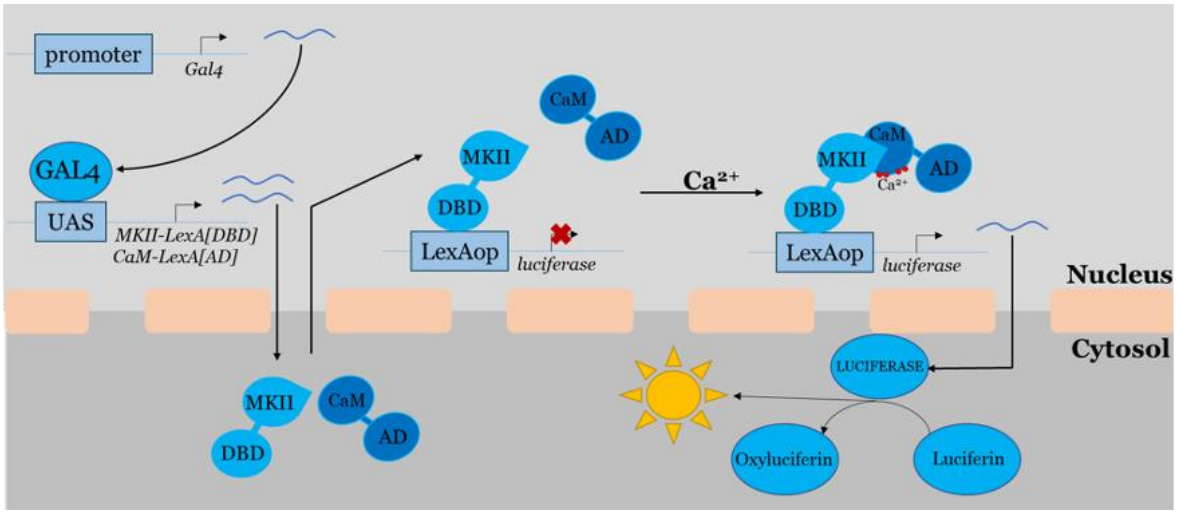

Figure 2.11.2 TRIC-LUC, the transcriptional reporter of intracellular Ca2+

CaLexA and TRIC systems are functionally similar; however, (Gao *et al.*, 2015) suggest that TRIC provides a stronger signal and a more representative expression pattern within neuronal populations. (Gao *et al.*, 2015). demonstrate this by looking at the expression pattern of CaLexA vs TRIC within the antennal lobe when driven by the antennal lobe projection neuron driver GH146-GAL4 (Figure 2.11.3). TRIC shows strong expression within projection neurons, whereas the CaLexA signal is much weaker. Therefore, at least within this context, the TRIC reporter captures the desired expression pattern more accurately in vivo.

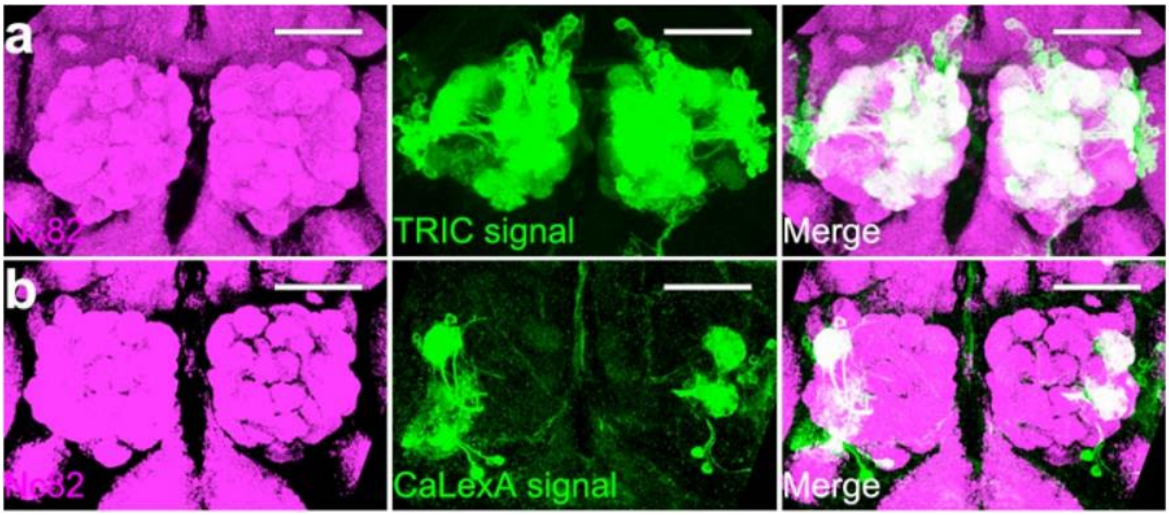

Figure 2.11.3 Comparing Calcium sensitive reporters CaLexA and TRIC

Image of a representative fly brain centred on the antennal lobe for TRIC **(A)**, and CaLexA **(B)**. The leftmost images show Nc82/Bruchpilot staining of the antennal lobe. The middle images show the GFP expression pattern for the respective reporter when driven in the antennal lobe projection neurons. The rightmost images show the two images merged. Image taken from Supplemental Figure 4a&b of (Gao *et al.*, 2015).

2.11.3 CRE/*tim*-LUC

The final reporter systems I tested were direct promoter-Luciferase reporters (Figure 2.11.4). The first was a cAMP response element binding protein (CREB) reporter termed CRE-LUC. dCREB2 is the *Drosophila* homolog of CREB and is implicated in learning and memory and circadian rhythms (Belvin, Zhou and Yin, 1999; Tubon *et al.*, 2013). The original CRE-LUC is a fusion of the firefly *luciferase* gene with cAMP response elements (CRE) upstream. The second is a *timeless* (*tim*) promoter-controlled Luciferase reporter, which outputs a bioluminescence signal from CLK:CYC transcriptional activity. These reporter constructs are modified to contain a flippase recognition target (FRT) flanked cassette between the CRE/*tim* promoter and the *luciferase* gene (CRE/tim-{FRT-STOP-FRT}-*luciferase*). This leads to a non-functional reporter as the stop codon within the cassette prevents luciferase transcription.

A recombinase (FLP) can be provided, which causes the flipping out of the FRT-flanked cassette, producing a functional CRE/tim-*luciferase* construct. The spatiotemporal targeting comes from the use of the GAL4/UAS system (Brand and Dormand, 1995). In this case, the FLP recombinase, which is not naturally found in flies, is controlled by a UAS element (UAS-FLP). A specific promoter-Gal4 can be used to target the expression of FLP to specific subsets of cells. As a result, bioluminescence should only be generated from these cells. A modified FLP was used, which contains a destabilising domain attached (Sethi and Wang, 2017). The presence of the destabilising domain leads to the degradation of the FLP by the proteasome, a process that is blocked by adding trimethoprim (TMP) to the diet. In this thesis, I will use CRE-LUC and *tim*-LUC as shorthand for these FRT flanked recombinase controlled constructs, although it should be noted that the original CRE-LUC in the literature does not contain the FRT flanked cassette (Belvin, Zhou and Yin, 1999).

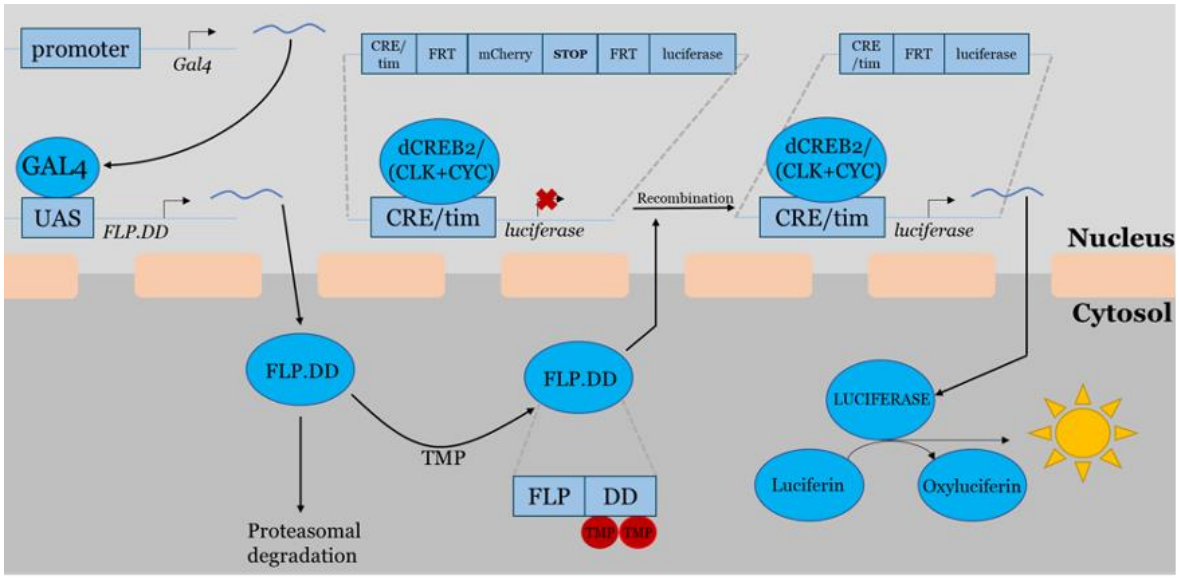

Figure 2.11.4 Using a destabilising domain FLP to control recombination of promoter-Luciferase constructs

The CRE/*tim*-LUC systems report direct transcriptional activity of dCREB2/CLK:CYC. These constructs contain an FRT-flanked cassette containing two stop codons before the luciferase open reading frame, thus preventing transcription. The presence of a flippase (FLP) within specific cells leads to site-specific recombination between the FRT sites, removing the stop codon-containing cassette and allowing for the dCREB2/CLK:CYC mediated transcription of luciferase (Tanenhaus, Zhang and Yin, 2012). In addition, the flippase is modified by adding a destabilising domain (DD) from *E.coli*, whereby the FLP.DD undergoes proteasomal degradation unless trimethoprim (TMP) is supplemented in the diet, at which point the FLP.DD is stabilised and can perform the site-specific recombination (Sethi and Wang, 2017).

2.12 Luciferase screen

For testing CaLexA-LUC and TRIC-LUC, promoter-GAL4 lines were selected that have been previously implicated in sleep/wake regulation (Table 2.2.1 Fly Strains. These were found by searching the literature using PubMed, with search terms ((‘Sleep’ OR ‘Circadian) AND ‘*Drosophila’*). I also tested some widely expressing drivers. However, due to major infrastructural issues, only a handful of the promoter-GAL4 lines were tested in this preliminary screen.

2.13 Luciferase assay

In vivo luciferase recordings for the bioluminescence screens were performed as previously described (Brandes *et al.*, 1996; Plautz *et al.*, 1997). 100µl of 5% sugar, 1% agar, 0. 7% Tegosept (10% w/v), and 1.5mM D-luciferin solution was added to every other well of a white 96-well microplate (Optiplate, Perkin Elmer). Adjacent wells were left empty to limit signal leakage from a neighbouring well. For the CRE/CREB reporter luciferase experiments, 10 mM Trimethoprim (TMP) was added to the sugar agar luciferin solution. For the NanoLuc-based reporter experiments, three concentrations (0.05, 0.1, and 0.67mM) of the substrate, fluorofurimazine (FFz, Nano-glo©, received from Promega), were tested in place of D-luciferin.

2- to 5-day-old, entrained flies were anaesthetised with CO_2 and placed into individual, food-containing, wells. A trimmed PCR cap was placed over each fly to reduce Z-axis movement and signal noise (Ralf Stanewsky *et al.*, 1997). Each microplate was covered with PCR film, and two holes were pierced into the caps and film to allow for gaseous exchange. The PCR film was trimmed to remove any excess overhanging film which may otherwise cause plate handling errors. An identification barcode was placed on the side of each microplate, which the TopCount NXT Scintillation and Luminescence Counter (PerkinElmer, Waltham, MA) reads. A transparent microplate (Optiplate, Perkin Elmer) was placed at the beginning, with a barcode specifying the assay type for the TopCount to read. An additional microplate, with two barcodes, was placed as the final plate to signal to the TopCount that it has reached the end and can begin the next cycle. Clear microplates were placed between each experimental microplate to act as spacer plates to allow light exposure. Before each experiment began, a calibration plate was used to calibrate the luminescence counter against a plate of known luminescence. Once calibrated, the calibration plate was removed, and the microplates were placed into a stacker and loaded into the TopCount, which was subjected to a 12:12 LD cycle at 20˚C with 70% humidity. The TopCount selects one plate at a time from the stacker. Once an experimental plate has been selected, it is taken into the recording chamber and held for one minute before the recording begins. The machine records the bioluminescence from each experimental well for 17 seconds, two wells at a time. An experiment

consisting of five experimental plates (plus start, stop and spacer plates) would take ~1 hour to complete a cycle. Bioluminescence readings were typically recorded for 7-10 days.

The raw bioluminescence data was uploaded to BioDare2 (biodare2.ed.ac.uk, (Zielinski *et al.*, 2014)). BioDare2 provides a platform to visualise bioluminescence recordings of each fly, allowing for the omission of data from flies that had died or showed unnaturally high spikes of bioluminescence. While deaths were rare, these usually occurred due to fungal contamination of the food source.

Raw bioluminescence counts were detrended (baseline and amplitude detrend) to account for the signal changes occurring due to luciferin availability. Detrended data was normalised (using the '[-1,1]' method) to account for varying overall levels between individual flies. Python was used to visualise and analyse the bioluminescence data. For rhythmic analysis, autocorrelation was performed on the averaged bioluminescence data as previously described (Levine *et al.*, 2002). Autocorrelation computes the similarity (correlation) of a time series (first copy) with itself (second copy). The second copy is then lagged hourly with respect to the first, and the correlation between the two is calculated for each lagged implementation. If there is no rhythmic pattern within the raw data, the correlation will begin at 1 (when no lag has been implemented) and quickly fall to low levels of correlation with subsequent lagged amounts. If a time series is rhythmic, a high correlation peak will occur at the lag amount corresponding to the time series' rhythmic period. Following the convention suggested by (Levine *et al.*, 2002), I extracted the correlation value corresponding to the third harmonic peak to represent the rhythmic index (RI). To perform rhythmic analysis, I utilised a forward-fill method for the initial screening to fill in the short sections of missing data. For follow-up work where I look at individual driver>CaLexA-LUC lines, I selected only the bioluminescence values following missing data.

For period analysis, Maximum Entropy Spectral Analysis (MESA) was used as previously described (Burg, 1972; Levine *et al.*, 2002; Zielinski *et al.*, 2014). MESA is a stochastic modelling technique which generates a power spectral density (PSD) for a given time series. Peaks in the PSD correspond to the associated frequencies (or period, which is the inverse of frequency) present within the time series. It is worth noting, however, that a peak at a specific period length does not inherently confirm that the time series is rhythmic, as MESA itself does not provide confidence intervals around the PSD measurement. If autocorrelation analysis does not suggest rhythmicity, then MESA is not necessary.

2.14 DAM locomotor assay

The DAM Locomotor assay was performed as previously described (Driscoll, Hyland and Sitaraman, 2019). Single 2- to 5-day old, entrained flies were anaesthetised and placed into glass tubes (65mm length x 5mm diameter) containing 5% sugar, 1% agar, and 0.07% Tegosept solution. The glass tubes were loaded into DAM2 activity monitors (DAMsystem – TriKinetics Inc, Waltham, MA USA). These monitors were placed within the same room as the TopCount to minimise environmental differences, such as humidity, temperature, and light levels. As with the TopCount assay, flies were subjected to a 12:12 LD cycle at 20˚C and 70% humidity. The locomotor activity of each fly is measured by the number of times the fly interrupts an infrared beam by crossing the midpoint of the tube. This locomotor activity is recorded for each minute of the experiment over a period of 7-10 days. The recorded activity data was trimmed to begin from the first minute after lights on (8:01 am) on the first full day and end at the last minute (8:00 am). Sleep length and architecture were calculated using the Sleep and Circadian Analysis MATLAB Program (SCAMP), whereby periods of inactivity lasting 5 minutes or more are classified as 'sleep'. The data was subsequently visualised and analysed in Python.

2.15 NanoLuc constructs

Since the introduction of NanoLuc (NLuc; (England, Ehlerding and Cai, 2016)), various genetic constructs have been made utilising NLuc. For testing in flies, I focused on five NLuc-based constructs. The first is called Antares, a fusion between NLuc and two orange fluorescent proteins (CyOFP1; (Chu *et al.*, 2016)). The CyOFP1 domains act as acceptors of resonant energy transfer from the blue light emitting NLuc and emit orange/red wavelengths of light. This is beneficial as red-shifted light penetrates tissue more effectively than blue-shifted light (Zhao *et al.*, 2005). The following two are green (GeNL) and red-shifted (GeNL) NLUC constructs that were created via the fusion of NLuc to mNeonGreen (Shaner *et al.*, 2013) and tdTomato (Shaner *et al.*, 2004), respectively (Suzuki *et al.*, 2016). These three constructs function as a regular luciferase and can be used comparably to current FLuc. For example, a GeNL construct with a LexAop promoter upstream could be used with CaLexA.

In addition, I also selected a calcium-sensitive GeNL, named 'GeNLCa' whose NLuc has been split into two sections by the addition of calmodulin and M13 domains (Kaihara, Umezawa and Furukawa, 2008; Suzuki *et al.*, 2016). When calcium is present within the cell, a conformation change occurs within calmodulin-M13, which brings the two halves of NLuc together to reconstitute the functional enzyme. Finally, I selected a calcium-sensitive Antares, named 'CaMBI',

which also utilises the calmodulin-M13 domains (Oh *et al.*, 2019). Instead of a transcriptional reporter of neuronal activity, these are directly sensitive to intracellular calcium levels and will, therefore, require fewer genetic constructs (compared to CaLexA with Luciferase) and theoretically have improved temporal resolution.

To create flies expressing these constructs, I first extracted the raw sequences from the research papers described above and visualised them using SnapGene software (www.snapgene.com). I next codon optimised the sequence for *Drosophila* within the SnapGene software and visualised the plasmid maps that these constructs would be inserted into. I employed VectorBuilder (vectorbuilder.com) first to synthesise the sequences and then to subclone these sequences into a plasmid. The calcium-sensitive NLuc-based reporters were subcloned into the JFRC7-20XUAS-IVS-mCD8::GFP plasmid (Genscript Item ID: 694639-5, www.genscript.com) by using XhoI/Xbal restriction sites. This results in these reporters being controlled by the UAS promoter. The non calcium-sensitive NLuc-based reporters were also subcloned into the JFRC7-20XUAS-IVS-mCD8::GFP plasmid (Genscript Item ID: 694639-5, www.genscript.com) by using XhoI/Xbal restriction sites. Additionally, these three non calcium-sensitive NLuc-based reporters were subcloned into the pJFRC19-13XLexAop2-IVS-myr::GF (Genscript Item ID: U0994BL070-9, www.genscript.com) by using XhoI/Xbal restriction sites. This results in these reporters being controlled by either the UAS promoter or the LexAop promoter. Finally, I ordered the completed plasmids containing the NLuc transgenes to be injected into embryos using the site-specific bacteriophage PhiC31 integrase technique via BestGene Inc (www.thebestgene.com). The NLuc transgenes were integrated into the third chromosome, and the miniwhite marker was used to select successful injection. In short, the white-eyed geneotype (due to a mutated *white* gene, otherwise known as w*) is used for the injection. A fragment of the *white* gene, named *miniwhite* is included in the NLuc transgene injection construct. If the construct is successfully integrated, the resulting flies will have orange/red eyes due to the presence of a function *miniwhite* gene (Silicheva *et al.*, 2010). The resulting flies had a general genotype of w*;;NLucBasedReporter/TM3-Sb[1].

Chapter 3 Characterising the Trumelan Assay

Sleep in *Drosophila* is studied as a correlate of gross locomotion. As an offshoot from circadian research, much of the initial studies into sleep utilised the same *Drosophila* Activity Monitor (DAM) assays which were successful in studying locomotor behaviour as an output of the circadian clock (See Chapter 1.2 & 1.6.2 for more information). These assays function by recording how often a fly crosses the midpoint of a glass tube, and a lack of midpoint crossing is considered a correlate to the fly sleeping. While this assay is cheap and simple to set up and analyse, it has major limitations in spatial, temporal, and informational resolution. Even though these drawbacks can have a significant impact on interpreting results, many laboratories still utilise these assays for studying sleep. In response to the drawbacks of DAM, video tracking assays (See Chapter 1.6.3 for more information) are becoming increasingly popular for studying fly behaviour (Zimmerman *et al.*, 2008; Donelson *et al.*, 2012; Gilestro, 2012; Faville *et al.*, 2015; Garbe *et al.*, 2015; Geissmann *et al.*, 2017). As anticipated, comparing video-tracking to DAM illustrated that DAM overestimates sleep to different extents based on a variety of factors (Zimmerman *et al.*, 2008). One drawback of the current published tracking systems, and a reason for this chapter, is that video-tracking assays record flies from a top-down (or bottom-up) perspective. This limits the ability to measure aspects of position and posture which I am interested in.

In this thesis, I am interested in studying fly behaviour from a side-on perspective to allow for analysis of postural changes, as well as an additional dimension of location (Y-dimension). In this chapter, I aim to first demonstrate a new behavioural tracking assay and compare its behavioural output to the commonly used DAM assay. For this purpose (and the rest of the thesis), I focused on males and females from three wild-type strains. I believe that providing data from both sexes and several wild-type strains is important. Studies often focus on one wild-type strain and one sex, however, there are differences between wild types and sex. For example, the white-eyed mutant fly w^{1118} is a common wild-type strain. While not technically wild-type (as it has a mutated *white* gene), these flies are otherwise wild-type and considered a common strain to use. These are especially useful as a way to mark whether a genetic construct has been successfully inserted into the genome, as genetic constructs are often tagged with a *miniwhite* genetic element (restoring the *white* gene function). Therefore, by utilising a w^{1118} background, flies with red eyes are known to contain the genetic construct of interest. These w^{1118} flies are then often used as a control in subsequent experiments. Research has demonstrated, however, that beyond a lack of eye pigmentation, *white* mutant flies also have climbing deficits, a shortened life span, and a reduction in stress resistance (Ferreiro *et al.*, 2018). Similarly, research on dietary restriction in flies found that wild-type strains have significantly varying lifespans (Grandison *et al.*, 2009). Another study tested three wild-type strains (Oregon-R, Canton-S, and w^{1118}) for their sensitivity

to cisplatin treatment (a cancer treatment which can cause chemotherapy-induced peripheral neuropathy) (Groen *et al.*, 2018). Flies treated with cisplatin have climbing deficits and reduced fertility. Interestingly, Groen *et al*., (2018) found strong differences in climbing ability, survival, and fertility defects across the three wild-type strains. For example, Oregon-R flies typically had the highest survival rates and least fertility defects for most cisplatin concentrations tested. Canton-S and w^{1118} on the other hand had reduced survival and more fertility defects with cisplatin treatment, illustrating that genetic background can have a strong impact on behaviour and physiology.

As with differences between wild types, much research typically focuses on one sex (often males). However, sexual dimorphism is present across a range of *Drosophila* behaviours (Manoli *et al.*, 2013; Asahina, 2018). Sex determination involves the expression of sex-specific splice variants of two transcription factors *fruitless* (*fru*) and *doublesex* (*dsx*) (Rideout *et al.*, 2010). One key area of sexual dimorphism is in reproductive behaviour. Male flies actively engage in courtship behaviour which can be broken down into chasing, tapping her abdomen with his foreleg, courtship song generated from his wing vibration, and licking the female's genitalia (Yamamoto and Koganezawa, 2013). These are male-specific behaviours which require the male variants of FRU and DSX and specific masculinised neural pathways (Yamamoto and Koganezawa, 2013; Asahina, 2018). In contrast, female-specific behaviour involves oviposition (egg release). Aggression is another sexually dimorphic behaviour. Both males and females will fight other individuals of the same sex. Interestingly, how each sex fights is substantially different. For example, males will often use lunging and boxing patterns of fighting, while females will shove and head-butt one another (Vrontou *et al.*, 2006). In addition, a large difference is that males form dominance hierarchies such that a male who wins the first aggressive interaction against another male will continue to win future interactions. In contrast, females do not form such hierarchies and instead will have an even chance (assuming similar fitness) of winning the next aggressive interaction even after losing the initial one. This male-specific process involves the male FRU variant (Vrontou *et al.*, 2006).

Within the context of sleep, sexual dimorphism is also clearly present. A typical wild-type sleep graph consists of two major periods of sleep, with a period during the middle of the day (termed a 'siesta') and a large amount of sleep during most of the night. This siesta period is significantly different between males and females, with males sleeping much more than females (Huber, Hill, *et al.*, 2004; Andretic and Shaw, 2005). Interestingly, virgin females' siesta sleep is similar to males, while mated females have greatly reduced siesta sleep and are instead more active (Isaac *et al.*, 2010). This reduction in siesta sleep was found to occur as a result of the male sex peptide that the female receives during copulation (Isaac *et al.*, 2010). The behavioural switch is thought of as a mechanism to promote egg-laying and feeding/foraging behaviour. Male flies also experience less sleep when housed with females and instead perform more courtship behaviour

(Machado *et al.*, 2017). The choice between courtship and sleep involves a subset of octopaminergic neurons (MS1). When MS1 neurons are activated, male flies will reduce their sleep even when isolated. In contrast, inhibiting MS1 neurons while male flies are in the presence of females results in males sleeping more (reduced inhibition of sleep) and having impaired mating success. While MS1 neurons do not express FRU, MS1 neurons interact with FRU-expressing neuronal circuits (Machado *et al.*, 2017). Finally, the circadian DN1 neurons, which have a role in sleep-wake regulation, are considered sexually dimorphic, in terms of number of neurons (males have more) and differences in daily activity patterns (Hanafusa *et al.*, 2013; Guo *et al.*, 2016).

Here, and in future chapters, my work separates analyses into males and females to allow sex-specific differences to become apparent. In addition, my work separates wild-type strains and then analyses the behavioural changes seen when averaging across all three strains used, to better understand typical wild-type behaviour.

3.1 Concept and design

Here, I am interested in utilising a novel video tracking assay, which records flies from a side-on perspective, to study fly behaviour, positioning, and posture. For this purpose, current and prior members of my laboratory (Dr. James Stewart, Dr. Stanislav Ott, and Prof. Adam Claridge-Chang) designed and created a new video tracking assay called 'Trumelan' Figure 3.1.1A, also see Chapter 2.3). The name 'Trumelan' was based on 'The Truman Show' as the flies are watched while they do their business. In brief, the assay functions by recording individually housed flies and tracking various metrics about the fly, such as their x-position, y-position, and the angle of their body/direction they are facing Figure 3.1.1A-B.

When starting my thesis, the Trumelan assay had been created; however, the outputs from running the assay were in binary files and thus not easily readable. The assay outputs two binary files per fly recorded. The first contains various selected metrics (such as those shown in Figure 3.1.1B) for each time point per fly. The second provides all the possible metrics recorded and image arrays for each frame of recording such that a small image vignette of each fly can be reconstructed for each frame (See the images shown in Figure 3.1.1C as examples of the vignettes).

To begin with, I created Python code to take these binary files and convert the data. I converted this code into functions such that any user of Trumelan can record an experiment, input the binary files into a given function and output readable data in the form of .csv files (readable in

standard programs such as Excel or coding languages). I also created functions to extract the raw image files from the pixel values stored within the binary files. Due to the nature of studying behaviour within a novel assay, there was no pre-made analysis package/software to analyse the behavioural outputs from Trumelan. A significant portion of my studies required first learning how to code (using Python) and then writing code/functions to explore the data generated and to analyse and plot the results of interest.

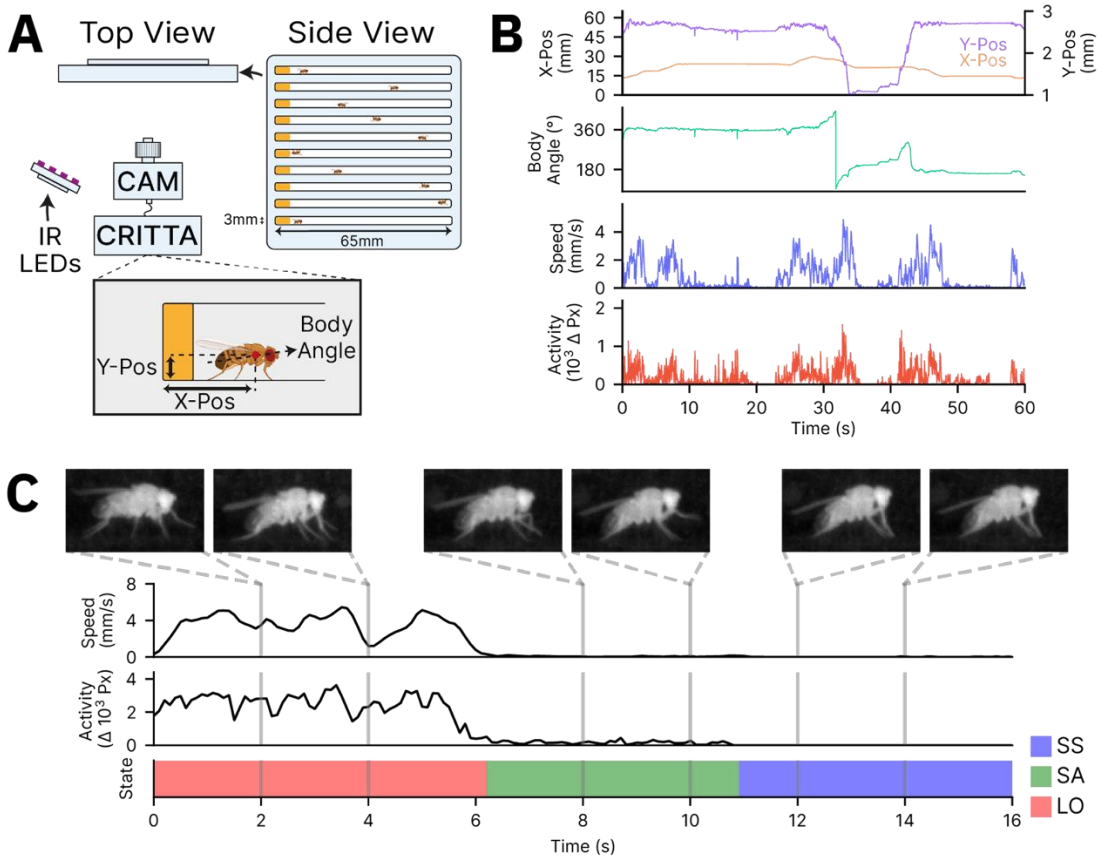

Figure 3.1.1 Trumelan Assay

(A) Schematic for the Trumelan behavioural tracking assay. Flies are individually housed in chambers and viewed from a side by a near-infrared high-quality video camera. **(B)** An example section of recording from one fly illustrates a few of the critical behavioural metrics that video tracking generates. **(C)** An example period of manual annotation where one fly performs all three behaviours.

3.2 Trumelan behavioural classifier

As mentioned, Trumelan records each fly's position, speed, pixel change (per frame), and various other metrics. A video tracking assay typically utilises metrics, such as speed, to classify the behaviour the fly is performing. For example, an assay may record behaviour as locomotor (movement) or rest (non-movement). In this example, a threshold for the distance the fly moved from frame to frame (or speed) may be used to classify a locomotive fly versus a resting fly. For Trumelan, the original designers of the assay decided to split fly behaviour into three primary overarching behaviours (Figure 3.1.1C). These three behavioural states are:

1. Locomotive (LO). The fly moves around the recording chamber in either the x-dimension, y-dimension, or both.
2. Stationary Active (SA). The fly is not moving location but is still performing coordinated limb movements. These can include front or rear leg movements, wing movements, or head/proboscis movements.
3. Stationary Static (SS). The fly is not moving location or performing coordinated limb movements.

The three primary states were considered sufficient at this preliminary stage. To create the behavioural classifier (automatic behaviour detection), I first created an annotated dataset (See Methods: State classification for more information regarding how this was done). I analysed thousands of video frames and manually annotated each for the fly's behaviour. After completing much of the subsequent work at 45 frames per second (fps) recordings, I decided to test a reduced frame rate (10 fps), hoping to improve classification accuracy. I therefore performed a second round of annotation (albeit a smaller sample size) with 10 fps data. The final annotated data (both for 45 and 10 fps) were separated into training, test, and validation subsets.

To begin with, the original designers of Trumelan utilised simple thresholding for classifying behaviour (Figure 3.2.1A). Fly behaviour was first separated into LO or stationary using the speed metric. A speed of 1 mm/sec was the threshold, whereby flies above 1 mm/sec were considered LO. A pixel change (otherwise termed 'activity level') threshold of 10 was used to separate flies into SA versus SS. In essence, this means that from frame to frame, if more than 10 pixels change (and the fly is not locomotive), the fly is considered SA. Otherwise, the fly is considered SS. By testing these thresholds against the annotated dataset, I found that classification accuracy at 45 fps was 81%. This was separated into 80% for LO, 71% for SA, and 93% for SS (Figure 3.2.1B). At 10 fps, the accuracy of classification increased to 87%. This was separated into 76% for LO, 91% for SA, and 96% for SS (Figure 3.2.1C).

I used simple machine learning algorithms to generate behavioural classifier models to improve classification accuracy. For this purpose, I tested five algorithms (Scikit-learn; (Pedregosa *et al.*, 2012)). The first two algorithms were a simple multinomial logistic regression and a decision tree. These are considered transparent methods in that the logic used to classify is openly available and straightforward to understand for the user. For example, a decision tree performs the same way as our initial thresholding task, except the algorithm now uses the training data to decide on the optimum thresholds. These models, however, only generated modest increases from the simple threshold model. Multinomial logistic regression generated overall accuracy scores of 79.2% at 45 fps (Figure 3.2.1D) and 90.2% at 10 fps (Figure 3.2.1I). The decision tree model was slightly better, with overall accuracy scores of 81.6% at 45 fps (Figure 3.2.1E) and 90.7% at 10 fps (Figure 3.2.1J).

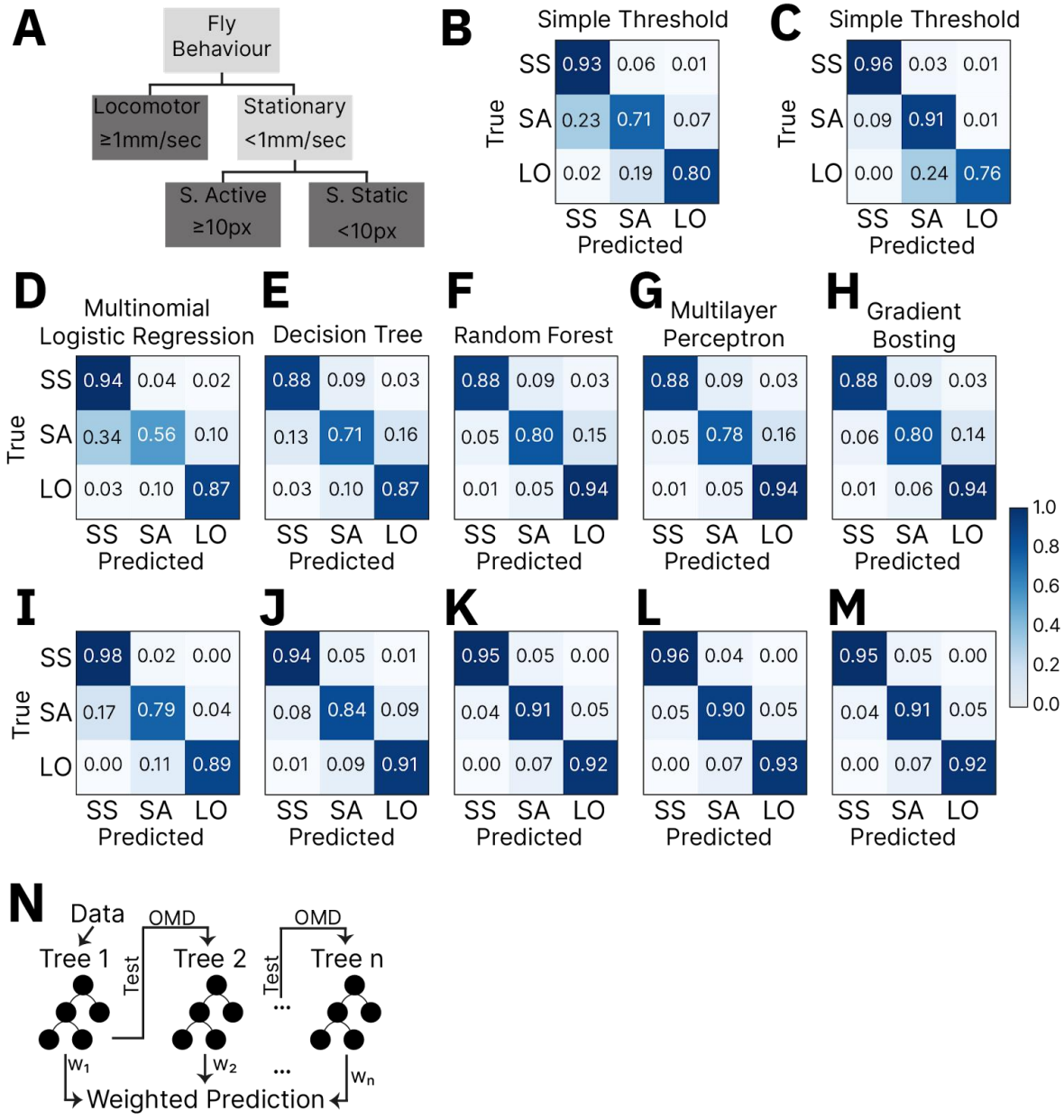

Figure 3.2.1 Creating a behavioural classifier

(A) The initial thresholds used to classify behaviour based on flies' speed and activity level. **(B-C)** The normalised confusion matrices for validating the simple threshold model at 45 fps **(B)** and 10 fps video **(C)**. **(D-H)** Normalised confusion matrices for 45 fps video with **(D)** Multinomial Logistic Regression, **(E)** Decision Tree, **(F)** Random Forest, **(G)** MultiLayer Perceptron, and **(H)** Gradient boosting models. **(I-M)** Same as for (D-H) but for 10 fps video. The predicted labels are labels the model has predicted, while the true labels are the manually annotated labels. **(N)** Illustration of how the gradient boosting model functions. OMD stands for over-weight misclassified data.

Subsequently, I tested less transparent methods (typically called 'black-box methods') and found an increased accuracy with all three. The random forest model generated overall accuracy scores of 87.3% at 45 fps (Figure 3.2.1F) and 93.7% at 10 fps (Figure 3.2.1K). The multilayer perceptron model generated overall accuracy scores of 86.8% at 45 fps (Figure 3.2.1G) and 93.3% at 10 fps (Figure 3.2.1L). Finally, the gradient boosting model generated overall accuracy scores of 87.4% at 45 fps (Figure 3.2.1H) and 93.8% at 10 fps (Figure 3.2.1M). All three black-box models had similar accuracies, so I continued with the gradient-boosting model (Figure 3.2.1N). This model was initially slow to train, but it generated predictions rapidly and performed the best (marginally) in my testing. The gradient-boosting method is an ensemble method whereby the training data is used to train a weak decision tree model. Misclassified cases when compared to the test data are taken and represented with greater weight (over-weight misclassified data, OMD) for training the next weak decision tree model. This process continues for multiple rounds of training and many decision trees are generated. To predict results, each decision tree provides a classification decision alongside a weight associated with each decision tree. The later the decision tree (in the training process), the higher the weight associated with its classification decision. All the classifications and associated weights are combined to create a weighted classification.

3.3 Basic fly behaviour patterns

I next wanted to study fly behaviour within the Trumelan assay. For this purpose, I analysed females and males from three common wild-type fly strains: Berlin-K (BK), Canton-S (CS), and w*. Flies were entrained and subsequently recorded in a 12:12 Light:Dark (LD) cycle where their behaviour was tracked for 26–50 hours (typically 48 h).

I observed a clear 24-hour pattern of activity in male flies, which was crepuscular, with strong locomotor peaks occurring in the lead-up to dawn (ZT0) and dusk (ZT12) (Figure 3.3.1). Conversely, the prevalence of the SS state was consolidated into two peaks, one during the day

(akin to the 'siesta' state as commonly referred to in sleep studies, e.g., (Dubowy and Sehgal, 2017)) and an extended period during the night. As expected, there are troughs of SS at dawn and dusk when LO behaviour is high. Interestingly, the SA state makes up a significant portion of the 24-hour period (Figure 3.3.1). Females also had similar patterns of Trumelan classified behaviour (Figure 3.3.1). Female flies had two major peaks of LO at dawn and dusk and two significant peaks of SS during the siesta and the night. The SA state also makes up a significant portion of the 24-hour period in females.

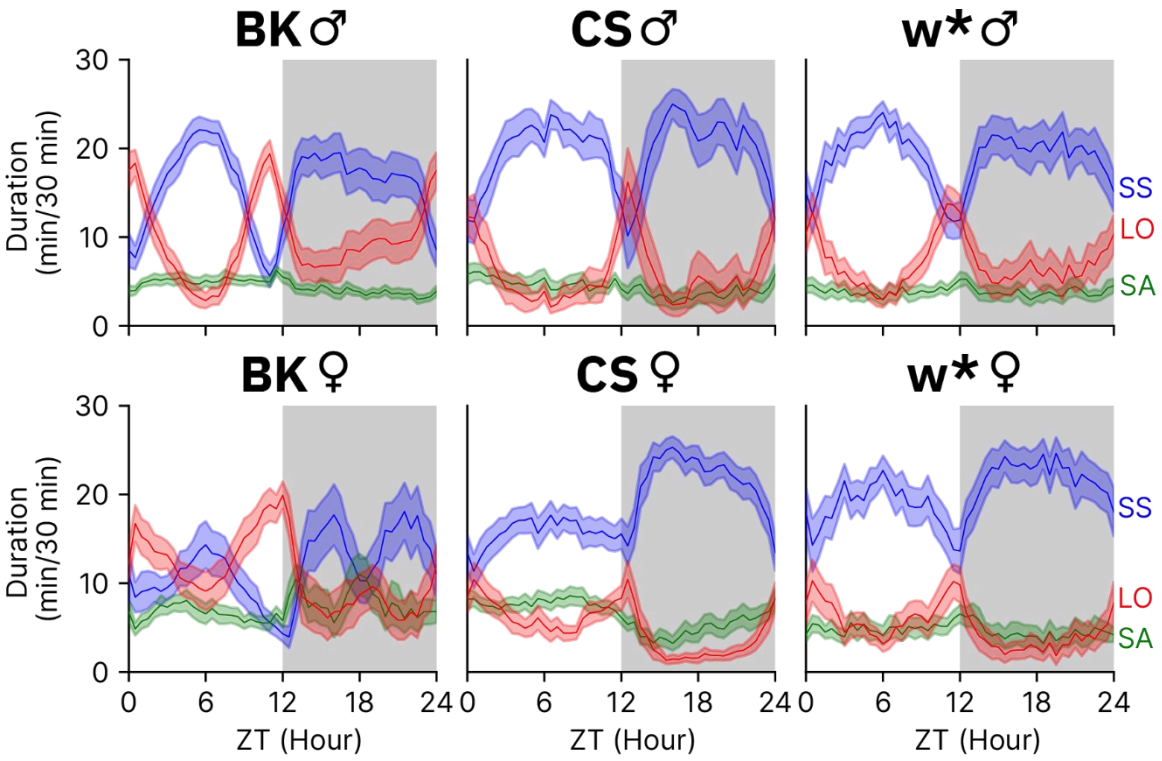

Figure 3.3.1 Trumelan can record typical daily patterns of behaviour in wild-type flies

Time series plots of wild-type males and females in a 12:12 LD cycle for the three overarching states that the Trumelan behavioural classifier records. Raw data is averaged into a 24-hour day with 30-minute bins (ZT: Zeitgeber Time, ZT0 is lights on, ZT12 is lights off). The solid lines indicate the mean of the population, while the shaded area represents the 95% CI around the mean. The sample sizes were 60 for BK males, 30 for BK females, 30 for CS males, 59 for CS females, 49 for w* males, and 38 for w* females.

The time series plots in Figure 3.3.1A-B suggest that the average percentage time spent in LO and SS during a 30-minute interval is inversely correlated. At the same time, SA duration is not particularly correlated with either LO or SS. I calculated the correlation of the average time spent in each behaviour against one another for each 30-minute interval of the averaged fly data. I found that the SS pattern was almost perfectly inversely correlated with LO (R = -0.99 for BK

males, -0.98 for CS males, and -0.99 for w* males; Appendix A Figure 1A). Females also had a highly inversely correlated LO vs. SS (R = -0.93 for BK females, -0.94 for CS females, and -0.98 for w* females; Appendix A Figure 1A). LO and SA, on the other hand, were not strongly correlated, with an R of -0.06 for BK males, -0.37 for BK females, 0.37 for CS males, and 0.62 for CS females, w* males, and w* females (Appendix A Figure 1B). SS and SA were not consistently correlated (Appendix A Figure 1C). In some genotypes, there was very little correlation (R= -0.11 for BK males, -0.01 for BK females). In others, there was an inverse correlation (R= -0.56 for CS males, R= -0.84 for CS females, -0.72 for w* males, and -0.77 for w* females).

Prior research has suggested that changes in the arousal threshold and activity of a fly's brain occur as early as 60 seconds from being inactive (Tainton-Heap *et al.*, 2021). Here, I decided to further separate the SS state into brief SS (SSB) and long SS (SSL), based on a 60-second threshold. SSB and SSL both make up a significant portion of the SS state in males and females (Figure 3.3.2).

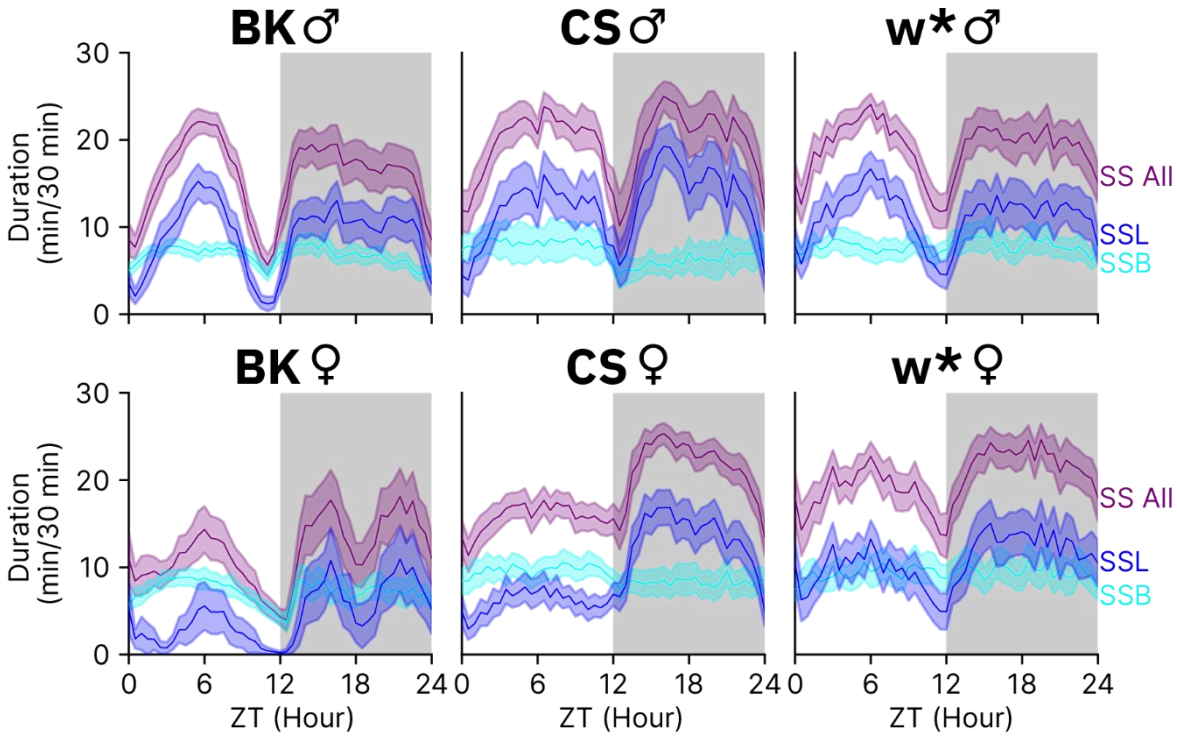

Figure 3.3.2 SS can be separated into short and long rest

Time series plots of wild-type males and females in a 12:12 LD cycle for SS (as in Figure 3.3.1), but also separated into short (SSB) and long rest (SSL). Raw data is averaged into a 24-hour day with 30-minute bins. The solid lines indicate the mean of the population, while the shaded area represents the 95% CI around the mean. The sample sizes were 60 for BK males, 30 for BK females, 30 for CS males, 59 for CS females, 49 for w* males, and 38 for w* females.

As the plots in Figure 3.3.2 suggest, there was a strong positive correlation between the waveform of the averaged SS and SSL binned into 30-minute sections, with an R (Mean±CI) of 0.91±0.01 for BK males, 0.83±0.06 for BK females, 0.87±0.07 for CS males, 0.85±0.05 for CS females, 0.83±0.04 for w* males, and 0.78±0.06 for w* females (Figure 3.3.3A). In comparison, there was no consistent correlation between SS and SSB, with an R (Mean±CI) of 0.27±0.08 for BK males, 0.37±0.15 for BK females, 0.02±0.10 for CS males, -0.02±0.09 for CS females, 0.10±0.10 for w* males, and 0.10±0.12 for w* females (Figure 3.3.3B). Finally, there was a mild negative correlation between SSL and SSB, with an R (Mean±CI) of -0.10±0.08 for BK males, -0.15±0.11 for BK females, -0.38±0.10 for CS males, -0.46±0.07 for CS females, -0.38±0.10 for w* males, and -0.45±0.09 for w* females (Figure 3.3.3C). The data from Figure 3.3.2 and Figure 3.3.3 suggest that the waveform of SS behaviour is mainly a result of SSL, while SSB is present across the whole 24-hour period but without much variation. The distinction of SS into SSB and SSL was kept for subsequent analyses. For this thesis, I use the term 'rest' rather than 'sleep' when discussing SSL. This is due to not having arousal threshold testing data to justify that the Trumelan behaviour adheres to a strict definition of sleep.

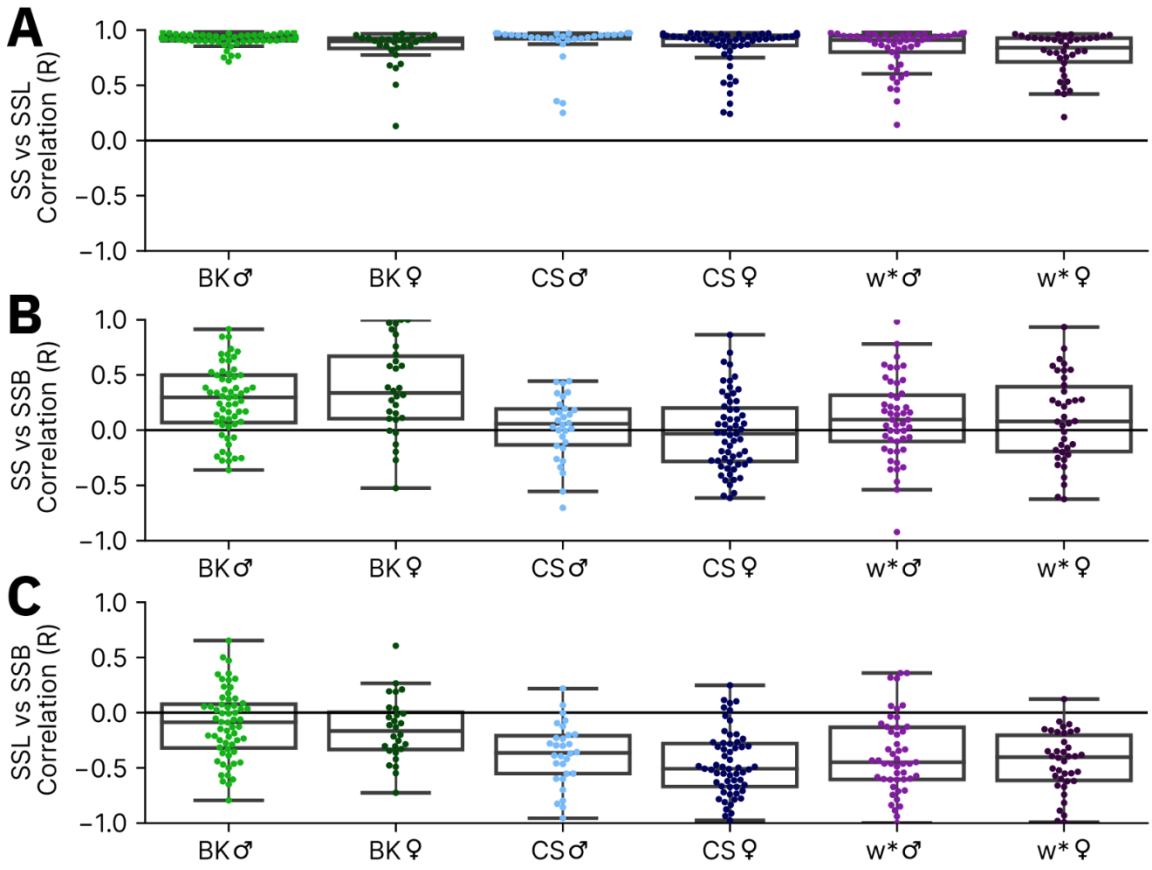

Figure 3.3.3 The correlation between SS states

The correlation between SS and SSL **(A)**, SS and SSB **(B)**, and SSL and SSB **(C)**. Each dot represents one fly's correlation of percentage time spent in a behavioural state against another per 30-

minute bin from raw data averaged over a 24-hour day for individual flies. Box plots are overlaid to represent the spread of the data. The sample sizes for (A-C) were 60 for BK males, 30 (28 for SSL) for BK females, 30 for CS males, 59 for CS females, 49 for w* males, and 38 for w* females. The summary data is shown in Appendix A Table 1.

Another noticeable thing from the plots in Figure 3.3.1A-B was that there were apparent differences between males and females of the same genotype regarding the duration of each behaviour. Here, I analysed each behaviour lasting longer than 1 second (to remove the fragmented bouts). I compared both the duration and architecture of behaviour (number of bouts and average bout duration) between females and males using estimation statistics with the DABEST software package (For more information on this analysis method, see Chapter 2.6).

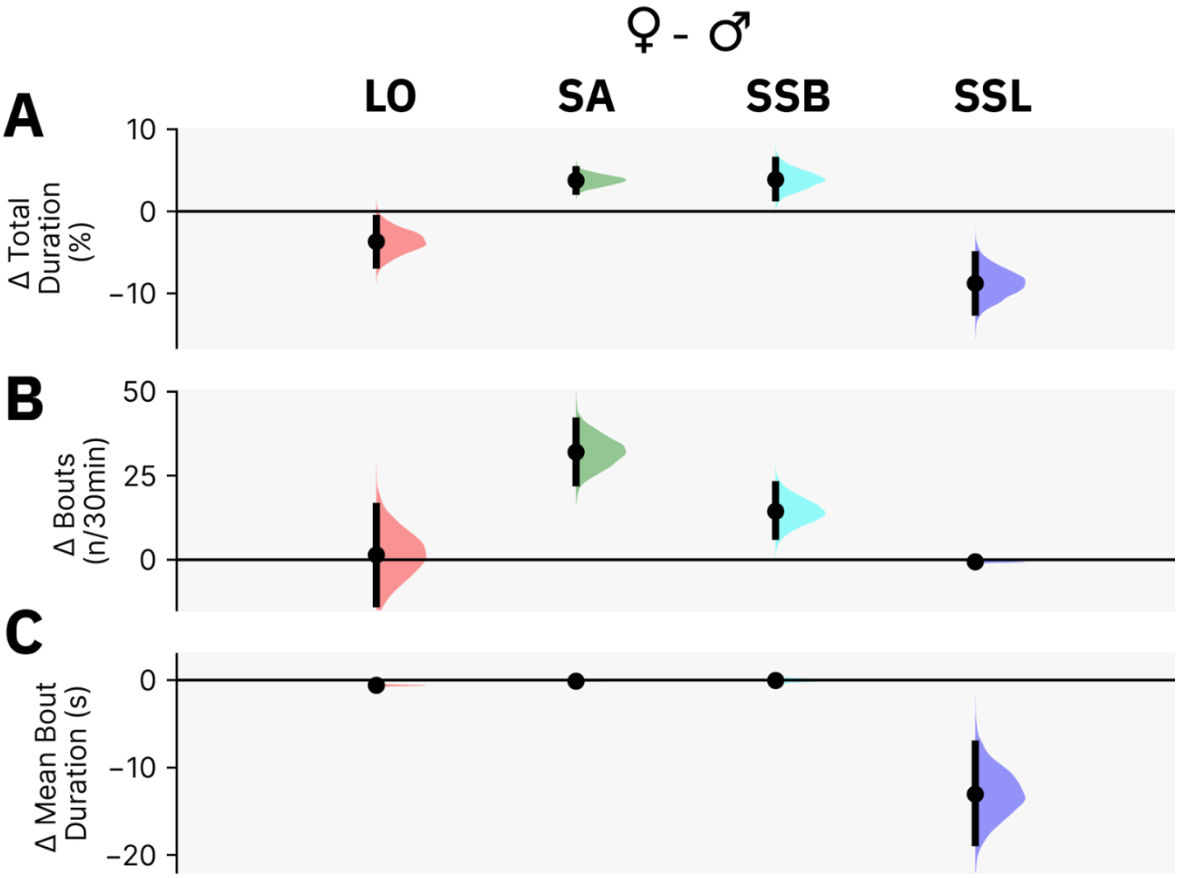

Figure 3.3.4 Changes in behaviour duration and architecture for females vs. males

Forest plots of the weighted deltas for the difference in percentage time **(A)**, number of bouts **(B)**, and mean bout duration **(C)** for each behaviour state. Each curve represents the weighted delta from three DABEST comparisons between females versus males (one for each wild-type genotype; BK, CS, w*). The weighted delta curve represents the weighted mean difference with 95% confidence intervals (CI) around the mean difference generated via bootstrap resampling. The sample sizes for (A-C) were 60 for BK males, 30 for BK females, 30 for CS males, 59 for CS females,

49 for w* males, and 38 for w* females. The expanded raw plots are shown in Appendix A Figure 2-5.

I found that across the whole 24-hour period, there was a minor decrease in the total duration of LO in females compared to males, with a weighted mean difference (Δ %) across all three genotypes of -3.69 [95%CI -6.53, -0.85] (Figure 3.3.4A). By analysing the number of bouts and the average bout duration, I found that the decrease in LO was primarily due to the reduced duration of LO bouts. The weighted mean difference (Δ number of bouts / 30 mins) for the number of bouts was 1.45 [95%CI -13.10, 15.87] (Figure 3.3.4B), while the weighted mean difference (Δ seconds) for the mean bout duration was -0.59 [95%CI -0.73, -0.46] (Figure 3.3.4C). In contrast, females spent more time in the SA state than males, with a weighted mean difference (Δ %) across all three genotypes of 3.76 [95%CI 2.44, 5.06] (Figure 3.3.4A). This increase in SA is due to an increase in bout number rather than duration. The weighted mean difference (Δ number of bouts / 30 mins) for the number of bouts was 31.99 [95%CI 22.85, 41.23] (Figure 3.3.4B), while the weighted mean difference (Δ seconds) for the mean bout duration was -0.12 [95%CI -0.20, -0.04] (Figure 3.3.4C).

SSB was also minorly increased in females, with a weighted mean difference (Δ %) across all three genotypes of 3.87 [95%CI 1.65, 6.21] (Figure 3.3.4A). As with SA, the increase in SSB was due to increased bouts rather than a change in bout duration. The weighted mean difference (Δ number of bouts / 30 mins) for the number of bouts was 14.38 [95%CI 6.98, 22.29] (Figure 3.3.4B), while the weighted mean difference (Δ seconds) for the mean bout duration was -0.04 [95%CI -0.40, 0.32] (Figure 3.3.4C). SSL, on the other hand, was reduced in females, with a weighted mean difference (Δ %) across all three genotypes of -8.77 [95%CI -12.27, -5.28] (Figure 3.3.4A). The reduction in SSL was primarily due to a decrease in bout duration. The weighted mean difference (Δ number of bouts / 30 mins) for the number of bouts was -0.61 [95%CI -0.99, -0.21] (Figure 3.3.4B), while the weighted mean difference (Δ seconds) for the mean bout duration was -13.04 [95%CI -18.57, -7.30] (Figure 3.3.4C).

Alongside the 24-hour waveforms, the plots in Figure 3.3.1 suggest that total durations of Trumelan behaviour may differ between day and night. As before, I subsequently analysed each behaviour lasting longer than 1 second. In male flies, there were no consistent differences in LO between the day and night, with a weighted mean difference (Δ %) across all three genotypes of -0.03 [95%CI -3.34, 3.46] (Figure 3.3.5A). In addition, there was very little change in the bout number and mean bout duration. The weighted mean difference (Δ number of bouts / 30 mins) for the number of bouts was -9.47 [95%CI -24.39, 5.71] (Figure 3.3.5B), while the weighted mean difference (Δ seconds) for the mean bout duration was 0.19 [95%CI 0.05, 0.33] (Figure 3.3.5C).

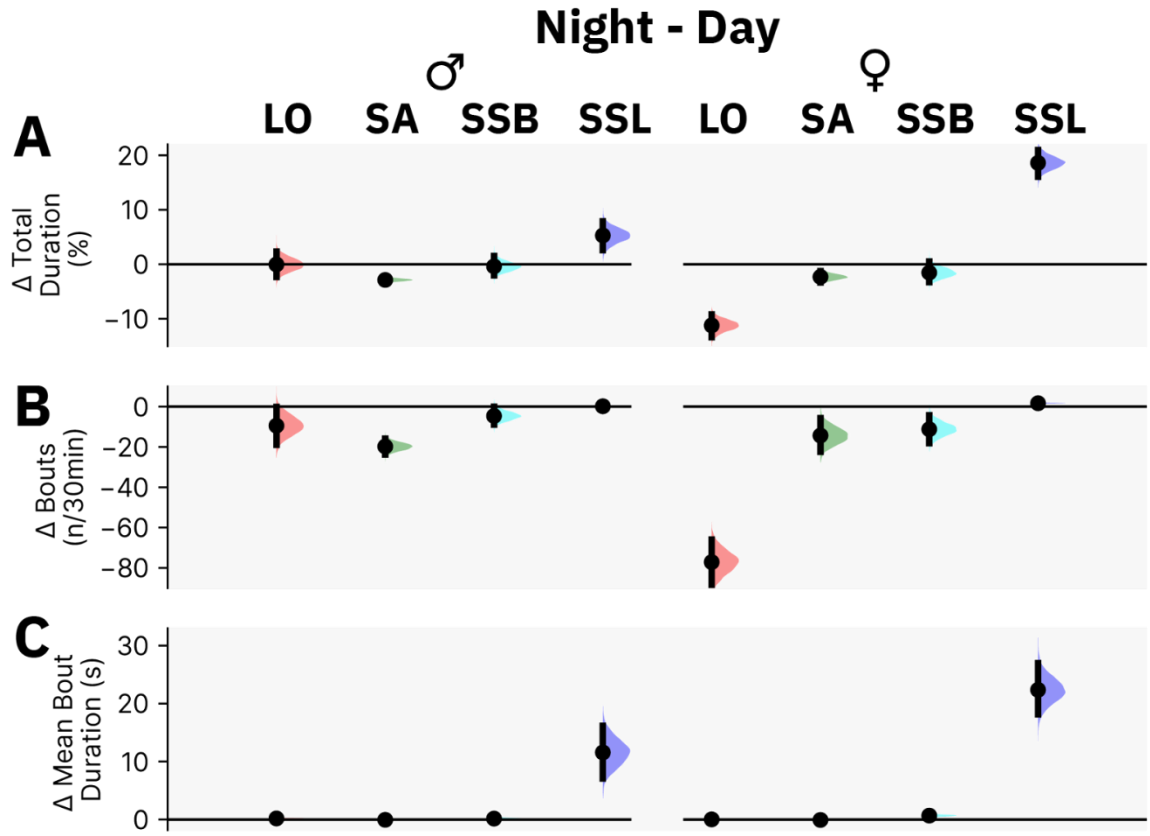

Figure 3.3.5 Behaviour durations and architecture for night vs. day

Forest plots of the weighted deltas for the difference in percentage time **(A)**, number of bouts **(B)**, and mean bout duration **(C)** for each behaviour state for night versus day. Each curve represents the weighted delta from three DABEST comparisons (one for each wild-type genotype; BK, CS, w*). The weighted delta curve represents the weighted mean difference with 95% confidence intervals (CI) around the mean difference generated via bootstrap resampling. The sample sizes for (A-C) were 60 (59 for C) for BK males, 30 (28 for C) for BK females, 30 for CS males, 59 for CS females, 49 (48 for C) for w* males, and 38 for w* females. The expanded raw plots are shown in Appendix A Figure 6-13.

SA behaviour was reduced during the night, with a weighted mean difference (Δ %) across all three genotypes of -2.86 [95%CI -3.81, -1.95] (Figure 3.3.5A). The reduction in SA was due to a reduction in bouts rather than a reduction in bout duration. The weighted mean difference (Δ number of bouts / 30 mins) for the number of bouts was -19.80 [95%CI -27.50, -12.60] (Figure 3.3.5B), while the weighted mean difference (Δ seconds) for the mean bout duration was -0.04 [95%CI -0.11, 0.02] (Figure 3.3.5C). SSB remained unchanged between the day and night, with a weighted mean difference (Δ %) across all three genotypes of -0.38 [95%CI -2.65, 1.93] (Figure 3.3.5A). There was also no significant change in SSB architecture. The weighted mean difference

(Δ number of bouts / 30 mins) for the number of bouts was -4.66 [95%CI -12.03, 2.41] (Figure 3.3.5B), while the weighted mean difference (Δ seconds) for the mean bout duration was 0.15 [95%CI -0.24, 0.52] (Figure 3.3.5C). SSL, on the other hand, increased at night, with a weighted mean difference (Δ %) across all three genotypes of 5.29 [95%CI 1.48, 8.95] (Figure 3.3.5A). The increase in SSL at night was due to increased bout duration rather than the number of bouts. The weighted mean difference (Δ number of bouts / 30 mins) for the number of bouts was 0.16 [95%CI -0.27, 0.59] (Figure 3.3.5B), while the weighted mean difference (Δ seconds) for the mean bout duration was 11.57 [95%CI 5.43, 17.30] (Figure 3.3.5C).

Females, on the other hand, had more extreme differences in behaviour between day and night. LO was reduced during the night, with a weighted mean difference (Δ %) across all three genotypes of -11.21 [95%CI -14.14, -8.32] (Figure 3.3.5A). The reduction in LO at night was due to a reduced number of bouts rather than a change in the average bout duration. The weighted mean difference (Δ number of bouts / 30 mins) for the number of bouts was -77.12 [95%CI -93.95, -59.44] (Figure 3.3.5B), while the weighted mean difference (Δ seconds) for the mean bout duration was 0.03 [95%CI -0.09, 0.16] (Figure 3.3.5C). As with male flies, SA was reduced at night, with a weighted mean difference (Δ %) across all three genotypes of -2.30 [95%CI -4.05, -0.65] (Figure 3.3.5A). The reduction in SA at night was due to a reduced number of bouts rather than a change in the average bout duration. The weighted mean difference (Δ number of bouts / 30 mins) for the number of bouts was -14.34 [95%CI -27.08, -1.93] (Figure 3.3.5B), while the weighted mean difference (Δ seconds) for the mean bout duration was -0.06 [95%CI -0.14, 0.02] (Figure 3.3.5C). SSB remained unchanged in terms of total duration, with a weighted mean difference (Δ %) across all three genotypes of -1.53 [95%CI -4.36, 1.49] (Figure 3.3.5A). However, there were slight changes in the architecture of SSB, with a reduced number of bouts at night but a slightly longer average duration. The weighted mean difference (Δ number of bouts / 30 mins) for the number of bouts was -11.24 [95%CI -21.43, -1.15] (Figure 3.3.5B), while the weighted mean difference (Δ seconds) for the mean bout duration was 0.67 [95%CI 0.27, 1.07] (Figure 3.3.5C). SSL, on the other hand, significantly increased during the night with a weighted mean difference (Δ %) across all three genotypes of 18.61 [95%CI 14.58, 22.36] (Figure 3.3.5A). The increase in SSL at night was due to an increased bout number and average bout duration. The weighted mean difference (Δ number of bouts / 30 mins) for the number of bouts was 1.64 [95%CI 1.22, 2.06] (Figure 3.3.5B), while the weighted mean difference (Δ seconds) for the mean bout duration was 22.37 [95%CI 16.57, 27.91] (Figure 3.3.5C).

3.4 Comparing Trumelan to DAM

Drosophila activity monitors (DAM; TriKinetics) are the most commonly used assay for *Drosophila* sleep and circadian research (Dubowy and Sehgal, 2017; Beckwith and French, 2019). Video tracking assays are widely considered an improvement over DAM by demonstrating that DAM overestimates sleep (For example, (Zimmerman *et al.*, 2008)). Utilising Trumelan, I wanted to study how behavioural tracking compares to a DAM-style analysis. For this purpose, I utilised the recordings of various wild-type flies in Trumelan (From Chapter 3.3). I analysed their behaviour via the Trumelan behavioural classifier and a DAM style analysis (See Chapter 2.7 for more information). In brief, the DAM-style analysis was performed by mimicking a DAM using a simulated vertical beam through the midpoint of the chamber. As with SSL, I use 'rest' rather than 'sleep' when discussing DAM classified 5 minutes or longer of no beam breaks within Trumelan. This is due to not having arousal threshold testing data to justify that the virtual DAM assay adheres to a strict definition of sleep.

To begin with, I found that wild-type flies appeared visually similar to the Trumelan recordings in Chapter 3.3 when analysed with a DAM-style method. There were strong peaks in locomotor activity (as measured via virtual DAM beam breaks) in anticipation of dawn and dusk, as is typical of flies with a functional circadian clock. The number of virtual beam breaks per 30-minute bin nicely tracks the locomotor activity recorded via the Trumelan behavioural classifier (Figure 3.4.1A). There was a strong correlation between the duration of LO and the number of virtual beam breaks in almost all flies tested (Appendix A Figure 14 and Appendix A Table 11). w* males had the strongest average correlation (Pearson's R; Mean±CI) of 0.97±0.01, while w* females had the weakest average correlation of 0.90±0.06. A positive correlation is unsurprising, given that locomotive flies are more likely to cross the midpoint of the chamber. It is, however, a positive sign to see such a high correlation and points to the robustness of DAM for locomotor experiments (such as in circadian studies).

These correlation analyses also address possible concerns that DAM results may not be accurate due to missing short-range locomotor activity movements that do not involve crossing the midpoint of the chamber. Given the high correlation between LO and virtual beam breaks, such concerns appear unfounded. I next separated the data into day and night and analysed the correlation between LO and virtual beam breaks. As the overall correlation data suggested, there was a robust correlation between LO and virtual beam break events for daytime and nighttime behaviour (Appendix A Figure 14 and Appendix A Table 11).

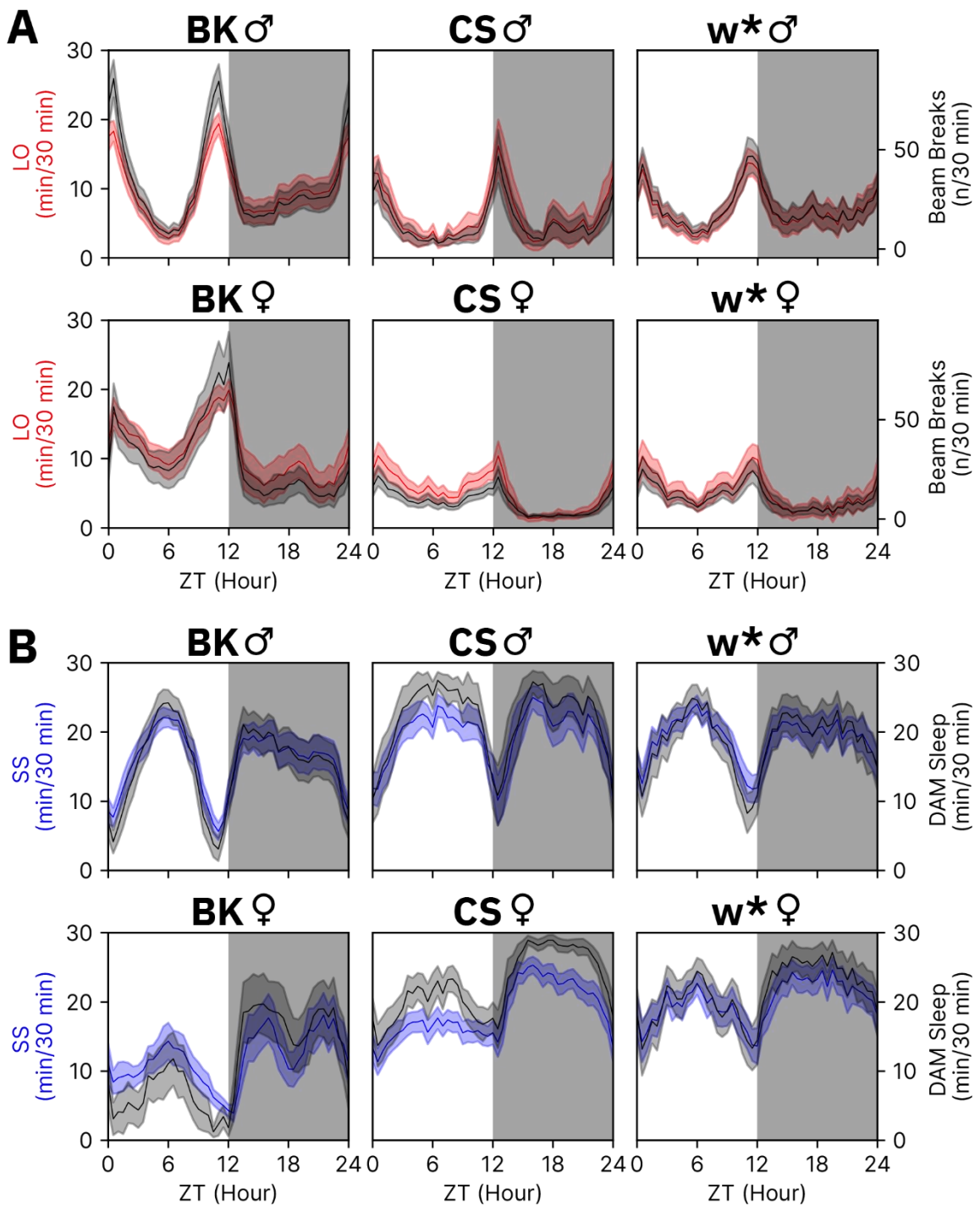

Figure 3.4.1 Simulating DAM in Trumelan

(A) Time series plots of Trumelan classified LO alongside beam break events as measured via a virtual DAM for the same wild-type flies. **(B)** Time series plots of Trumelan classified SS alongside DAM sleep as measured via a virtual DAM for the same wild-type flies. Beam break events, DAM rest, and Trumelan behaviour are averaged into a 24-hour day with 30-minute bins. Beam breaks are recorded as the number of times the fly crosses the midpoint of the chamber. DAM rest is considered present if a fly does not cross the midpoint for at least five minutes. The sample sizes were 60 for BK males, 30 for BK females, 30 for CS males, 59 for CS females, 49 for w* males, and 38 for w* females.

The virtual DAM measured rest also appeared to visually track the SS state well (Figure 3.4.1B). The correlation between all stationary static behaviour versus virtual DAM rest varied between genotypes (Appendix A Figure 15A, Appendix A Table 12). In some genotypes, the correlation (Pearson's R) was strong. For example, BK males had an R (Mean±CI) of 0.93±0.01. On the other hand, other genotypes had weaker correlations between SS and virtual DAM rest. For example, BK females had an R (Mean±CI) of 0.73±0.06. Similarly, varied correlations were seen between SSL and virtual DAM rest (Appendix A Figure 15B, Appendix A Table 12). Using the same examples as above, BK males had an R (Mean±CI) of 0.86±0.02, while BK females had an R (Mean±CI) of 0.67±0.06 (Appendix A Table 12).

Two key things stand out from these correlation plots in Appendix A Figure 15. Firstly, the plots suggest that the virtual DAM rest does not correlate as well in females as in males. To further illustrate this point, I plotted the unpaired comparison between males and females of each genotype and then computed the weighted delta across all three wild-type genotypes. Here, it was evident that virtual DAM rest does not track SS as well as in females, with a weighted delta mean difference (Δ R) of -0.13 [95%CI -0.17, -0.10] (Figure 3.4.2A).

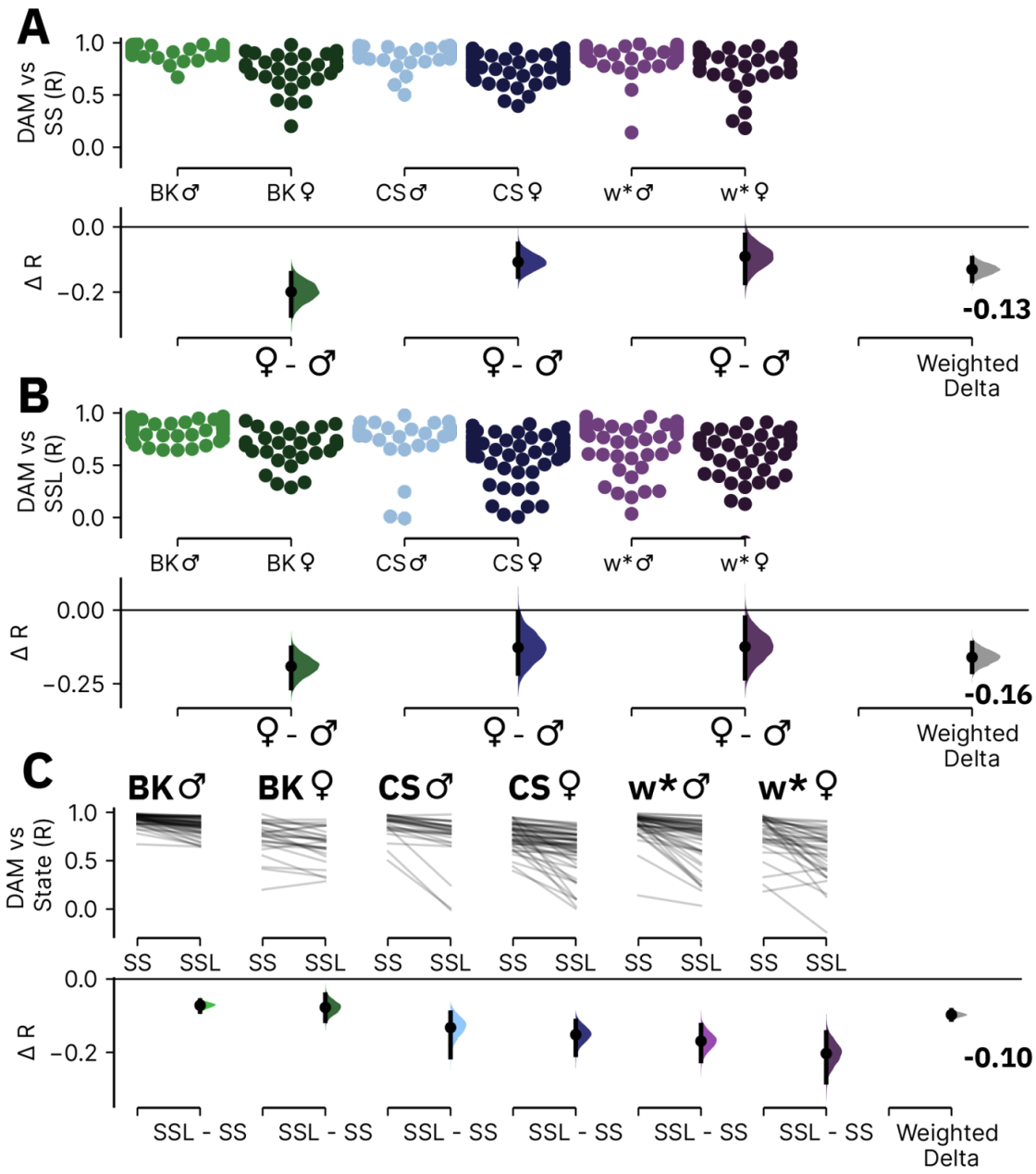

Figure 3.4.2 The correlation of stationary static versus virtual DAM rest in females vs. males

(A-B) The difference in correlation of SS **(A)** or SSL **(B)** versus virtual DAM rest for females versus males of the same genotype. **(C)** DABEST plot of the correlation between SSL and virtual DAM rest versus SS and virtual DAM rest for each genotype. The top section of all the plots shows the raw data, with each dot/line indicating an individual. The bottom section shows the mean difference with 95% confidence intervals (CI) around the mean difference generated via bootstrap resampling. The final DABEST curve represents the weighted delta. The sample sizes in (A-B) were 60 for BK males, 30 (28 in B) for BK females, 30 for CS males, 59 for CS females, 49 for w* males, and 38 for w* females. The sample sizes in (C) were 60 for BK males, 28 for BK females, 30 for CS males, 59 for CS females, 49 for w* males, and 38 for w* females. The tabulated comparisons are shown in for Appendix A Table 13 (A&B) and for Appendix A Table 14 (C).

Virtual DAM rest also does not correlate as well to SSL in females, with a weighted mean difference (Δ R) of -0.16 [95%CI -0.21, -0.11] (Figure 3.4.2B). These results suggest that the virtual DAM assay is less accurate as a correlate of rest in females than in males.

The second thing that stands out from the correlation plots in Appendix A Figure 15 is that virtual DAM rest does not correlate as well to SSL as SS. Paired plots for each genotype further demonstrate this, whereby the correlation (Pearson's R) of SSL versus virtual DAM rest is significantly lower than SS versus virtual DAM rest (Figure 3.4.2C). The weighted mean difference (Δ R) across genotypes was -0.10 [95%CI -0.11, -0.09] (Figure 3.4.2C).

While correlation provides a comparison of waveforms, I was next interested in comparing the duration of rest as described by the virtual DAM assay to the Trumelan behavioural classifier. By overlaying virtual DAM rest with SSL, SSB, and total SS, it was clear that virtual DAM rest tends to overestimate rest (Figure 3.4.3A). The pattern throughout the 24-hour period is similar, as mentioned earlier; however, the overall levels of rest differ. Notably, virtual DAM rest most closely resembled all SS rather than SSL. SSL includes only rest bouts longer than 60 seconds, suggesting that DAM rest overestimates the long rest that it is considered to be a correlate of. A few interesting features become apparent by plotting the difference between SSL or SS versus virtual DAM rest for each 30-minute time point (Figure 3.4.3B). Firstly, virtual DAM rest overestimates long rest across the whole day. Secondly, virtual DAM rest sometimes even overestimates total rest, while at other times, it underestimates total rest.

Thirdly, the amount of difference varies throughout the 24-hour period. On one hand, this makes sense, given that total amounts of rest vary in a circadian manner. Therefore, periods of low amounts of total rest (e.g., around dawn and dusk) will tend to have lower differences between rest. However, this was not always the case, as there are periods when the flies have less rest, yet the difference between virtual DAM and SS/SSL is more significant than periods when the same genotype rests more. For example, in CS females, the overall amount of rest (seen as either SS, SSL, or virtual DAM) is lower during the day than at night, yet the difference between virtual DAM rest and SS or SSL is more significant during the day than at night. To illustrate this, I created a Bland-Altman plot (Altman and Bland, 1983; Bland and Altman, 1986) for comparing virtual DAM rest to SS (Appendix A Figure 16A) or SSL (Appendix A Figure 16B). Some genotypes, such as BK males, have a strong linear relationship between the mean of the two measuring techniques and the difference between virtual DAM and SS or SSL. This represents the case whereby as the amount of rest increases, the difference between measuring techniques increases. In other words, as rest increases, rest overestimation increases. Other genotypes, such as CS females,

clearly do not follow this pattern, demonstrating that DAM can overestimate rest to different degrees at different times of the day.

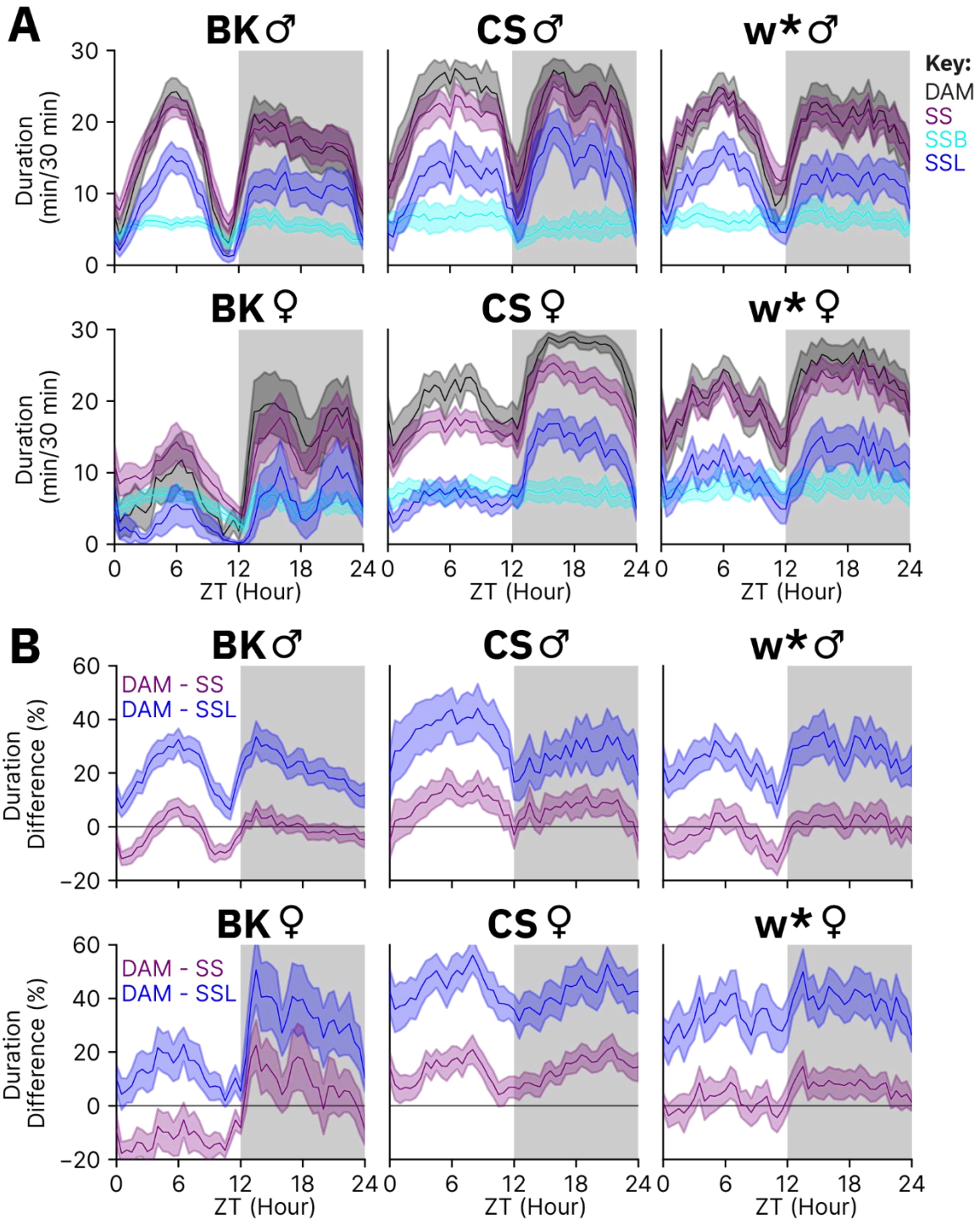

Figure 3.4.3 Comparing durations of DAM rest to Trumelan SS and SSL

(A) Duration of virtual DAM rest versus stationary static behaviours. **(B)** The difference in rest duration when measuring rest via virtual DAM versus all SS or SSL. (A-B) Raw data is averaged into

a 24-hour day with 30-minute bins. The sample sizes were 60 for BK males, 30 for BK females, 30 for CS males, 59 for CS females, 49 for w* males, and 38 for w* females.

Finally, there was significant variation, across genotypes and between individuals, in the difference between virtual DAM rest and SS or SSL. By utilising Bland-Altman plots, it becomes apparent that some genotypes tend to have more significant differences between virtual DAM rest and SS (Appendix A Figure 17A) or between virtual DAM rest and SSL (Appendix A Figure 17B). Compared to SS, however, this is mainly due to differences in the average duration of rest. This was different with the comparison to SSL. For example, w* males and females had similar levels of total rest, but w* females had a much more significant difference between virtual DAM rest and SSL. In addition, there were significant differences across individuals, as seen from the data spread in Appendix A Figure 17. Within each genotype, there was a large spread of average duration of rest across individuals. Interestingly, there was also a large spread in the difference between virtual DAM rest and SS or SSL between individuals of the same genotype with roughly the same average duration of rest. This is clearly seen in each genotype whereby dots that are aligned vertically have the same means (mean of virtual DAM rest and SS or SSL) but with vastly differing differences between the two methods.

To round off my comparison between the virtual DAM assay and Trumelan, I wanted to see what behaviours, as measured by the Trumelan behavioural classifier, typically occur when DAM classifies a period as active or rest. First, I broadly looked at periods of DAM active and DAM rest, quantified the percentage time spent in each Trumelan recorded state for each fly, and then averaged across genotypes. For periods of virtual DAM rest, I found that these were dominated by both SSB and SSL (Figure 3.4.4A). For example, in BK males, 55.60±3.20% (Mean±CI) of virtual DAM rest was comprised of SSL, while 23.93±1.62% was SSB (Appendix A Table 15). While most virtual DAM rest was comprised of Trumelan classified SSB/SSL, a large percentage of virtual DAM rest was filled with SA and, to a lesser extent, LO. For example, the same BK males had 13.71±1.52% of the time spent in SA and 2.85±0.36% in LO (Appendix A Table 15). Comparable patterns were seen across each wild-type genotype tested. CS males spent 57.53±4.83% of the time in SSL, 21.09±4.24% in SSB, 13.39±1.80% in SA, and 4.28±0.62% in LO. Similarly, w* males spent 53.72±4.38% of the time in SSL, 25.88±3.55% in SSB, 12.46±1.95% in SA, and 3.11±0.47% in LO.

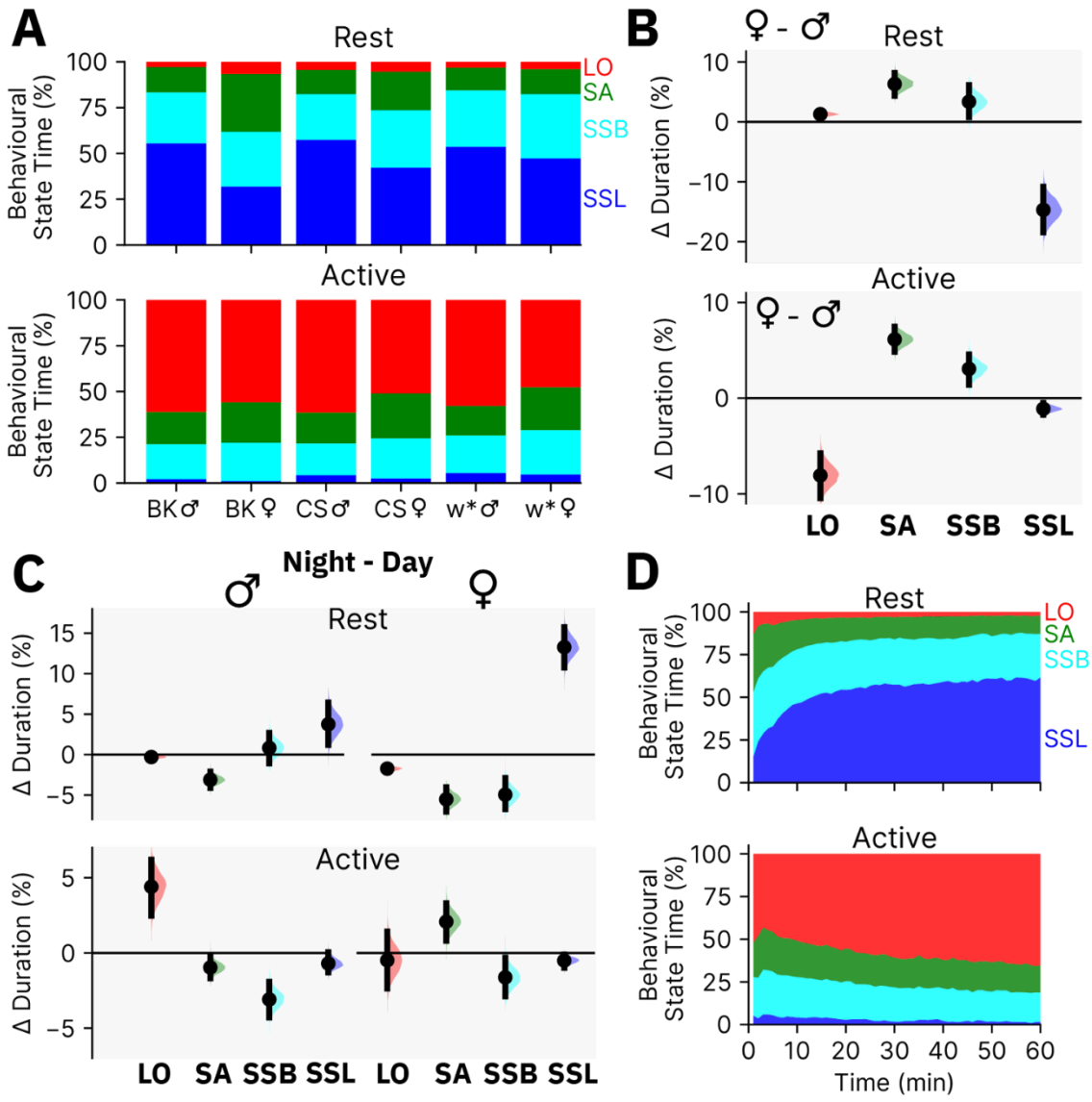

Figure 3.4.4 Composition of behaviour in virtual DAM rest and active periods

(A) The percentage of each Trumelan behaviour that occurs during virtual DAM rest and active periods for each genotype averaged across all bouts. The summary data is shown in Appendix A Table 15. **(B)** Forest plots of the weighted deltas for the difference in the percentage of behavioural stage present during virtual DAM rest or active periods in females vs. male flies. Each genotype is analysed separately, and the weighted difference is calculated across the three wild-type genotypes. The expanded raw plots and summary data is shown in Appendix A Figure 18-19 **(C)** Forest plots of the weighted deltas for the paired difference in percentage of behavioural stage present during virtual DAM rest or active periods during the night vs. day. Each curve represents the weighted delta from three paired comparisons between night and day (one for each wild-type genotype; BK, CS, w*), and the data is split by sex. (B-C) The weighted delta curve represents the weighted mean difference with 95% confidence intervals (CI) around the mean

difference generated via bootstrap resampling. The expanded raw plots and summary data is shown in Appendix A Figure 21-22. **(D)** The percentage of each Trumelan behaviour that occurs during each minute of DAM rest or activity, averaged for all bouts across all genotypes. Zero indicates the start of the DAM rest, or the start of DAM activity after a rest bout. The sample sizes for (A-D) were 60 for BK males, 30 for BK females, 30 for CS males, 59 for CS females, 49 for w* males, and 38 for w* females.

Interestingly, compared to males of the same genotype, female flies appear to have more SA behaviour during virtual DAM rest at the expense of SSL (Figure 3.4.4A). By comparing the differences in sex across all three genotypes, I found that during virtual DAM rest, females have marginally increased LO compared to males, with a weighted difference (Δ %) of 1.29 [95%CI 0.75, 1.86] (Figure 3.4.4B). As the plots in Figure 3.4.4A suggested, SA was significantly increased, with a weighted difference (Δ %) of 6.32 [95%CI 4.34, 8.19] (Figure 3.4.4B). In addition, SSB was mildly increased, with a weighted difference (Δ %) of 3.36 [95%CI 0.79, 6.12] (Figure 3.4.4B). SSL, on the other hand, was heavily reduced in females as compared to males, with a weighted difference (Δ %) of -14.68 [95%CI -18.44, -10.82] (Figure 3.4.4B). The data suggest that virtual DAM rest more accurately tracks long rest (as measured via the Trumelan behavioural classifier) in males than females. This also ties back into the previous data I showed, whereby virtual DAM rest did not correlate as well to SS/SSL in female flies as in males.

In contrast, during DAM active periods, females have reduced LO compared to males, with a weighted difference (Δ %) of -8.07 [95%CI -10.46, -5.76] (Figure 3.4.4B). SA behaviour was more abundant in females during DAM active periods, with a weighted difference (Δ %) of 6.14 [95%CI 4.85, 7.47] (Figure 3.4.4B). Only small differences were seen for SSB and SSL, with weighted differences (Δ %) of 3.06 [95%CI 1.40, 4.56] (Figure 3.4.4B) and -1.11 [95%CI -1.73, -0.51] (Figure 3.4.4B), respectively.

As the composition of virtual DAM rest/active periods could differ based on the time of day, I separated the plot of Figure 3.4.4A into day versus night. Only minor differences were noticeable when comparing the composition of DAM rest between day and night (Appendix A Figure 20, Appendix A Table 15). I next compared the difference between day and night in individual flies and recorded the weighted difference across the three wild-type genotypes tested. To account for differences between males and females, day versus night differences were analysed in each sex separately. In male flies, paired analysis for each fly (night - day) showed that the amount of LO during virtual DAM rest is unchanged, with a weighted difference (Δ %) of -0.30 [95%CI -0.61, 0.05] (Figure 3.4.4C). SA, on the other hand, was reduced at night with a weighted difference (Δ %) of -3.10 [95%CI -4.11,-2.11] (Figure 3.4.4C). SSB also had no change, with a weighted difference

(Δ %) of 0.83 [95%CI -1.08, 2.69] (Figure 3.4.4C). As the plots in Appendix A Figure 20 suggested, SSL is increased during virtual DAM rest at night, with a weighted difference (Δ %) of 3.75 [95%CI 1.20, 6.43] (Figure 3.4.4C).

In female flies, the paired analysis showed that the amount of LO during virtual DAM rest was marginally lower during the night, with a weighted difference (Δ %) of -1.73 [95%CI -2.17, -1.29] (Figure 3.4.4C). SA and SSB were both also reduced at night with weighted differences (Δ %) of -5.51 [95%CI -7.05, -4.03] and -4.94 [95%CI -6.73, -2.88], respectively (Figure 3.4.4C). As with males, SSL was increased during virtual DAM rest at night, with a weighted difference (Δ %) of 13.27 [95%CI 10.76, 15.74] (Figure 3.4.4C). The data suggests that virtual DAM rest more accurately represents rest during the night. This was especially true for female flies, whereby the increase in percentage SSL present during virtual DAM rest was over three times that of males.

During DAM active periods, only minor changes in composition were seen between day and night in males and females (Figure 3.4.4C). The main finding was that in males, LO increased in prevalence during DAM active periods at night, with a weighted difference (Δ %) of 4.40 [95%CI 2.48, 6.19] (Figure 3.4.4C). This increase came at the expense of minor reductions in all three stationary states. Females, on the other hand, had little change in all behavioural states.

DAM measures the number of beam breaks per minute; therefore, virtual DAM rest is recorded per minute (if no beam breaks for at least five minutes). A previous study found that flies become less responsive to a mechanical stimulus during each minute of DAM rest until around five minutes, after which responsiveness plateaus (Huber, Hill, *et al.*, 2004). I, therefore, wanted to see if the composition of virtual DAM rest, measured via the states from the Trumelan behavioural classifier, changes with the duration of the virtual DAM rest bout. To begin with, I grouped all genotypes and plotted the percentage time spent in each Trumelan classified behaviour per minute of virtual DAM rest or active periods (Figure 3.4.4D). In the grouped analysis, the beginning of virtual DAM rest is composed of moderate amounts (Mean±CI) of SSL (15.40±0.61%), a large amount of SSB and SA (37.80±0.56% and 33.95±0.53%, respectively), and a moderate amount of LO (12.85±0.27%) (Figure 3.4.4D, Appendix A Table 20). As anticipated, the structure of virtual DAM rest changes as the duration increases. The percentage of SSL in virtual DAM rest increases over time, while both SA and LO reduce in percentage time (Figure 3.4.4D, Appendix A Table 20). For example, at the five-minute timepoint, SSL increased to 33.01±0.80% while SA and LO reduced to 24.36±0.52% and 7.77±0.25%, respectively. SSB, on the other hand, remained relatively unchanged (34.86±0.62%).

Similarly, at the ten-minute timepoint, SSL increased to 46.51±1.10%, while SA and LO continued to reduce to 17.15±0.62% and 4.70±0.25%, respectively. At the five-minute timepoint, SSB only minorly reduced at ten minutes of virtual DAM rest, with an average percentage of 31.63±0.84%.

These changes during virtual DAM rest were broadly seen in all the wild-type genotypes tested (Appendix A Figure 23A). As was seen in the earlier analysis of females versus males, the graphs in Appendix A Figure 23A illustrate that females have significantly more SA present during virtual DAM rest than males. To account for potential time-of-day differences, I separated virtual DAM rest into day versus night; however, very little difference was seen in the composition of virtual DAM rest (Appendix A Figure 24), suggesting the changes in composition are broadly similar across the 24-hour day.

Alongside quantifying the composition of virtual DAM rest periods, I could also quantify the composition of DAM active periods. After a DAM rest period, the analysis starts at the first DAM active minute. Compared to a DAM rest period, however, active periods showed little change as the duration of activity increased (Figure 3.4.4D, Appendix A Figure 24). Some differences were seen across genotypes (Appendix A Figure 23B). For example, some genotypes, such as BK males and CS males, showed increases in LO as the duration of DAM-classified activity increased at the expense of SSB. Meanwhile, other genotypes, such as BK females, w* males, and w* females, had very little change in the composition of Trumelan classified behaviour as duration of DAM activity increased. As with virtual DAM rest, DAM active periods show very little difference in the composition between day and night (Appendix A Figure 25), suggesting the changes in composition are broadly similar across the 24-hour day.

3.5 Chapter 3 Discussion

Trumelan is a video-tracking assay that can record fly behaviour at high frame rates over multiple days. While Trumelan uses tracking metrics to classify behaviour, a simple classification threshold was initially used and had not been validated. I show that Trumelan can accurately identify three overarching behavioural states in flies using simple machine-learning algorithms. I settled on a gradient-boosting algorithm as it had the highest classification accuracy and was a model that could rapidly predict results.

While the classification accuracy was high, there is potential for improvement. Machine learning models can only be as good as the manually annotated input dataset is. I tried to create an accurately annotated dataset; however, misclassification was possible. Firstly, this can occur as a result of human error. The annotation process is tedious, and it takes a long time to manually click through hundreds of thousands of video images and individually select the behavioural state performed for each one. Therefore, some annotated images may have been misclassified. Secondly, some images were unclear regarding which behaviour the fly was performing. As I

hypothesised, the classifiers were more accurate at 10 fps recording rather than 45 fps. Reduced accuracy with higher fps likely stems from very little time passing between frames, so there are more ambiguous frames where only minor changes have happened. Behavioural states are chosen per frame, so ambiguity is challenging to manage. An improved method could be to utilise a rolling window of frames whereby if a sufficient number of frames of a given state are present within that window, the current frame is assigned that behavioural state. Additional laboratory members should perform manual annotation on the same data to validate the accuracy of classification. A second annotation set would demonstrate the difference in classification between human annotators and provide a more accurate representation of the effectiveness of the behavioural classification. This was, however, not feasible during my studies (primarily due to time constraints and other members being busy with their projects).

I found that Trumelan can record the behaviour of flies over multiple days and produces time series data for each classified behaviour that fits what has been described in the literature regarding wild-type flies. Wild-type flies are crepuscular, exhibiting prominent peaks of activity/locomotion around dawn and dusk. This characteristic was present in the LO behavioural state in all wild-type flies. Wild-type flies are also considered to have two significant periods of sleep, as defined by 5 minutes of not crossing the midpoint of the chamber in a DAM assay. The siesta is a substantial sleep period during the day and is typically more extensive in males. The second significant period of sleep occurs during most of the night. Both these peaks of inactivity were noticeable in the rest state SS.

I defined long rest based on a 60-second threshold due to research from the van Swinderen lab suggesting changes in brain activity associated with sleep can occur from as early as 60 seconds (van Alphen *et al.*, 2013; Tainton-Heap *et al.*, 2021). A perfect threshold likely differs for different genotypes or between individuals within a specific genotype. However, it was clear from utilising a 60-second threshold that short and long rest have distinct properties. Both are highly present; however, long rest correlates much better with total rest than short rest. While long rest follows overall rest with a clear daytime and nighttime peak in behaviour, short rest had a minimal pattern throughout the 24-hour day. The data suggest that short and long rest may represent different states controlled by differing mechanisms.

Interestingly, the time a fly spends in SS and LO states during a given 30-minute bin was almost perfectly inversely correlated. Given that one is locomotion and the other is rest, it is understandable to be inversely correlated. However, when a fly is not LO, it could be in SA or SS. Therefore, such a high correlation between LO and SS was unexpected. SA, on the other hand, was not highly correlated to either LO or SS. The correlation suggests that the majority of the behaviour is taken up by either SS or LO for a given point in time. This results in patterns whereby

LO and SS appear as two sides of the same behaviour, while SA occurs in an unrelated pattern throughout the day. A previous video-tracking study found similar results, whereby another wild-type genotype, *iso31+*, had strongly inversely correlated long rest and locomotion, while grooming did not correlate well with any other behaviour (B. Qiao *et al.*, 2018).

I found that the SA state takes up a significant portion of the 24-hour period. SA was more prevalent in females than males, which could be explained, in part, by the increased feeding need of females (Wong *et al.*, 2009). Given that a recent paper suggested that grooming behaviours take up a significant portion of the day (B. Qiao *et al.*, 2018), it could also be that female flies perform more grooming behaviour than males. For example *iso31+* flies were found to perform grooming behaviours around 6% of the time and feeding (defined by correlation with proximity to the food) 3% of the time (B. Qiao *et al.*, 2018). Unfortunately, Qiao *et al.*, 2018 only used male flies, so a comparison of grooming between males and females was not performed. For my data, the increase in SA in females was due to an increased number of bouts rather than an increase in the average duration. This suggests that females initiate more feeding and/or grooming behaviour than males rather than spending longer per SA event. Improving Trumelan to separate SA into feeding and grooming (or more detailed) would be an achievable future direction to take.

The increased prevalence of SA in females came at the expense of SSL. This follows what can be seen in the time series plots and in the literature whereby the siesta period (of SSL in this case) is reduced compared to males. Unlike SA, the reduced SSL in females resulted from reduced average duration rather than quantity. Given the time series plots and the DABEST comparisons between day and night, much of this difference in SSL resulted from females having reduced average durations of siesta rest. Interestingly, short rest was increased in females compared to males, further demonstrating that short and long rest had characteristic differences.

I next decided to compare Trumelan to DAM style recordings. DAMs are the most commonly used assays for studying sleep and circadian rhythms in flies; however, they lack spatial and temporal resolution. Video tracking assays improve these two factors and provide a more accurate representation of fly behaviour. When demonstrating a new video tracking assay, it is valuable to show how it contrasts with DAM, as DAM is widely considered to overestimate rest (Zimmerman *et al.*, 2008). The virtual DAM assay within Trumelan generated robust patterns in wild-type flies, which appeared visually similar in structure when measured with Trumelan behavioural classification. The duration of LO correlated well with the number of virtual beam breaks, confirming the robustness of beam breaking assays as a correlate for locomotor activity in circadian studies. The data suggest that if a fly is locomotive, it will generally walk the whole length of the chamber rather than remaining in a small region. I only tested a limited set of genotypes, so I cannot exclude the possibility that some genotypes may have altered locomotor

patterns (regarding walking location) without changes to overall locomotion, which a DAM assay would not detect.

I found that the waveform of virtual DAM rest correlated relatively well to SS/SSL behaviour. Interestingly, DAM rest correlates better to SS/SSL in males than females, which suggests that the shape of *Drosophila* rest (waveform) over the 24-hour day is less accurately represented in females when utilising DAM. This could be because females have more significant amounts of SA than males, which a DAM assay would not pick up. As SA appears higher in females and has a different waveform to SS/SSL, it would likely change the waveform of DAM-measured rest compared to SS. More evidence to back up this explanation came when analysing the composition of Trumelan-classified behaviours during DAM-classified rest, whereby females had increased amounts of SA compared to their male counterparts.

The main difference between virtual DAM and Trumelan was the duration of rest. DAM is supposed to correlate with long rest; however, the virtual DAM within my assay severely overestimated rest compared to SSL. Virtual DAM rest most closely resembled total SS. Rest overestimation differed with time-of-day, genotype, and across individuals, even when accounting for the total amount of measured rest. This confirms a prior study which showed variation in overestimation of rest by DAM, whereby they calculate DAM can overestimate rest by between 7-95% depending on time-of-day, age, sex, and genotype (Zimmerman *et al.*, 2008).

By analysing the composition of Trumelan behaviours that occur during DAM classified rest, it became clear that significant amounts of SA, and to a lesser extent LO, are present. Females had more SA behaviour occurring during DAM classified rest than males, providing further evidence that virtual DAM rest is less accurate as a correlate of long rest in females. In addition, SSB dominated the beginning of DAM-classified rest, although SSL significantly increased in percentage as the duration of DAM rest increased. My analysis here could explain why a previous study found that the responsiveness of flies to a mechanical stimulus decreases with the duration of DAM rest (Huber, Hill, *et al.*, 2004). During those first few minutes, many flies are likely in a short rest, SA, or even LO state. Therefore, a mechanical stimulus would be more likely to elicit a response and for the fly to cross the chamber's midpoint. As DAM rest increases, more flies are likely to be long resting, so the percentage of flies that respond to a stimulus decreases. They also found that, even with increasing DAM rest duration, the responsiveness to a stimulus plateau and many flies still respond. My data suggests that this is because, even during extremely long periods of DAM classified rest, a significant percentage of flies are not long resting and instead are short resting or in the SA state.

A future experiment could analyse virtual DAM rest versus Trumelan classified rest for data manually annotated for the actual behaviour of the fly. This would allow a true error rate to be

associated with DAM recording rather than just a comparison to the Trumelan metrics. Given that the accuracy of the Trumelan behavioural classifier was validated, the comparison between virtual DAM rest and the Trumelan metrics is still informative and heavily suggests that DAM overestimates rest.

Chapter 4 Fly Posture and Place Preference

Within the *Drosophila* sleep research field, sleep is defined by gross locomotor inactivity, with five minutes or more of no beam crossings within a DAM assay being associated with a lower arousal threshold in a specific wild-type fly population (Huber, Hill, *et al.*, 2004). In more recent studies, flies inactive for as short as one minute were found to have increased arousal thresholds when tested with higher-resolution video tracking (van Alphen *et al.*, 2013; Tainton-Heap *et al.*, 2021). Beyond gross inactivity, sleep is typically characterised by a set of behavioural features in organisms not amenable to EEG recordings, such as *Drosophila melanogaster*. A species-specific rest posture is considered one such behavioural hallmark of a sleep-like state. As discussed in Chapter 1.7, many organisms across the animal kingdom have been described to have a posture associated with rest, such as cockroaches and bees who lower themselves prone to their resting surface (Kaiser, 1988, 1995; Tobler and Neuner-Jehle, 1992). As with rest posture, a resting place preference can be widely seen across the animal kingdom, from the buffy-headed marmoset and many bird species sleeping in sheltered trees (Ferrari and Ferrari, 1990; Tisdale *et al.*, 2018), to a population of bees resting in an alcove of a cliff (Rau and Rau, 1916; Rau, 1938).

In *Drosophila*, a seminal paper described flies as having a very similar rest posture as in bees, with flies beginning in a supported upright posture and lowering over time until the fly becomes prone to the resting surface (Hendricks *et al.*, 2000). Similarly, flies were described to rest near, but facing away from, the food source when placed in a 65mm glass tube (Hendricks *et al.*, 2000). Subsequent studies provide additional evidence for flies resting near the food source (Zimmerman *et al.*, 2008; Donelson *et al.*, 2012). While rest posture and place preference have been described in *Drosophila*, there is limited (or none in the case of rest posture) quantitative data supporting this description. If a specific sleep posture and place preference are overt and consistent, they could become important features to help laboratories define a sleep state. While Trumelan does not currently have the arousal testing required to justify that specific postures are associated with sleep per se, the first step is to find whether any specific postures can be detectable during long rest periods. In addition, a place preference in terms of whether flies rest on the ground or the ceiling (right-side up, or upside-down) has never been shown. Given that many organisms, such as butterflies, bees, and bats are known to rest upside down, it could be interesting to see if flies have any preference for resting location. So far, I have illustrated a video-tracking assay which can accurately record behaviour from a side-on perspective. This provides the required context for studying both rest posture and place preference quantitatively. As with Chapter 3, I used both males and females from three wild-type strains, as postural and place preference changes may vary with sex or genetic background.

4.1 Flies do not substantially change their posture during prolonged rest

Rest posture in flies is thought to begin in an upright supported position, with flies subsequently lowering during the rest bout such that they end up prone flat on the ground (Hendricks *et al.*, 2000). To analyse starting posture and postural changes during rest, I utilised the side-on tracking nature of Trumelan to measure the y-position (Y-Pos) and normalised body angle (nBA) of individual flies during the SS state (Figure 4.1.1A). Briefly, Y-Pos is measured relative to the ground, and nBA measures the angle of the body perpendicular to the side-on view (sagittal plane), whereby 0° is parallel to the ground (See Chapter 2.8: Rest posture). To test for any potential changes in posture during prolonged rest, I separated SS into brief SS (SSB) and long SS (SSL) based on a 60-second threshold and analysed the starting position of wild-type flies.

As the original description of rest posture was based on prolonged resting flies on the ground, I analysed the starting posture of wild-type flies during SSL. I first extracted images from random SSL bouts from three example BK male flies. Here, at least in these examples, it was clear that flies typically begin in a supported upright position when resting on the ground (Figure 4.1.1B, Appendix B Table 1). These few examples had a Y-Pos (mm) of 1.18 to 1.27 and a nBA (°) of -7.93 to -18.56. Additional starting posture examples during ground-based SSL demonstrate an upright supported posture (Appendix B Figure 1, Appendix B Table 1). Ceiling-based SSL appeared to be a less angled resting position, with flies' bodies more parallel to the resting surface than ground-based rest (Figure 4.1.1B, Appendix B Table 1). These few examples had a Y-Pos (mm) of 2.71 to 2.75 and a nBA (°) of -0.18 to 4.10. nBA is flipped when flies are on the ceiling, so a more positive degree indicates an upright position relative to the ceiling where the head of the fly is further from the ceiling. Further examples also indicate that flies often begin long rest in a less supported position when on the ceiling (Appendix B Figure 2, Appendix B Table 2). However, given that the ceiling resting flies are upside down, a supported position would potentially be more energetically costly as the fly must hold its rear up against gravity.

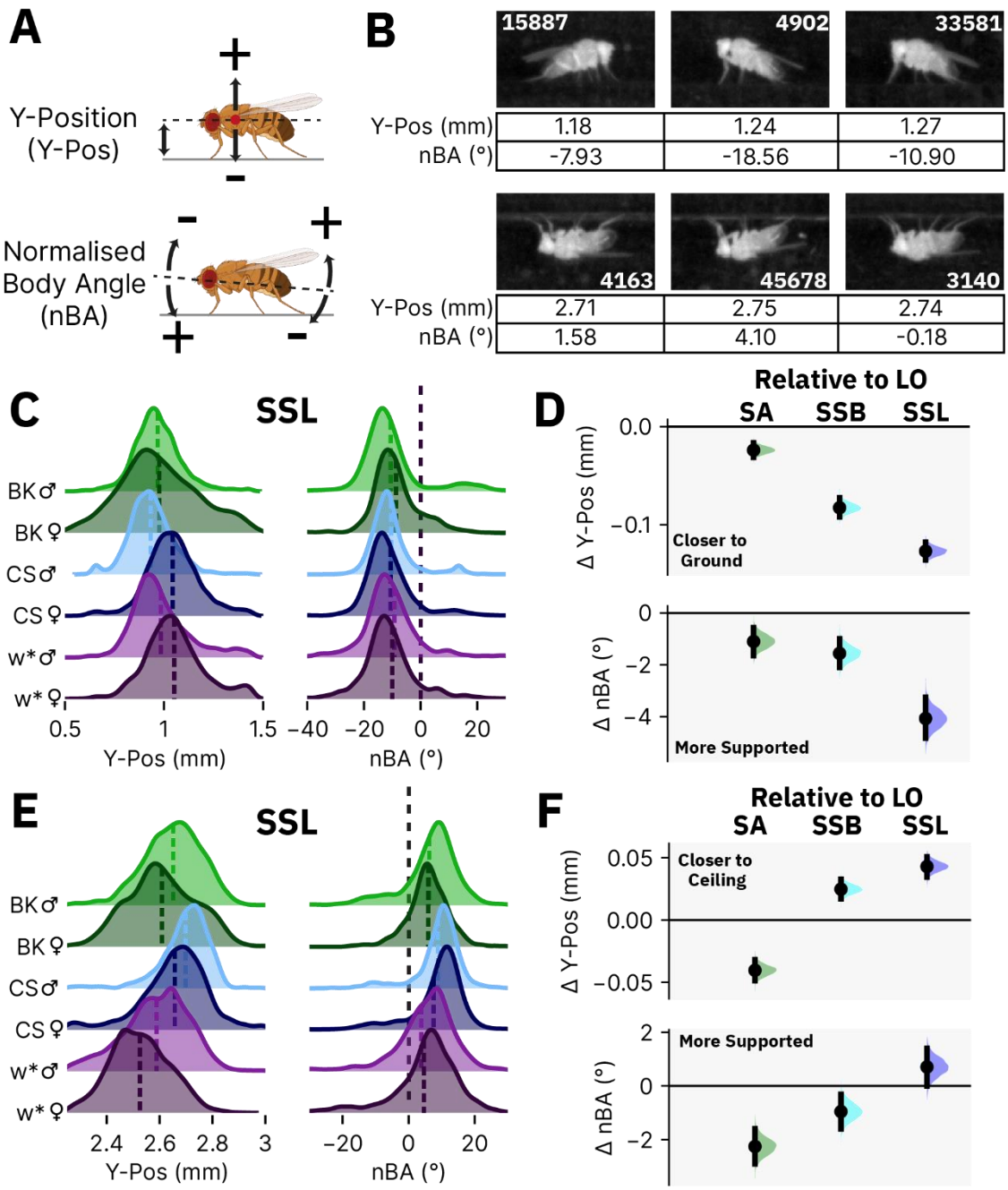

Figure 4.1.1 Starting posture of wild-type flies

(A) Illustration of the Y-Position (Y-Pos) and normalised body angle (nBA) metrics used to analyse fly posture. **(B)** An example image of the starting posture from three different BK male flies beginning SSL on the ground and the ceiling, with their respective raw Y-Pos and nBA values shown below. The white number on the image shows the bout number corresponding to the image, and the raw data can be found within Appendix B Table 1-2. **(C)** Distribution of starting Y-Pos and nBA for ground-based SSL in each genotype. The dotted line within each distribution illustrates the mean, and the dotted black line across the distributions for the nBA plots is the zero line. The sample sizes were 60 for BK males, 30 for BK females, 30 for CS males, 59 for CS females, 49 for w* males, and 38 for w* females. **(D)** Forest plots of the weighted deltas for the

difference in starting posture between each stationary behavioural state versus LO during ground-based behaviour. Each genotype is analysed separately, and the weighted difference is calculated across the three wild-type genotypes. The expanded raw plots and summary data is shown in Appendix B Figure 3-4. The weighted delta curve represents the weighted mean difference with 95% confidence intervals (CI) around the mean difference generated via bootstrap resampling. See Appendix B Table 3-4 for the sample sizes in (D). **(E-F)** Same as (C-D) but for ceiling-based behaviour. The expanded raw plots and summary data for (F) are shown in Appendix B Figure 6-7. See Appendix B Table 5-6 for the sample sizes in (F).

I next plotted the distribution of Y-Pos and nBA for each genotype/sex combination at the start of a long rest on the ground (Figure 4.1.1C). Here, I found significant variation in starting Y-Pos within and across genotypes. In addition, the distribution of nBA of flies on the ground illustrated what was seen in the images, whereby most long rest bouts began with a negative nBA, indicating a more upright supported position (Figure 4.1.1C). On average, flies beginning SSL started at a lower Y-Pos compared to during LO, with a weighted mean difference (Δ mm) across all genotype/sex combinations of -0.13 [95% CI -0.14, -0.12] (Figure 4.1.1D). While the difference between SSL and LO was large, flies beginning SA or SSB also had lower starting Y-Pos compared to LO, with weighted mean differences (Δ mm) of -0.02 [95% CI -0.03, -0.02] and -0.08 [95% CI -0.09, -0.07], respectively. Flies beginning SSL also had a more negative nBA compared to LO (Figure 4.1.1D), with a weighted mean difference (Δ °) of -4.07 [95% CI -4.83, -3.26]. Similarly, flies beginning SA or SSB also had a more negative nBA compared to LO, with weighted mean differences (Δ °) of -1.10 [95% CI -1.64, -0.57] and -1.56 [95% CI -2.10, -0.99], respectively.

The data suggest that ground-based stationary behaviours generally begin in a lower Y-Pos with a more supported upright posture. However, the difference between LO and stationary behaviours was the most extreme in flies about to begin a long rest. Plotting the starting Y-Pos of all four states, nevertheless, demonstrated that there is significant overlap between the distributions of each state, and therefore, a specific starting Y-Pos is likely not indicative of the behaviour the fly is beginning (Appendix B Figure 5). As with the Y-Pos distributions, plotting the distribution of nBA for all states uncovered that a negative nBA is typical across all behaviours (Appendix B Figure 5).

Flies on the ceiling also had variation in the starting Y-Pos of long rest within and between genotypes (Figure 4.1.1E) and significant overlap between behavioural states (Appendix B Figure 5). Flies beginning SSL did, however, have a marginally higher Y-Pos compared to LO, with a weighted mean difference (Δ mm) across all genotype/sex combinations of 0.04 [95% CI 0.03, 0.05] (Figure 4.1.1F). This suggests that flies begin SSL, on average, slightly closer to the ceiling than during LO. In contrast, SA typically began with a minorly lower Y-Pos than LO, with a

weighted mean difference (Δ mm) of -0.04 [95% CI -0.05, -0.03]. SSB followed the same trend as SSL, with a minorly increased Y-Pos compared to LO, with a weighted mean difference (Δ mm) of 0.02 [95% CI 0.02, 0.03].

While on the ceiling, flies also had a supported upright (relative to the ceiling, nBA is inverted) posture (Figure 4.1.1E). However, the distribution of nBA was less extreme for flies on the ceiling than on the ground. For example, the BK males used for comparing SSL to LO on the ground had a nBA (°) of -11.31±1.28 (Appendix B Table 4). In contrast, the BK males used for comparing SSL to LO on the ceiling had a nBA (°) of 6.79±1.40 (nBA is inverted when on the ceiling) (Appendix B Table 6). There was significant overlap in starting nBA between behaviour states (Appendix B Figure 5), and the difference in nBA between flies starting SSL versus LO was marginal, with a weighted mean difference (Δ °) of 0.71 [95% CI -0.01, 1.40] (Figure 4.1.1F).

Beyond the starting posture, a fundamental concept of rest posture is whether changes occur during the rest bout. To study this, I began by visualising the ending posture from the same randomly selected SSL bouts from which I visualised the starting. Surprisingly, the ending postures from these SSL bouts appeared visually identical (or almost identical) to the starting postures for ground (Appendix B Figure 8) and ceiling-based SSL (Appendix B Figure 9). There was no noticeable lowering of the body into a prone position as had been suggested, and instead, flies remained in their starting supported position. These bouts were not of insignificant duration, and thus, it appeared unlikely that the reason for minimal postural changes to have occurred was due to the rest bouts being too short in duration.

To further visualise the change in posture that occurs during SSL, I plotted the distributions of posture change (Δ Y-Pos and Δ nBA) for each genotype during ground-based SSL (Figure 4.1.2A). Here, I found that during ground-based SSL, flies of all genotypes often lowered their Y-Pos. This can be seen from the skewed distribution of ridgeline plots in Figure 4.1.2A. Most bouts centred around zero, indicating very little to no change in posture. Many bouts occurred with a slightly negative change in Y-Pos, while few bouts resulted in a raised Y-Pos. Averaging the start and end postures of each fly per genotype provided further evidence for a minor Y-Pos reduction, whereby the weighted mean difference (end - start posture, Δ µm) in Y-Pos across genotypes was -24.72 [95%CI -26.16, -23.25] (Appendix B Figure 10A).

Y-Pos lowering during ground-based SSL was accompanied by a minor reduction in nBA. The distribution of Δ nBA clearly shows that considerable variation in Δ nBA occurs, with many bouts resulting in a positive Δ nBA (more supported/upright posture) and many with a negative Δ nBA (more parallel to the ground/prone posture) (Figure 4.1.2A). Averaging the start and end postures of each fly per genotype showed that flies do typically have a minor reduction in nBA, whereby

the weighted mean difference (end - start nBA, Δ °) across genotypes was -0.65 [95%CI -0.74, -0.56] (Appendix B Figure 10B).

The data presented in Figure 4.1.2A shows that flies, on average, lower their Y-Pos and have a more negative nBA. I subsequently visualised the changes over time by plotting the average change in posture during the first 60 seconds of ground-based SSL bouts for each genotype. For both Y-Pos and nBA changes, the changes in posture appeared to follow a power-law-like structure, with most of the postural changes occurring at the beginning of the SSL bout. Then, the change in posture reduces rapidly over time (Figure 4.1.2B).

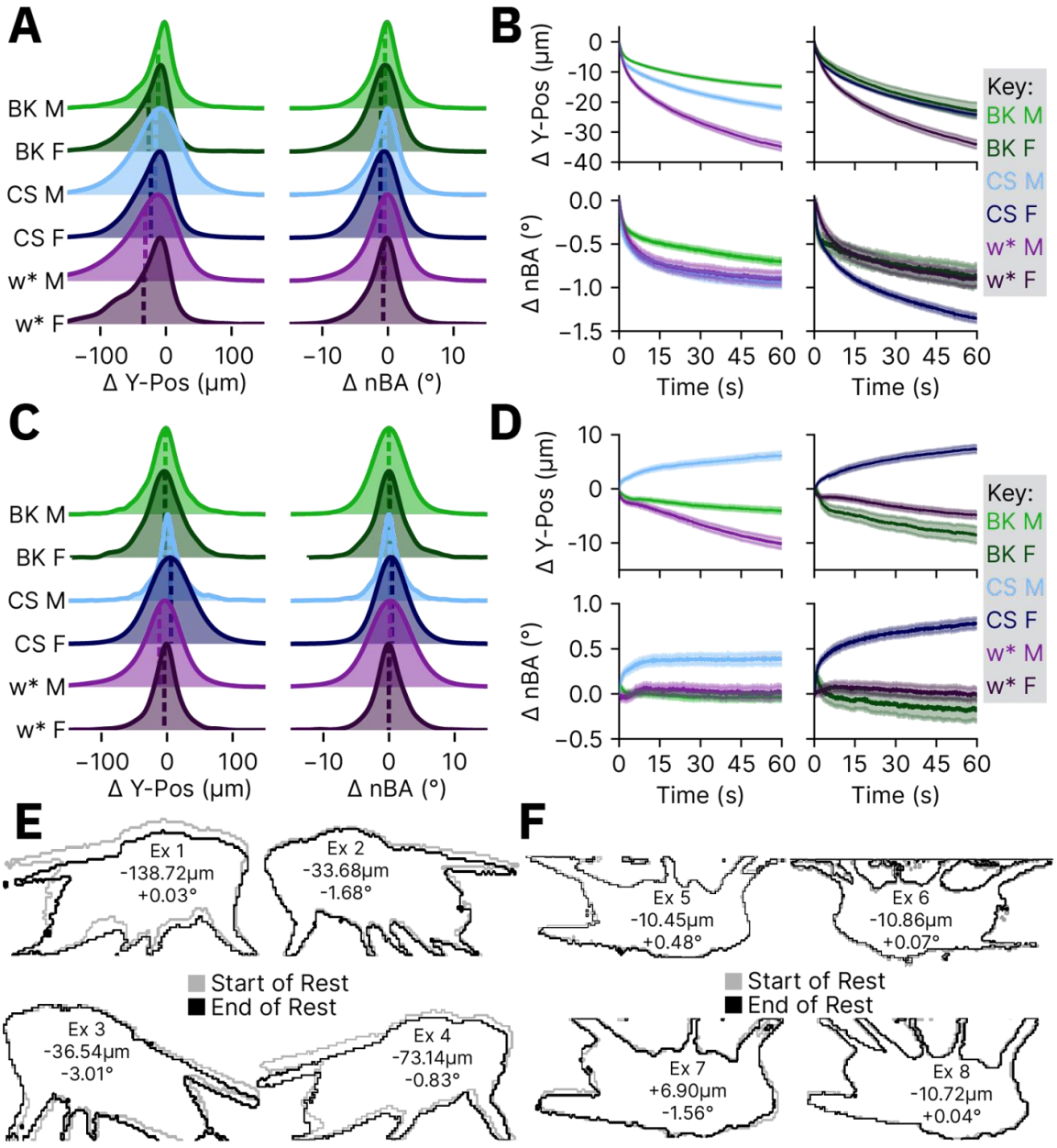

Figure 4.1.2 Minor changes in posture occur during SSL

(A) Distribution of change (end posture - start posture) in Y-Pos and nBA for ground-based SSL. Dotted lines indicate the mean value. **(B)** The change in Y-Pos and nBA during the first 60 seconds

of ground-based SSL (Mean±CI). **(C-D)** The same as for (A-B) but for ceiling-based SSL. **(E-F)** Example outlines from three BK male flies at the start (grey) versus the end (black) of an SSL bout on the ground **(E)** or on the ceiling **(F)**. The values inside each fly indicate the change in Y-Pos (µm) and nBA (°) between the start and end. The sample sizes for (A-D) were 60 for BK males, 30 for BK females, 30 for CS males, 59 for CS females, 49 for w* males, and 38 for w* females.

A question that arises is whether the duration of rest predicts the change in posture. Hendricks and colleagues posit that flies lower over the course of a few minutes (Hendricks *et al.*, 2000), which suggests that the duration of rest could predict changes in posture. For this purpose, I first focused on SSL bouts and found that, while the occasional fly had a strong correlation, most flies had no correlation between their duration of SSL and the change in posture (Appendix B Table 13). This lack of correlation was also evident if accounting for all rest durations (Appendix B Table 14) or just short rest bouts (Appendix B Table 15).

In contrast to ground-based SSL, the distribution of ceiling bouts appears to centre around zero and with minimal skew towards negative or positive Δ Y-Pos and Δ nBA (Figure 4.1.2C). Interestingly, plotting individual flies' average start and end postures for each genotype showed that some genotypes, such as CS males and females, increased Y-Pos during the SSL bout (Appendix B Figure 11A). This is surprising as these flies often become closer to the ceiling during rest. Other genotypes, however, show very little change or become less close to the ceiling during rest bouts. The weighted mean difference (Δ µm) across genotypes was 0.80 [95%CI -0.80, 2.27], suggesting no consistent change in Y-Pos occurs during ceiling-based SSL (Appendix B Figure 11A). Differences between genotypes can be seen when plotting the average change in posture during the first 60 seconds of ceiling-based SSL bouts for each genotype (Figure 4.1.2D). As with ground-based SSL, the ceiling plots also resemble power-law-like curves, demonstrating that most posture change occurs at the beginning of the SSL bout.

Similarly, some genotypes, such as CS females, have a positive change in nBA during ceiling-based SSL (Appendix B Figure 11B). This suggests that these flies have a posture that becomes more angled/less parallel, with their rear raising towards the ceiling. Across all genotypes, however, the weighted mean difference (Δ °) was 0.25 [95%CI 0.15, 0.34], suggesting the body angle change is exceptionally minor. As with Y-Pos, the change in nBA, when averaged across all bouts for each genotype, differs over time, with some having a positive change in nBA and most having very little change occurring (Figure 4.1.2D).

As with ground-based rest, there was no correlation between the duration of an SSL bout and the change in Y-Pos or nBA (Appendix B Table 14). As before, this was also the case when plotted for all rest bouts (Appendix B Table 14) or just for SSB bouts (Appendix B Table 15).

The averaged data suggests that changes in posture, albeit minor, occur during long rest bouts, especially on the ground. This begs the question of whether individual flies have a preferred change in posture that they typically do, but which may differ between individuals. To illustrate that this was not the case, I plotted the change in posture distributions for ten randomly selected individual flies from each genotype. For both ground (Appendix B Figure 12) and ceiling (Appendix B Figure 13) based SSL, the ridgeline plots show considerable variation in postural changes during SSL within individual flies. This suggests that individual flies do not have a consistent postural change.

One final unknown was whether changes in posture during SSL were specific to long rest or also occurred during short rest (SSB). Given that most postural change occurs during the first few seconds, it is unlikely to be long rest specific. Plotting the mean start and end posture for individual flies during ground-based SSB confirmed this, whereby the weighted mean difference (end-start, Δ µm or Δ°) was -14.40µm [95%CI -15.59, -13.33] (Appendix B Figure 14A), and -0.52° [95%CI -0.57, -0.47] (Appendix B Figure 14B). Short resting flies on the ground slightly lower their Y-Pos and become slightly more angled towards a supported upright position with a lowered rear. As with SSL, postural changes during ceiling-based SSB were less extreme than on the ground, with a weighted mean difference (Δ µm or Δ°) of 2.63µm [95%CI 1.88, 3.22] (Appendix B Figure 14C), and 0.26° [95%CI 0.21, 0.31] (Appendix B Figure 14D). This suggests that short resting flies, on average, marginally lower their body towards the ground and marginally raise their rear towards the ceiling/lower their head towards the ground.

In conclusion, changes in posture are minor for both ground and ceiling-resting flies. To illustrate that flies remain upright and changes in posture are marginal, I generated eight examples (four ground and four ceiling) of flies' start and end posture (Figure 4.1.2E-F, Appendix B Table 22). These examples are outlines of a fly whereby the start and end postures are overlaid to allow easy comparison. These hand-picked examples clearly show that postural changes are minor, even in the more extreme examples. For example, the first posture example shown Figure 4.1.2E has a Δ Y-Pos of 138.72µm (which is a much larger change than the averages seen in Appendix B Figure 10A), and yet visually, the change is minor.

4.2 Flies prefer to be stationary near the food port

Rest is associated with a specific place preference. In *Drosophila*, the original findings indicated that flies strongly prefer resting close to but facing away from the food (Hendricks *et al.*, 2000). To provide a quantitative analysis for place preference, I analysed the wild-type data generated in

Chapter 3. The x-position (X-Pos), y-position (Y-Pos), and the body angle (BA) during LO, SA, and SS were analysed. As before, I selected bouts of all behaviours longer than one second, and I separated SS into brief SS (SSB) and long SS (SSL) based on a 60-second threshold.

I found that both male and female wild-type flies have similar distributions of X-Pos (Figure 4.2.1A-F). During LO bouts, flies typically sampled the whole length of the chamber and showed some positional preference for both chamber ends. The small peaks at either end may be partially due to turning behaviour, which could elicit more fragmented locomotion (e.g., multiple short bouts). The small peak at the food port may also be due to flies walking around/on the food during feeding events, which can be seen when viewing fly behaviour. In contrast, the ridgeline plots suggest that flies prefer to stay close to the food port during stationary behaviours (SA, SSB, and SSL) (Figure 4.2.1A-F).

I next looked at the mean position for individual flies in each genotype/sex combination during each stationary state compared to during LO, separating the genotypes by sex. As the ridgeline plots suggest, the average position of the fly during all stationary states (SA, SSB, and SSL) is nearer to the food port than during LO in both males and females (Figure 4.2.1G). Male flies during SA had a weighted delta across the three wild-type genotypes tested (Δ mm) of -6.00 [95%CI -6.82, -5.19]. In addition, the weighted delta (Δ mm) during SSB compared to LO was -6.74 [95%CI -7.49, -5.90]. Finally, flies were also closer to the food port during SSL than LO, with a weighted delta (Δ mm) of -5.42 [95%CI -6.44, -4.38]. Female flies also had stationary behaviour closer to the food port than during LO. SA was closer to the food, with a weighted mean difference (Δ mm) of -11.46 [95%CI -12.27, -10.64]. SSB was also closer to the food port than LO, with a weighted mean difference (Δ mm) of -9.03 [95%CI -9.85, -8.19]. As with male flies, females during SSL were also closer to the food port but less extreme than SA or SSB, with a weighted mean difference (Δ mm) of -6.39 [95%CI -7.69, -5.01].

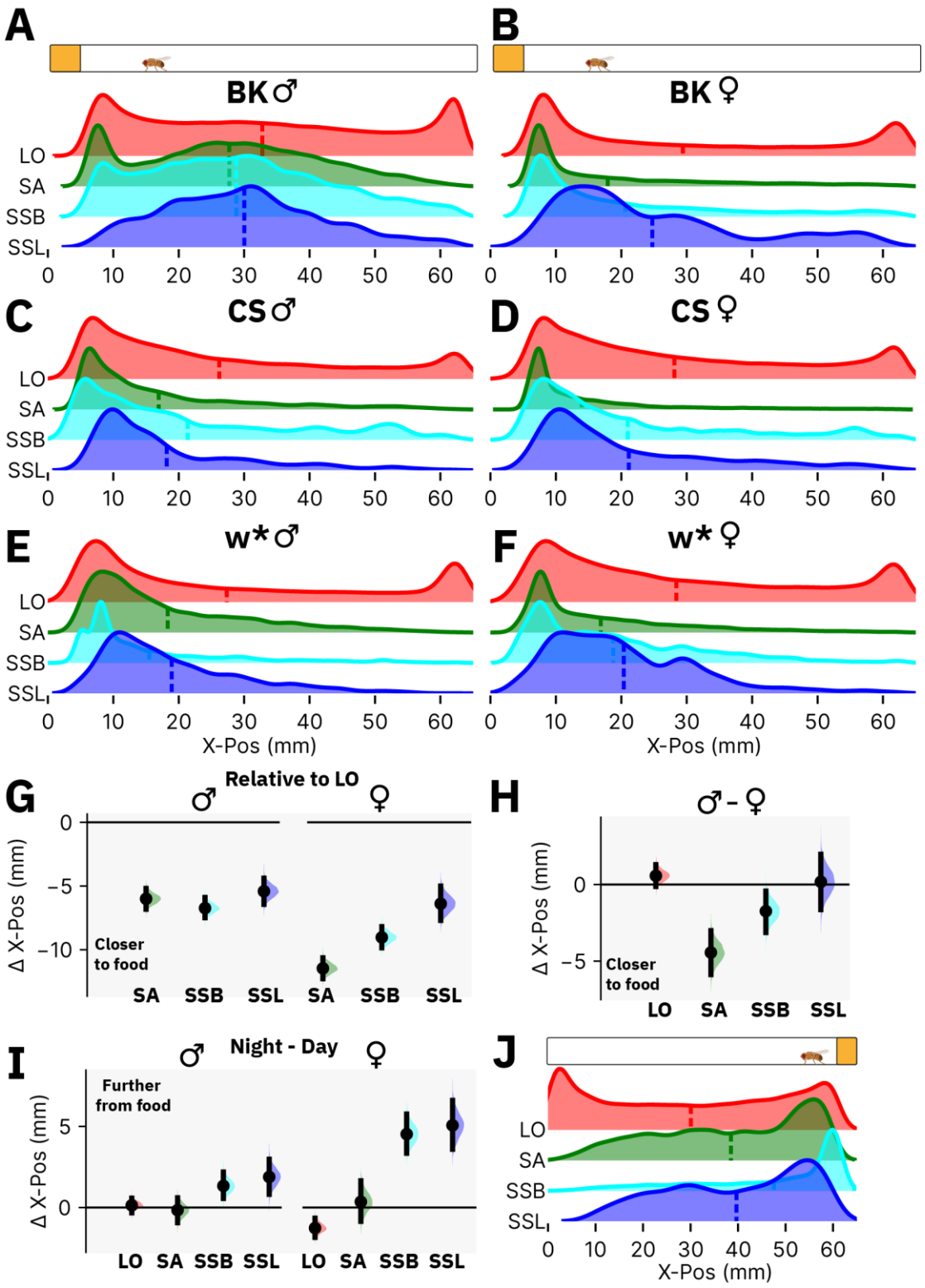

Figure 4.2.1 Flies prefer to be stationary near the food port

(A-F) Ridgeline plots showing the x-position distribution of bouts for each of the four recorded behaviours in BK males (n=60) **(A)**, BK females (n=30) **(B)**, CS males (n=30) **(C)**, CS females (n=59) **(D)**, w* males (n=49) **(E)**, and w* females (n=38) **(F)**. The dotted lines on each ridgeline curve indicates the mean of that distribution. Cartoons above (A-B) illustrate the location relative to the fly chamber. **(G-I)** Forest plots of the weighted deltas for the difference in mean x-position

between each stationary behavioural state vs. LO **(G)**, or for females vs. males for each behaviour state **(H),** or for night vs. day **(I)**. Each genotype is analysed separately, and the weighted difference is calculated across the three wild-type genotypes. The weighted delta curve represents the weighted mean difference with 95% confidence intervals (CI) around the mean difference generated via bootstrap resampling. The expanded raw plots and summary data is shown in Appendix B Figure 15 for (G), Appendix B Figure 16 for (H), and Appendix B Figure 18 for (I). The sample sizes are shown in Appendix B Table 23 for (G), Appendix B Table 24 for (H), and Appendix B Table 25 for (I). **(J)** Ridgeline plots showing the X-Position distribution of bouts for each of the four recorded behaviours in CS males (n=10) when food is placed on the other side of the chamber. Data from (J) was collected by a prior lab member (Dr. James Stewart) but I analysed the data.

Both the distribution of bouts seen in Figure 4.2.1A-F and the weighted comparisons in Figure 4.2.1G suggest that flies are typically closer to the food port during long rest than the average position during LO. However, this is also common across all stationary behaviours. In addition, both SA and SSB were more extreme in their closeness towards the food compared to SSL. Furthermore, flies during SSL exhibited increased variability in their X-Pos, as can be seen in the ridgeline plots (Figure 4.2.1A-F).

While males and females had similar X-Pos distributions, Figure 4.2.1G suggests that closeness to the food port is more extreme in female flies. To test this, I plotted unpaired comparisons between females and males for each genotype and computed the weighted delta for each behaviour state (Figure 4.2.1H). The analysis between females and males demonstrated that females had no change in average X-Pos during both LO and SSL, with weighted mean differences (Δ mm) of 0.57 [95%CI -0.13, 1.30] and 0.18 [95%CI -1.64, 1.97], respectively. In contrast, the mean SA position was much closer to the food port in females, with a weighted mean difference (Δ mm) of -4.44 [95%CI -5.88, -3.01]. SSB was also closer to the food port in females, with a weighted mean difference (Δ mm) of -1.74 [95%CI -3.13, -0.43].

Finally, to test for potential differences between day and night, I separated the analysis into these two categories. The ridgeline plots appear very similar between day and night, suggesting little difference (Appendix B Figure 17). To quantify the differences, I analysed the mean difference (Δ mm) of X-Pos during the night versus the day (Figure 4.2.1I). In males, there was no difference in average position between day and night during LO and SA, with weighted mean differences (Δ mm) of 0.14 [95%CI -0.33, 0.57] and -0.16 [95%CI -0.94, 0.60], respectively. Both SSB and SSL were slightly further away from the food port during the night, with weighted mean differences (Δ mm) of 1.33 [95%CI 0.56, 2.19] and 1.88 [95%CI 0.81,2.98], respectively.

Similar differences were also seen in females (Figure 4.2.1I). LO was slightly closer to the food port at night, with a weighted mean difference (Δ mm) of -1.27 [95%CI -1.84, -0.66]. Conversely, SA was unchanged, with a weighted mean difference (Δ mm) of 0.35 [95%CI -0.86, 1.64]. As with males, but to a more extreme extent, SSB and SSL were further from the food port during the night. The weighted mean differences (Δ mm) for SSB and SSL were 4.52 [95%CI 3.35, 5.76] and 5.07 [95%CI 3.60, 6.61], respectively.

When setting up a Trumelan experiment, fly diet is provided on the left-hand side of the chamber for each experiment. In general, flies prefer to be stationary near the left side of the chamber; however, this does not confirm that it is due to the food location. Although unlikely, given the locomotor data, it could be that the flies generally prefer resting on one side of the chamber. A simple experiment would be to test the place preference of flies when the food location has been switched to the opposite side. One such experiment was performed by a prior lab member (Dr. James Stewart), whereby ten CS males were recorded in Trumelan but with food on the opposite side of the chamber. I analysed the raw data and plotted the ridgeline distributions which clearly demonstrate that the fly position is shifted towards the food port, rather than a specific property of the Trumelan chamber itself (Figure 4.2.1J).

4.3 Flies prefer to face away from the food port during long rest

To investigate whether *Drosophila* faced away from the food during rest, I plotted the body angle (BA) of flies during each behavioural state. A fly with a BA value of ~180° faces towards the food port, and a fly with a BA of ~0°/360° faces away from the food port. By plotting the BA distributions as ridgeline plots, the BA data appeared bimodal in all wild-type flies (with peaks facing towards or away from the food port) (Figure 4.3.1A-F). At a population level, the ridgeline plots suggest that all flies have little preference for facing either direction during LO (red curves in Figure 4.3.1A-F). In contrast, SSL appeared to occur more often facing away from the food (blue curves in Figure 4.3.1A-F). To quantify this, I separated BA preference into facing towards or away from the food port and measured the percentage duration spent by each fly facing the food port during each state. LO flies typically had very little preference for the direction they face, with the average percentage for facing the food port across various genotype/sex combinations ranging from 49.31±0.69% in BK males to 43.16±1.34% in CS males (Appendix B Table 26).

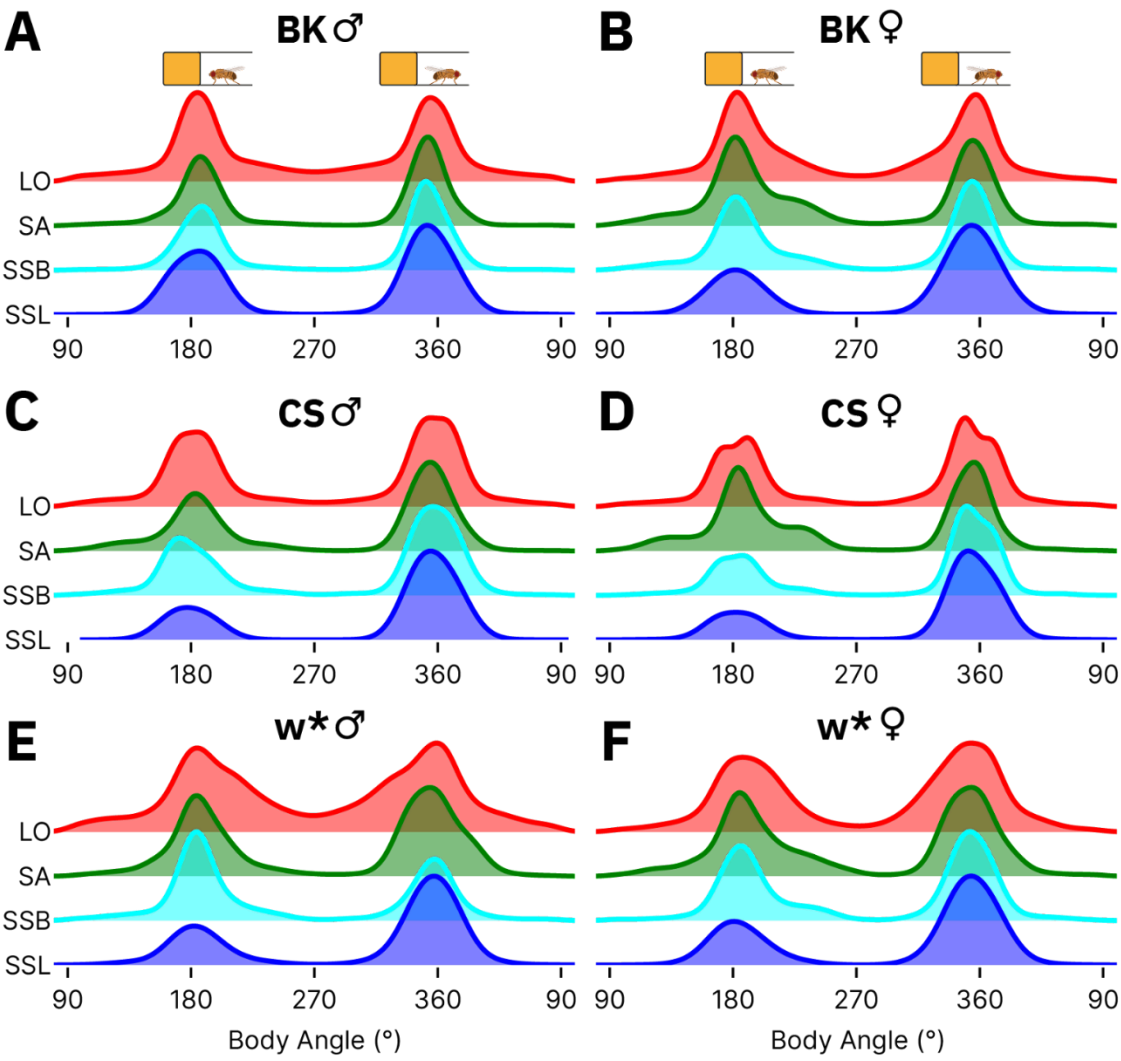

Figure 4.3.1 Long resting flies prefer to face away from the food port

Ridgeline plots of body angle showing the distribution of bouts for each of the four recorded behaviours in BK males (n=60) **(A)**, BK females (n=30) **(B)**, CS males (n=30) **(C)**, CS females (n=59) **(D)**, w* males (n=49) **(E)**, and w* females (n=38) **(F)**. As illustrated above (A-B), a body angle of 180° is facing the food port, while 0/360° is facing away.

As the ridgeline plots suggest, male flies preferred to face away from the food port more during SSL compared to LO, with a weighted mean difference (SSL - LO, Δ %) for facing towards the food port of -10.15 [95%CI -12.77, -7.53] (Figure 4.3.2A). Female flies preferred to face away from the food port compared to LO to an even greater extent, with a weighted mean difference (SSL - LO, Δ %) for facing towards the food port of -15.11 [95%CI -18.25, -11.70].

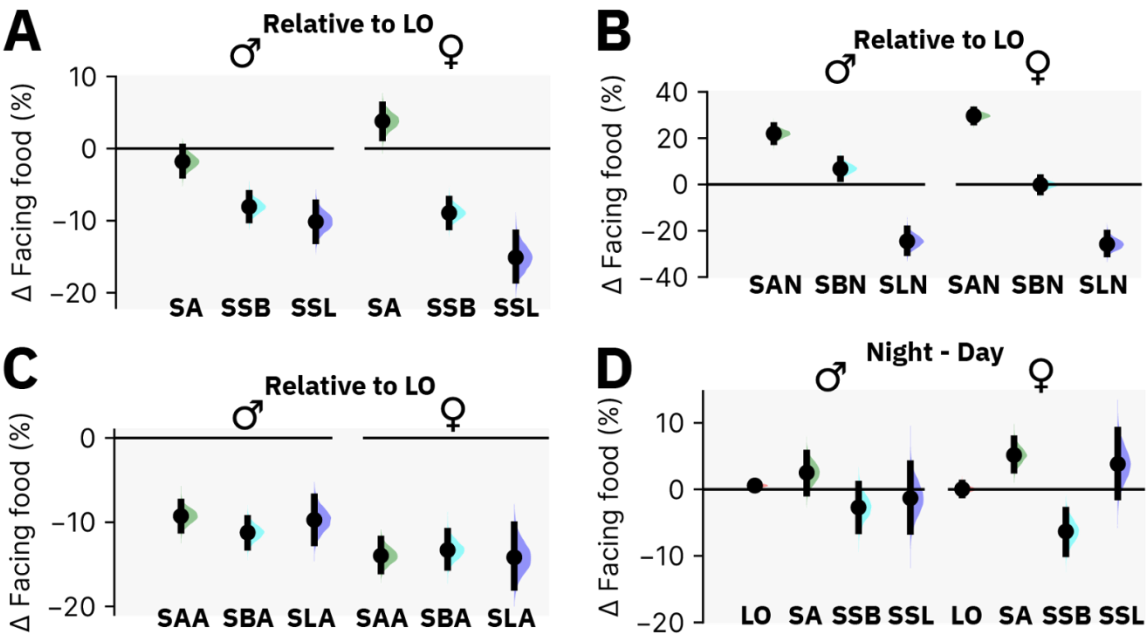

Figure 4.3.2 Long resting flies prefer to face away from the food port, while SA flies switch preference depending on location

(A-C) Forest plots of the weighted deltas for the difference in percentage time spent facing the food port during each stationary behavioural state for all areas of the fly chamber **(A)**, or bouts occurring near the food **(B)**, or bouts occurring away from the food port **(C)**, vs. LO in males and females. **(D)** Forest plot of the weighted deltas for the difference in percentage time spent facing the food port during the night vs. the day for each behavioural state for males and females. (A-D) Each genotype is analysed separately, and the weighted difference is calculated across the three wild-type genotypes. The weighted delta curve represents the weighted mean difference with 95% confidence intervals (CI) around the mean difference generated via bootstrap resampling. The expanded raw plots and summary data are shown in Appendix B Figure 19 for (A), Appendix B Figure 20-22 for (B-C), and Appendix B Figure 24 for (D). The sample sizes are shown in Appendix B Table 26 for (A), Appendix B Table 27-29 for (B-C), and Appendix B Table 30 for (D).

The preference for facing away from the food port was not specific to long rest as both male and female flies also preferred to face away from the food during short rest relative to LO (Figure 4.3.2A), with weighted mean differences (Δ %) of -8.07 [95%CI -9.91, -6.21] and -8.93 [95%CI -10.85, -7.03], respectively, for facing towards the food.

In contrast, male flies appeared to have no significant preference for direction facing during SA, with a weighted mean difference (Δ %) of -1.80 [95%CI -3.71, 0.20] for facing towards the food compared to during LO (Figure 4.3.2A). Similarly, female flies only had a minor increase in

percentage time facing towards the food relative to LO, with a weighted mean difference (Δ %) of 3.80 [95%CI 1.47, 6.05].

I hypothesised that SA facing direction could be affected by a difference in feeding versus grooming events that may have an opposing effect on direction preference. As previously mentioned, SA events are expected to encapsulate feeding and grooming events and any other stationary active behaviour. To test for this, I separated the analysis into when the fly is near the food port (<10 mm from the end of the chamber, roughly <5 mm from the food) and when the fly is away from the food port (≥ 10 mm from the end of the chamber).

By separating the SA bouts to account for location, I found that flies had a substantial preference for facing towards the food when near the food port. Both males and females had weighted mean differences for percentage time facing towards the food port (Δ %) compared to during LO of 21.97 [95%CI 18.47, 25.43] and 29.65 [95%CI 26.96, 32.27], respectively (Figure 4.3.2B). This difference is significantly more substantial in females, which further justifies the claim that the feeding events drive this preference. On the other hand, short rest near the food had only minor preference in males and no preference in females. For males, the weighted mean difference (Δ %) for the percentage facing time facing the food compared to LO was 6.77 [95%CI 2.48, 10.92], while in females it was -0.17 [95%CI -3.26, 2.91] (Figure 4.3.2B). The minor or lack of facing the food during short rest was surprising as the X-Pos data suggested flies spend a lot of their short rests near the food, and I had hypothesised that these could be partially due to breaks during feeding and grooming events. While short rests in this manner are likely present, the data here suggest that the majority are not breaks in between feeding events. Unlike SA and SSB, both male and female long resting flies maintain a preference for facing away from the food port even when nearby, with weighted mean differences (Δ %) for percentage facing time facing the food compared to LO of -24.54 [95%CI -29.56, -19.17] and -25.81 [95%CI -30.03, -20.99], respectively (Figure 4.3.2B).

In stark contrast, all behaviours occurred preferentially facing away from the food port relative to LO when flies were not near the food. In both males and females, SA bouts away from the food port had weighted mean differences of (Δ %) -9.27 [95%CI -10.95, -7.61] and -13.98 [95%CI -15.79, -12.00], respectively, compared to during LO (Figure 4.3.2C). Similarly, males and females preferred to face away from the food port during SSB when not near the food port, with weighted mean differences of (Δ %) -11.23 [95%CI -12.96, -9.54] and -13.31 [95%CI -15.37, -11.07], respectively, compared to during LO (Figure 4.3.2C). Finally, males and females maintained preference in SSL for facing away from the food port when not near the food port, with weighted mean differences of (Δ %) -9.73 [95%CI -12.46, -6.99] and -14.17 [95%CI -17.74, -10.29], respectively, compared to during LO (Figure 4.3.2C).

As with X-Pos preference, I analysed the body angle data between day and night. The general ridgeline plots suggested no significant changes between day and night (Appendix B Figure 23). Both male and female flies had minor/no preference difference between day and night, with weighted mean differences (Δ %) for facing the food port during night vs. day of 0.56 [95CI% 0.04, 1.08] and 0.03 [95CI% -0.85, 0.93], respectively (Figure 4.3.2D). Male flies had unchanged preference during SA between day and night, while females had a slight preference shift towards facing the food slightly more at night, with weighted differences of 2.50 [95CI% -0.55, 5.47] and 5.15 [95CI% 2.88, 7.60], respectively (Figure 4.3.2D). In contrast, both male and female flies during SSB slightly decreased their time spent facing the food port during the night, with weighted mean differences (Δ %) of -2.71 [95%CI -6.26, 0.78] and -6.33 [95%CI -9.70, -3.15], respectively, compared to during the day (Figure 4.3.2D). As with LO, both male and female flies during SSL had no shift in time spent facing the food port during the night, with weighted mean differences (Δ %) of -1.32 [95%CI -6.32, 3.86] and 3.80 [95%CI -1.14, 8.91], respectively, compared to during the day (Figure 4.3.2D).

One question that arose was whether the facing direction preference seen was specific to the food location or an inherent feature of the experiment chamber or incubator. As the food media had always been placed on the left-hand side of the fly chamber, this question had yet to be answered. To clarify this, I tested w* male flies utilising half-length chambers (32mm length), whereby half had food on the left-hand side of each chamber (same as the original experiments), and the other half had food on the right-hand side of the chamber. The ridgeline distribution of bouts for each state suggested that the facing direction preference is specific to the food location rather than the chamber itself (Figure 4.3.3A-B). Flies in the left and right-side food conditions had a minor preference for facing away from the food, with a percentage time facing food during LO of 45.13±2.77 and 43.17±2.18, respectively (Figure 4.3.3C). There was no significant difference between the two conditions, with a mean difference (Δ Facing food % Right - Left) of -1.96 [95%CI -5.11, 1.64] (Figure 4.3.3C). During SA, flies with food on the left and right food had a facing food percentage time of 44.50±4.22 and 50.68±4.45, respectively (Figure 4.3.3C). There was only a minor difference between the two conditions, with a mean difference (Δ Facing food % Right - Left) of 6.18 [95%CI 0.27, 11.87] (Figure 4.3.3C). For both SSB and SSL, flies preferred facing away from the food regardless of food location. During SSB, flies had a percentage time facing food for left and right-sided food of 29.96±4.73 and 35.97±4.35, respectively (Figure 4.3.3C). Similarly, during SSL, flies had a percentage time facing food for left and right-sided food of 37.80±8.99 and 35.59±6.04, respectively (Figure 4.3.3C). In both SSB and SSL, there was no significant difference between the two conditions, with a mean difference (Δ Facing food % Right - Left) of 6.01 [95%CI -1.00, 11.29] and -2.21 [95%CI -13.12, 7.76], respectively (Figure 4.3.3C).

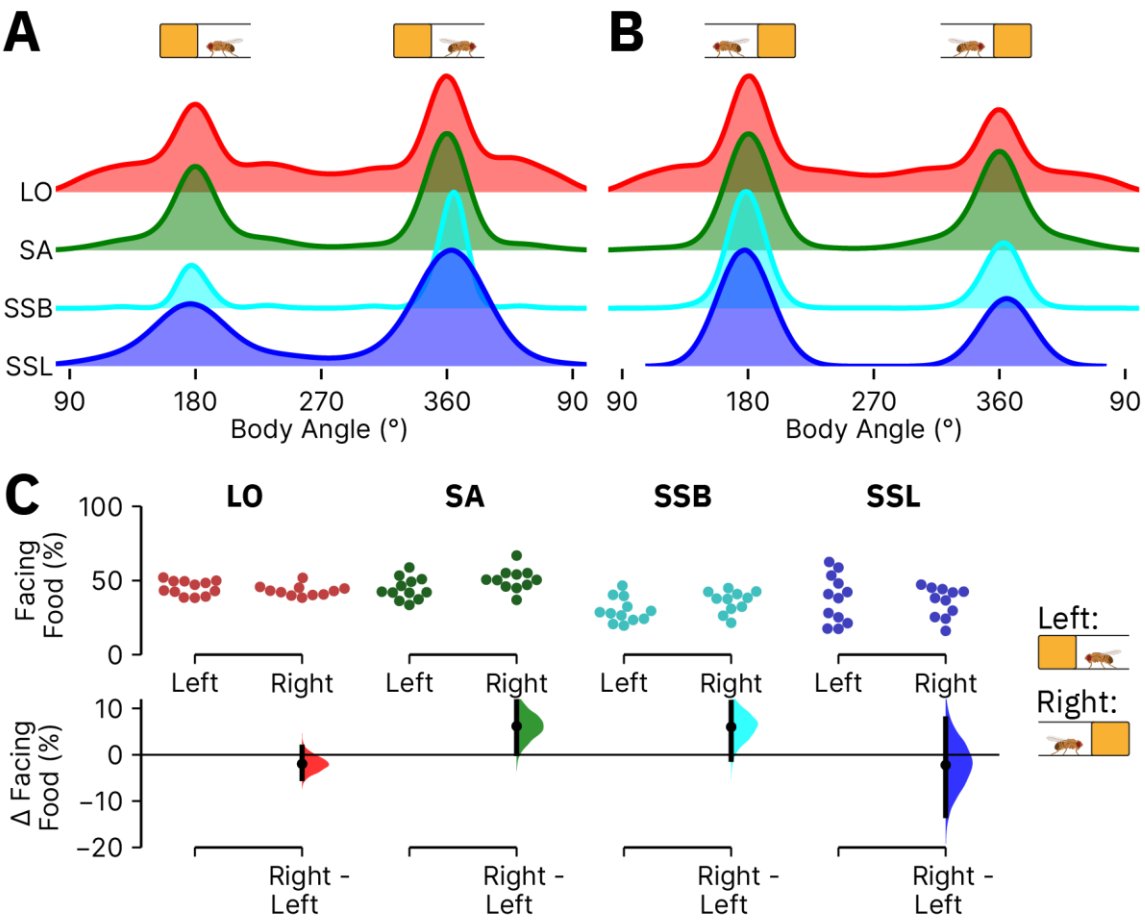

Figure 4.3.3 Facing direction preference is not due to chamber orientation

(A-B) Ridgeline plots of BA showing the distribution of bouts for each of the four recorded behaviours in w* males with food on the left side of the chamber (n=12) **(A)** or food on the right side of the chamber (n=11) **(B)**. As illustrated above (A-B), a body angle of 180° is facing the food port for (A) and facing away from the food port for (B), while 0/360° is the opposite. **(C)** DABEST plot of the percentage time facing the food port for food placed on the left side of the chamber versus the right side of the chamber, for all four behavioural states. The top section shows the raw unpaired data, with each dot indicating an individual. The bottom section shows the paired mean difference with 95% confidence intervals (CI) around the mean difference generated via bootstrap resampling. Each pair and associated DABEST curve represent one genotype/sex combination. The final DABEST curve represents the weighted delta. The summary data and sample sizes are shown in Appendix B Table 31.

4.4 Wild-type flies exhibit a time-of-day change in y-position place preference

I next studied whether flies have a y-position (Y-Pos) preference within Trumelan. This is an aspect of place preference that has not been described before. Within Trumelan, the Y-Pos of a fly can be measured at a fine (µm) resolution (as utilised for Chapter 4.1) or broadly (as in this case). For this purpose, flies can be separated into being on the ground of the chamber (described as 'ground'), on the ceiling of the chamber (described as 'ceiling'), or on the side walls of the chamber (described as 'wall') (Figure 4.4.1).

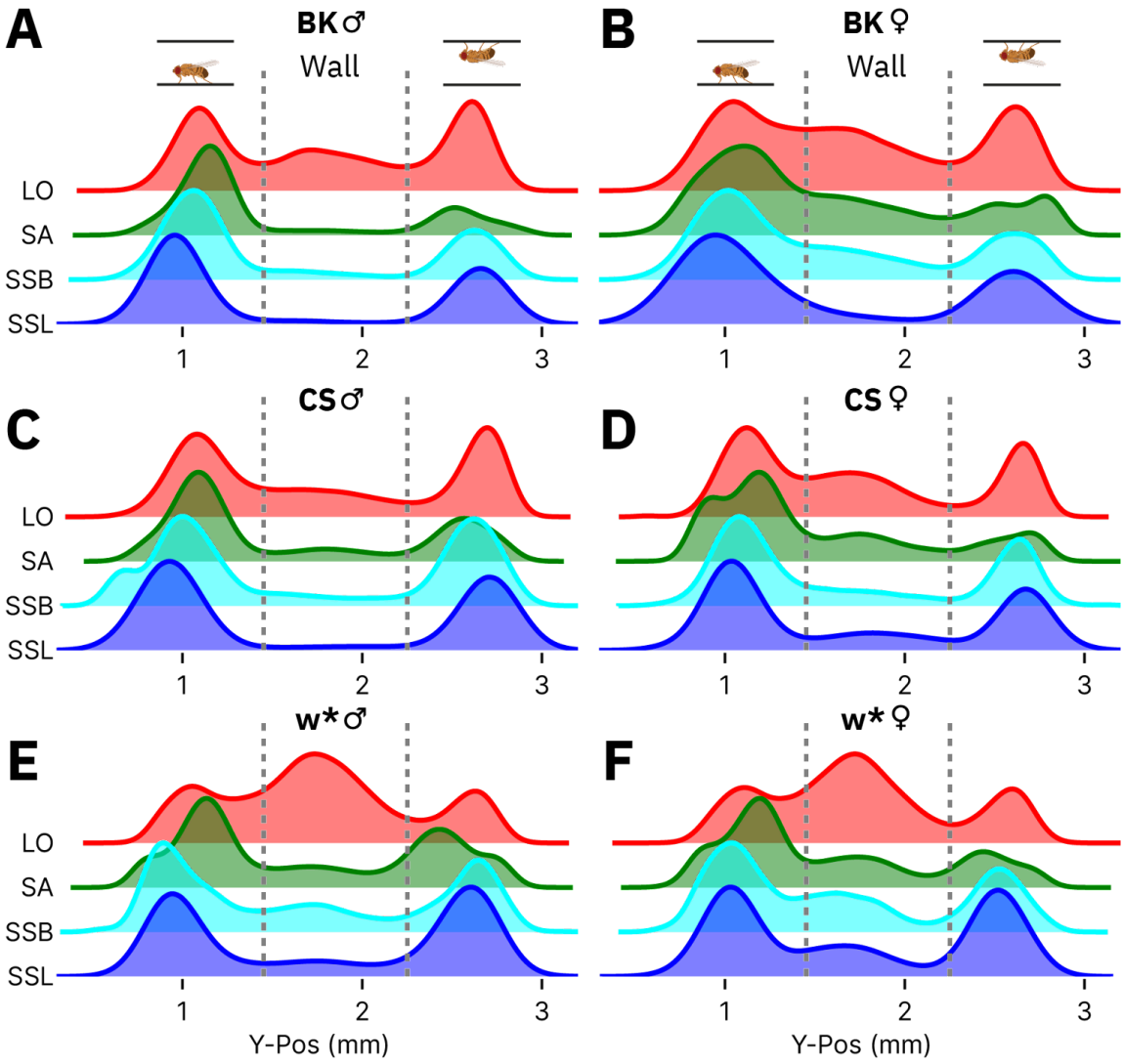

Figure 4.4.1 Wild-type flies perform stationary behaviours on the ground and the ceiling

Ridgeline plots showing the Y-Pos distribution of bouts for each of the behavioural states in BK males (n=60) **(A)**, BK females (n=30) **(B)**, CS males (n=30) **(C)**, CS females (n=59) **(D)**, w* males (n=49) **(E)**, and w* females (n=38) **(F).** The grey dotted lines indicate the boundaries for the three positions: Ground (low Y-Pos), Wall, and Ceiling (high Y-Pos). See Appendix B Table 32 for summary information.

During LO, both male and female flies spent significant time on all three Y-Pos compartments (Figure 4.4.1). For example, BK male flies, on average (Mean±CI), spent 32.80±1.50% on the ground, 31.05±1.68% on the walls, and 36.15±2.08% on the ceiling (Appendix B Table 32). This makes sense, given that flies are locomotive and like to explore the whole chamber. In contrast, flies rarely spent time on the wall during stationary behaviours and typically favoured being on the ground (Figure 4.4.1). Using the same BK males as an example, during SSL flies spent on average (Mean±CI) 66.02±5.38% of the time on the ground, only 2.98±1.15% on the wall, and 31.00±5.43% on the ceiling (Appendix B Table 32). By visually inspecting flies, it was apparent that they find being stationary on the wall challenging as they appear to slide down the wall and become locomotive again or remain on the ground. Interestingly, I found that flies spend a significant portion of their time stationary on the ceiling, reaching as high as 46.01±7.90% during SSL in CS males (Appendix B Table 32).

Unexpectedly, by separating the data into day versus night, I discovered a stark preference shift whereby all wild-type genotypes had increased time spent on the ceiling during the night compared to the day (Figure 4.4.2, described as ceiling occupancy). The differences in ceiling occupancy between day and night appeared consistent across males and females (Figure 4.4.2) and were thus grouped together for weighted delta calculations. By calculating the weighted difference across all wild-type genotypes/sex combinations, I found there was no difference in ceiling occupancy between day and night during LO, with a weighted mean difference (night - day, Δ %) of 0.62 [95%CI -0.31, 1.59] (Appendix B Figure 25A). However, during the three stationary behaviours (SA, SSB, and SSL), all wild-type flies consistently shifted towards more ceiling occupancy during the night (Appendix B Figure 25B-D). The weighted mean difference for night vs. day (Δ %) was 16.32 [95%CI 14.67, 18.11] for SA (Appendix B Figure 25B), 19.35 [95%CI 16.89, 21.87] for SSB (Appendix B Figure 25C), and 25.82 [95%CI 21.71, 29.88] for SSL (Appendix B Figure 25D). In almost all cases, SSL bouts had the most substantial time-of-day shift in Y-Pos place preference (Figure 4.4.2).

The ridgeline plots in Figure 4.4.2 suggest that flies spend most of their bouts on the ground during the day and shift towards more bouts on the ceiling at night. I plotted the wall occupancy data for night vs. day to confirm that the ceiling occupancy difference between day and night is at the expense of ground occupancy. I found only minor changes in occupancy from day to night (Appendix B Figure 26). Wall occupancy increased mildly for all four behaviours, with a weighted mean difference (Δ %) of 6.30 [95%CI 5.44, 7.17] for LO (Appendix B Figure 26A), 4.10 [95%CI 3.29, 4.89] for SA (Appendix B Figure 26B), 4.66 [95%CI 3.54, 5.83] for SSB (Appendix B Figure 26C), and 3.00 [95%CI 1.90, 4.29] for SSL (Appendix B Figure 26D).

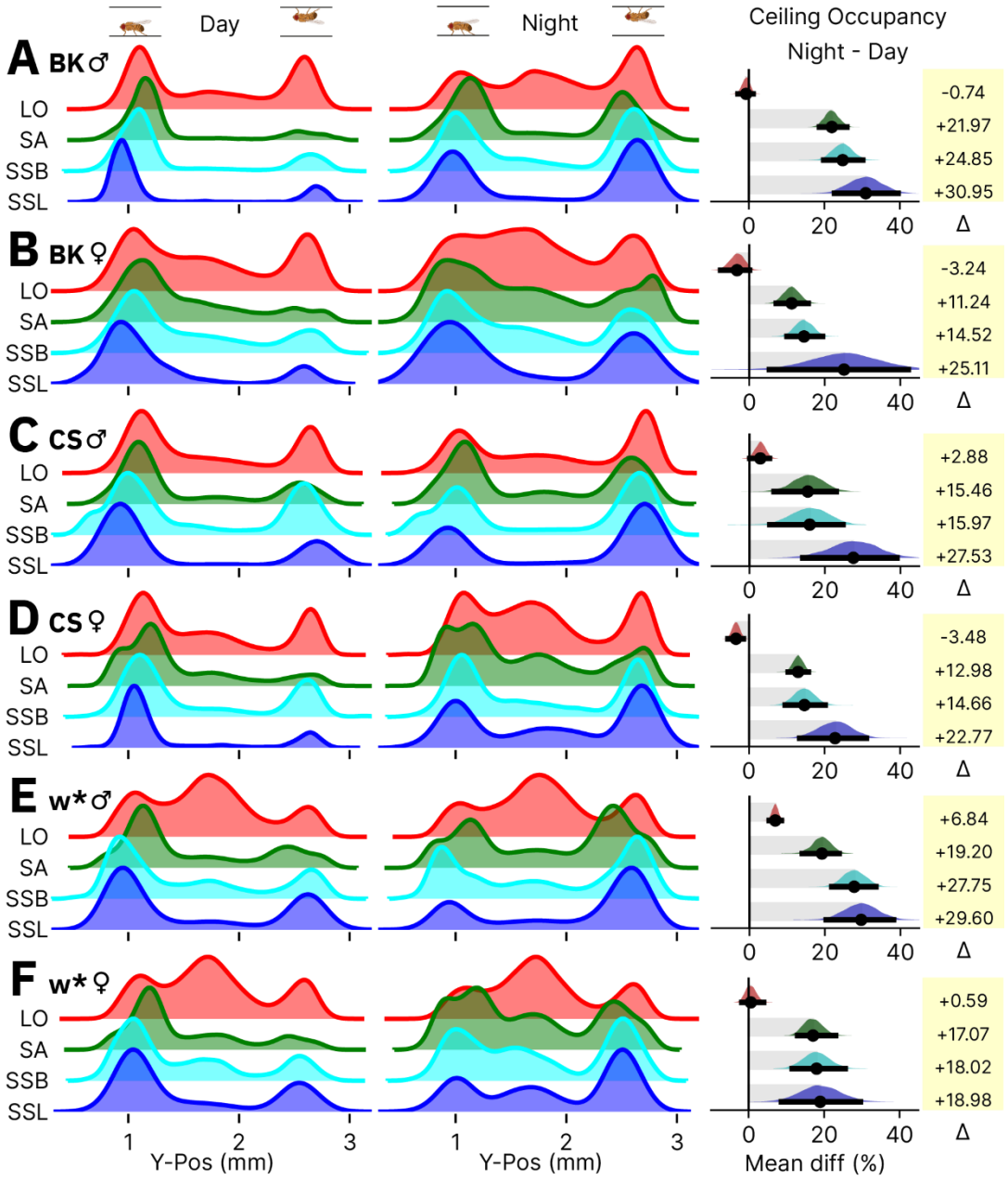

Figure 4.4.2 Y-position place preference during night vs. day in wild-type flies in an LD cycle

Left-Hand Side: Ridgeline plots showing the Y-Pos during each state for BK males (n=60) **(A)**, BK females (n=30) **(B)**, CS males (n=30) **(C)**, CS females (n=59) **(D)**, w* males (n=49) **(E)**, and w* females (n=38) **(F)**. Right-Hand Side: DABEST mean difference plots of percentage time spent on the ceiling during night vs day. The width of the bar and the black dot indicates the paired mean difference. Error bars show 95% CI of the mean difference estimate. The numerical value for mean difference (Δ) is shown to the right. The full DABEST plots are shown in Appendix B Figure 25.

My data suggest that flies spend most of their time on the ground during the day, which shifts to increased ceiling and minorly increased wall occupancy at night. Plotting the ground occupancy data further confirms this, as flies show a substantial loss of ground occupancy during the night (Appendix B Figure 27). Ground occupancy decreased minorly during LO, with a weighted mean difference (Δ %) of -6.56 [95%CI -7.54, -5.57] for LO (Appendix B Figure 27A). The data, therefore, suggest that the gain in wall occupancy during the night results from a loss of ground occupancy. As expected, ground occupancy decreased significantly for the stationary behaviours, with a weighted mean difference (Δ %) of -21.28 [95%CI -23.05, -19.58] for SA (Appendix B Figure 27B), -25.42 [95%CI -28.06, -22.75] for SSB (Appendix B Figure 27C), and -32.43 [95%CI -36.55, -28.33] for SSL (Appendix B Figure 27D).

To further study this preference shift, I analysed the light-dark wild-type fly data over shorter intervals of 1 hour rather than my initial analysis, which used a broad day versus night comparison. I plotted the behavioural time series data (as in Figure 3.3.1 except excluding < 1-second bouts) alongside ceiling occupancy time series data to be able to compare the waveforms directly. As the initial analysis suggested, LO shows very little change in pattern throughout the 24-hour day in all genotype/sex combinations tested, with flies typically spending more time on the ground/wall during LO (Figure 4.4.3A-F). All three stationary behaviours (SA, SSB, and SSL), on the other hand, showed a clear pattern in all genotype/sex combinations tested with low amounts of ceiling occupancy during the light phase (relative to the total time spent in the behavioural state), and increased amounts during the dark phase (Figure 4.4.3A-F). As stationary behaviour on the wall is much less common, flies prefer being stationary (whether SA, SSB, or SSL) on the ground during the light phase. In contrast, during the dark phase, flies consistently spent relatively more time on the ceiling than during the light phase (Figure 4.4.3A-F). Interestingly, while very little change in ceiling occupancy occurs during either the light or dark phase itself, the shift from low to increased ceiling occupancy occurred just before the lights come off (Figure 4.4.3A-F), suggesting an anticipation of the dark phase.

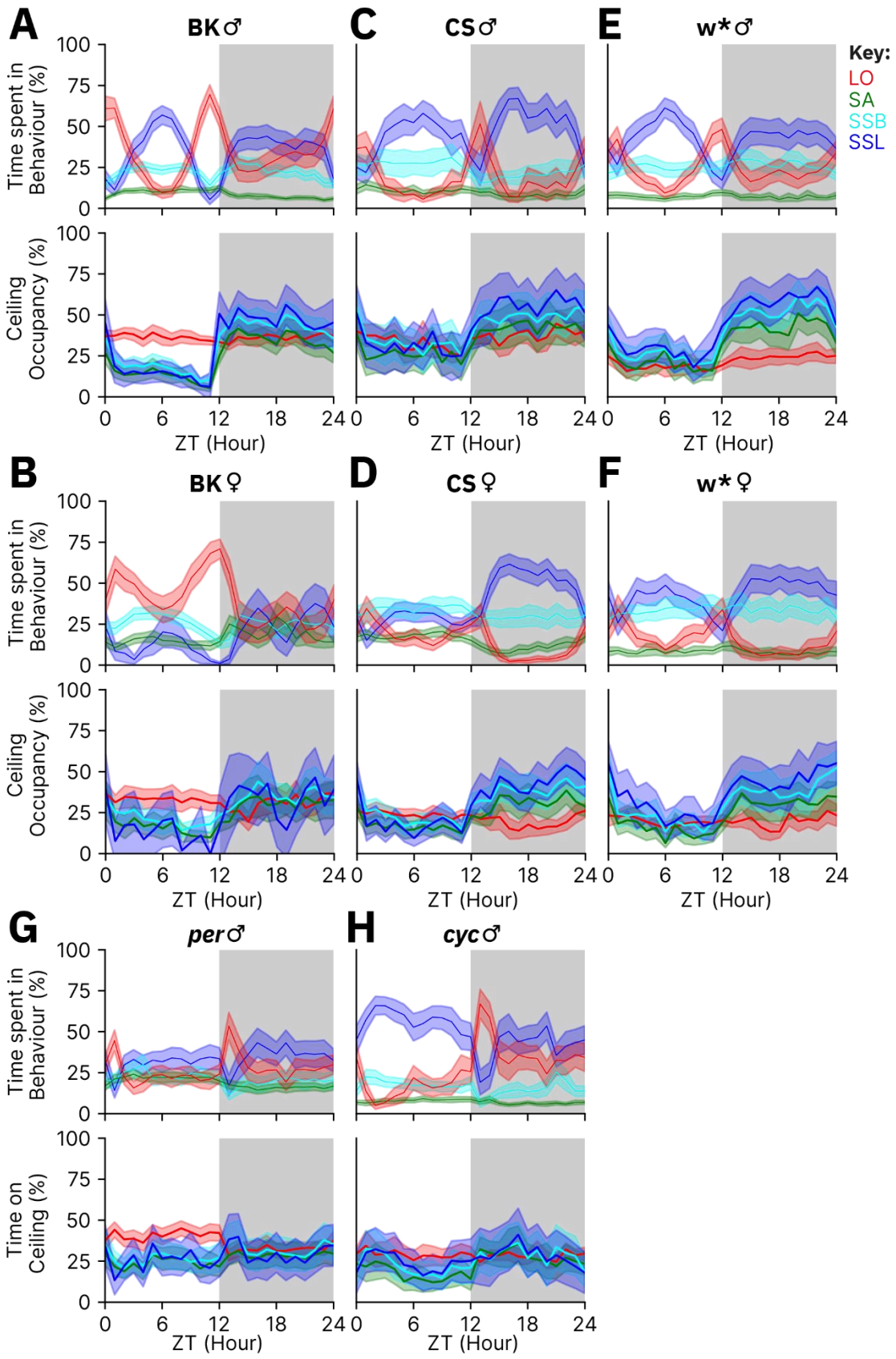

Figure 4.4.3 Time series plots of behaviour and ceiling occupancy in wild-type flies in an LD cycle

Time series plots of wild-type BK males (n=60) **(A)**, BK females (n=30) **(B)**, CS males (n=30) **(C)**, CS females (n=59) **(D)**, w* males (n=49) **(E)**, w* females (n=38) **(F)**, *per*^{01} males (n=41) **(G)**, and *cyc*^{01} males (n=30) **(H)**, recorded in a 12:12 light-dark cycle. The top plot shows the percentage

(Mean±CI) of each 60-min time point (ZT: Zeitgeber Time) spent in each behavioural state for each respective genotype. The bottom plot shows the time spent on the chamber ceiling for each state as a percentage of total time. The same data were used for top and bottom panels and the flies were kept in a LD cycle.

4.5 The ceiling occupancy shift is maintained in free-running conditions but lost in circadian mutants

The ceiling occupancy data elucidated a novel wild-type place preference and raised the question of whether this ceiling occupancy shift is a circadian-controlled process. To test whether the circadian clock controls this time-of-day-dependent behaviour, I first analysed the behaviour of the circadian mutants per^{01} and cyc^{01} (Konopka and Benzer, 1971; Rutila *et al.*, 1998). These two genotypes lack a functional circadian clock due to the loss of function of either positive (cyc^{01}) or negative (per^{01}) transcriptional regulators in the molecular clock (see Chapter 1.3.1). To begin with, I recorded both circadian mutants in light-dark cycles and compared these to BK males (replotted from Figure 4.4.3A for ease of comparison).

As previously shown, wild-type flies have a substantial ceiling occupancy shift from day to night during stationary behaviours (Figure 4.4.3A-F). Compared to BK, CS, or w* flies, both circadian mutants tested showed a significantly reduced change in ceiling occupancy Figure 4.4.3G-H). per^{01} flies had a ceiling occupancy change (night - day, Δ%) of -10.57 [95%CI -13.45, -8.02] for LO, 4.83 [95%CI 1.66, 8.56] for SA, 6.87 [95%CI 1.13, 13.30] for SSB, and 2.86 [95%CI -6.29, 12.3] for SSL (Appendix B Figure 28). Similarly, cyc^{01} flies had a ceiling occupancy change (night - day, Δ%) of -2.25 [95%CI -4.78, 0.49] for LO, 11.02 [95%CI 4.91, 17.31] for SA, 6.23 [95%CI -3,98, 17.14] for SSB, and 9.93 [95%CI -2.31, 22.0] for SSL (Appendix B Figure 28).

Given time constraints for this work, I decided to focus BK males as these had the strongest preference shift, as well as the male circadian mutants. As previously shown, BK males have a strong pattern of locomotor activity peaking around dawn and dusk (Figure 4.5.1A). In addition, BK flies had a clear pattern in SSL, with two significant periods of SSL occurring during the middle of the day and throughout most of the night (Figure 4.5.1A). Both SA and SSB were more minor states, although they still appeared to have some changes in amplitude throughout the circadian day.

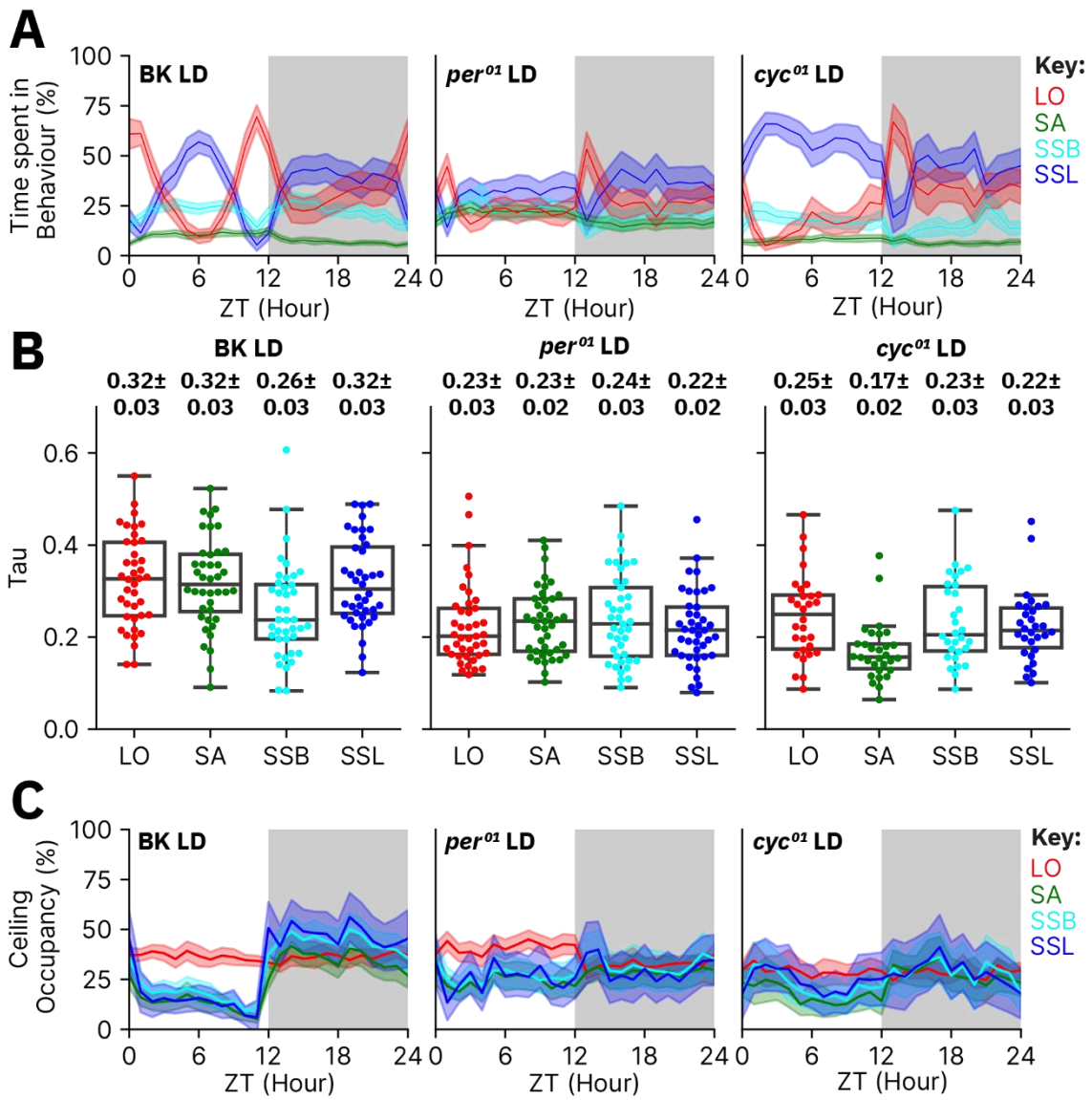

Figure 4.5.1 Time series data for BK and circadian mutants in an LD cycle

(A) Time series plots of the percentage (Mean±CI) of each 60-min time point from raw data averaged over a 24-hour day (ZT: Zeitgeber Time) spent in each behavioural state for each respective genotype. **(B)** Rhythmicity analysis of male BK (n=40), *per*^{01} (n=41), and *cyc*^{01} (n=30) flies' total behaviour in an LD cycle. Rhythmicity was analysed for each recorded behaviour state. The empirical JTK-Cycle with asymmetry search was employed to perform the analysis. The summary data is shown in Appendix B Table 37-39. **(C)** Time series plots of the percentage (Mean±CI) time spent on the chamber ceiling for each state for each 60-min time point from raw data averaged over a 24-hour day (ZT: Zeitgeber Time). The sample sizes for (A&C) were 60 for BK males, 41 for *per*^{01}, and 30 for *cyc*^{01}.

To test for rhythmicity, I analysed the raw data (in 30-minute bins) using an 'empirical JTK Cycle with asymmetry search' method (described here as eJTK_Cycle; see Chapter 2.10 for more

information). In brief, eJTK_Cycle works well on short time series data and tests against various waveforms. The tau metric generated by eJTK_Cycle represents the highest correlation the input data has against a set of rhythmic curves. Tau=1 would indicate a perfect correlation, while Tau=0 would be no correlation at all. The empirical p-value generated provides the likelihood of obtaining this tau value or greater if the null hypothesis of no rhythmicity is true.

By testing the BK behavioural data, I found that these flies had a Tau (Mean±CI) of 0.32±0.03 for LO, 0.32±0.03 for SA, 0.26±0.03 for SSB, and 0.32±0.03 for SSL (Figure 4.5.1B). Utilising a threshold of p<0.01, 80.0% of LO, 82.5% of SA, 45.0% of SSB, and 85.0% of SSL time series are considered rhythmic in BK flies (Appendix B Table 37). As expected from a circadian mutant in an LD cycle, per^{01} flies had no major pattern in behaviour throughout the circadian day except for peaks of LO (and troughs in SSL) at dawn and dusk (Figure 4.5.1A). These peaks occur in response to the light transitions (light to dark and dark to light), which indicates a startle response. Rhythmic analysis of per^{01} flies in an LD cycle generated a Tau (Mean±CI) of 0.23±0.03 for LO, 0.23±0.02 for SA, 0.24±0.03 for SSB, and 0.22±0.02 for SSL (Figure 4.5.1B). Utilising a threshold of p<0.01, 31.7% of LO, 43.9% of SA, 46.3% of SSB, and 31.7% of SSL time series are considered rhythmic in per^{01} flies (Appendix B Table 38). While per^{01} flies lack a functional clock, they can appear rhythmic within an LD cycle due to the consistent startle responses at lights on and off. cyc^{01} flies, on the other hand, had a minor nocturnality phenotype of increased LO and reduced SSL at night compared to during the day (Figure 4.5.1A). This was as expected given the prior understanding of cyc^{01} male flies within an LD cycle (Lee *et al.*, 2013). Rhythmic analysis of cyc^{01} flies in an LD cycle generated a Tau (Mean±CI) of 0.25±0.03 for LO, 0.17±0.02 for SA, 0.23±0.03 for SSB, and 0.22±0.03 for SSL (Figure 4.5.1B). Utilising a threshold of p<0.01, 50.0% of LO, 6.7% of SA, 40.0% of SSB, and 33.3% of SSL time series are considered rhythmic in cyc^{01} flies (Appendix B Table 39).

The hourly time series data provided further evidence that no significant ceiling occupancy change occurred over the 24-hour day in circadian mutants' four recorded behaviours. As seen in Figure 4.4.3A, BK males had a clear ceiling occupancy pattern in stationary behaviours of low occupancy during the day, rising during the hour before lights off and remaining higher during the night (Figure 4.5.1C). Both circadian mutants, on the other hand, had no overt waveform in ceiling occupancy over the 24-hour day (Figure 4.5.1C).

One thing that stood out from the wild-type time series plots in Figure 4.4.3 and Figure 4.5.1 is that all three stationary behaviours follow the same waveform and rough amounts of ceiling occupancy. In contrast, LO appears not to follow these waveforms. To follow up, I quantified the correlation of mean ceiling occupancy between behaviour states in BK males. I found that the ceiling occupancy pattern of LO did not correlate with any of the other stationary behaviours (Pearson's R; R=-0.06 for LO vs. SA, R=-0.07 for LO vs. SSB, and R=-0.11 for LO vs. SSL) (Figure

4.5.2A). In contrast, all three stationary behaviours were almost perfectly correlated with each other (R=0.96 for SSL vs. SA, R=0.98 for SSL vs. SSB, R=0.99 for SA vs. SSB) (Figure 4.5.2A).

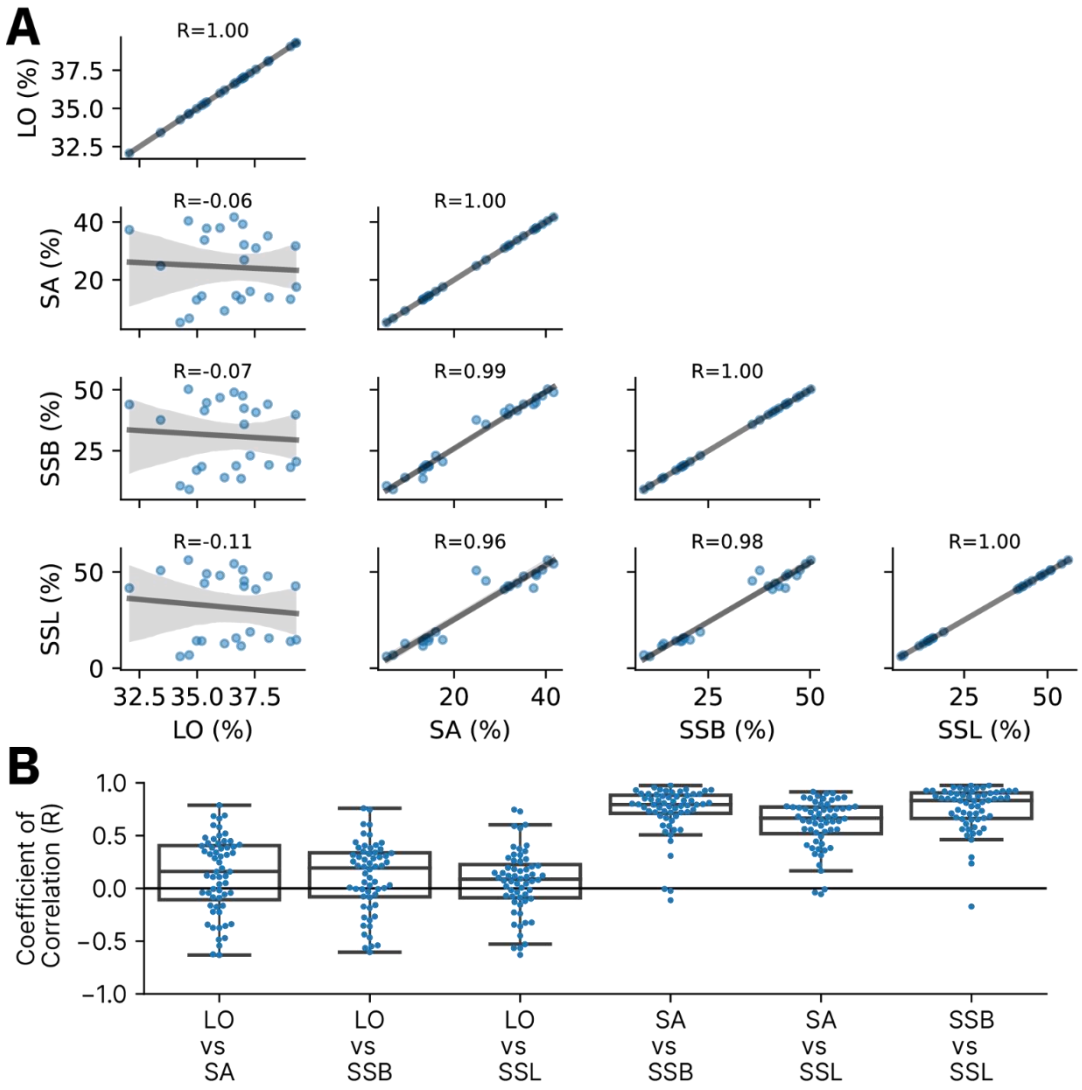

Figure 4.5.2 Ceiling occupancy is highly correlated between stationary behaviours in BK males

Cross-correlation plots of the ceiling occupancy of each behavioural state, for the averaged data across all BK flies **(A)** or for individual BK flies **(B)**. The sample size for **(A-B)** was n=60. The summary data for (B) is shown in Appendix B Table 40.

As these correlation plots utilised the mean values for each behaviour state, I also analysed individual flies. This was more problematic than utilising the mean values due to the nature of how ceiling occupancy was recorded. As ceiling occupancy is the percentage of time spent in a given state on the ceiling relative to the total state duration, this becomes more problematic in SSL when a fly only performs a small number of SSL bouts. When analysed for individual flies, SSL

has more extreme values (e.g., 0 or 100%) or missing values (NaNs) compared to SA or SSB. Nevertheless, there was a strong correlation (Mean±CI) between SSL and SSB (R= 0.76±0.05), SSL and SA (R= 0.61±0.06), and SA and SSB (R= 0.74±0.06) (Figure 4.5.2B). As with the averaged data, there was no correlation between LO and SA (R= 0.13±0.09), LO and SSB (R= 0.11±0.08), and LO and SSL (R= 0.06±0.08) (Figure 4.5.2B).

As a result of the similarity between all three stationary states, I grouped the behaviours into an overarching state which I termed 'roosting'. I next analysed the rhythmicity of the ceiling occupancy of this roosting state and compared it to the rhythmicity of LO ceiling occupancy. I first replotted the ceiling occupancy data from Figure 4.5.1C but with the collective roosting state instead of the three separate stationary states (Figure 4.5.3A).

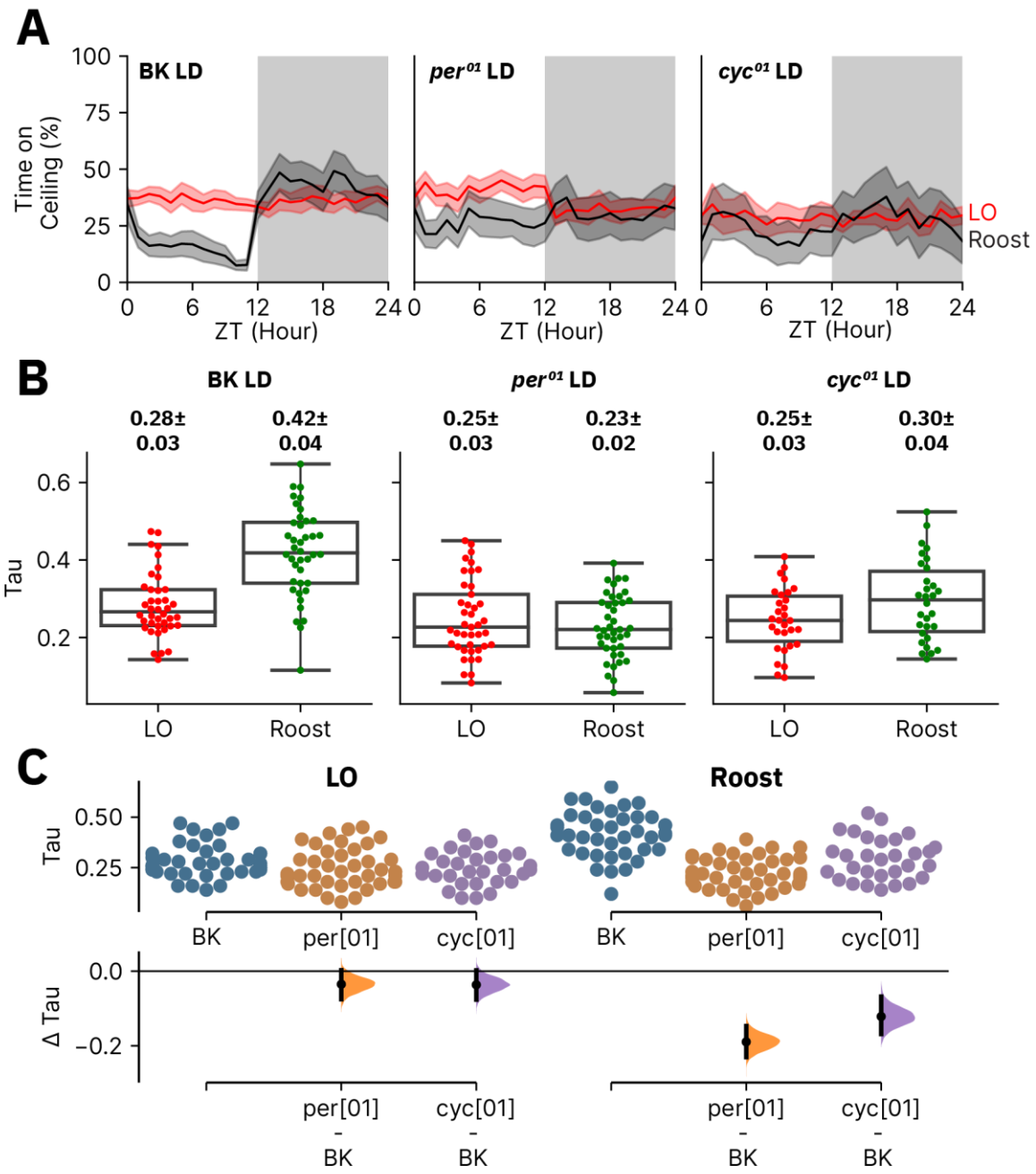

Figure 4.5.3 Rhythmic analysis of ceiling occupancy in LD conditions

(A) Time series plots of the percentage (Mean±CI) of each 60-min time point from raw data averaged over a 24-hour day (ZT: Zeitgeber Time) spent on the ceiling for LO and Roost for BK males (n=60), *per*^{01} males (n=41), and *cyc*^{01} males (n=40). **(B)** Rhythmicity (Tau), as measured by eJTK_Cycle, of LO and Roost ceiling occupancy, for BK males (n=40), *per*^{01} males (n=41), and *cyc*^{01} males (n=40). The summary data for (B) are shown in Appendix B Table 41. **(C)** Unpaired DABEST plot comparing the rhythmicity of circadian mutants vs. BK for LO and Roost ceiling occupancy. The top section shows the raw unpaired data, with each dot indicating an individual. The bottom section shows the mean difference between comparisons with 95% confidence intervals (CI) around the mean difference generated via bootstrap resampling. The summary data for (C) are

shown in Appendix B Table 42. The sample sizes were 40 for BK males, 41 for *per*^{01} males, and 40 for *cyc*^{01} males.

I next analysed the rhythmicity of ceiling occupancy behaviour using eJTK_Cycle as before. In BK males, the mean Tau for LO was 0.28±0.03, while the mean for the roosting state 'Roost' was 0.42±0.04. Utilising a threshold of p<0.01, 40% of flies were considered rhythmic in LO ceiling occupancy, while 87.5% were considered rhythmic in Roost ceiling occupancy (Figure 4.5.3B, Appendix B Table 41). *per*^{01} flies had a mean tau for LO of 0.25±0.03, while the mean Tau for Roost was 0.23±0.02. Utilising a threshold of p<0.01, 34.1% of flies were considered rhythmic in LO ceiling occupancy, while 31.7% were considered rhythmic in Roost ceiling occupancy (Figure 4.5.3B, Appendix B Table 41). *cyc*^{01} flies also had lower rhythmicity, with a mean tau for LO of 0.25±0.03, while the mean Tau for Roost was 0.30±0.04. Utilising a threshold of p<0.01, 26.7% of flies were considered rhythmic in LO ceiling occupancy, while 43.3% were considered rhythmic in Roost ceiling occupancy (Figure 4.5.3B, Appendix B Table 41). I subsequently compared the mean difference in Tau between BK and the circadian mutants. Mean Tau was relatively unchanged for LO between BK and *per*^{01} or *cyc*^{01}, with mean differences (Δ Tau) of -0.03 [95%CI -0.08, 0.00] and -0.04 [95%CI -0.08, 0.00], respectively (Figure 4.5.3C). In contrast, Tau was reduced in both *per*^{01} or *cyc*^{01} as compared to BK, with mean differences (Δ Tau) of -0.19 [95%CI -0.23, -0.15] and -0.12 [95%CI -0.17, -0.07], respectively (Figure 4.5.3C).

The LD data suggest that the circadian clock could control the ceiling occupancy rhythm. All wild-type flies tested had an evident ceiling occupancy change from day to night, while both circadian mutants tested had minor/no change in ceiling occupancy. A key feature of circadian rhythms is that they remain in free-running conditions. If it is a circadian controlled process, rather than directly due to light, the ceiling occupancy rhythm should remain. Therefore, an important test to justify this claim is whether the ceiling occupancy rhythm remains if entrained flies are placed in constant darkness. To this end, I recorded BK, *per*^{01}, and *cyc*^{01} males after placing them in constant darkness. As in an LD cycle, BK males in constant darkness (DD) demonstrated an apparent ceiling occupancy change in stationary behaviours. This was evident in the broad subjective night vs. subjective day comparison (Figure 4.5.4), with a ceiling occupancy increase (subjective night - subjective day, Δ%) of 16.81 [95%CI 11.86, 22.24] for SA, 24.55 [95%CI 16.98, 32.84] for SSB, and 21.29 [95%CI 8.32, 36.33] for SSL, compared to 5.63 [95%CI 3.82, 7.46] for LO (Appendix B Figure 29). Both circadian mutants, on the other hand, showed no major time-of-day ceiling occupancy shift (Figure 4.5.4). *per*^{01} flies had a ceiling occupancy change (subjective night - subjective day, Δ%) of 1.34 [95%CI -0.53, 3.19] for LO, 2.98 [95%CI 0.68, 5.50] for SA, 1.90 [95%CI -2.65, 6.39] for SSB, and 1.26 [95%CI -4.53, 7.07] for SSL (Appendix B Figure 29). Similarly, *cyc*^{01}

flies had a ceiling occupancy change (subjective night - subjective day, Δ%) of -0.74 [95%CI -2.40, 0.69] for LO, 1.94 [95%CI -0.02, 4.92] for SA, 0.92 [95%CI -2.41, 5.10] for SSB, and -1.97 [95%CI -7.59, 8.82] for SSL (Appendix B Figure 29).

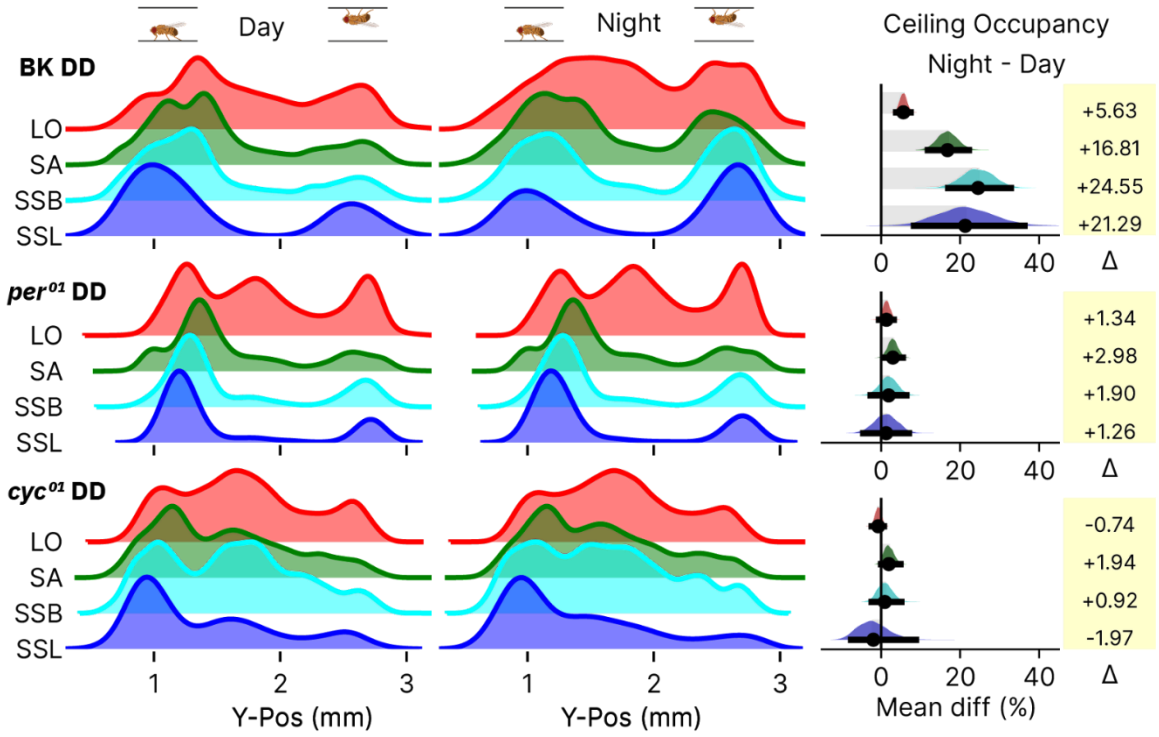

Figure 4.5.4 Differences in ceiling occupancy between BK and circadian mutants remains in free-running conditions

Left-Hand Side: Ridgeline plots showing the Y-Position during each state for male BK flies (n=31), and male circadian mutants *per*^{01} (n=22) and *cyc*^{01} (n=20) during DD conditions. Right-Hand Side: DABEST plots of percentage time spent on the ceiling during night vs. day (ceiling occupancy). The width of the bar and the black dot indicates the paired mean difference. Error bars show 95% CI of the mean difference estimate. The numerical value for mean difference (Δ) is shown to the right. Expanded DABEST plots are shown in Appendix B Figure 29.

Time series plots demonstrated that BK behaviour during DD is similar to during LD, with peaks of LO around dawn and dusk and two main periods of SSL during the middle of the subjective day and broadly during the subjective night (Figure 4.5.5A). On the other hand, both circadian mutants had no major observable patterns in behaviour during DD (Figure 4.5.5A).

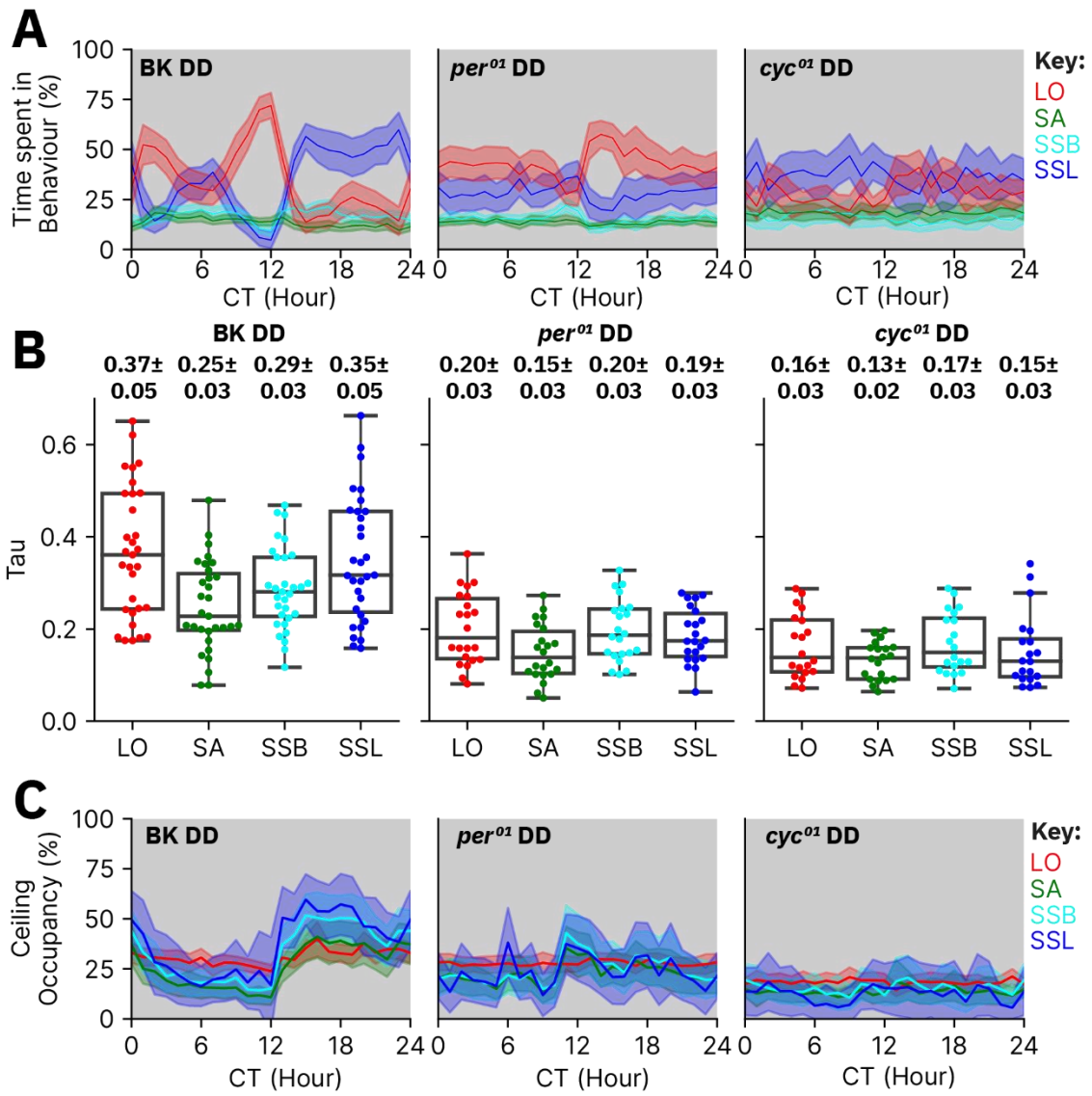

Figure 4.5.5 Time series data for BK and circadian mutants in DD conditions

(A) Time series plots of the percentage (Mean±CI) of each 60-min time point from raw data averaged over a 24-hour day (CT: Circadian Time) spent in each behavioural state for each respective genotype. **(B)** Rhythmicity analysis of male BK (n=31), *per*^{01} (n=22), and *cyc*^{01} (n=20) flies' total behaviour in a DD cycle. Rhythmicity was analysed for each recorded behaviour state. The empirical JTK-Cycle with asymmetry search was employed to perform the analysis. The summary data is shown in Appendix B Table 44-46. **(C)** Time series plots of the percentage (Mean±CI) time spent on the chamber ceiling for each state for each 60-min time point from raw data averaged over a 24-hour day (CT: Circadian Time). The sample sizes for (A-C) were 31 for BK males, 22 for *per*^{01} males, and 20 for *cyc*^{01} males.

As in LD cycles, rhythmic analysis of BK behaviour in DD generated Tau scores (Mean±CI) of 0.37±0.05 for LO, 0.25±0.03 for SA, 0.29±0.03 for SSB, and 0.35±0.05 for SSL (Figure 4.5.5B). Utilising a threshold of p<0.01, 77.4% of LO, 45.2% of SA, 67.7% of SSB, and 74.2% of SSL time series are considered rhythmic (Appendix B Table 44). Rhythmic analysis of *per*^{01} fly behaviour in

DD generated Tau scores (Mean ±CI) of 0.20±0.03 for LO, 0.15±0.03 for SA, 0.20±0.03 for SSB, and 0.19±0.03 for SSL (Figure 4.5.5B). Utilising a threshold of p<0.01, 31.8% of LO, 9.1% of SA, 27.3% of SSB, and 22.7% of SSL time series are considered rhythmic (Appendix B Table 45). Similarly, rhythmic analysis of *cyc*^{01} fly behaviour in DD generated Tau scores (Mean ±CI) of 0.16±0.03 for LO, 0.13±0.02 for SA, 0.17±0.03 for SSB, and 0.15±0.03 for SSL (Figure 4.5.5B). Utilising a threshold of p<0.01, 20.0% of LO, 0.0% of SA, 20.0% of SSB, and 15.0% of SSL time series are considered rhythmic (Appendix B Table 46). There was a clear reduction in Tau in both circadian mutants in DD compared to LD, as is expected, given that the light transitions are no longer present. In addition, there was a clear reduction in Tau between BK flies and circadian mutants in LD and DD conditions (Figure 4.5.1B and Figure 4.5.5B).

BK flies within DD conditions also have a noticeable ceiling occupancy rhythm as in LD (Figure 4.5.5C). The waveform appears more varied than in LD, but a difference in ceiling occupancy between day and night is apparent. On the other hand, both circadian mutants had no noticeable ceiling occupancy rhythm in DD (Figure 4.5.5C). Separating ceiling occupancy states into LO and Roost further demonstrated the noticeable pattern in BK males and the lack of overt pattern in circadian mutants (Figure 4.5.6A).

Rhythmic analysis of ceiling occupancy behaviour was analysed in the same manner as for LD conditions. In BK males, the mean Tau for LO was 0.29±0.03, while for the roosting state, 'Roost' was 0.32±0.05. Utilising a threshold of p<0.01, 58.1% of flies were considered rhythmic in LO ceiling occupancy and Roost ceiling occupancy (Figure 4.5.6B, Appendix B Table 47). *per*^{01} flies had lower rhythmicity than BK flies, with a mean Tau for LO and Roost of 0.20±0.03 and 0.23±0.03, respectively. Utilising a threshold of p<0.01, 22.7% of flies were considered rhythmic in LO ceiling occupancy, while 36.4% were considered rhythmic in Roost ceiling occupancy (Figure 4.5.6B, Appendix B Table 47). *cyc*^{01} flies also had lower rhythmicity, with a mean Tau for LO of 0.16±0.02, while the mean tau for Roost was 0.19±0.02. Utilising a threshold of p<0.01, 0.0% of flies were considered rhythmic in LO ceiling occupancy, while 10.0% were considered rhythmic in Roost ceiling occupancy (Figure 4.5.6B, Appendix B Table 47). I subsequently compared the mean difference in Tau between BK and the circadian mutants. Mean Tau of LO was reduced in *per*^{01} or *cyc*^{01} as compared to BK, with mean differences (Δ Tau) of -0.10 [95%CI -0.14, -0.06] and -0.14 [95%CI -0.17, -0.11], respectively (Figure 4.5.6C). Similarly, Tau of Roost was reduced in both *per*^{01} or *cyc*^{01} as compared to BK, with mean differences (Δ Tau) of -0.09 [95%CI -0.15, -0.03] and -0.13 [95%CI -0.18, -0.08], respectively (Figure 4.5.6C).

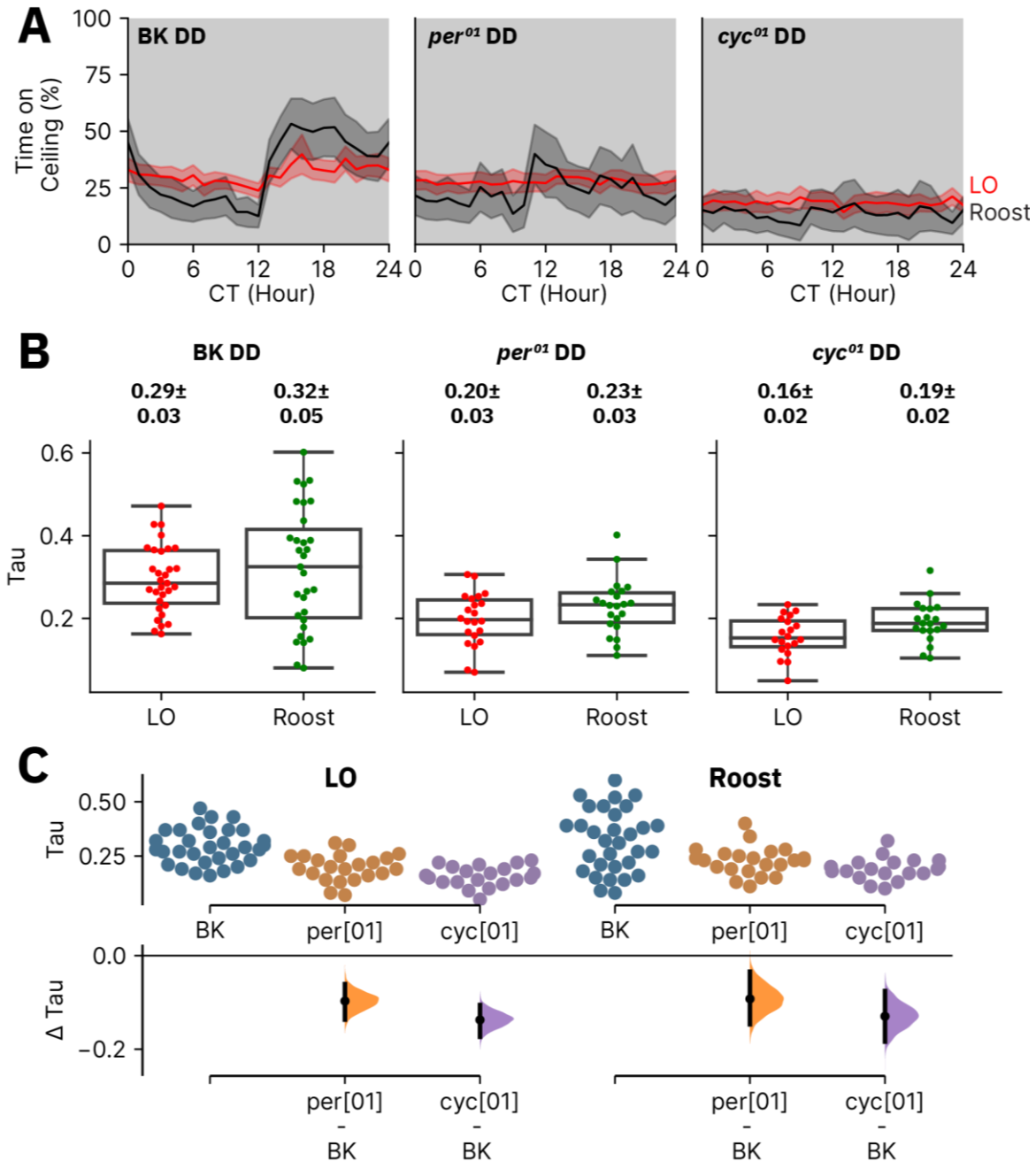

Figure 4.5.6 Rhythmic analysis of ceiling occupancy in DD conditions

(A) Time series plots of the percentage (Mean±CI) of each 60-min time point from raw data averaged over a 24-hour day (CT: Circadian Time) spent on the ceiling for LO and Roost for BK males (n=31), *per*^{01} males (n=22), and *cyc*^{01} males (n=20). **(B)** Rhythmicity (Tau), as measured by eJTK_Cycle, of LO and Roost ceiling occupancy, for BK males (n=31), *per*^{01} males (n=22), and *cyc*^{01} males (n=20). The summary data for (B) are shown in Appendix B Table 47. **(C)** DABEST plots comparing the rhythmicity of circadian mutants vs. BK for LO and Roost ceiling occupancy. The top section shows the raw unpaired data, with each dot indicating an individual. The bottom section shows the mean difference between comparisons with 95% confidence intervals (CI) around the mean difference generated via bootstrap resampling. Each DABEST curve represents

one comparison. The summary data for (C) are shown in Appendix B Table 48. The sample sizes for (A-C) were 31 for BK males, 22 for *per*^{01} males, and 20 for *cyc*^{01} males.

From the LD and DD data, it is clear that the ceiling occupancy shift remains in free-running conditions in wild-type flies. The data also hinted that light may have a small effect, as BK males had a reduced effect size and increased variation in DD compared to LD. To quantify the effect of light on the ceiling occupancy shift, I used the 'delta-delta' feature of DABEST (Ho *et al.*, 2019), which computes the change in effect size of ceiling occupancy shift (from night minus day) for the LD data versus the DD data. This analysis method allows for computing the effect that light has on the ceiling occupancy shift during the night. Here, I focused on the effect on ceiling occupancy during Roost and found that light has no noticeable impact, with delta-delta values of 9.66% [95%CI -7.04, 25.6] for BK males (Figure 4.5.7A), 1.6% [95%CI -9.45, 12.5] for *per*^{01} (Figure 4.5.7B), and 11.9% [95%CI -2.45, 25.7] for *cyc*^{01} (Figure 4.5.7C).

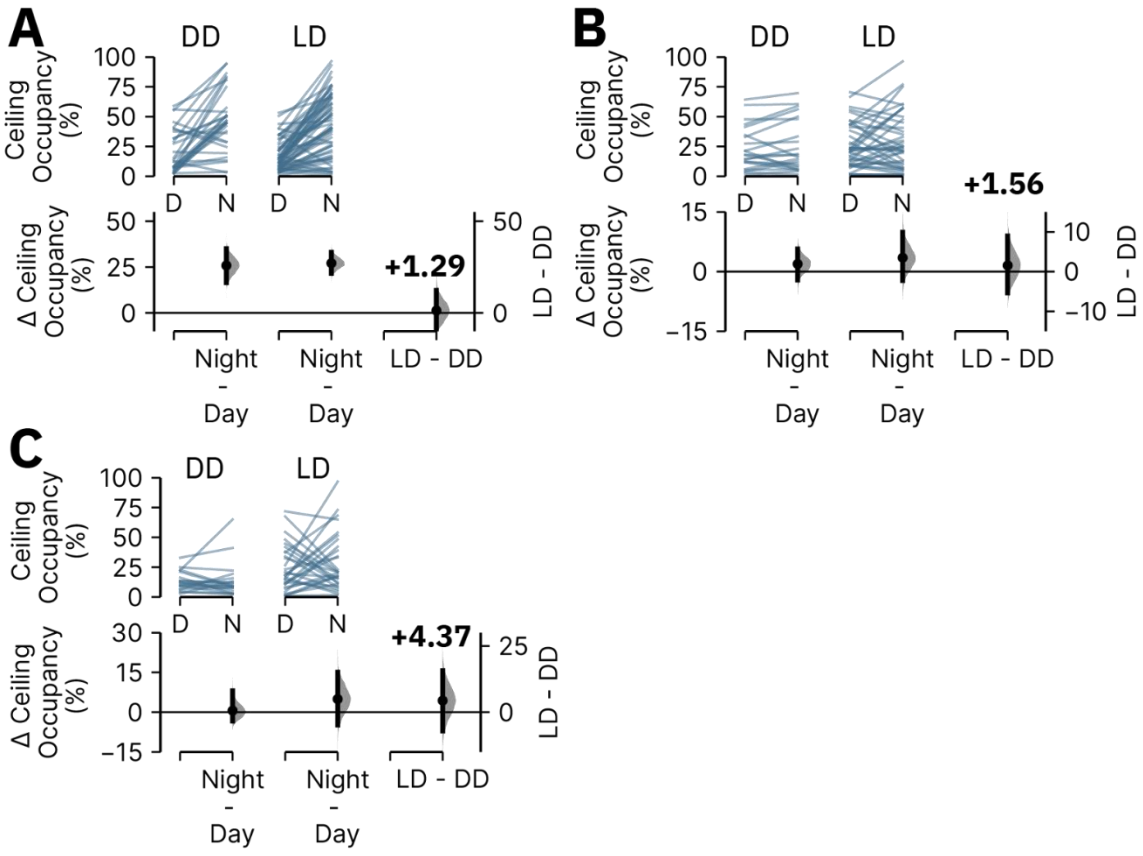

Figure 4.5.7 Light has no effect on magnitude of daily ceiling occupancy shift

Delta-Delta DABEST plots for Roost percentage ceiling occupancy during night versus day for LD versus DD experiments in BK **(A)**, *per*^{01} **(B)**, and *cyc*^{01} males **(C)**. The top section shows the raw paired data, with each line indicating an individual. The bottom section shows the paired mean difference with 95% confidence intervals (CI) around the mean difference generated via bootstrap

resampling. The summary data, including sample sizes, are shown in Appendix B Table 49. The first level of analysis computes the difference between night and day for ceiling occupancy of Roost data in LD and DD conditions. The delta-delta computes the difference between the LD and DD experimental deltas.

4.6 Chapter 4 Discussion

In flies, ground-based rest was described as beginning in a supported upright position and lowering to become prone (flat) to the ground (Hendricks *et al.*, 2000). My quantitative analysis found that long-resting flies on the ground typically began in a supported upright position. The supported posture is where the flies' rear is low/on the ground, and their front legs are extended, keeping their body upright (resulting in a sizeable negative nBA). The posture of ceiling-based rest had yet to be described. Here, flies long-resting on the ceiling began in a slightly less supported position, which is likely explained by the additional energy cost to keep their rear close to the ceiling. Instead, flies long-resting on the ceiling had a more parallel body angle, and their rear was visually off the ceiling.

While flies typically began long rest in a supported upright position, rest was associated with various starting postures, and there was no correlation between the starting posture and the duration of the rest. In addition, fly posture was generally consistent across behavioural states, as flies began all behaviours from various poses with significant overlap in distribution between behaviours. It follows, therefore, that the starting posture of a fly cannot accurately inform the viewer (or a behavioural classifier) of the behaviour that the fly is about to perform. Visual inspection of fly behaviour quickly confirmed this, as the supported upright position was ubiquitous.

Alongside a supported upright starting posture, changes in posture do occur during a long rest bout. This was most evident for ground-based long rest, where all genotypes had a consistent average posture change of lowering the body. While fly lowering over time appears consistent with the original description, (Hendricks *et al.*, 2000) suggest that flies lower to a prone position flat against the ground. This would result in a significantly negative Y-Pos and a sizeable positive nBA. In addition, the end images of flies would show them resting prone on the ground. My quantitative work here suggests that this is not the case. Flies did lower their body; however, the amount was marginal and, in most cases, not noticeable to the human eye. Alongside minor lowering, flies remained in a supported upright position. The data here is unlike the initial suggestion of flies becoming prone (parallel to the ground). Long-resting flies on the ground had a

slightly negative nBA over time, suggesting that flies remained in a supported upright position. Given the minor Y-Pos change and the raw images of start and end posture, this is likely via the rear lowering towards the ground slightly while the front legs remain extended to keep the fly body pointing upwards. Long rest on the ceiling was less consistent, with each genotype having different postural changes. Altogether, ceiling-based long rest was not associated with any significant changes in posture.

Validation of the body angle metric (see Methods: Chapter 2.8), demonstrated that there were some minor differences in measurement of a fly's posture when compared to human annotation. It is worth noting, however, that the difference in human annotation versus video tracking was relatively consistent across test images, suggesting more of a systematic error rather than random issues with tracking. As a result, this provides confidence that this will not have a large impact on the change in posture data. In addition, I found that the video tracking tends to suggest flies are in a more parallel posture than when measured by human annotation. Therefore, this adds more weight to the finding that flies do not become parallel/prone to the ground during rest, and that flies start with a supported upright posture. Nonetheless, future work could look to utilise an additional measure of body angle, such as via an alternative body pose estimation software (such as DeepLabCut; (Mathis *et al.*, 2018)) to provide further evidence for the lack of a distinct rest posture in flies.

One potential alternative explanation for why flies do not appear to become prone to the ground could be that the tracking is too sensitive. If the movement of the fly lowering was flagged as SA or LO, it would break up rest bouts. This is unlikely, however:

- While training the Trumelan behavioural state classifier, I was mindful of allowing small movements, such as twitches, to be included as SS.
- Lowering into a prone position rapidly would likely not occur; otherwise, the fly may be jolted awake. Hendricks and colleagues suggest it occurs over multiple minutes (Hendricks *et al.*, 2000). Thus, the movement per frame (45 fps) would be insignificant and unlikely to cause the tracker to misinterpret the lowering as SA/LO.
- Many long rest bouts lead to no change or raising the fly body relative to the ground.
- The nBA becoming more negative suggests the fly remains in a supported upright position rather than progressing to becoming prone to the ground.

Suppose flies eventually become prone, but tracking issues broke up the lowering. In that case, many rest bouts should begin in a prone position low to the ground. This is not the case, as seen in the images of flies and the visual inspection of thousands of flies during my studies. Many Trumelan recorded rest bouts were of significant duration, suggesting that the tracking was not fragmenting rest bouts. If becoming prone is not seen in these more prolonged bouts, then it is

likely not typical for such postural changes to happen, even if some rest bouts are being fragmented.

Finally, postural changes did not correlate with the duration of rest, suggesting that the lowering seen in the averaged data is inconsistent. The time series plots of postures suggest that changes in posture occur most prominently at the beginning of a bout and rapidly wane to no change in posture over time. While flies had minor postural changes, I hypothesise that these were due to general properties of fly biomechanics when a fly is stationary (and not actively performing an action) rather than long rest per se. One piece of evidence for this is that short-resting flies also had similar postural changes over time. As both short and long resting flies had postural changes, it suggests that neither starting nor change in posture can be used to identify a long rest bout. Further work to confirm this could include testing the arousal threshold of flies during rest bouts and seeing if specific postural changes are associated with a heightened arousal threshold. This is currently not possible within the Trumelan assay; however, it could be done using air puffs or other arousing stimuli.

In addition to resting posture, flies are thought to rest near a food source. I show that flies prefer this; however, there are some caveats. Firstly, long resting near the food port does not appear to be a universal phenomenon as one of the wild-type strains (BK males) showed no significant preference for resting near the food port and instead spent most of their time in the middle of the chamber. Secondly, while flies tend to long rest near the food port, many bouts still occurred away from the food port, resulting in the place preference being much less extreme than initially described (Hendricks *et al.*, 2000). Hendricks and colleagues suggest that most long rest (96%) occurs in a third of the chamber near the food port. My quantitative analysis confirms the general concept but tempers the extremeness of the preference. Flies tended to rest near the food port; however, a vast number of bouts occurred across the whole length of the chamber. If I were to plot the location of 96% of the rest episodes recorded via Trumelan, it would cover most of the length of the chamber.

Thirdly, resting near the food port was not specific to long rest. SA bouts occurred primarily by the food port, which could be explained by the fact that SA likely encompasses feeding events. An interesting difference between X-Pos place preference in males and females was in SA. One explanation for why females tend to be closer during SA could be that SA encompasses feeding events. As female flies are known to feed more than males (Wong *et al.*, 2009), and feeding can only occur at the food port, this could skew SA behaviour towards the food port more so in females than males. In addition, SA encompasses fly grooming, which could occur before, during, or after feeding events. Short-resting flies also preferred being near the food, suggesting that being near the food is a common preference for all stationary behaviour. It appears that flies

generally prefer to be near a food source; therefore, they remain near the food when they are not locomotive.

I also found that long-resting flies preferred to face away from the food port, as previously suggested (Hendricks *et al.*, 2000). While flies preferred to face away from the food on average, it was not entirely specific to long rest. A preference for facing away from the food was also seen for the other stationary behaviours (short rest or SA) that occurred away from the food port. This was an interesting finding as both SA and short rest appeared to have little or no preference for facing either direction when all the data was analysed. Being near the food is associated with potential feeding events, and it was noteworthy to see that while flies were away from the food port, they preferred to face away from the food port regardless of the stationary behaviour being performed. However, the tendency to face away from the food port was strongest in long-resting flies. In addition, while flies near the food port tended to face the food during SA or short rest, long-resting flies near the food port still preferred to face away from the food port.

As described above, the preference for facing the food during SA periods near the food could be explained by feeding events, which inevitably require facing the food port. Meanwhile, when away from the food, perhaps flies prefer to face away from the food port like in long rest. Short rest near the food appeared to have a minor preference for facing the food or no preference for either direction. Some of these short rests near the food could represent brief pauses before, during, or after feeding events, which would inevitably be facing towards the food port. The facing direction preference difference between long and short rest provides further evidence that these two states are functionally different.

My data suggest that a preference for being near but facing away from the food source may be more of a preference during all stationary behaviour unrelated to feeding. To further study this, an informative upgrade to Trumelan could involve integrating a feeding assay into the current setup such that feeding events can be recorded concurrently with behavioural tracking. This would allow for greater precision with behavioural analyses. It could provide vital information about the behaviours occurring near the food. For example, whether short rest near the food is associated with occurring before, during, or after feeding events. Another example would be that it could separate SA into feeding versus non-feeding SA behaviour.

Unexpectedly, I discovered that wild-type flies also had a y-position preference. All wild-type flies tested had a similar pattern with little stationary time on the ceiling (ceiling occupancy) during the day and greater ceiling occupancy at night. The waveform of ceiling occupancy for each behaviour differed from the pattern of the behaviour itself, suggesting a different regulation mechanism. For example, even though the amount of SSL varies substantially throughout the day, the ceiling occupancy percentage remains low until dusk. Interestingly, the waveform of ceiling occupancy

appeared similar across all stationary behaviours, and I found these were highly correlated in both average and individual fly data. The strong correlation between stationary behaviours and lack of correlation to locomotion suggests an underlying mechanism that controls the location of where a fly chooses to be stationary. As a result, I combined these behaviours into one overarching state called 'Roosting' ('Roost'). While strongly correlated ceiling occupancy patterns could be due to these behaviours occurring consecutively (e.g., if grooming happens after/before SS), amounts of SA and SS were not correlated in my preliminary analysis.

As the ceiling occupancy pattern changed between day and night, I hypothesised that the circadian clock was controlling this location preference. To follow up, I compared BK flies to two circadian mutants in an LD cycle. Unlike wild-type flies, circadian mutants lacked an overt change in ceiling occupancy throughout the day. This suggested that the circadian clock may be involved. Rhythmic analysis indicated that most BK flies had rhythmic ceiling occupancy in Roost and moderate levels in LO. In contrast, fewer circadian mutant flies were rhythmic during Roost, justifying the patterns seen in the averaged waveforms.

To account for the potential of a direct light response rather than circadian regulation, I also tested flies in constant darkness. When in constant darkness, fewer BK flies were rhythmic in the Roost state than in LD, but the rhythmicity of Roost and LO was significantly more robust in BK flies than for circadian mutants. While fewer flies had rhythmic Roost ceiling occupancy in BK flies in DD, their behaviour was also less rhythmic in DD. The waveform of Roost appeared to have a similar pattern to that in LD, and there was still a significant difference in the percentage of rhythmic flies between BK and circadian mutant flies in DD. The constant dark experiments suggest that light may affect the rhythmicity of Roost ceiling occupancy; however, the difference in ceiling occupancy between day and night was unaffected by light.

The y-position discovery was unexpected and is a preliminary finding. Studying males and females from three wild-type genotypes provides some confidence that the ceiling occupancy shift between day and night is a typical wild-type phenomenon. The data also demonstrate, however, that there is a large amount of variation between these genotypes (or even between sexes). BK males, for example, had very low amounts of ceiling occupancy during the day with higher levels at night. Other genotypes still had a day/night difference in ceiling occupancy but had higher amounts of ceiling occupancy during the day as compared to BK males. Similarly, both circadian mutants spend more time on the ceiling during the day as compared to BK males. The variability in ceiling occupancy across genotypes raises the question of whether the lack of ceiling occupancy change in the circadian mutants is really due to lack of circadian clock, or purely noise and/or a result of these flies already having a reasonably high ceiling occupancy during the day. With that being said, some wild-type genotypes tested also had similar levels of ceiling occupancy during

the day (e.g., CS males), but still had an increase at night. Nonetheless, future work is needed to better elucidate whether the clock is involved. This would include reducing confounds in the genetic background. For example, both circadian mutants lack a direct wild-type comparison (i.e., A genotype with the same genetic background as the circadian mutant except for the specific mutation). This could be achieved via many rounds of backcrossing of the circadian mutants with a chosen wild-type background. An alternative approach to this situation could be to utilise RNAi to specifically perturb clock gene function. This would provide an experiment which illustrates the ceiling occupancy behaviour before and after the circadian clock is perturbed. One issue with RNAi is that the knockdown efficiency is typically below 100% (H.-H. Qiao *et al.*, 2018), which could result in the molecular clock continuing to function. More efficient methods, such as CRISPR have arisen and are commonly used in flies to knockout specific genes of interest (Gratz *et al.*, 2015). With this approach, we could specifically target circadian clock genes with high efficiency. In addition, the commonly used UAS/GAL4 system could be used to target CRISPR to specific cells of interest, which could further help elucidate the cells necessary and sufficient for ceiling occupancy rhythms.

Many additional follow-up experiments could be performed to understand this behaviour further. Due to time constraints, only male BK and circadian mutants were tested in LD and DD. Further work to test additional wild-type genotypes could be performed. In addition, testing flies in constant light (LL) experiments would be a valuable way to disrupt the molecular clock within wild-type flies. I would hypothesise that these flies would lose any ceiling occupancy rhythm when in LL. While all wild-type flies had a daily ceiling occupancy shift, further tests are needed to clarify how robust the phenotype is and the potential impact of genetic backgrounds. In the future, discovering whether specific circadian clocks (brain or peripheral) are involved in this phenotype is also possible.

Chapter 5 Bioluminescent correlates of neuronal activity

A key aspect of studying sleep is discovering the role of specific neurons and circuits involved. To achieve this objective, many laboratories studying *Drosophila* sleep utilise thermo, chemo, or optogenetics to manipulate (whether that be activation or inhibition) specific cells or circuits. Locomotor assays, whether that be DAM or video-tracking approaches, are then used to record the behaviour of flies before, during, and after the manipulation occurs, and the resulting gross locomotor effects are recorded. Pioneered by the van Swinderen lab, an improved method for studying the role of cell populations in sleep has arisen (Nitz *et al.*, 2002; van Alphen *et al.*, 2013; Bushey, Tononi and Cirelli, 2015; Tainton-Heap *et al.*, 2021). Here, the local field potentials within the fly brain, or calcium activity within specific cell populations by utilising two-photon microscopy, can be recorded from a tethered fly, while simultaneously recording the fly's behaviour on an air-supported walking-ball via video-tracking. Fly behaviour can then be correlated to brain activity, which provides insight into which neurons or circuits are active during behaviour. Before these techniques in *Drosophila*, similar techniques had become commonplace in mammalian models to study the role of specific neurons in sleep control. For example, utilising EEG and EMG recordings to record sleep and micropipettes to record single-unit brain activity, researchers found that orexinergic neurons were active during waking and silent during sleep in head-fixed rats (Lee, Hassani and Jones, 2005).

While van Swinderen's approach is considered the current gold standard for recording brain activity and discovering neural correlates of sleep, this method has drawbacks (As mentioned in Chapter 1.6.4). A key issue is that flies are head tethered which begs the question of whether the fly's behaviour and neuronal activation patterns are consistent with a naturalist context. Logistically, the experimental setup is also expensive, technically challenging, and the experiments have low throughput. An ideal assay would involve recording brain activity with concurrent behavioural tracking but in a non-invasive manner in freely moving flies. Higher throughput would be an important additional breakthrough.

Luciferase reporter assays have the potential to be a viable alternative approach for recording neuronal activity in freely moving flies. Luciferases are a class of oxidative enzymes which generate bioluminescence and are found within a variety of organisms such as the firefly. Firefly Luciferase functions by catalysing the oxidation of luciferin (the substrate) to oxyluciferin with the help of ATP and mg2+ as a cofactor. This oxidation step results in oxyluciferin being in an excited state, which then returns to the ground state thereby releasing a photon of light. This light can then be detected by a sensitive luminometer or a charge-coupled device (CCD) camera. Luciferase assays were initially performed in a circadian context in *Drosophila*, whereby the coding region of

firefly Luciferase is expressed downstream of a circadian promoter of interest, such as the period gene promoter (Brandes *et al.*, 1996; R. Stanewsky *et al.*, 1997). This inserted into the fly then results in a fly which expresses Luciferase as a result of period promoter activity (due to CLOCK:CYCLE transcriptional activity) and generates bioluminescence downstream (with the addition of D-luciferin). As firefly Luciferase has a half-life of around three hours (Thompson, Hayes and Lloyd, 1991), rhythms in bioluminescence can be detected which correspond to rhythms in period transcription. This technique has been used extensively for studying circadian gene expression, whereby experiments can be performed over multiple days in freely moving flies (Tataroglu and Emery, 2014).

Beyond firefly Luciferase (FLuc), NanoLuc (NLuc) was recently discovered in *Oplophorus gracilirostris* and has been shown to generate orders of magnitude greater bioluminescence signals compared to FLuc (England, Ehlerding and Cai, 2016). NLuc also differs in multiple ways from FLuc (England, Ehlerding and Cai, 2016). Firstly, NLuc utilises furimazine (or analogues) as a substrate rather than D-luciferin for FLuc. Secondly, NLuc is substantially smaller in molecular weight (19 versus 61kDA for NLuc and FLuc, respectively). Thirdly, NLuc has an emission wavelength of 460nm (blue) versus 560nm (yellow-green) for FLuc. Finally, while FLuc requires both ATP and an mg2+ ion cofactor to convert luciferin to oxyluciferin and light, NLuc does not require additional factors in the conversion of furimazine to furimamide and light (England, Ehlerding and Cai, 2016). NLuc has yet to be introduced into Drosophila and it is currently unknow whether the luciferin substrate will be able to enter the fly brain.

In flies, two genetic constructs were created which can be expressed in specific cells of interest, are calcium sensitive, and lead to the downstream transcription of a gene of interest (Masuyama *et al.*, 2012; Gao *et al.*, 2015). In principle, these constructs can be combined with a Luciferase construct to create flies which express Luciferase within specific cells of interest as a result of high calcium activity within those cells. As calcium activity is a correlate of neuronal activity (Baker, Hodgkin and Ridgway, 1971; Tank *et al.*, 1988; Kerr *et al.*, 2000; Sabatini, Oertner and Svoboda, 2002), this provides a mechanism of using bioluminescence patterns to detect patterns of neuronal activity over time. This concept was shown to elicit rhythmic patterns of bioluminescence in specific circadian neuronal populations targeted (Guo *et al.*, 2016; Guo, Chen and Rosbash, 2017). However, beyond these two studies and their limited experimentation, there is currently no evidence that calcium signals can be detected within a variety of neuronal populations.

For this initial work, I aimed to study whether firefly Luciferase reporters could be used to detect rhythmic calcium activity (a correlate of neuronal activity) in various neuronal populations which have been implicated in sleep-wake regulation. This current method does not directly compete

with the gold-standard tethered fly brain recordings as transcriptional Luciferase assays detect broad patterns over longer timescales, while van Swinderen's techniques detect immediate changes over short timescales. Instead, the initial aim here is to study whether broad rhythmic patterns of brain activity can be found as correlates of sleep. As rest/sleep in flies occurs primarily in two major overarching periods over a 24-hour day (a siesta during the middle of the day, and a large period during most of the night), broad rhythmic patterns may be detectable during these periods from neurons involved in promoting sleep (or vice versa). In addition, I aimed to perform preliminary testing with novel NanoLuc expressing flies to test whether NanoLuc could become a viable alternative to firefly Luciferase.

5.1 CaLexA-LUC can generate rhythmic luciferase activity

Discovering neural correlates of sleep is an area of interest for the *Drosophila* sleep research field. Currently, the gold standard for recording brain activity and discovering neural correlates of sleep involves two-photon imaging with a tethered fly; however, this has drawbacks (See Chapter 1.8). Here, I looked to use an alternative approach to record brain activity in freely moving flies over long periods using luciferase reporter assays. For this purpose, I focused on CaLexA-LUC and TRIC-LUC which are two transcriptional reporters of calcium levels (See Chapter 2.11.1-2 for more information about the constructs). Both reporters function as calcium-sensitive transcription factors, leading to downstream luciferase expression in response to high calcium levels within the cell. The concept of calcium reporters comes from the biological principle that neuronal activity leads to increases in intracellular calcium (Baker, Hodgkin and Ridgway, 1971; Tank *et al.*, 1988; Kerr *et al.*, 2000; Sabatini, Oertner and Svoboda, 2002). CaLexA and TRIC have been previously demonstrated to successfully monitor rhythmic bioluminescence signals within circadian neurons in the fly brain (Guo *et al.*, 2016; Guo, Chen and Rosbash, 2017).

I began by selecting promoter-GAL4 drivers, which have been implicated in sleep-wake regulation, alongside some broadly expressing drivers (See Chapter 2.12 for more information). These drivers were then crossed to CaLexA-LUC or TRIC-LUC. The offspring were tested within a bioluminescence assay as previously described (Brandes *et al.*, 1996; Plautz *et al.*, 1997); see Chapter 2.13 for more info). In brief, each fly's bioluminescence was recorded around once per hour, and experiments were performed typically for more than five days. As previously shown, the raw bioluminescence values were detrended and normalised for each fly ((Levine *et al.*, 2002); See Chapter 2.13 for more info). This allowed flies to be averaged per genotype and subsequently compared across genotypes.

During the initial stages of this work, I struggled to maintain TRIC-LUC flies as they appeared poorly and did not survive well in our fly vials (See Chapter 5.4 for more information). I managed

to produce some promoter>TRIC-LUC flies that I tested in the bioluminescence assay. I found that the majority of driver>TRIC-LUC lines tested had bioluminescence levels that were not significantly above the driverless control (Ctr>TRIC-LUC; Appendix C Figure 1). While bioluminescence levels were low, some driver>TRIC-LUC lines had visually rhythmic patterns of normalised bioluminescence (Appendix C Figure 2). However, due to the issues with TRIC-LUC, I shifted my focus to CaLexA-LUC, whose flies were much healthier.

I first tabulated all tested driver>CaLexA-LUC for their average bioluminescence (relative light units RLU) from the detrended but non-normalised data against the rhythmic index (RI) of the normalised data averaged per genotype. Due to infrastructural issues with the bioluminescence plate reader, many driver>CaLexA-LUC experiments had sections of missing data. For the initial screen, these were filled (with the least intrusive forward fill method) to allow rhythmic analysis to be performed. The RI provides a value of how rhythmic a time series is considered to be, performed via autocorrelation as previously demonstrated ((Levine *et al.*, 2002); See Chapter 2.13 for more info). Some drivers were found to have high levels of bioluminescent signal (Table 5.1.1). As expected, these corresponded to broadly expressing drivers such as pan-neuronal (elav::GAL4), pan-glial (repo-GAL4), and pan-dopaminergic neurons (ple-GAL4). Concerningly, most driver>CaLexA-LUC lines had low levels of bioluminescence around the levels of the CaLexA-LUC control (Table 5.1.1).

Table 5.1.1 Many driver>CaLexA-LUC flies have low bioluminescence but strong 24-hour rhythmicity

The mean bioluminescence of raw (detrended) signal for the average of each genotype is compared with the rhythmic index (RI) of the detrended and normalised bioluminescence signal. Rhythmic index values above the threshold to be considered rhythmic are illustrated in bold.

Genotype	Expresses in	Sex	Sample Size (n)	Bioluminescence Mean (RLU)	Bioluminescence 95%CI (RLU)	Rhythmic Index	Rhythmic Index 95% CI Threshold (Above this is considered rhythmic)
Ctr	NA	M	13	73.58	14.27	**0.2519**	0.1426
Ctr	NA	F	13	99.80	13.39	0.1165	0.1426
MB504B	subset of PPL1 dopaminergic neurons	M	15	54.08	14.50	**0.4467**	0.1276
MB504B	subset of PPL1 dopaminergic neurons	F	15	67.74	11.30	**0.3029**	0.1276

Genotype	Expresses in	Sex	Sample Size (n)	Bioluminescence Mean (RLU)	Bioluminescence 95%CI (RLU)	Rhythmic Index	Rhythmic Index 95% CI Threshold (Above this is considered rhythmic)
MB461B	α'/β' lobes of the MB	M	23	71.84	16.48	**0.3490**	0.1411
MB461B	α'/β' lobes of the MB	F	22	48.62	6.26	0.1393	0.1411
LKR	Leucokinin receptor neurons	M	14	170.37	58.04	**0.4344**	0.1414
LKR	Leucokinin receptor neurons	F	14	419.31	127.41	**0.2533**	0.1414
ChAT	Pan cholinergic	M	10	63.69	12.11	**0.2964**	0.1426
ChAT	Pan cholinergic	F	10	130.54	28.80	**0.1686**	0.1426
Clk	Pan clock neurons	M	12	49.52	9.56	**0.3746**	0.1279
Clk	Pan clock neurons	F	17	94.91	28.31	**0.3298**	0.1279
Ilp2		M	7	1103.00	317.14	**0.1698**	0.1279
Ilp2		F	5	692.49	450.63	**0.2422**	0.1279
OK371	Pan glutamatergic	M	16	709.50	171.65	**0.2595**	0.1414
OK371	Pan glutamatergic	F	18	854.22	336.92	**0.2387**	0.1414
ple	Pan dopaminergic	M	8	1896.38	920.28	0.0877	0.1426
ple	Pan dopaminergic	F	12	1650.00	605.42	**0.3625**	0.1426
R23E10	dFB neurons	M	19	69.88	20.71	**0.3581**	0.1279
R23E10	dFB neurons	F	15	81.32	15.58	**0.4420**	0.1279
R54G12	Pan GABAergic	M	24	50.56	10.23	**0.3530**	0.1426
R54G12	Pan GABAergic	F	19	63.24	16.37	**0.3562**	0.1426
R56H10	R1-4 EB ring neurons	M	20	202.32	88.40	**0.3566**	0.1276
R56H10	R1-4 EB ring neurons	F	25	153.90	41.43	**0.3893**	0.1279
R70F10	Widely expressed in fly brain	M	13	92.41	33.46	**0.3652**	0.1276
R70F10	Widely expressed in fly brain	F	23	76.26	11.54	**0.4060**	0.1276
R92E10	Widely expressed in fly brain	M	18	121.64	56.39	**0.2753**	0.1411

Genotype	Expresses in	Sex	Sample Size (n)	Bioluminescence Mean (RLU)	Bioluminescence 95%CI (RLU)	Rhythmic Index	Rhythmic Index 95% CI Threshold (Above this is considered rhythmic)
R92E10	Widely expressed in fly brain	F	18	112.51	18.75	**0.3582**	0.1411
R92G05	Dopaminergic PPM3-EB neurons	M	11	48.40	7.30	**0.4283**	0.1279
R92G05	Dopaminergic PPM3-EB neurons	F	15	87.35	24.29	0.0884	0.1279
repo	Pan glial	M	9	2921.57	1032.58	**0.4006**	0.1429
repo	Pan glial	F	10	2044.14	840.17	**0.2817**	0.1429
elav	Pan neuronal	F	17	826.36	158.17	**0.4887**	0.1426

In the initial analysis, the CaLexA-LUC control (Ctr>CaLexA-LUC) males were considered rhythmic (Table 5.1.1). The normalised bioluminescence pattern over the experiment suggested that male and female Ctr>CaLexA-LUC flies have some visually rhythmic patterns (Figure 5.1.1A).

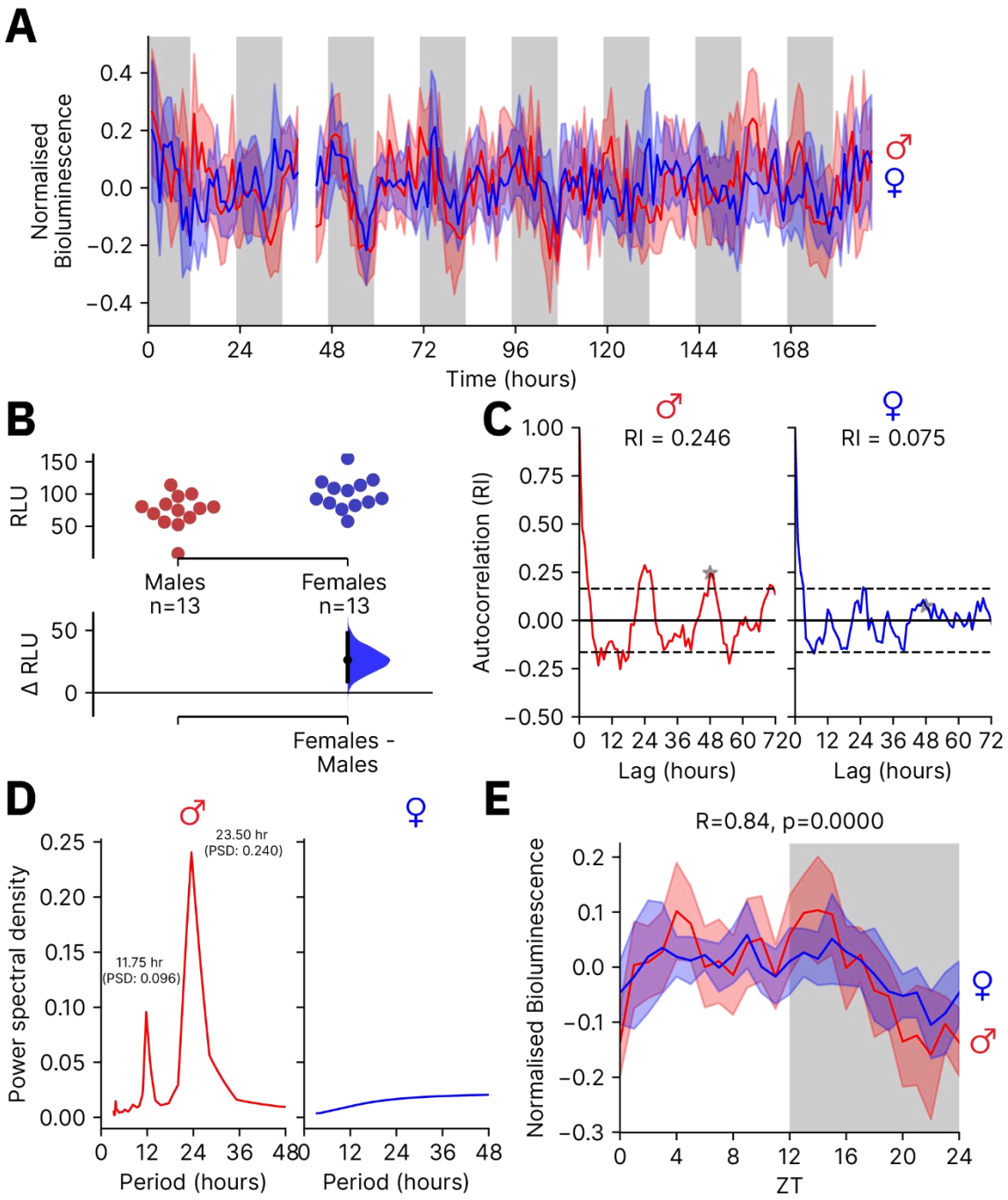

Figure 5.1.1 Control>CaLexA-LUC flies have some rhythmicity

(A) Average normalised and detrended bioluminescence signal from control>CaLexA-LUC males and females over the course of the experiment. Recordings are taken once per hour per fly. The solid line indicates the mean and the shaded area indicates the 95%CI. **(B)** DABEST plot comparing the mean bioluminescence (RLU) for female vs. male Control>CaLexA-LUC flies. The top section shows the raw data, with each dot indicating an individual flies' average bioluminescence from the detrended data. The bottom section shows the paired mean difference with 95% confidence intervals (CI) around the mean difference generated via bootstrap resampling. The summary data for (B) are shown in Appendix C Table 2. **(C)** Autocorrelation plots analysing the rhythmicity of males and females. Peaks of RI above the black dotted (95%CI) line suggest a rhythmic signal is

present. **(D)** MESA plot of the power spectral density at each potential period length for a given time series. Peaks at a given period(s) suggest that a periodic signal at this period length may be present. **(E)** Normalised bioluminescence for a given genotype averaged across all flies and all days for a typical 24-hour pattern of calcium activity. Pearson's R correlation coefficient and associated p-value was computed for the waveform of males and females and displayed above the plot. The sample size for (A-E) was 13 for control males and 13 for control females.

Females had slightly higher average raw bioluminescence (RLU), with a mean difference (Δ RLU) of 26.22 [95%CI 9.22, 47.57] (Figure 5.1.1B). Autocorrelation analysis suggested that males had an RI of 0.246, while females had an RI of 0.075 (Figure 5.1.1C). To confirm the period of a rhythm, I performed Maximum Entropy Spectral Analysis (MESA, See Chapter 2.13 for more info). MESA suggested a peak at 23.50 hours for male flies with a power spectral density (PSD) of 0.240 and a second peak at 11.75 hours with a PSD of 0.096 (Figure 5.1.1D). As the RI suggested, females had no noticeable period seen in MESA (Figure 5.1.1D). While the rhythmic analysis suggested that no noticeable rhythm in females could be detected, the pattern across the 24-hour day was similar to that of males, with a Pearson's correlation coefficient of 0.84 (Figure 5.1.1E).

During this preliminary CaLexA-LUC screen, I found that pan-neuronal expression (with elav::GAL4) had strong bioluminescence signal and a high RI (Table 5.1.1). While I was only able to test females during this preliminary screen, these flies had a visually rhythmic pattern of bioluminescence (Figure 5.1.2A). Compared to the driverless CaLexA female control (Ctr>CaLexA-LUC), the bioluminescence signal was significantly greater in elav>CaLexA-LUC, with a mean difference (Δ RLU, each fly is averaged across the whole experiment), of 726.56 [95%CI 587.42, 896.97] (Figure 5.1.2B). Autocorrelation analysis demonstrated an RI of 0.550 (Figure 5.1.2C), while MESA suggested a period of 24.33 hours with a PSD of 0.173 (Figure 5.1.2D). MESA also suggested a period of 12.17 with a PSD of 0.104.

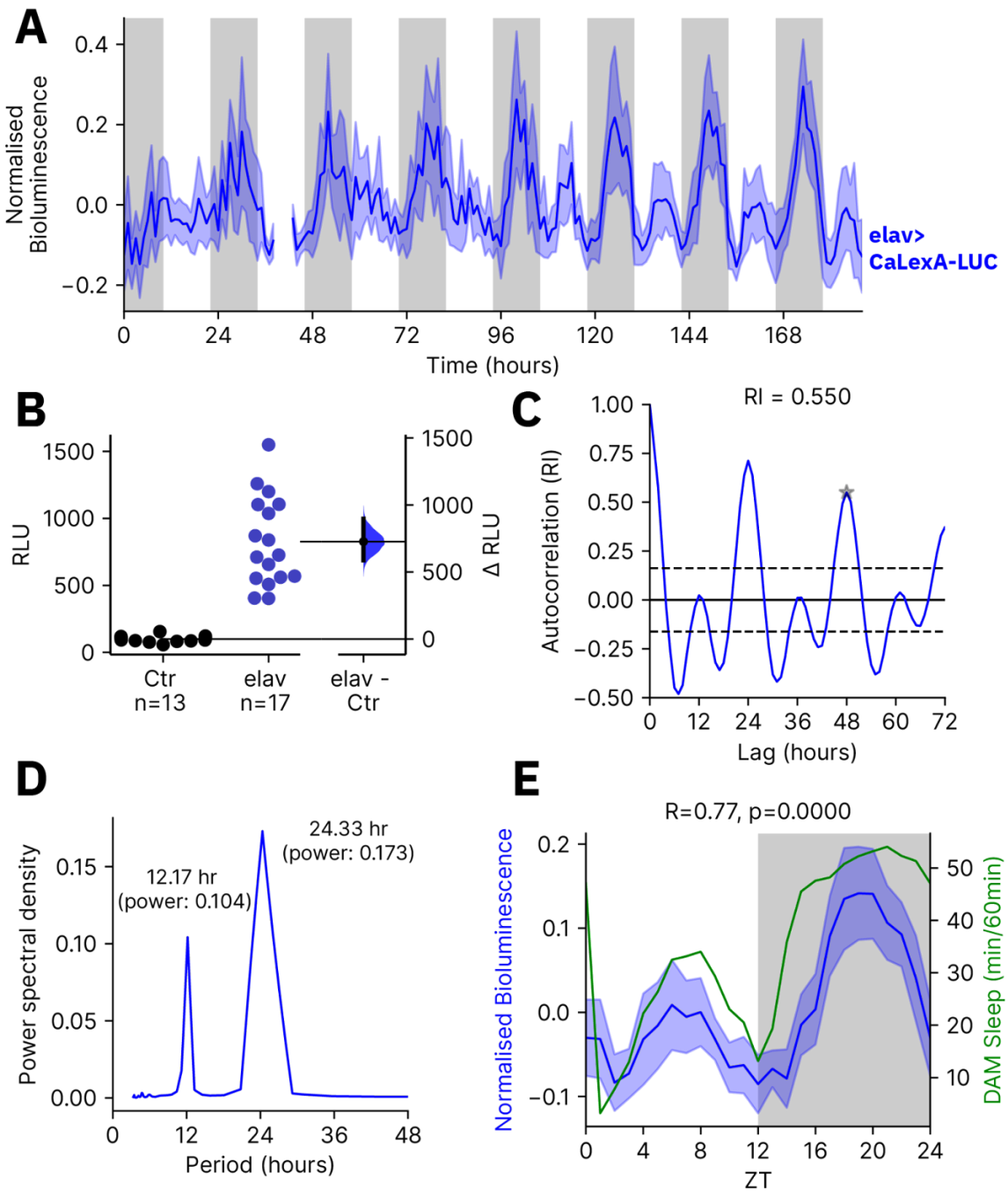

Figure 5.1.2 Pan-neuronal calcium activity is highly rhythmic

(A) Average normalised and detrended bioluminescence signal from elav>CaLexA-LUC females over the course of the experiment. Recordings are taken once per hour per fly. The solid line indicates the mean and the shaded area indicates the 95%CI. **(B)** DABEST plot comparing the mean bioluminescence (RLU) for female elav>CaLexA-LUC vs. female Ctr>CaLexA-LUC flies. The top section shows the raw data, with each dot indicating an individual flies' average bioluminescence from the detrended data. The bottom section shows the paired mean difference with 95% confidence intervals (CI) around the mean difference generated via bootstrap resampling. The summary data for (B) are shown in Appendix C Table 3. **(C)** Autocorrelation plots analysing the rhythmicity of the normalised and averaged bioluminescence. Peaks of RI above the

black dotted (95%CI) line suggest a rhythmic signal is present. The third peak is selected for the RI metric **(D)** MESA plot of the power spectral density at each potential period length for a given time series. Peaks at a given period(s) suggest that a periodic signal at this period length may be present. **(E)** Normalised bioluminescence for elav>CaLexA-LUC averaged across all flies and all days for a typical 24-hour pattern of calcium activity, compared against levels of DAM measured sleep for the same genotype. Pearson's R correlation coefficient and associated p-value was computed for the comparison and displayed above the plot. The sample size for (A, C, &D) was 17 female flies. The sample size for elav>CaLexA-LUC female flies tested in DAM was 32.

The normalised time series plots demonstrated the presence of two peaks in bioluminescence, one during the day and a major one at night (Figure 5.1.2A). MESA also suggested a substantial period of around 12 hours (Figure 5.1.2D). This was interesting as the daily waveform of bioluminescence resembled a daily sleep/inactivity recording of wild-type flies (e.g., via 5-min inactivity in DAM or SS/SSL in Trumelan). To further illustrate this similarly, I wanted to test whether the behaviour of these flies correlates to the bioluminescence. The ideal experiment would be to record the behaviour of flies during the luciferase assay experiments; however, this was not currently possible. As these experiments were performed in a different location to the Trumelan behavioural assay, this could also not be used. I, therefore, tested the same genotype (elav>CaLexA-LUC) within a DAM assay within the same room and with the same conditions that the luciferase assay was performed (See Chapter 2.14 for more information). As hypothesised, the bioluminescence pattern had a relatively strong correlation with the levels of DAM recorded sleep averaged over a 24-hour day, with a correlation coefficient (Pearson's R) of 0.77 (Figure 5.1.2E).

Next, I wondered if other driver>CaLexA-LUC lines had a waveform similar to elav>CaLexA-LUC. I performed cross-correlation of the 24-hour averaged bioluminescence patterns across genotypes. I generated a heatmap of the cross-correlation (Pearson's R). I utilised the heatmap with a hierarchical clustering option (Seaborn clustermap) to illustrate the groups of genotypes with similar waveforms (Figure 5.1.3). There were clear clusters of genotypes with correlated calcium activity patterns in both males and females. While I hypothesised that clusters of similar calcium activity patterns would correspond to the putative role of the cells targeted, I found that this was not the case in either males (Figure 5.1.3A) or females (Figure 5.1.3B).

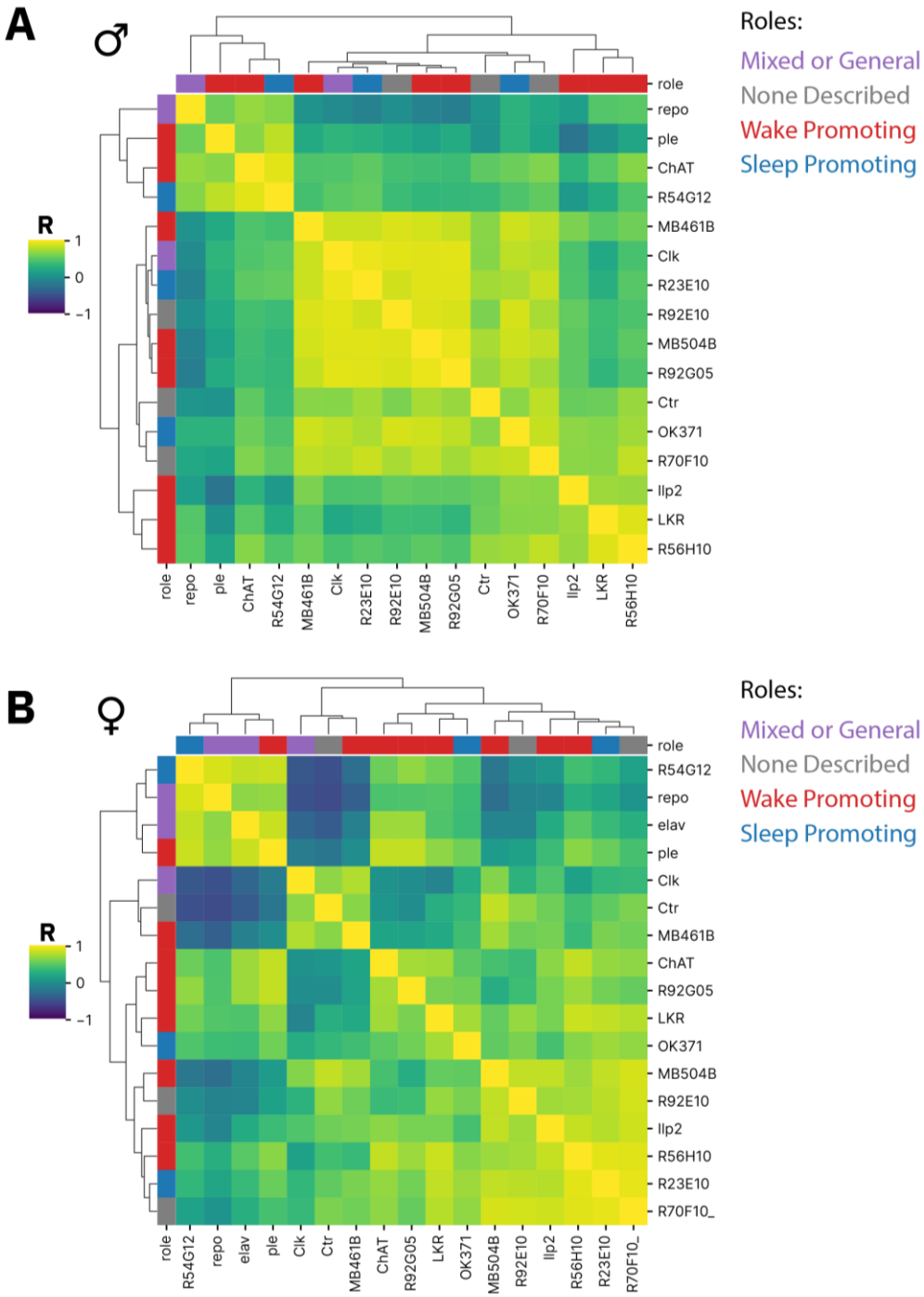

Figure 5.1.3 Cross-correlation illustrates pockets of correlated driver>CaLexA-LUC calcium activity patterns

The correlation coefficient (Pearson's R) for each genotype compared to each other and displayed as a clustered heatmap for males **(A)** and females **(B)**. The normalised bioluminescence for each genotype is averaged across all flies and all days for a typical 24-hour pattern of calcium activity. These are then compared against one another to compute the Pearson's R correlation coefficients. The putative role for each driver (in terms of sleep-wake regulation) is shown alongside the heatmap. The sample sizes for each driver>CaLexA-LUC line is found in Table 5.1.1.

The cross-correlation heatmap in Figure 5.1.3B suggested that a collection of drivers had correlated daily calcium activity patterns to elav>CaLexA-LUC. I plotted elav>CaLexA-LUC alongside the three lines suggested in the correlation heatmap to be highly similar (Figure 5.1.4)

Interestingly, one was the GABAergic driver R54G12-GAL4 (Figure 5.1.4A). GABA is a sleep-promoting neurotransmitter in both mammals (Gallopin *et al.*, 2000; Gong *et al.*, 2004; Benedetto, Chase and Torterolo, 2012) and *Drosophila* (Agosto *et al.*, 2008; Dissel *et al.*, 2015). The pan-glial driver, repo-GAL4, also had highly similar daily calcium activity patterns as pan-neuronal (Figure 5.1.4B). The calcium activity pattern was highly similar but lagged relative to elav::GAL4 by around an hour. Glial cells are known to be involved in sleep-wake regulation in both mammals (Halassa *et al.*, 2009; Schmitt *et al.*, 2012; Xie *et al.*, 2013) and *Drosophila* (Seugnet *et al.*, 2011; Farca Luna, Perier and Seugnet, 2017), although this field of study is less well studied than for neuronal populations. The pan-dopaminergic driver ple-GAL4 also had a similar daily calcium activity pattern (Figure 5.1.4C). This was unexpected given that dopaminergic neurons are considered wake-promoting (Liu *et al.*, 2012; Ueno *et al.*, 2012; Sitaraman, Aso, Rubin, *et al.*, 2015).

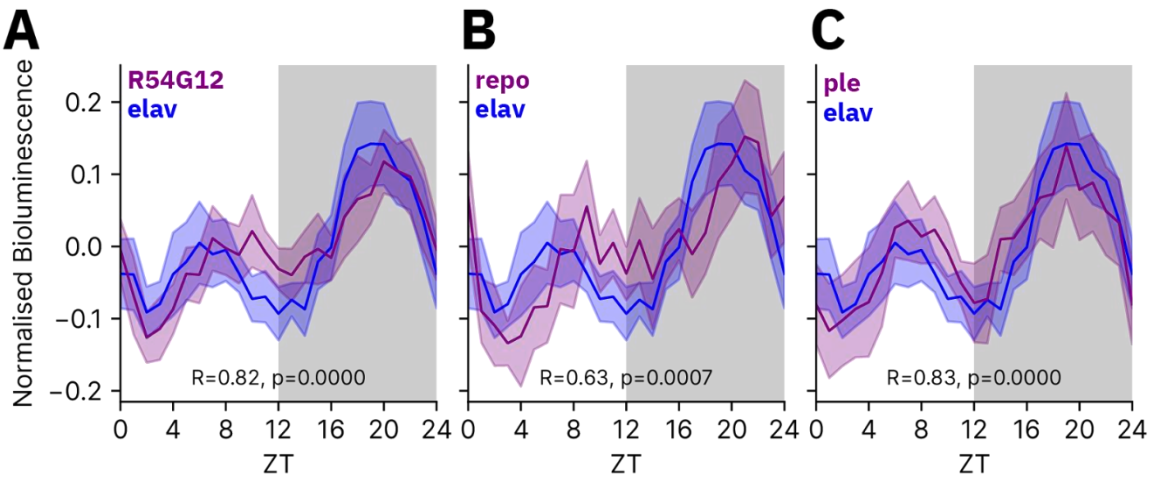

Figure 5.1.4 Pan-neuronal, GABAergic, glial, and dopaminergic calcium activity are highly correlated

The comparison of average daily calcium activity in elav>CaLexA-LUC (n=17) vs. R54G12>CaLexA-LUC (n=19) **(A)**, repo>CaLexA-LUC (n=10) **(B)**, or ple>CaLexA-LUC (n=12) **(C)**. The normalised bioluminescence for each genotype was averaged across all flies and all days for a typical 24-hour pattern of calcium activity, compared against levels of DAM measured sleep for the same genotype. Pearson's R correlation coefficient and associated p-value was computed for the comparison and displayed above the plot. The solid line indicates the mean and the shaded area indicates the 95%CI.

The cross-correlation heatmaps also highlighted two additional features of the driver>CaLexA calcium activity patterns recorded. Firstly, there appeared to be various sets of waveforms, which is seen by the different clusters of correlations. Secondly, the heatmaps were not consistent between males and females, suggesting that the waveforms of a given driver>CaLexA-LUC line may differ between sex. Research studies using *Drosophila* often focus on one sex (typically males). A recent study showed that the calcium profile of a subset of circadian neurons differs between males and females (Guo *et al.*, 2016). They suggest that the sexual dimorphism in the calcium pattern was not seen in other driver>CaLexA-LUC lines, although the data was not shown. As I had tested most of the driver>CaLexA-LUC combinations in males and females, this provided an interesting avenue to analyse whether the rhythmic calcium signals were consistent across sex. For this purpose, I compared the 24-hour averaged patterns of normalised bioluminescence across each genotype and computed the correlation (Pearson's R; Figure 5.1.5). In addition, I measured the peak and trough locations for each genotype (Table 5.1.2). Here, I found that some drivers, such as the cholinergic driver ChAT-GAL4, had relatively consistent patterns between males and females. ChAT>CaLexA-LUC males and females had two major bioluminescence peaks and troughs (Figure 5.1.5). The troughs were consistent, with a trough at ZT1 for both sexes and a trough at ZT11 in females and 12 in males (Table 5.1.2). Both sexes had a major peak of bioluminescence signal at ZT16, while the first peak differed between the sexes, with a peak at ZT4 in males and ZT7 in females. Similarly, R56H10>CaLexA-LUC flies had relatively consistent two peaks of bioluminescence signal (Figure 5.1.5), with a major peak of at ZT15 in males and ZT16 in females, and troughs of ZT11 and ZT23 in both sexes. As with ChAT> CaLexA-LUC, males had an earlier peak of bioluminescence at ZT4, while this peak occurred at ZT8 in females. Many drivers, however, had sexually dimorphic patterns of normalised bioluminescence. For example, the glial driver repo-GAL4 had strong bimodal peaks during the middle of the day and middle of the night in males (Figure 5.1.5). These bioluminescence peaks occurred at ZT5 and ZT16, with troughs at ZT12 and ZT0/24 (Table 5.1.2). In contrast, females had lower calcium activity during the day and peaked late at night as the male's calcium activity declined. These bioluminescence peaks occurred at ZT9 and ZT21, with troughs at ZT3 and ZT14 (Table 5.1.2).

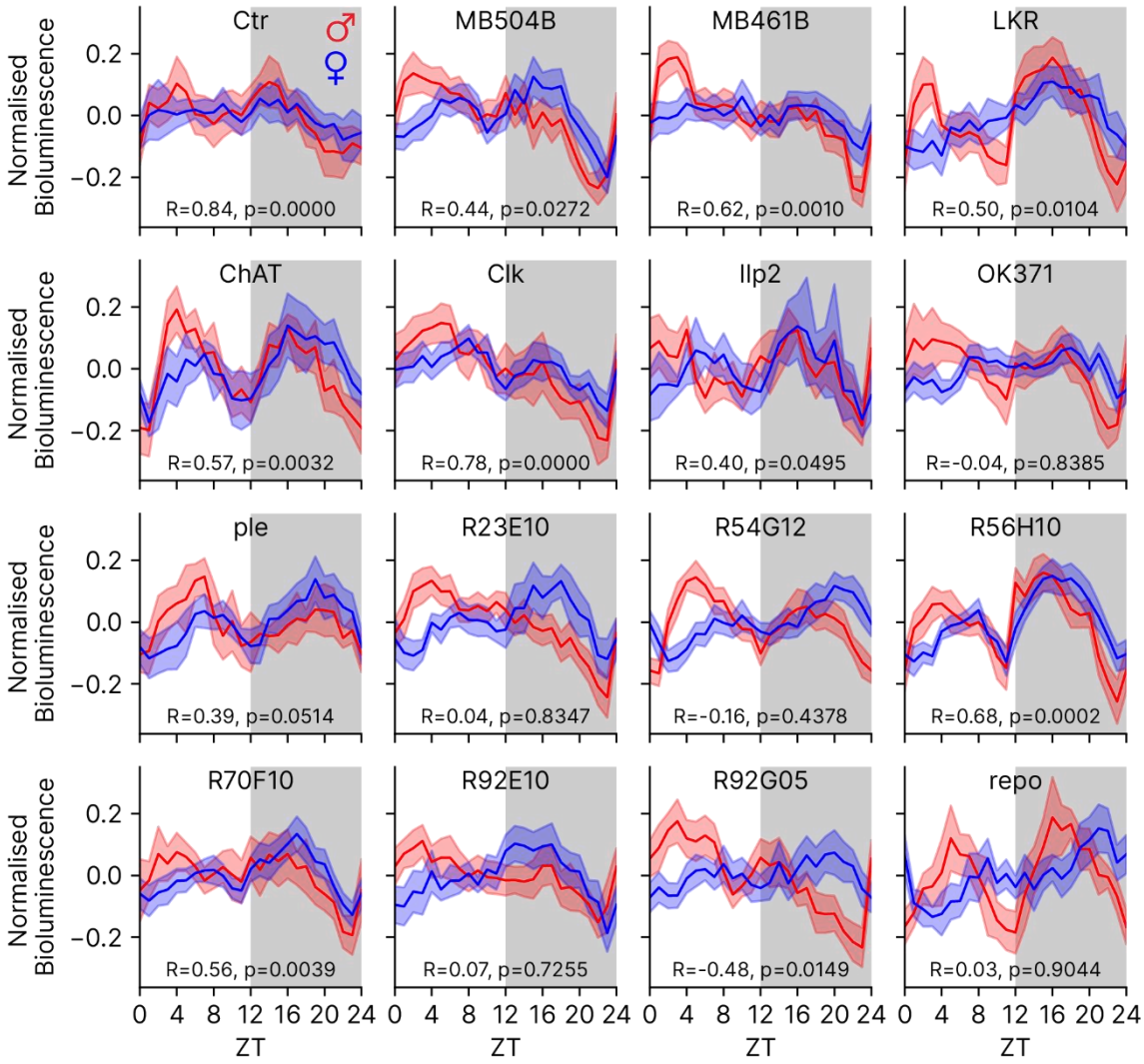

Figure 5.1.5 Many cell populations have sexually dimorphic daily patterns of calcium activity

The normalised bioluminescence for a given driver>CaLexA-LUC genotype averaged across all flies and all days for a typical 24-hour pattern of calcium activity. Both sexes are displayed on the same subplot, and the correlation coefficient (Pearson's R) and associated p-value between the two is shown. The solid line indicates the mean and the shaded area indicates the 95%CI.

Table 5.1.2 Waveform parameters for the 24-hour averaged bioluminescence data for driver>CaLexA-LUC lines illustrated in Figure 5.1.5. Peaks and troughs were located by visual inspection.

Genotype	Sex	Sample Size (n)	Number of peaks	Peak Location 1 (ZT)	Peak Location 2 (ZT)	Number of Troughs	Trough Location 1 (ZT)	Trough Location 2 (ZT)
Ctr>CaLexA-LUC	M	13	2	4	14	2	8	22
Ctr>CaLexA-LUC	F	13	0	NA	NA	0	NA	NA
MB504B>CaLexA-LUC	M	15	2	2	12	2	9	22
MB504B>CaLexA-LUC	F	15	2	7	15	2	10	23
MB461B>CaLexA-LUC	M	23	1	3	NA	1	23	NA
MB461B>CaLexA-LUC	F	22	1	10	NA	1	23	NA
LKR>CaLexA-LUC	M	14	2	3	16	2	11	23
LKR>CaLexA-LUC	F	14	1	16	NA	1	4	NA
ChAT>CaLexA-LUC	M	10	2	4	16	2	1	12
ChAT>CaLexA-LUC	F	10	2	7	16	2	1	11
Clk>CaLexA-LUC	M	12	2	6	16	2	11	23
Clk>CaLexA-LUC	F	17	2	8	15	2	12	23
Ilp2>CaLexA-LUC	M	7	2	4	16	2	6	23
Ilp2>CaLexA-LUC	F	5	2	5	16	2	12	23
OK371>CaLexA-LUC	M	16	2	1	17	2	11	22
OK371>CaLexA-LUC	F	18	2	7	18	1	23	NA
ple>CaLexA-LUC	M	8	2	7	19	2	11	24
ple>CaLexA-LUC	F	12	2	7	19	2	1	12
R23E10>CaLexA-LUC	M	19	1	4	NA	1	23	NA
R23E10>CaLexA-LUC	F	15	2	7	18	2	11	23
R54G12>CaLexA-LUC	M	24	2	5	17	2	1	12
R54G12>CaLexA-LUC	F	19	2	10	20	2	2	11
R56H10>CaLexA-LUC	M	20	2	4	15	2	11	23
R56H10>CaLexA-LUC	F	25	2	8	16	2	11	23
R70F10>CaLexA-LUC	M	13	2	4	16	2	11	23

R70F10>CaLexA-LUC	F	23	2	8	17	2	11	23
R92E10>CaLexA-LUC	M	18	1	3	NA	1	22	NA
R92E10>CaLexA-LUC	F	18	1	17	NA	1	23	NA
R92G05>CaLexA-LUC	M	11	2	3	12	2	9	23
R92G05>CaLexA-LUC	F	15	2	8	20	2	12	24
repo>CaLexA-LUC	M	9	2	5	16	2	12	24
repo>CaLexA-LUC	F	10	2	9	21	2	3	14

Alongside broadly expressing drivers, I tested some drivers with more restricted expression within only a few neurons in the brain. During the CaLexA-LUC screen, the restricted driver MB540B stood out as having a highly rhythmic signal in male flies (Table 5.1.1, orange arrow). Unfortunately, large chunks of time points at the beginning of the experiment were lost due to infrastructural errors with the bioluminescence plate reader. These chunks were removed for follow-up analysis, and the autocorrelation and MESA were performed on the subsequent data. Both males and females appeared to have rhythmic activity throughout the experiment (Figure 5.1.6A).

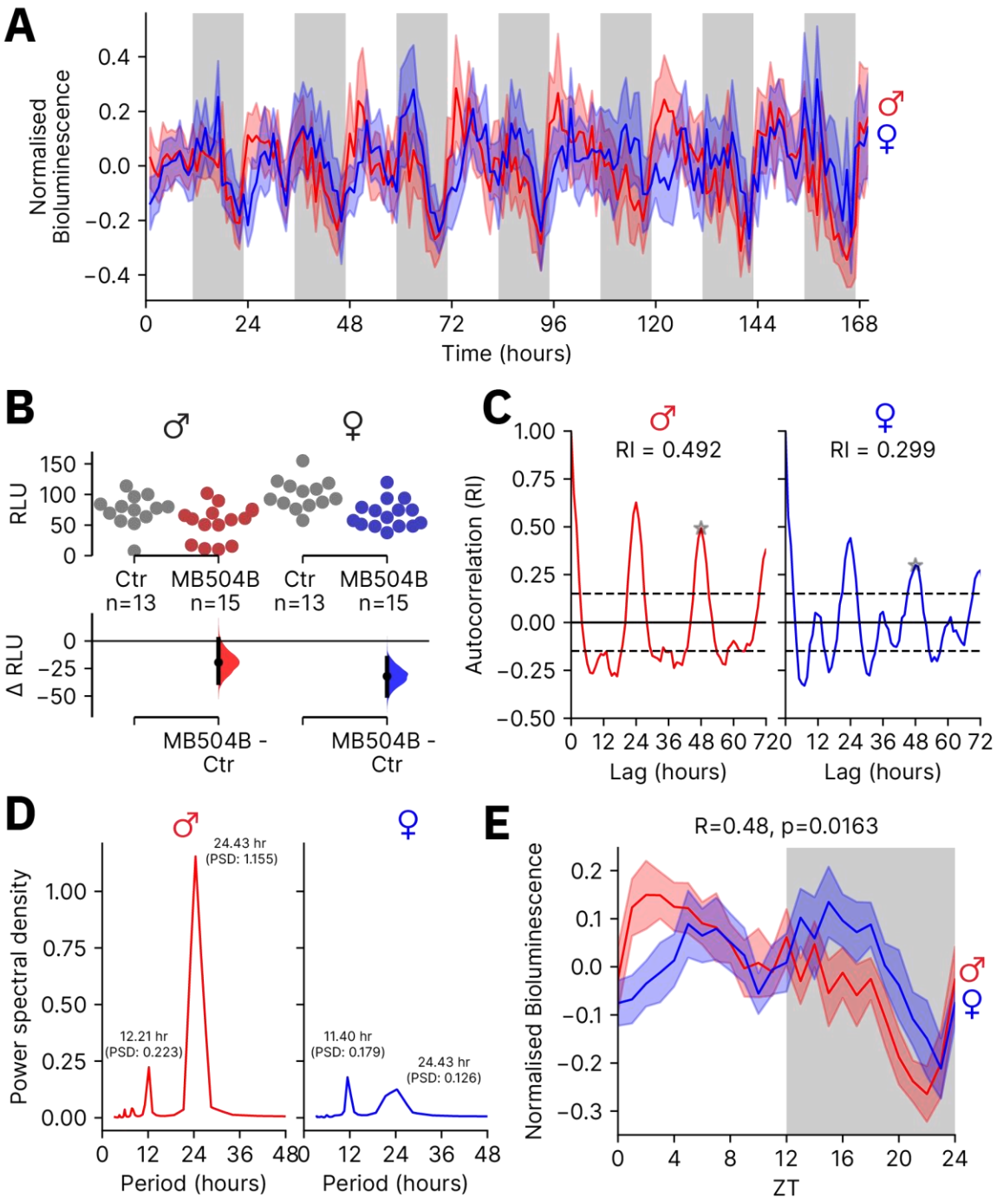

Figure 5.1.6 Highly rhythmic signal can be uncovered in restricted driver>CaLexA-LUC lines such as MB504B

(A) Average normalised and detrended bioluminescence signal from MB504B>CaLexA-LUC males and females over the course of the experiment. Recordings are taken once per hour per fly. The solid line indicates the mean and the shaded area indicates the 95%CI. **(B)** DABEST plot comparing the mean bioluminescence (RLU) for male and female MB504B>CaLexA-LUC flies vs. the Ctr>CaLexA-LUC flies of the same sex. The top section shows the raw data, with each dot indicating an individual flies' average bioluminescence from the detrended data. The bottom section shows the paired mean difference with 95% confidence intervals (CI) around the mean

difference generated via bootstrap resampling. The summary data for **(B)** are shown in Appendix C Table 4. **(C)** Autocorrelation plots analysing the rhythmicity of males and females. Peaks of RI above the black dotted (95%CI) line suggest a rhythmic signal is present. **(D)** MESA plot of the power spectral density at each potential period length for a given time series. Peaks at a given period(s) suggest that a periodic signal at this period length may be present. **(E)** Normalised bioluminescence for a given genotype averaged across all flies and all days for a typical 24-hour pattern of calcium activity. Pearson's R correlation coefficient and associated p-value was computed for the waveform of males and females and displayed above the plot. The sample sizes for (A, C, & D-E) were 15 for MB504B>CaLexA-LUC males, and 15 for MB504B>CaLexA-LUC females.

As the initial screening plot suggested, the overall signal strength for both males and females was around the same or lower than in the sex-matched Ctr>CaLexA-LUC, with mean differences (Δ RLU) of -19.5 [95%CI -38.04, 1.75] and -32.06 [95%CI -49.72, -15.44], respectively (Figure 5.1.6B). The autocorrelation analysis suggested that males and females were highly rhythmic, with an RI of 0.492 and 0.299, respectively (Figure 5.1.6C). MESA confirmed a period of around 24 hours was seen in both cases, with males having a peak of 1.155 PSD at 24.43 hours and a peak at 12.21 hours with a PSD of 0.223 (Figure 5.1.6D). Females had a weaker signal, but peaks at 24.43 and 11.40 were seen, with PSDs of 0.126 and 0.179, respectively (Figure 5.1.6D). By overlaying the two time series plots of the daily calcium activity patterns, it was clear that there were some similarities between males and females, such as both having a sharp decline and trough of activity late at night (Figure 5.1.6E). However, there were also some differences, with males having a more substantial peak during the early day while females had more of a bimodal calcium activity pattern.

5.2 NanoLuc-based reporters as a potential upgrade to firefly Luciferase

The preliminary luciferase testing illustrated that broadly expressed drivers, such as pan-neuronal or a broad dopaminergic driver, can elicit strong bioluminescence signals well above background levels. Restricted drivers such as MB504B demonstrated that a rhythmic signal could be detected; however, the signal was low. The signal was as low in MB504B>CaLexA-LUC as in Control>CaLexA-LUC. While rhythmic signal was still seen with MB504B, the low signal strength suggests that firefly luciferase is not ideal for restricted populations of cells.

NanoLuc (NLuc) is a recently discovered luciferase that generates orders of magnitude greater bioluminescence signal than firefly luciferase (FLuc) (England, Ehlerding and Cai, 2016). I decided to test whether NLuc-based reporters could be a viable alternative and improvement over FLuc-based ones. These NLuc-based reporters (and NLuc in general) have not yet been demonstrated in *Drosophila*. As a result, it was unclear whether the substrate would be able to cross the fly blood-brain barrier and what the characteristics of any signal generated would be. I selected three NLuc-based reporters, which are fusions of NLuc to fluorescent proteins (Chu *et al.*, 2016; Suzuki *et al.*, 2016). I also selected two NLuc-based reporters that were further modified to be calcium-sensitive by adding calmodulin and M13 domains (Suzuki *et al.*, 2016; Oh *et al.*, 2019).

As the NLuc-based reporters had not been created in flies before, I began by creating these flies (See Chapter 2.15 for more information). At the time of this line of work, I was based in Singapore and could not test the NLuc-based reporter flies. My Singapore-based laboratory (and the surrounding laboratories) did not have a suitable bioluminescence plate reader to perform tests on these flies. As a result, I shipped the NLuc-based reporter flies to my laboratory in Southampton (Herman Wijnen Lab), and final-year undergraduate students performed the subsequent experiments.

Due to limitations in substrate availability (high cost), it was decided to limit testing to GeNL and GeNLCa as these are the most similar to firefly luciferase in terms of the wavelength of photons emitted. I suggested that elav::GAL4 should be used for the driver, as I already had clear data showing it produces strong rhythmic activity with CaLexA-LUC; however, the preliminary testing was performed with nsyb-GAL4. nsyb-GAL4 (n-synaptobrevin) is a pan-neuronal driver (Bushey, Tononi and Cirelli, 2009). The students first recorded the bioluminescence profiles of nsyb>CaLexA-LUC (method as previously described, Chapter 2.13). I first plotted the students' raw bioluminescence data for nsyb>CaLexA-LUC (Figure 5.2.1). The bioluminescence began with RLU peaks of around 1000 or less in both males and females. The bioluminescence signal rapidly dropped until a steady state was reached around 10-30 hours from the start of the experiment.

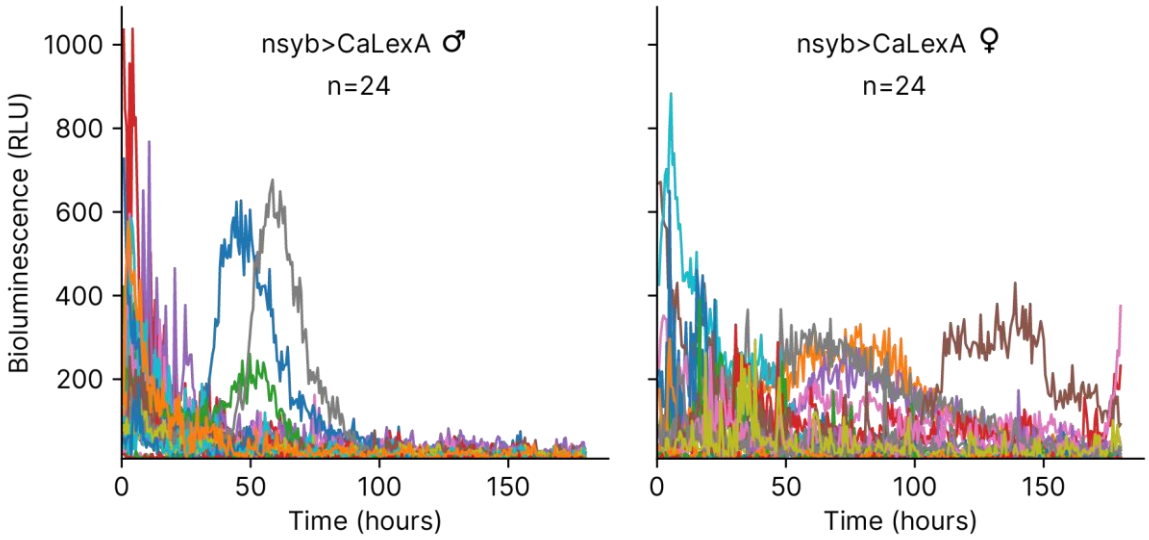

Figure 5.2.1 Raw bioluminescence for individual nsyb>CaLexA-LUC flies

The raw bioluminescence (RLU) over time for individual nsyb>CaLexA-LUC males and females. Experiments were carried out as per Chapter 2.13 by third year undergraduate students as part of their final year laboratory projects.

I next analysed the students' raw bioluminescence data for nsyb>GeNL (Figure 5.2.2). These flies should directly convert nsyb promoter activity to a bioluminescence output via GeNL. Three sets of experiments with GeNL were performed, one with a low level of the substrate FFz (0.05mM, Figure 5.2.2A), one with a medium level (0.1mM, Figure 5.2.2B), and one with a high level (0.67mM, Figure 5.2.2C). As with nsyb>CaLexA-LUC, individual male and female flies were plotted. In contrast to nsyb>CaLexA-LUC, nsyb>GeNL produced orders of magnitude greater signals in all three levels of FFz substrate addition (Figure 5.2.2 compared to Figure 5.2.1).

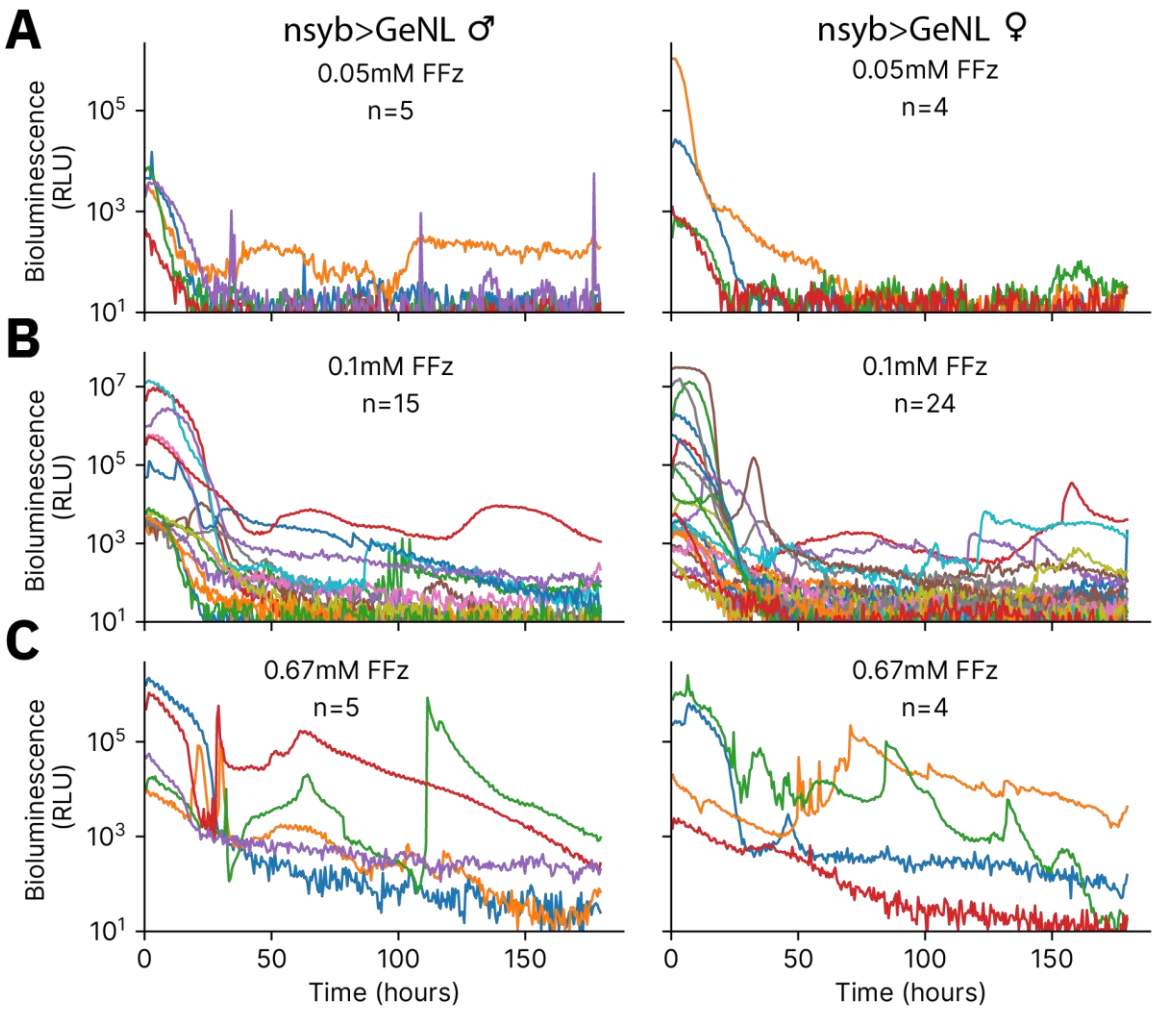

Figure 5.2.2 Raw bioluminescence for individual nsyb>GeNL flies

The raw bioluminescence (RLU) over time for individual nsyb>GeNL males and females with the addition of 0.05mM FFz **(A)**, 0.1mM FFz **(B)**, or 0.67mM FFz **(C)**. Experiments were carried out as per Chapter 2.13 by third year undergraduate students as part of their final year laboratory projects.

During the first ten hours of recording, nsyb>GeNL male flies with 0.05mM, 0.1mM, or 0.67mM concentrations of FFz had significantly higher bioluminescence than nsyb>CaLexA-LUC, with mean differences (Δ log10 RLU) of 1.14 [95%CI 0.48, 1.47] and 2.47 [95%CI 1.87, 3.26] and 2.84 [95%CI 2.08, 3.77], respectively (Figure 5.2.3A). Similarly, nsyb>GeNL female flies with low, medium, or high concentrations of FFz had significantly higher bioluminescence than nsyb>CaLexA-LUC, with mean differences (Δ log10 RLU) of 2.077 [95%CI 1.02, 3.37] and 2.36 [95%CI 1.78, 3.05] and 2.96 [95%CI 1.80, 4.01], respectively (Figure 5.2.3A).

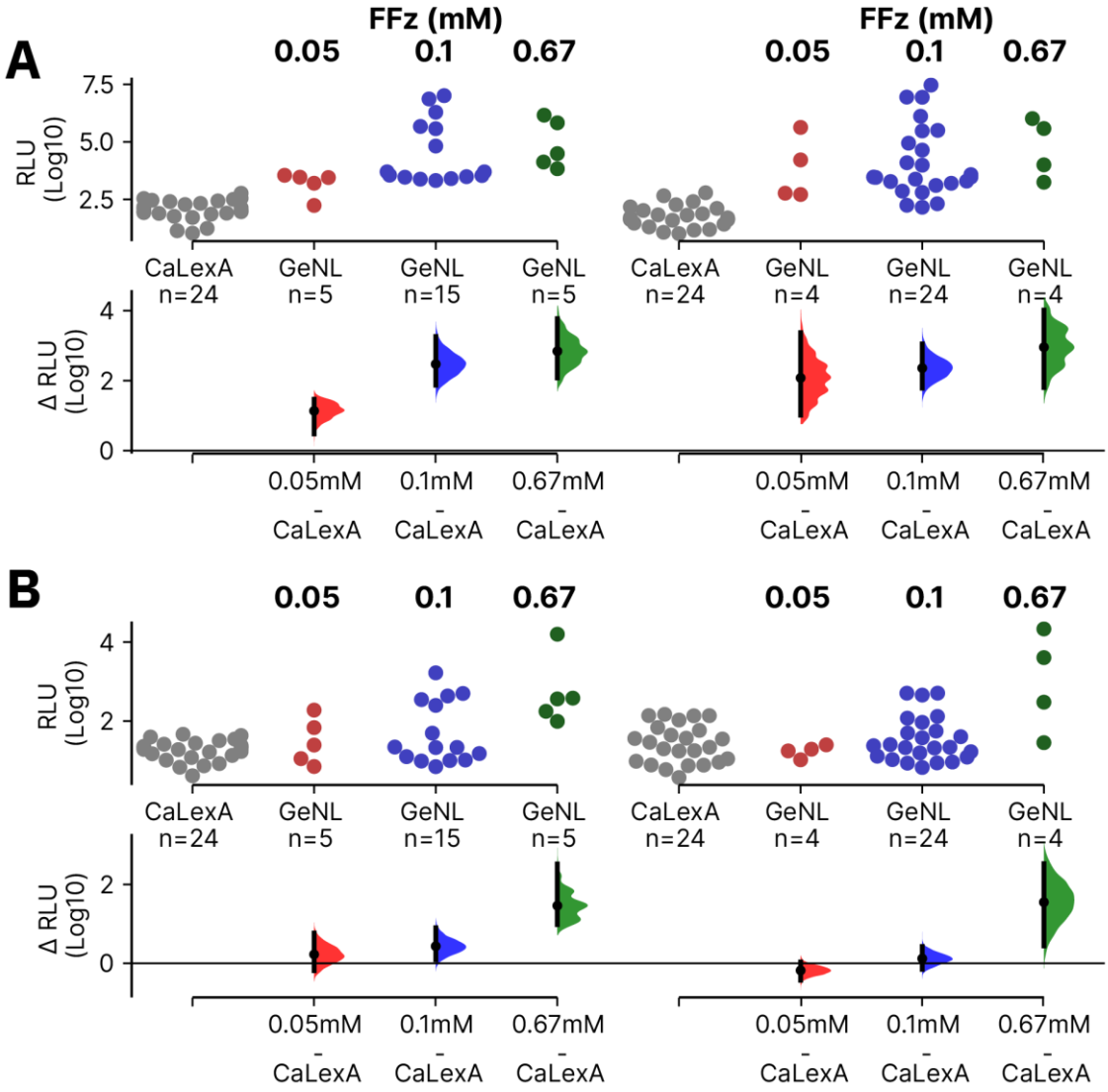

Figure 5.2.3 GeNL signal rapidly decays to FLuc levels

DABEST comparison of average raw bioluminescence (RLU) for the first ten hours of recording **(A)** and during a late stage of the experiment (100-115 hours from the start) **(B)** in nsyb>CaLexA-LUC versus nsyb>GeNL with three varying concentrations of FFz. Data was analysed from the raw bioluminescence data collected by third year undergraduate students as part of their final year laboratory projects. (A-B) The top section shows the raw unpaired data, with each dot indicating an individual. The bottom section shows the mean difference with 95% confidence intervals (CI) around the mean difference between comparisons generated via bootstrap resampling. The summary data for (A-B) are shown in Appendix C Table 5-6.

However, while the signal began high, it rapidly declined to FLuc levels within the first few hours of the experiment (Figure 5.2.2). As a comparison, during the hundredth to hundred and tenth hours of recording, nsyb>GeNL male flies with low, medium, or high concentrations of FFz had similar bioluminescence levels to nsyb>CaLexA-LUC, with mean differences (Δ log10 RLU) of 0.22

[95%CI -0.19, 0.77] and 0.43 [95%CI 0.09, 0.90] and 1.46 [95%CI 0.98, 2.52], respectively (Figure 5.2.3B). Similarly, nsyb>GeNL female flies with low, medium, or high concentrations of FFz had similar bioluminescence levels to nsyb>CaLexA-LUC, with mean differences (Δ log10 RLU) of -0.18 [95%CI -0.43, 0.03] and 0.12 [95%CI -0.15, 0.43] and 1.55 [95%CI 0.44, 2.53], respectively (Figure 5.2.3B).

The student's raw bioluminescence data for nsyb>GeNLCa showed similar results to the GeNL testing (Figure 5.2.4). These flies should be comparable to CaLexA-LUC in that the bioluminescence should result from calcium activity within the cells expressing the construct. Experiments with GeNLCa were performed with the same three concentrations of FFz. As with nsyb>GeNL, nsyb>GeNLCa produced high bioluminescence counts with all three concentrations of FFz substrate addition (Figure 5.2.4).

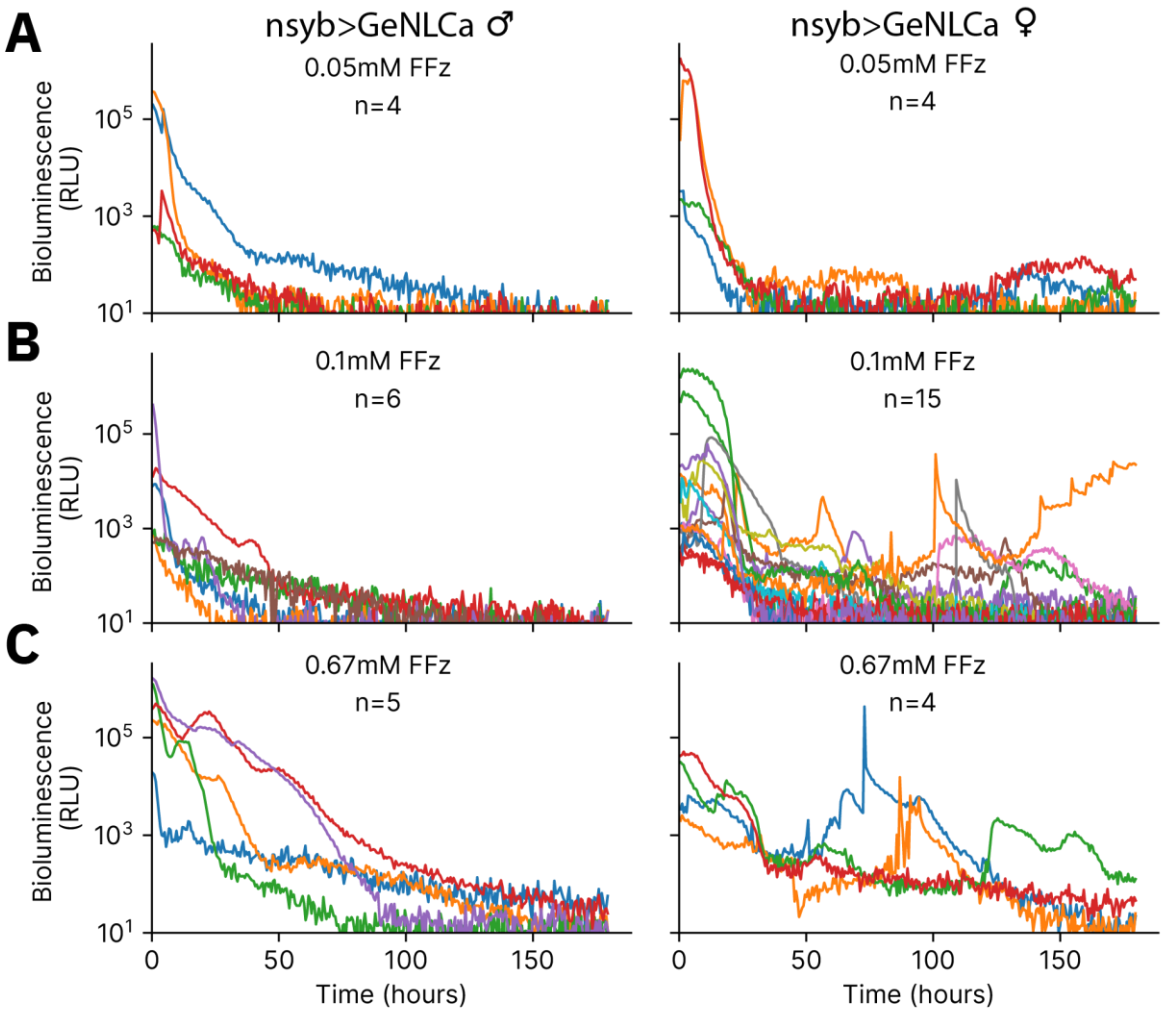

Figure 5.2.4 Raw bioluminescence for individual nsyb>GeNLCa flies

The raw bioluminescence (RLU) over time for individual nsyb>GeNLCa males and females with the addition of 0.05mM FFz **(A)**, 0.1mM FFz **(B)**, or 0.67mM FFz **(C)**. Experiments were carried out as

per Chapter 2.13 by third year undergraduate students as part of their final year laboratory projects.

During the first ten hours of recording, nsyb>GeNLCa male flies with 0.05mM, 0.1mM, or 0.67mM of FFz had significantly higher bioluminescence than nsyb>CaLexA-LUC, with mean differences (Δ log10 RLU) of 1.84 [95%CI 0.72, 2.97] and 1.30 [95%CI 0.70, 2.11] and 3.06 [95%CI 2.05, 3.55], respectively (Figure 5.2.5A). Similarly, nsyb>GeNLCa female flies with 0.05mM, 0.1mM, or 0.67mM of FFz had significantly higher bioluminescence than nsyb>CaLexA-LUC, with mean differences (Δ log10 RLU) of 2.63 [95%CI 1.34, 3.89] and 1.91 [95%CI 1.45, 2.65] and 2.14 [95%CI 1.62, 2.66], respectively (Figure 5.2.5A). Similarly, while the signal began high, it rapidly declined to FLuc levels within the first few hours of the experiment. As a comparison, during the hundredth to hundred and tenth hours of recording, nsyb>GeNLCa male flies with 0.05mM, 0.1mM, or 0.67mM of FFz had similar bioluminescence levels to nsyb>CaLexA-LUC, with mean differences (Δ log10 RLU) of -0.18 [95%CI -0.44, 0.18] and -0.09 [95%CI -0.25, 0.12] and 0.45 [95%CI -0.01, 0.86], respectively (Figure 5.2.5B). Similarly, nsyb>GeNLCa female flies with 0.05mM, 0.1mM, or 0.67mM of FFz had similar bioluminescence levels to nsyb>CaLexA-LUC, with mean differences (Δ log10 RLU) of -0.23 [95%CI -0.42, 0.02] and 0.21 [95%CI -0.17, 0.78] and 1.00 [95%CI 0.56, 1.51], respectively (Figure 5.2.5B).

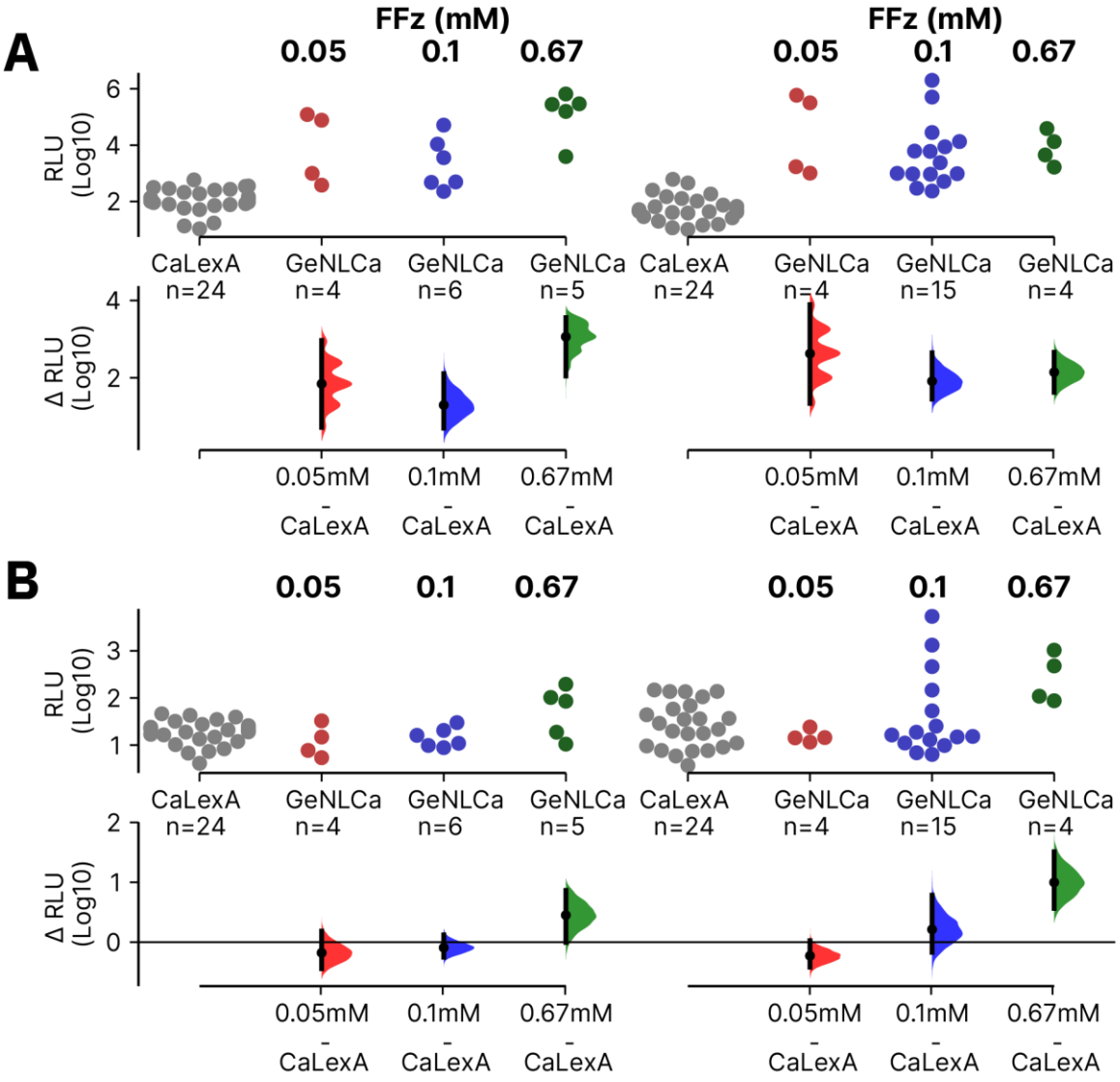

Figure 5.2.5 GeNLCa signal rapidly decays to FLuc levels

DABEST comparison of average raw bioluminescence (RLU) for the first ten hours of recording **(A)** and during a late stage of the experiment (100-115 hours from the start) **(B)** in nsyb>CaLexA-LUC versus nsyb>GeNLCa with three varying concentrations of FFz. Data was analysed from the raw bioluminescence data collected by third year undergraduate students as part of their final year laboratory projects. (A-B) The top section shows the raw unpaired data, with each dot indicating an individual. The bottom section shows the mean difference with 95% confidence intervals (CI) around the mean difference between comparisons generated via bootstrap resampling. The summary data for (A-B) are shown in Appendix C Table 7-8.

5.3 The destabilising domain controlled FLP is incompatible with CRE or TIM-Luciferase

To conclude my thesis, I wanted to test whether a new destabilising domain FLP could be used to improve the targeting of direct promoter-Luciferase constructs to specific cells of interest. Direct promoter-Luciferase constructs can be modified via the use of FLP/FRT and GAL4/UAS systems to allow targeting of the reporter to specific cells within the brain (Golic and Lindquist, 1989; Brand and Dormand, 1995; Tanenhaus, Zhang and Yin, 2012). This was demonstrated for a Luciferase reporter controlled by a cAMP response element (CRE). CRE-Luciferase reports cAMP response element binding protein (CREB) activity as a bioluminescence signal (Tanenhaus, Zhang and Yin, 2012). CRE-Luciferase can be targeted to different regions of the fly brain and can record rhythmic patterns of bioluminescence, which are under both circadian control and downstream of neural activity (Tanenhaus, Zhang and Yin, 2012). A current issue with this system is high background noise levels (Tanenhaus, Zhang and Yin, 2012). This is most noticeable when targeting CRE-Luciferase to more restricted populations rather than across the whole brain (Tanenhaus, Zhang and Yin, 2012). The high background is likely due to the nature of the construct, whereby once the cassette is flipped out, the CRE-Luciferase will always be functional within that specific cell. Misexpression of FLP within cells will cause irreversible flipping, leading to bioluminescence signals during experiments that may not represent the underlying biology. If the flipping occurred early in development, many unwanted cells would end up with the functional CRE-Luciferase construct. In addition, FLP could be misexpressed even in the absence of a cell-specific promoter-Gal4 if the UAS-FLP has leaky expression. While the signal-to-noise ratio is still large for broadly expressing drivers, the ability to target a promoter-Luciferase construct to a restricted set of neurons in the fly brain is appealing.

Recently, a modified FLP, which has a destabilising domain (FLP.DD), from dihydrofolate reductase of *E.coli* fused to it was created (Sethi and Wang, 2017). The destabilising domain targets FLP to be degraded by the proteasome, a process that is blocked by adding trimethoprim (TMP) to the diet. Misexpressed FLP should be rapidly degraded before irreversibly flipping out the FRT-flanked cassette, and thus, the signal-to-noise ratio of our bioluminescence values should be significantly improved. Here, I wanted to test whether the recently created FLP.DD can be utilised to lower the noise of promoter-luciferase reporters. For this purpose, I began with a *tim*-Luciferase reporter construct and the modified FLP.DD (*tim*-LUC, See Chapter 2.11.3 for more info). This functions similarly to the CRE-Luciferase but with a *timeless* promoter which reports the transcriptional activity of the core circadian clock proteins CLK:CYCLE. I first tested tim-LUC flies without a promoter-GAL4 (Ctr>*tim*-LUC) with or without the addition of TMP (+/-TMP). I found that Ctr>*tim*-LUC flies had low levels of bioluminescence signal in both males and females with no TMP

addition (Figure 5.3.1A-B). The average bioluminescence (RLU) for male and female Ctr>*tim*-LUC -TMP flies was 44.17±11.84 and 45.32±22.14, respectively. In contrast, the line plots in Figure 5.5.1A-B suggested that Ctr>*tim*-LUC flies with TMP added to the experimental food media had slightly increased bioluminescence for both males and females. The mean difference (Δ RLU) with the addition of TMP compared to without TMP in males and females was 48.64 [95%CI 12.01, 104.65] and 53.39 [10.85, 168.13], respectively (Figure 5.3.1C). This suggests that there is some leaky expression of the UAS-FLP.DD and TMP is functioning to stabilise the flippase, allowing increased levels of recombination to occur.

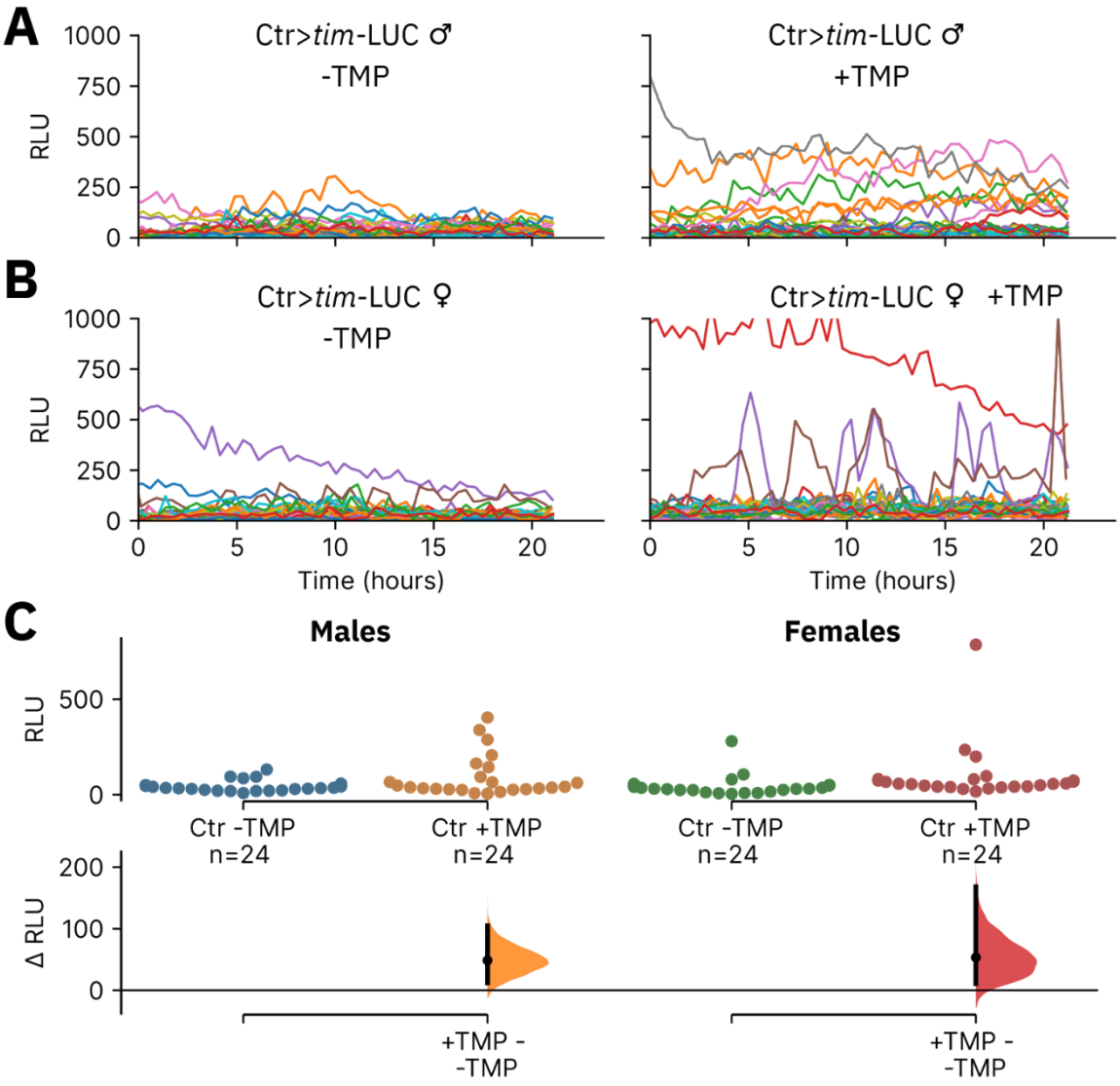

Figure 5.3.1 TMP addition has a minor impact on Ctr>*tim*-LUC flies

(A-B) Line plots of the raw bioluminescence (RLU) over time for *tim*-LUC flies lacking a promoter-GAL4 with or without the addition of TMP in the experimental food media, in males **(A)** and females **(B)**. **(C)** The comparison of average bioluminescence (RLU) for Ctr>*tim*-LUC with or without TMP addition to the food media, in both males and females. The top section shows the raw unpaired data, with each dot indicating an individual. The bottom section shows the mean

difference with 95% confidence intervals (CI) around the mean difference generated via bootstrap resampling. The summary data for (C) are shown in Appendix C Table 9. The sample size for (A-C) was 24 for Control>*tim*-LUC males and females, with and without TMP addition.

I next tested *tim*-LUC with a circadian driver tim(UAS)-GAL4, which broadly expresses within the circadian neurons in the fly brain (Blau and Young, 1999). Compared to the *tim*-LUC flies lacking the promoter-GAL4 and lacking TMP (replotted from Figure 5.3.1), tim>*tim*-LUC flies had much greater levels of bioluminescence with or without TMP (Figure 5.3.2A-B). tim>*tim*-LUC flies lacking TMP in the experimental food media had mean differences (Δ Log10 RLU) compared to Ctr>*tim*-LUC for males and females of 1.97 [95%CI 1.78, 2.18] and 1.21 [95%CI 1.00, 1.37], respectively (Figure 5.3.2C). This suggests that the UAS-FLP.DD functions strongly even without the addition of the stabilising drug TMP. The addition of TMP to tim>*tim*-LUC flies further increased average bioluminescence levels in both males and females, with mean differences (Δ Log10 RLU) compared to Ctr>*tim*-LUC of 2.29 [95%CI 2.12, 2.41] and 1.65 [95%CI 1.49, 1.79], respectively (Figure 5.3.2C). The data suggest that the addition of TMP has a further effect on increasing bioluminescence levels but that even without TMP, the FLP recombinase is highly active.

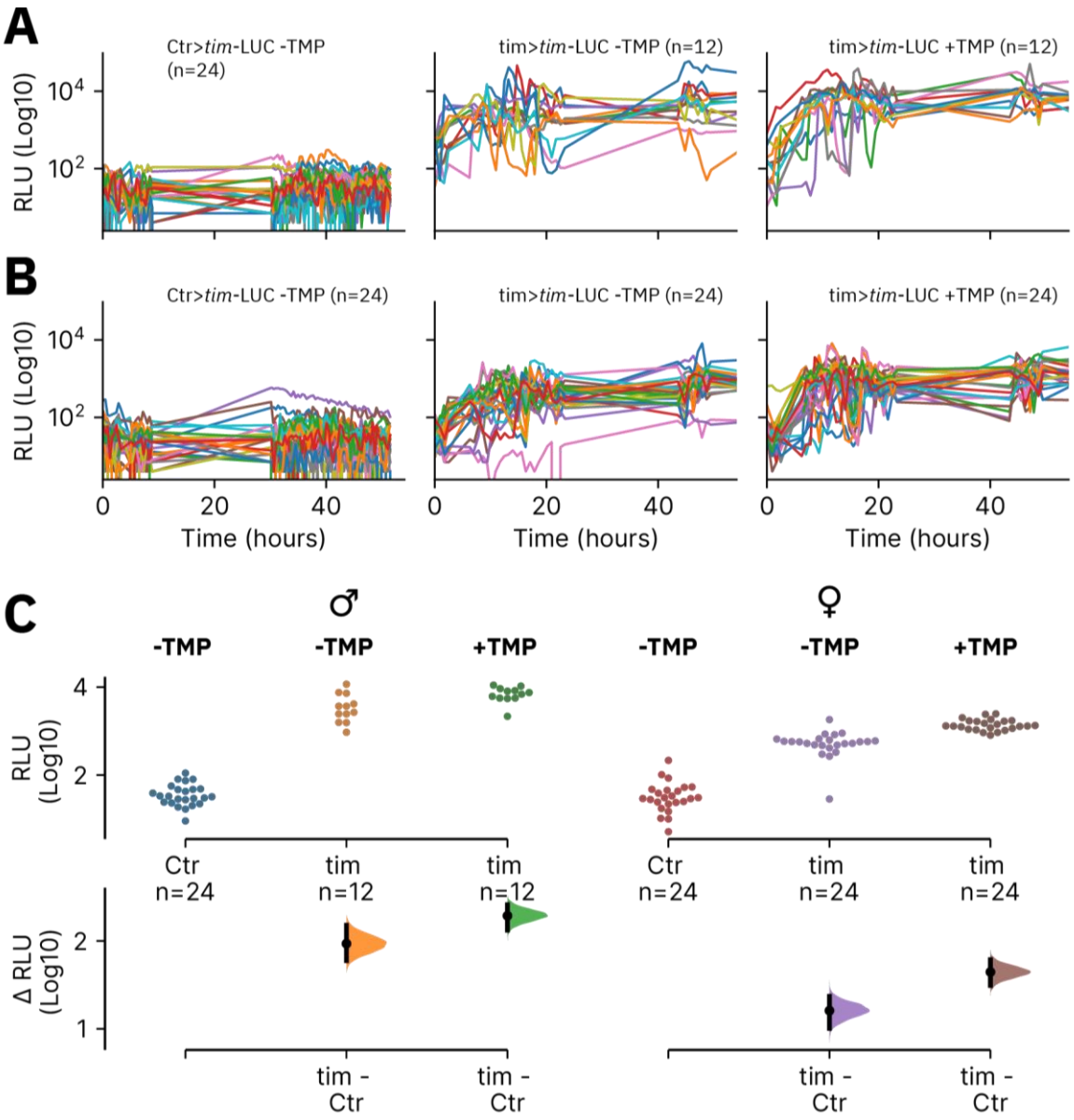

Figure 5.3.2 The FLP.DD recombinase functions without TMP in tim>*tim*-LUC flies

(A-B) Line plots of the raw bioluminescence (RLU) over time for *tim*-LUC flies lacking a promoter-GAL4 and lacking TMP, *tim*-LUC flies expressed with the tim(UAS)-GAL4 promoter but lacking TMP, or *tim*-LUC flies expressed with the tim(UAS)-GAL4 promoter with TMP addition to the food media, in males **(A)** and females **(B)**. **(C)** The comparison of average bioluminescence (RLU) for tim>*tim*-LUC with or without TMP addition to the food media versus Ctr>*tim*-LUC flies, in both males and females. The top section shows the raw unpaired data, with each dot indicating an individual. The bottom section shows the mean difference with 95% confidence intervals (CI) around the mean difference generated via bootstrap resampling. The summary data for (C) are shown in Appendix C Table 10.

I next tested the CRE-LUC reporter construct that (Tanenhaus, Zhang and Yin, 2012) demonstrated but with FLP.DD (CRE-LUC; See Chapter 2.11.3 for more info; (Tanenhaus, Zhang and Yin, 2012)). I began by testing the CRE-LUC reporter in TopCount assays with two strongly expressing promoter-Gal4 drivers. The first driver I tested was the glutamatergic driver OK371-GAL4 (Mahr and Aberle, 2006), as this expressed strongly with CaLexA-LUC (Table 5.1.1). I found that control flies which lacked a promoter-GAL4 (Ctr>CRE-LUC) had low levels of bioluminescence signal in both males and females (Figure 5.3.3A-B). The average bioluminescence for male and female Ctr>CRE-LUC were 21.90±2.52 RLU and 22.63±4.64 RLU, respectively. The experimental OK371>CRE-LUC flies, which lacked TMP in the food media, had higher levels of bioluminescence signal but remained low in both males and females (Figure 5.3.3A-B). The mean difference (Δ RLU) between OK371>CRE-LUC lacking TMP and Ctr>CRE-LUC for males and females was 25.34 [95%CI 19.76, 30.85] and 33.44 [95%CI 14.08, 69.27], respectively (Figure 5.3.3C). This is only a mild increase indicating FLP.DD is not performing much erroneous recombination. However, testing OK371>CRE-LUC with TMP addition in the food media resulted in little change in signal compared to those lacking TMP for both males and females (Figure 5.3.3A-B). Like the -TMP experiment, the mean difference (Δ RLU) between OK371>CRE-LUC with TMP and Ctr>CRE-LUC lacking TMP for males and females was 31.04 [95%CI 18.58, 52.70] and 60.18 [95%CI 31.16, 101.83], respectively (Figure 5.3.3C). The data suggest that while the FLP.DD construct appears to limit undesired recombination events; the addition of the stabilising drug TMP has little effect on increasing the recombination events.

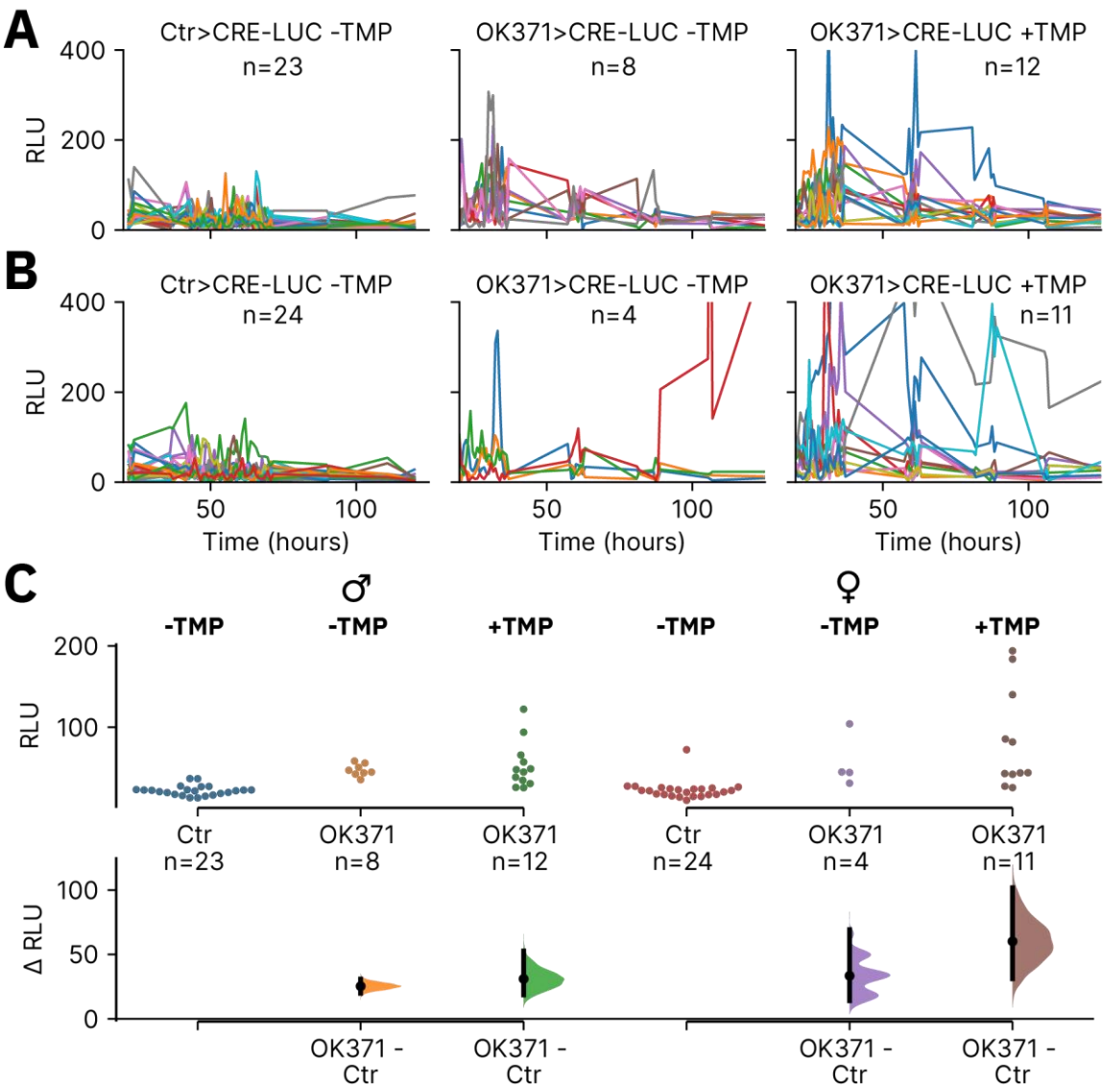

Figure 5.3.3 TMP addition has little impact on OK371>CRE-LUC flies

(A-B) Line plots of the raw bioluminescence (RLU) over time for CRE-LUC flies lacking a promoter-GAL4 and lacking TMP, CRE-LUC flies expressed with the OK371-GAL4 promoter but lacking TMP, or CRE-LUC flies expressed with the OK371-GAL4 promoter with TMP addition to the food media, in males **(A)** and females **(B)**. **(C)** The comparison of average bioluminescence (RLU) for OK371>CRE-LUC with or without TMP addition to the food media versus Ctr>CRE-LUC flies, in both males and females. The top section shows the raw unpaired data, with each dot indicating an individual. The bottom section shows the mean difference with 95% confidence intervals (CI) around the mean difference generated via bootstrap resampling. The summary data for (C) are shown in Appendix C Table 11.

To test whether the lack of effect with TMP addition was specific to the driver used, I tested an additional driver, kurs58-GAL4, which had a strong bioluminescence signal with CaLexA-LUC

(Table 5.1.1). I first replotted the Ctr>CRE-LUC flies from Figure 5.3.3A-B, alongside kurs58>CRE-LUC flies with or without TMP in the food media (Figure 5.3.4A-B). The line plots suggested that, as with OK371>CRE-LUC, the addition of the kurs58-GAL4 increased the bioluminescence signal by a small amount. However, the further addition of TMP had very little additional increase in bioluminescence. The mean difference (Δ RLU) between kurs58>CRE-LUC lacking TMP and Ctr>CRE-LUC for males and females was 6.38 [95%CI 2.02, 11.73] and 16.77 [95%CI 8.33, 29.40], respectively (Figure 5.3.4C). Similarly, the mean difference (Δ RLU) between kurs58>CRE-LUC with TMP in the food media compared to Ctr>CRE-LUC for males and females was 27.08 [95%CI 10.84, 83.29] and 22.70 [95%CI 8.44, 45.46], respectively (Figure 5.3.4C).

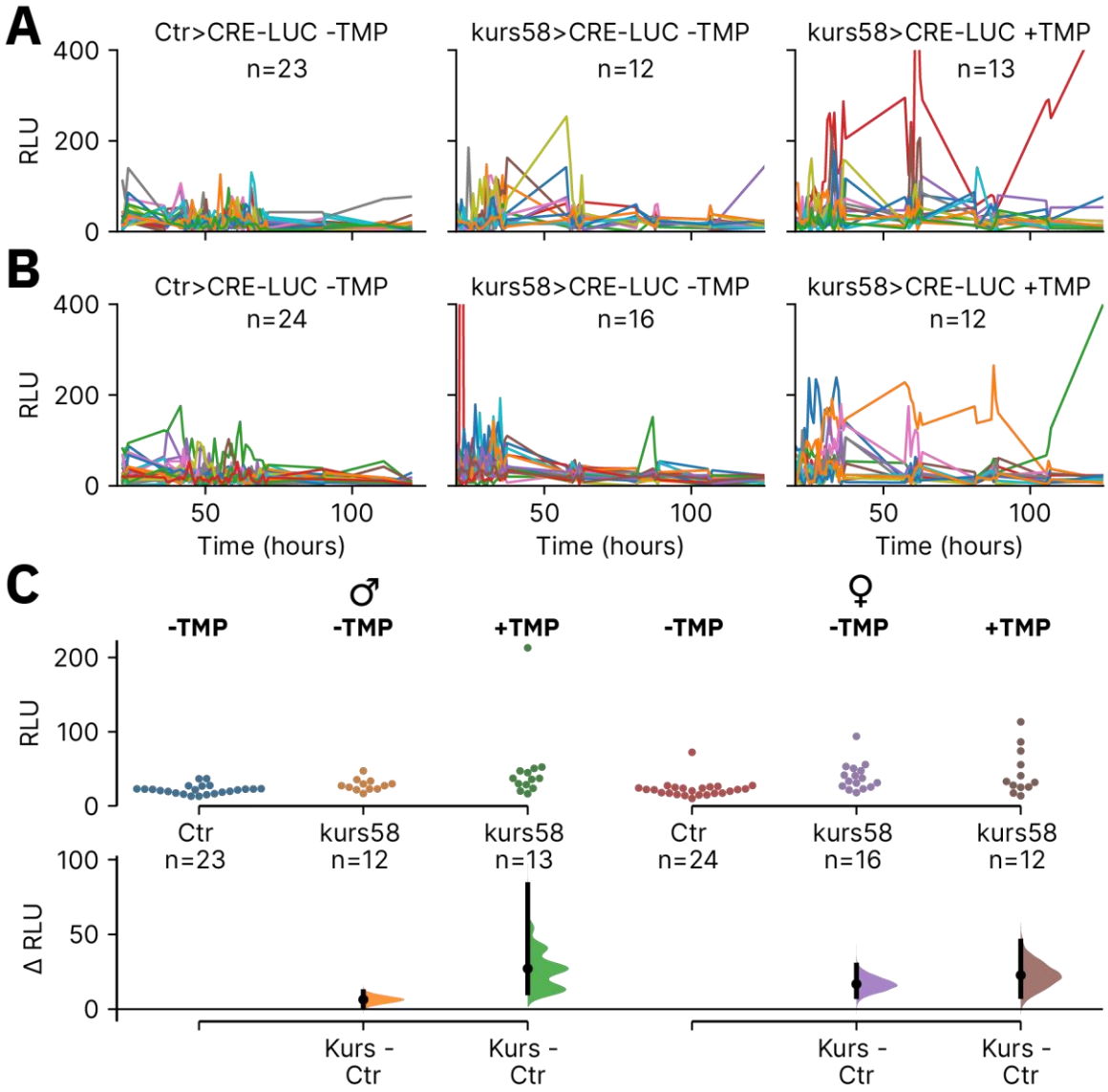

Figure 5.3.4 TMP addition has little impact on kurs58>CRE-LUC flies

(A-B) Line plots of the raw bioluminescence (RLU) over time for CRE-LUC flies lacking a promoter-GAL4 and lacking TMP, CRE-LUC flies expressed with the kurs58-GAL4 promoter but lacking TMP,

or CRE-LUC flies expressed with the kurs58-GAL4 promoter with TMP addition to the food media, in males **(A)** and females **(B)**. **(C)** The comparison of average bioluminescence (RLU) for kurs58>CRE-LUC with or without TMP addition to the food media versus Ctr>CRE-LUC flies, in both males and females. The top section shows the raw unpaired data, with each dot indicating an individual. The bottom section shows the mean difference with 95% confidence intervals (CI) around the mean difference generated via bootstrap resampling. The summary data for (C) are shown in Appendix C Table 12.

The prior experiments were performed with TMP addition to the luciferase food media. A question that arose was whether TMP requires longer time to act to stabilise FLP.DD and allow recombination to occur for CRE-LUC. To follow this up, I tested whether the addition of TMP during development would result in an increased bioluminescence signal due to a longer duration of TMP action on stabilising FLP.DD. The line plots of bioluminescence throughout the experiments suggested that the signal was low in OK371>CRE-LUC flies lacking TMP during development (dTMP) or during the experiment (eTMP) (Figure 5.5.5A). The addition of TMP during the experiment appeared to have no impact on bioluminescence (Figure 5.5.5A). The mean difference (Δ RLU) of -dTMP +eTMP versus -dTMP -eTMP was -0.40 [95%CI -7.05, 4.24] (Figure 5.5.5B). The addition of TMP only during development (+dTMP -eTMP) also had no noticeable effect on bioluminescence levels (Figure 5.5.5A), with a mean difference compared to -dTMP -eTMP of 8.17 [95%CI -2.39, 25.22] (Figure 5.5.5B). Finally, the addition of TMP during both development and the experiment (+dTMP +eTMP) did not affect bioluminescence levels (Figure 5.5.5A), with a mean difference compared to -dTMP -eTMP of 4.09 [95%CI -2.47, 13.64] (Figure 5.5.5B).

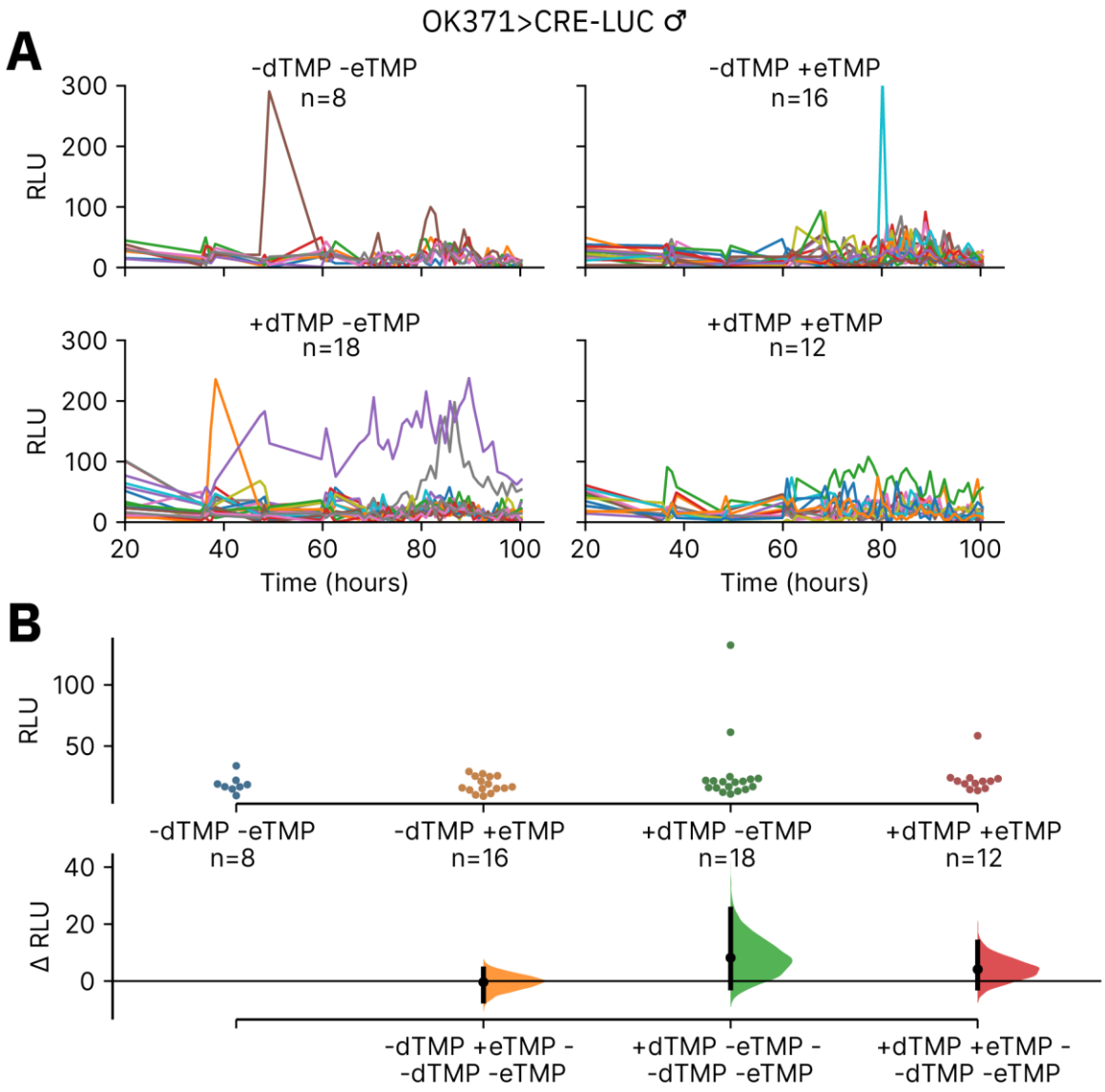

Figure 5.3.5 Developmental TMP addition has no impact on OK371>CRE-LUC male flies

(A) Line plots of the raw bioluminescence (RLU) over time for male OK371>CRE-LUC flies with varied conditions of TMP added during development (dTMP) and or in the experimental food media (eTMP). **(B)** The comparison of average bioluminescence (RLU) for male OK371>CRE-LUC with or without TMP addition to the food media during development and or the experimental media versus control conditions of no developmental or experimental TMP addition. The top section shows the raw unpaired data, with each dot indicating an individual. The bottom section shows the mean difference with 95% confidence intervals (CI) around the mean difference generated via bootstrap resampling. The summary data for (B) are shown in Appendix C Table 13.

5.4 Chapter 5 Discussion

Luciferase assays are commonly used for recording circadian gene expression in freely behaving animals over long periods. Recent studies have utilised calcium-sensitive transcriptional reporters with luciferase to study the calcium activity of circadian neurons. I was interested in testing whether these calcium-sensitive transcriptional reporters could be used to screen for neural correlates of sleep in freely moving flies.

While I began with two calcium-sensitive reporters, CaLexA and TRIC, I found the TRIC reporter problematic. I had significant difficulties maintaining the TRIC stock of flies, as they did not survive well in the food media. This was the case for two different laboratories where I tried to maintain the flies (Singapore and the UK). Although unpublished findings, additional lab members within my Singapore-based laboratory (Adam Claridge-Chang Laboratory) were also unable to maintain TRIC flies (acquired separately from my copy), suggesting a common issue with this stock. One potential reason for this is that the TRIC construct consists of two separate genetic constructs inserted on the second chromosome, and these flies have a balancer chromosome as the second and third chromosomal pair (See Chapter 2.1 for more information on balancers). Personal observations and observations from other fly researchers suggested that flies with multiple transgenes and two balancer chromosomes often appear less healthy and can be more challenging to maintain. Despite these issues, I note that visually rhythmic bioluminescence could be detected, for example with R54G12>TRIC-LUC. This activity, although not formally compared, appeared visually similar to the R54G12>CaLexA-LUC pattern of bioluminescence.

In contrast to TRIC, my CaLexA flies were much healthier. I therefore focused on CaLexA to express luciferase downstream (CaLexA-LUC) when calcium levels are high within the cells of interest. Here, I performed a preliminary screen of drivers, some of which had widespread expression in the fly brain and others with more restricted expression. The preliminary screen aimed first to discover rhythmic populations of cells which may be a correlate of sleep. For this purpose, I tested drivers ascribed to have a role in sleep-wake regulation, as well as some broadly expressing drivers. Surprisingly, most driver lines tested had rhythmic, ~24-hour calcium activity patterns.

An interesting finding was that pan-neuronal expression of CaLexA-LUC generated strong calcium activity rhythms. The elav (Embryonic lethal abnormal vision) driver used here is an enhancer trap (Gal4 sequence inserted into the *elav* promoter, otherwise described as elav[c155] allele; (Brand and Perrimon, 1993; Lin and Goodman, 1994), and is expressed in all post-mitotic neurons (Robinow and White, 1988, 1991). The elav>CaLexA experimental line, therefore, provided a way to measure calcium signalling from all neurons of the fly brain. While the overall

bioluminescence level for this line was significantly higher than controls, it was surprisingly lower than more restricted drivers, such as the dopaminergic driver (ple-GAL4) or Ilp2-GAL4 which drives only in the insulin-producing cells of the pars intercerebralis. One potential reason for this could be that the *elav* is weakly expressed, and so there may be lower levels of CaLexA-LUC within the fly brain compared to other promoter-GAL4s, which may be expressed more strongly. The elav::GAL4 [c155] line I used has previously been described to show weaker expression than an alternative elav-Gal4 line (Kim, Kolodziej and Chiba, 2002).

The daily activity profile of elav>CaLexA-LUC indicated two significant peaks of bioluminescence, one during the middle of the day and one during the middle of the night. This strongly resembled a typical inactivity/sleep profile that can be seen by analysing wild-type flies with Trumelan or DAM recordings. By testing elav>CaLexA-LUC in a DAM assay, there was a relatively strong correlation between the bioluminescence pattern and the general DAM sleep behaviour. This appeared surprising as sleep is considered a time of lowered activity in *Drosophila*, associated with synaptic downscaling (Tononi and Cirelli, 2014). Several drivers, such as pan-glial and pan-dopaminergic neurons, also had a similar pattern with two significant peaks of bioluminescence. At first glance, these appear like a typical inactivity/sleep profile; however, this requires further testing. While the elav>CaLexA-LUC bioluminescence signal and elav>CaLexA-LUC DAM sleep had two significant peaks during the day and night, the timing of the two peaks were different. This was most apparent during the night, whereby the prominent peak of bioluminescence occurs during the middle of the night, while the DAM sleep measure begins much earlier and ends much later than the bioluminescence peak. This could indicate that the elav>CaLexA-LUC Luciferase activity is not tracking sleep. However, the differences seen could also be because the DAM assay was performed on different flies at a different time, and DAM is a low resolution assay which overestimates sleep (Zimmerman *et al.*, 2008). An ideal experiment would be to record the Luciferase activity while using Trumelan to record behaviour concurrently; however, this is currently not possible.

MESA suggested that elav>CaLexA-LUC had a strong 12-hour rhythmic component in the signal, associated with the dual peaks of bioluminescence. Upon revisiting the literature, prior studies utilising luciferase assays discovered similar two 12-hour peaks in bioluminescence rhythms. One study found that *per*-LUC flies had a secondary, 12-hour peak in bioluminescence signal, which they ascribed to a secondary peak of *per* transcription (Brandes *et al.*, 1996). Subsequent work by found that the 12-hour peak was not specific to *per* transcription as it was seen in other luciferase reporter lines (R. Stanewsky *et al.*, 1997). Stanewsky and colleagues suggest that the two peak 12-hour may be a behavioural artefact downstream of the circadian clock, which is likely to be feeding (Koksharov, 2022). Therefore, the elav>CaLexA-LUC two peak signal may be a feeding rhythm rather than relevant to sleep. This may also be the case for additional driver>CaLexA-LUC

lines with a similar two-peak bioluminescence signal. In addition to feeding rhythms, movement can also lead to significant changes in the bioluminescence signal (Koksharov, 2022). A follow-up experiment could test bioluminescence signals from an ex-vivo brain preparation of elav>CaLexA-LUC flies. This would remove the possibility of rhythmic behaviour, such as feeding or gross locomotion, to impact the bioluminescence signal while still allowing a rhythmic signal relevant to sleep to be potentially detected.

Another question is whether the promoters themselves are rhythmic. Given that the core circadian clock transcription factors CLK and CYC promote rhythmic transcription of a wide variety of clock-controlled genes (Patke, Young and Axelrod, 2020), it would be a valuable experiment to test whether the promoter-GAL4 lines themselves are rhythmically expressed as this would lead to rhythmically expressed genetic constructs downstream of UAS elements. In the case of CaLexA-LUC, a rhythmic promoter-GAL4 would lead to rhythmically expressed GAL4 protein and downstream transcription of CaLexA. However, even if CaLexA is rhythmically transcribed, it is unknown if this would lead to rhythmic luciferase transcription and bioluminescence signal downstream. For example, the stability/half-life of CaLexA has yet to be shown. If CaLexA remains within cells for prolonged durations, rhythmic transcription of CaLexA would be dampened over time as the total levels of CaLexA build up. It would be informative to see whether CaLexA protein levels cycle rhythmically.

As a result of the caveats with bioluminescence assays, careful interpretation of rhythmic bioluminescence signals from CaLexA-LUC is required. The concept for this project was to perform a preliminary screen of a wide variety of cell populations to first discover rhythmic bioluminescence signals within otherwise wild-type flies. While I initially planned to perform a broad screening of many driver lines and then a subsequent screening of follow-up results, there were complications. I could only complete a few experiments due to issues with the bioluminescence plate reader (TopCount) and months of COVID lockdowns/limited lab access. Most importantly, the TopCount had major infrastructural problems throughout my studies. The TopCount had errors (plate handling errors) occurring, which prevented experiments from occurring and could not be fixed by multiple rounds of engineering support. Even in this preliminary screen, it must be noted that many of the experiments were partially fragmented due to errors, resulting in many missing time points. This was most problematic for my PhD research, which was split over two distant laboratories (Singapore and UK).

Due to the aforementioned issues, completing the original aims for this chapter was not possible. Once cell populations with rhythmic calcium activity were discovered, I planned to test whether these rhythms were downstream of the circadian clock or relevant to sleep-wake regulation. For this purpose, I planned to use the circadian mutant cyc^{01}. Core circadian mutants, such as per^{01}

and *cyc*^{01}, lack a functional molecular clock. In addition, circadian mutants typically have arrhythmic behaviour (except for a startle response within a light:dark cycle). The benefit of *cyc*^{01} is that males lack a circadian clock but have a nocturnality phenotype within a light:dark cycle (Lee *et al.*, 2013). My Trumelan experiments also showed this when testing cyc^{01} behaviour in LD conditions. This means that *cyc*^{01} males have increased levels of inactivity/sleep during the day compared to lower levels during the night. The *cyc*^{01} nocturnality phenotype, therefore, allows a method for testing the cell populations with rhythmic calcium activity. These cell populations can be recombined into *cyc*^{01} background such that the flies should behaviourally have a nocturnal phenotype alongside a non-functional circadian clock. A secondary screen can then be performed with driver>CaLexA-LUC flies in a *cyc*^{01} background. Suppose rhythmic patterns of calcium activity are found within the secondary screen. In that case, it provides more evidence that these cell populations may be relevant to sleep-wake regulation rather than directly due to a functional circadian clock. The cell populations discovered within the secondary screen can subsequently be recorded in the high-resolution Trumelan assay I previously demonstrated. Using standard tools to manipulate cellular activity, such as optogenetics or thermogenetics, while recording in Trumelan, the role of the cell populations discovered in the screening process can be elucidated. The high resolution of Trumelan will allow for a better understanding of the targeted cells' role, as it will be apparent if the cells targeted promote rest or other behaviours, which DAM assays may not detect.

One driver that was an interesting discovery from the preliminary screen was MB504B. The MB504B driver is expressed in a restricted set of dopaminergic neurons and is involved in regulating memory consolidation (Feng *et al.*, 2021). During a screening of dopaminergic neurons with inputs to the mushroom body, the MB504B driver was mildly sleep-promoting (although they suggest not statistically significant) when activated by the temperature sensitive cation channel TrpA1 (Sitaraman, Aso, Rubin, *et al.*, 2015). In my CaLexA-LUC data, MB504B males and females had highly rhythmic bioluminescence signals. In addition, MB504B males had a strongly rhythmic 24-hour bioluminescence pattern without the aforementioned strong 12-hour rhythmic peak, potentially indicative of a feeding rhythm. Regardless of whether MB504B has a role in sleep-wake regulation, MB504B is relevant to memory consolidation, and so the highly rhythmic signal is interesting and could be worth following up.

A major issue encountered with CaLexA-LUC was the low overall bioluminescence levels. The driverless CaLexA-LUC control flies had relatively low levels of bioluminescence, although an empty plate without a fly generates much lower levels (not shown, typically around 10 RLU). This suggesting some leaky CaLexA-LUC expression resulted in bioluminescence counts above background. A follow-up experiment to provide evidence that this was due to leaky would be to test the bioluminescence counts of flies expressing only the driver. These should have background

levels of bioluminescence. An alternative method could be to express a fluorescent protein (e.g., GFP) downstream of CaLexA (CaLexA-GFP) and image the fluorescence levels across the fly brain and ventral nerve cord.

Compared to the controls, some broadly expressing drivers had strong bioluminescence signals, such as pan-neuronal elav::GAL4 or pan-glial repo-GAL4. Unfortunately, more restricted drivers had low signal levels comparable to the driverless controls. For example, MB504B, expressed in a handful of dopaminergic neurons, had bioluminescence counts lower than the driverless control. Less restricted drivers such as R23E10-GAL4, which expresses in at least 31 neurons in the brain and some in the ventral nerve cord (Hulse *et al.*, 2021; Jones *et al.*, 2023), also had bioluminescence levels comparable to the driverless control. This suggests that either many driver lines express weakly or that firefly luciferase is not sensitive enough within small populations. Given that many of the drivers tested are widely used for *Drosophila* studies, they can produce strong phenotypes with genetic manipulations (e.g. activating R23E10 cells with a temperature-sensitive cation channel; (Jones *et al.*, 2023)), and targeting a fluorescent protein to such populations (e.g. R23E10>GFP; (Jones *et al.*, 2023)) produces a strong signal, it is unlikely that the driver is too weak.

The data, therefore, demonstrates a major issue with firefly luciferase. Most of the promoter-GAL4s tested in this preliminary screen had bioluminescence counts around the level of the driverless control. This makes it difficult to know how much of the bioluminescence recorded is signal rather than noise. While many promoter-GAL4 lines led to rhythmic signals, the low overall bioluminescence relative to the control raises the question of how much of the signal or rhythm is coming specifically from the neurons targeted. This was also the case for the TRIC-LUC tests, whereby the majority of drivers tested had bioluminescence levels around that of the driverless controls. A potential option for improving the bioluminescence signal is to increase the number of FLuc copies used. During the initial testing of CaLexA, increasing the copy number of GFP (used instead of luciferase in this case) increased the sensitivity of the CaLexA reporter (Masuyama *et al.*, 2012). Increasing the luciferin concentration would also be an avenue for increasing the signal strength.

Recent advances in Luciferase discovery led me to determine whether an alternative Luciferase could be viable for bioluminescence assays. The most promising Luciferase recently engineered is NanoLuc (NLuc), which was shown to produce orders of magnitude more significant signal over firefly luciferase (England, Ehlerding and Cai, 2016). The drawback was that it had never been shown to work in *Drosophila*. In addition, whether the substrate (FFz) could enter the fly brain was unknown. Here, I created flies with various NLuc-based constructs, and final year undergraduate project students crossed these flies to a pan-neuronal driver nsyb-GAL4 and tested

the offspring in the same manner as for firefly luciferase (FLuc). While this thesis only includes preliminary testing with GeNL and GeNLCa, informative results were found.

The initial signal strength of both GeNL and GeNLCa was significantly higher than for FLuc. The signal from the TopCount was the highest that our laboratory had ever seen from in vivo bioluminescence recordings. This showed that the substrate can enter the brain and that NLuc-based constructs can work in *Drosophila*. A major stumbling block, however, was that the signal rapidly decays until around FLuc levels or even to background levels. While FLuc also has a bioluminescence decay state, it is followed by a relatively steady state where rhythmic patterns can be discovered. Unfortunately, these initial tests showed no consistent steady state for the NLuc-based constructs. The rapid decline in signal was seen for all three concentrations of FFz tested. One possibility is that the substrate is not stable within the experimental media. Additional testing with different experimental media could be performed, such as altering the pH. The fly feeding and defecating on the food likely alters the pH of the media, which may impact the stability of FFz. For example, NLuc has reduced activity at lower pH levels (Hall *et al.*, 2012; England, Ehlerding and Cai, 2016). However, FLuc is also considered to be inactive/less active at low pH (England, Ehlerding and Cai, 2016). Additional work should be done to test the other NLuc-based reporters created, as these may be more effective. In addition, alternative substrates (e.g., FFz analogues) may function better for *Drosophila* based studies.

Finally, direct promoter-Luciferase reporters with spatial targeting have been demonstrated as a promising method for analysing the activity of a promoter within specific cells of interest. A promoter downstream of neuronal activity, such as CRE, may be utilised as an alternative method to calcium-sensitive transcriptional reporters. The current method, however, involves a FLP recombinase, which can lead to high background noise, likely due to leaky expression of FLP and undesired recombination events. Here, I tested whether a novel destabilising domain FLP recombinase (FLP.DD) can be used with direct promoter-luciferase reporters to lower the background noise of spatial targeting.

Unfortunately, my testing with FLP.DD had mixed results. I began by testing the construct with *tim*-LUC and found that flies lacking a driver had low bioluminescence signal, indicating that if leaky expression of FLP.DD is occurring, only a few recombination events occurred. This suggests that the destabilising domain may be having some effect on lowering the background signal. Adding a broad circadian driver (tim(UAS)-GAL4) greatly increased bioluminescence levels irrespective of whether the stabilising drug, TMP, was added. On the one hand, the low background with no driver is an important finding, as the driverless control is typically the only control used in such experiments, and these are the ones that showed high background noise in the original paper (Tanenhaus, Zhang and Yin, 2012). On the other hand, my findings with *tim*-LUC

suggest that the UAS-FLP.DD may be stable enough without TMP to lead to recombination events. While these two findings seem at odds with one another, it may be that in controls, the low levels of FLP via leaky expression allows the destabilising domain to promote proteasomal degradation. Meanwhile, in flies with a strongly expressing driver, the levels of FLP become elevated, which may allow recombination events to occur before proteasomal degradation of FLP can occur. Further evidence for this is that adding TMP further increased the bioluminescence levels of tim>*tim*-LUC females from flies lacking TMP in the experimental food media. To further study this aspect, a few more experiments are required. For example, testing Ctr>*tim*-LUC with the standard UAS-FLP to see how the background noise compares to UAS-FLP.DD. In addition, testing with other driver lines would be necessary to gauge whether these findings are consistent across various drivers with high signal in driver>*tim*-LUC lines. Even if the addition of TMP has no significant effect, if the destabilising domain can lower background noise in driverless controls, this would be an important finding and potential upgrade to the existing method.

In addition to the *tim*-LUC reporter, I tested the CRE-LUC reporter demonstrated by (Tanenhaus, Zhang and Yin, 2012) but with the destabilising domain tagged flippase. As with tim-LUC, I found that the driverless control of CRE-LUC had low bioluminescence counts, suggesting that the background is low. The addition of a driver, however, only had a minor effect on bioluminescence levels. I first tested with OK371-GAL4, which is widely expressed in glutamatergic neurons. OK371>CRE-LUC flies had increased bioluminescence relative to the driverless control, with or without TMP. This followed the findings of *tim*-LUC with an apparent lack of TMP sensitivity. However, the signal strength with OK371 was extremely low for CRE-LUC and barely increased from the driverless control. In addition, compared to OK371>CaLexA-LUC, the signal was over ten times less with the CRE-LUC reporter. Follow-up work with an additional driver, kurs58-GAL4, demonstrated similar findings of low background noise but also low signal.

These data open up a few potential interpretations. Firstly, the CRE-LUC reporter could be relatively weak, irrespective of the FLP.DD, resulting in a low signal compared to other reporters with the same driver. As with *tim*-LUC, a simple experiment would be to use the standard UAS-FLP to test the signal strength of OK371>CRE-LUC or kurs58>CRE-LUC. If the reporter itself is weak, there should not be an increase when utilising the standard FLP. The original CRE-LUC construct, which did not have the spatial targeting FRT flanked modification had strong activity, suggesting that the CRE promoter itself is not weak (Belvin, Zhou and Yin, 1999).

The alternative option is that the destabilising domain may be functioning too strongly, providing low background noise in driverless controls but repressing much of the FLP activity (and, therefore, recombination) even in the presence of TMP. If the signal of a driver>CRE-LUC with the standard FLP is much greater than for FLP.DD, it suggests that the destabilising domain is having a

negative impact by lowering the signal in experimental conditions. In the original (Tanenhaus, Zhang and Yin, 2012) paper, elav>CRE-LUC (with UAS-FLP) generated bioluminescence counts similar to my testing of elav>CaLexA-LUC. This suggests the destabilising domain may be the problem, as both OK371>CRE-LUC and kurs58>CRE-LUC with UAS-FLP.DD led to a substantially lower signal than with CaLexA-LUC. However, these two methods measure separate processes. While elav>CaLexA-LUC measures calcium activity patterns within elav-expressing neurons, elav>CRE-LUC expresses the CRE-LUC construct within elav-expressing neurons but reads out CRE promoter activity. The *tim*-LUC reporter generated strong bioluminescence levels in experimental flies, suggesting the issue may be the promoter strength of CRE. However, I only tested one broad driver, and it could be that the tim-LUC signal is still being heavily repressed by the FLP.DD, irrespective of the strength of the reporter itself. Additional testing with the standard FLP should elucidate the reason. An additional follow-up test could be to modify the concentrations of TMP and test whether an increased concentration is required in this case. This seemed unlikely at the time as the original paper illustrating FLP.DD tested the kinetics of the destabilising domain and the concentrations of TMP that are relevant (Sethi and Wang, 2017). They found that increasing the TMP concentration only up to 1mM increased the number of cells expressing a fluorescent protein due to recombination events.

Chapter 6 Conclusion

6.1 Flies spend a significant amount of time in behaviours undetectable to DAM or low-resolution assays

In this thesis, I characterise a novel video-tracking assay named Trumelan, which can record flies from a side-on perspective. I demonstrate that Trumelan can record high-quality position, posture, and behavioural data. My data corroborates previous findings about the drawbacks of utilising DAM assays for studying sleep (Zimmerman *et al.*, 2008; Donelson *et al.*, 2012), whereby DAM severely overestimates rest to differing extents at different times of day and in different genotypes or individuals. My data supports that DAM provides a robust system for measuring broad locomotor patterns but does not accurately measure *Drosophila* long rest. Furthermore, my data suggests that as stationary active behaviours increase, the accuracy of the waveform of DAM rest and the amount of total DAM rest reduces. This is concerning as DAM assays are often used to justify whether a specific *Drosophila* mutant has sleep/wake deficits, or neuronal population is involved in sleep/wake regulation. A mutant or neuronal population that leads to changes in stationary active or short rest would not be accurately picked up by a DAM assay and would lead to a potentially incorrect conclusion if further checks (e.g., video recording) are not performed. This was certainly the case for the 104y>TrpA1 experiment described in Chapter 1.4.1, whereby DAM suggested activating these neurons leads to sleep (as correlated by no beam breaks), while visual inspection clearly illustrated that the flies had a seizure-like phenotype (De *et al.*, 2023). Stationary active behaviour would also be problematic for low-resolution video-tracking assays, which only record x-position or locomotion rather than more complex behaviours. Due to females typically performing more SA behaviours than males, it also results in DAM being a less accurate measure of rest in females.

While I record fly behaviour as three overarching states, fly behaviour could be further separated into many more specific states, such as front leg grooming, head grooming, feeding, and proboscis extension-retraction movements. An improvement to the Trumelan behavioural classifier could be to split the SA state into grooming and feeding (or even finer detail). Another possibility could be to add a feeding capillary into the Trumelan assay. This would allow for a much finer resolution of feed events as compared to using a classifier. A capillary setup embedded into Trumelan would allow for the total quantity of food being ingested to be recorded, the number of feed events, and the quantity of ingested food for each bout. Providing higher resolution of fly behaviour could be an interesting future direction to improve Trumelan. This would be a big task to perform, however. A substantial issue with increasing the behavioural resolution is that it would require

significantly more time to annotate behaviour, train models, and test these classifiers. Multi-behaviour assays have already been developed; for example, the Branson laboratory developed an automated assay to detect individual and group-housed flies (Branson *et al.*, 2009). An assay that integrates posture, high-quality behavioural classification, and high-quality feeding information would be novel and of great value to the field.

6.2 Flies do not have an overt rest posture

Beyond correlating sleep with prolonged inactivity, the notion of a sleep posture and place preference in *Drosophila* suggested a potential way to improve the way a sleeping fly is defined (Hendricks *et al.*, 2000). If flies have an overt postural or positional change during rest, this could be easily noticeable and recordable by Trumelan, providing the possibility of an improved way to measure sleep. While current high-resolution video-tracking assays can accurately detect behaviour, recording orientation precludes postural analyses. Trumelan records flies from a side-on perspective, allowing for a quantitative analysis of fly posture and place preference.

The original description of rest posture in flies is similar to what was previously described for resting bees (Kaiser, 1988, 1995) and cockroaches (Tobler and Neuner-Jehle, 1992). Unlike the initial suggestion by (Hendricks *et al.*, 2000), I was unable to uncover any significant postural changes during rest in *Drosophila*. I found that flies began rest in a supported upright position while on the ground; however, this was not specific to long rest, and all behavioural states' distributions of starting posture were highly overlapping. On average, resting flies lowered in y-position slightly over time; however, this was not lowering prone to the ground as initially described (Hendricks *et al.*, 2000). Even though flies lowered on average, many bouts did not follow this pattern, and average lowering occurred for both short and long rest bouts. On average, ground-resting flies lower their rear marginally while remaining in a supported upright position. The rest posture for flies on the ceiling (upside down) had not been previously described, and I found that flies began rest in a more parallel starting posture compared to ground-based flies. At the same time, no consistent postural changes occurred during rest itself.

My findings suggest that overt changes in posture do not occur during rest, which precludes the possibility of using posture as an additional marker of a sleep state. While Trumelan is a high-resolution assay, there is potential that extremely minor changes in posture were undetectable or missed by this analysis of posture. In addition, I tested flies during rest rather than specifically testing the arousal threshold of flies and correlating postural changes with arousal threshold levels. Therefore, minor postural changes associated with a heightened arousal threshold may

occur during rest. Future studies on posture using arousal threshold testing and even higher biomechanical analysis would elucidate this further. Nevertheless, my data demonstrates that overt postural changes, as initially described, do not occur. Flies typically remain in a supported upright position, and I did not see flies prone on the ground during my studies.

6.3 Flies prefer to rest near the food while facing away from the food port

Drosophila are associated with a preference for resting near the food port (Hendricks *et al.*, 2000; Zimmerman *et al.*, 2008; Donelson *et al.*, 2012). The initial studies on rest place preference utilised Canton-S and w* flies and suggested that these wild-type genotypes strongly prefer to rest near the food port. In addition, Donelson *et al.*, 2012 suggested that *CASK*-β mutant flies, which have locomotor defects (Slawson *et al.*, 2011), remain near the middle of the tube. They conclude that rest place could be a valuable metric for assessing mutant flies.

My analysis corroborates prior findings that Canton-S and w* flies prefer to be near the food port when stationary. However, I found that Berlin-K males preferred to long rest in the middle of the chamber. This suggests that resting near the food is not a consistent characteristic of a long rest place preference. In addition, while flies typically prefer to long rest near the food port, the distribution of fly location was broad such that a significant amount of long rest was performed near the middle of the chamber. This differed from previous studies of rest place preference (Hendricks *et al.*, 2000; Zimmerman *et al.*, 2008; Donelson *et al.*, 2012). However, a significant difference between my work and the previous studies on rest place is that Trumelan can separate stationary active behaviours from rest. The two video-tracking studies cited above used low-resolution tracking, which cannot detect SA events. While Donelson *et al.*, 2012 suggest that feeding events are associated with locomotion, I found that SA events make up a significant portion of the day and are strongly associated with being performed near the food. My results here represent a more accurate measure of x-position place preference and suggest that flies typically have a mild preference for being near the food whenever they are not locomotive.

In addition to an x-position preference, flies were initially described to prefer facing away from the food port (Hendricks *et al.*, 2000). As Trumelan can measure fly posture, the facing direction of flies can also be recorded. Surprisingly, I found that flies prefer to face away from the food port during long rest, regardless of location within the chamber. In addition, stationary active behaviour and short rest away from the food port were also associated with facing away from the

food port. This suggests that the facing direction preference is seen across all non-locomotive behaviours unrelated to food/feeding.

6.4 Flies change their resting location between day and night

A significant finding of my thesis was that flies have a y-position place preference. To my knowledge, the y-position of flies is an aspect of fly behaviour that has not yet been studied. This is likely because typical video-tracking assays occur from a top-down (or bottom-up) perspective and cannot accurately measure the y-position. Unexpectedly, I found that wild-type flies prefer to be stationary on the ground during the day and shift their preference at night to spend more time on the ceiling. This ceiling occupancy shift remained in constant dark conditions but was absent in circadian mutants.

The follow-up work involved narrowing down the genotypes used (e.g., Using Berlin-K males or only circadian mutant males). This was done due to time constraints. As my PhD research was split between two separate laboratories and was heavily impacted by the COVID-19 pandemic, there was not enough time to feasibly test all possible fly genotype/sex combinations. While I focused on male flies for testing circadian mutants, this work could be broadened in the future to include females and additional genotypes. That said, given that the wild-type flies show no significant differences between males and females in ceiling occupancy, circadian mutant females would not be predicted to have a significantly different phenotype.

The ceiling occupancy rhythm begs the question of what the function may be. I hypothesise that the ceiling occupancy increase is associated with flies (in the wild) preferring to rest in a more protected location at night, for example, under a leaf. This would be a safer place to evade predators and protect the fly from poor weather conditions. To my knowledge, the resting location of insects or small organisms in general has not been widely studied. Many organisms choose a resting location to protect from predators (Shukla, Kilpatrick and Beltran, 2021). For example, the buffy-headed marmoset is known to use resting location (in a tree) as a mechanism of predator avoidance (Ferrari and Ferrari, 1990). Diurnal birds often choose an elevated sleeping location to protect from ground-based mammalian predators (Tisdale *et al.*, 2018). Interestingly, Tisdale and colleagues found that pigeons which were allowed to sleep on an elevated resting perch had increased levels of REM sleep and increased slow wave sleep intensity compared to pigeons sleeping on the ground.

In field observations, various insect species are also known to rest (often described as roosting or sleeping) in locations that protect the environment and predators (Rau and Rau, 1916; Rau, 1938).

For example, blue wasps were discovered resting underneath a rockface during a heavily cloudy dark morning. Another population of blue wasps were found to rest on the ceiling of a cowshed at night specifically. These wasps were not present at this location during the day but began to arrive at the cowshed ceiling around dusk and remained during the night (Rau and Rau, 1916). While both sexes were present, the author suggests that no mating occurred while on the ceiling, and these wasps were deeply resting (as suggested by seemingly high arousal thresholds). Fire ants were also found to sometimes rest on the ceiling of an artificial nest chamber (Cassill *et al.*, 2009). While ground-based rest was the most abundant, ceiling-based rest was associated with increased rest durations, suggesting a deeper rest state.

Whether a y-position place preference is specific to Trumelan or can be seen in alternative assays is unknown. It must be noted that Trumelan chambers have a slightly different design than DAM assays. While the sizes of both assay chambers are comparable, DAM assays use cylindrical tubes, and Trumelan uses cuboid chambers. The y-position preference may look slightly different in a DAM assay; however, the cuboid shape is a more natural chamber for a fly to experience than a tube. Further work to test in other arena sizes would be interesting to see whether a ceiling occupancy rhythm still occurs.

My data suggest that daytime and nighttime rest are associated with different location preferences. Ceiling occupancy remains low during the day, increases at dusk, and remains relatively high at night. *Drosophila* are known to have two main rest periods, which is also seen in my data for all wild-type flies. The daytime bout of rest is thought of as a light rest (commonly called ‘siesta’), while nighttime rest is thought of as a deeper state (Shafer and Keene, 2021). For example, daytime rest is less consolidated with shorter rest bouts (Andretic, van Swinderen and Greenspan, 2005). In addition, nighttime rest is associated with higher arousal thresholds (van Alphen *et al.*, 2013). Therefore, being in a protected location during the deeper, more consolidated rest at night would benefit survival.

There are many potential future directions for this work. Testing additional *Drosophila* or other invertebrate species, such as mosquitos, would be interesting to see whether this ceiling occupancy rhythm is a conserved process. An informative experiment to test this protected location hypothesis would be to set up a more naturalistic assay. A laboratory insect cage could be used to give flies space to fly and explore more naturally. Plants could be put within the cage, and video cameras could be used to track the fly’s positioning. The time spent at various locations could be recorded. If my hypothesis is correct, I expect increased fly occupancy levels underneath the plant at night (relative to total time resting).

The protected location hypothesis also begs the question of whether a sleep deprivation protocol elicits an increase in ceiling occupancy during rest rebound in Trumelan. If ceiling rest is

associated with a deeper state, an increase in ceiling occupancy during rest rebound would be expected. In addition, the effect of environmental conditions on ceiling occupancy has not been characterised. For example, does temperature affect ceiling occupancy? Does changing the day length (e.g., <12 hours of light per 24-hour cycle) lead to a change in ceiling occupancy? While the y-position preference data is an interesting finding, further work is required to understand the underlying mechanisms.

6.5 Calcium-sensitive luciferase reporters can detect rhythmic signal in restricted cell populations but do not produce strong signals

In addition to high-quality video-tracking, I aimed to establish whether in vivo luciferase assays can be used for discovering neural correlates of sleep in *Drosophila*. Luciferase assays have been an important tool for studying circadian clock function within freely behaving flies (Tataroglu and Emery, 2014). Recent studies have engineered calcium-sensitive transcriptional reporters of luciferase to study calcium activity as a correlate of neural activity, within specific cells of interest in the fly brain (Masuyama *et al.*, 2012; Gao *et al.*, 2015; Guo *et al.*, 2016; Guo, Chen and Rosbash, 2017).

While my experiments were unfortunately heavily disrupted by infrastructural issues as well as the COVID-19 pandemic, some valuable results were found. I first found that broadly expressing drivers such as pan-neuronal expression (elav>CaLexA-LUC) lead to strong highly rhythmic signal. Interestingly, the luciferase activity correlated well with the general daily 'sleeping' pattern of the same genotype when tested in a DAM assay. This is exciting as an in vivo whole brain activity monitor that functions in freely moving flies and correlates with sleep would be of great interest to the research field. However, there are major caveats and much further work would be required to demonstrate this. Prior studies have illustrated that feeding rhythms can result in rhythmic luciferase activity with similar patterns to what I see here for elav>CaLexA-LUC (Brandes *et al.*, 1996; Plautz *et al.*, 1997; Stanewsky *et al.*, 1998; Koksharov, 2022).

Further work would be required to dissect whether the signal of elav>CaLexA-LUC is relevant to sleep. Firstly, a direct elav>Luciferase experiment would demonstrate whether the *elav* promoter itself is rhythmically expressed. Secondly, an elav>CaLexA-LUC experiment in cultured/dissected fly brains would remove rhythmic Luciferase activity as a result of locomotor or feeding behaviour, while allowing sleep relevant signals to remain. Finally, as rhythmic activity could be indicative of circadian control, a follow up test should utilise elav>CaLexA-LUC in a cyc^{01} background. cyc^{01} flies lack a functional circadian clock, but the males are nocturnal within an LD

cycle (Lee *et al.*, 2013). If rhythmic Luciferase activity is still seen in elav>CaLexA-LUC in a *cyc*^{01} background, this provides further evidence for a neural correlate of sleep.

Similarly, I found that in vivo calcium sensitive luciferase assays can detect rhythmic luciferase activity within highly restricted populations of neurons, such as the four PPL1 dopaminergic neurons captured by the MB504B split GAL4 driver. MB504B is relevant to memory consolidation (Feng *et al.*, 2021), and so the highly rhythmic signal is interesting and could be worth following up. As with elav>CaLexA-LUC, follow up experiments would be required to justify whether a rhythmic Luciferase activity pattern is a neural correlate of sleep.

6.6 NanoLuc-based reporters function in *Drosophila*

A major issue with CaLexA-LUC approach was that the signal strength with restricted drivers was around the level of the driverless controls, suggesting firefly Luciferase may not be suitable for restricted experiments. This led me to test whether an alternative Luciferase could be used in place of firefly Luciferase.

Luciferase assay development is an active area of research and many novel luciferases have been discovered (Liu *et al.*, 2021). NanoLuc is an exciting prospect as it has a low molecular weight, it can be modified to have a short half-life and it produces orders of magnitude greater bioluminescence than Firefly Luciferase (England, Ehlerding and Cai, 2016). In-vivo NanoLuc assays typically function by injection of the substrate (e.g., FFz) directly into the mouse brain. For *Drosophila*, however, firefly Luciferase assays can be performed by adding D-luciferin to the experimental food media. It was unknown whether FFz would be able to enter the brain via feeding, and whether a bioluminescence signal would be detectable.

The initial findings demonstrated here was undertaken by final-year undergraduate project students. The data suggests that NanoLuc-based reporters can function in *Drosophila* and that the substrate can enter the brain. The primary issue with the two NanoLuc-based reporters tested was that the bioluminescence signal rapidly dropped to FLuc levels or baseline. It must be noted that these are preliminary findings, and much additional work is required. Testing all the NanoLuc-based reporter flies I created would be valuable, as alternative reporters may function better for *Drosophila*. In addition, multiple substrates and analogues have been shown to work with NanoLuc (Coutant *et al.*, 2020). An informative study would be to test all the possible substrates that NanoLuc-based reporters can use for *Drosophila*-based assays. The current substrate, FFz, is considered the most suitable substrate for in-vivo imaging in mice via injection of the substrate into the brain (Su *et al.*, 2020; Gaspar *et al.*, 2021). However, it may be that for *Drosophila* and

given the difference in uptake method (ingestion rather than injection), another substrate proves to be more effective. Another current drawback for NanoLuc-based reporters is that FFz is neither as readily available nor cheap as D-luciferin. This was one reason for the limited testing of the NanoLuc-based constructs.

The field of neuroscience, especially in *Drosophila*, has progressed to studying individual neurons (Scheffer *et al.*, 2020). My findings with CaLexA-LUC suggest that firefly Luciferase does not provide a strong enough signal for these purposes. The high level of bioluminescence with NanoLuc-based reporters is exciting as it demonstrates that alternative luciferases such as NanoLuc could be engineered for use in *Drosophila*. Given time, lowered costs, and further refinements, alternative luciferase reporters could become an integral tool for *Drosophila* bioluminescence studies. These may have the signal strength required to one-day record signal, whether calcium sensitive or direct promoter activity, from individual cells or small subsets of cells. In addition, it would open the way for more accessible methods for recording bioluminescence in *Drosophila*. Currently, a highly sensitive bioluminescence plate reader, such as a TopCount, is required to detect low bioluminescence signals, such as firefly Luciferase recordings. Alternative detection methods, such as charge-coupled device cameras, may also be possible. This could open further avenues, such as tracking behaviour while recording bioluminescence.

While writing this thesis, a novel Luciferase (Akaluc), engineered via directed evolution of firefly Luciferase, was demonstrated to function within *Drosophila* and produce much stronger signals than firefly Luciferase (Chihara *et al.*, 2023). It will be informative to see whether Akaluc can be used as an alternative to firefly luciferase for detecting rhythmic signals in Luciferase activity within restricted populations of cells, as this has yet to be demonstrated. Given the wide array of potential Luciferases and substrates (Liu *et al.*, 2021), the future is looking bright for an optimised bioluminescence assay for *Drosophila*-based studies.

6.7 Future Directions

Within the *Drosophila* neurobehavioural field, discovering the role of specific neurons and circuits in controlling behaviour is a key objective. This continues to be challenging in the context of *Drosophila* rest/sleep studies, whereby most laboratories are stuck with inferring the role of a set of neurons by manipulating these and recording the resulting gross locomotor patterns. The study of sleep homeostasis and the role of the dorsal fan-shaped body (dFB) neurons are a prominent example of how much research has been performed yet how unclear our understanding remains.

As discussed extensively in Chapter 1.4.1, initial studies found that activating a set of neurons which mostly project to the dFB leads to behavioural inactivity and these have a key role as the sleep homeostat within a homeostatically regulated circuit in the central complex of the fly brain (Donlea *et al.*, 2011, 2018; Donlea, Pimentel and Miesenböck, 2014; Pimentel *et al.*, 2016). Interestingly, recent studies have called both the role of the dFB neurons as sleep-promoting and as being involved in sleep homeostasis into question (De *et al.*, 2023; Jones *et al.*, 2023). Understanding the role of sleep homeostasis and knowing whether the central complex houses a centralised sleep homeostat is an important area of study in *Drosophila*.

I believe studying brain activity will help uncover the role of these neurons and circuits, as well as the role of various circuits in controlling sleep-wake behaviour. As mentioned, the current gold standard in *Drosophila* involves recording calcium imaging from head-tethered flies via a 2-photon microscope while simultaneously recording behaviour. By studying the dFB neurons with this method, van Swinderen's group found that activating dFB neurons (with optogenetics) elicits total brain activity that most closely resembles brain activity during wakefulness and that flies are less responsive to visual stimuli (Tainton-Heap *et al.*, 2021). They suggest that these neurons are involved in sleep-wake regulation, but perhaps a different 'active' sleep state. An issue with this gold standard approach is that it is unknown how unrestricted flies would behave and whether their brain activity would be different. In addition, fluorescence imaging (as used in 2-photon microscopy) can lead to photobleaching and phototoxicity, which limits recording durations. I believe it would be informative to have an assay which can record the activity of specific populations of neurons during naturalistic freely moving behaviour over extended periods of time. In the case of the dFB neurons, it would be highly informative to record the activity of dFB neurons themselves while flies are performing naturalistic behaviour, as well as during sleep deprivation and subsequent rebound sleep. Such an assay would also provide the potential to discover sleep-wake regulating neurons/circuits by screening for sleep or wake-active neurons akin to current methods in larger model organisms such as rats and mice.

To accomplish these goals, an improved gold standard assay would be able to record brain activity in unconstrained freely moving flies with concurrent behavioural tracking. Here, I attempted to lay the foundation for the role of Luciferase assays for this approach. So far, I have demonstrated a high-resolution video-tracking assay which can accurately detect behaviour. In addition, I demonstrated that calcium-sensitive transcriptional reporters of Luciferase can be used to record broad neuronal activity in various neuronal populations. While firefly Luciferase is effective for broad neuronal populations over long photon capturing durations, it is unable to generate strong signal in restricted neuronal populations. In addition, a calcium-sensitive transcriptional reporter of Luciferase naturally functions as a long exposure signal, rather than being able to record rapid changes in neuronal activity.

First, a stronger signal from Luciferase is required to adapt this approach for future studies. This could come about by finetuning the current firefly Luciferase system, utilising the modified firefly Luciferase 'AkaLuc' (Chihara *et al.*, 2023), or by utilising an alternative Luciferase such as NanoLuc (England, Ehlerding and Cai, 2016). A stronger signal is required, as it would be important to study the brain activity within restricted populations of neurons rather than just whole brain activity. Secondly, a directly calcium sensitive Luciferase should be used, such as a Luciferase split into two sections with a calmodulin and M13 linker. This would allow for high temporal resolution of Luciferase activity as the protein would only become active in the presence of calcium. My preliminary data with the NanoLuc-based constructs GeNL and GeNLCa provide the first pieces of evidence to suggest that these tools could work in flies. Both constructs generated much greater bioluminescence signals than firefly Luciferase, suggesting that luciferin (FFz) can enter the brain (which was previously unknown). In addition, GeNLCa represents a calcium-dependent Luciferase which will be an important construct to further test. Testing was extremely limited due to substrate availability during my PhD; however, future work should expand on this with additional testing of different constructs and substrates to narrow down the most effective Luciferase/luciferin combination. Thirdly, a high-quality CCD camera should be used to allow Luciferase recordings to take place with simultaneous behavioural recording. A similar concept has recently been employed in C. elegans, whereby a high-resolution CCD camera was used to record bioluminescence signal, as a correlate of neuronal activity, within specific neurons while recording behaviour (Morales-Curiel *et al.*, 2022). Importantly, they were able to record worms at a reasonable frame rate (1-10 fps) while achieving a good signal-to-noise ratio with the use of machine learning techniques. Such an assay in flies would be extremely useful and I believe my work sets an initial foundation to adapt this approach to flies.

My work here also discovered a potentially novel behavioural pattern by using side-on recording, whereby flies rest more on the ceiling at night, which we termed inverted roosting. The circadian clock may control the alternation between ground and ceiling-based roosting; however, more experiments are needed to justify this. Future work should look to better understand this phenomenon, including more controls and testing circadian clock knockdown, knockout, or rescue. The alternation between roosting location between day and night also suggests there may be distinct brain-activity patterns during these times. The current tools available are not suitable to test this hypothesis, as brain activity imaging during behaviour is currently limited to individual tethered flies. This means that with the current gold standard in flies, it would not be possible to study brain activity in inverted roosting or freely moving flies. To address this hypothesis, I suggest that the Luciferase recording with a behavioural tracking approach will be an important future direction to go in.

Appendix A Chapter 3

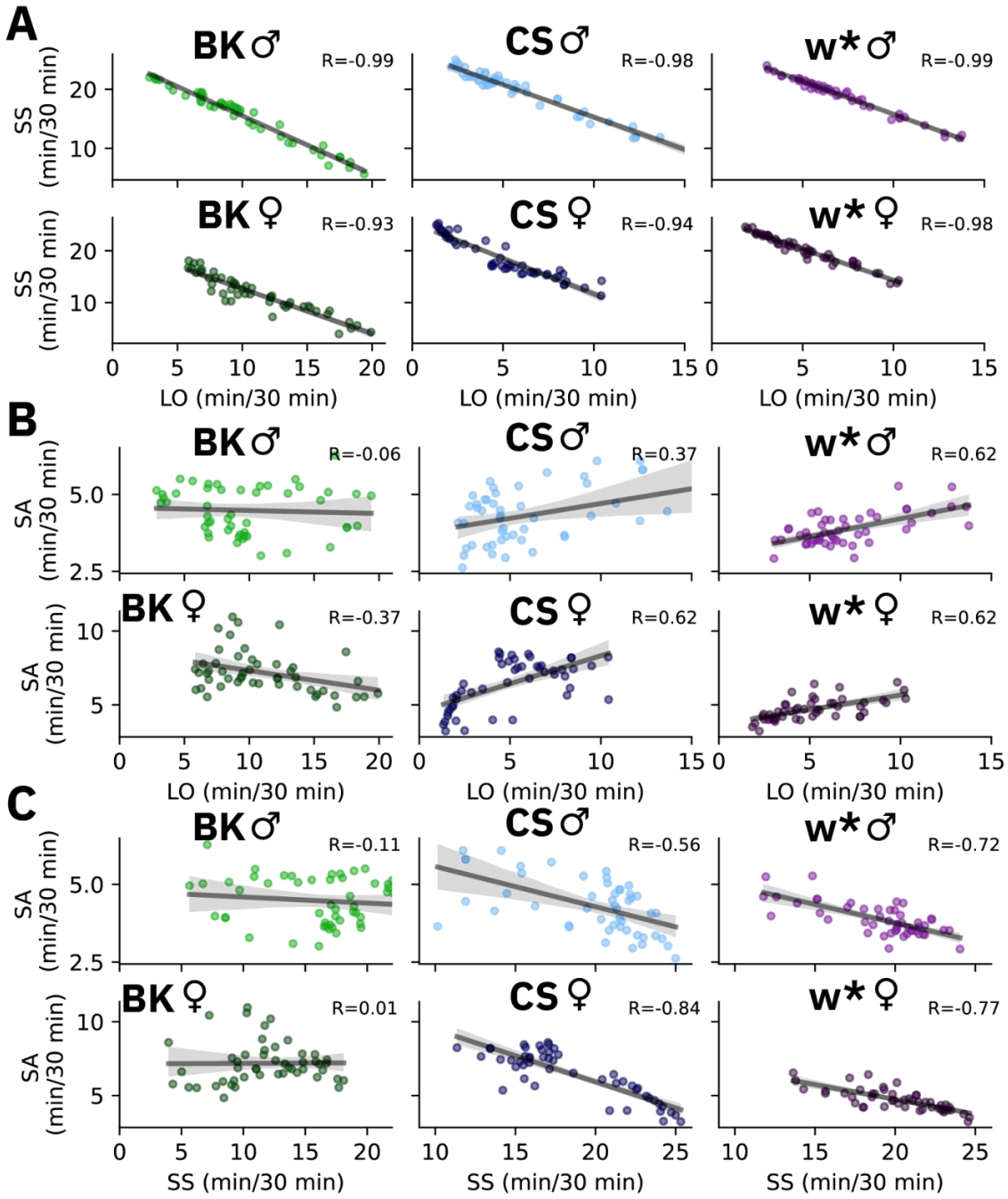

Appendix A Figure 1 The correlation between Trumelan behaviours for averaged data

The correlation between LO and SS **(A)**, LO and SA **(B)**, and SS and SA **(C)** for averaged wild-type fly data. Raw data is averaged for 30-minute bins over the 24-hour day; each dot indicates one bin. The black line and shaded area represent the fitted regression model. The correlation coefficient (R) is shown for each plot. The number of flies used for the averaged data in (A-C) was 60 for BK males, 30 for BK females, 30 for CS males, 59 for CS females, 49 for w* males, and 38 for w* females. SS and LO have strong inverse correlation, while SA and LO or SS have varied correlations depending on genotype.

Appendix A Table 1 The correlation between SS states for individual wild-type flies

The table is pertinent to Figure 3.3.3. The percentage time spent in a stationary static behavioural state was correlated against another stationary static behaviour state per 30-minute bin from raw data averaged over a 24-hour day for individual flies. The Pearson's R (Mean±CI) is shown for each comparison alongside the associated sample size.

Genotype	Sex	Comparison	Sample Size (n)	R Mean±CI
BK	M	SS vs SSL	60	0.91±0.01
BK	M	SS vs SSB	60	0.27±0.08
BK	M	SSL vs SSB	60	-0.10±0.08
BK	F	SS vs SSL	28	0.83±0.06
BK	F	SS vs SSB	30	0.37±0.15
BK	F	SSL vs SSB	28	-0.15±0.11
CS	M	SS vs SSL	30	0.87±0.07
CS	M	SS vs SSB	30	0.02±0.10
CS	M	SSL vs SSB	30	-0.38±0.10
CS	F	SS vs SSL	59	0.85±0.05
CS	F	SS vs SSB	59	-0.02±0.09
CS	F	SSL vs SSB	59	-0.46±0.07
w*	M	SS vs SSL	49	0.83±0.05
w*	M	SS vs SSB	49	0.10±0.10
w*	M	SSL vs SSB	49	-0.38±0.10
w*	F	SS vs SSL	38	0.78±0.06
w*	F	SS vs SSB	38	0.10±0.12
w*	F	SSL vs SSB	38	-0.45±0.09

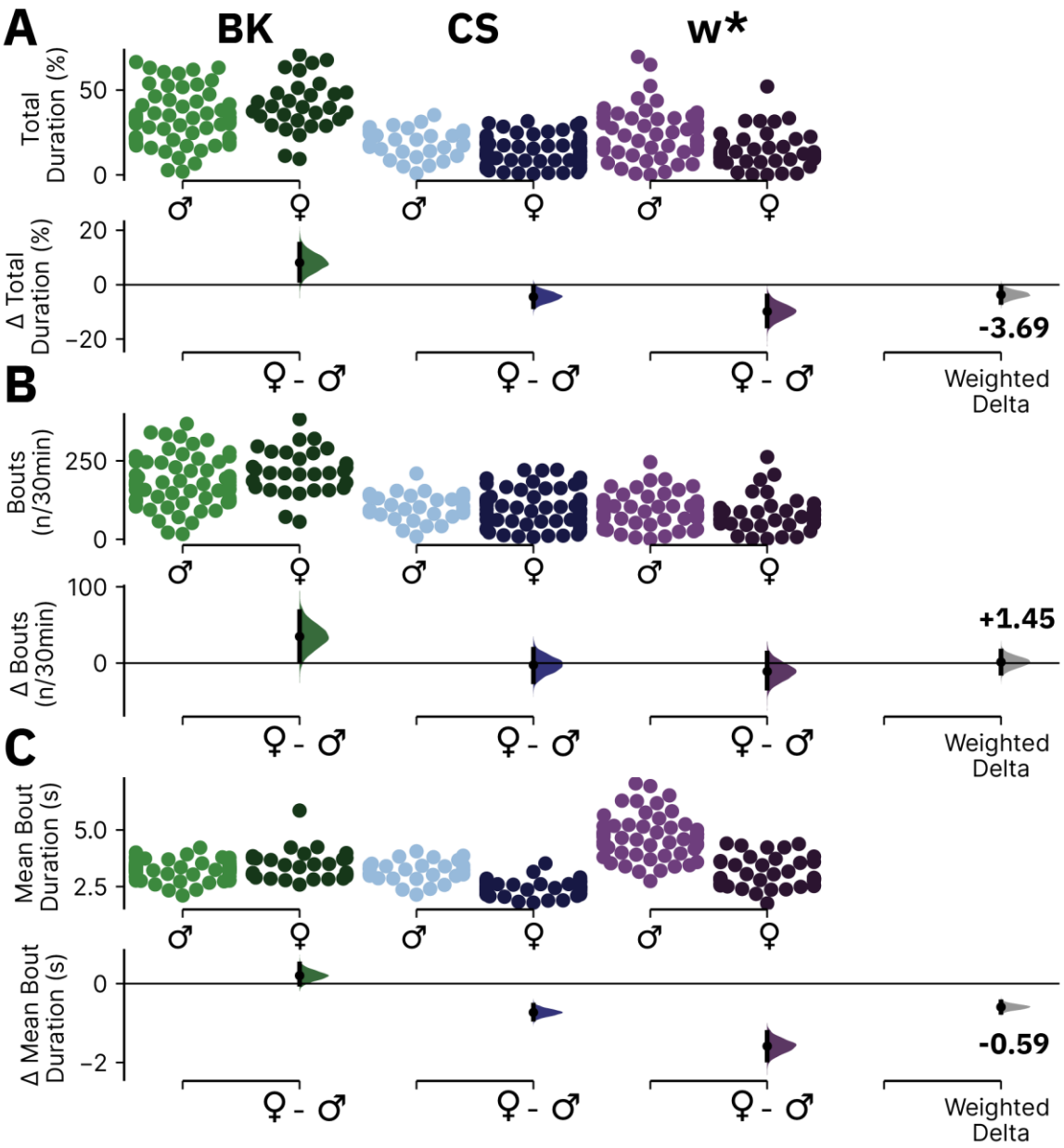

Appendix A Figure 2 The characteristics of LO for wild-type females vs. males

DABEST plots comparing percentage total duration **(A)**, number of bouts per 30 minutes **(B)**, and mean bout duration **(C)** for LO averaged over the 24-hour day in wild-type females vs. male flies of the same genotype. The sample sizes for (A-C) were 60 for BK males, 30 for BK females, 30 for CS males, 59 for CS females, 49 for w* males, and 38 for w* females. The summary data for these plots are shown in Appendix A Table 2-4. See Chapter 2.6 for more information about the structure of DABEST plots.

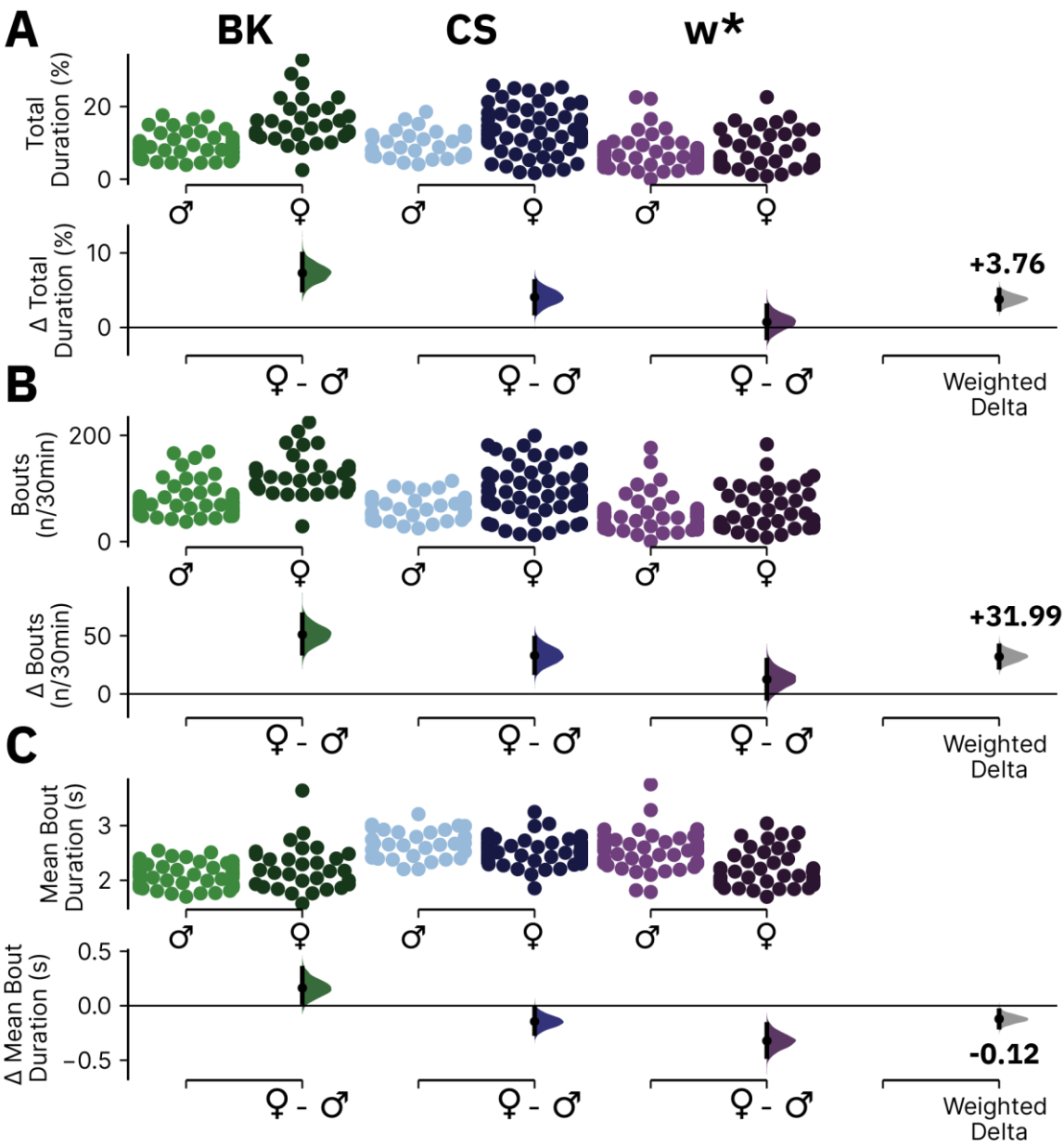

Appendix A Figure 3 The characteristics of SA for wild-type females vs. males

DABEST plots comparing percentage total duration **(A)**, number of bouts per 30 minutes **(B)**, and mean bout duration **(C)** for SA averaged over the 24-hour day in wild-type females vs. male flies of the same genotype. The sample sizes for (A-C) were 60 for BK males, 30 for BK females, 30 for CS males, 59 for CS females, 49 for w* males, and 38 for w* females. The summary data for these plots are shown in Appendix A Table 2-4. See Chapter 2.6 for more information about the structure of DABEST plots.

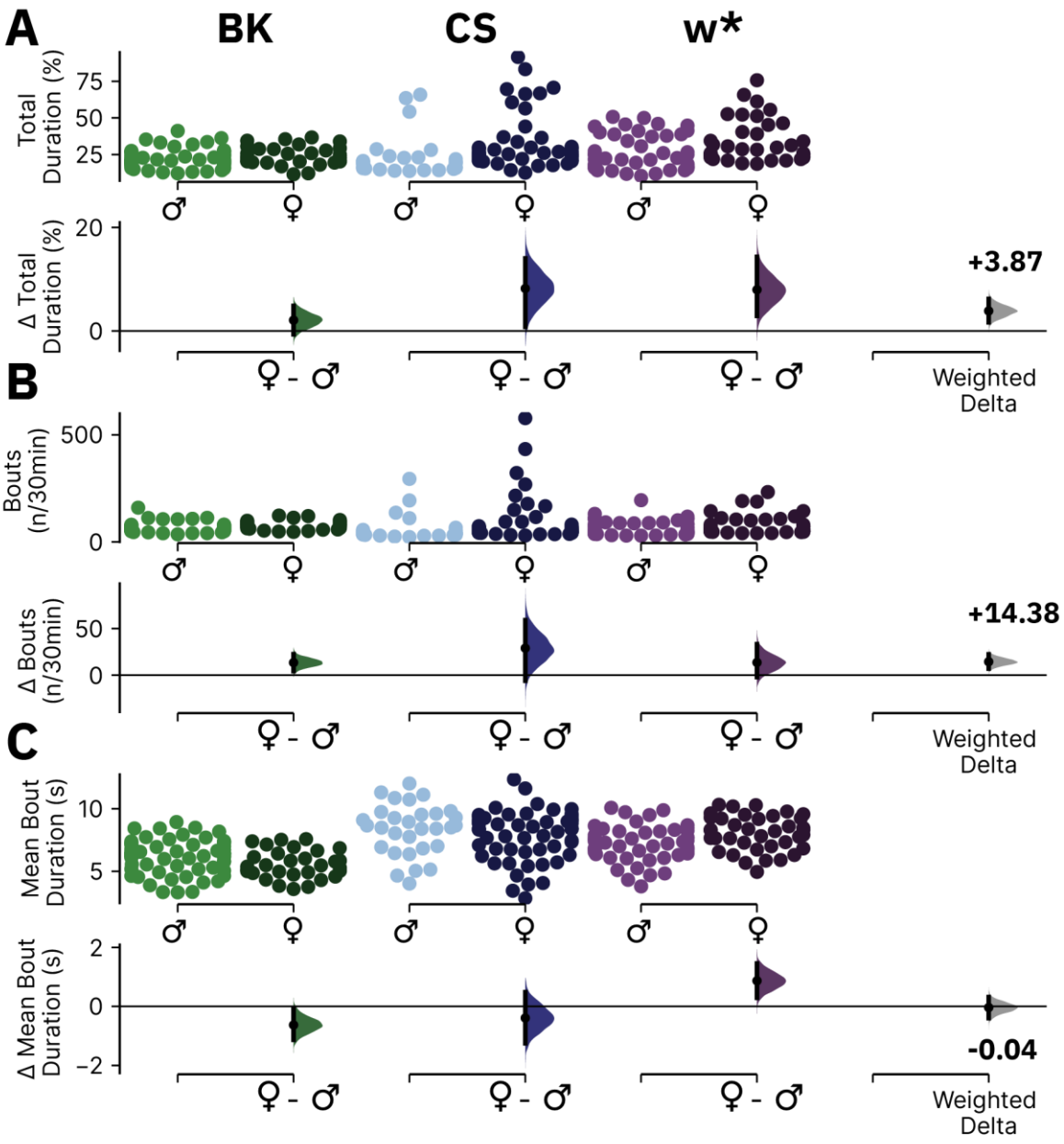

Appendix A Figure 4 The characteristics of SSB for wild-type females vs. males

DABEST plots comparing percentage total duration **(A)**, number of bouts per 30 minutes **(B)**, and mean bout duration **(C)** for SSB averaged over the 24-hour day in wild-type females vs. male flies of the same genotype. The sample sizes for (A-C) were 60 for BK males, 30 for BK females, 30 for CS males, 59 for CS females, 49 for w* males, and 38 for w* females. The summary data for these plots are shown in Appendix A Table 2-4. See Chapter 2.6 for more information about the structure of DABEST plots.

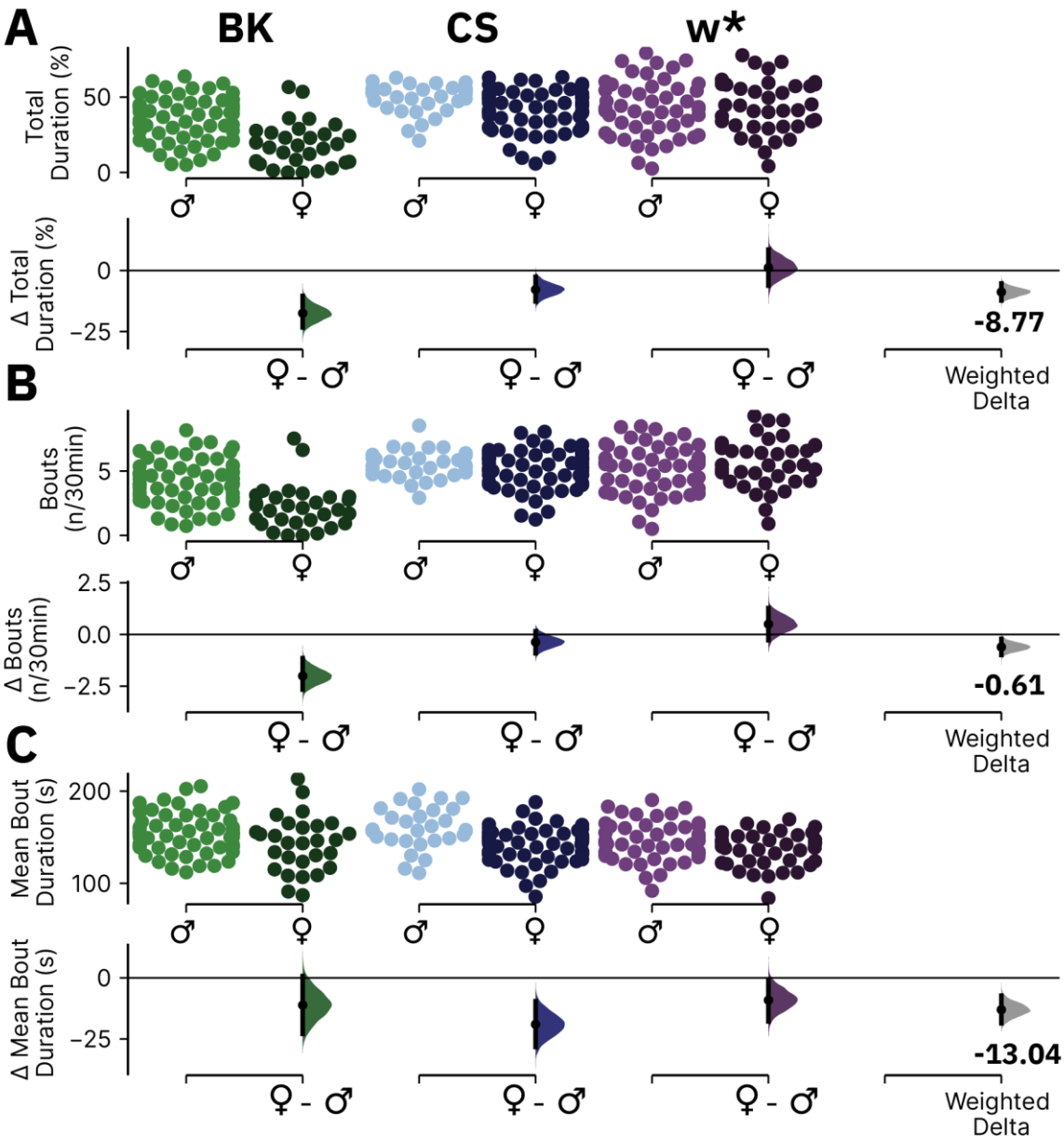

Appendix A Figure 5 The characteristics of SSL for wild-type females vs. males

DABEST plots comparing percentage total duration **(A)**, number of bouts per 30 minutes **(B)**, and mean bout duration **(C)** for SSL averaged over the 24-hour day in wild-type females vs. male flies of the same genotype. The sample sizes for (A-C) were 60 for BK males, 30 for BK females, 30 for CS males, 59 for CS females, 49 for w* males, and 38 for w* females. The summary data for these plots are shown in Appendix A Table 2-4. See Chapter 2.6 for more information about the structure of DABEST plots.

Appendix A Table 2 Behavioural state durations for wild-type females vs. males

The table is pertinent to Appendix A Figure 2-5. Each row illustrates a DABEST comparison of the percentage time spent in a given behavioural state in wild-type females vs. males. See Chapter 2.6 for more information about DABEST plots.

Genotype	State	Ctr / Test	Ctr (n)	Test (n)	Ctr Mean±CI (%)	Test Mean±CI (%)	Delta (%)	Delta-CI (%)	Delta+CI (%)	p-value
BK	LO	M / F	60	30	33.15±4.00	41.25±5.45	8.09	1.59	14.91	0.0246
CS	LO	M / F	30	59	18.68±3.02	14.20±2.19	-4.47	-8.13	-0.89	0.0242
w*	LO	M / F	49	38	24.60±4.31	14.74±3.48	-9.86	-15.18	-4.16	0.0010
Weighted Delta	LO	M / F	139	127	NA	NA	-3.69	-6.53	-0.85	0.0186
BK	SA	M / F	60	30	8.62±0.82	15.92±2.30	7.30	5.01	9.85	0.0000
CS	SA	M / F	30	59	9.39±1.33	13.45±1.66	4.07	1.94	6.17	0.0026
w*	SA	M / F	49	38	7.17±1.29	7.89±1.72	0.72	-1.41	2.91	0.4980
Weighted Delta	SA	M / F	139	127	NA	NA	3.76	2.44	5.06	0.0000
BK	SSB	M / F	60	30	22.30±1.55	24.38±2.31	2.08	-0.65	4.83	0.1362
CS	SSB	M / F	30	59	23.08±4.86	31.28±4.34	8.20	0.79	14.02	0.0272
w*	SSB	M / F	49	38	25.53±3.27	33.49±4.59	7.96	2.90	14.30	0.0054
Weighted Delta	SSB	M / F	139	127	NA	NA	3.87	1.65	6.21	0.0004
BK	SSL	M / F	60	30	35.93±3.73	18.45±5.26	-17.48	-23.33	-10.43	0.0000
CS	SSL	M / F	30	59	48.86±3.62	41.06±3.51	-7.79	-12.64	-2.55	0.0072
w*	SSL	M / F	49	38	42.70±5.19	43.88±5.61	1.18	-6.17	8.61	0.7682
Weighted Delta	SSL	M / F	139	127	NA	NA	-8.77	-12.27	-5.28	0.0000

Appendix A Table 3 Behavioural state bout number for wild-type females vs. males

Data is pertinent to Appendix A Figure 2-5. Each row illustrates a DABEST comparison of the mean number of bouts of a given behavioural state per 30-minute bin in wild-type females vs. males. See Chapter 2.6 for more information about DABEST plots.

Genotype	State	Ctr / Test	Ctr (n)	Test (n)	Ctr Mean±CI (n/30min)	Test Mean±CI (n/30min)	Delta (n/30min)	Delta-CI (n/30min)	Delta+CI (n/30min)	p-value
BK	LO	M / F	60	30	180.74±20.45	215.59±25.67	34.86	3.29	67.55	0.0476
CS	LO	M / F	30	59	103.90±15.80	101.49±15.05	-2.41	-24.37	18.32	0.8532
w*	LO	M / F	49	38	92.62±14.84	81.79±17.76	-10.83	-32.70	13.24	0.3686
Weighted Delta	LO	M / F	139	127	NA	NA	1.45	-13.10	15.87	0.8516
BK	SA	M / F	60	30	75.55±7.65	126.48±14.70	50.92	34.95	68.04	0.0000
CS	SA	M / F	30	59	63.82±8.76	96.82±12.09	33.01	18.23	47.87	0.0008
w*	SA	M / F	49	38	50.98±9.40	63.49±13.30	12.51	-3.66	29.05	0.1286
Weighted Delta	SA	M / F	139	127	NA	NA	31.99	22.85	41.23	0.0000
BK	SSB	M / F	60	30	66.86±5.34	80.28±7.41	13.42	4.23	22.45	0.0040
CS	SSB	M / F	30	59	58.31±20.48	87.21±24.82	28.91	-6.07	59.02	0.1430
w*	SSB	M / F	49	38	66.37±9.52	79.95±14.83	13.58	-2.15	33.17	0.1232
Weighted Delta	SSB	M / F	139	127	NA	NA	14.38	6.98	22.29	0.0008
BK	SSL	M / F	60	30	4.20±0.44	2.19±0.61	-2.01	-2.67	-1.15	0.0000
CS	SSL	M / F	30	59	5.51±0.40	5.14±0.38	-0.37	-0.92	0.15	0.2188
w*	SSL	M / F	49	38	5.12±0.54	5.62±0.60	0.49	-0.29	1.27	0.2378
Weighted Delta	SSL	M / F	139	127	NA	NA	-0.61	-0.99	-0.21	0.0044

Appendix A Table 4 Behavioural state mean bout duration for wild-type females vs. males

The table is pertinent to Appendix A Figure 2-5. Each row illustrates a DABEST comparison of the mean bout duration of a given behavioural state in wild-type females vs. males. See Chapter 2.6 for more information about DABEST plots.

Genotype	State	Ctr / Test	Ctr (n)	Test (n)	Ctr Mean±CI (s)	Test Mean±CI (s)	Delta (s)	Delta-CI (s)	Delta+CI (s)	p-value
BK	LO	M / F	60	30	3.24±0.10	3.44±0.23	0.20	-0.02	0.50	0.0790
CS	LO	M / F	30	59	3.18±0.16	2.45±0.08	-0.73	-0.90	-0.55	0.0000
w*	LO	M / F	49	38	4.69±0.28	3.11±0.21	-1.58	-1.94	-1.24	0.0000
Weighted Delta	LO	M / F	139	127	NA	NA	-0.59	-0.73	-0.46	0.0000
BK	SA	M / F	60	30	2.07±0.05	2.23±0.15	0.16	0.03	0.34	0.0120
CS	SA	M / F	30	59	2.66±0.09	2.52±0.06	-0.15	-0.26	-0.03	0.0110
w*	SA	M / F	49	38	2.54±0.09	2.22±0.11	-0.32	-0.47	-0.17	0.0000
Weighted Delta	SA	M / F	139	127	NA	NA	-0.12	-0.20	-0.04	0.0022
BK	SSB	M / F	60	30	6.19±0.34	5.56±0.40	-0.63	-1.13	-0.08	0.0292
CS	SSB	M / F	30	59	8.35±0.73	7.96±0.49	-0.39	-1.25	0.48	0.3790
w*	SSB	M / F	49	38	7.18±0.39	8.05±0.44	0.87	0.29	1.46	0.0042
Weighted Delta	SSB	M / F	139	127	NA	NA	-0.04	-0.40	0.32	0.8480
BK	SSL	M / F	60	30	153.88±5.35	142.71±11.11	-11.17	-22.91	0.72	0.0480
CS	SSL	M / F	30	59	160.27±8.09	141.23±4.87	-19.03	-28.32	-9.59	0.0000
w*	SSL	M / F	49	38	145.93±5.91	136.78±6.01	-9.14	-17.82	-1.03	0.0418
Weighted Delta	SSL	M / F	139	127	NA	NA	-13.04	-18.57	-7.30	0.0000

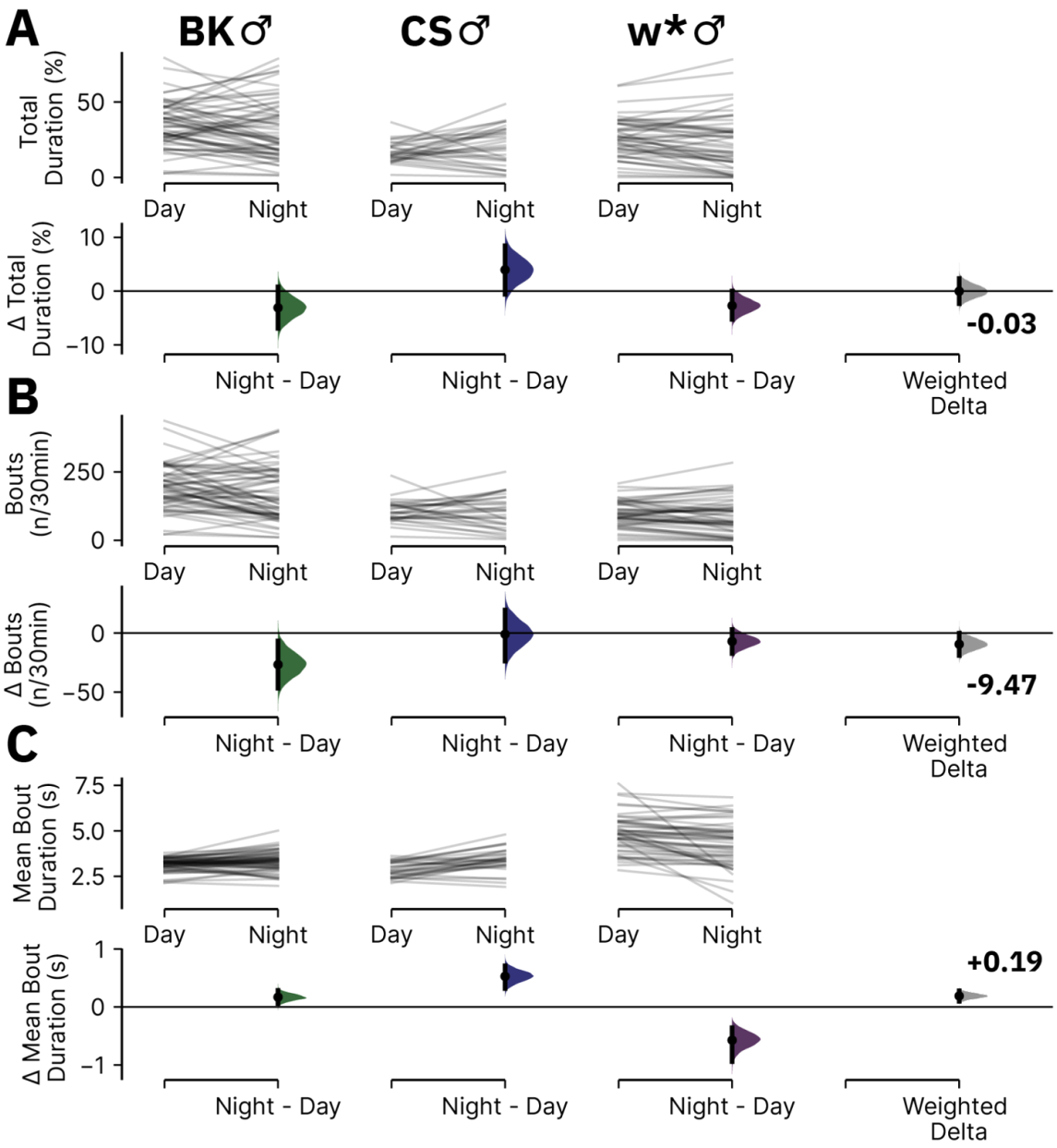

Appendix A Figure 6 The characteristics of LO during night vs. day in wild-type male flies

DABEST plots comparing percentage total duration **(A)**, number of bouts per 30 minutes **(B)**, and mean bout duration **(C)** for LO during night versus day in wild-type male flies. The sample sizes for (A-C) were 60 for BK males, 30 for CS males, 49 for w* males. The summary data for these plots are shown in Appendix A Table 5-7. See Chapter 2.6 for more information about the structure of DABEST plots.

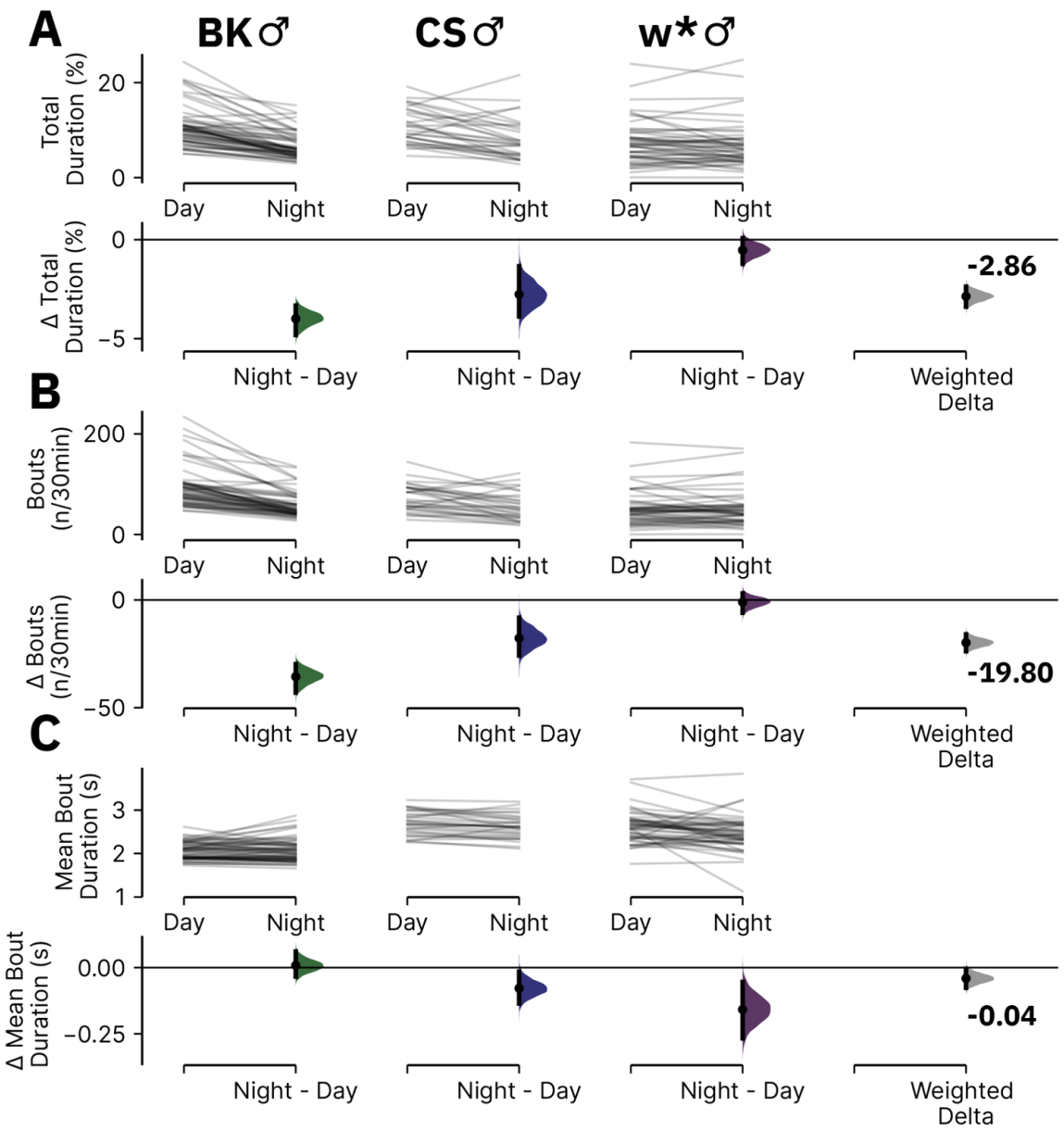

Appendix A Figure 7 The characteristics of SA during night vs. day in wild-type male flies

DABEST plots comparing percentage total duration **(A)**, number of bouts per 30 minutes **(B)**, and mean bout duration **(C)** for SA during night versus day in wild-type male flies. The sample sizes for (A-C) were 60 for BK males, 30 for CS males, 49 for w* males. The summary data for these plots are shown in Appendix A Table 5-7. See Chapter 2.6 for more information about the structure of DABEST plots.

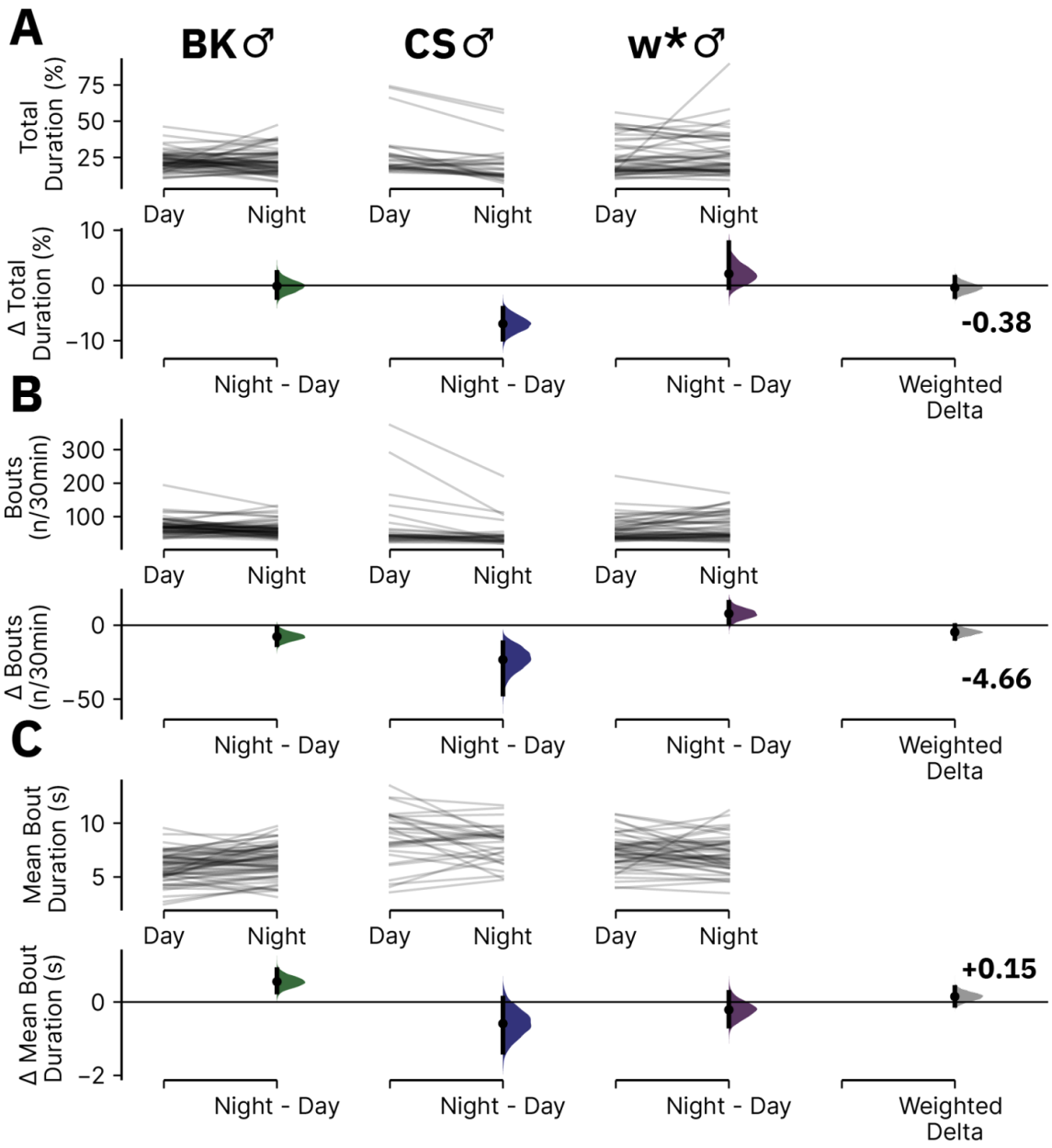

Appendix A Figure 8 The characteristics of SSB during night vs. day in wild-type males

DABEST plots comparing percentage total duration **(A)**, number of bouts per 30 minutes **(B)**, and mean bout duration **(C)** for SSB during night versus day in wild-type male flies. The sample sizes for (A-C) were 60 for BK males, 30 for CS males, 49 for w* males. The summary data for these plots are shown in Appendix A Table 5-7. See Chapter 2.6 for more information about the structure of DABEST plots.

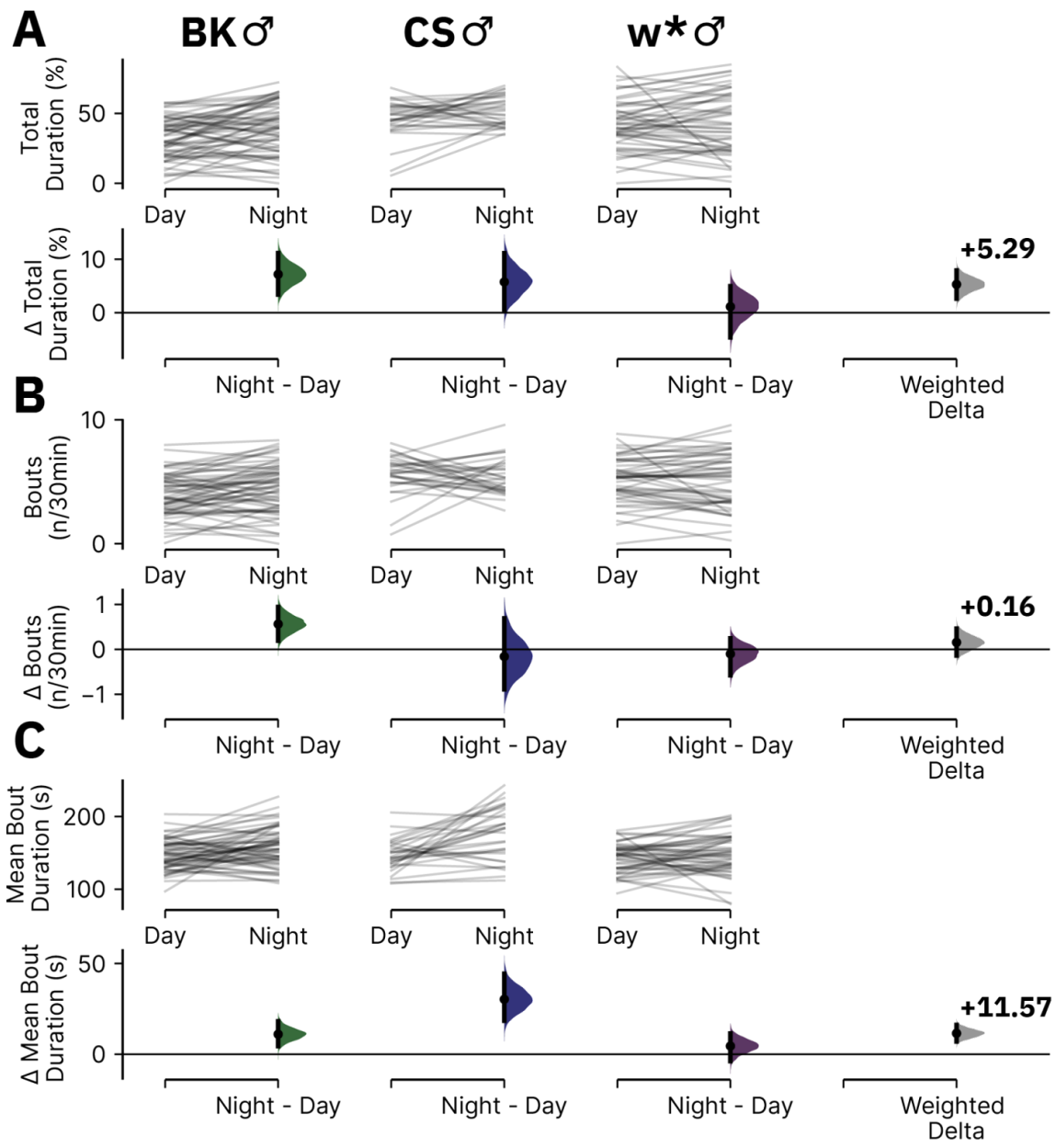

Appendix A Figure 9 The characteristics of SSL during night vs. day in males

DABEST plots comparing percentage total duration **(A)**, number of bouts per 30 minutes **(B)**, and mean bout duration **(C)** for SSL during night versus day in male flies. The sample sizes for (A-C) were 60 for BK males, 30 for CS males, 49 for w* males. The summary data for these plots are shown in Appendix A Table 5-7. See Chapter 2.6 for more information about the structure of DABEST plots.

Appendix A Table 5 Behavioural state durations for night vs. day in wild-type male flies

The table is pertinent to Appendix A Figure 6-9. Each row illustrates a DABEST comparison of the percentage time spent in a given behavioural state during night vs. day in wild-type male flies. See Chapter 2.6 for more information about DABEST plots.

Genotype	State	Ctr / Test	Ctr (n)	Test (n)	Ctr Mean±CI (%)	Test Mean±CI (%)	Delta (%)	Delta-CI (%)	Delta+CI (%)	p-value
BK	LO	Day / Night	60	60	34.85±3.91	31.75±4.91	-3.10	-9.22	3.51	0.3440
CS	LO	Day / Night	30	30	16.75±2.45	20.71±4.65	3.96	-1.20	9.25	0.1486
w*	LO	Day / Night	49	49	26.05±3.76	23.34±5.12	-2.71	-8.80	3.96	0.4114
Weighted Delta	LO	Day / Night	139	139	NA	NA	-0.03	-3.34	3.46	0.9880
BK	SA	Day / Night	60	60	10.67±1.07	6.68±0.71	-3.99	-5.36	-2.81	0.0000
CS	SA	Day / Night	30	30	10.88±1.35	8.11±1.58	-2.77	-4.64	-0.57	0.0108
w*	SA	Day / Night	49	49	7.45±1.31	6.92±1.35	-0.53	-2.41	1.39	0.6010
Weighted Delta	SA	Day / Night	139	139	NA	NA	-2.86	-3.81	-1.95	0.0000
BK	SSB	Day / Night	60	60	22.38±1.68	22.29±2.12	-0.09	-2.67	2.68	0.9488
CS	SSB	Day / Night	30	30	26.75±5.71	19.80±4.48	-6.94	-14.93	-0.34	0.0618
w*	SSB	Day / Night	49	49	24.62±3.44	26.73±4.15	2.12	-3.05	8.09	0.4390
Weighted Delta	SSB	Day / Night	139	139	NA	NA	-0.38	-2.65	1.93	0.7604
BK	SSL	Day / Night	60	60	32.10±3.68	39.28±4.64	7.18	0.89	12.84	0.0162
CS	SSL	Day / Night	30	30	45.63±5.03	51.38±3.83	5.75	0.13	12.80	0.0774
w*	SSL	Day / Night	49	49	41.88±5.03	43.00±6.22	1.12	-6.62	9.30	0.7902
Weighted Delta	SSL	Day / Night	139	139	NA	NA	5.29	1.48	8.95	0.0072

Appendix A Table 6 Behavioural state bout number for night vs. day in wild-type male flies

The table is pertinent to Appendix A Figure 6-9. Each row illustrates a DABEST comparison of the mean number of bouts of a given behavioural state per 30-minute bin during night vs. day in wild-type male flies. See Chapter 2.6 for more information about DABEST plots.

Genotype	State	Ctr / Test	Ctr (n)	Test (n)	Ctr Mean±CI (n/30min)	Test Mean±CI (n/30min)	Delta (n/30min)	Delta-CI (n/30min)	Delta+CI (n/30min)	p-value
BK	LO	Day / Night	60	60	195.04±20.85	168.32±24.53	-26.72	-58.11	6.55	0.1058
CS	LO	Day / Night	30	30	105.30±14.73	104.31±22.43	-0.99	-27.35	26.11	0.9460
w*	LO	Day / Night	49	49	96.58±13.12	89.51±17.88	-7.08	-28.31	16.14	0.5332
Weighted Delta	LO	Day / Night	139	139	NA	NA	-9.47	-24.39	5.71	0.2306
BK	SA	Day / Night	60	60	93.86±10.15	58.27±6.24	-35.60	-48.61	-24.96	0.0000
CS	SA	Day / Night	30	30	73.43±9.70	55.69±10.03	-17.73	-30.87	-3.93	0.0150
w*	SA	Day / Night	49	49	51.56±9.50	50.61±9.85	-0.95	-14.78	12.76	0.8970
Weighted Delta	SA	Day / Night	139	139	NA	NA	-19.80	-27.50	-12.60	0.0000
BK	SSB	Day / Night	60	60	70.95±6.34	63.25±5.82	-7.70	-16.40	0.78	0.0852
CS	SSB	Day / Night	30	30	70.67±28.15	47.34±14.31	-23.33	-62.59	2.42	0.1658
w*	SSB	Day / Night	49	49	62.61±9.97	70.49±10.52	7.88	-7.31	21.74	0.2902
Weighted Delta	SSB	Day / Night	139	139	NA	NA	-4.66	-12.03	2.41	0.2146
BK	SSL	Day / Night	60	60	3.89±0.43	4.46±0.51	0.56	-0.15	1.22	0.0984
CS	SSL	Day / Night	30	30	5.57±0.58	5.41±0.53	-0.16	-0.87	0.71	0.6902
w*	SSL	Day / Night	49	49	5.15±0.52	5.05±0.62	-0.10	-0.88	0.72	0.8160
Weighted Delta	SSL	Day / Night	139	139	NA	NA	0.16	-0.27	0.59	0.4850

Appendix A Table 7 Behavioural state mean bout duration for night vs. day in wild-type male flies

The table is pertinent to Appendix A Figure 6-9. Each row illustrates a DABEST comparison of the mean bout duration of a given behavioural state during night vs. day in wild-type male flies. See Chapter 2.6 for more information about DABEST plots.

Genotype	State	Ctr / Test	Ctr (n)	Test (n)	Ctr Mean±CI (s)	Test Mean±CI (s)	Delta (s)	Delta-CI (s)	Delta+CI (s)	p-value
BK	LO	Day / Night	60	60	3.16±0.09	3.32±0.14	0.17	0.00	0.34	0.0524
CS	LO	Day / Night	30	30	2.86±0.15	3.39±0.23	0.53	0.26	0.79	0.0004
w*	LO	Day / Night	49	49	4.83±0.29	4.26±0.35	-0.57	-1.02	-0.12	0.0146
Weighted Delta	LO	Day / Night	139	139	NA	NA	0.19	0.05	0.33	0.0094
BK	SA	Day / Night	60	60	2.06±0.05	2.07±0.07	0.01	-0.07	0.09	0.8474
CS	SA	Day / Night	30	30	2.70±0.10	2.62±0.10	-0.08	-0.21	0.05	0.2654
w*	SA	Day / Night	49	49	2.61±0.10	2.46±0.11	-0.16	-0.32	-0.01	0.0428
Weighted Delta	SA	Day / Night	139	139	NA	NA	-0.04	-0.11	0.02	0.2246
BK	SSB	Day / Night	60	60	5.91±0.36	6.47±0.39	0.56	0.04	1.10	0.0390
CS	SSB	Day / Night	30	30	8.66±0.89	8.07±0.65	-0.59	-1.66	0.49	0.3120
w*	SSB	Day / Night	49	49	7.33±0.45	7.11±0.46	-0.21	-0.87	0.40	0.5136
Weighted Delta	SSB	Day / Night	139	139	NA	NA	0.15	-0.24	0.52	0.4596
BK	SSL	Day / Night	59	59	147.07±5.34	158.14±6.80	11.07	2.13	19.61	0.0146
CS	SSL	Day / Night	30	30	146.75±7.89	177.03±13.11	30.28	14.73	44.95	0.0008
w*	SSL	Day / Night	48	48	143.09±5.71	147.64±7.96	4.56	-5.26	14.02	0.3604
Weighted Delta	SSL	Day / Night	137	137	NA	NA	11.57	5.43	17.30	0.0004

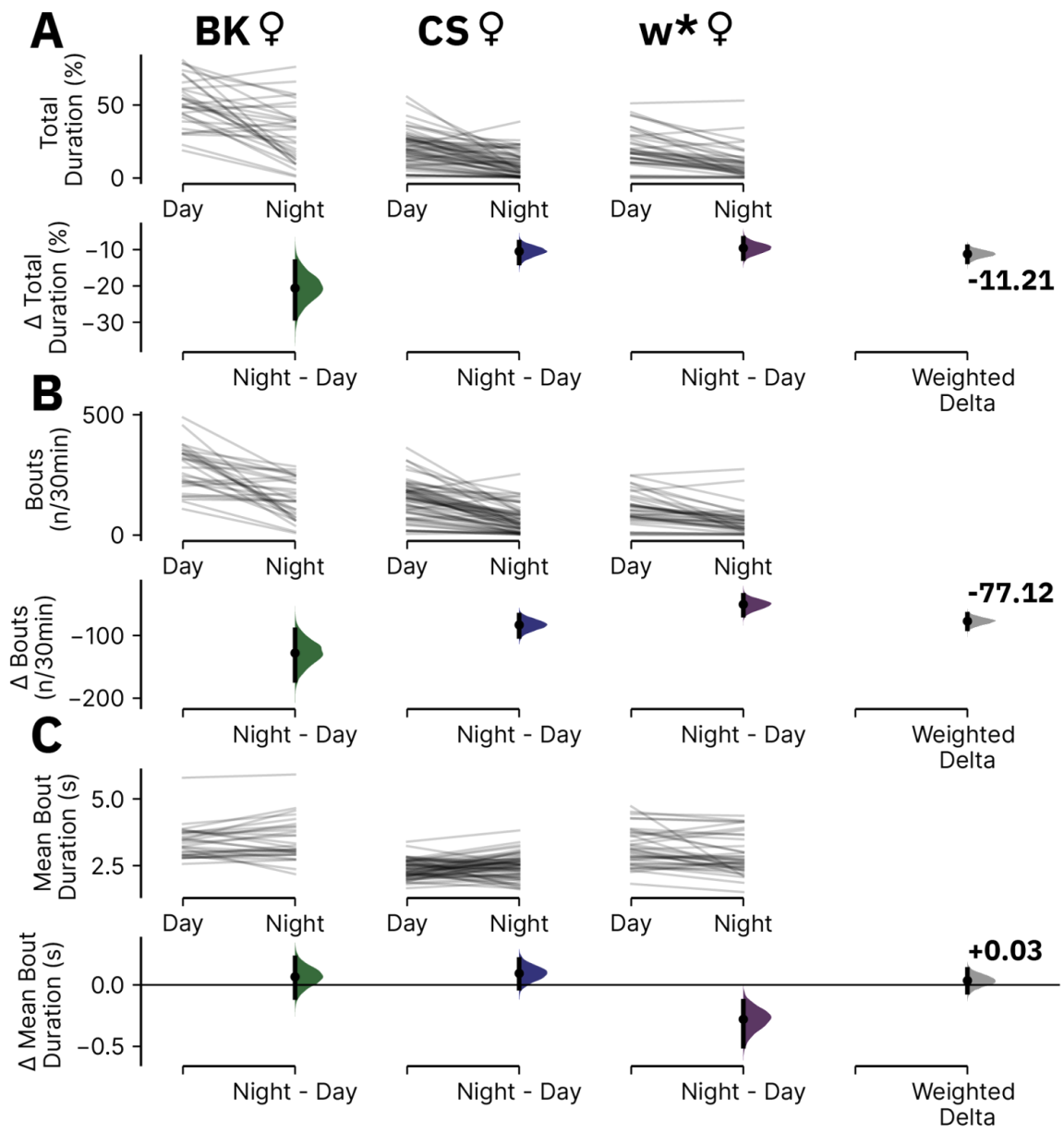

Appendix A Figure 10 The characteristics of LO during night vs. day in wild-type female flies

DABEST plots comparing percentage total duration **(A)**, number of bouts per 30 minutes **(B)**, and mean bout duration **(C)** for LO during night vs. day in wild-type female flies. The sample sizes for (A-C) were 30 for BK females, 59 for CS females, and 38 for w* females. The summary data for these plots are shown in Appendix A Table 8-10. See Chapter 2.6 for more information about the structure of DABEST plots.

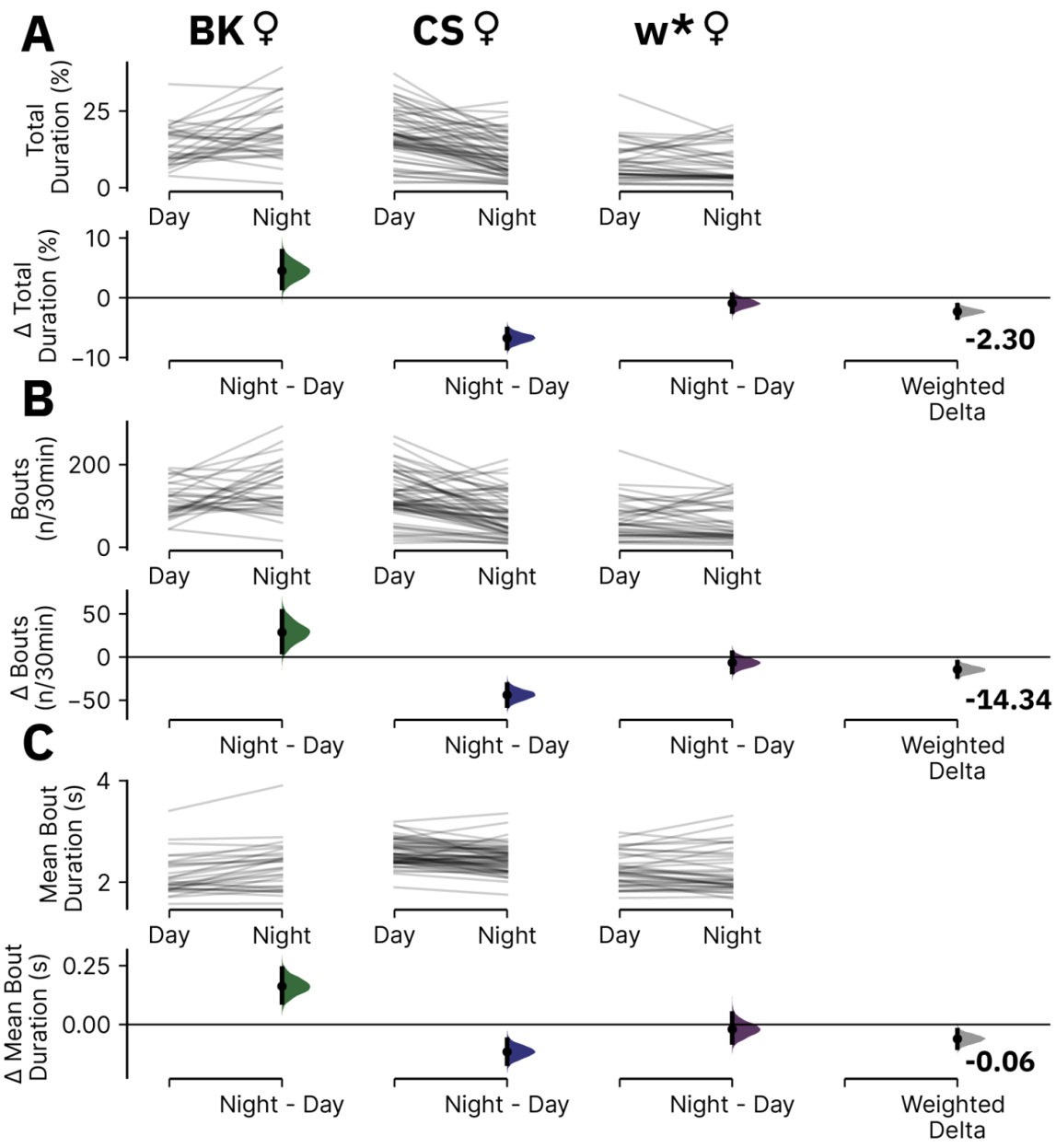

Appendix A Figure 11 The characteristics of SA during night vs. day in wild-type female flies

DABEST plots comparing percentage total duration **(A)**, number of bouts per 30 minutes **(B)**, and mean bout duration **(C)** for SA during night vs. day in wild-type female flies. The sample sizes for (A-C) were 30 for BK females, 59 for CS females, and 38 for w* females. The summary data for these plots are shown in Appendix A Table 8-10. See Chapter 2.6 for more information about the structure of DABEST plots.

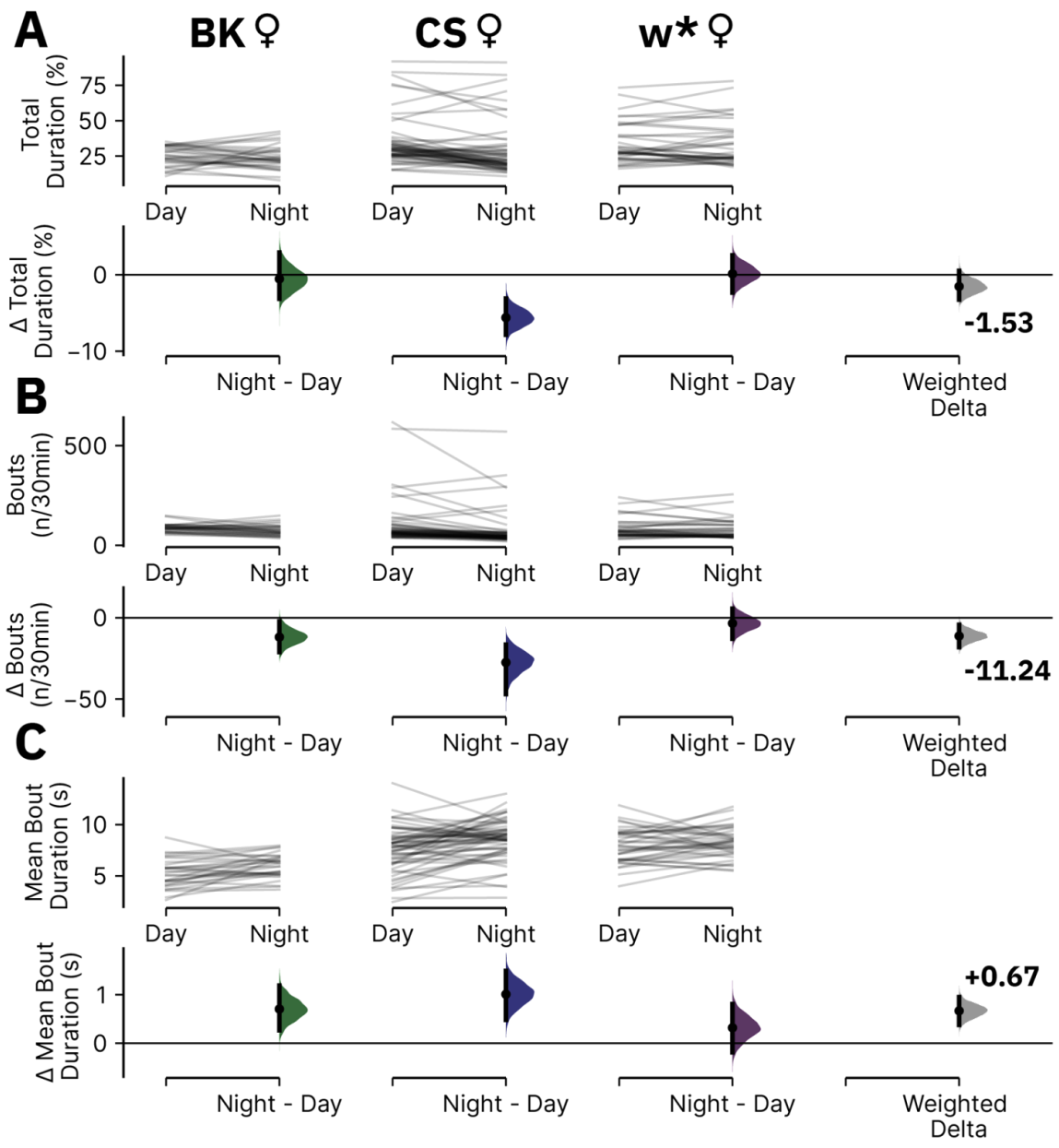

Appendix A Figure 12 The characteristics of SSB during night vs. day in wild-type female flies

DABEST plots comparing percentage total duration **(A)**, number of bouts per 30 minutes **(B)**, and mean bout duration **(C)** for SSB during night vs. day in female flies. The sample sizes for (A-C) were 30 for BK females, 59 for CS females, and 38 for w* females. The summary data for these plots are shown in Appendix A Table 8-10. See Chapter 2.6 for more information about the structure of DABEST plots.

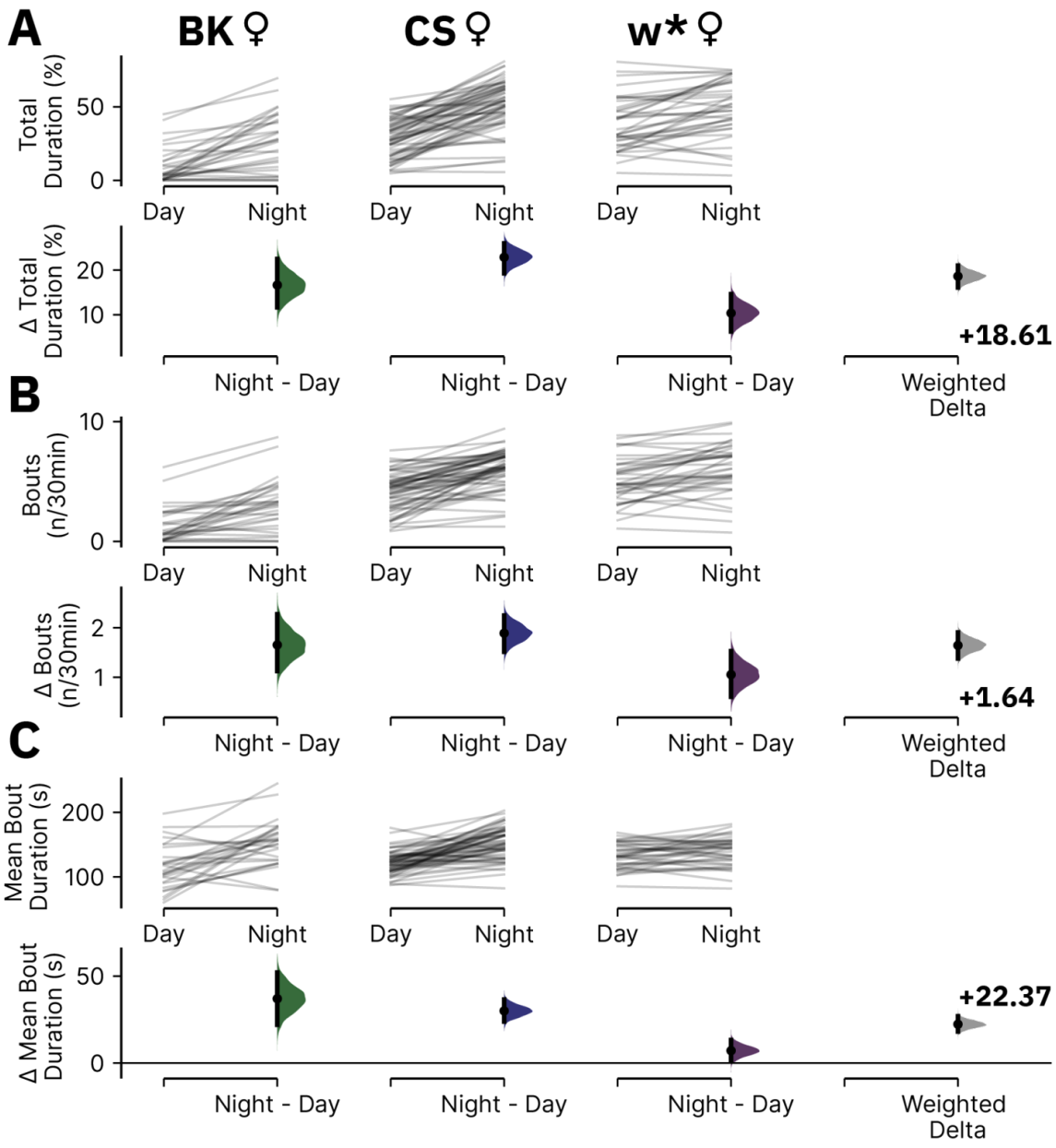

Appendix A Figure 13 The characteristics of SSL during night vs. day in wild-type female flies

DABEST plots comparing percentage total duration **(A)**, number of bouts per 30 minutes **(B)**, and mean bout duration **(C)** for SSL during night vs. day in wild-type female flies. The sample sizes for (A-C) 30 for BK females, 59 for CS females, and 38 for w* females. The summary data for these plots are shown in Appendix A Table 8-10. See Chapter 2.6 for more information about the structure of DABEST plots.

Appendix A Table 8 Behavioural state durations for night vs. day in wild-type female flies

The table is pertinent to Appendix A Figure 10-13. Each row illustrates a DABEST comparison of the percentage time spent in a given behavioural state during night vs. day in wild-type female flies. See Chapter 2.6 for more information about DABEST plots.

Genotype	State	Ctr / Test	Ctr (n)	Test (n)	Ctr Mean±CI (%)	Test Mean±CI (%)	Delta (%)	Delta-CI (%)	Delta+CI (%)	p-value
BK	LO	Day / Night	30	30	51.45±5.95	30.84±7.16	-20.61	-29.61	-11.05	0.0002
CS	LO	Day / Night	59	59	19.94±3.04	9.43±2.15	-10.51	-14.29	-6.91	0.0000
w*	LO	Day / Night	38	38	19.77±4.09	10.19±3.40	-9.59	-14.58	-4.00	0.0000
Weighted Delta	LO	Day / Night	127	127	NA	NA	-11.21	-14.14	-8.32	0.0000
BK	SA	Day / Night	30	30	13.82±2.30	18.32±3.14	4.50	0.71	8.33	0.0268
CS	SA	Day / Night	59	59	17.18±2.05	10.43±1.65	-6.75	-9.41	-4.12	0.0000
w*	SA	Day / Night	38	38	8.45±1.95	7.53±1.84	-0.91	-3.71	1.54	0.5090
Weighted Delta	SA	Day / Night	127	127	NA	NA	-2.30	-4.05	-0.65	0.0110
BK	SSB	Day / Night	30	30	24.78±2.53	24.24±3.01	-0.54	-4.22	3.62	0.8046
CS	SSB	Day / Night	59	59	34.29±4.36	28.68±4.62	-5.60	-11.84	0.66	0.0870
w*	SSB	Day / Night	38	38	33.43±4.51	33.55±4.98	0.12	-6.28	7.06	0.9746
Weighted Delta	SSB	Day / Night	127	127	NA	NA	-1.53	-4.36	1.49	0.3212
BK	SSL	Day / Night	30	30	9.95±4.49	26.60±6.94	16.64	8.39	24.54	0.0010
CS	SSL	Day / Night	59	59	28.60±3.33	51.46±4.26	22.86	17.27	27.98	0.0000
w*	SSL	Day / Night	38	38	38.35±5.71	48.73±6.17	10.38	1.66	18.18	0.0166
Weighted Delta	SSL	Day / Night	127	127	NA	NA	18.61	14.58	22.36	0.0000

Appendix A Table 9 Behavioural state bout number for night vs. day in wild-type female flies

The table is pertinent to Appendix A Figure 10-13. Each row illustrates a DABEST comparison of the mean number of bouts of a given behavioural state per 30-minute bin during night vs. day in wild-type female flies. See Chapter 2.6 for more information about DABEST plots.

Genotype	State	Ctr / Test	Ctr (n)	Test (n)	Ctr Mean±CI (n/30min)	Test Mean±CI (n/30min)	Delta (n/30min)	Delta-CI (n/30min)	Delta+CI (n/30min)	p-value
BK	LO	Day / Night	30	30	279.12±33.80	151.11±29.55	-128.01	-171.71	-82.09	0.0000
CS	LO	Day / Night	59	59	146.75±20.33	63.62±13.99	-83.13	-107.50	-59.04	0.0000
w*	LO	Day / Night	38	38	108.42±20.97	58.07±17.96	-50.35	-76.16	-20.99	0.0002
Weighted Delta	LO	Day / Night	127	127	NA	NA	-77.12	-93.95	-59.44	0.0000
BK	SA	Day / Night	30	30	113.61±14.80	142.30±22.40	28.69	2.83	55.80	0.0384
CS	SA	Day / Night	59	59	121.11±14.77	77.35±12.55	-43.76	-63.75	-24.67	0.0000
w*	SA	Day / Night	38	38	67.47±14.95	61.06±14.26	-6.41	-27.59	12.54	0.5480
Weighted Delta	SA	Day / Night	127	127	NA	NA	-14.34	-27.08	-1.93	0.0320
BK	SSB	Day / Night	30	30	86.67±7.77	74.79±9.94	-11.89	-24.92	0.35	0.0688
CS	SSB	Day / Night	59	59	102.36±28.26	74.88±23.73	-27.48	-65.66	6.55	0.1454
w*	SSB	Day / Night	38	38	81.98±15.45	78.56±15.79	-3.42	-24.50	19.57	0.7672
Weighted Delta	SSB	Day / Night	127	127	NA	NA	-11.24	-21.43	-1.15	0.0386
BK	SSL	Day / Night	30	30	1.34±0.55	2.99±0.77	1.65	0.74	2.60	0.0014
CS	SSL	Day / Night	59	59	4.11±0.41	6.00±0.42	1.89	1.30	2.46	0.0000
w*	SSL	Day / Night	38	38	5.05±0.61	6.11±0.67	1.05	0.12	1.92	0.0260
Weighted Delta	SSL	Day / Night	127	127	NA	NA	1.64	1.22	2.06	0.0000

Appendix A Table 10 Behavioural state mean bout duration for night vs. day in wild-type female flies

The table is pertinent to Appendix A Figure 10-13. Each row illustrates a DABEST comparison of the mean bout duration of a given behavioural state during night vs. day in wild-type female flies. See Chapter 2.6 for more information about DABEST plots.

Genotype	State	Ctr / Test	Ctr (n)	Test (n)	Ctr Mean±CI (s)	Test Mean±CI (s)	Delta (s)	Delta-CI (s)	Delta+CI (s)	p-value
BK	LO	Day / Night	30	30	3.38±0.22	3.44±0.28	0.07	-0.28	0.43	0.7226
CS	LO	Day / Night	59	59	2.37±0.09	2.47±0.12	0.09	-0.05	0.24	0.2022
w*	LO	Day / Night	38	38	3.17±0.22	2.89±0.23	-0.28	-0.59	0.04	0.0970
Weighted Delta	LO	Day / Night	127	127	NA	NA	0.03	-0.09	0.16	0.5728
BK	SA	Day / Night	30	30	2.13±0.14	2.30±0.17	0.16	-0.04	0.39	0.1430
CS	SA	Day / Night	59	59	2.57±0.06	2.46±0.07	-0.12	-0.21	-0.02	0.0142
w*	SA	Day / Night	38	38	2.23±0.10	2.21±0.13	-0.02	-0.18	0.15	0.8204
Weighted Delta	SA	Day / Night	127	127	NA	NA	-0.06	-0.14	0.02	0.1370
BK	SSB	Day / Night	30	30	5.24±0.51	5.95±0.41	0.70	0.05	1.34	0.0384
CS	SSB	Day / Night	59	59	7.56±0.57	8.57±0.50	1.01	0.25	1.79	0.0104
w*	SSB	Day / Night	38	38	7.93±0.53	8.25±0.48	0.32	-0.38	1.05	0.3940
Weighted Delta	SSB	Day / Night	127	127	NA	NA	0.67	0.27	1.07	0.0016
BK	SSL	Day / Night	28	28	115.38±12.98	152.45±13.47	37.07	18.43	55.37	0.0000
CS	SSL	Day / Night	59	59	121.91±4.58	151.98±6.39	30.07	21.93	37.57	0.0000
w*	SSL	Day / Night	38	38	132.46±6.29	139.63±7.19	7.17	-2.39	16.19	0.1508
Weighted Delta	SSL	Day / Night	125	125	NA	NA	22.37	16.57	27.91	0.0000

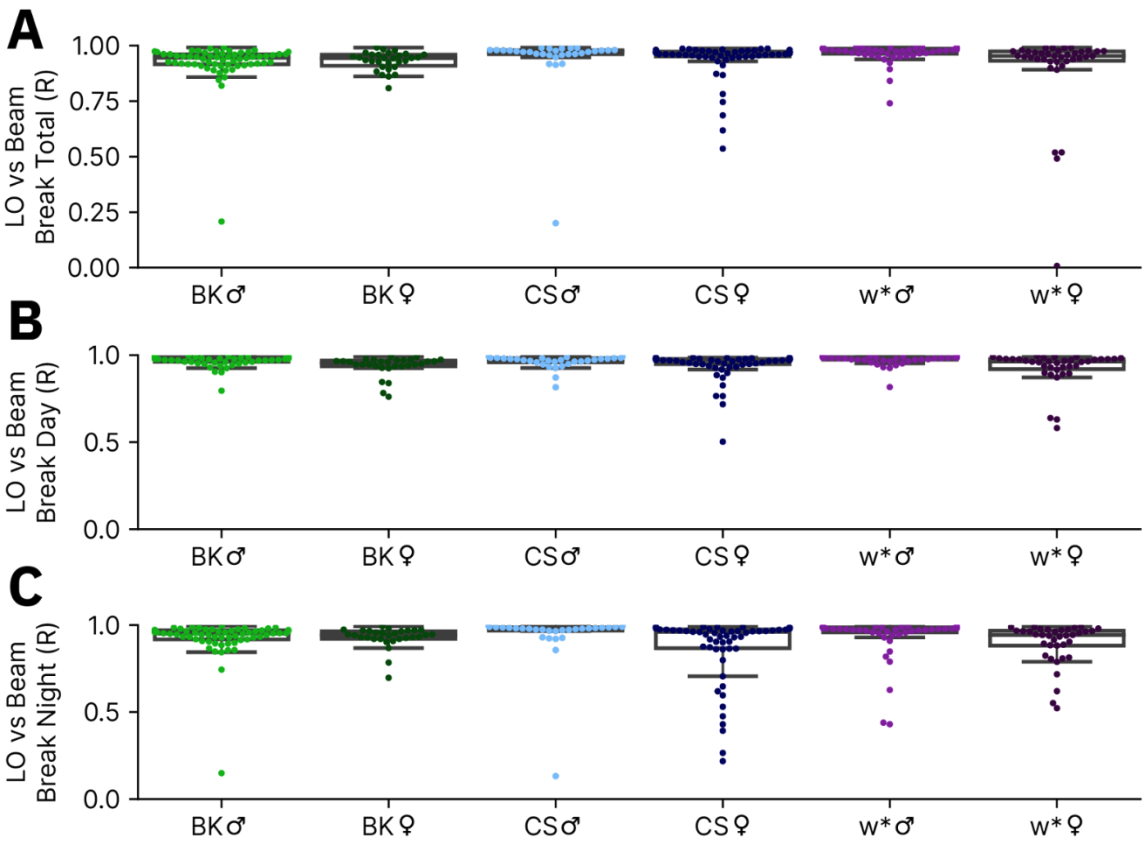

Appendix A Figure 14 The correlation of virtual DAM beam breaks with LO

The correlation (Pearson's R) of LO versus the number of beam breaking events per 30-minute bin for whole day **(A)**, day time **(B)**, or night time **(C)**. Raw data was averaged over a 24-hour day and separated into 30-minute bins. Each dot is an individual flies of a given genotype and box plots are drawn underneath to represent the quartiles of the data. The summary data and sample sizes are shown in Appendix A Table 11.

Appendix A Table 11 The correlation of virtual DAM beam breaks with LO

The table is pertinent to Appendix A Figure 14. The correlation (Pearson's R) of locomotor behaviour (LO) versus the number of beam breaking events, per 30-minute bin for individual flies. Data is grouped into the daytime, nighttime, or total. The sample size is shown in a list, for each comparison (Total, Day, Night).

Genotype	Sex	Comparison	Sample Size (n)	Total R Mean±CI	Day R Mean±CI	Night R Mean±CI
BK	M	LO vs Beam Break	[60, 60, 60]	0.92±0.03	0.97±0.01	0.92±0.03
BK	F	LO vs Beam Break	[30, 30, 30]	0.93±0.01	0.94±0.02	0.93±0.02
CS	M	LO vs Beam Break	[30, 30, 30]	0.94±0.05	0.96±0.01	0.94±0.06
CS	F	LO vs Beam Break	[59, 59, 58]	0.94±0.02	0.94±0.02	0.87±0.05
w*	M	LO vs Beam Break	[49, 49, 48]	0.97±0.01	0.98±0.01	0.94±0.03
w*	F	LO vs Beam Break	[38, 38, 37]	0.90±0.06	0.90±0.06	0.89±0.04

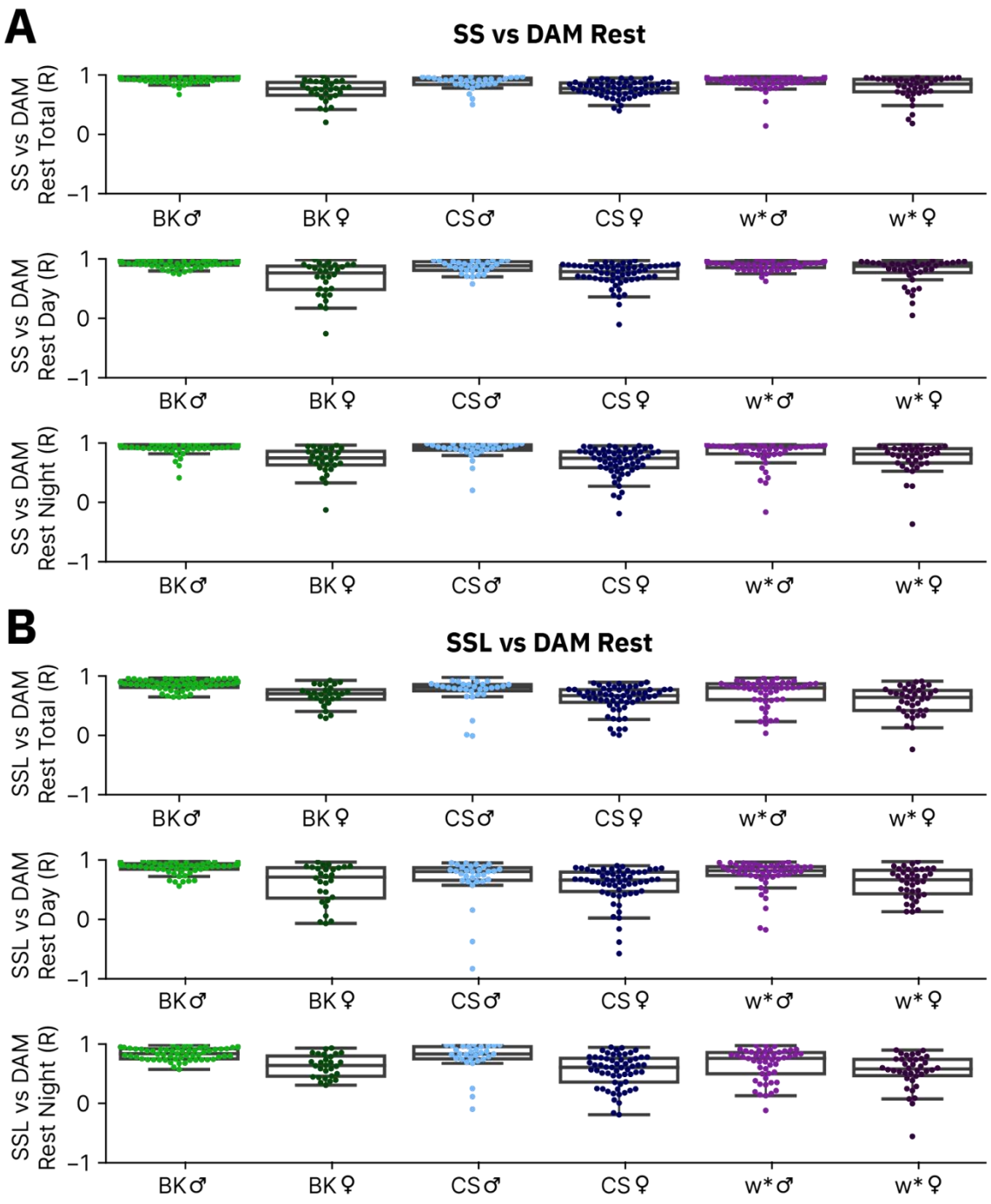

Appendix A Figure 15 The correlation of stationary static behaviour with virtual DAM rest

The correlation (Pearson's R) of SS **(A)** or SSL **(B)** versus virtual DAM rest. Raw data was averaged over a 24-hour day and separated into 30-minute bins. Each dot is an individual flies of a given genotype and box plots are drawn underneath to represent the quartiles of the data. The sample sizes and summary data are shown in Appendix A Table 12.

Appendix A Table 12 The correlation of stationary static behaviour with virtual DAM rest

The table is pertinent to Appendix A Figure 15. The correlation (Pearson's R) of total stationary static (SS) or long bouts of SS (SSL) versus DAM classified sleep per 30-minute bin for individual flies. The sample size is shown in a list for each comparison (Total, Day, Night).

Genotype	Sex	Comparison	Sample Size (n)	Total R Mean±CI	Day R Mean±CI	Night R Mean±CI
BK	M	SS vs DAM	[60, 60, 60]	0.93±0.01	0.92±0.02	0.92±0.02
BK	M	SSL vs DAM	[60, 60, 59]	0.86±0.02	0.87±0.03	0.84±0.03
BK	F	SS vs DAM	[30, 30, 30]	0.73±0.06	0.66±0.11	0.70±0.08
BK	F	SSL vs DAM	[28, 28, 28]	0.67±0.06	0.59±0.12	0.63±0.07
CS	M	SS vs DAM	[30, 30, 30]	0.87±0.04	0.86±0.04	0.88±0.06
CS	M	SSL vs DAM	[30, 30, 30]	0.74±0.09	0.68±0.14	0.78±0.09
CS	F	SS vs DAM	[59, 59, 59]	0.77±0.03	0.74±0.05	0.68±0.06
CS	F	SSL vs DAM	[59, 59, 59]	0.61±0.06	0.58±0.08	0.55±0.07
w*	M	SS vs DAM	[49, 49, 49]	0.88±0.04	0.89±0.02	0.84±0.06
w*	M	SSL vs DAM	[49, 48, 48]	0.71±0.06	0.75±0.07	0.65±0.08
w*	F	SS vs DAM	[38, 38, 38]	0.79±0.06	0.79±0.07	0.75±0.08
w*	F	SSL vs DAM	[38, 38, 38]	0.58±0.08	0.61±0.08	0.54±0.09

Appendix A Table 13 The comparison of females vs. males for correlation of stationary static behaviour with virtual DAM rest

The table is pertinent to Figure 3.4.2A-B, illustrating the comparison of females vs. males of each genotype for their correlation (Pearson's R) between stationary static behaviour measured via the Trumelan behavioural classifier with virtual DAM rest. Behavioural state durations are summed into 30-minute bins and the correlation between SSL or SS and virtual DAM rest is analysed for individual flies. See Chapter 2.6 for more information about DABEST plots.

Genotype	Comparison	Ctr	Test	Ctr (n)	Test (n)	Ctr Mean±CI (R)	Test Mean±CI (R)	Delta (R)	Delta-CI (R)	Delta+CI (R)	p-value
BK	SS vs DAM	Male	Female	60	30	0.93±0.01	0.73±0.06	-0.20	-0.27	-0.14	0.0000
CS	SS vs DAM	Male	Female	30	59	0.87±0.04	0.77±0.03	-0.11	-0.15	-0.05	0.0000
w*	SS vs DAM	Male	Female	49	38	0.88±0.04	0.79±0.06	-0.09	-0.17	-0.02	0.0128
Weighted Delta	SS vs DAM	Male	Female	139	127	NA	NA	-0.13	-0.17	-0.10	0.0000

Genotype	Comparison	Ctr	Test	Ctr (n)	Test (n)	Ctr Mean±CI (R)	Test Mean±CI (R)	Delta (R)	Delta-CI (R)	Delta+CI (R)	p-value
BK	SSL vs DAM	Male	Female	60	28	0.86±0.02	0.67±0.06	-0.19	-0.26	-0.13	0.0000
CS	SSL vs DAM	Male	Female	30	59	0.74±0.09	0.61±0.06	-0.13	-0.22	-0.01	0.0166
w*	SSL vs DAM	Male	Female	49	38	0.71±0.06	0.58±0.08	-0.12	-0.23	-0.03	0.0184
Weighted Delta	SSL vs DAM	Male	Female	139	125	NA	NA	-0.16	-0.21	-0.11	0.0000

Appendix A Table 14 The comparison between SS and SSL correlated to virtual DAM rest for all genotypes

The table is pertinent to Figure 3.4.2C, illustrating the comparison of SSL vs. SS for correlation to virtual DAM rest in each genotype. Behavioural state durations are summed into 30-minute bins and the correlation between SSL or SS and virtual DAM rest is analysed for individual flies. See Chapter 2.6 for more information about DABEST plots.

Genotype	Ctr	Test	Sample Size (n)	Ctr Mean±CI (R)	Test Mean±CI (R)	Delta (R)	Delta-CI (R)	Delta+CI (R)	p-value
BK M	SS	SSL	60	0.93±0.01	0.86±0.02	-0.07	-0.09	-0.06	0.0000
BK F	SS	SSL	28	0.74±0.06	0.67±0.06	-0.08	-0.11	-0.04	0.0006
CS M	SS	SSL	30	0.87±0.04	0.74±0.09	-0.13	-0.21	-0.09	0.0000
CS F	SS	SSL	59	0.77±0.03	0.61±0.06	-0.15	-0.21	-0.11	0.0000
w* M	SS	SSL	49	0.88±0.04	0.71±0.06	-0.17	-0.22	-0.13	0.0000
w* F	SS	SSL	38	0.79±0.06	0.58±0.08	-0.20	-0.28	-0.15	0.0000
Weighted Delta	SS	SSL	264	NA	NA	-0.10	-0.11	-0.09	0.0000

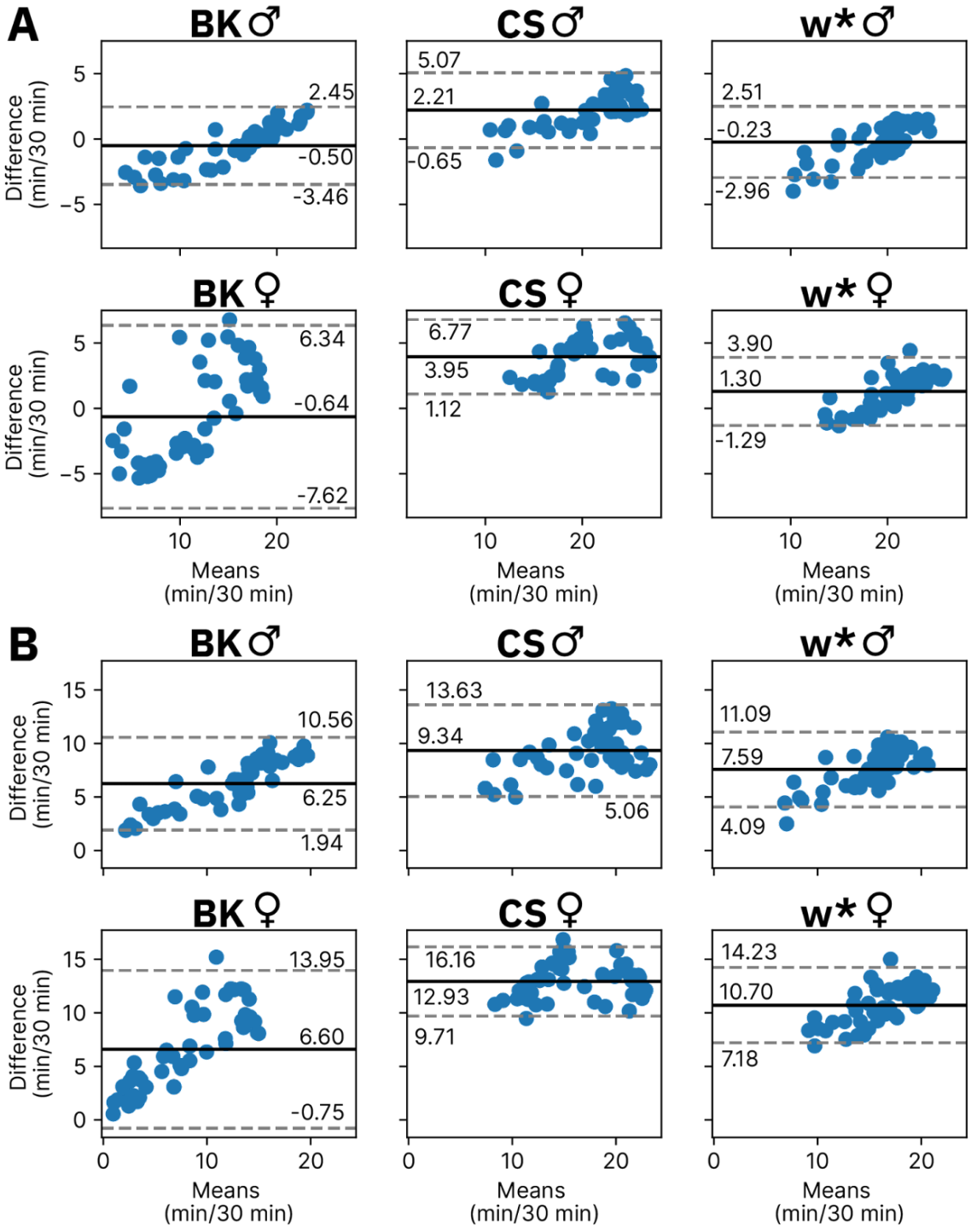

Appendix A Figure 16 The comparison between virtual DAM rest vs. SS or SSL for grouped fly data

Bland-Altman compares the differences in rest as measured by virtual DAM vs. SS **(A)**, or SSL **(B)**. Each dot indicates one time point (30-min bin) for the averaged 24-hour data of each genotype. The Y-axis indicates the difference between the two methods, while the X-axis indicates the mean of the two methods. The solid horizontal line indicates the mean difference, while the dotted lines indicate the 95% CIs.

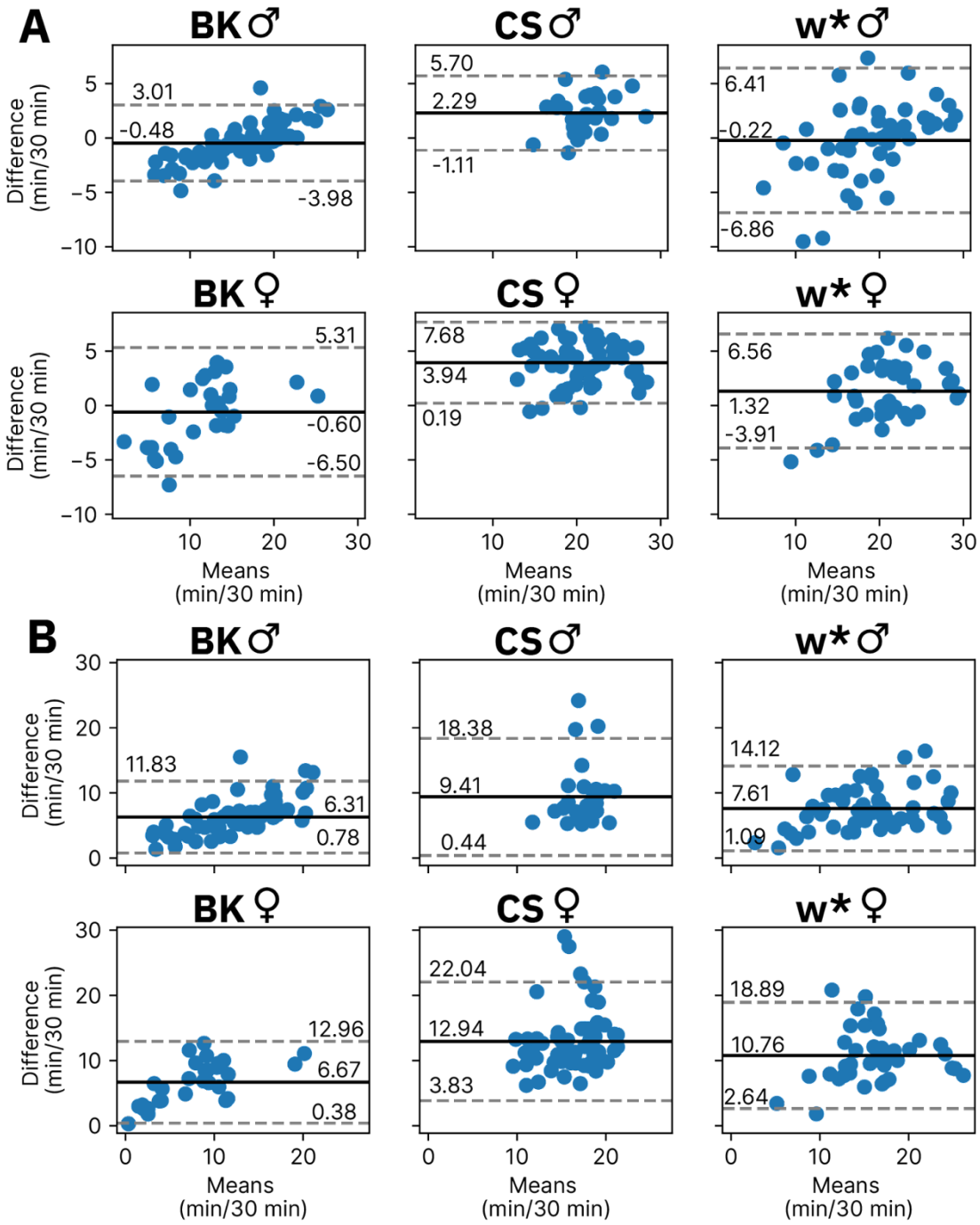

Appendix A Figure 17 The comparison between virtual DAM rest vs. SS or SSL for individual fly data

Bland-Altman plot compares the differences in rest as measured by virtual DAM vs. SS **(A)**, or SSL **(B)**. Each dot indicates the average of an all data from an individual fly. The Y-axis indicates the difference between the two methods, while the X-axis indicates the mean of the two methods. The solid horizontal line indicates the mean difference, while the dotted lines indicate the 95% CIs.

Appendix A Table 15 The percentage time spent in Trumelan recorded states during virtual DAM active periods or virtual DAM rest for each genotype, separated into day, night or total

The table is pertinent to Figure 3.4.4A and Appendix A Figure 20.

Genotype	DAM	Time of Day	LO (% Time)	SA (% Time)	SSB (% Time)	SSL (% Time)
BK M	Active	Total	61.17±2.41	17.60±1.10	13.56±1.20	2.12±0.56
BK F	Active	Total	55.87±2.65	22.13±1.68	16.02±1.82	1.05±0.39
CS M	Active	Total	61.49±4.36	16.91±1.64	13.07±2.03	4.29±1.71
CS F	Active	Total	51.06±2.24	24.53±1.55	15.03±1.30	2.60±0.55
w* M	Active	Total	57.83±2.46	16.15±1.79	15.63±2.47	5.48±1.50
w* F	Active	Total	47.71±3.38	23.41±2.72	18.42±2.74	4.79±1.65
BK M	Active	Day	58.42±2.44	18.67±1.28	14.65±1.18	2.37±0.56
BK F	Active	Day	55.81±3.25	20.92±1.89	17.16±2.00	1.20±0.54
CS M	Active	Day	56.90±3.76	18.14±1.39	15.07±2.17	5.00±1.57
CS F	Active	Day	49.39±2.24	24.99±1.58	15.70±1.47	2.86±0.72
w* M	Active	Day	56.67±2.65	15.48±1.89	16.59±2.76	6.30±1.71
w* F	Active	Day	49.08±3.38	22.28±2.64	18.08±2.67	5.08±2.03
BK M	Active	Night	64.09±2.87	16.69±1.14	12.10±1.60	1.97±0.75
BK F	Active	Night	52.91±3.47	26.52±2.59	14.63±2.38	0.70±0.29
CS M	Active	Night	63.91±5.75	16.50±2.21	12.12±2.55	3.63±2.54
CS F	Active	Night	52.98±3.04	23.90±1.99	14.54±1.60	2.62±1.03
w* M	Active	Night	58.50±3.40	17.79±1.92	14.35±2.27	4.27±1.55
w* F	Active	Night	44.62±3.64	26.78±3.40	18.96±3.61	3.39±0.87
BK M	Rest	Total	2.85±0.36	13.71±1.52	23.93±1.62	55.60±3.20
BK F	Rest	Total	6.64±1.52	31.49±5.28	23.22±2.81	32.00±6.54
CS M	Rest	Total	4.28±0.62	13.39±1.80	21.09±4.24	57.53±4.83
CS F	Rest	Total	5.34±0.72	21.08±2.05	26.10±3.70	42.19±3.49
w* M	Rest	Total	3.11±0.47	12.46±1.95	25.88±3.55	53.72±4.38
w* F	Rest	Total	3.93±0.62	13.71±2.28	30.48±4.92	47.33±5.02
BK M	Rest	Day	2.86±0.30	16.72±2.20	22.61±1.41	53.37±3.65
BK F	Rest	Day	8.45±2.30	30.73±6.22	26.21±3.71	27.50±8.55

Appendix A

Genotype	DAM	Time of Day	LO (% Time)	SA (% Time)	SSB (% Time)	SSL (% Time)
CS M	Rest	Day	5.29±0.96	15.59±1.92	23.42±5.00	51.01±5.84
CS F	Rest	Day	6.80±0.88	27.10±2.54	28.11±3.71	30.57±3.31
w* M	Rest	Day	3.15±0.48	12.57±2.05	24.84±4.26	54.56±4.82
w* F	Rest	Day	4.49±0.83	14.16±2.55	30.52±4.94	45.96±5.37
BK M	Rest	Night	3.03±0.59	12.03±1.98	25.15±2.22	56.13±4.12
BK F	Rest	Night	6.31±1.62	31.56±5.82	21.66±3.04	34.06±7.40
CS M	Rest	Night	3.08±0.53	11.08±2.25	18.59±3.92	64.59±5.31
CS F	Rest	Night	4.31±0.66	16.70±2.17	24.60±3.90	50.64±4.25
w* M	Rest	Night	3.14±0.54	12.31±2.03	27.70±3.80	52.27±5.01
w* F	Rest	Night	3.51±0.63	13.11±2.51	30.64±5.18	48.48±5.49

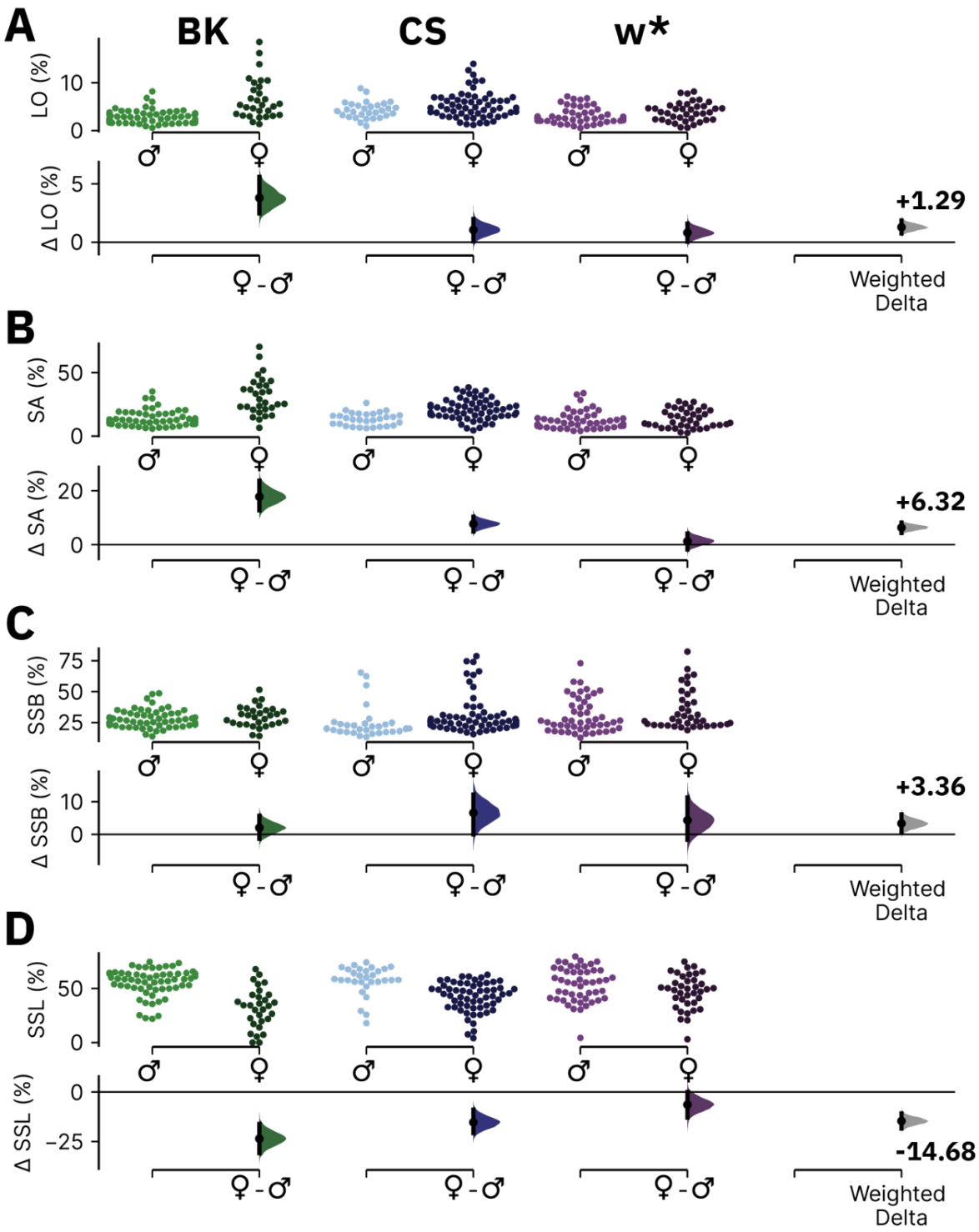

Appendix A Figure 18 Time spent in each state during virtual DAM rest in females vs. males

DABEST plots comparing the time spent in LO **(A)**, SA **(B)**, SSB **(C)**, or SSL **(D)** during virtual DAM classified rest, in females vs. males for each genotype. The sample sizes for (A-C) were 60 for BK males, 30 for BK females, 30 for CS males, 59 for CS females, 49 for w* males, and 38 for w* females. The summary data for these plots are shown in Appendix A Table 16. See Chapter 2.6 for more information about the structure of DABEST plots.

Appendix A Table 16 Time spent in each state during DAM rest in females vs. males

The table is pertinent to Appendix A Figure 18. Each row illustrates a DABEST comparison of percentage time spent in a given state in females vs. males for a given genotype during virtual DAM rest periods. See Chapter 2.6 for more information about DABEST plots.

Genotype	State	Ctr / Test	Ctr (n)	Test (n)	Ctr Mean±CI (%)	Test Mean±CI (%)	Delta (%)	Delta-CI (%)	Delta+CI (%)	p-value
BK	LO	M / F	60	30	2.85±0.36	6.64±1.52	3.80	2.47	5.60	0.0000
CS	LO	M / F	30	59	4.28±0.62	5.34±0.72	1.05	0.08	1.98	0.0642
w*	LO	M / F	49	38	3.11±0.47	3.93±0.62	0.81	0.04	1.60	0.0400
Weighted Delta	LO	M / F	139	127	NA	NA	1.29	0.75	1.86	0.0000
BK	SA	M / F	60	30	13.71±1.52	31.49±5.28	17.78	12.76	23.68	0.0000
CS	SA	M / F	30	59	13.39±1.80	21.08±2.05	7.69	4.86	10.33	0.0000
w*	SA	M / F	49	38	12.46±1.95	13.71±2.28	1.26	-1.79	4.11	0.4184
Weighted Delta	SA	M / F	139	127	NA	NA	6.32	4.34	8.19	0.0000
BK	SSB	M / F	60	30	27.85±1.84	29.87±3.00	2.03	-1.34	5.72	0.2512
CS	SSB	M / F	30	59	24.79±4.76	31.39±3.94	6.59	0.00	12.22	0.0496
w*	SSB	M / F	49	38	30.71±3.90	35.03±5.12	4.32	-1.61	11.32	0.1840
Weighted Delta	SSB	M / F	139	127	NA	NA	3.36	0.79	6.12	0.0174
BK	SSL	M / F	60	30	55.60±3.20	32.00±6.54	-23.60	-30.91	-16.08	0.0000
CS	SSL	M / F	30	59	57.53±4.83	42.19±3.49	-15.34	-20.77	-8.89	0.0000
w*	SSL	M / F	49	38	53.72±4.38	47.33±5.02	-6.39	-12.98	0.01	0.0688
Weighted Delta	SSL	M / F	139	127	NA	NA	-14.68	-18.44	-10.82	0.0000

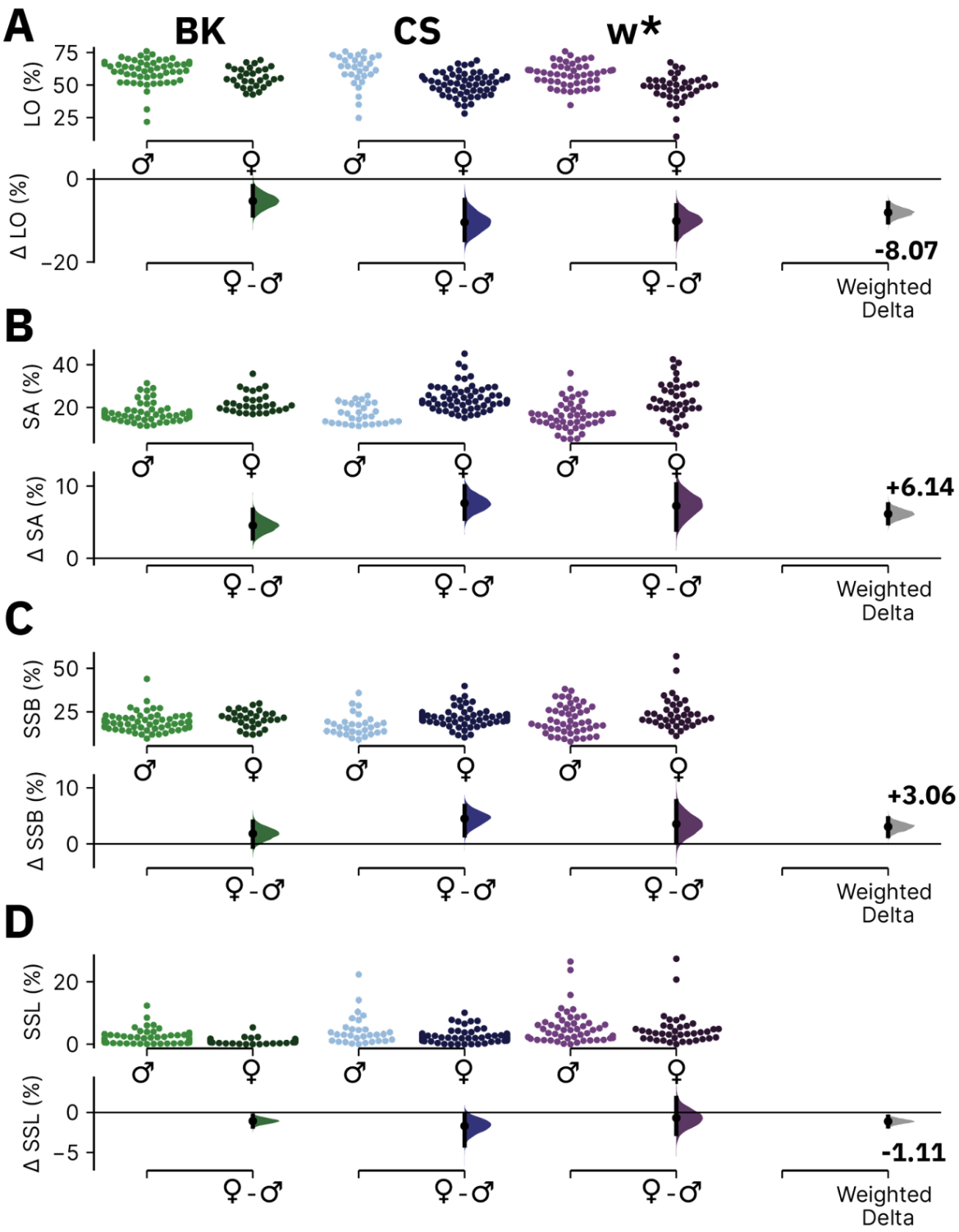

Appendix A Figure 19 Time spent in each state during virtual DAM active periods in females vs. males

DABEST plots comparing the time spent in LO **(A)**, SA **(B)**, SSB **(C)**, or SSL **(D)** during virtual DAM active periods, in females vs. males for each genotype. The sample sizes for (A-C) were 60 for BK males, 30 for BK females, 30 for CS males, 59 for CS females, 49 for w* males, and 38 for w* females. The summary data for these plots are shown in Appendix A Table 17. See Chapter 2.6 for more information about the structure of DABEST plots.

Appendix A Table 17 Time spent in each state during virtual DAM active periods in females vs. males

The table is pertinent to Appendix A Figure 19. Each row illustrates a DABEST comparison of percentage time spent in a given state in females vs. males for a given genotype during virtual DAM active periods. See Chapter 2.6 for more information about DABEST plots.

Genotype	State	Ctr / Test	Ctr (n)	Test (n)	Ctr Mean±CI (%)	Test Mean±CI (%)	Delta (%)	Delta-CI (%)	Delta+CI (%)	p-value
BK	LO	M / F	60	30	61.17±2.41	55.87±2.65	-5.30	-8.77	-1.68	0.0100
CS	LO	M / F	30	59	61.49±4.36	51.06±2.24	-10.44	-14.70	-5.02	0.0002
w*	LO	M / F	49	38	57.83±2.46	47.71±3.38	-10.12	-14.50	-6.31	0.0000
Weighted Delta	LO	M / F	139	127	NA	NA	-8.07	-10.46	-5.76	0.0000
BK	SA	M / F	60	30	17.60±1.10	22.13±1.68	4.54	2.75	6.73	0.0000
CS	SA	M / F	30	59	16.91±1.64	24.53±1.55	7.62	5.47	9.97	0.0000
w*	SA	M / F	49	38	16.15±1.79	23.41±2.72	7.26	3.95	10.25	0.0000
Weighted Delta	SA	M / F	139	127	NA	NA	6.14	4.85	7.47	0.0000
BK	SSB	M / F	60	30	19.11±1.38	20.94±1.75	1.83	-0.51	3.96	0.1264
CS	SSB	M / F	30	59	17.30±2.21	21.81±1.39	4.51	1.54	6.78	0.0012
w*	SSB	M / F	49	38	20.54±2.29	24.08±2.87	3.55	0.24	7.61	0.0568
Weighted Delta	SSB	M / F	139	127	NA	NA	3.06	1.40	4.56	0.0000
BK	SSL	M / F	60	30	2.12±0.56	1.05±0.39	-1.07	-1.77	-0.41	0.0086
CS	SSL	M / F	30	59	4.29±1.71	2.60±0.55	-1.69	-4.11	-0.34	0.0184
w*	SSL	M / F	49	38	5.48±1.50	4.79±1.65	-0.68	-2.69	1.81	0.5678
Weighted Delta	SSL	M / F	139	127	NA	NA	-1.11	-1.73	-0.51	0.0018

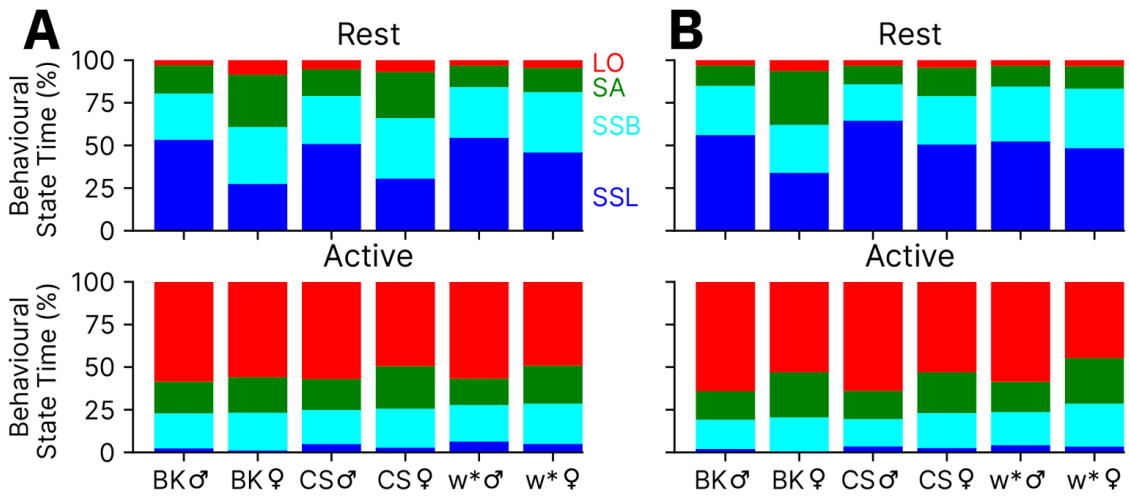

Appendix A Figure 20 Composition of Trumelan behaviours during virtual DAM rest and active periods separated into day and night

The percentage time spent in each Trumelan recorded behaviour during virtual DAM rest and active periods for each genotype during the day **(A)** or during the night **(B)**. The summary data is shown in Appendix A Table 15.

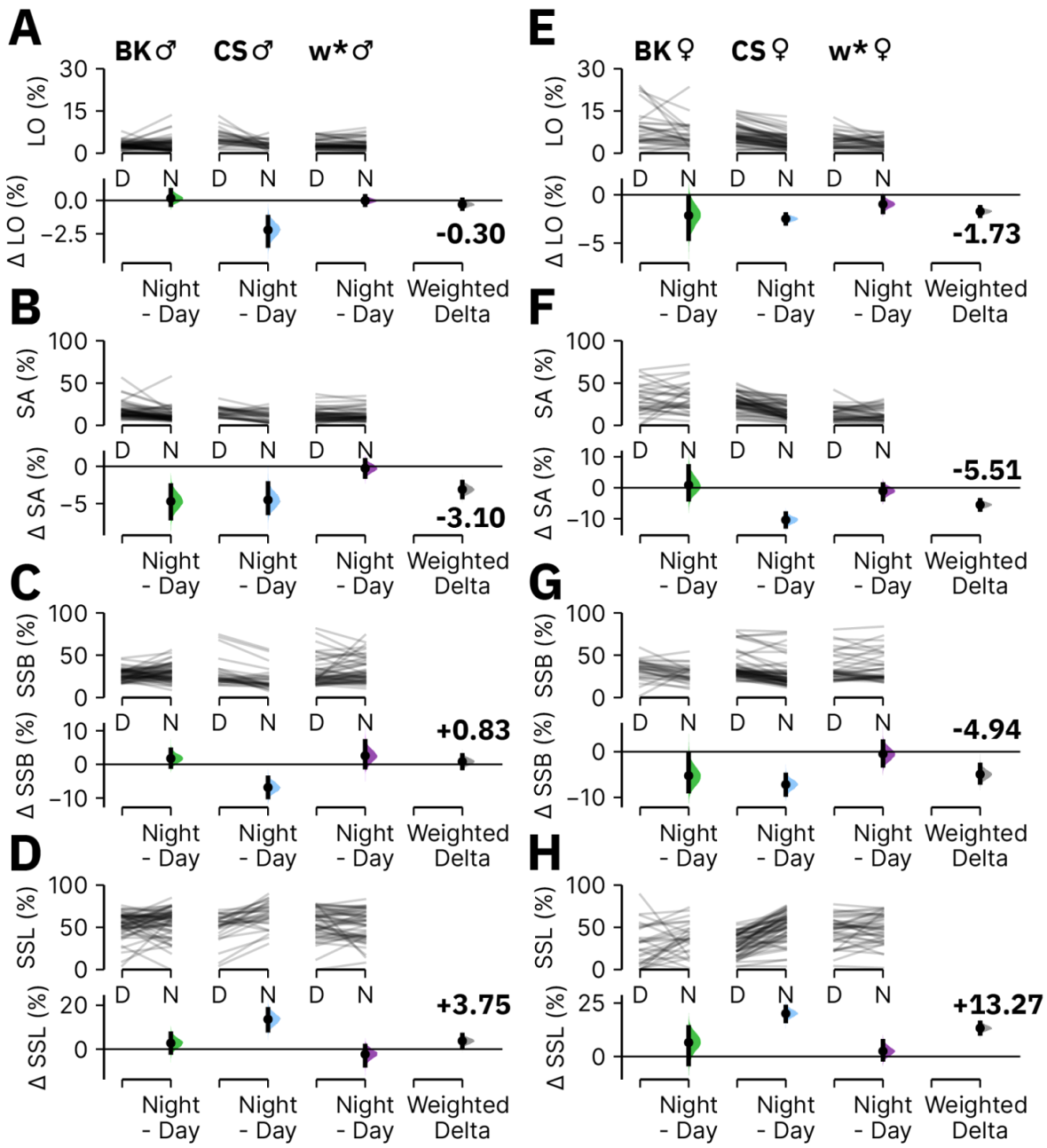

Appendix A Figure 21 Composition of Trumelan behaviours during virtual DAM rest during night vs. day

(A-D) DABEST plots comparing the time spent in LO **(A)**, SA **(B)**, SSB **(C)**, or SSL **(D)** during virtual DAM rest periods during the night vs. the day for male flies. **(E-H)** Same as (A-D) but for female flies. The summary data and sample sizes for this plot is shown in Appendix A Table 18. See Chapter 2.6 for more information about the structure of DABEST plots.

Appendix A Table 18 Composition of Trumelan recorded behaviours during virtual DAM rest during night vs. day

The table is pertinent to Appendix A Figure 21. Each row illustrates a DABEST comparison of percentage time spent in a given state during night vs. day for a given genotype during virtual DAM rest periods. See Chapter 2.6 for more information about DABEST plots.

Genotype	Sex	State	Ctr / Test	Sample Size (n)	Ctr Mean±CI (%)	Test Mean±CI (%)	Delta (%)	Delta-CI (%)	Delta+CI (%)	p-value
BK	M	LO	Day / Night	60	2.86±0.30	3.03±0.59	0.17	-0.32	0.78	0.5516
CS	M	LO	Day / Night	30	5.29±0.96	3.08±0.53	-2.21	-3.39	-1.25	0.0004
w*	M	LO	Day / Night	49	3.15±0.48	3.14±0.54	-0.01	-0.32	0.31	0.9666
Weighted Delta	M	LO	Day / Night	139	NA	NA	-0.30	-0.61	0.05	0.0890
BK	M	SA	Day / Night	60	16.72±2.20	12.03±1.98	-4.69	-6.95	-2.57	0.0000
CS	M	SA	Day / Night	30	15.59±1.92	11.08±2.25	-4.51	-6.25	-2.29	0.0000
w*	M	SA	Day / Night	49	12.57±2.05	12.31±2.03	-0.26	-1.36	0.82	0.6462
Weighted Delta	M	SA	Day / Night	139	NA	NA	-3.10	-4.11	-2.11	0.0000
BK	M	SSB	Day / Night	60	27.05±1.71	28.81±2.44	1.76	-0.64	4.33	0.1570
CS	M	SSB	Day / Night	30	28.11±5.71	21.26±4.34	-6.85	-9.71	-3.99	0.0002
w*	M	SSB	Day / Night	49	29.72±4.53	32.28±4.29	2.57	-0.80	6.87	0.1956
Weighted Delta	M	SSB	Day / Night	139	NA	NA	0.83	-1.08	2.69	0.4040
BK	M	SSL	Day / Night	60	53.37±3.65	56.13±4.12	2.77	-1.53	7.04	0.2088
CS	M	SSL	Day / Night	30	51.01±5.84	64.59±5.31	13.58	8.61	18.16	0.0000
w*	M	SSL	Day / Night	49	54.57±4.82	52.27±5.01	-2.30	-7.33	1.45	0.3072
Weighted Delta	M	SSL	Day / Night	139	NA	NA	3.75	1.20	6.43	0.0114

Appendix A

Genotype	Sex	State	Ctr / Test	Sample Size (n)	Ctr Mean±CI (%)	Test Mean±CI (%)	Delta (%)	Delta-CI (%)	Delta+CI (%)	p-value
BK	F	LO	Day / Night	30	8.45±2.30	6.31±1.62	-2.14	-4.56	-0.32	0.0510
CS	F	LO	Day / Night	59	6.80±0.88	4.31±0.66	-2.49	-2.97	-2.04	0.0000
w*	F	LO	Day / Night	38	4.49±0.83	3.51±0.63	-0.98	-1.78	-0.32	0.0098
Weighted Delta	F	LO	Day / Night	127	NA	NA	-1.73	-2.17	-1.29	0.0000
BK	F	SA	Day / Night	30	30.73±6.22	31.56±5.82	0.83	-3.73	6.89	0.7742
CS	F	SA	Day / Night	59	27.11±2.54	16.70±2.17	-10.40	-12.46	-8.37	0.0000
w*	F	SA	Day / Night	38	14.16±2.55	13.11±2.51	-1.05	-3.72	1.03	0.4114
Weighted Delta	F	SA	Day / Night	127	NA	NA	-5.51	-7.05	-4.03	0.0000
BK	F	SSB	Day / Night	30	33.32±4.04	28.07±3.43	-5.25	-8.62	-0.36	0.0166
CS	F	SSB	Day / Night	59	35.53±3.89	28.35±4.17	-7.18	-9.35	-5.09	0.0000
w*	F	SSB	Day / Night	38	35.39±5.13	34.90±5.42	-0.49	-2.96	2.23	0.7254
Weighted Delta	F	SSB	Day / Night	127	NA	NA	-4.94	-6.73	-2.88	0.0000
BK	F	SSL	Day / Night	30	27.50±8.55	34.06±7.40	6.55	-3.51	13.62	0.1396
CS	F	SSL	Day / Night	59	30.57±3.31	50.64±4.25	20.07	16.60	23.16	0.0000
w*	F	SSL	Day / Night	38	45.96±5.37	48.48±5.49	2.52	-1.31	7.15	0.2452
Weighted Delta	F	SSL	Day / Night	127	NA	NA	13.27	10.76	15.74	0.0000

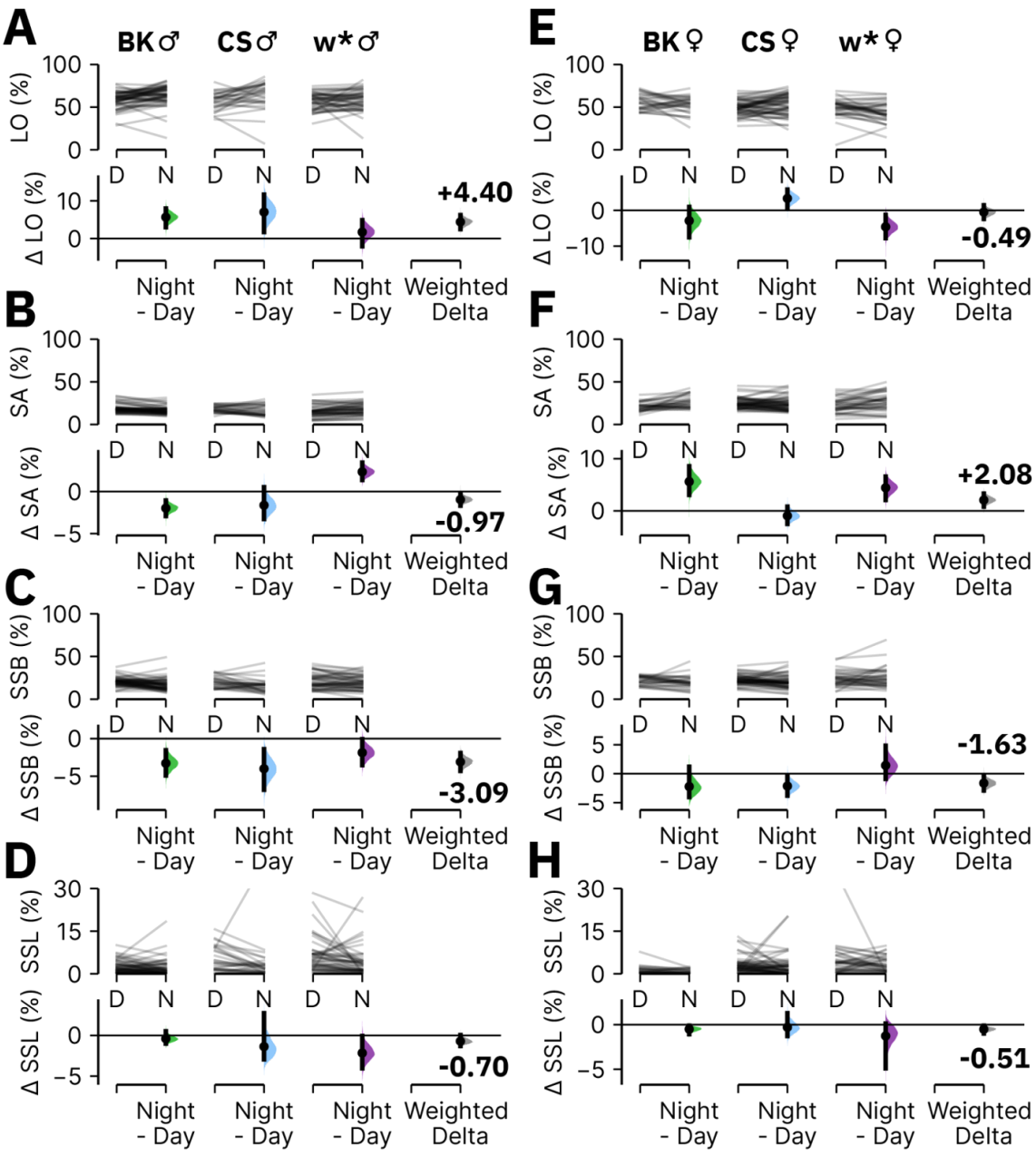

Appendix A Figure 22 Composition of Trumelan recorded behaviours during virtual DAM active periods during night vs. day

(A-D) DABEST plots comparing the time spent in LO **(A)**, SA **(B)**, SSB **(C)**, or SSL **(D)** during virtual DAM active periods during the night versus the day for male flies. **(E-H)** Same as (A-D) but for female flies. The summary data and sample sizes for this plot is shown in Appendix A Table 19. See Chapter 2.6 for more information about the structure of DABEST plots.

Appendix A Table 19 Composition of Trumelan recorded behaviours during virtual DAM active periods during night vs. day

The table is pertinent to Appendix A Figure 22. Each row illustrates a DABEST comparison of percentage time spent in a given state during night vs. day for a given genotype during virtual DAM active periods. See Chapter 2.6 for more information about DABEST plots.

Genotype	Sex	State	Ctr / Test	Sample Size (n)	Ctr Mean±CI (%)	Test Mean±CI (%)	Delta (%)	Delta-CI (%)	Delta+CI (%)	p-value
BK	M	LO	Day / Night	60	58.43±2.44	64.09±2.87	5.66	3.00	7.97	0.0000
CS	M	LO	Day / Night	30	56.90±3.76	63.91±5.75	7.01	1.69	11.63	0.0122
w*	M	LO	Day / Night	48	56.81±2.69	58.50±3.40	1.69	-2.05	4.86	0.3400
Weighted Delta	M	LO	Day / Night	138	NA	NA	4.40	2.48	6.19	0.0000
BK	M	SA	Day / Night	60	18.67±1.27	16.69±1.14	-1.98	-2.91	-1.07	0.0000
CS	M	SA	Day / Night	30	18.14±1.39	16.50±2.21	-1.63	-3.27	0.50	0.0972
w*	M	SA	Day / Night	48	15.46±1.93	17.79±1.92	2.33	1.36	3.41	0.0002
Weighted Delta	M	SA	Day / Night	138	NA	NA	-0.97	-1.68	-0.26	0.0184
BK	M	SSB	Day / Night	60	20.53±1.32	17.26±1.80	-3.28	-4.91	-1.55	0.0004
CS	M	SSB	Day / Night	30	19.96±2.35	15.95±2.81	-4.00	-6.81	-1.39	0.0074
w*	M	SSB	Day / Night	48	21.30±2.50	19.43±2.32	-1.86	-3.52	-0.08	0.0312
Weighted Delta	M	SSB	Day / Night	138	NA	NA	-3.09	-4.29	-1.92	0.0000
BK	M	SSL	Day / Night	60	2.37±0.56	1.97±0.75	-0.40	-1.01	0.52	0.2926
CS	M	SSL	Day / Night	30	5.00±1.57	3.63±2.54	-1.37	-2.93	2.74	0.3172
w*	M	SSL	Day / Night	48	6.43±1.72	4.27±1.55	-2.16	-4.04	-0.08	0.0282
Weighted Delta	M	SSL	Day / Night	138	NA	NA	-0.70	-1.29	0.04	0.0344

Genotype	Sex	State	Ctr / Test	Sample Size (n)	Ctr Mean±CI (%)	Test Mean±CI (%)	Delta (%)	Delta-CI (%)	Delta+CI (%)	p-value
BK	F	LO	Day / Night	30	55.81±3.25	52.91±3.47	-2.89	-7.52	0.97	0.1930
CS	F	LO	Day / Night	58	49.64±2.23	52.98±3.04	3.35	0.71	5.84	0.0138
w*	F	LO	Day / Night	37	49.22±3.46	44.62±3.64	-4.60	-7.78	-1.24	0.0064
Weighted Delta	F	LO	Day / Night	125	NA	NA	-0.49	-2.37	1.42	0.6396
BK	F	SA	Day / Night	30	20.92±1.89	26.52±2.59	5.61	3.07	8.56	0.0008
CS	F	SA	Day / Night	58	24.83±1.58	23.90±1.99	-0.93	-2.50	0.81	0.2856
w*	F	SA	Day / Night	37	22.35±2.71	26.78±3.40	4.43	2.11	6.56	0.0008
Weighted Delta	F	SA	Day / Night	125	NA	NA	2.08	0.81	3.30	0.0038
BK	F	SSB	Day / Night	30	22.08±1.81	19.86±2.69	-2.22	-4.04	1.21	0.0892
CS	F	SSB	Day / Night	58	22.62±1.48	20.49±1.96	-2.13	-3.80	-0.23	0.0228
w*	F	SSB	Day / Night	37	23.77±2.82	25.21±3.73	1.44	-0.90	4.83	0.3354
Weighted Delta	F	SSB	Day / Night	125	NA	NA	-1.63	-2.89	-0.32	0.0176
BK	F	SSL	Day / Night	30	1.20±0.54	0.70±0.29	-0.50	-1.06	-0.11	0.0332
CS	F	SSL	Day / Night	58	2.90±0.73	2.62±1.03	-0.29	-1.28	1.29	0.6496
w*	F	SSL	Day / Night	37	4.65±1.91	3.39±0.87	-1.26	-4.90	0.12	0.2842
Weighted Delta	F	SSL	Day / Night	125	NA	NA	-0.51	-0.99	-0.10	0.0240

Appendix A Table 20 Percentage of Trumelan behaviours present over time during the first sixty minutes of virtual DAM classified rest in all genotypes combined

The table is pertinent to Figure 3.4.4D.

Duration (Min)	Bouts (n)	LO (%) Mean±CI	SA (%) Mean±CI	SSB (%) Mean±CI	SSL (%) Mean±CI
1	10990	12.85±0.27	33.95±0.53	37.80±0.56	15.40±0.61
2	10990	8.07±0.23	30.74±0.55	36.88±0.60	24.31±0.73
3	10990	7.05±0.22	27.80±0.54	36.44±0.61	28.71±0.77
4	10990	6.68±0.22	25.88±0.53	35.65±0.62	31.79±0.79
5	10990	7.77±0.25	24.36±0.52	34.86±0.62	33.01±0.80
6	9636	6.88±0.25	22.13±0.54	33.65±0.67	37.35±0.88
7	8573	6.08±0.25	20.72±0.57	32.61±0.72	40.59±0.95
8	7798	5.57±0.26	19.40±0.59	31.92±0.76	43.10±1.01
9	7154	4.90±0.24	18.16±0.61	31.43±0.80	45.52±1.06
10	6652	4.70±0.25	17.15±0.62	31.63±0.84	46.51±1.10
11	6202	4.48±0.25	16.55±0.63	31.79±0.87	47.17±1.14
12	5797	4.18±0.25	15.64±0.64	31.44±0.91	48.75±1.17
13	5447	3.80±0.25	15.55±0.66	30.56±0.93	50.10±1.21
14	5161	3.57±0.24	14.98±0.68	30.27±0.96	51.18±1.24
15	4917	3.89±0.27	14.47±0.68	29.28±0.98	52.37±1.28
16	4684	3.53±0.27	14.17±0.69	29.53±1.01	52.76±1.31
17	4456	3.43±0.27	14.58±0.73	29.90±1.04	52.10±1.34
18	4242	3.35±0.27	14.30±0.74	28.80±1.05	53.55±1.37
19	4071	3.20±0.26	13.88±0.74	28.36±1.08	54.55±1.40
20	3919	3.40±0.28	14.01±0.77	28.11±1.10	54.48±1.43
21	3756	3.31±0.28	13.53±0.76	28.54±1.12	54.62±1.45
22	3608	3.33±0.29	13.08±0.76	28.21±1.14	55.38±1.48
23	3460	3.08±0.28	12.96±0.78	27.99±1.16	55.96±1.51
24	3350	3.35±0.31	12.89±0.80	28.52±1.19	55.24±1.53
25	3218	3.45±0.33	13.20±0.82	26.56±1.18	56.79±1.56
26	3077	2.96±0.30	13.17±0.85	26.41±1.21	57.47±1.60
27	2967	2.80±0.30	12.56±0.85	27.44±1.26	57.20±1.62

Duration (Min)	Bouts (n)	LO (%) Mean±CI	SA (%) Mean±CI	SSB (%) Mean±CI	SSL (%) Mean±CI
28	2872	2.85±0.30	12.61±0.86	26.39±1.26	58.15±1.65
29	2772	2.77±0.30	12.49±0.86	27.06±1.30	57.68±1.69
30	2680	3.10±0.33	12.95±0.90	26.58±1.31	57.37±1.72
31	2607	2.81±0.31	12.23±0.90	27.50±1.34	57.46±1.72
32	2507	2.75±0.33	12.88±0.94	28.05±1.39	56.31±1.78
33	2429	2.78±0.33	13.07±0.95	27.33±1.39	56.83±1.81
34	2348	2.92±0.34	13.29±0.98	26.08±1.39	57.70±1.83
35	2264	2.93±0.34	12.66±0.97	26.44±1.42	57.98±1.86
36	2197	2.58±0.32	12.74±1.00	26.64±1.44	58.04±1.87
37	2130	2.50±0.31	12.74±1.01	27.26±1.48	57.49±1.91
38	2070	2.67±0.35	12.69±1.02	26.61±1.50	58.02±1.95
39	2019	2.59±0.32	13.29±1.07	25.62±1.50	58.51±1.98
40	1964	2.57±0.34	13.22±1.09	25.16±1.50	59.06±1.99
41	1907	2.53±0.34	12.90±1.08	24.91±1.51	59.65±2.02
42	1858	2.45±0.33	13.44±1.13	25.41±1.55	58.70±2.05
43	1815	2.56±0.37	12.85±1.12	26.04±1.60	58.55±2.09
44	1763	2.44±0.35	12.34±1.10	25.92±1.60	59.30±2.10
45	1715	2.43±0.36	12.19±1.11	26.49±1.63	58.89±2.14
46	1672	2.20±0.35	11.64±1.10	25.90±1.68	60.26±2.17
47	1634	2.15±0.33	11.06±1.07	27.90±1.73	58.89±2.17
48	1593	1.99±0.32	10.61±1.08	26.92±1.75	60.47±2.19
49	1556	2.27±0.38	10.61±1.09	26.08±1.74	61.04±2.21
50	1519	2.23±0.33	11.98±1.19	24.88±1.74	60.91±2.25
51	1493	2.12±0.34	11.47±1.16	25.59±1.75	60.83±2.26
52	1458	2.18±0.39	10.64±1.12	25.58±1.79	61.59±2.30
53	1428	2.03±0.35	10.75±1.13	27.33±1.85	59.90±2.31
54	1390	2.00±0.37	11.38±1.19	26.58±1.85	60.05±2.35
55	1362	2.22±0.41	10.22±1.13	25.87±1.87	61.68±2.38
56	1341	2.14±0.37	9.94±1.08	26.32±1.84	61.60±2.35
57	1318	1.99±0.34	10.66±1.17	26.15±1.90	61.19±2.42

Duration (Min)	Bouts (n)	LO (%) Mean±CI	SA (%) Mean±CI	SSB (%) Mean±CI	SSL (%) Mean±CI
58	1285	2.48±0.44	10.27±1.15	26.80±1.92	60.46±2.43
59	1252	2.23±0.42	10.69±1.20	27.34±1.97	59.74±2.48
60	1222	2.07±0.41	10.79±1.26	25.54±1.95	61.61±2.48

Appendix A Table 21 Percentage of Trumelan behaviours present over time during the first sixty minutes of virtual DAM classified active periods in all genotypes combined

The table is pertinent to Figure 3.4.4D.

Duration (Min)	Bouts (n)	LO (%) Mean±CI	SA (%) Mean±CI	SSB (%) Mean±CI	SSL (%) Mean±CI
1	10991	51.88±0.44	20.27±0.29	22.60±0.39	5.25±0.30
2	8672	48.00±0.57	24.44±0.42	23.88±0.47	3.67±0.34
3	7112	43.00±0.66	24.80±0.50	26.24±0.55	5.95±0.49
4	6495	44.53±0.70	23.62±0.51	25.84±0.57	6.00±0.52
5	5954	45.58±0.72	23.28±0.52	25.66±0.59	5.48±0.51
6	5476	48.37±0.74	22.37±0.51	24.70±0.59	4.55±0.48
7	4991	49.19±0.78	21.97±0.53	24.78±0.64	4.06±0.48
8	4591	49.31±0.82	21.85±0.56	24.04±0.65	4.80±0.56
9	4254	49.90±0.86	21.79±0.58	23.80±0.67	4.50±0.55
10	3961	50.94±0.88	21.21±0.60	23.69±0.70	4.17±0.55
11	3705	51.63±0.91	20.73±0.59	23.63±0.72	4.00±0.56
12	3471	52.44±0.94	20.44±0.61	23.16±0.72	3.96±0.57
13	3250	52.93±0.97	20.04±0.61	22.71±0.74	4.33±0.62
14	3084	53.68±1.00	19.85±0.64	22.12±0.75	4.35±0.63
15	2905	53.93±1.03	20.16±0.67	22.00±0.78	3.91±0.63
16	2757	53.21±1.07	19.99±0.68	22.62±0.80	4.18±0.66
17	2619	54.57±1.09	19.64±0.69	21.98±0.83	3.80±0.65
18	2472	55.10±1.09	19.25±0.67	22.23±0.85	3.42±0.63
19	2355	56.59±1.11	18.67±0.68	21.66±0.85	3.08±0.61
20	2257	55.30±1.17	19.24±0.71	22.62±0.92	2.84±0.59

Duration (Min)	Bouts (n)	LO (%) Mean±CI	SA (%) Mean±CI	SSB (%) Mean±CI	SSL (%) Mean±CI
21	2159	55.82±1.19	18.83±0.73	22.29±0.92	3.07±0.65
22	2079	57.66±1.21	18.72±0.74	20.53±0.88	3.08±0.67
23	2005	58.03±1.24	18.32±0.76	20.47±0.92	3.18±0.67
24	1940	58.18±1.26	18.24±0.76	20.30±0.95	3.28±0.68
25	1859	58.85±1.26	17.79±0.75	20.67±0.97	2.68±0.65
26	1784	59.30±1.26	18.47±0.79	20.17±0.92	2.07±0.58
27	1730	59.01±1.31	18.12±0.78	20.69±0.99	2.19±0.58
28	1671	58.70±1.31	18.55±0.81	20.28±0.98	2.47±0.67
29	1622	59.99±1.29	17.87±0.79	20.19±0.99	1.94±0.59
30	1570	60.74±1.33	17.42±0.78	20.14±1.00	1.69±0.56
31	1520	61.30±1.35	17.37±0.79	19.67±1.02	1.66±0.57
32	1468	61.64±1.37	16.96±0.79	19.35±1.03	2.04±0.61
33	1427	61.24±1.38	17.23±0.81	19.49±1.01	2.04±0.65
34	1395	61.11±1.40	17.79±0.86	18.95±1.05	2.14±0.65
35	1357	59.25±1.49	18.32±0.90	19.66±1.12	2.78±0.78
36	1323	61.16±1.48	17.47±0.88	18.63±1.06	2.74±0.79
37	1300	61.69±1.45	17.15±0.88	18.47±1.01	2.69±0.80
38	1266	60.92±1.49	17.58±0.89	18.47±1.05	3.03±0.85
39	1229	61.02±1.52	17.08±0.88	18.81±1.12	3.09±0.84
40	1205	62.11±1.51	16.70±0.87	19.05±1.12	2.14±0.71
41	1176	62.12±1.56	17.11±0.92	19.17±1.17	1.60±0.64
42	1149	60.70±1.55	17.78±0.97	19.79±1.14	1.72±0.67
43	1120	62.12±1.58	17.72±0.98	18.72±1.16	1.44±0.61
44	1098	62.09±1.58	17.78±0.98	18.38±1.12	1.75±0.69
45	1068	62.37±1.60	17.18±0.96	18.16±1.15	2.29±0.81
46	1042	63.50±1.53	17.48±0.95	17.50±1.09	1.51±0.64
47	1029	63.11±1.58	16.69±0.93	17.60±1.13	2.60±0.87
48	1006	62.93±1.63	16.78±0.95	17.98±1.15	2.30±0.81
49	984	62.86±1.63	17.56±1.00	17.92±1.17	1.67±0.69
50	961	63.53±1.65	17.18±1.03	17.48±1.16	1.82±0.76

Appendix A

Duration (Min)	Bouts (n)	LO (%) Mean±CI	SA (%) Mean±CI	SSB (%) Mean±CI	SSL (%) Mean±CI
51	943	63.00±1.68	16.78±0.98	18.55±1.25	1.67±0.72
52	929	62.90±1.69	17.10±0.98	18.33±1.24	1.67±0.70
53	906	64.14±1.65	15.83±0.88	17.95±1.20	2.08±0.85
54	893	64.23±1.65	16.97±1.00	17.21±1.16	1.60±0.71
55	880	64.52±1.67	16.47±0.96	17.43±1.28	1.58±0.73
56	863	64.84±1.67	16.21±0.97	17.51±1.22	1.44±0.71
57	850	64.08±1.71	17.05±1.03	17.49±1.25	1.39±0.69
58	835	65.13±1.65	16.34±0.96	17.62±1.24	0.91±0.52
59	823	65.68±1.69	15.41±0.93	17.47±1.29	1.44±0.75
60	810	65.30±1.75	15.95±1.04	17.12±1.31	1.63±0.75

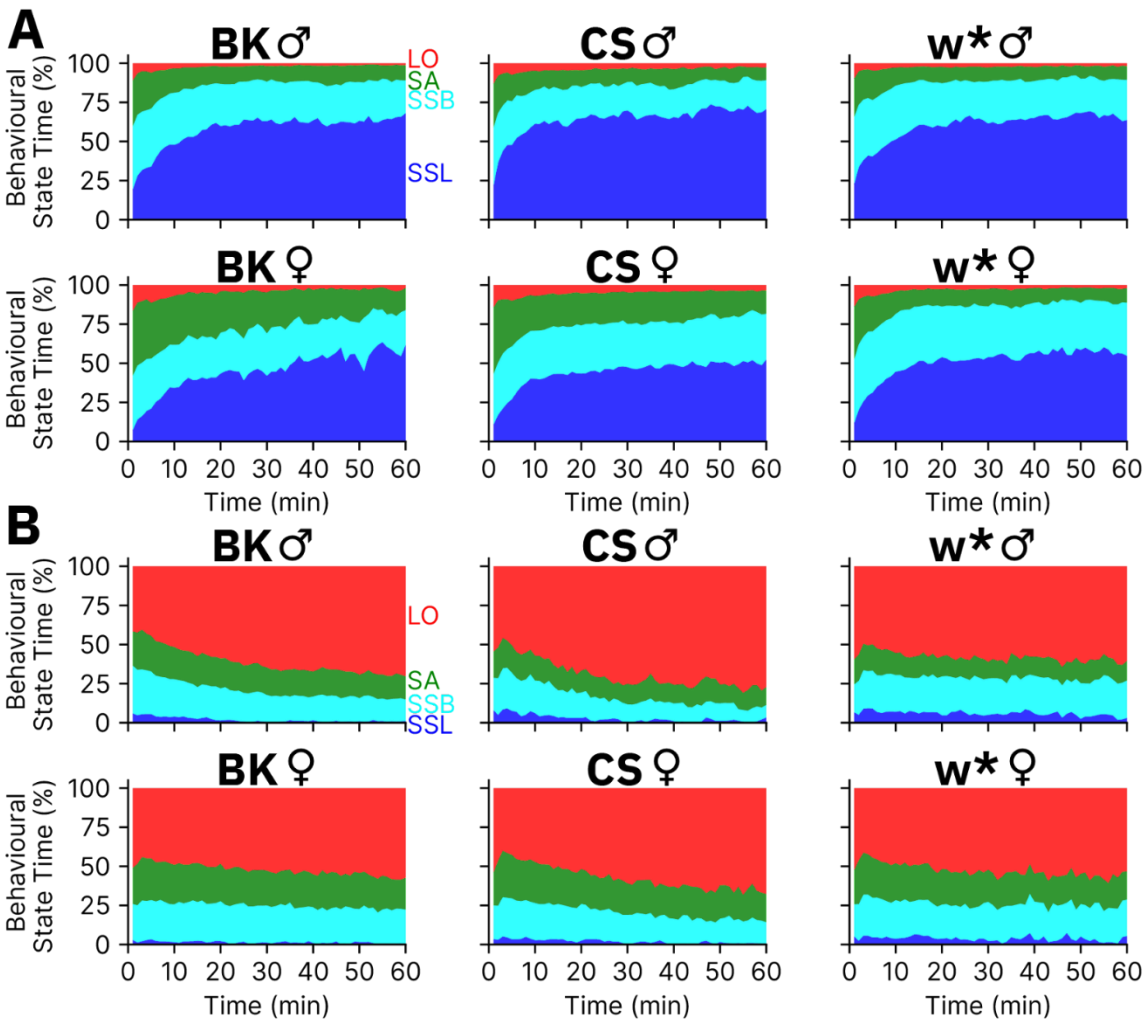

Appendix A Figure 23 Composition of Trumelan behaviours during virtual DAM rest or active periods for each genotype

The percentage of each Trumelan behaviour that occurs during each minute of virtual DAM rest **(A)** or activity **(B)**, averaged for all bouts for each genotype. Data starts as the first minute of virtual DAM rest, active periods after rest. The number of flies used for (A-B) were 60 for BK males, 30 for BK females, 30 for CS males, 59 for CS females, 49 for w* males, and 38 for w* females.

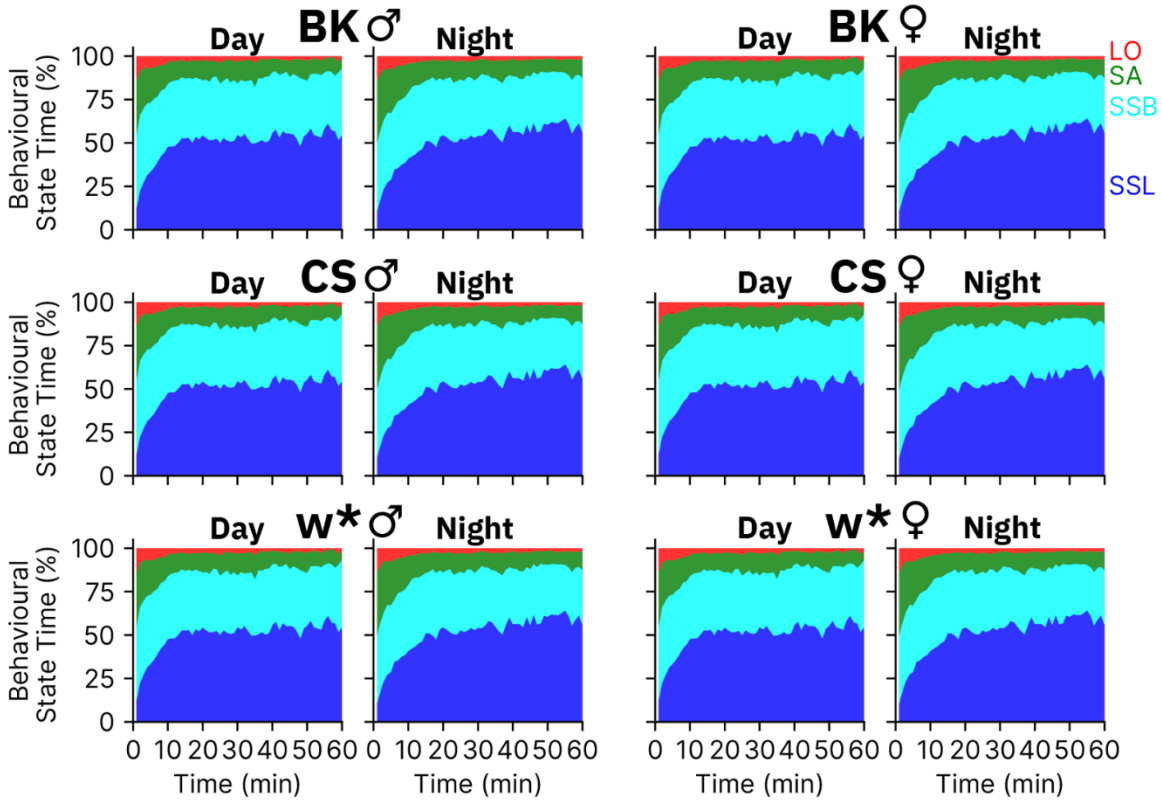

Appendix A Figure 24 Composition of Trumelan behaviours during virtual DAM recorded rest for day and night

The percentage of each Trumelan behaviour that occurs during each minute of virtual DAM rest, averaged for all bouts during the day or night for each genotype. Data starts as the first minute of virtual DAM rest. The number of flies used was 60 for BK males, 30 for BK females, 30 for CS males, 59 for CS females, 49 for w* males, and 38 for w* females.

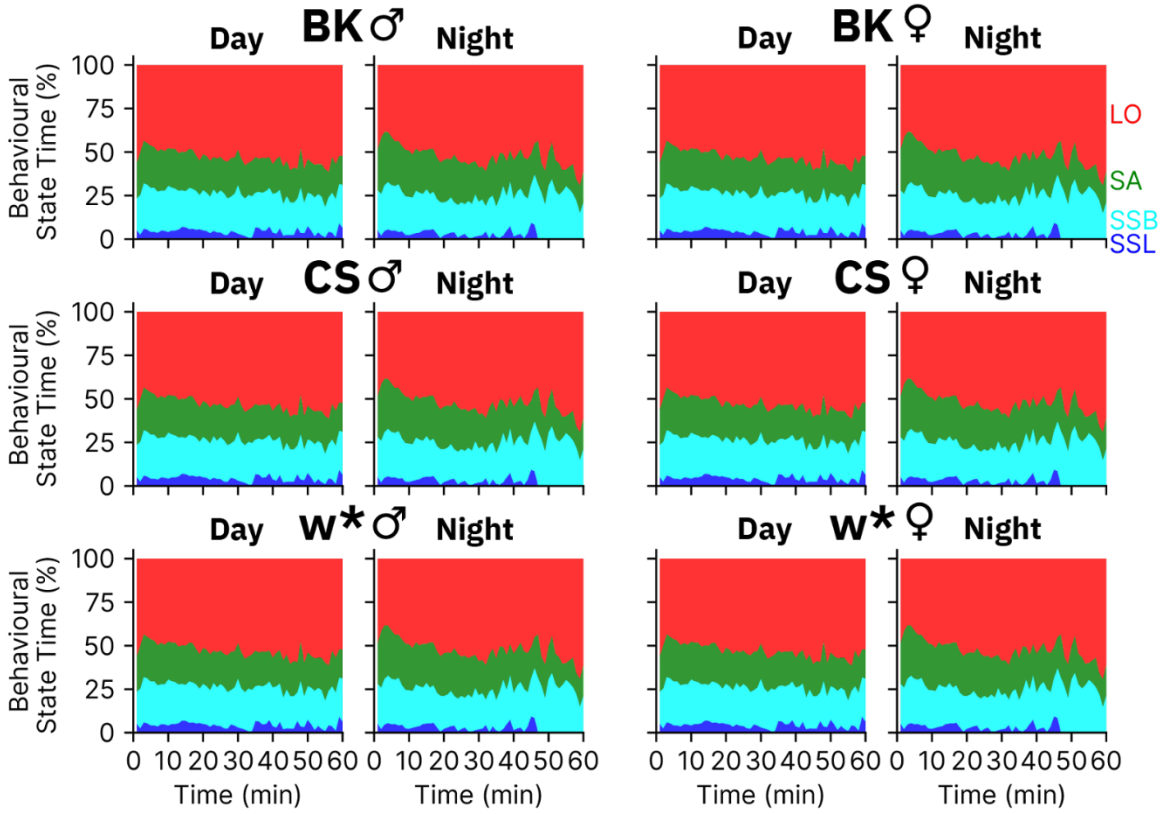

Appendix A Figure 25 Composition of Trumelan behaviours during virtual DAM recorded active periods for day and night

The percentage of each Trumelan behaviour that occurs during each minute of virtual DAM active periods, averaged for all bouts during the day or night for each genotype. Data starts as the first minute of active periods after a virtual DAM rest period ends. The number of flies used was 60 for BK males, 30 for BK females, 30 for CS males, 59 for CS females, 49 for w* males, and 38 for w* females.

Appendix B Chapter 4

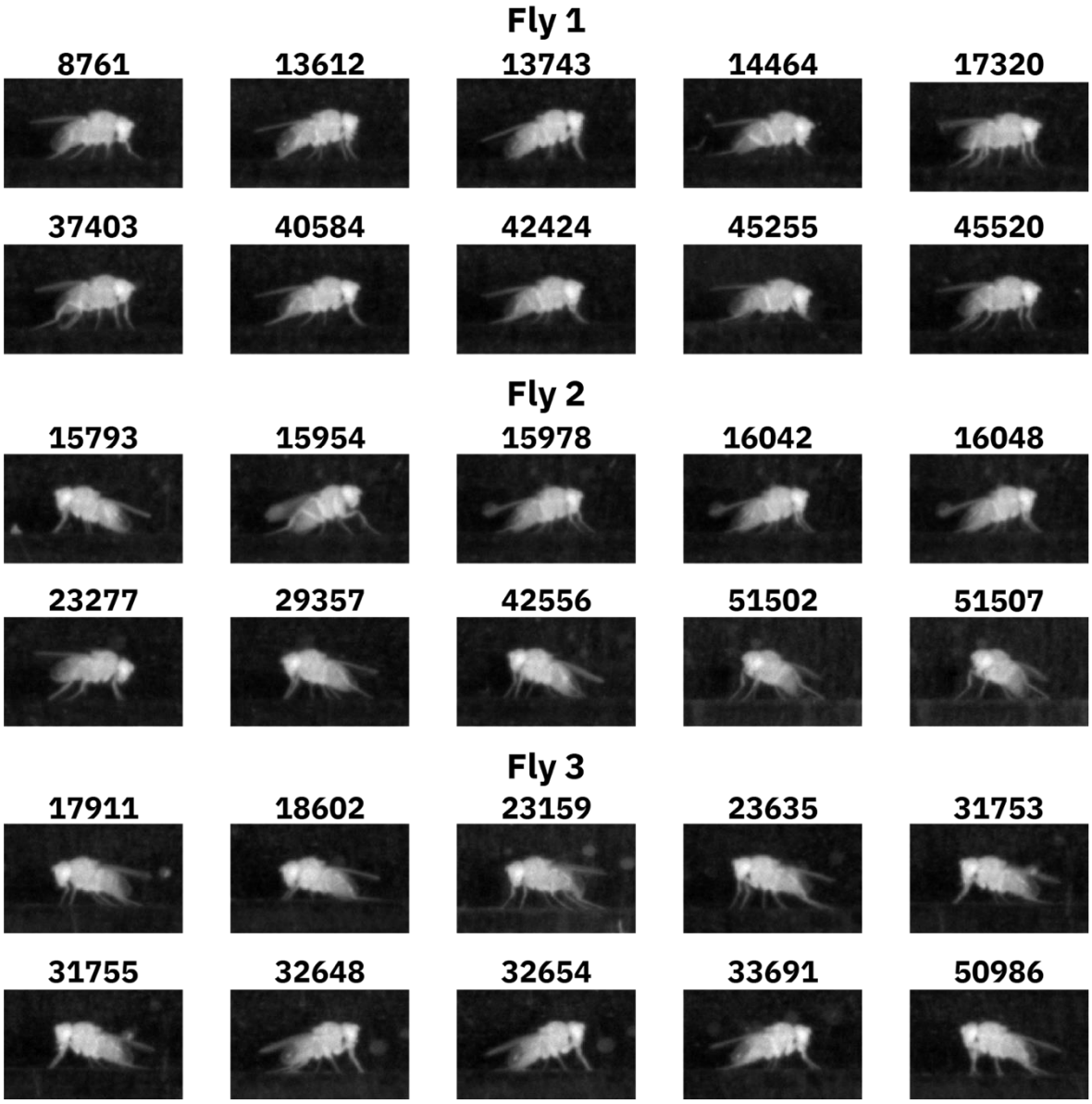

Appendix B Figure 1 Starting posture examples from ground-based SSL

Ten randomly selected example images of the starting posture (first frame) from three Berlin-K male flies performing ground-based SSL. The number above each image corresponds to the bout number, and the values associated with these images (such as starting Y-Pos, nBA, and the duration of the bout can be found in Appendix B Table 1.

Appendix B Table 1 Starting posture examples from ground-based SSL

The table represents the raw data for the starting posture and duration of the SSL bout for the images shown in Figure 4.1.1B and Appendix B Figure 1.

Fly	Bout	Duration (s)	Y-Pos (mm)	nBA (°)
1	8761	62.138	1.21	-4.23
1	13612	114.769	1.23	-12.45
1	13743	68.641	1.23	-15.93
1	14464	263.057	1.09	-7.66
1	15887	79.648	1.18	-7.93
1	17320	68.34	1.32	-5.56
1	37403	145.087	1.35	-7.66
1	40584	73.044	1.21	-7.06
1	42424	357.914	1.15	-9.87
1	45255	84.251	1.04	-3.85
1	45520	73.243	1.32	-8.37
2	4902	182.209	1.24	-18.56
2	15793	194.716	1.16	-14.70
2	15954	61.337	1.19	-11.89
2	15978	366.82	1.13	-11.35
2	16042	199.52	1.13	-10.93
2	16048	258.055	1.13	-11.69
2	23277	66.74	1.28	-4.39
2	29357	163.098	1.23	-10.65
2	42556	366.019	1.20	-16.71
2	51502	335.902	1.22	-18.71
2	51507	295.577	1.24	-25.61
3	17911	200.62	1.24	-10.05
3	18602	139.284	1.07	-9.19
3	23159	145.687	1.34	-10.92
3	23635	90.855	1.33	-12.79
3	31753	236.841	1.18	-9.62

Fly	Bout	Duration (s)	Y-Pos (mm)	nBA (°)
3	31755	72.543	1.16	-11.12
3	32648	188.514	1.25	-11.29
3	32654	110.267	1.21	-13.83
3	33581	64.039	1.27	-10.90
3	33691	102.161	1.17	-12.21
3	50986	123.874	1.32	-15.61

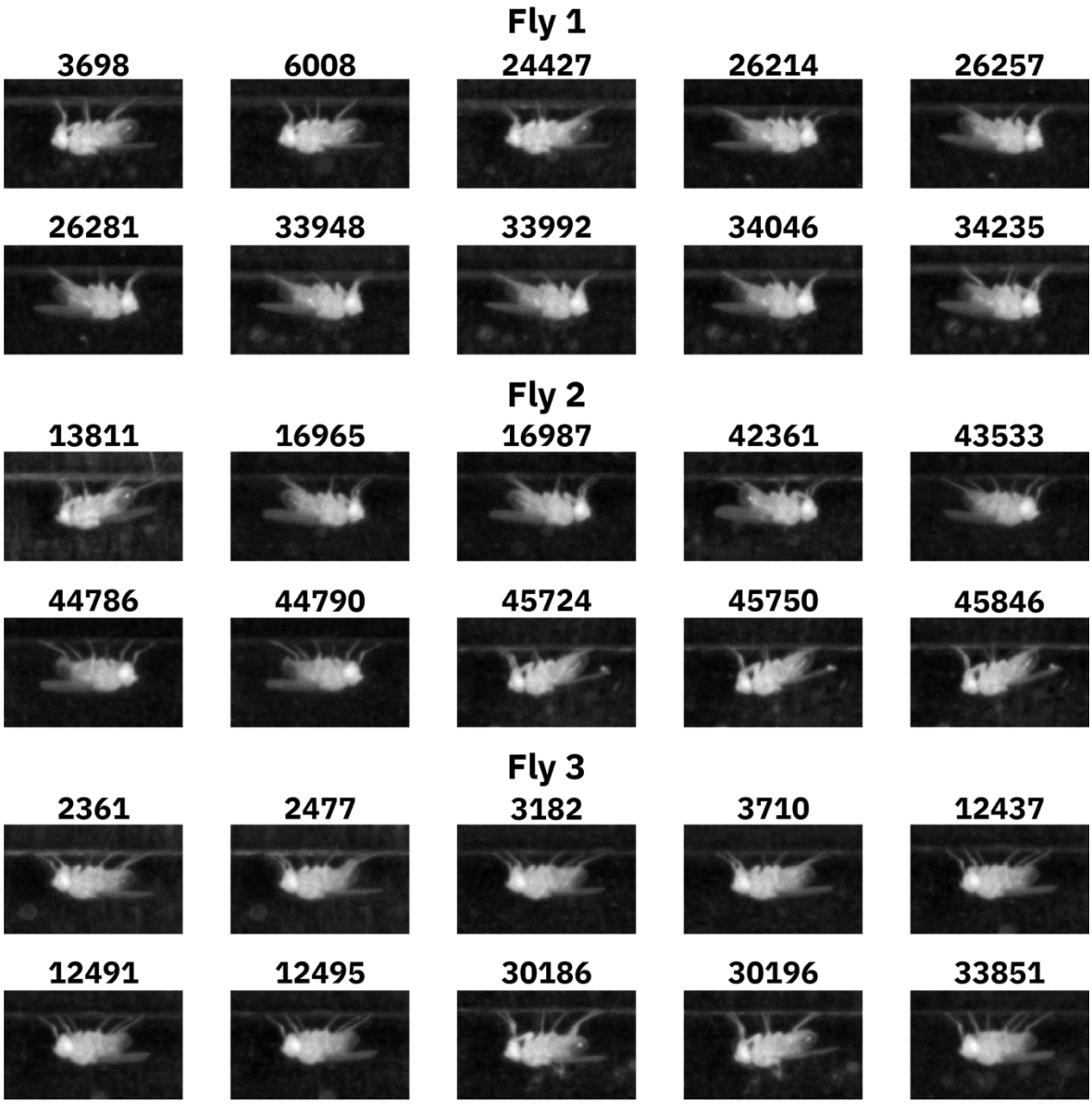

Appendix B Figure 2 Starting posture examples from ceiling-based SSL

Ten randomly selected example images of the starting posture (first frame) from three Berlin-K male flies performing ceiling-based SSL. The number above each image corresponds to the bout number, and the values associated with these images (such as starting Y-Pos, nBA, and the duration of the bout can be found in Appendix B Table 2.

Appendix B Table 2 Starting posture from examples of ceiling-based SSL

The table represents the raw data for the starting posture and duration of the SSL bout for the images shown in Figure 4.1.1B and Appendix B Figure 2.

Fly	Bout	Duration (s)	Y-Pos (mm)	nBA (°)
1	3698	530.819	2.59	4.40
1	4163	106.163	2.71	1.58
1	6008	305.383	2.59	1.61
1	24427	142.786	2.68	5.24
1	26214	60.437	2.83	1.04
1	26257	74.744	2.78	1.97
1	26281	114.369	2.68	-0.02
1	33948	60.236	2.83	2.10
1	33992	194.917	2.80	2.28
1	34046	84.05	2.78	-0.22
1	34235	303.183	2.62	-2.20
2	13811	64.839	2.72	12.91
2	16965	111.967	2.70	1.28
2	16987	184.111	2.69	0.41
2	42361	69.641	2.72	-1.44
2	43533	264.958	2.71	-0.43
2	44786	89.054	2.63	-1.15
2	44790	65.239	2.65	-2.47
2	45678	176.506	2.75	4.10
2	45724	187.713	2.82	7.21
2	45750	150.189	2.79	12.30
2	45846	96.359	2.76	9.66
3	2361	270.664	2.79	-2.35
3	2477	490.194	2.80	1.28
3	3140	77.145	2.74	-0.18
3	3182	506.303	2.80	-2.45
3	3710	100.26	2.80	-0.71

Appendix B

Fly	Bout	Duration (s)	Y-Pos (mm)	nBA (°)
3	12437	89.553	2.72	-3.86
3	12491	171.803	2.73	-4.55
3	12495	217.33	2.72	-4.69
3	30186	92.554	2.57	0.88
3	30196	61.437	2.65	3.50
3	33851	120.672	2.65	-4.39

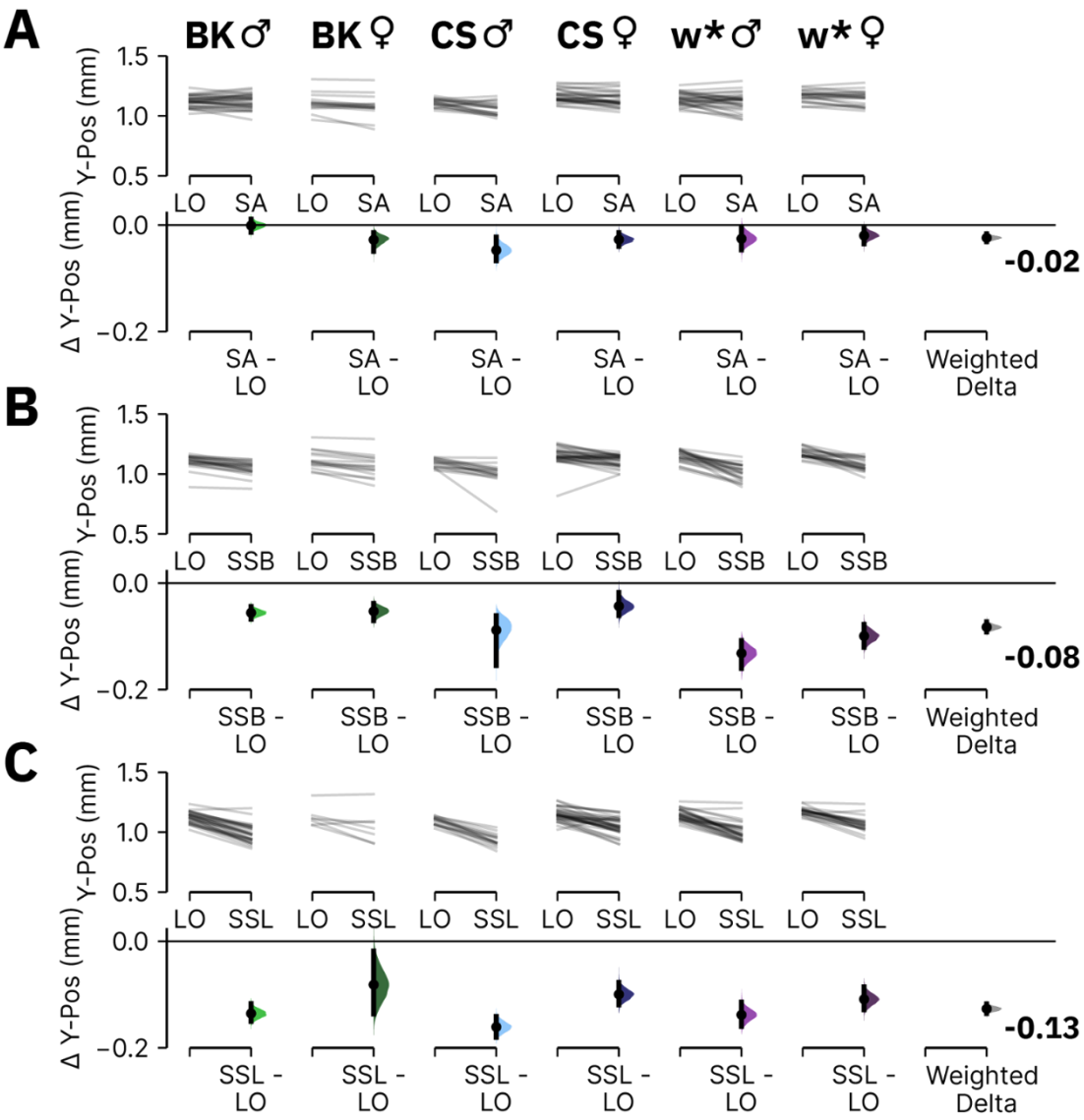

Appendix B Figure 3 Flies begin each stationary behaviour on the ground with a lower Y-Pos compared to LO

DABEST plots of the average starting Y-Pos for ground-based SA **(A)**, SSB **(A)**, or SSL **(C)** vs. LO bouts. Summary information and sample sizes are shown in Appendix B Table 3. See Chapter 2.6 for more information about the structure of DABEST plots.

Appendix B Table 3 Comparison of starting Y-Pos for ground-based stationary behaviour vs. LO

The table is pertinent to Appendix B Figure 3, illustrating the DABEST comparisons of Y-Pos between stationary states and LO bouts for a given genotype. See Chapter 2.6 for more information about DABEST plots.

Genotype	Sex	Ctr / Test	Sample Size (n)	Ctr Mean±CI (mm)	Test Mean±CI (mm)	Delta (mm)	Delta-CI (mm)	Delta+CI (mm)	p-value
BK	M	LO / SA	31	1.12±0.02	1.12±0.02	0.00	-0.01	0.01	0.8812
BK	F	LO / SA	15	1.11±0.04	1.08±0.05	-0.03	-0.05	-0.01	0.0042
CS	M	LO / SA	19	1.11±0.02	1.06±0.02	-0.05	-0.07	-0.02	0.0016
CS	F	LO / SA	29	1.17±0.02	1.14±0.02	-0.03	-0.04	-0.01	0.0010
w*	M	LO / SA	29	1.14±0.02	1.11±0.03	-0.03	-0.05	0.00	0.0362
w*	F	LO / SA	21	1.17±0.02	1.15±0.03	-0.02	-0.04	-0.01	0.0138
Weighted Delta	M/F	LO / SA	144	NA	NA	-0.02	-0.03	-0.02	0.0000
BK	M	LO / SSB	22	1.10±0.02	1.05±0.02	-0.06	-0.07	-0.04	0.0000
BK	F	LO / SSB	15	1.12±0.04	1.07±0.05	-0.05	-0.07	-0.04	0.0000
CS	M	LO / SSB	16	1.09±0.02	1.00±0.05	-0.09	-0.15	-0.06	0.0000
CS	F	LO / SSB	31	1.15±0.03	1.11±0.02	-0.04	-0.06	-0.02	0.0000
w*	M	LO / SSB	23	1.15±0.02	1.01±0.03	-0.13	-0.16	-0.11	0.0000
w*	F	LO / SSB	22	1.18±0.02	1.08±0.02	-0.10	-0.12	-0.08	0.0000
Weighted Delta	M/F	LO / SSB	129	NA	NA	-0.08	-0.09	-0.07	0.0000
BK	M	LO / SSL	31	1.12±0.02	0.99±0.03	-0.14	-0.15	-0.12	0.0000
BK	F	LO / SSL	7	1.13±0.06	1.05±0.10	-0.08	-0.14	-0.02	0.0662
CS	M	LO / SSL	16	1.09±0.02	0.93±0.03	-0.16	-0.18	-0.14	0.0000
CS	F	LO / SSL	35	1.15±0.02	1.05±0.02	-0.10	-0.12	-0.08	0.0000
w*	M	LO / SSL	30	1.15±0.02	1.01±0.03	-0.14	-0.16	-0.11	0.0000
w*	F	LO / SSL	23	1.17±0.01	1.07±0.03	-0.11	-0.13	-0.09	0.0000
Weighted Delta	M/F	LO / SSL	142	NA	NA	-0.13	-0.14	-0.12	0.0000

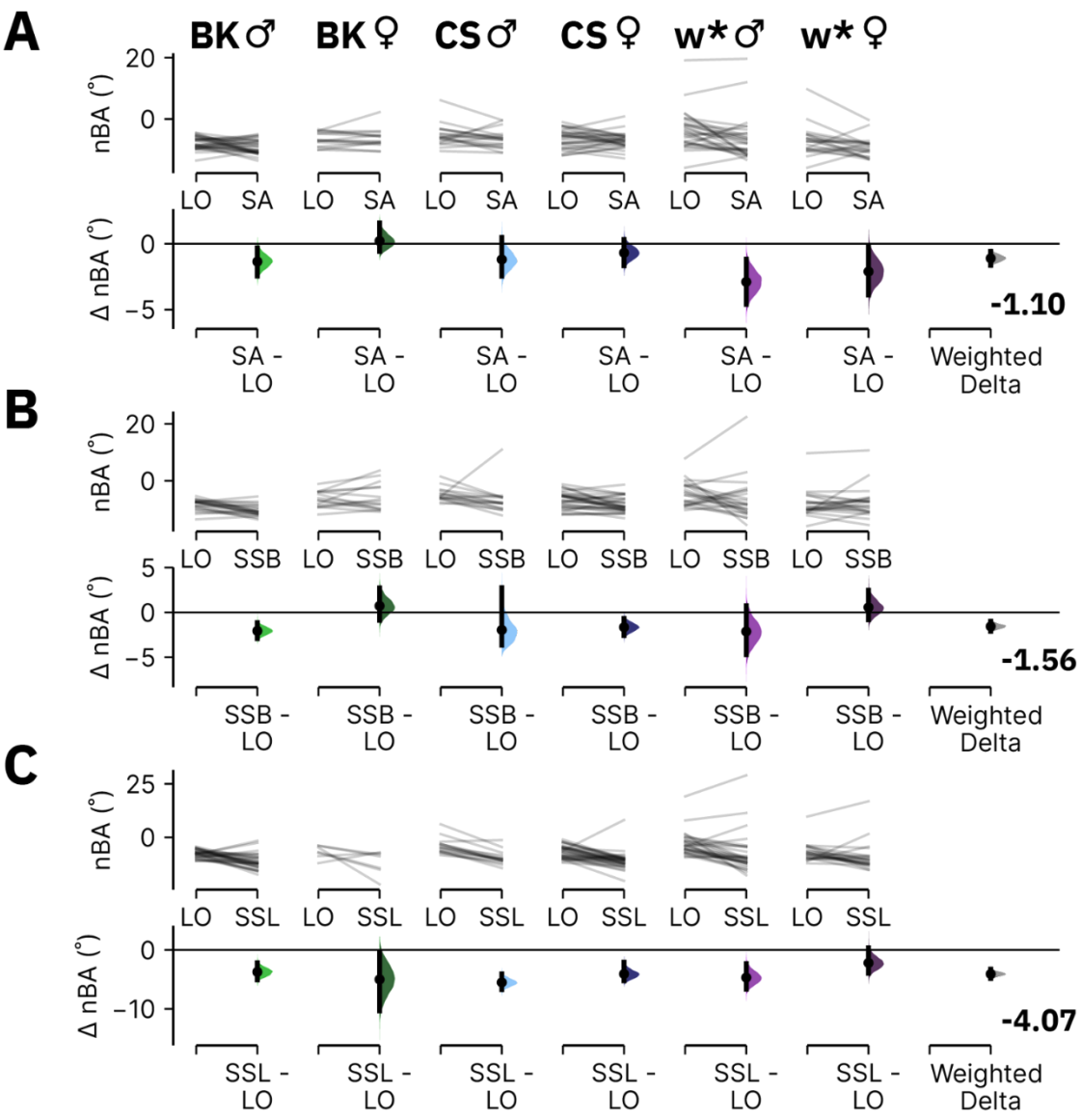

Appendix B Figure 4 Flies begin stationary behaviours on the ground with a more negative body angle compared to LO

DABEST plots of the average starting nBA for ground-based SA **(A)**, SSB **(A)**, or SSL **(C)** versus LO bouts. Summary information and sample sizes are shown in Appendix B Table 4. See Chapter 2.6 for more information about the structure of DABEST plots.

Appendix B Table 4 Comparison of starting nBA for ground-based stationary behaviour versus LO

The table is pertinent to Appendix B Figure 4, illustrating the DABEST comparison of nBA between stationary behaviours and LO bouts for a given genotype. See Chapter 2.6 for more information about DABEST plots.

Genotype	Sex	Ctr / Test	Sample Size (n)	Ctr Mean±CI (°)	Test Mean±CI (°)	Delta (°)	Delta-CI (°)	Delta+CI (°)	p-value
BK	M	LO / SA	31	-7.76±0.74	-9.11±0.81	-1.35	-2.44	-0.31	0.0160
BK	F	LO / SA	15	-6.55±1.20	-6.34±1.57	0.21	-0.57	1.57	0.7356
CS	M	LO / SA	19	-5.28±1.61	-6.48±1.37	-1.19	-2.46	0.47	0.1494
CS	F	LO / SA	29	-6.37±1.12	-7.06±0.95	-0.69	-1.67	0.33	0.1978
w*	M	LO / SA	29	-3.54±2.33	-6.43±2.58	-2.89	-4.60	-1.17	0.0068
w*	F	LO / SA	21	-6.97±2.15	-9.08±1.41	-2.11	-3.88	-0.23	0.0348
Weighted Delta	M/F	LO / SA	144	NA	NA	-1.10	-1.64	-0.57	0.0006
BK	M	LO / SSB	22	-8.38±0.82	-10.44±0.81	-2.06	-2.91	-1.15	0.0002
BK	F	LO / SSB	15	-6.42±1.47	-5.69±2.40	0.73	-0.88	2.73	0.4544
CS	M	LO / SSB	16	-4.77±1.19	-6.73±2.51	-1.96	-3.65	2.75	0.1652
CS	F	LO / SSB	31	-6.72±1.05	-8.37±0.95	-1.65	-2.58	-0.67	0.0046
w*	M	LO / SSB	23	-4.42±1.80	-6.54±3.15	-2.12	-4.71	0.76	0.1480
w*	F	LO / SSB	22	-8.13±2.04	-7.56±2.27	0.57	-0.81	2.47	0.5396
Weighted Delta	M/F	LO / SSB	129	NA	NA	-1.56	-2.10	-0.99	0.0000
BK	M	LO / SSL	31	-7.58±0.67	-11.31±1.28	-3.73	-5.08	-2.17	0.0002
BK	F	LO / SSL	7	-6.78±2.19	-11.78±4.11	-5.00	-10.34	-0.55	0.1108
CS	M	LO / SSL	16	-4.08±1.79	-9.59±1.55	-5.51	-6.73	-4.06	0.0000
CS	F	LO / SSL	35	-6.83±0.98	-10.90±1.37	-4.07	-5.22	-2.09	0.0000
w*	M	LO / SSL	30	-2.94±2.00	-7.62±3.31	-4.68	-6.65	-2.31	0.0000
w*	F	LO / SSL	23	-6.99±1.78	-9.19±2.78	-2.19	-3.97	0.36	0.0468
Weighted Delta	M/F	LO / SSL	142	NA	NA	-4.07	-4.83	-3.26	0.0000

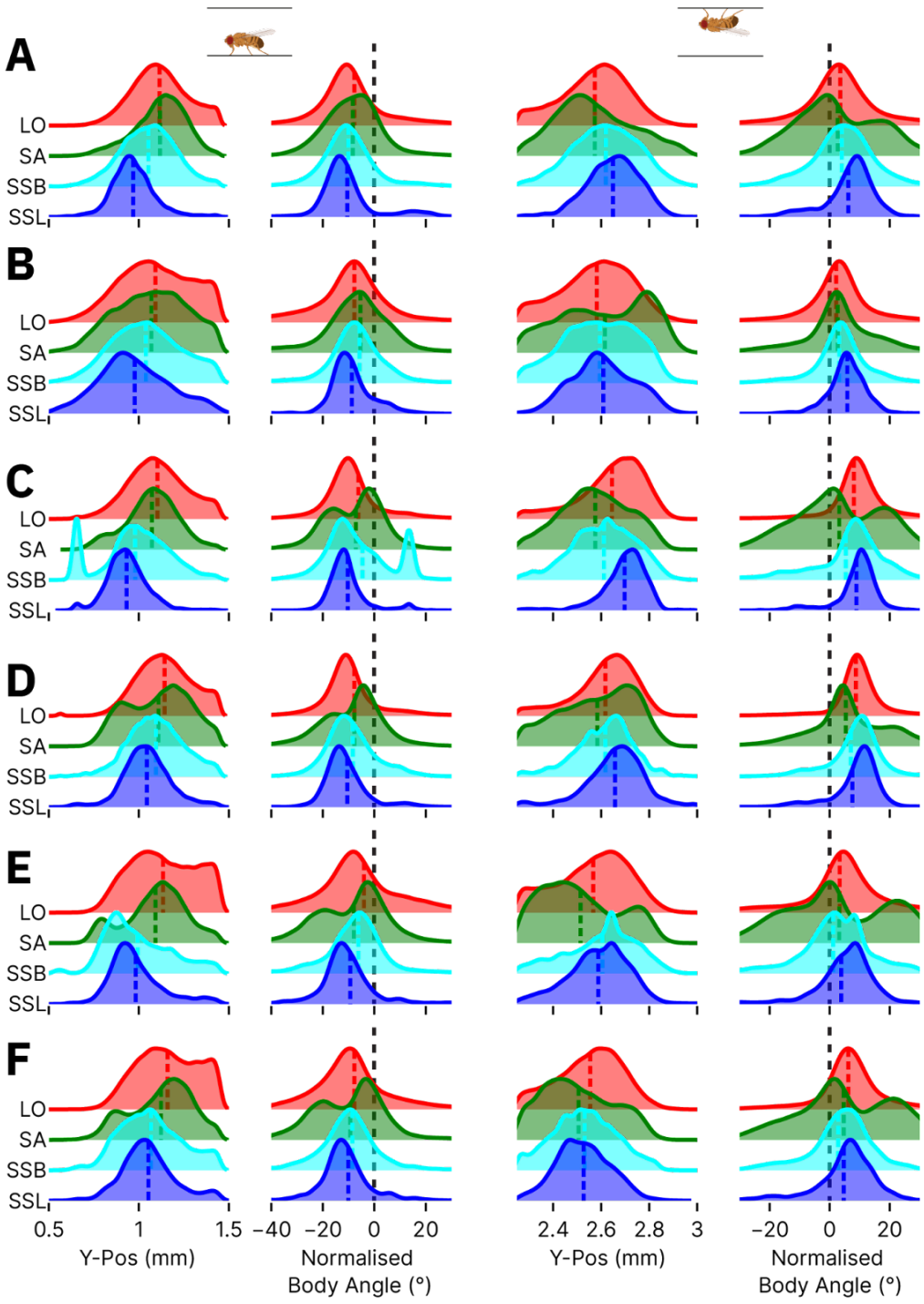

Appendix B Figure 5 The distribution of starting postures for each behavioural state demonstrates the high variability and overlap (between states) in starting posture

Ridgeline plots demonstrating the distribution of starting Y-Pos (mm) and nBA (°) of BK males **(A)**, BK females **(B)**, CS males **(C)**, CS females **(D)**, w* males **(E)**, and w* females **(F)**. Ridgeline curves are shown for all four behavioural states (LO, SA, SSB, and SSL) on the ground and the ceiling. The dotted lines within the distributions indicate the mean of that distribution. The dotted black line on the nBA subplots indicates the zero line.

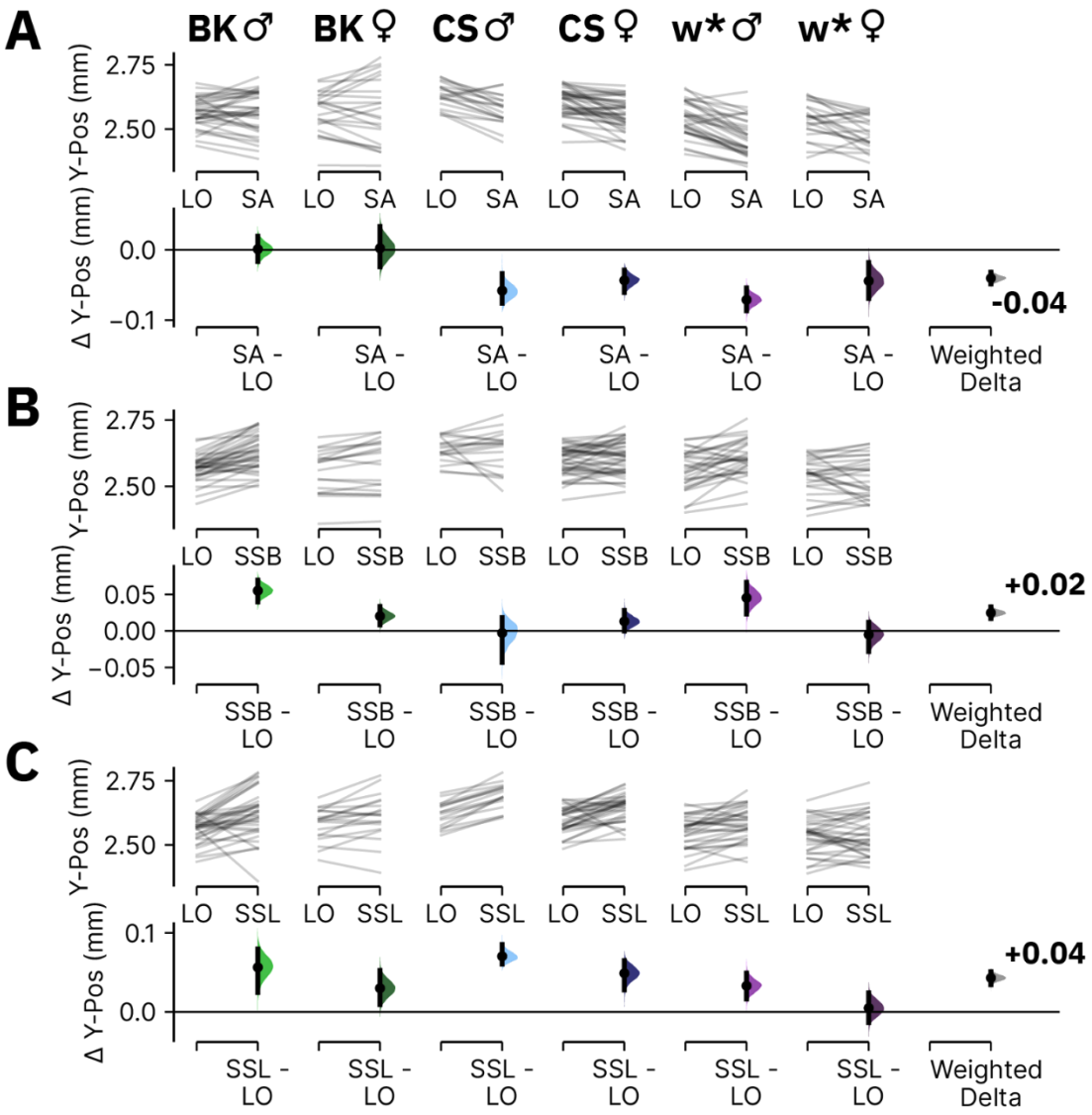

Appendix B Figure 6 Flies begin long rest closer to the ceiling compared to LO

DABEST plots of the average starting Y-Pos for ceiling-based SA **(A)**, SSB **(A)**, or SSL **(C)** vs. LO bouts. Summary information and sample sizes are shown in Appendix B Table 5. See Chapter 2.6 for more information about the structure of DABEST plots.

Appendix B Table 5 Comparison of starting Y-Pos for ceiling-based stationary behaviour vs. LO

The table is pertinent to Appendix B Figure 6, illustrating the DABEST comparison of Y-Pos between stationary states and LO bouts for a given genotype. See Chapter 2.6 for more information about DABEST plots.

Genotype	Sex	Ctr / Test	Sample Size (n)	Ctr Mean±CI (mm)	Test Mean±CI (mm)	Delta (mm)	Delta-CI (mm)	Delta+CI (mm)	p-value
BK	M	LO / SA	35	2.56±0.02	2.56±0.03	0.00	-0.02	0.02	0.9166
BK	F	LO / SA	22	2.57±0.03	2.57±0.05	0.00	-0.02	0.03	0.8858
CS	M	LO / SA	19	2.63±0.02	2.57±0.03	-0.06	-0.08	-0.03	0.0002
CS	F	LO / SA	39	2.60±0.02	2.56±0.02	-0.04	-0.06	-0.03	0.0000
w*	M	LO / SA	32	2.54±0.02	2.47±0.03	-0.07	-0.09	-0.05	0.0000
w*	F	LO / SA	23	2.54±0.03	2.49±0.03	-0.04	-0.07	-0.02	0.0024
Weighted Delta	M/F	LO / SA	170	NA	NA	-0.04	-0.05	-0.03	0.0000
BK	M	LO / SSB	37	2.57±0.02	2.62±0.02	0.06	0.04	0.07	0.0000
BK	F	LO / SSB	19	2.56±0.04	2.58±0.04	0.02	0.01	0.03	0.0066
CS	M	LO / SSB	18	2.64±0.02	2.64±0.04	0.00	-0.04	0.02	0.8766
CS	F	LO / SSB	42	2.59±0.02	2.61±0.02	0.01	0.00	0.03	0.0754
w*	M	LO / SSB	30	2.56±0.03	2.61±0.02	0.05	0.02	0.07	0.0004
w*	F	LO / SSB	27	2.54±0.03	2.54±0.03	-0.01	-0.03	0.01	0.6286
Weighted Delta	M/F	LO / SSB	173	NA	NA	0.02	0.02	0.03	0.0000
BK	M	LO / SSL	35	2.57±0.02	2.62±0.03	0.06	0.02	0.08	0.0002
BK	F	LO / SSL	19	2.58±0.03	2.61±0.04	0.03	0.01	0.05	0.0188
CS	M	LO / SSL	17	2.62±0.02	2.69±0.02	0.07	0.06	0.09	0.0000
CS	F	LO / SSL	33	2.60±0.02	2.65±0.02	0.05	0.03	0.06	0.0000
w*	M	LO / SSL	31	2.55±0.02	2.58±0.02	0.03	0.02	0.05	0.0000
w*	F	LO / SSL	33	2.54±0.02	2.54±0.03	0.00	-0.01	0.02	0.6326
Weighted Delta	M/F	LO / SSL	168	NA	NA	0.04	0.03	0.05	0.0000

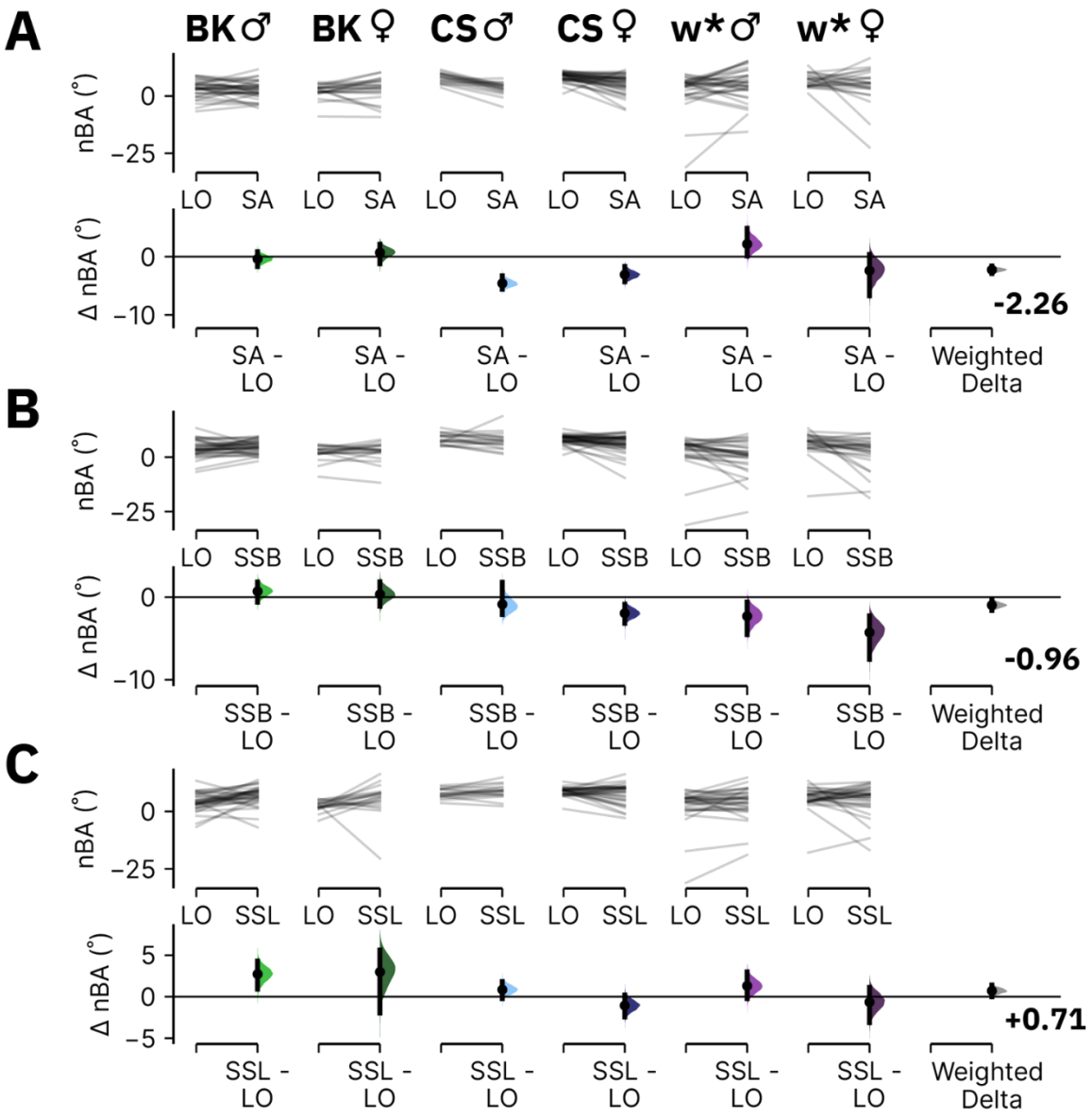

Appendix B Figure 7 Flies have varied starting body angles during ceiling based stationary behaviour compared to LO

DABEST plots of the average starting nBA for ceiling-based SA **(A)**, SSB **(A)**, or SSL **(C)** vs. LO bouts. Summary information and sample sizes are shown in Appendix B Table 6. See Chapter 2.6 for more information about the structure of DABEST plots.

Appendix B Table 6 Comparison of starting nBA for ceiling-based stationary behaviour vs. LO

The table is pertinent to Appendix B Figure 7, illustrating the DABEST comparison of nBA between stationary states and LO bouts for a given genotype. See Chapter 2.6 for more information about DABEST plots.

Genotype	Sex	Ctr / Test	Sample Size (n)	Ctr Mean±CI (°)	Test Mean±CI (°)	Delta (°)	Delta-CI (°)	Delta+CI (°)	p-value
BK	M	LO / SA	35	3.09±1.28	2.69±1.28	-0.40	-1.69	0.84	0.5474
BK	F	LO / SA	22	2.15±1.34	2.83±2.20	0.69	-1.22	2.11	0.4366
CS	M	LO / SA	19	7.88±0.98	3.31±1.24	-4.58	-5.58	-3.27	0.0000
CS	F	LO / SA	39	8.40±0.63	5.32±1.30	-3.08	-4.30	-1.69	0.0000
w*	M	LO / SA	32	2.64±2.73	4.79±2.46	2.15	0.10	4.84	0.0778
w*	F	LO / SA	23	6.61±1.17	4.21±3.35	-2.39	-6.73	0.39	0.2000
Weighted Delta	M/F	LO / SA	170	NA	NA	-2.26	-2.91	-1.60	0.0000
BK	M	LO / SSB	37	3.94±1.30	4.66±0.97	0.72	-0.60	1.84	0.2684
BK	F	LO / SSB	19	1.99±1.60	2.35±2.02	0.36	-1.10	1.85	0.6440
CS	M	LO / SSB	18	8.48±1.13	7.62±1.84	-0.86	-2.11	1.80	0.4018
CS	F	LO / SSB	42	8.21±0.62	6.27±1.25	-1.94	-3.17	-0.85	0.0018
w*	M	LO / SSB	30	2.47±2.84	0.16±2.72	-2.30	-4.51	-0.58	0.0234
w*	F	LO / SSB	27	6.19±2.11	1.92±2.84	-4.27	-7.54	-2.25	0.0002
Weighted Delta	M/F	LO / SSB	173	NA	NA	-0.96	-1.60	-0.31	0.0062
BK	M	LO / SSL	35	4.07±1.34	6.79±1.40	2.73	0.91	4.30	0.0040
BK	F	LO / SSL	19	2.38±1.02	5.35±3.32	2.98	-1.98	5.61	0.1146
CS	M	LO / SSL	17	7.83±1.01	8.67±1.47	0.84	-0.23	1.83	0.1336
CS	F	LO / SSL	33	8.66±0.66	7.60±1.51	-1.06	-2.45	0.20	0.1378
w*	M	LO / SSL	31	2.46±2.79	3.75±2.44	1.30	-0.24	2.98	0.1272
w*	F	LO / SSL	33	5.86±1.73	5.21±2.29	-0.65	-3.11	1.13	0.5626
Weighted Delta	M/F	LO / SSL	168	NA	NA	0.71	-0.01	1.40	0.0652

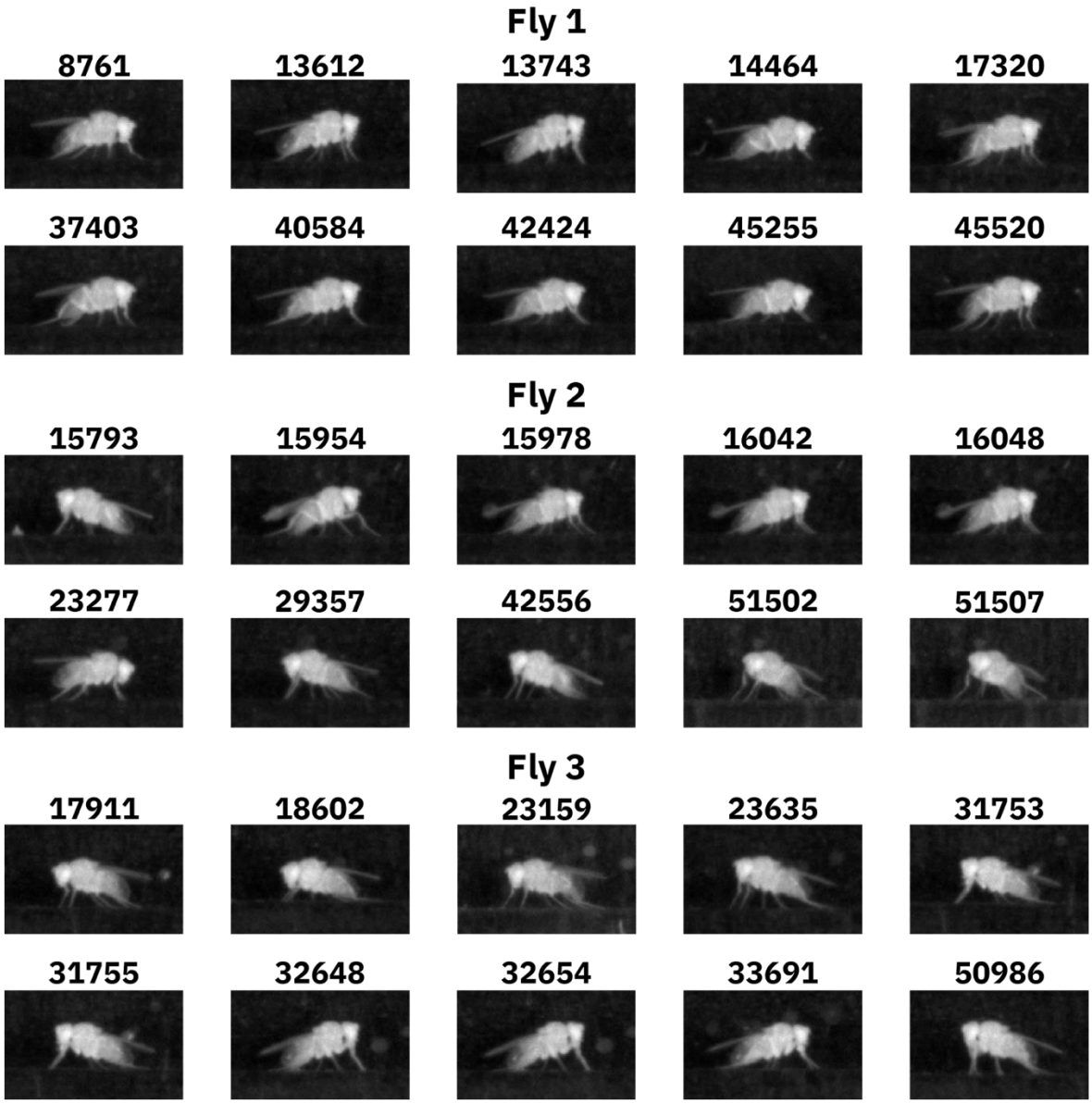

Appendix B Figure 8 Images of end posture of ground-based SSL

Ten randomly selected example images (same selection as for Appendix B Figure 1) of the ending posture (last frame) from three Berlin-K male flies performing ground-based SSL. The number above each image corresponds to the bout number, and the values associated with these images (such as change in Y-Pos, nBA, and the duration of the bout) can be found in Appendix B Table 7.

Appendix B Table 7 Change in posture for ground-based SSL examples

The table represents the raw data for the change in posture and duration of the SSL bout for the images shown in Appendix B Figure 8.

Fly	Bout	Duration (s)	Δ Y-Pos (µm)	Δ nBA (°)
1	8761	62.138	-32.1	-0.65
1	13612	114.769	-1.34	-0.41
1	13743	68.641	-13.18	0.71
1	14464	263.057	-12.05	-0.99
1	15887	79.648	-7.94	-0.23
1	17320	68.34	-98.3	-2.32
1	37403	145.087	-133.83	0.28
1	40584	73.044	-39.06	-1.86
1	42424	357.914	-20.05	2.84
1	45255	84.251	-4.62	-2.35
1	45520	73.243	-20.82	-0.14
2	4902	182.209	-34.35	-0.82
2	15793	194.716	-6.96	-0.61
2	15954	61.337	2.44	-0.06
2	15978	366.82	-7.23	-0.81
2	16042	199.52	-6.27	0.36
2	16048	258.055	1.49	-0.26
2	23277	66.74	-53.65	-2.10
2	29357	163.098	-11.5	-0.69
2	42556	366.019	-12.27	-1.03
2	51502	335.902	-25.87	-3.50
2	51507	295.577	-36.25	5.42
3	17911	200.62	19.26	0.41
3	18602	139.284	8.26	0.10
3	23159	145.687	-54.35	-2.01
3	23635	90.855	-31.78	-1.94
3	31753	236.841	-31.15	-2.08
3	31755	72.543	-11.14	-0.74
3	32648	188.514	-37.07	-2.09
3	32654	110.267	-6.23	0.30

Appendix B

Fly	Bout	Duration (s)	Δ Y-Pos (µm)	Δ nBA (°)
3	33581	64.039	-44.22	-3.43
3	33691	102.161	-32.45	-0.85
3	50986	123.874	-8.95	-0.14

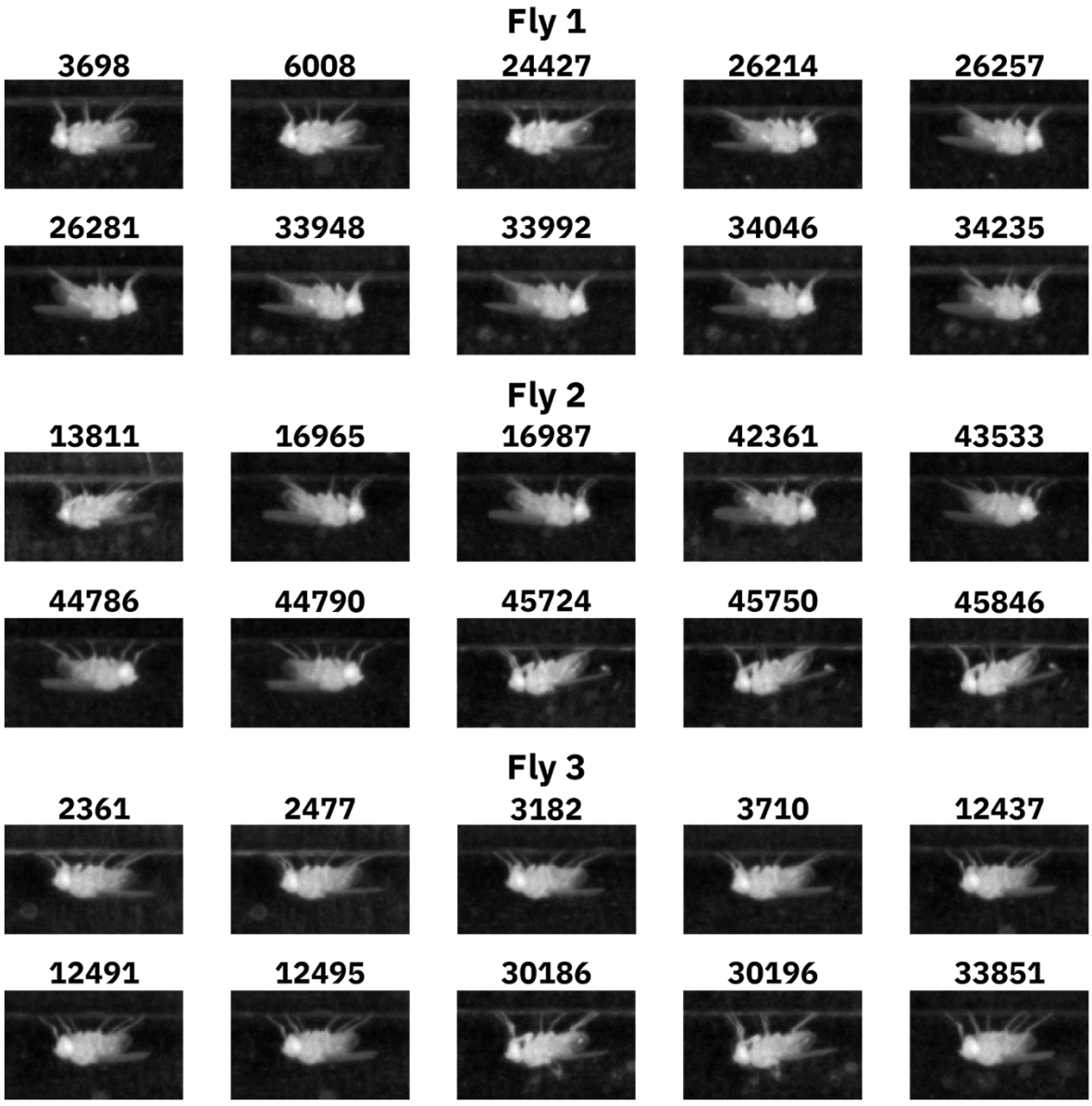

Appendix B Figure 9 Images of starting posture for ceiling-based SSL

Ten randomly selected example images (same selection as for Appendix B Figure 2) of the ending posture (last frame) from three Berlin-K male flies performing ceiling-based SSL. The number above each image corresponds to the bout number, and the values associated with these images (such as change in Y-Pos, nBA, and the duration of the bout can be found in Appendix B Table 8.

Appendix B Table 8 Change in posture for ceiling-based SSL examples

The table represents the raw data for the change in posture and duration of the SSL bout for the images shown in Appendix B Figure 9.

Fly	Bout	Duration (s)	Δ Y-Pos (µm)	Δ nBA (°)
1	3698	530.819	-8.72	-5.06
1	4163	106.163	33.16	0.47
1	6008	305.383	9.49	-0.48
1	24427	142.786	-14.81	-1.15
1	26214	60.437	0.86	0.11
1	26257	74.744	-10.41	0.34
1	26281	114.369	3.39	-0.01
1	33948	60.236	-5.57	-0.08
1	33992	194.917	9.31	-0.05
1	34046	84.05	-6.69	-0.73
1	34235	303.183	22.33	-1.01
2	13811	64.839	16.06	-6.26
2	16965	111.967	-1.5	0.18
2	16987	184.111	20.14	0.73
2	42361	69.641	-17.05	-1.24
2	43533	264.958	37.64	0.66
2	44786	89.054	25.16	0.37
2	44790	65.239	-13.17	-0.23
2	45678	176.506	-4.86	-0.93
2	45724	187.713	-20.39	-0.42
2	45750	150.189	-15.09	-3.03
2	45846	96.359	-28.47	-1.25
3	2361	270.664	-1.41	-0.71
3	2477	490.194	17.37	0.84
3	3140	77.145	-5.59	-1.57
3	3182	506.303	-14.09	-0.56
3	3710	100.26	5.23	-0.55
3	12437	89.553	0.49	-0.84
3	12491	171.803	3.75	0.34
3	12495	217.33	0.77	-0.24

Fly	Bout	Duration (s)	Δ Y-Pos (µm)	Δ nBA (°)
3	30186	92.554	54.13	2.92
3	30196	61.437	-17.04	-1.48
3	33851	120.672	-3.33	0.65

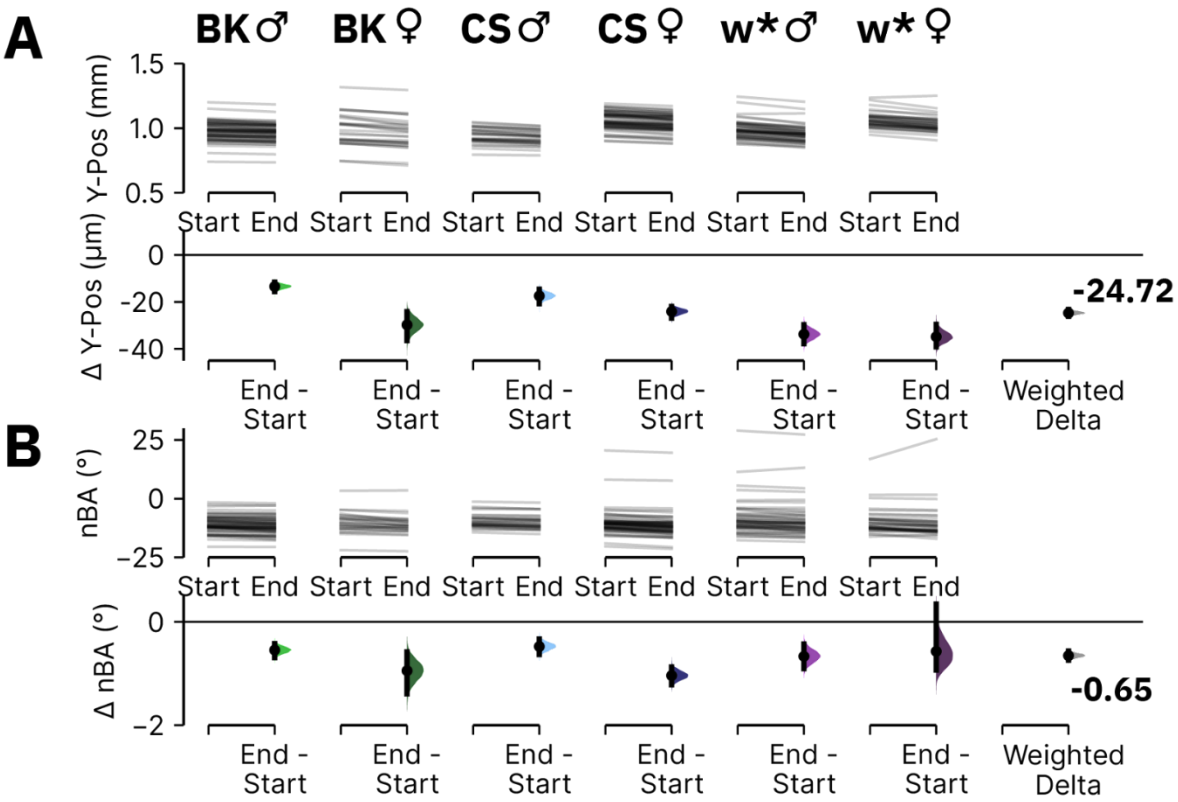

Appendix B Figure 10 Wild-type flies marginally lower and have a more angled body during ground-based SSL

DABEST plots comparing the mean Y-Pos **(A)** or nBA **(B)** from the final frame of ground-based SSL versus the first frame (end - start posture). Summary information and sample sizes are shown in Appendix B Table 9-10. See Chapter 2.6 for more information about the structure of DABEST plots.

Appendix B Table 9 End vs. start Y-Pos for ground-based SSL

The table is pertinent to Appendix B Figure 10. Each row is a DABEST comparison of the end vs. start Y-Pos for a given genotype. See Chapter 2.6 for more information about DABEST plots.

Genotype	Sex	Ctr	Test	Sample Size (n)	Ctr Mean±CI (mm)	Test Mean±CI (mm)	Delta (µm)	Delta-CI (µm)	Delta+CI (µm)	p-value
BK	M	Start	End	60	0.98±0.02	0.96±0.02	-13.44	-15.55	-11.60	0.0000
BK	F	Start	End	26	0.99±0.05	0.96±0.05	-29.77	-36.47	-24.13	0.0000
CS	M	Start	End	30	0.94±0.02	0.92±0.02	-17.44	-20.80	-14.60	0.0000
CS	F	Start	End	59	1.06±0.02	1.03±0.02	-24.09	-26.89	-21.89	0.0000
w*	M	Start	End	48	0.99±0.02	0.96±0.02	-33.76	-37.86	-29.68	0.0000
w*	F	Start	End	38	1.06±0.02	1.03±0.02	-34.83	-39.14	-29.54	0.0000
Weighted Delta	M/F	Start	End	261	NA	NA	-24.72	-26.16	-23.25	0.0000

Appendix B Table 10 End vs. start nBA for ground-based SSL

Data is pertinent to Appendix B Figure 10. Each row is a DABEST comparison of the end vs. start nBA for a given genotype. See Chapter 2.6 for more information about DABEST plots.

Genotype	Sex	Ctr	Test	Sample Size (n)	Ctr Mean±CI (°)	Test Mean±CI (°)	Delta (°)	Delta-CI (°)	Delta+CI (°)	p-value
BK	M	Start	End	60	-10.87±0.92	-11.41±0.96	-0.54	-0.69	-0.42	0.0000
BK	F	Start	End	26	-10.13±1.75	-11.07±1.71	-0.94	-1.39	-0.58	0.0000
CS	M	Start	End	30	-9.46±1.09	-9.94±1.12	-0.48	-0.63	-0.33	0.0000
CS	F	Start	End	59	-10.27±1.44	-11.31±1.47	-1.04	-1.21	-0.87	0.0000
w*	M	Start	End	48	-8.26±2.22	-8.92±2.24	-0.67	-0.91	-0.43	0.0000
w*	F	Start	End	38	-10.11±2.12	-10.68±2.46	-0.57	-0.93	0.35	0.0354
Weighted Delta	M/F	Start	End	261	NA	NA	-0.65	-0.74	-0.56	0.0000

Appendix B Table 11 Correlation of Δ Y-Pos and Δ nBA for SSL bouts

The coefficient of determination (Pearson's R^2) between change in Y-Pos and change in nBA for SSL bouts is shown as the Mean±CI calculated from individual flies for each genotype.

Genotype	Sex	Location	State	Sample Size (n)	R^2 Mean±CI
BK	M	Ground	SSL	60	0.10±0.03
BK	M	Ceiling	SSL	56	0.13±0.04
BK	F	Ground	SSL	26	0.24±0.08
BK	F	Ceiling	SSL	23	0.23±0.10
CS	M	Ground	SSL	30	0.12±0.05
CS	M	Ceiling	SSL	30	0.09±0.05
CS	F	Ground	SSL	59	0.15±0.04
CS	F	Ceiling	SSL	59	0.13±0.05
w*	M	Ground	SSL	47	0.16±0.04
w*	M	Ceiling	SSL	47	0.18±0.04
w*	F	Ground	SSL	38	0.17±0.04
w*	F	Ceiling	SSL	38	0.20±0.06

Appendix B Table 12 Correlation of start posture and Δ posture for SSL bouts

The coefficient of determination (Pearson's R^2) for start posture with change in posture is shown as the Mean±CI calculated from individual flies for each genotype.

Genotype	Sex	Location	State	Sample Size (n)	sY-Pos vs Δ Y-Pos R^2 Mean±CI	snBA vs Δ nBA R^2 Mean±CI
BK	M	Ground	SSL	60	0.24±0.04	0.09±0.03
BK	M	Ceiling	SSL	56	0.21±0.05	0.16±0.05
BK	F	Ground	SSL	26	0.24±0.08	0.19±0.07
BK	F	Ceiling	SSL	23	0.23±0.07	0.27±0.07
CS	M	Ground	SSL	30	0.23±0.04	0.14±0.05
CS	M	Ceiling	SSL	30	0.13±0.05	0.13±0.05
CS	F	Ground	SSL	59	0.16±0.04	0.07±0.02
CS	F	Ceiling	SSL	59	0.10±0.03	0.15±0.05

Genotype	Sex	Location	State	Sample Size (n)	sY-Pos vs Δ Y-Pos R^2 Mean±CI	snBA vs Δ nBA R^2 Mean±CI
w*	M	Ground	SSL	47	0.22±0.04	0.14±0.03
w*	M	Ceiling	SSL	47	0.09±0.03	0.10±0.03
w*	F	Ground	SSL	38	0.18±0.03	0.12±0.05
w*	F	Ceiling	SSL	38	0.11±0.03	0.14±0.04

Appendix B Table 13 Correlation of duration and Δ posture for SSL bouts

The coefficient of determination (Pearson's R^2) for the duration of SSL with the change in posture is shown as the Mean±CI calculated from individual flies for each genotype.

Genotype	Sex	Location	State	Sample Size (n)	Duration vs Δ Y-Pos R^2 Mean±CI	Duration vs Δ nBA R^2 Mean±CI
BK	M	Ground	SSL	60	0.01±0.00	0.01±0.00
BK	M	Ceiling	SSL	56	0.04±0.02	0.03±0.02
BK	F	Ground	SSL	26	0.05±0.05	0.03±0.02
BK	F	Ceiling	SSL	23	0.09±0.06	0.08±0.05
CS	M	Ground	SSL	30	0.02±0.01	0.01±0.01
CS	M	Ceiling	SSL	30	0.01±0.01	0.01±0.01
CS	F	Ground	SSL	59	0.04±0.02	0.02±0.01
CS	F	Ceiling	SSL	59	0.04±0.01	0.03±0.01
w*	M	Ground	SSL	47	0.02±0.01	0.02±0.01
w*	M	Ceiling	SSL	47	0.05±0.03	0.03±0.02
w*	F	Ground	SSL	38	0.03±0.01	0.02±0.01
w*	F	Ceiling	SSL	38	0.03±0.01	0.04±0.03

Appendix B Table 14 Correlation of duration and Δ posture for all rest bouts

The coefficient of determination (Pearson's R^2) for the duration of all rest bouts with the change in posture is shown as the Mean±CI calculated from individual flies for each genotype. The analysis is the same as for Appendix B Table 13 but for all durations of rest.

Genotype	Sex	Location	State	Sample Size (n)	Duration vs Δ Y-Pos R^2 Mean±CI	Duration vs Δ nBA R^2 Mean±CI
BK	M	Ground	SSB+SSL	60	0.00±0.00	0.00±0.00
BK	M	Ceiling	SSB+SSL	60	0.01±0.00	0.00±0.00
BK	F	Ground	SSB+SSL	30	0.03±0.01	0.01±0.00
BK	F	Ceiling	SSB+SSL	30	0.01±0.01	0.01±0.01
CS	M	Ground	SSB+SSL	30	0.01±0.00	0.00±0.00
CS	M	Ceiling	SSB+SSL	30	0.01±0.00	0.00±0.00
CS	F	Ground	SSB+SSL	59	0.02±0.01	0.01±0.00
CS	F	Ceiling	SSB+SSL	59	0.01±0.00	0.01±0.00
w*	M	Ground	SSB+SSL	48	0.03±0.01	0.01±0.00
w*	M	Ceiling	SSB+SSL	49	0.03±0.01	0.01±0.00
w*	F	Ground	SSB+SSL	38	0.03±0.01	0.01±0.00
w*	F	Ceiling	SSB+SSL	38	0.02±0.01	0.01±0.01

Appendix B Table 15 Correlation of duration and Δ posture for SSB bouts

The coefficient of (Pearson's R^2) for the duration of SSB bouts with the change in posture is shown as the Mean±CI calculated from individual flies for each genotype. The analysis is the same as for Appendix B Table 13 but for only short rest.

Genotype	Sex	Location	State	Sample Size (n)	Duration vs Δ Y-Pos R^2 Mean±CI	Duration vs Δ nBA R^2 Mean±CI
BK	M	Ground	SSB	60	0.01±0.00	0.00±0.00
BK	M	Ceiling	SSB	60	0.01±0.01	0.00±0.00
BK	F	Ground	SSB	30	0.06±0.02	0.02±0.01
BK	F	Ceiling	SSB	30	0.02±0.01	0.02±0.01
CS	M	Ground	SSB	30	0.01±0.00	0.00±0.00
CS	M	Ceiling	SSB	30	0.01±0.00	0.00±0.00
CS	F	Ground	SSB	59	0.02±0.01	0.01±0.00

Genotype	Sex	Location	State	Sample Size (n)	Duration vs Δ Y-Pos R^2 Mean±CI	Duration vs Δ nBA R^2 Mean±CI
CS	F	Ceiling	SSB	59	0.01±0.00	0.01±0.00
w*	M	Ground	SSB	48	0.03±0.01	0.01±0.00
w*	M	Ceiling	SSB	49	0.02±0.01	0.00±0.00
w*	F	Ground	SSB	38	0.04±0.01	0.01±0.01
w*	F	Ceiling	SSB	38	0.01±0.00	0.01±0.01

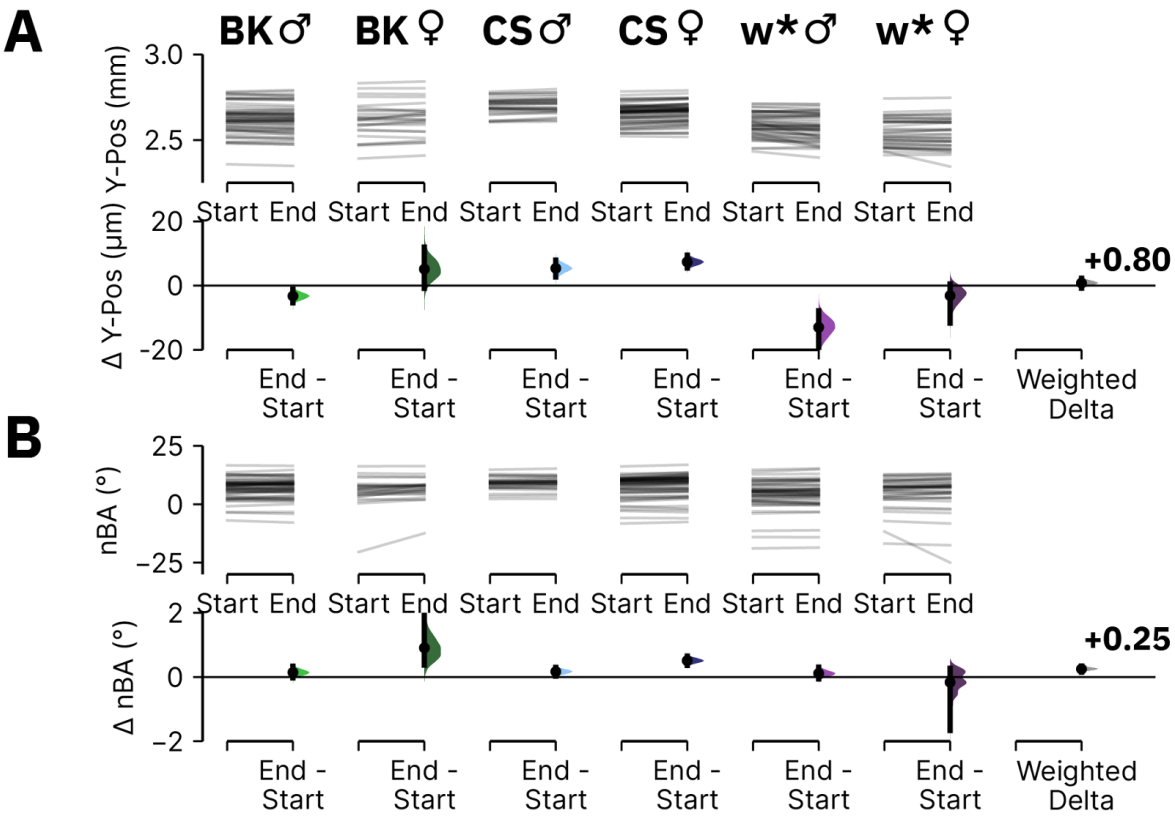

Appendix B Figure 11 End vs. start posture for ceiling-based SSL

DABEST plots comparing the mean Y-Pos **(A)** or nBA **(B)** from the final frame of ceiling-based SSL vs. the first frame (end - start posture). Summary information and sample sizes are shown in Appendix B Table 16-17. See Chapter 2.6 for more information about the structure of DABEST plots.

Appendix B Table 16 End vs. start Y-Pos for ceiling-based SSL

The table is pertinent to Appendix B Figure 11A. Each row is a DABEST comparison of the end vs. start Y-Pos for a given genotype. See Chapter 2.6 for more information about DABEST plots.

Genotype	Sex	Ctr	Test	Sample Size (n)	Ctr Mean±CI (mm)	Test Mean±CI (mm)	Delta (µm)	Delta-CI (µm)	Delta+CI (µm)	p-value
BK	M	Start	End	56	2.62±0.02	2.62±0.02	-3.25	-5.36	-1.18	0.0048
BK	F	Start	End	25	2.62±0.04	2.63±0.04	5.13	-0.83	11.99	0.1284
CS	M	Start	End	30	2.70±0.02	2.70±0.02	5.38	2.67	7.93	0.0000
CS	F	Start	End	59	2.65±0.02	2.66±0.02	7.38	5.46	9.48	0.0000
w*	M	Start	End	49	2.59±0.02	2.58±0.02	-13.00	-20.12	-7.83	0.0000
w*	F	Start	End	38	2.54±0.03	2.54±0.03	-3.13	-11.69	0.51	0.2980
Weighted Delta	M/F	Start	End	257	NA	NA	0.80	-0.80	2.27	0.3888

Appendix B Table 17 End vs. start nBA for ceiling-based SSL

Data is pertinent to Appendix B Figure 11B. Each row is a DABEST comparison of the end vs. start nBA for a given genotype. See Chapter 2.6 for more information about DABEST plots.

Genotype	Sex	Ctr	Test	Sample Size (n)	Ctr Mean±CI (°)	Test Mean±CI (°)	Delta (°)	Delta-CI (°)	Delta+CI (°)	p-value
BK	M	Start	End	56	6.77±1.16	6.91±1.19	0.14	-0.03	0.34	0.1300
BK	F	Start	End	25	5.61±2.58	6.51±2.02	0.91	0.37	2.00	0.0066
CS	M	Start	End	30	8.90±0.96	9.07±0.97	0.17	0.03	0.30	0.0294
CS	F	Start	End	59	7.38±1.23	7.89±1.29	0.51	0.36	0.65	0.0000
w*	M	Start	End	49	4.20±1.79	4.31±1.83	0.11	-0.06	0.31	0.2184
w*	F	Start	End	38	5.04±2.04	4.88±2.50	-0.16	-1.67	0.27	0.9458
Weighted Delta	M/F	Start	End	257	NA	NA	0.25	0.15	0.34	0.0000

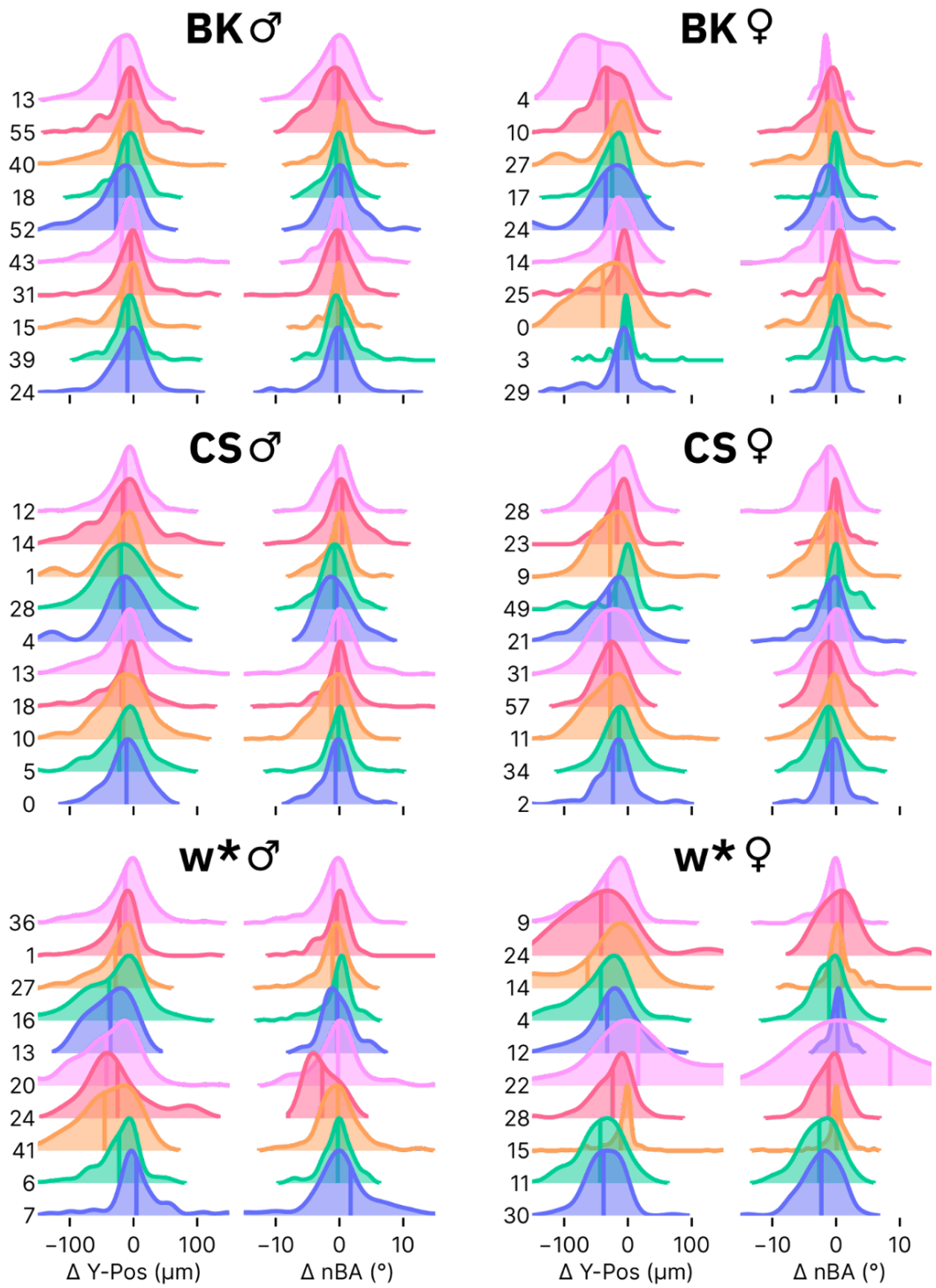

Appendix B Figure 12 Change in posture for ground-based SSL of randomly selected individual flies

Ridgeline plots for the distribution of posture change (End - Start) of ground-based long rest bouts for ten randomly selected flies from each genotype. The y-axis number is a label of the fly that the ridgeline is associated with.

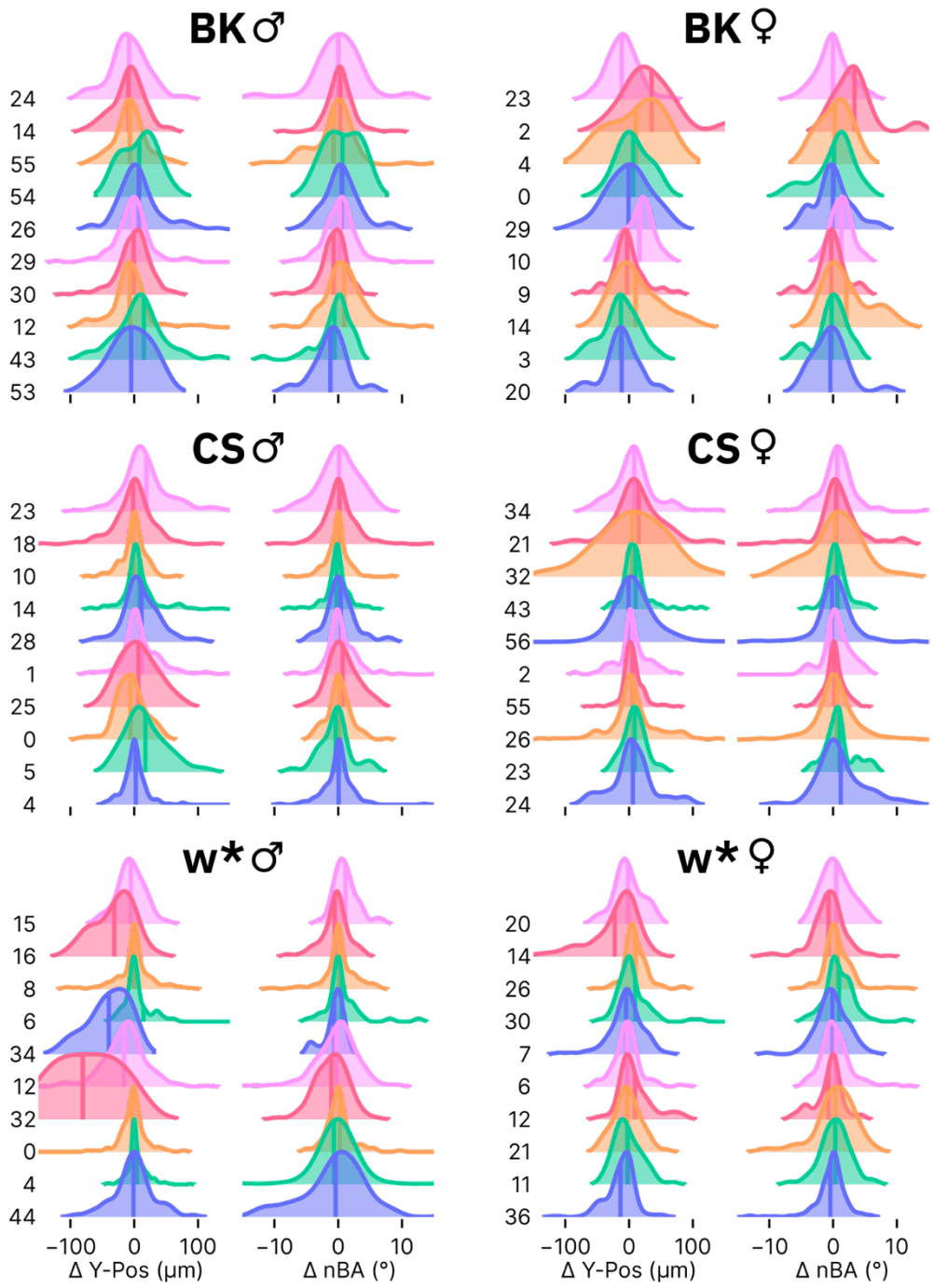

Appendix B Figure 13 Change in posture for ceiling-based SSL of randomly selected individual flies

Ridgeline plots for the distribution of posture change (End - Start) of ceiling-based long rest bouts for ten randomly selected flies from each genotype. The y-axis number is a label of the fly that the ridgeline is associated with.

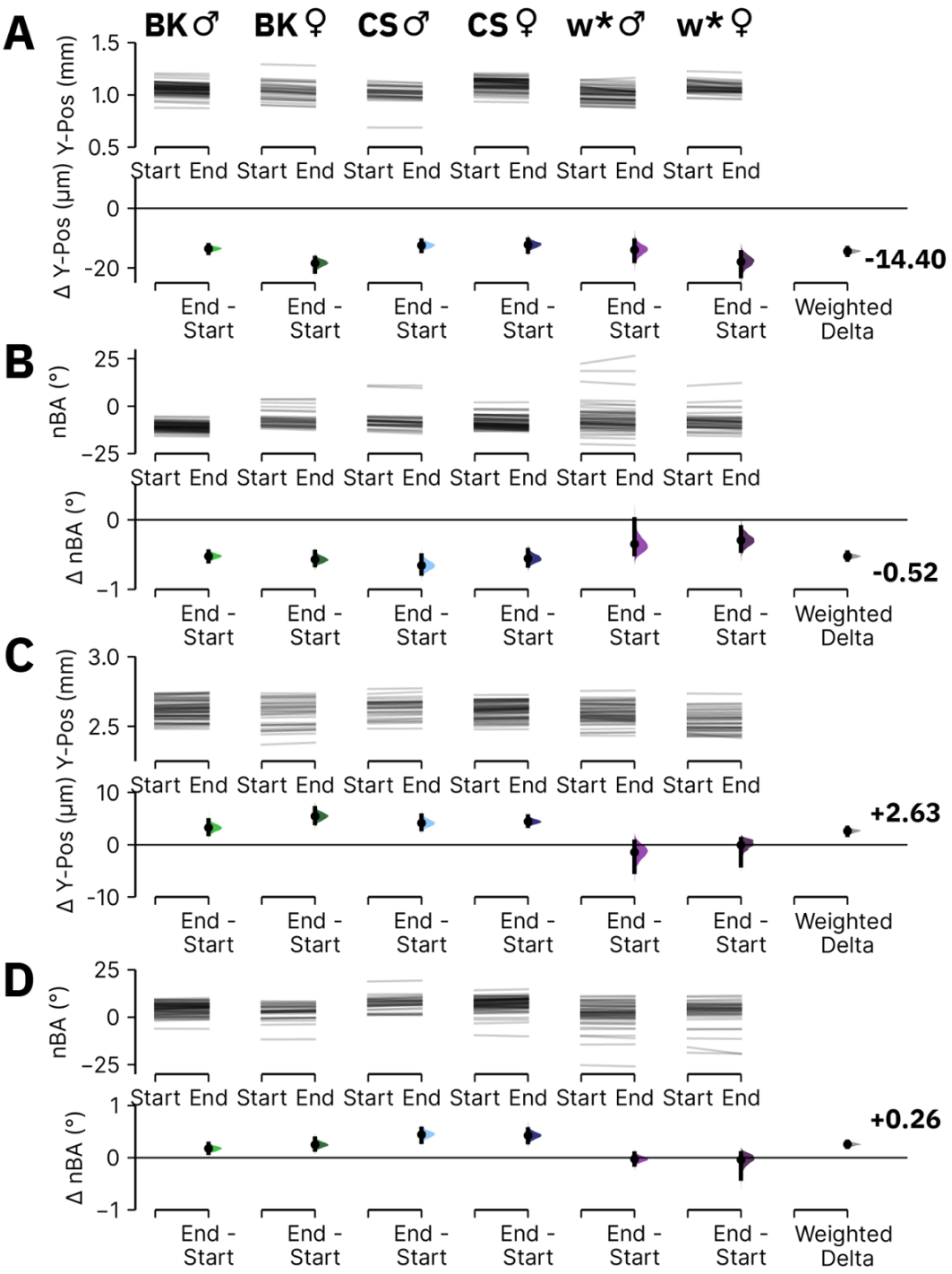

Appendix B Figure 14 End vs. start posture for SSB

(A-B) DABEST plots comparing the mean Y-Pos **(A)** or nBA **(B)** from the final frame of ground based SSB versus the first frame (end - start posture). **(C-D)** The same as (A-B) but for ceiling based SSB. Summary information and sample sizes are shown in Appendix B Table 18-21. See Chapter 2.6 for more information about the structure of DABEST plots.

Appendix B Table 18 End vs. start Y-Pos for ground-based SSB

The table is pertinent to Appendix B Figure 14A. Each row is a DABEST comparison of the end vs. start Y-Pos for a given genotype. See Chapter 2.6 for more information about DABEST plots.

Genotype	Sex	Ctr / Test	Sample Size (n)	Ctr Mean±CI (mm)	Test Mean±CI (mm)	Delta (µm)	Delta-CI (µm)	Delta+CI (µm)	p-value
BK	M	Start / End	60	1.06±0.01	1.05±0.01	-13.53	-14.95	-12.32	0.0000
BK	F	Start / End	30	1.05±0.03	1.03±0.03	-18.41	-21.22	-16.61	0.0000
CS	M	Start / End	30	1.02±0.03	1.01±0.03	-12.45	-14.34	-10.78	0.0000
CS	F	Start / End	59	1.10±0.02	1.09±0.02	-12.21	-14.53	-10.48	0.0000
w*	M	Start / End	49	1.01±0.02	1.00±0.02	-13.92	-17.66	-10.76	0.0000
w*	F	Start / End	38	1.08±0.02	1.06±0.02	-17.91	-22.75	-14.75	0.0000
Weighted Delta	M/F	Start / End	266	NA	NA	-14.40	-15.59	-13.33	0.0000

Appendix B Table 19 End vs. start nBA for ground-based SSB

The table is pertinent to Appendix B Figure 14B. Each row is a DABEST comparison of the end vs. start nBA for a given genotype. See Chapter 2.6 for more information about DABEST plots.

Genotype	Sex	Ctr / Test	Sample Size (n)	Ctr Mean±CI (°)	Test Mean±CI (°)	Delta (°)	Delta-CI (°)	Delta+CI (°)	p-value
BK	M	Start / End	60	-10.52±0.55	-11.04±0.57	-0.52	-0.60	-0.46	0.0000
BK	F	Start / End	30	-6.64±1.53	-7.21±1.58	-0.57	-0.65	-0.46	0.0000
CS	M	Start / End	30	-7.35±1.92	-8.00±1.95	-0.66	-0.77	-0.51	0.0000
CS	F	Start / End	59	-8.33±0.81	-8.89±0.84	-0.56	-0.66	-0.43	0.0000
w*	M	Start / End	49	-6.27±2.18	-6.62±2.27	-0.35	-0.50	0.01	0.0014
w*	F	Start / End	38	-8.30±1.82	-8.59±1.90	-0.29	-0.45	-0.11	0.0024
Weighted Delta	M/F	Start / End	266	NA	NA	-0.52	-0.57	-0.47	0.0000

Appendix B Table 20 End vs. start Y-Pos for ceiling-based SSB

The table is pertinent to Appendix B Figure 14C. Each row is a DABEST comparison of the end vs. start Y-Pos for a given genotype. See Chapter 2.6 for more information about DABEST plots.

Genotype	Sex	Ctr / Test	Sample Size (n)	Ctr Mean±CI (mm)	Test Mean±CI (mm)	Delta (µm)	Delta-CI (µm)	Delta+CI (µm)	p-value
BK	M	Start / End	60	2.61±0.02	2.62±0.02	3.25	2.04	4.69	0.0000
BK	F	Start / End	30	2.59±0.03	2.60±0.03	5.46	4.13	6.99	0.0000
CS	M	Start / End	30	2.63±0.02	2.63±0.02	4.15	2.98	5.57	0.0000
CS	F	Start / End	59	2.61±0.01	2.62±0.02	4.43	3.62	5.42	0.0000
w*	M	Start / End	49	2.60±0.02	2.59±0.02	-1.44	-5.21	0.56	0.3166
w*	F	Start / End	38	2.54±0.02	2.54±0.02	-0.06	-3.96	1.07	0.9950
Weighted Delta	M/F	Start / End	266	NA	NA	2.63	1.88	3.22	0.0000

Appendix B Table 21 End vs. start nBA for ceiling-based SSB

The table is pertinent to Appendix B Figure 14D. Each row is a DABEST comparison of the end vs. start nBA for a given genotype. See Chapter 2.6 for more information about DABEST plots.

Genotype	Sex	Ctr / Test	Sample Size (n)	Ctr Mean±CI (°)	Test Mean±CI (°)	Delta (°)	Delta-CI (°)	Delta+CI (°)	p-value
BK	M	Start / End	60	4.33±0.82	4.51±0.81	0.18	0.09	0.27	0.0002
BK	F	Start / End	30	2.82±1.47	3.07±1.46	0.25	0.15	0.37	0.0000
CS	M	Start / End	30	7.05±1.33	7.49±1.36	0.44	0.30	0.55	0.0000
CS	F	Start / End	59	6.56±0.98	6.98±1.02	0.43	0.30	0.54	0.0000
w*	M	Start / End	49	1.60±1.84	1.58±1.89	-0.03	-0.13	0.08	0.6456
w*	F	Start / End	38	2.60±2.06	2.56±2.18	-0.04	-0.40	0.09	0.8896
Weighted Delta	M/F	Start / End	266	NA	NA	0.26	0.21	0.31	0.0000

Appendix B Table 22 Change in posture outline examples

The table is pertinent to Figure 4.1.2E-F. Each row is the postural and duration data for a given example bout of ground- or ceiling-based SSL.

				Y-Pos (mm)			nBA (°)		
Example	**Fly**	**Bout**	**Duration (s)**	**Start**	**End**	**Δ (µm)**	**Start**	**End**	**Δ (°)**
1	2	42422	449.37	1.28	1.15	-138.72	-8.21	-8.19	0.03
2	2	2991	82.25	1.32	1.29	-33.68	-6.80	-8.49	-1.68
3	4	4910	261.06	1.22	1.18	-36.54	-16.09	-19.10	-3.01
4	5	4605	195.72	1.27	1.20	-73.14	-9.38	-10.20	-0.83
5	2	34575	78.35	2.72	2.71	-10.45	-0.49	-0.01	0.48
6	2	3232	90.75	2.76	2.75	-10.86	0.52	0.59	0.07
7	4	16957	387.33	2.68	2.69	6.90	2.71	1.15	-1.56
8	5	1997	61.94	2.64	2.63	-10.72	3.26	3.30	0.04

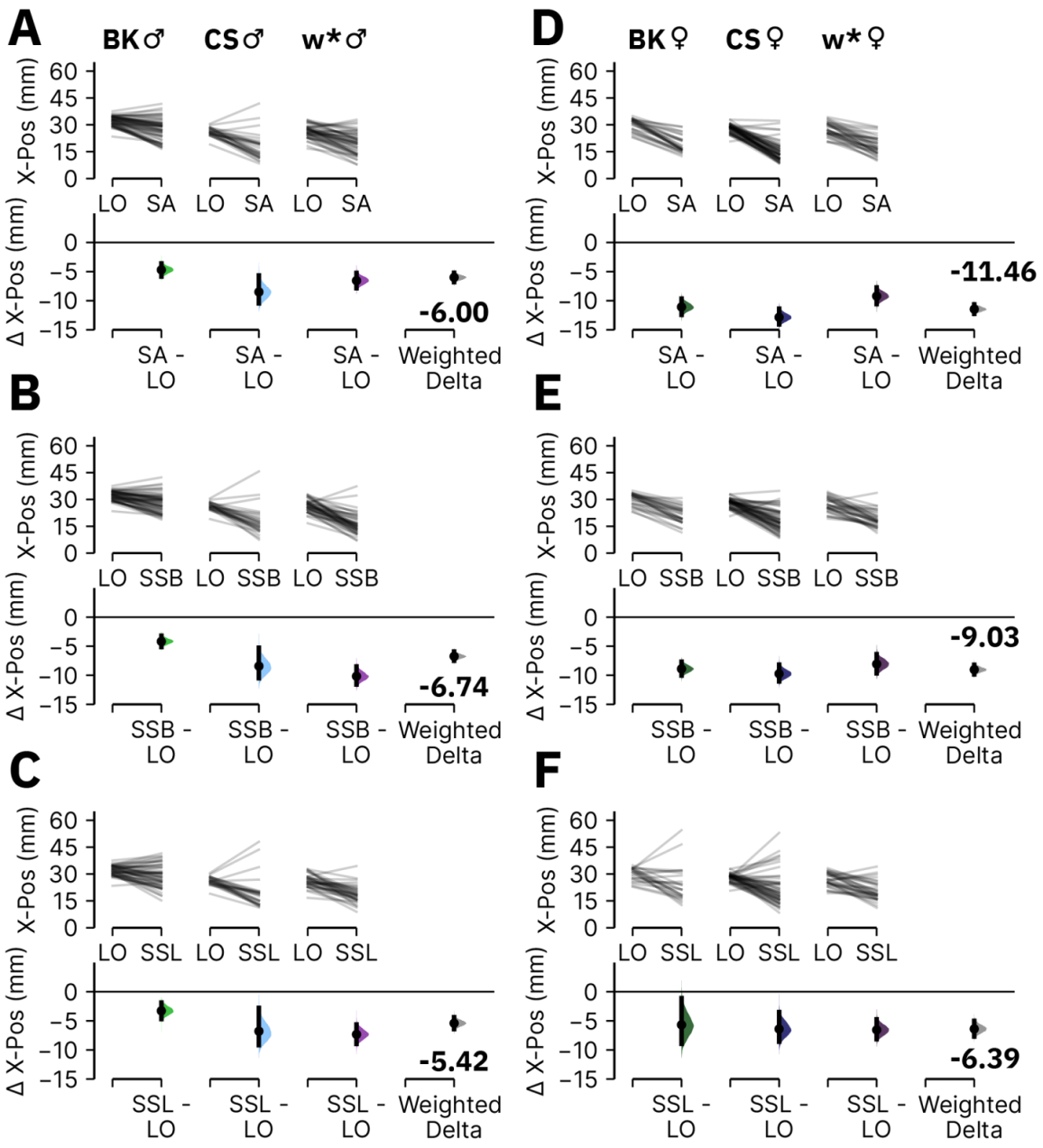

Appendix B Figure 15 Flies prefer to be nearer the food during stationary behaviour than during LO

(A-C) DABEST plots of the mean X-Pos (mm) during SA **(A)**, SSB **(B)**, or SSL **(C)** vs. LO for wild-type male flies. **(D-F)** the same as (A-C) but for wild-type female flies. The summary data, including sample sizes, are shown in Appendix B Table 23. See Chapter 2.6 for more information about the structure of DABEST plots.

Appendix B Table 23 Flies prefer to be nearer the food during stationary behaviour than during LO

The table is pertinent to Appendix B Figure 15. Each row is a DABEST comparison of the mean X-Pos of flies during a given stationary behaviour compared to during LO in a given genotype. See Chapter 2.6 for more information about DABEST plots.

Genotype	Sex	Ctr / Test	Sample Size (n)	Ctr Mean±CI (mm)	Test Mean±CI (mm)	Delta (mm)	Delta-CI (mm)	Delta+CI (mm)	p-value
BK	M	LO / SA	58	32.14±0.66	27.44±1.57	-4.70	-5.84	-3.59	0.0000
CS	M	LO / SA	29	26.18±0.83	17.68±2.72	-8.49	-10.47	-5.66	0.0000
w*	M	LO / SA	49	26.30±0.99	19.74±1.72	-6.55	-7.84	-5.24	0.0000
Weighted Delta	M	LO / SA	136	NA	NA	-6.00	-6.82	-5.19	0.0000
BK	M	LO / SSB	58	32.08±0.66	27.90±1.36	-4.18	-5.14	-3.19	0.0000
CS	M	LO / SSB	29	26.29±0.81	17.87±2.82	-8.42	-10.51	-5.25	0.0000
w*	M	LO / SSB	47	26.50±0.98	16.33±1.65	-10.16	-11.58	-8.47	0.0000
Weighted Delta	M	LO / SSB	134	NA	NA	-6.74	-7.49	-5.90	0.0000
BK	M	LO / SSL	51	32.02±0.72	28.74±1.74	-3.28	-4.70	-1.87	0.0000
CS	M	LO / SSL	27	26.28±0.87	19.49±3.42	-6.79	-9.19	-2.78	0.0002
w*	M	LO / SSL	37	26.18±1.16	18.85±1.59	-7.33	-8.98	-5.64	0.0000
Weighted Delta	M	LO / SSL	115	NA	NA	-5.42	-6.44	-4.38	0.0000
BK	F	LO / SA	29	30.22±1.25	19.14±1.70	-11.08	-12.43	-9.65	0.0002
CS	F	LO / SA	58	27.89±0.60	15.04±1.39	-12.85	-14.07	-11.37	0.0000
w*	F	LO / SA	35	27.46±1.26	18.24±1.65	-9.21	-10.58	-7.72	0.0000
Weighted Delta	F	LO / SA	122	NA	NA	-11.46	-12.27	-10.64	0.0000
BK	F	LO / SSB	30	30.18±1.21	21.29±1.68	-8.90	-10.05	-7.67	0.0000
CS	F	LO / SSB	57	27.99±0.62	18.26±1.54	-9.73	-11.05	-8.17	0.0000
w*	F	LO / SSB	34	27.14±1.37	19.07±1.55	-8.07	-9.66	-6.37	0.0000
Weighted Delta	F	LO / SSB	121	NA	NA	-9.03	-9.85	-8.19	0.0000
BK	F	LO / SSL	24	30.04±1.44	24.35±4.01	-5.68	-8.96	-1.09	0.0122
CS	F	LO / SSL	51	28.02±0.61	21.61±2.55	-6.41	-8.58	-3.49	0.0004
w*	F	LO / SSL	34	26.95±1.29	20.38±1.80	-6.56	-8.17	-4.75	0.0000
Weighted Delta	F	LO / SSL	109	NA	NA	-6.39	-7.69	-5.01	0.0000

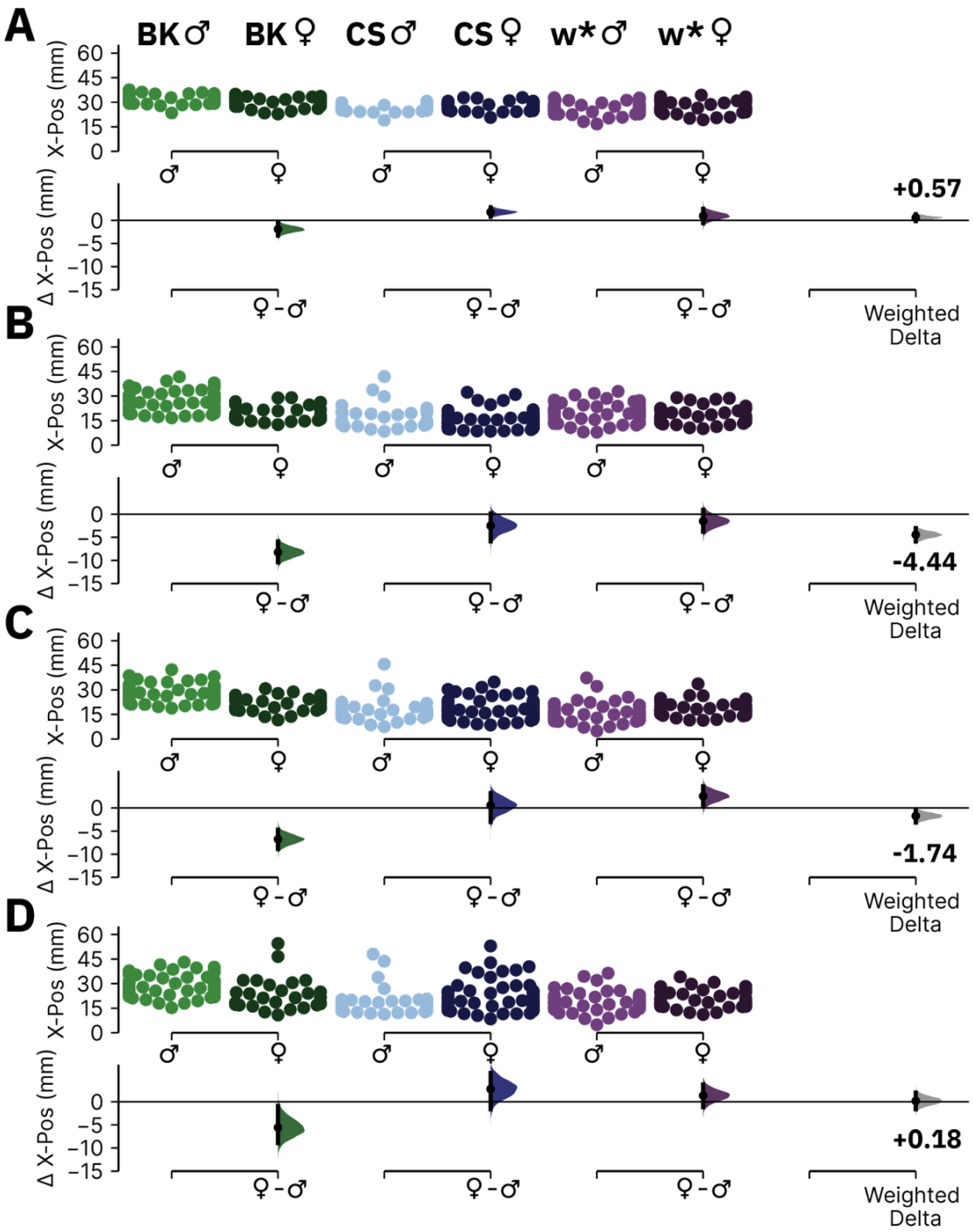

Appendix B Figure 16 Comparing the mean X-Pos of Trumelan behaviours in females vs. males

DABEST plots of the mean X-Pos (mm) during LO **(A)**, SA **(B)**, SSB **(C)**, or SSL **(D)** in wild-type females vs. males. The summary data, including sample sizes, are shown in Appendix B Table 24. See Chapter 2.6 for more information about the structure of DABEST plots.

Appendix B Table 24 Comparing the mean X-Pos of Trumelan behaviours in females vs. males

The table is pertinent to Appendix B Figure 16. Comparing the mean X-Pos of flies during each behaviour in females vs. males. See Chapter 2.6 for more information about DABEST plots.

Genotype	State	Ctr / Test	Ctr (n)	Test (n)	Ctr Mean±CI (mm)	Test Mean±CI (mm)	Delta (mm)	Delta-CI (mm)	Delta+CI (mm)	p-value
BK	LO	M / F	60	30	32.09±0.64	30.18±1.21	-1.91	-3.29	-0.61	0.0036
CS	LO	M / F	30	59	26.21±0.80	27.97±0.61	1.76	0.79	2.79	0.0008
w*	LO	M / F	49	38	26.30±0.99	27.25±1.26	0.95	-0.62	2.47	0.2368
Weighted Delta	LO	M / F	139	127	NA	NA	0.57	-0.13	1.30	0.1338
BK	SA	M / F	60	30	27.25±1.55	19.00±1.67	-8.25	-10.40	-5.91	0.0000
CS	SA	M / F	30	59	17.57±2.64	15.07±1.36	-2.49	-5.86	0.13	0.0642
w*	SA	M / F	49	38	19.74±1.72	18.23±1.64	-1.52	-3.81	0.92	0.2224
Weighted Delta	SA	M / F	139	127	NA	NA	-4.44	-5.88	-3.01	0.0000
BK	SSB	M / F	60	30	28.05±1.33	21.29±1.68	-6.76	-8.87	-4.72	0.0000
CS	SSB	M / F	30	59	17.93±2.72	18.48±1.55	0.55	-3.03	3.21	0.7010
w*	SSB	M / F	49	38	16.18±1.66	18.71±1.49	2.54	0.32	4.69	0.0340
Weighted Delta	SSB	M / F	139	127	NA	NA	-1.74	-3.13	-0.43	0.0212
BK	SSL	M / F	60	28	28.98±1.66	23.40±3.61	-5.58	-8.92	-0.90	0.0024
CS	SSL	M / F	30	59	19.03±3.12	21.78±2.33	2.75	-1.63	6.20	0.1776
w*	SSL	M / F	49	38	19.05±1.72	20.38±1.73	1.34	-1.19	3.72	0.3022
Weighted Delta	SSL	M / F	139	125	NA	NA	0.18	-1.64	1.97	0.8544

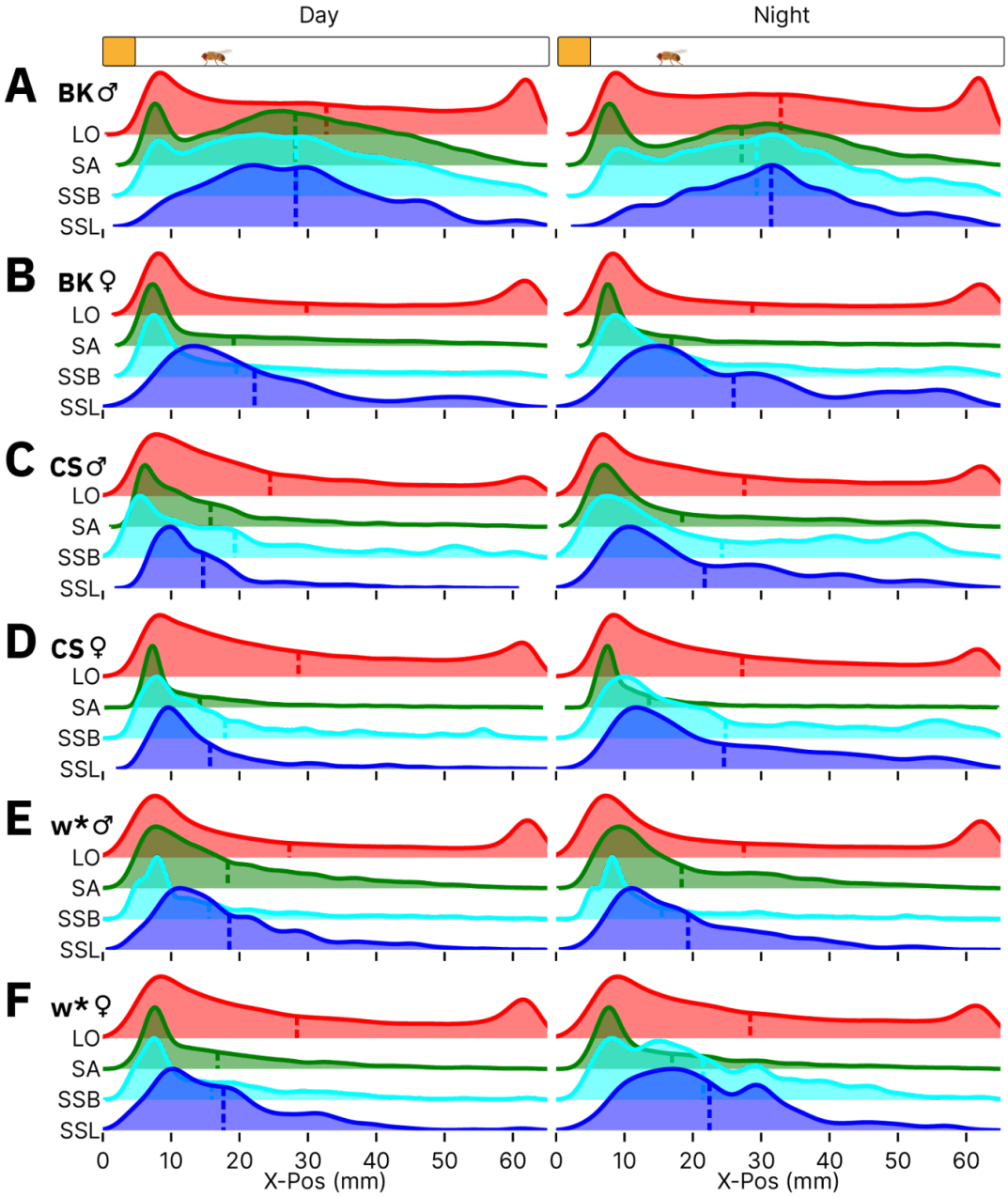

Appendix B Figure 17 Flies have no major differences in X-Pos place preference between day and night

The X-Pos distribution of bouts during the day (left plots) and during the night (right plots) for each of the four recorded behaviours in BK males (n=60) **(A)**, BK females (n=30) **(B)**, CS males (n=30) **(C)**, CS females (n=59) **(D)**, w* males (n=49) **(E)**, and w* females (n=38) **(F)**. The dotted lines on each ridgeline curve indicates the mean of that distribution. Cartoons above (A) illustrate the location relative to the fly chamber. There are no major differences in X-Pos place preference seen when separating data into day and night.

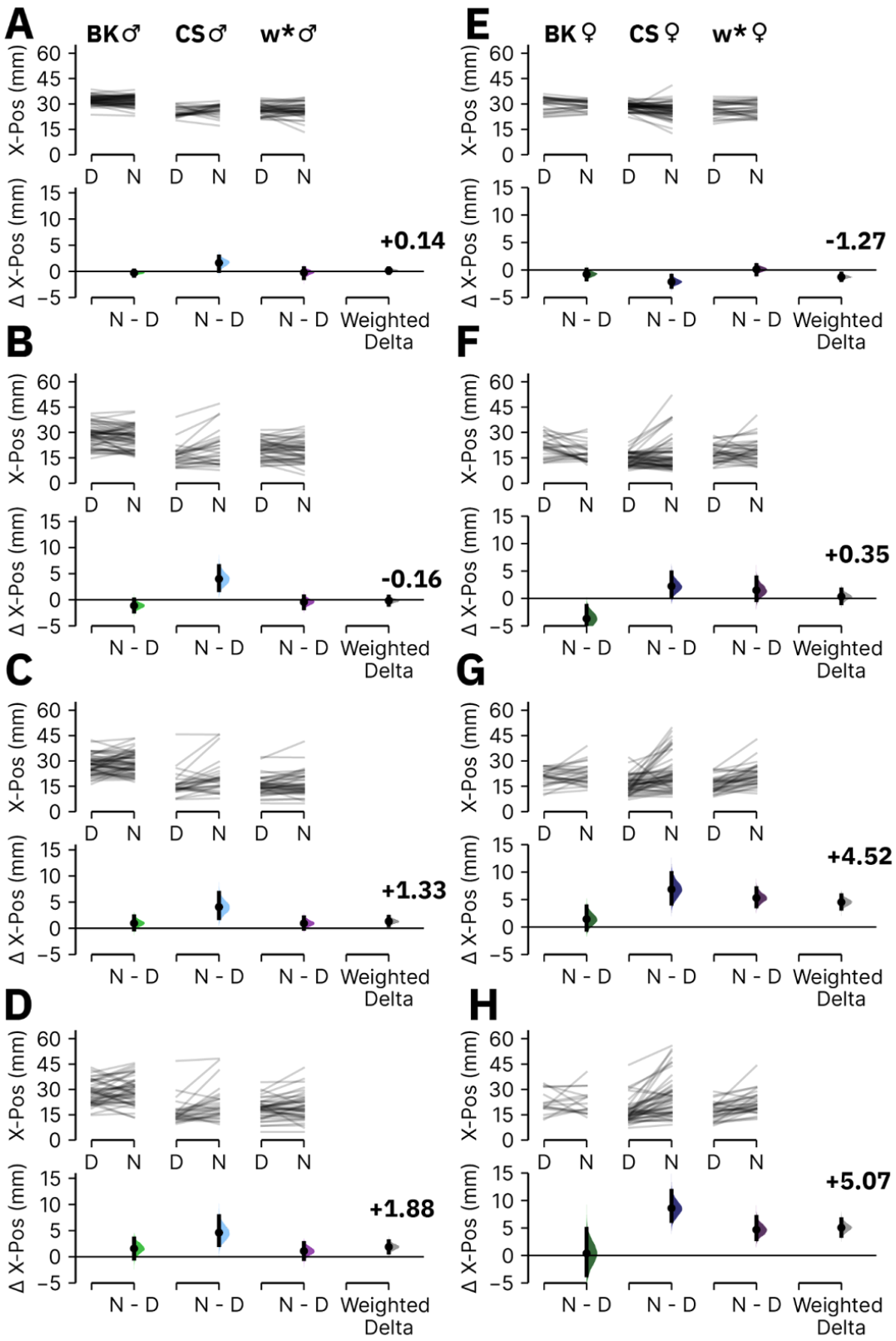

Appendix B Figure 18 There are only minor differences in mean X-Pos during night vs. day

(A-D) DABEST plots of the mean X-Pos (mm) during LO **(A)** SA **(B)**, SSB **(C)**, or SSL **(D)** during the night vs. day in wild-type male flies **(E-H)** The same as (A-D) but for wild-type females. The summary data, including sample sizes, are shown in Appendix B Table 25. See Chapter 2.6 for more information about the structure of DABEST plots.

Appendix B Table 25 There are only minor differences in mean X-Pos during night vs. day

The table is pertinent to Appendix B Figure 18. Comparing the mean X-Pos of flies during each behaviour during the night vs. the day. Each row is a DABEST comparison of the mean X-Pos of a given behavioural during the night vs. the day for a given genotype. See Chapter 2.6 for more information about DABEST plots.

Genotype	Sex	State	Ctr / Test	Sample Size (n)	Ctr Mean±CI (mm)	Test Mean±CI (mm)	Delta (mm)	Delta-CI (mm)	Delta+CI (mm)	p-value
BK	M	LO	Day / Night	59	32.20±0.63	31.90±0.77	-0.31	-0.84	0.16	0.2224
CS	M	LO	Day / Night	29	25.05±1.00	26.67±1.20	1.62	0.07	2.82	0.0260
w*	M	LO	Day / Night	45	26.69±0.94	26.46±1.20	-0.22	-1.30	0.59	0.6494
Weighted Delta	M	LO	Day / Night	133	NA	NA	0.14	-0.33	0.57	0.5642
BK	M	SA	Day / Night	58	27.92±1.59	26.80±1.74	-1.12	-2.22	0.04	0.0582
CS	M	SA	Day / Night	28	16.31±2.33	20.30±3.72	4.00	1.85	6.43	0.0016
w*	M	SA	Day / Night	46	19.85±1.60	19.43±1.89	-0.42	-1.62	0.66	0.4830
Weighted Delta	M	SA	Day / Night	132	NA	NA	-0.16	-0.94	0.60	0.6848
BK	M	SSB	Day / Night	59	27.63±1.39	28.60±1.58	0.97	-0.21	2.27	0.1198
CS	M	SSB	Day / Night	29	16.13±2.65	20.20±3.57	4.07	1.94	6.79	0.0024
w*	M	SSB	Day / Night	44	15.43±1.59	16.38±2.03	0.95	-0.11	2.12	0.1054
Weighted Delta	M	SSB	Day / Night	132	NA	NA	1.33	0.56	2.19	0.0024
BK	M	SSL	Day / Night	48	27.87±1.94	29.45±2.27	1.58	-0.36	3.49	0.1168
CS	M	SSL	Day / Night	28	16.64±2.73	21.26±3.73	4.62	2.25	7.77	0.0012
w*	M	SSL	Day / Night	43	18.64±1.75	19.74±2.32	1.10	-0.45	2.63	0.1830
Weighted Delta	M	SSL	Day / Night	119	NA	NA	1.88	0.81	2.98	0.0004
BK	F	LO	Day / Night	29	30.11±1.46	29.34±1.01	-0.77	-1.70	0.06	0.0978

Genotype	Sex	State	Ctr / Test	Sample Size (n)	Ctr Mean±CI (mm)	Test Mean±CI (mm)	Delta (mm)	Delta-CI (mm)	Delta+CI (mm)	p-value
CS	F	LO	Day / Night	58	28.47±0.61	26.33±1.17	-2.14	-3.06	-1.04	0.0002
w*	F	LO	Day / Night	33	27.11±1.41	27.24±1.45	0.13	-0.79	0.91	0.7808
Weighted Delta	F	LO	Day / Night	120	NA	NA	-1.27	-1.84	-0.66	0.0002
BK	F	SA	Day / Night	28	21.66±2.28	17.99±2.02	-3.67	-6.09	-1.35	0.0070
CS	F	SA	Day / Night	57	14.28±0.96	16.53±2.42	2.25	0.49	4.74	0.0372
w*	F	SA	Day / Night	36	17.53±1.62	19.03±2.18	1.50	-0.28	3.82	0.1636
Weighted Delta	F	SA	Day / Night	121	NA	NA	0.35	-0.86	1.64	0.6118
BK	F	SSB	Day / Night	28	20.45±1.78	21.87±2.24	1.42	-0.48	3.76	0.2018
CS	F	SSB	Day / Night	55	15.86±1.33	22.71±2.73	6.85	4.28	9.82	0.0000
w*	F	SSB	Day / Night	37	16.16±1.43	21.45±2.00	5.29	3.78	7.05	0.0000
Weighted Delta	F	SSB	Day / Night	120	NA	NA	4.52	3.35	5.76	0.0000
BK	F	SSL	Day / Night	16	22.33±3.38	22.70±3.67	0.38	-3.60	4.86	0.8724
CS	F	SSL	Day / Night	49	16.89±1.91	25.50±3.37	8.61	6.29	11.76	0.0000
w*	F	SSL	Day / Night	33	17.28±1.70	21.97±2.18	4.69	2.98	7.01	0.0000
Weighted Delta	F	SSL	Day / Night	98	NA	NA	5.07	3.60	6.61	0.0000

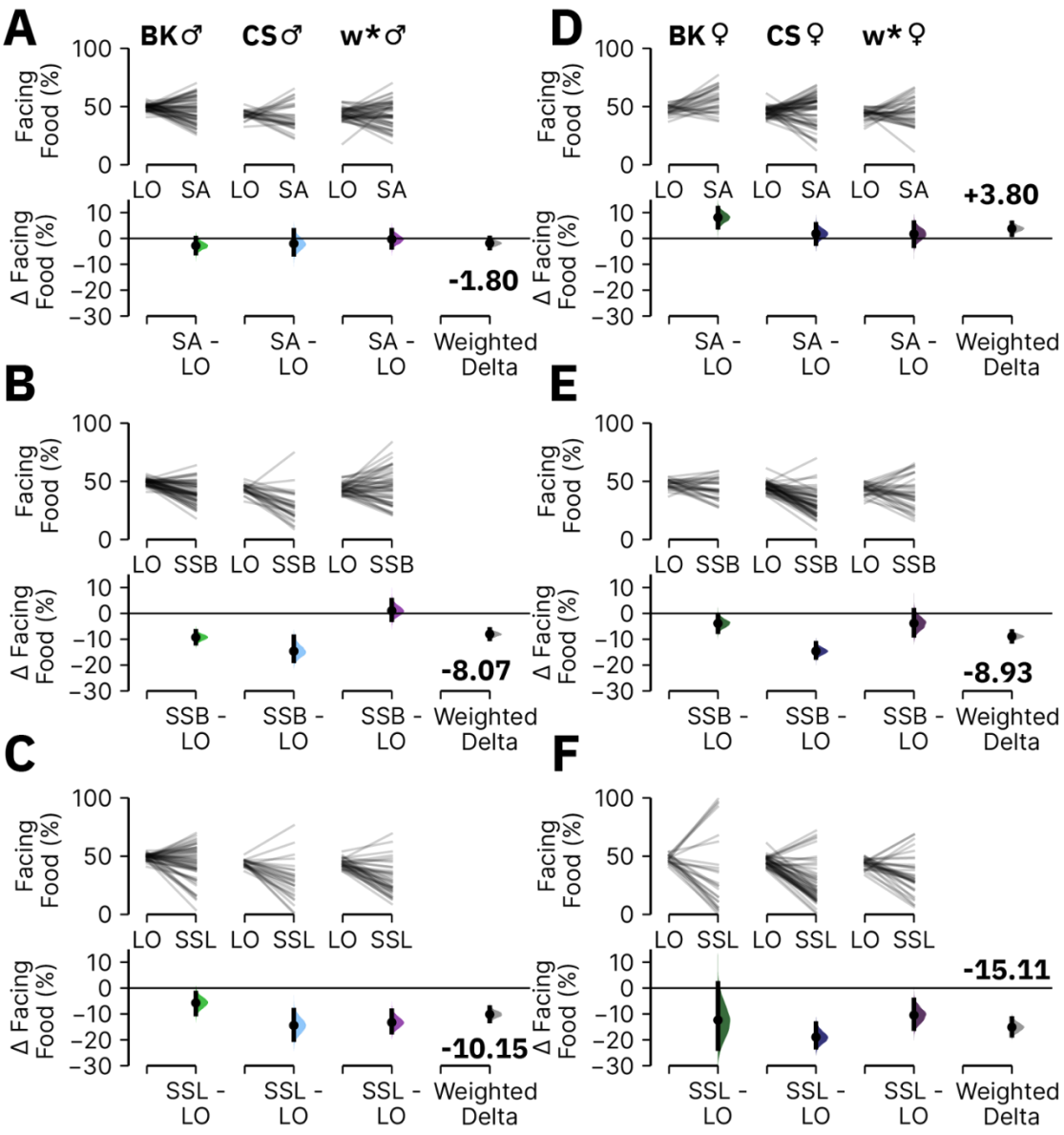

Appendix B Figure 19 Time spent facing the food port during stationary behaviours vs. LO

(A-C) DABEST plots of the percentage time spent facing the food port during SA **(A)** or SSB **(B)** or SSL **(C)** versus LO for wild-type male flies. **(D-F)** The same as for (A-C) but for wild-type female flies. The summary data, including sample sizes, are shown in Appendix B Table 26. See Chapter 2.6 for more information about the structure of DABEST plots.

Appendix B Table 26 Time spent facing the food port during stationary behaviours vs. LO

The table is pertinent to Figure 4.3.2A and Appendix B Figure 19. Each row is a DABEST comparison of the mean time spent facing the food during a given stationary behaviour vs. during LO for a given genotype. See Chapter 2.6 for more information about DABEST plots.

Genotype	Sex	Ctr / Test	Sample Size (n)	Ctr Mean±CI (%)	Test Mean±CI (%)	Delta (%)	Delta-CI (%)	Delta+CI (%)	p-value
BK	M	LO / SA	58	49.31±0.69	46.53±2.90	-2.78	-5.68	0.20	0.0784
CS	M	LO / SA	29	43.16±1.34	41.18±4.18	-1.98	-6.11	3.15	0.4122
w*	M	LO / SA	49	43.33±1.59	43.03±3.17	-0.30	-3.47	3.17	0.8718
Weighted Delta	M	LO / SA	136	NA	NA	-1.80	-3.71	0.20	0.0928
BK	M	LO / SSB	58	49.26±0.69	39.97±2.41	-9.29	-11.61	-6.94	0.0000
CS	M	LO / SSB	29	43.44±1.39	28.80±4.86	-14.64	-18.37	-9.04	0.0002
w*	M	LO / SSB	47	43.86±1.26	44.85±4.29	0.99	-2.50	5.09	0.6160
Weighted Delta	M	LO / SSB	134	NA	NA	-8.07	-9.91	-6.21	0.0000
BK	M	LO / SSL	51	49.20±0.72	43.48±4.28	-5.72	-10.03	-1.87	0.0076
CS	M	LO / SSL	27	43.77±1.11	29.35±6.43	-14.43	-19.95	-8.54	0.0002
w*	M	LO / SSL	37	43.59±1.28	30.33±4.62	-13.26	-17.00	-8.77	0.0000
Weighted Delta	M	LO / SSL	115	NA	NA	-10.15	-12.77	-7.53	0.0000
BK	F	LO / SA	29	47.46±1.42	55.57±3.82	8.12	4.35	11.73	0.0002
CS	F	LO / SA	58	45.29±1.08	47.14±3.52	1.86	-2.01	5.44	0.3328
w*	F	LO / SA	35	43.58±1.46	45.31±3.93	1.73	-2.85	6.11	0.4540
Weighted Delta	F	LO / SA	122	NA	NA	3.80	1.47	6.05	0.0034
BK	F	LO / SSB	30	47.43±1.37	43.52±3.17	-3.90	-7.10	-0.70	0.0250
CS	F	LO / SSB	57	45.38±1.08	30.75±2.82	-14.63	-17.10	-11.60	0.0000

Genotype	Sex	Ctr / Test	Sample Size (n)	Ctr Mean±CI (%)	Test Mean±CI (%)	Delta (%)	Delta-CI (%)	Delta+CI (%)	p-value
w*	F	LO / SSB	34	43.25±1.57	39.37±4.73	-3.89	-8.52	1.21	0.1240
Weighted Delta	F	LO / SSB	121	NA	NA	-8.93	-10.85	-7.03	0.0000
BK	F	LO / SSL	24	47.62±1.38	35.24±13.19	-12.37	-23.38	1.85	0.0728
CS	F	LO / SSL	51	45.58±1.16	26.64±4.84	-18.94	-22.88	-13.72	0.0000
w*	F	LO / SSL	34	43.72±1.38	33.26±5.61	-10.46	-15.65	-4.59	0.0018
Weighted Delta	F	LO / SSL	109	NA	NA	-15.11	-18.25	-11.70	0.0000

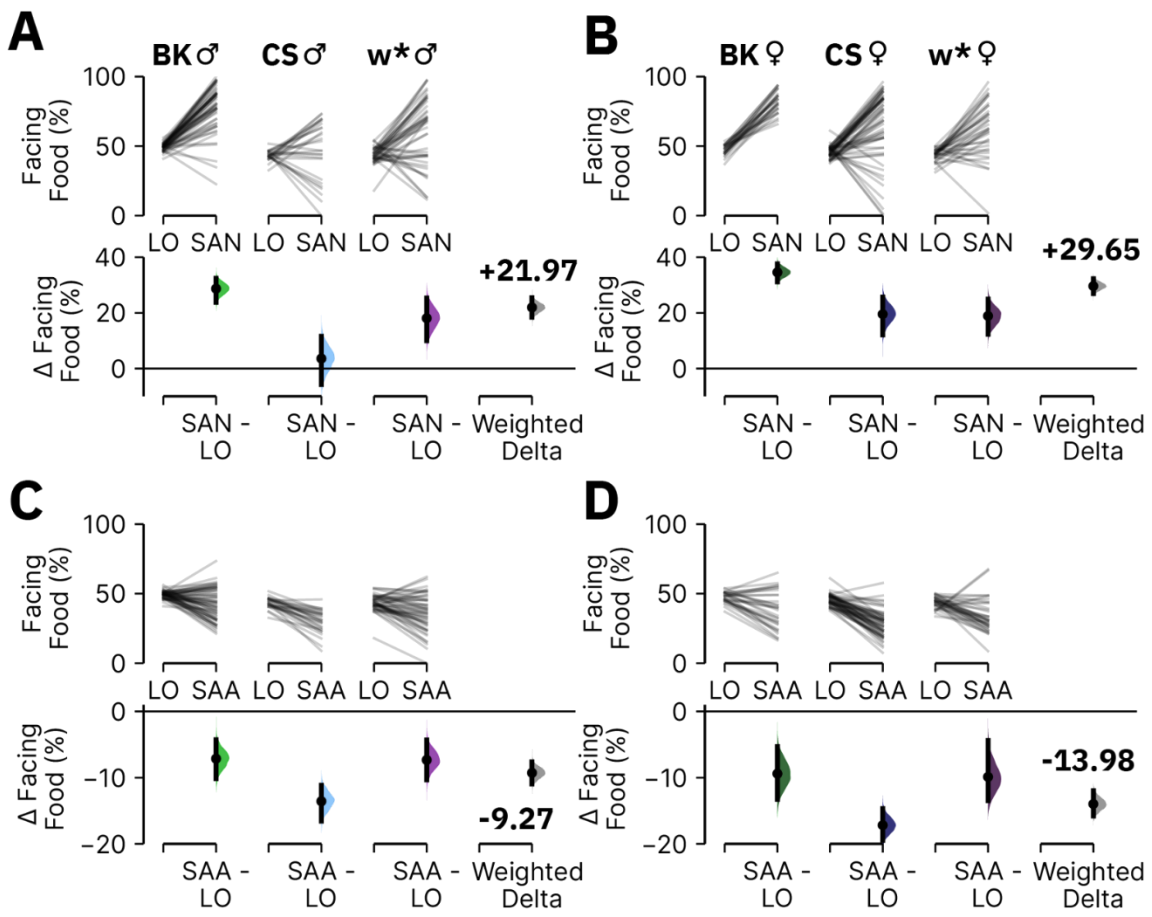

Appendix B Figure 20 Time spent facing the food port during SA near or away from the food as compared to during LO

(A-B) DABEST plots of the percentage time spent facing the food port when near the food port during SA compared to general LO for wild-type males **(A)** or females **(B)**. **(C-D)** The same as for (A-B) but with SA away from the food port. The summary data, including sample sizes, are shown in Appendix B Table 27. See Chapter 2.6 for more information about the structure of DABEST plots.

Appendix B Table 27 Time spent facing the food port during SA near or away from the food as compared to during LO

The table is pertinent to Appendix B Figure 20. Each row is a DABEST comparison of the mean time spent facing the food during SA near the food (SAN) or away (SAA) from the food compared to during LO. See Chapter 2.6 for more information about DABEST plots.

Genotype	Sex	Ctr / Test	Sample Size (n)	Ctr Mean±CI (%)	Test Mean±CI (%)	Delta (%)	Delta-CI (%)	Delta+CI (%)	p-value
BK	M	LO / SAN	54	49.36±0.72	78.07±4.47	28.70	23.82	32.42	0.0000
CS	M	LO / SAN	26	43.36±1.40	46.93±8.30	3.56	-5.78	11.57	0.4156
w*	M	LO / SAN	43	43.27±1.78	61.35±7.30	18.08	9.99	25.33	0.0000
Weighted Delta	M	LO / SAN	123	NA	NA	21.97	18.47	25.43	0.0000
BK	M	LO / SAA	59	49.36±0.67	42.22±2.94	-7.13	-10.15	-4.28	0.0000
CS	M	LO / SAA	28	43.38±1.45	29.81±3.17	-13.56	-16.57	-11.15	0.0000
w*	M	LO / SAA	49	43.33±1.59	36.00±3.75	-7.32	-10.33	-4.33	0.0000
Weighted Delta	M	LO / SAA	136	NA	NA	-9.27	-10.95	-7.61	0.0000
BK	F	LO / SAN	28	47.23±1.40	81.83±2.91	34.60	31.20	37.67	0.0000
CS	F	LO / SAN	57	45.56±1.06	65.10±6.54	19.54	12.10	25.64	0.0000
w*	F	LO / SAN	36	43.47±1.42	62.38±6.47	18.90	12.34	24.93	0.0000
Weighted Delta	F	LO / SAN	121	NA	NA	29.65	26.96	32.27	0.0000
BK	F	LO / SAA	30	47.43±1.37	38.03±4.87	-9.40	-13.29	-5.30	0.0000
CS	F	LO / SAA	55	45.43±1.10	28.25±2.57	-17.18	-19.47	-14.68	0.0000
w*	F	LO / SAA	36	43.75±1.35	33.86±3.98	-9.88	-13.46	-4.39	0.0000
Weighted Delta	F	LO / SAA	121	NA	NA	-13.98	-15.79	-12.00	0.0000

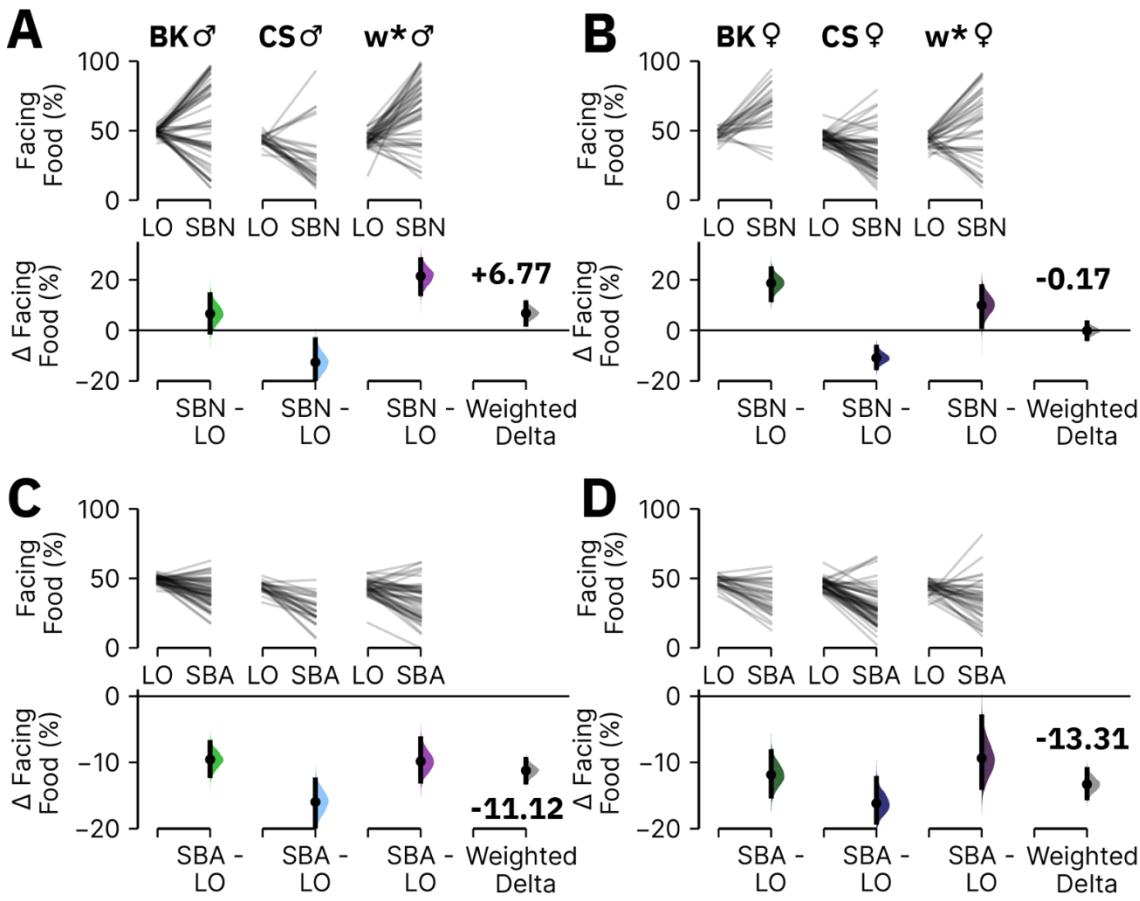

Appendix B Figure 21 Time spent facing the food port during SSB near or away from the food as compared to during LO

(A-B) DABEST plots of the percentage time spent facing the food port when near the food port during SSB (SBN) compared to during LO for wild-type males **(A)** or females **(B)**. **(C-D)** The same as for (A-B) but with SSB away from the food port (SBA). The summary data, including sample sizes, are shown in Appendix B Table 28. See Chapter 2.6 for more information about the structure of DABEST plots.

Appendix B Table 28 Time spent facing the food port during SSB near or away from the food as compared to during LO

The data is pertinent to Appendix B Figure 21. Each row is a DABEST comparison of the mean time spent facing the food during SSB near the food (SBN) or away (SBA) from the food compared to during LO. See Chapter 2.6 for more information about DABEST plots.

Genotype	Sex	Ctr / Test	Sample Size (n)	Ctr Mean±CI (%)	Test Mean±CI (%)	Delta (%)	Delta-CI (%)	Delta+CI (%)	p-value
BK	M	LO / SBN	53	49.20±0.75	55.79±7.72	6.58	-0.73	14.09	0.0870
CS	M	LO / SBN	28	43.48±1.37	30.85±7.81	-12.63	-19.23	-3.69	0.0038
w*	M	LO / SBN	47	43.39±1.64	64.82±6.67	21.44	14.47	27.92	0.0000
Weighted Delta	M	LO / SBN	128	NA	NA	6.77	2.48	10.92	0.0064
BK	M	LO / SBA	56	49.17±0.67	39.61±2.58	-9.56	-12.00	-6.98	0.0000
CS	M	LO / SBA	28	43.57±1.38	27.59±3.67	-15.98	-19.62	-12.67	0.0000
w*	M	LO / SBA	47	43.34±1.66	33.50±3.98	-9.84	-12.82	-6.43	0.0000
Weighted Delta	M	LO / SBA	131	NA	NA	-11.23	-12.96	-9.54	0.0000
BK	F	LO / SBN	26	47.38±1.54	66.07±6.17	18.70	12.12	24.33	0.0000
CS	F	LO / SBN	55	45.15±1.11	34.24±4.07	-10.91	-14.77	-6.65	0.0000
w*	F	LO / SBN	36	43.27±1.50	53.24±8.42	9.96	1.54	17.22	0.0174
Weighted Delta	F	LO / SBN	117	NA	NA	-0.17	-3.26	2.91	0.9350
BK	F	LO / SBA	30	47.43±1.37	35.55±4.13	-11.87	-15.07	-8.37	0.0000
CS	F	LO / SBA	56	45.44±1.08	29.25±3.43	-16.19	-19.02	-12.41	0.0000
w*	F	LO / SBA	36	43.50±1.49	34.13±4.95	-9.37	-13.80	-3.13	0.0010
Weighted Delta	F	LO / SBA	122	NA	NA	-13.31	-15.37	-11.07	0.0000

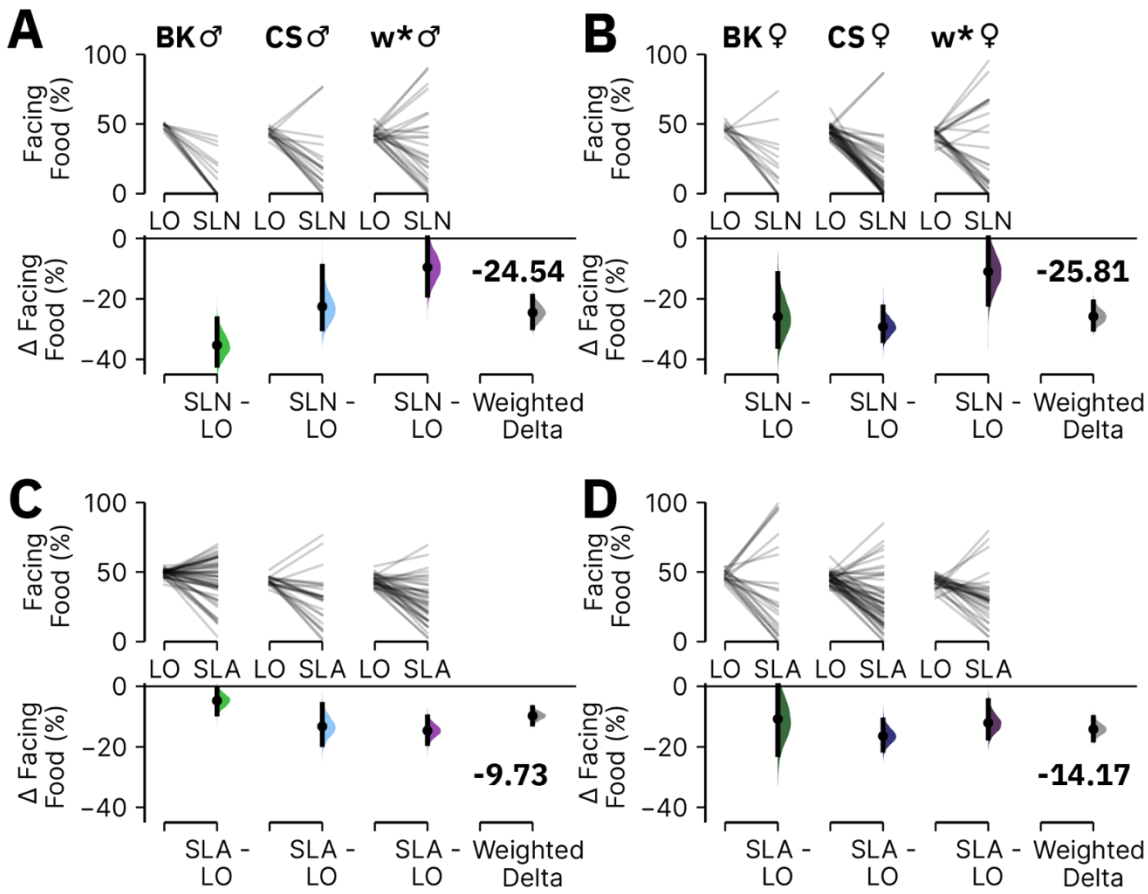

Appendix B Figure 22 Time spent facing the food port during SSL near or away from the food as compared to during LO

(A-B) DABEST plots of the percentage time spent facing the food port when near the food port during SSL (SLN) compared to general LO for wild-type males **(A)** or females **(B)**. **(C-D)** The same as for (A-B) but with SSL away from the food port (SLA). The summary data, including sample sizes, are shown in Appendix B Table 29. See Chapter 2.6 for more information about the structure of DABEST plots.

Appendix B Table 29 Time spent facing the food port during SSL near or away from the food as compared to during LO

The data is pertinent to Appendix B Figure 22. Each row is a DABEST comparison of the mean time spent facing the food during SSL near the food (SLN) or away (SLA) from the food compared to during LO. See Chapter 2.6 for more information about DABEST plots.

Genotype	Sex	Ctr / Test	Sample Size (n)	Ctr Mean±CI (%)	Test Mean±CI (%)	Delta (%)	Delta-CI (%)	Delta+CI (%)	p-value
BK	M	LO / SLN	14	48.35±1.09	13.02±8.23	-35.32	-41.93	-26.61	0.0000
CS	M	LO / SLN	19	43.85±1.32	21.30±10.09	-22.54	-29.86	-9.24	0.0010
w*	M	LO / SLN	27	42.79±1.48	33.23±10.35	-9.56	-18.77	0.91	0.0776
Weighted Delta	M	LO / SLN	60	NA	NA	-24.54	-29.56	-19.17	0.0000
BK	M	LO / SLA	53	49.24±0.69	44.51±4.24	-4.73	-9.17	-0.99	0.0282
CS	M	LO / SLA	26	43.65±1.12	30.40±7.10	-13.25	-19.22	-6.01	0.0014
w*	M	LO / SLA	41	43.62±1.22	29.00±4.76	-14.63	-18.85	-10.07	0.0000
Weighted Delta	M	LO / SLA	120	NA	NA	-9.73	-12.46	-6.99	0.0000
BK	F	LO / SLN	14	46.75±1.75	20.85±11.53	-25.90	-35.70	-11.68	0.0020
CS	F	LO / SLN	46	45.13±1.24	15.91±5.65	-29.22	-33.84	-22.72	0.0000
w*	F	LO / SLN	26	42.14±1.64	31.15±11.92	-11.00	-21.76	1.19	0.0820
Weighted Delta	F	LO / SLN	86	NA	NA	-25.81	-30.03	-20.99	0.0000
BK	F	LO / SLA	24	47.45±1.39	36.66±13.79	-10.78	-22.57	4.10	0.1308
CS	F	LO / SLA	53	45.33±1.17	28.91±5.18	-16.42	-21.09	-11.10	0.0000
w*	F	LO / SLA	35	43.03±1.46	30.97±5.64	-12.06	-17.10	-4.70	0.0010
Weighted Delta	F	LO / SLA	112	NA	NA	-14.17	-17.74	-10.29	0.0000

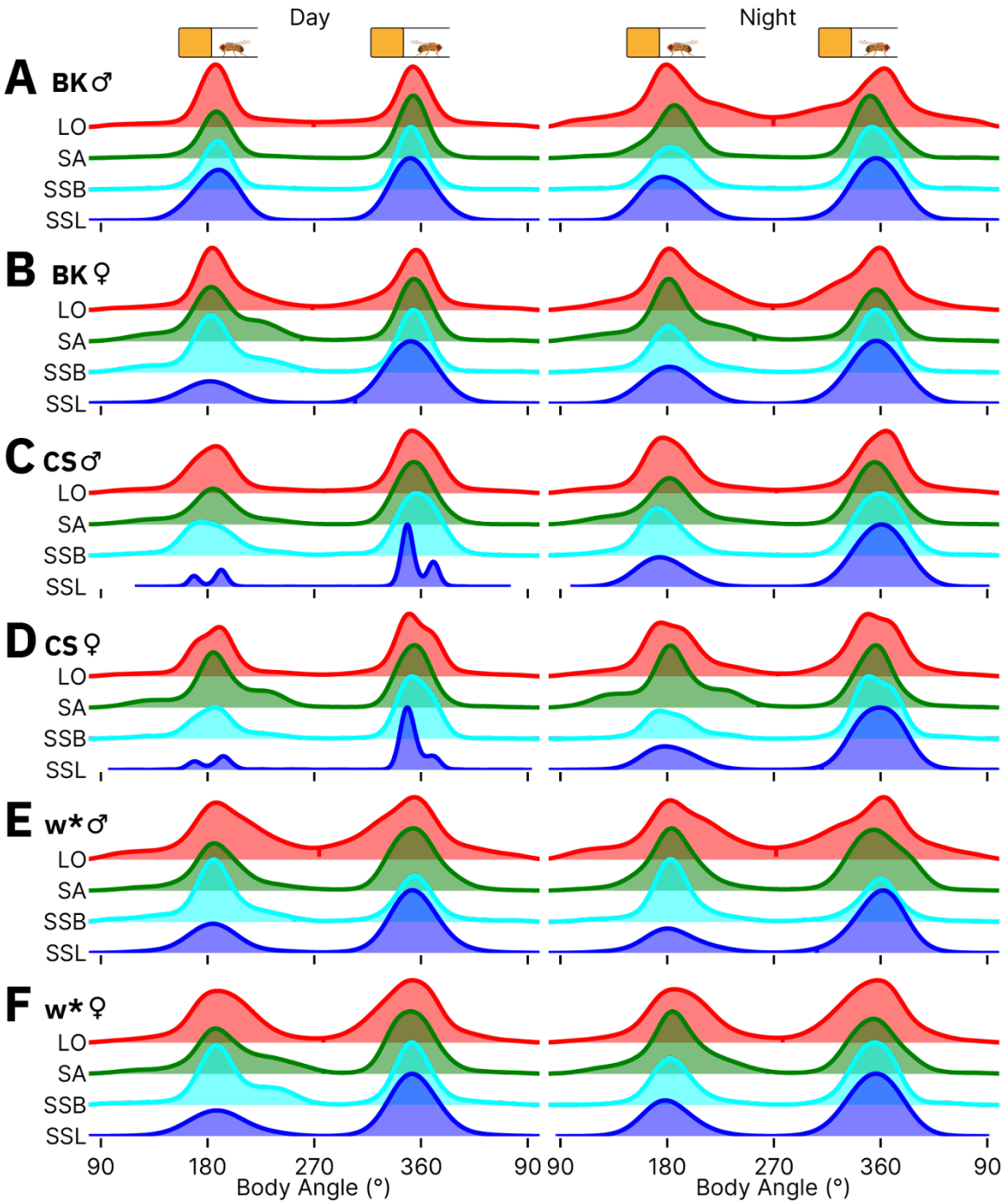

Appendix B Figure 23 No major difference in body angle between day and night

Ridgeline plots showing the body angle distribution of bouts during the day (left plots) and during the night (right plots) for each of the four recorded behaviours in BK males (n=60) **(A)**, BK females (n=30) **(B)**, CS males (n=30) **(C)**, CS females (n=59) **(D)**, w* males (n=49) **(E)**, and w* females (n=38) **(F)**. The dotted lines on each ridgeline curve indicates the mean of that distribution. Cartoons above (A) illustrate the location relative to the fly chamber.

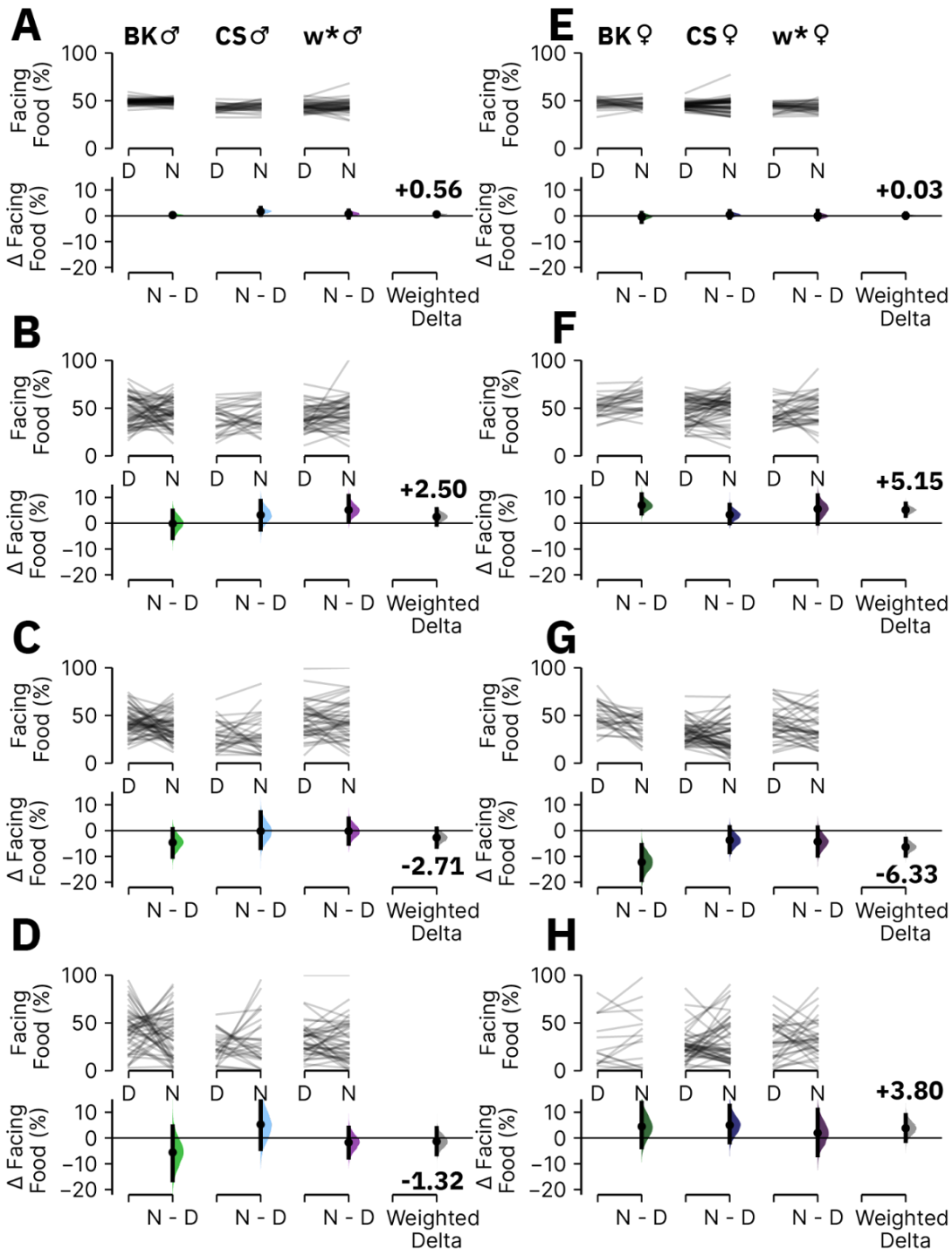

Appendix B Figure 24 No major difference in facing direction preference for night vs. day

(A-D) DABEST plots of the mean percentage time spent facing the food (%) during LO **(A)** SA **(B)**, SSB **(C)**, or SSL **(D)** during the night vs. day in wild-type male flies. **(E-H)** The same as for **(A-D)** but with female flies. The summary data, including sample sizes, are shown in Appendix B Table 30. See Chapter 2.6 for more information about the structure of DABEST plots.

Appendix B Table 30 No major difference in facing direction preference for night vs. day

The table is pertinent to Appendix B Figure 24. Each row is a DABEST comparison of the mean time spent facing the food for a given behaviour during the night vs. day for a given genotype. See Chapter 2.6 for more information about DABEST plots.

Genotype	Sex	State	Ctr / Test	Sample Size (n)	Ctr Mean±CI (%)	Test Mean±CI (%)	Delta (%)	Delta-CI (%)	Delta+CI (%)	p-value
BK	M	LO	Day / Night	59	49.16±0.75	49.43±0.73	0.26	-0.38	0.87	0.4212
CS	M	LO	Day / Night	29	42.30±1.39	44.00±1.68	1.70	0.31	3.05	0.0228
w*	M	LO	Day / Night	45	43.55±1.39	44.30±1.84	0.75	-0.71	2.04	0.3030
Weighted Delta	M	LO	Day / Night	133	NA	NA	0.56	0.04	1.08	0.0420
BK	M	SA	Day / Night	58	45.96±4.06	45.83±3.52	-0.13	-5.79	4.85	0.9612
CS	M	SA	Day / Night	28	39.20±5.12	42.39±5.17	3.19	-2.47	8.69	0.2766
w*	M	SA	Day / Night	46	40.43±3.59	45.54±4.52	5.11	1.05	10.58	0.0290
Weighted Delta	M	SA	Day / Night	132	NA	NA	2.50	-0.55	5.47	0.1136
BK	M	SSB	Day / Night	59	42.94±3.50	38.34±3.65	-4.61	-10.14	0.60	0.1030
CS	M	SSB	Day / Night	29	29.77±5.33	29.55±6.78	-0.21	-6.79	7.15	0.9548
w*	M	SSB	Day / Night	44	45.50±5.23	45.30±5.91	-0.20	-5.06	4.70	0.9392
Weighted Delta	M	SSB	Day / Night	132	NA	NA	-2.71	-6.26	0.78	0.1394
BK	M	SSL	Day / Night	48	43.41±6.32	37.85±6.99	-5.57	-16.35	4.49	0.3176
CS	M	SSL	Day / Night	28	24.93±5.55	30.18±9.65	5.25	-4.26	18.32	0.3664
w*	M	SSL	Day / Night	43	32.64±5.52	30.93±6.49	-1.71	-7.58	4.01	0.5948
Weighted Delta	M	SSL	Day / Night	119	NA	NA	-1.32	-6.32	3.86	0.6302
BK	F	LO	Day / Night	29	47.26±1.65	46.88±1.67	-0.37	-2.33	1.12	0.6962
CS	F	LO	Day / Night	58	45.08±0.91	45.50±1.88	0.42	-0.75	1.82	0.5156
w*	F	LO	Day / Night	33	43.69±1.44	43.65±1.69	-0.04	-1.36	1.93	0.9710

Genotype	Sex	State	Ctr / Test	Sample Size (n)	Ctr Mean±CI (%)	Test Mean±CI (%)	Delta (%)	Delta-CI (%)	Delta+CI (%)	p-value
Weighted Delta	F	LO	Day / Night	120	NA	NA	0.03	-0.85	0.93	0.9376
BK	F	SA	Day / Night	28	51.29±3.62	58.26±4.37	6.98	3.76	11.21	0.0010
CS	F	SA	Day / Night	57	46.98±3.50	50.27±3.95	3.29	0.00	7.10	0.0740
w*	F	SA	Day / Night	36	43.22±3.79	48.76±5.13	5.55	-0.13	10.79	0.0494
Weighted Delta	F	SA	Day / Night	121	NA	NA	5.15	2.88	7.60	0.0000
BK	F	SSB	Day / Night	28	50.15±5.01	37.93±4.66	-12.22	-19.20	-5.54	0.0018
CS	F	SSB	Day / Night	55	32.11±2.98	28.40±4.39	-3.71	-8.35	1.32	0.1356
w*	F	SSB	Day / Night	37	41.89±5.62	37.61±5.50	-4.28	-9.71	1.19	0.1476
Weighted Delta	F	SSB	Day / Night	120	NA	NA	-6.33	-9.70	-3.15	0.0008
BK	F	SSL	Day / Night	16	27.35±12.71	31.80±14.91	4.45	-3.59	13.63	0.3226
CS	F	SSL	Day / Night	49	26.04±4.57	31.01±6.43	4.97	-1.71	12.45	0.1688
w*	F	SSL	Day / Night	33	32.55±6.81	34.49±6.64	1.94	-6.69	10.95	0.6610
Weighted Delta	F	SSL	Day / Night	98	NA	NA	3.80	-1.14	8.91	0.1398

Appendix B Table 31 Facing direction preference is not due to chamber orientation

The table is pertinent to Figure 4.3.3. Each row is a DABEST comparison of the mean time facing the food for a given behaviour in w* male flies with food on the right side of the chamber vs. flies with food on the left side. See Chapter 2.6 for more information about DABEST plots.

Genotype	Sex	State	Ctr / Test	Ctr (n)	Test (n)	Ctr Mean±CI (%)	Test Mean±CI (%)	Delta (%)	Delta-CI (%)	Delta+CI (%)	p-value
w*	M	LO	Left/Right	12	11	45.13±2.77	43.17±2.18	-1.96	-5.11	1.64	0.2838
w*	M	SA	Left/Right	12	11	44.50±4.22	50.68±4.45	6.18	0.27	11.87	0.0628
w*	M	SSB	Left/Right	12	11	29.96±4.73	35.97±4.35	6.01	-1.00	11.29	0.0810
w*	M	SSL	Left/Right	12	11	37.80±8.99	35.59±6.04	-2.21	-13.12	7.76	0.6944

Appendix B Table 32 Wild-type flies occupy all three y-position locations within a chamber

Each row indicates the percentage time spent on each Y-Pos compartment for a given behaviour for a given wild-type genotype.

Genotype	Sex	Behaviour State	Sample Size (n)	Ground Occupancy Mean±CI (%)	Wall Occupancy Mean±CI (%)	Ceiling Occupancy Mean±CI (%)
BK	M	LO	60	32.80±1.50	31.05±1.68	36.15±2.08
BK	M	SA	60	71.24±3.65	6.23±0.95	22.54±3.07
BK	M	SSB	60	61.22±3.89	6.33±1.20	32.45±4.04
BK	M	SSL	60	66.02±5.38	2.98±1.15	31.00±5.43
BK	F	LO	30	36.74±4.62	30.81±3.03	32.45±4.36
BK	F	SA	30	55.87±6.27	20.69±3.54	23.43±5.58
BK	F	SSB	30	55.91±5.65	16.93±3.20	27.16±4.82
BK	F	SSL	28	57.32±10.15	7.07±3.26	35.61±10.12
CS	M	LO	30	38.95±1.92	24.97±2.32	36.08±2.81
CS	M	SA	30	58.04±7.02	10.10±2.83	31.86±6.08
CS	M	SSB	30	54.33±7.03	6.70±2.18	38.97±6.71
CS	M	SSL	30	50.09±8.45	3.90±1.85	46.01±7.90
CS	F	LO	59	41.31±2.58	33.11±2.22	25.58±2.05
CS	F	SA	59	62.32±2.99	17.11±2.02	20.57±2.93
CS	F	SSB	59	56.24±4.17	14.58±2.27	29.19±4.19
CS	F	SSL	59	45.03±5.48	17.52±3.42	37.45±5.49
w*	M	LO	49	28.20±2.51	50.44±3.12	21.36±2.70
w*	M	SA	49	49.52±4.40	17.98±3.59	32.50±4.94
w*	M	SSB	49	42.83±4.69	17.24±3.38	39.93±5.47
w*	M	SSL	49	43.80±5.81	12.27±3.30	43.93±5.80
w*	F	LO	38	27.95±2.82	51.09±3.04	20.96±1.93
w*	F	SA	38	56.84±4.57	21.18±3.95	21.99±3.03
w*	F	SSB	38	48.30±4.32	22.52±4.24	29.18±4.22
w*	F	SSL	38	41.47±5.08	21.39±5.17	37.14±5.63

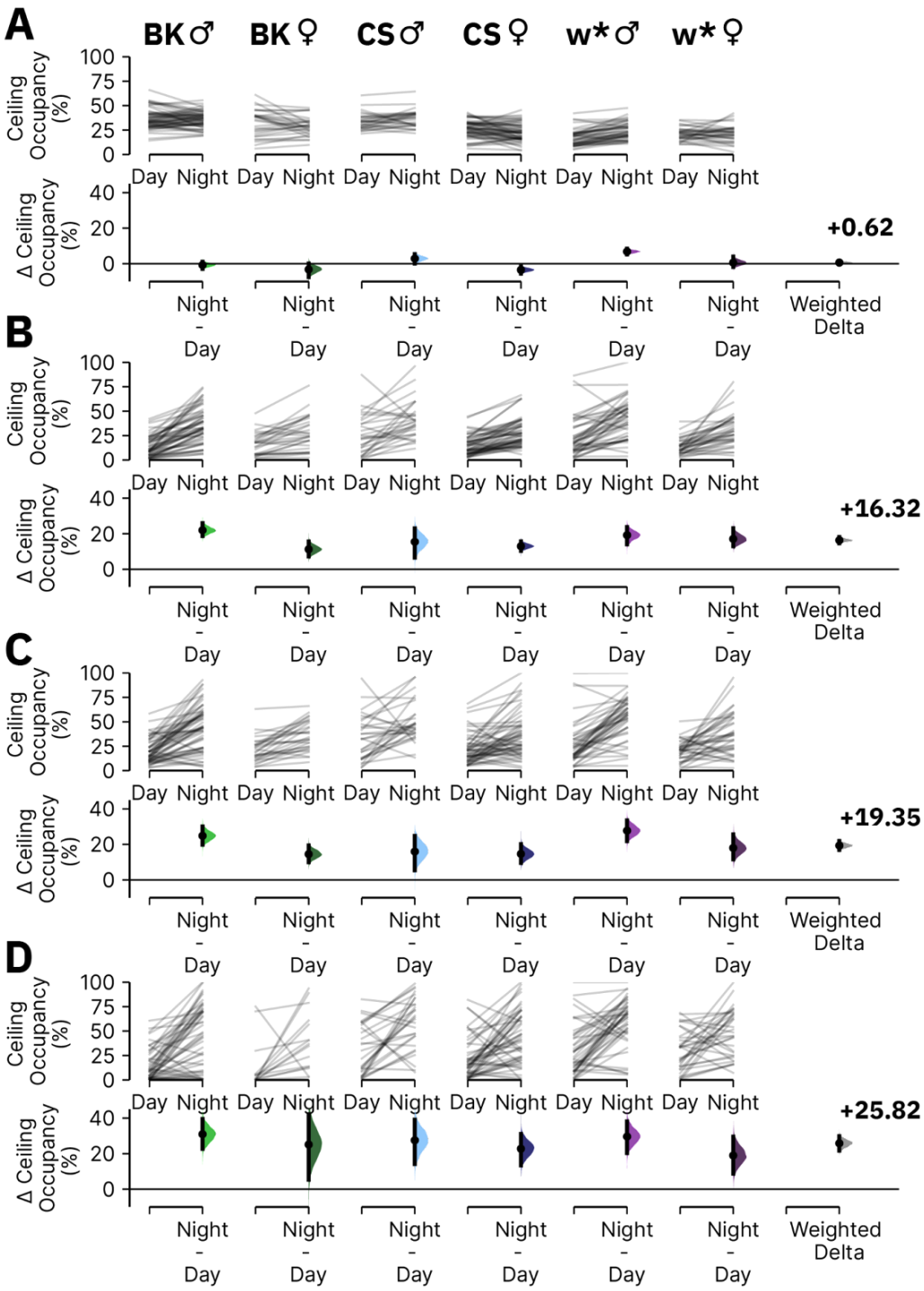

Appendix B Figure 25 Ceiling occupancy during night vs. day

DABEST plots of the percentage time spent on the ceiling during LO **(A)** SA **(B)**, SSB **(C)**, or SSL **(D)** during the night versus day. The summary data, including sample sizes, are shown in Appendix B Table 33. See Chapter 2.6 for more information about the structure of DABEST plots.

Appendix B Table 33 Ceiling occupancy during night vs. day

The table is pertinent to Appendix B Figure 25. Each row is DABEST comparison of the percentage time spent on the ceiling during a given behaviour during the night vs. day for a given genotype. See Chapter 2.6 for more information about DABEST plots.

Genotype	Sex	State	Ctr / Test	Sample Size (n)	Ctr Mean±CI (%)	Test Mean±CI (%)	Delta (%)	Delta-CI (%)	Delta+CI (%)	p-value
BK	M	LO	Day / Night	59	36.47±2.58	35.73±2.11	-0.74	-2.89	1.13	0.4636
BK	F	LO	Day / Night	29	32.08±5.05	28.84±3.52	-3.24	-7.57	0.06	0.1116
CS	M	LO	Day / Night	29	34.00±3.14	36.88±3.29	2.88	0.09	5.33	0.0470
CS	F	LO	Day / Night	58	26.18±2.25	22.70±2.34	-3.48	-5.56	-1.50	0.0006
w*	M	LO	Day / Night	45	17.32±2.43	24.16±2.53	6.84	5.23	8.46	0.0000
w*	F	LO	Day / Night	33	20.95±2.23	21.53±2.99	0.59	-1.80	3.97	0.7080
Weighted Delta	M/F	LO	Day / Night	253	NA	NA	0.62	-0.31	1.59	0.2588
BK	M	SA	Day / Night	58	13.55±2.68	35.52±4.57	21.97	18.70	25.96	0.0000
BK	F	SA	Day / Night	28	16.39±4.25	27.64±6.50	11.24	7.20	15.62	0.0000
CS	M	SA	Day / Night	28	25.73±7.64	41.19±7.28	15.46	6.52	22.99	0.0008
CS	F	SA	Day / Night	57	14.75±2.56	27.73±3.58	12.98	10.36	15.70	0.0000
w*	M	SA	Day / Night	46	23.45±5.81	42.65±5.72	19.20	14.04	23.78	0.0000
w*	F	SA	Day / Night	36	13.93±2.67	31.00±5.41	17.07	13.00	23.07	0.0000
Weighted Delta	M/F	SA	Day / Night	253	NA	NA	16.32	14.67	18.11	0.0000
BK	M	SSB	Day / Night	59	19.77±3.14	44.62±5.89	24.85	19.85	30.13	0.0000
BK	F	SSB	Day / Night	28	21.31±4.81	35.83±5.68	14.52	10.00	19.41	0.0000
CS	M	SSB	Day / Night	29	33.44±8.39	49.41±7.51	15.97	5.42	24.75	0.0030
CS	F	SSB	Day / Night	55	22.02±4.05	36.67±5.95	14.66	9.58	20.15	0.0000
w*	M	SSB	Day / Night	44	27.06±6.53	54.80±6.27	27.75	21.84	33.50	0.0000
w*	F	SSB	Day / Night	37	19.95±3.46	37.97±7.02	18.02	11.56	25.60	0.0000
Weighted Delta	M/F	SSB	Day / Night	252	NA	NA	19.35	16.89	21.87	0.0000
BK	M	SSL	Day / Night	48	14.90±4.61	45.85±9.07	30.95	22.69	39.50	0.0000
BK	F	SSL	Day / Night	16	12.46±12.07	37.57±15.07	25.11	5.32	42.15	0.0154
CS	M	SSL	Day / Night	28	31.16±9.71	58.69±9.96	27.53	14.16	39.06	0.0002
CS	F	SSL	Day / Night	49	21.34±5.84	44.11±7.63	22.77	13.43	31.07	0.0000
w*	M	SSL	Day / Night	43	29.92±7.67	59.52±7.36	29.60	20.31	38.13	0.0000
w*	F	SSL	Day / Night	33	29.60±7.16	48.58±8.30	18.98	8.73	29.60	0.0004

Genotype	Sex	State	Ctr / Test	Sample Size (n)	Ctr Mean±CI (%)	Test Mean±CI (%)	Delta (%)	Delta-CI (%)	Delta+CI (%)	p-value
Weighted Delta	M/F	SSL	Day / Night	217	NA	NA	25.82	21.71	29.88	0.0000

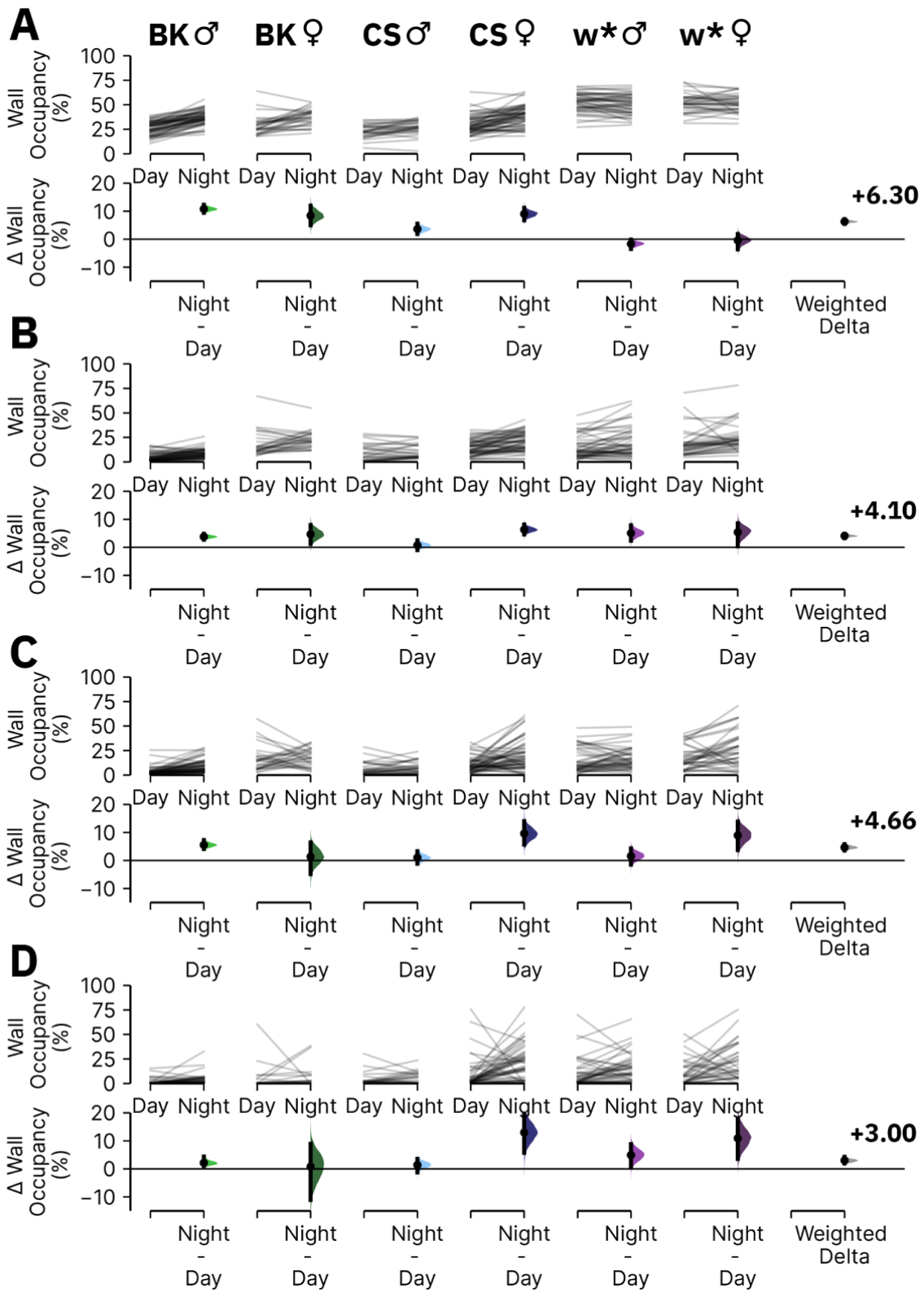

Appendix B Figure 26 Wall occupancy during night vs. day

DABEST plots of the percentage time spent on the wall during LO **(A)** SA **(B)**, SSB **(C)**, or SSL **(D)** during the night versus day. The summary data, including sample sizes, are shown in Appendix B Table 34. See Chapter 2.6 for more information about the structure of DABEST plots.

Appendix B Table 34 Wall occupancy during night vs. day

The table is pertinent to Appendix B Figure 26. Each row is DABEST comparison of the percentage time spent on the wall during a given behaviour during the night vs. day for a given genotype. See Chapter 2.6 for more information about DABEST plots.

Genotype	Sex	State	Ctr / Test	Sample Size (n)	Ctr Mean±CI (%)	Test Mean±CI (%)	Delta (%)	Delta-CI (%)	Delta+CI (%)	p-value
BK	M	LO	Day / Night	59	26.22±1.77	37.00±1.82	10.78	9.42	12.30	0.0000
BK	F	LO	Day / Night	29	29.17±3.67	37.58±3.04	8.41	4.99	11.93	0.0000
CS	M	LO	Day / Night	29	23.04±2.47	26.65±2.69	3.61	1.84	5.54	0.0002
CS	F	LO	Day / Night	58	29.73±2.38	38.74±2.59	9.01	6.78	11.20	0.0000
w*	M	LO	Day / Night	45	51.99±2.82	50.31±2.93	-1.68	-3.52	-0.19	0.0498
w*	F	LO	Day / Night	33	51.79±3.37	51.37±3.06	-0.42	-3.63	1.84	0.7838
Weighted Delta	M/F	LO	Day / Night	253	NA	NA	6.30	5.44	7.17	0.0000
BK	M	SA	Day / Night	58	4.72±1.09	8.50±1.18	3.79	2.71	4.88	0.0000
BK	F	SA	Day / Night	28	18.14±4.76	22.83±3.30	4.68	1.22	7.96	0.0124
CS	M	SA	Day / Night	28	9.22±3.20	9.96±2.73	0.74	-0.97	2.52	0.4288
CS	F	SA	Day / Night	57	14.70±1.99	21.03±2.40	6.33	4.62	8.21	0.0000
w*	M	SA	Day / Night	46	14.77±3.18	19.87±4.34	5.10	2.41	7.88	0.0004
w*	F	SA	Day / Night	36	18.90±4.71	24.30±4.62	5.39	0.34	8.60	0.0104
Weighted Delta	M/F	SA	Day / Night	253	NA	NA	4.10	3.29	4.89	0.0000
BK	M	SSB	Day / Night	59	3.63±1.12	9.17±1.71	5.55	4.10	7.30	0.0000
BK	F	SSB	Day / Night	28	16.61±4.86	17.96±3.32	1.35	-4.82	6.46	0.6490
CS	M	SSB	Day / Night	29	6.31±2.52	7.34±2.22	1.04	-1.15	3.32	0.3700
CS	F	SSB	Day / Night	55	10.45±2.03	20.06±4.01	9.61	5.66	14.02	0.0002
w*	M	SSB	Day / Night	44	15.00±3.66	16.57±3.23	1.57	-1.47	4.34	0.2994
w*	F	SSB	Day / Night	37	18.00±3.94	26.97±5.79	8.97	3.72	13.91	0.0012
Weighted Delta	M/F	SSB	Day / Night	252	NA	NA	4.66	3.54	5.83	0.0000
BK	M	SSL	Day / Night	48	1.32±0.93	3.47±1.63	2.15	1.00	4.36	0.0008
BK	F	SSL	Day / Night	16	7.03±7.56	7.83±6.00	0.79	-11.10	8.94	0.8972
CS	M	SSL	Day / Night	28	3.48±2.50	4.87±2.25	1.39	-1.28	3.54	0.2644
CS	F	SSL	Day / Night	49	8.64±4.41	21.63±4.98	12.99	5.71	19.38	0.0000
w*	M	SSL	Day / Night	43	10.48±4.48	15.41±4.28	4.93	0.49	8.83	0.0294
w*	F	SSL	Day / Night	33	11.69±4.53	22.62±6.40	10.92	3.55	17.97	0.0068

Genotype	Sex	State	Ctr / Test	Sample Size (n)	Ctr Mean±CI (%)	Test Mean±CI (%)	Delta (%)	Delta-CI (%)	Delta+CI (%)	p-value
Weighted Delta	M/F	SSL	Day / Night	217	NA	NA	3.00	1.90	4.29	0.0000

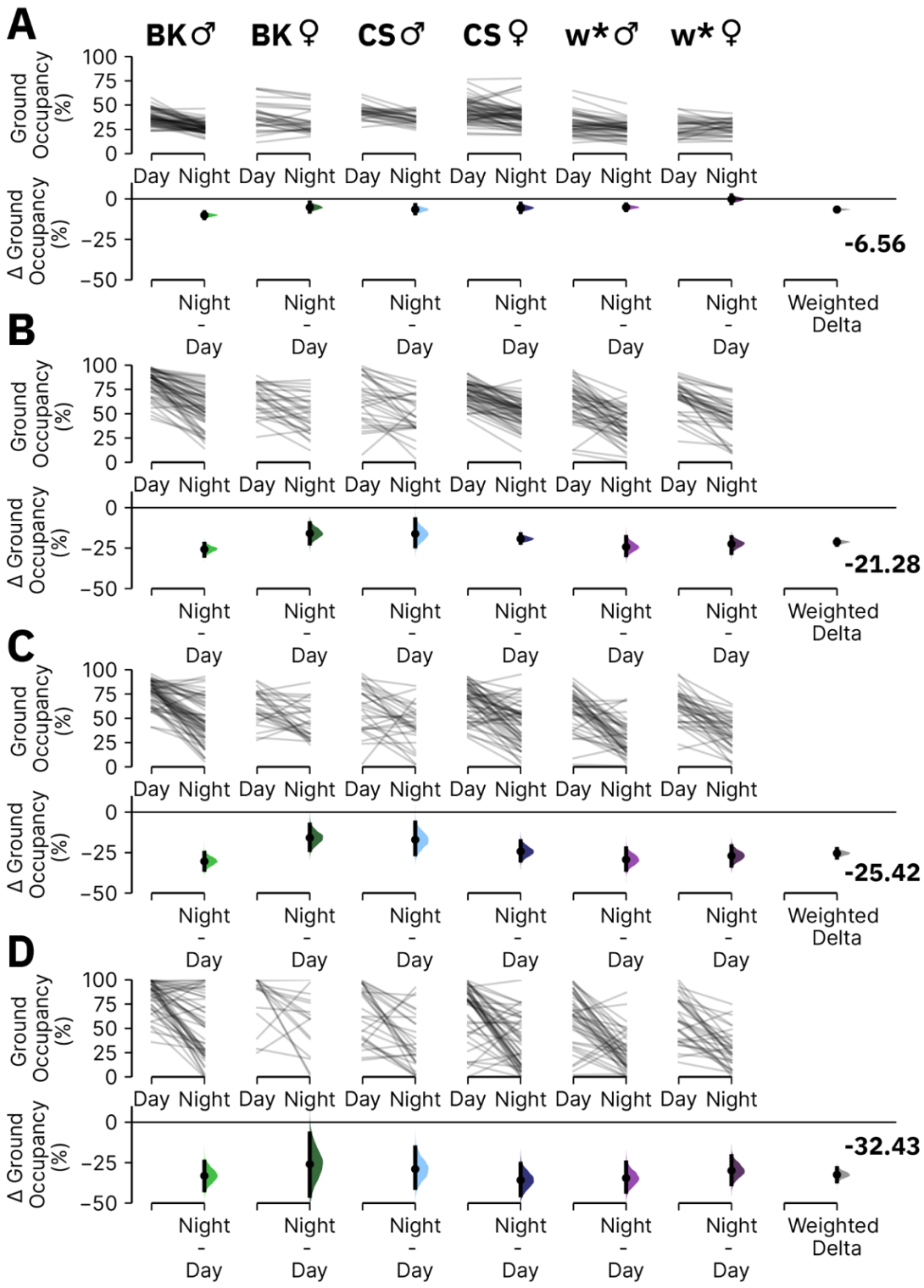

Appendix B Figure 27 Ground occupancy during night vs. day

DABEST plot of the percentage time spent on the ground during LO **(A)** SA **(B)**, SSB **(C)**, or SSL **(D)** during the night versus day. The summary data, including sample sizes, are shown in Appendix B Table 35. See Chapter 2.6 for more information about the structure of DABEST plots.

Appendix B Table 35 Ground occupancy during night vs. day

The table is pertinent to Appendix B Figure 27. Each row is DABEST comparison of the percentage time spent on the ground during a given behaviour during the night vs. day for a given genotype. See Chapter 2.6 for more information about DABEST plots.

Genotype	Sex	State	Ctr / Test	Sample Size (n)	Ctr Mean±CI (%)	Test Mean±CI (%)	Delta (%)	Delta-CI (%)	Delta+CI (%)	p-value
BK	M	LO	Day / Night	59	37.31±1.96	27.28±1.43	-10.04	-11.91	-8.19	0.0000
BK	F	LO	Day / Night	29	38.75±5.20	33.58±4.63	-5.17	-7.84	-2.19	0.0036
CS	M	LO	Day / Night	29	42.96±2.49	36.46±2.27	-6.49	-8.97	-3.70	0.0000
CS	F	LO	Day / Night	58	44.09±2.97	38.56±3.02	-5.53	-8.04	-2.93	0.0002
w*	M	LO	Day / Night	45	30.70±3.16	25.53±2.36	-5.16	-6.88	-3.45	0.0000
w*	F	LO	Day / Night	33	27.27±3.10	27.10±2.46	-0.17	-2.59	2.15	0.8898
Weighted Delta	M/F	LO	Day / Night	253	NA	NA	-6.56	-7.54	-5.57	0.0000
BK	M	SA	Day / Night	58	81.73±3.40	55.98±4.96	-25.76	-29.78	-22.30	0.0000
BK	F	SA	Day / Night	28	65.46±5.87	49.53±7.10	-15.93	-22.16	-9.65	0.0000
CS	M	SA	Day / Night	28	65.06±9.08	48.86±7.38	-16.20	-23.96	-7.22	0.0004
CS	F	SA	Day / Night	57	70.55±2.93	51.24±3.47	-19.31	-21.77	-16.53	0.0000
w*	M	SA	Day / Night	46	61.79±5.81	37.49±4.79	-24.30	-29.41	-18.20	0.0000
w*	F	SA	Day / Night	36	67.16±5.19	44.70±5.97	-22.46	-28.01	-18.30	0.0000
Weighted Delta	M/F	SA	Day / Night	253	NA	NA	-21.28	-23.05	-19.58	0.0000
BK	M	SSB	Day / Night	59	76.60±3.24	46.21±5.66	-30.39	-35.62	-25.10	0.0000
BK	F	SSB	Day / Night	28	62.08±6.22	46.21±6.58	-15.87	-23.44	-7.63	0.0016
CS	M	SSB	Day / Night	29	60.25±8.67	43.25±7.53	-17.00	-25.98	-6.34	0.0024
CS	F	SSB	Day / Night	55	67.54±4.62	43.27±5.68	-24.27	-29.91	-17.94	0.0000
w*	M	SSB	Day / Night	44	57.94±6.40	28.63±5.16	-29.31	-35.68	-22.36	0.0000
w*	F	SSB	Day / Night	37	62.04±5.56	35.06±5.14	-26.98	-33.04	-21.05	0.0000
Weighted Delta	M/F	SSB	Day / Night	252	NA	NA	-25.42	-28.06	-22.75	0.0000
BK	M	SSL	Day / Night	48	83.78±4.66	50.68±9.24	-33.10	-42.06	-24.36	0.0000
BK	F	SSL	Day / Night	16	80.51±13.05	54.60±15.17	-25.91	-45.50	-6.98	0.0238
CS	M	SSL	Day / Night	28	65.36±10.49	36.44±10.24	-28.92	-40.53	-15.54	0.0002
CS	F	SSL	Day / Night	49	70.02±7.58	34.26±7.33	-35.76	-45.17	-25.72	0.0000
w*	M	SSL	Day / Night	43	59.60±8.40	25.07±5.96	-34.53	-42.93	-24.85	0.0000

Genotype	Sex	State	Ctr / Test	Sample Size (n)	Ctr Mean±CI (%)	Test Mean±CI (%)	Delta (%)	Delta-CI (%)	Delta+CI (%)	p-value
w*	F	SSL	Day / Night	33	58.71±8.03	28.81±6.54	-29.90	-38.35	-21.02	0.0000
Weighted Delta	M/F	SSL	Day / Night	217	NA	NA	-32.43	-36.55	-28.33	0.0000

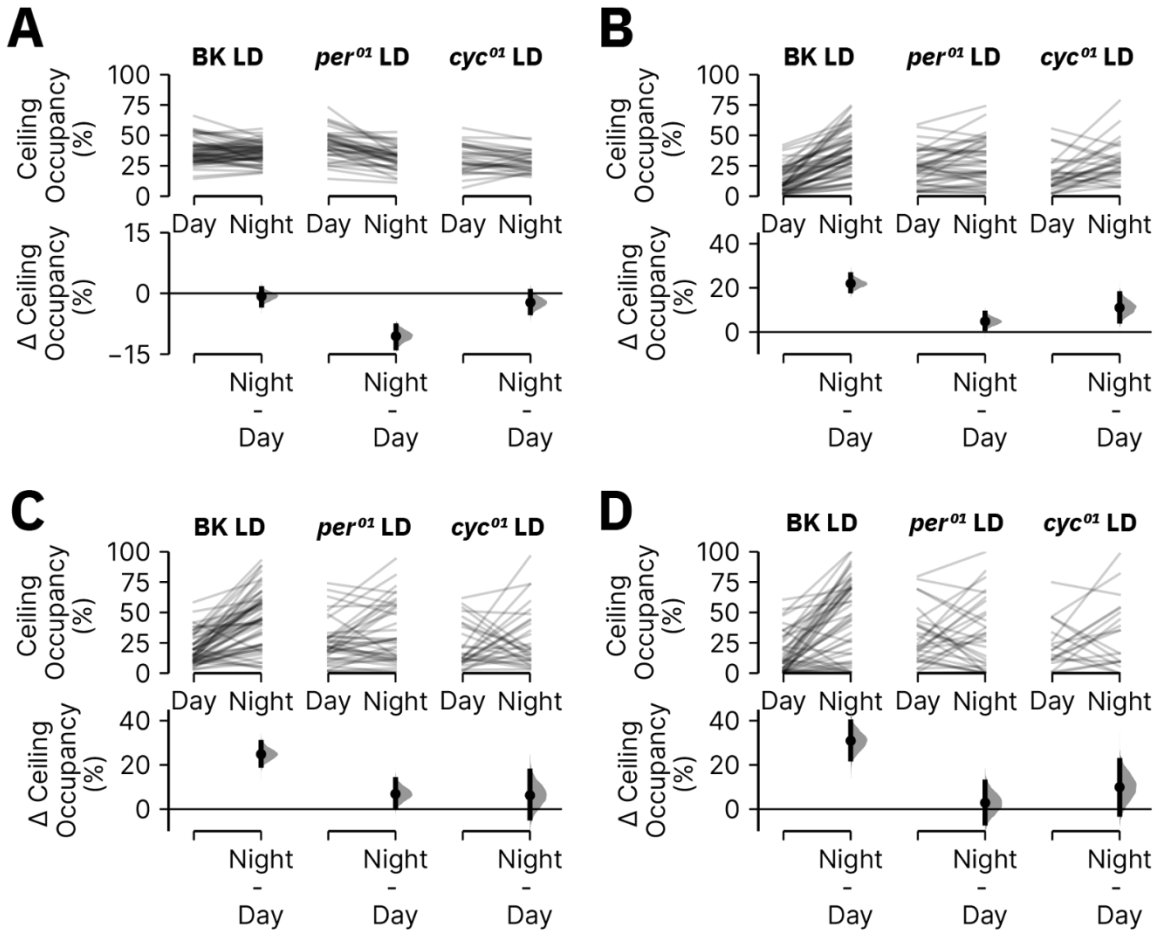

Appendix B Figure 28 Ceiling occupancy during night vs. day for male BK, *per*^{01}, and *cyc*^{01} flies in an LD cycle

DABEST plot of the percentage time spent on the ceiling during LO **(A)** SA **(B)**, SSB **(C)**, or SSL **(D)** during the night versus day for BK, *per*^{01}, and *cyc*^{01} males in LD. The summary data, including sample sizes, are shown in Appendix B Table 36. See Chapter 2.6 for more information about the structure of DABEST plots.

Appendix B Table 36 Ceiling occupancy during night vs. day for male BK, *per*^{01}, and *cyc*^{01} flies

The table is pertinent to Appendix B Figure 28. Each row is a DABEST comparison of the percentage time spent on the ceiling during a given behaviour during the night vs. day in BK, *per*^{01}, or *cyc*^{01} male flies in an LD cycle. See Chapter 2.6 for more information about DABEST plots.

Genotype	Sex	State	Ctr / Test	Sample Size (n)	Ctr Mean±CI (%)	Test Mean±CI (%)	Delta (%)	Delta-CI (%)	Delta+CI (%)	p-value
BK	M	LO	Day / Night	59	36.47±2.58	35.73±2.11	-0.74	-2.89	1.13	0.464
BK	M	SA	Day / Night	58	13.55±2.68	35.52±4.57	21.97	18.70	25.96	0.000
BK	M	SSB	Day / Night	59	19.77±3.14	44.62±5.89	24.85	19.85	30.13	0.000
BK	M	SSL	Day / Night	48	14.90±4.61	45.85±9.07	30.95	22.69	39.50	0.000
per^{01}	M	LO	Day / Night	40	42.35±3.70	31.78±2.94	-10.57	-13.45	-8.02	0.000
per^{01}	M	SA	Day / Night	41	23.45±4.42	28.27±5.42	4.83	1.66	8.56	0.012
per^{01}	M	SSB	Day / Night	39	25.31±5.73	32.19±7.82	6.87	1.13	13.30	0.032
per^{01}	M	SSL	Day / Night	32	27.19±7.95	30.05±9.99	2.86	-6.29	12.31	0.564
cyc^{01}	M	LO	Day / Night	30	30.96±4.07	28.71±2.95	-2.25	-4.78	0.49	0.117
cyc^{01}	M	SA	Day / Night	29	17.22±4.92	28.23±5.87	11.02	4.91	17.31	0.002
cyc^{01}	M	SSB	Day / Night	29	22.57±6.60	28.80±8.73	6.23	-3.98	17.14	0.268
cyc^{01}	M	SSL	Day / Night	20	21.70±8.50	31.63±12.59	9.93	-2.31	22.03	0.127

Appendix B Table 37 Rhythmic analysis of BK behaviour in an LD cycle

The table is pertinent to Figure 4.5.1B. Each row indicates an individual BK male fly's rhythmic analysis of all four Trumelan behaviours via eJTK_Cycle. See Chapter 2.10 for more information.

	LO		SA		SSB		SSL	
Fly	Tau	emp p	Tau	emp p	Tau	emp p	Tau	emp p
1	0.49	0.00001	0.48	0.00001	0.48	0.00001	0.27	0.00193
2	0.20	0.04577	0.28	0.00130	0.33	0.00005	0.24	0.00761
3	0.24	0.00709	0.22	0.01940	0.20	0.04618	0.22	0.01953
4	0.33	0.00003	0.33	0.00004	0.32	0.00007	0.40	0.00001
5	0.32	0.00009	0.30	0.00029	0.26	0.00281	0.34	0.00003
6	0.55	0.00001	0.47	0.00001	0.61	0.00001	0.49	0.00001
7	0.33	0.00005	0.38	0.00001	0.33	0.00003	0.39	0.00001
8	0.14	0.36687	0.20	0.04619	0.08	0.90871	0.16	0.24062

	LO		SA		SSB		SSL	
9	0.47	0.00001	0.30	0.00031	0.34	0.00003	0.49	0.00001
10	0.21	0.03928	0.13	0.46256	0.24	0.01065	0.25	0.00635
11	0.25	0.00626	0.36	0.00002	0.26	0.00301	0.26	0.00289
12	0.14	0.36625	0.36	0.00002	0.30	0.00032	0.25	0.00435
13	0.27	0.00205	0.22	0.02692	0.08	0.89943	0.27	0.00208
14	0.30	0.00034	0.18	0.11685	0.22	0.02029	0.28	0.00099
15	0.27	0.00152	0.09	0.85610	0.33	0.00003	0.26	0.00341
16	0.28	0.00080	0.24	0.00978	0.16	0.18948	0.29	0.00039
17	0.44	0.00001	0.44	0.00001	0.31	0.00011	0.24	0.00929
18	0.41	0.00001	0.38	0.00001	0.21	0.03018	0.43	0.00001
19	0.37	0.00001	0.30	0.00022	0.16	0.18875	0.32	0.00002
20	0.41	0.00001	0.30	0.00020	0.37	0.00001	0.39	0.00001
21	0.36	0.00001	0.34	0.00001	0.20	0.04850	0.33	0.00001
22	0.33	0.00001	0.30	0.00017	0.15	0.32474	0.27	0.00126
23	0.24	0.00801	0.24	0.00926	0.22	0.02351	0.12	0.54274
24	0.30	0.00016	0.17	0.15782	0.21	0.03219	0.23	0.01265
25	0.38	0.00001	0.44	0.00001	0.20	0.06246	0.33	0.00001
26	0.25	0.00523	0.30	0.00016	0.13	0.43716	0.22	0.01919
27	0.28	0.00121	0.26	0.00253	0.22	0.02377	0.34	0.00003
28	0.45	0.00001	0.34	0.00003	0.29	0.00046	0.46	0.00001
29	0.18	0.10806	0.52	0.00001	0.16	0.22062	0.27	0.00185
30	0.42	0.00001	0.38	0.00001	0.31	0.00010	0.43	0.00001
31	0.45	0.00001	0.24	0.00725	0.30	0.00035	0.49	0.00001
32	0.21	0.02862	0.33	0.00003	0.22	0.01872	0.19	0.08980
33	0.36	0.00002	0.36	0.00002	0.20	0.06216	0.34	0.00003
34	0.35	0.00003	0.36	0.00002	0.14	0.36893	0.43	0.00001
35	0.44	0.00001	0.44	0.00001	0.36	0.00002	0.44	0.00001
36	0.34	0.00003	0.26	0.00308	0.24	0.01032	0.29	0.00069
37	0.41	0.00001	0.33	0.00005	0.41	0.00001	0.42	0.00001
38	0.20	0.05342	0.47	0.00001	0.24	0.01020	0.24	0.00741
39	0.33	0.00005	0.39	0.00001	0.15	0.25321	0.34	0.00003
40	0.22	0.02736	0.30	0.00033	0.30	0.00022	0.31	0.00010

Appendix B Table 38 Rhythmic analysis of *per*^{01} behaviour in an LD cycle

The data is pertinent to Figure 4.5.1B. Each row indicates an individual *per*^{01} male fly's rhythmic analysis of all four Trumelan behaviours via eJTK_Cycle. See Chapter 2.10 for more information.

	LO		SA		SSB		SSL	
Fly	**Tau**	**emp p**	**Tau**	**emp p**	**Tau**	**emp p**	**Tau**	**emp p**
1	0.13	0.51126	0.12	0.58828	0.11	0.73156	0.17	0.16369
2	0.15	0.32073	0.15	0.35550	0.15	0.32608	0.11	0.68985
3	0.20	0.07030	0.25	0.00750	0.36	0.00002	0.24	0.01208
4	0.17	0.15455	0.17	0.20209	0.29	0.00086	0.19	0.07818
5	0.16	0.25652	0.22	0.02490	0.16	0.25100	0.13	0.50005
6	0.13	0.48875	0.15	0.33011	0.20	0.05569	0.15	0.27924
7	0.21	0.04989	0.20	0.05667	0.36	0.00002	0.16	0.23818
8	0.30	0.00042	0.27	0.00230	0.23	0.01447	0.31	0.00023
9	0.20	0.06688	0.18	0.11526	0.20	0.06741	0.09	0.87096
10	0.35	0.00002	0.24	0.00879	0.39	0.00002	0.30	0.00038
11	0.28	0.00127	0.24	0.01193	0.36	0.00002	0.31	0.00022
12	0.47	0.00001	0.33	0.00004	0.48	0.00001	0.34	0.00003
13	0.27	0.00243	0.17	0.18234	0.32	0.00009	0.19	0.08730
14	0.16	0.23818	0.26	0.00344	0.36	0.00002	0.22	0.03381
15	0.16	0.25020	0.18	0.13675	0.27	0.00185	0.17	0.18808
16	0.18	0.15003	0.25	0.00741	0.13	0.46975	0.19	0.09181
17	0.19	0.10228	0.24	0.01283	0.24	0.00931	0.21	0.05072
18	0.40	0.00001	0.37	0.00002	0.21	0.03822	0.30	0.00038
19	0.21	0.05034	0.15	0.30994	0.15	0.35257	0.25	0.00616
20	0.17	0.16634	0.31	0.00010	0.24	0.00915	0.08	0.94172
21	0.18	0.11862	0.29	0.00045	0.31	0.00014	0.18	0.11927
22	0.17	0.20561	0.15	0.31353	0.12	0.56569	0.16	0.23943
23	0.31	0.00012	0.32	0.00006	0.20	0.07005	0.37	0.00001
24	0.23	0.01713	0.39	0.00001	0.27	0.00259	0.16	0.26301
25	0.20	0.05753	0.29	0.00039	0.16	0.22049	0.20	0.07322
26	0.26	0.00451	0.16	0.26663	0.22	0.02731	0.16	0.25694
27	0.14	0.42630	0.16	0.23587	0.17	0.16059	0.13	0.45040
28	0.22	0.02502	0.18	0.14518	0.28	0.00085	0.23	0.01807
29	0.23	0.01637	0.22	0.02924	0.23	0.01822	0.25	0.00698

	LO		SA		SSB		SSL	
30	0.23	0.01951	0.28	0.00114	0.14	0.39505	0.22	0.03076
31	0.34	0.00004	0.10	0.78029	0.32	0.00011	0.23	0.02186
32	0.26	0.00356	0.28	0.00106	0.26	0.00435	0.27	0.00266
33	0.14	0.37878	0.16	0.23440	0.13	0.44877	0.22	0.02286
34	0.18	0.10982	0.31	0.00020	0.35	0.00002	0.34	0.00004
35	0.22	0.02676	0.23	0.02253	0.09	0.87795	0.27	0.00294
36	0.51	0.00001	0.28	0.00107	0.42	0.00001	0.46	0.00001
37	0.13	0.53303	0.19	0.08368	0.22	0.03225	0.22	0.03512
38	0.16	0.22048	0.24	0.00944	0.26	0.00419	0.20	0.06083
39	0.27	0.00183	0.41	0.00001	0.11	0.71389	0.30	0.00042
40	0.12	0.61823	0.23	0.01475	0.15	0.32425	0.10	0.83904
41	0.25	0.00568	0.17	0.16196	0.18	0.11810	0.23	0.01652

Appendix B Table 39 Rhythmic analysis of *cyc*^{01} behaviour in an LD cycle

The data is pertinent to Figure 4.5.1B. Each row indicates an individual *cyc*^{01} male fly's rhythmic analysis of all four Trumelan behaviours via eJTK_Cycle. See Chapter 2.10 for more information.

	LO		SA		SSB		SSL	
Fly	**Tau**	**emp p**	**Tau**	**emp p**	**Tau**	**emp p**	**Tau**	**emp p**
1	0.17	0.20011	0.22	0.03076	0.19	0.08969	0.10	0.78932
2	0.16	0.23095	0.21	0.04715	0.14	0.43752	0.26	0.00465
3	0.16	0.22512	0.14	0.39573	0.34	0.00003	0.11	0.66984
4	0.20	0.07114	0.13	0.51344	0.19	0.09458	0.22	0.02261
5	0.31	0.00013	0.18	0.11182	0.20	0.06546	0.27	0.00252
6	0.27	0.00196	0.16	0.23270	0.31	0.00013	0.24	0.01160
7	0.11	0.68099	0.21	0.04293	0.14	0.42581	0.13	0.48048
8	0.24	0.01172	0.17	0.16617	0.33	0.00004	0.17	0.20094
9	0.29	0.00060	0.16	0.25652	0.34	0.00003	0.25	0.00659
10	0.17	0.16654	0.11	0.66171	0.17	0.18655	0.21	0.03973
11	0.11	0.67692	0.06	0.98798	0.25	0.00799	0.14	0.39085
12	0.15	0.30829	0.10	0.80752	0.13	0.49710	0.19	0.09834
13	0.30	0.00024	0.11	0.69607	0.12	0.62366	0.29	0.00069

14	0.22	0.03085	0.18	0.12801	0.20	0.06349	0.23	0.01844
15	0.09	0.90377	0.13	0.53220	0.19	0.09879	0.12	0.60304
16	0.42	0.00001	0.38	0.00002	0.36	0.00002	0.27	0.00203
17	0.20	0.06306	0.18	0.13011	0.15	0.27981	0.22	0.02925
18	0.29	0.00076	0.15	0.28527	0.21	0.04362	0.22	0.02310
19	0.31	0.00013	0.15	0.28230	0.30	0.00052	0.28	0.00131
20	0.28	0.00157	0.16	0.26975	0.16	0.26428	0.27	0.00271
21	0.39	0.00001	0.12	0.64584	0.48	0.00001	0.41	0.00001
22	0.20	0.06565	0.14	0.39179	0.23	0.01527	0.16	0.24710
23	0.29	0.00071	0.22	0.02283	0.09	0.89845	0.20	0.06767
24	0.26	0.00358	0.15	0.32936	0.30	0.00042	0.21	0.04802
25	0.27	0.00191	0.15	0.32440	0.18	0.14682	0.21	0.04138
26	0.22	0.02420	0.33	0.00006	0.32	0.00013	0.17	0.16205
27	0.28	0.00117	0.21	0.04093	0.26	0.00374	0.20	0.06307
28	0.47	0.00001	0.09	0.86873	0.35	0.00002	0.45	0.00001
29	0.18	0.12584	0.19	0.10735	0.17	0.15640	0.20	0.05357
30	0.36	0.00002	0.18	0.15053	0.22	0.03287	0.27	0.00216

Appendix B Table 40 Correlation of ceiling occupancy across behaviour states

Summary table for the cross-correlation analysis in Figure 4.5.2B. The correlation coefficient (Pearson's R) is computed for each individual fly, whereby the ceiling occupancy data (raw data averaged into a 24-hour day in 60-minute bins) is compared for each behavioural state against one another.

Genotype	Sex	Comparison	Sample Size (n)	R Mean±CI
BK	M	LO vs SA	60	0.13±0.09
BK	M	LO vs SSB	60	0.11±0.08
BK	M	LO vs SSL	60	0.06±0.08
BK	M	SA vs SSB	60	0.74±0.06
BK	M	SA vs SSL	60	0.61±0.06
BK	M	SSB vs SSL	60	0.76±0.05

Appendix B Table 41 Rhythmic analysis of ceiling occupancy for BK, *per*^{01}, and *cyc*^{01} male flies in LD conditions

The table is pertinent to Figure 4.5.3D-F. The tau and associated empirical p-value via eJTK_Cycle for analysis of LO and Roost ceiling occupancy rhythms for BK, *per*^{01} and *cyc*^{01} males in LD conditions. See Chapter 2.10 for more information.

	BK LD				***per*^{01} LD**				***cyc*^{01} LD**			
	LO		**Roost**		**LO**		**Roost**		**LO**		**Roost**	
Fly	**Tau**	**emp p**	**Tau**	**emp p**	**Tau**	**emp p**	**Tau**	**emp p**	**Tau**	**emp p**	**Tau**	**emp p**
1	0.24	0.05752	0.50	0.00001	0.40	0.00011	0.25	0.08005	0.25	0.09427	0.29	0.02755
2	0.26	0.03785	0.55	0.00001	0.17	0.22617	0.35	0.00001	0.22	0.11628	0.23	0.08093
3	0.25	0.03922	0.46	0.00001	0.26	0.11819	0.13	0.87088	0.23	0.10147	0.25	0.05074
4	0.36	0.00012	0.51	0.00001	0.23	0.02139	0.32	0.00026	0.18	0.49145	0.16	0.63686
5	0.44	0.00001	0.34	0.00004	0.38	0.00001	0.12	0.57717	0.41	0.00002	0.23	0.05714
6	0.32	0.00019	0.49	0.00001	0.29	0.00195	0.23	0.03361	0.24	0.15475	0.31	0.02770
7	0.33	0.00010	0.46	0.00001	0.44	0.00002	0.34	0.00122	0.21	0.15180	0.31	0.00521
8	0.26	0.02896	0.30	0.00543	0.21	0.15729	0.35	0.00048	0.17	0.44565	0.23	0.10477
9	0.25	0.09989	0.24	0.12178	0.14	0.47116	0.17	0.24238	0.26	0.06118	0.26	0.05421
10	0.25	0.02650	0.53	0.00001	0.29	0.01108	0.32	0.00351	0.33	0.01092	0.33	0.01155
11	0.22	0.35863	0.12	0.95875	0.10	0.92471	0.27	0.03072	0.27	0.07371	0.52	0.00001
12	0.47	0.00006	0.65	0.00001	0.26	0.01411	0.22	0.06831	0.10	0.85672	0.44	0.00001
13	0.36	0.00001	0.37	0.00001	0.34	0.00013	0.19	0.12266	0.24	0.15825	0.40	0.00071
14	0.14	0.43181	0.45	0.00001	0.18	0.22024	0.18	0.21634	0.12	0.71019	0.49	0.00001
15	0.47	0.00034	0.50	0.00009	0.23	0.26002	0.16	0.71602	0.32	0.00195	0.42	0.00002
16	0.16	0.39579	0.23	0.07670	0.16	0.28437	0.14	0.52749	0.23	0.05788	0.35	0.00028
17	0.38	0.00047	0.41	0.00010	0.22	0.03488	0.39	0.00001	0.13	0.81578	0.17	0.48861
18	0.23	0.11526	0.40	0.00011	0.21	0.10715	0.22	0.06081	0.10	0.94021	0.20	0.29354
19	0.41	0.00223	0.31	0.05947	0.18	0.29190	0.30	0.00648	0.31	0.01834	0.17	0.57644
20	0.23	0.09371	0.46	0.00001	0.17	0.33362	0.15	0.43404	0.17	0.42506	0.16	0.52942
21	0.21	0.20965	0.45	0.00002	0.18	0.17611	0.31	0.00090	0.21	0.14382	0.21	0.15780
22	0.27	0.01150	0.59	0.00001	0.33	0.00079	0.17	0.33495	0.35	0.00066	0.32	0.00299
23	0.29	0.00403	0.41	0.00001	0.18	0.20154	0.20	0.11050	0.32	0.00334	0.38	0.00015
24	0.23	0.20574	0.43	0.00015	0.31	0.00055	0.21	0.07170	0.18	0.24400	0.19	0.21824
25	0.26	0.01696	0.56	0.00001	0.42	0.00001	0.14	0.44210	0.22	0.15127	0.39	0.00022

	BK LD				*per*^{01} LD				*cyc*^{01} LD			
26	0.32	0.00322	0.39	0.00011	0.28	0.00239	0.29	0.00114	0.30	0.00870	0.31	0.00494
27	0.44	0.00001	0.34	0.00091	0.21	0.11259	0.24	0.04072	0.28	0.00751	0.26	0.01598
28	0.24	0.05423	0.34	0.00048	0.24	0.01529	0.21	0.05405	0.38	0.00003	0.33	0.00012
29	0.32	0.00013	0.59	0.00001	0.39	0.00001	0.29	0.00737	0.37	0.00012	0.43	0.00001
30	0.27	0.02151	0.40	0.00006	0.37	0.00008	0.09	0.93947	0.29	0.05095	0.14	0.77344
31	0.24	0.01185	0.50	0.00001	0.28	0.00518	0.20	0.12050	N/A	N/A	N/A	N/A
32	0.27	0.01647	0.32	0.00208	0.21	0.04549	0.18	0.12357	N/A	N/A	N/A	N/A
33	0.29	0.00049	0.40	0.00001	0.37	0.00002	0.22	0.05353	N/A	N/A	N/A	N/A
34	0.16	0.28812	0.46	0.00001	0.21	0.08156	0.35	0.00010	N/A	N/A	N/A	N/A
35	0.28	0.00094	0.24	0.00976	0.23	0.04248	0.28	0.00536	N/A	N/A	N/A	N/A
36	0.22	0.07425	0.32	0.00104	0.08	0.96480	0.10	0.88186	N/A	N/A	N/A	N/A
37	0.30	0.00147	0.41	0.00001	0.10	0.92394	0.20	0.22364	N/A	N/A	N/A	N/A
38	0.22	0.03851	0.57	0.00001	0.14	0.72721	0.29	0.02947	N/A	N/A	N/A	N/A
39	0.16	0.32279	0.42	0.00001	0.14	0.45412	0.30	0.00074	N/A	N/A	N/A	N/A
40	0.29	0.04397	0.28	0.07230	0.45	0.00001	0.06	0.99503	N/A	N/A	N/A	N/A
41	N/A	N/A	N/A	N/A	0.18	0.24893	0.22	0.06967	N/A	N/A	N/A	N/A

Appendix B Table 42 Rhythmic amplitude of ceiling occupancy for BK, *per*^{01}, and *cyc*^{01} male flies in LD conditions

The table is pertinent to Figure 4.5.3C. Each row is a DABEST comparison of the rhythmic amplitude (Tau) of either LO or Roost ceiling occupancy in circadian mutant males vs. BK males. See Chapter 2.6 for more information about DABEST plots.

State	Ctr / Test	Sample Size Ctr (n)	Sample Size Test (n)	Ctr Mean±CI (Tau)	Test Mean±CI (Tau)	Delta (Tau)	Delta-CI (Tau)	Delta+CI (Tau)	p-value
LO	BK / *per*^{01}	40	41	0.28±0.03	0.25±0.03	-0.03	-0.08	0.00	0.0864
LO	BK / *cyc*^{01}	40	30	0.28±0.03	0.25±0.03	-0.04	-0.08	0.00	0.0734
Roost	BK / *per*^{01}	40	41	0.42±0.04	0.23±0.02	-0.19	-0.23	-0.15	0.0000
Roost	BK / *cyc*^{01}	40	30	0.42±0.04	0.30±0.04	-0.12	-0.17	-0.07	0.0000

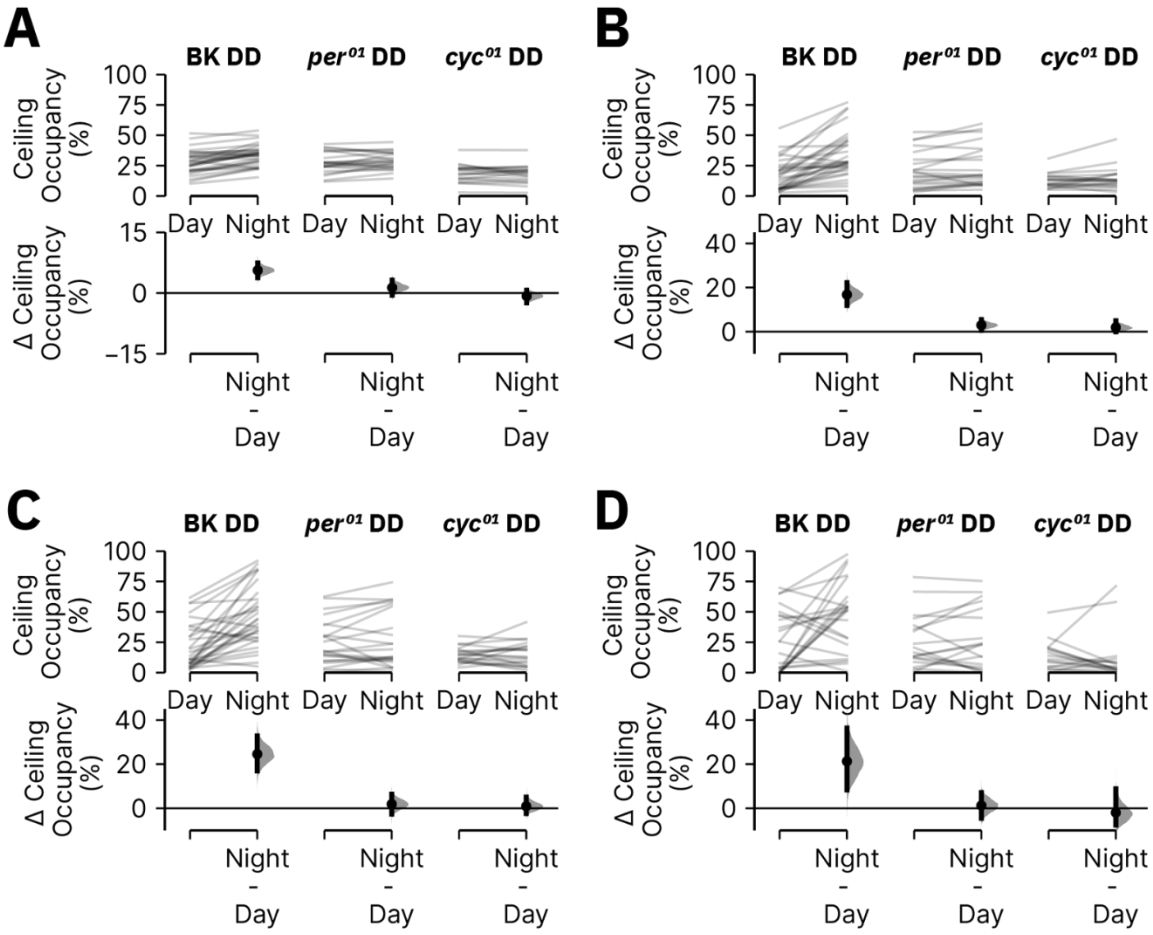

Appendix B Figure 29 Ceiling occupancy during night vs. day for male BK, *per*^{01}, and *cyc*^{01} flies in DD conditions

DABEST plots of the percentage time spent on the ceiling during LO **(A)** SA **(B)**, SSB **(C)**, or SSL **(D)** during the night versus the day for BK, *per*^{01}, and *cyc*^{01} males in DD. The summary data, including sample sizes, are shown in Appendix B Table 43. See Chapter 2.6 for more information about the structure of DABEST plots.

Appendix B Table 43 Ceiling occupancy during night versus day for male BK, *per*^{01}, and *cyc*^{01} flies in DD conditions

The table is pertinent to Figure 4.5.4 and Appendix B Figure 29. Each row is a DABEST comparison of the percentage time spent on the ceiling during a given behaviour during the night vs. day in BK, *per*^{01}, or *cyc*^{01} male flies in DD conditions. See Chapter 2.6 for more information about DABEST plots.

Genotype	Sex	State	Ctr / Test	Sample Size (n)	Ctr Mean±CI (%)	Test Mean±CI (%)	Delta (%)	Delta-CI (%)	Delta+CI (%)	p-value
BK	M	LO	Day / Night	31	27.89±3.41	33.51±3.08	5.63	3.82	7.46	0.000
BK	M	SA	Day / Night	31	17.14±4.57	33.95±6.62	16.81	11.86	22.24	0.000
BK	M	SSB	Day / Night	30	21.44±6.65	46.00±8.88	24.55	16.98	32.84	0.000
BK	M	SSL	Day / Night	23	26.24±10.24	47.53±11.64	21.29	8.32	36.33	0.007
per^{01}	M	LO	Day / Night	22	27.49±3.64	28.83±3.04	1.34	-0.53	3.19	0.182
per^{01}	M	SA	Day / Night	22	21.14±6.28	24.12±7.17	2.98	0.68	5.5	0.028
per^{01}	M	SSB	Day / Night	22	24.93±7.82	26.84±9.66	1.9	-2.65	6.39	0.430
per^{01}	M	SSL	Day / Night	20	23.80±9.79	25.07±11.28	1.26	-4.53	7.07	0.675
cyc^{01}	M	LO	Day / Night	19	18.75±3.43	18.01±3.37	-0.74	-2.4	0.69	0.392
cyc^{01}	M	SA	Day / Night	19	12.74±2.75	14.68±4.35	1.94	-0.02	4.92	0.142
cyc^{01}	M	SSB	Day / Night	19	14.61±2.96	15.53±4.66	0.92	-2.41	5.1	0.661
cyc^{01}	M	SSL	Day / Night	17	13.69±5.93	11.73±9.72	-1.97	-7.59	8.82	0.664

Appendix B Table 44 Rhythmic analysis of BK behaviour in DD conditions

The table is pertinent to Figure 4.5.5B. Each row indicates an individual BK male fly's rhythmic analysis of all four Trumelan behaviours via eJTK_Cycle. See Chapter 2.10 for more information.

	LO		SA		SSB		SSL	
Fly	Tau	emp p	Tau	emp p	Tau	emp p	Tau	emp p
1	0.49	0.00001	0.15	0.28410	0.29	0.00052	0.48	0.00001
2	0.37	0.00002	0.08	0.94631	0.30	0.00042	0.30	0.00025
3	0.36	0.00002	0.17	0.15405	0.17	0.16616	0.31	0.00013
4	0.24	0.00853	0.14	0.37928	0.21	0.04105	0.16	0.21957
5	0.40	0.00001	0.14	0.44632	0.18	0.11283	0.42	0.00001

	LO		SA		SSB		SSL	
6	0.39	0.00002	0.35	0.00003	0.19	0.08572	0.34	0.00003
7	0.65	0.00001	0.48	0.00001	0.37	0.00001	0.59	0.00001
8	0.52	0.00001	0.20	0.07441	0.28	0.00122	0.46	0.00001
9	0.56	0.00001	0.27	0.00243	0.45	0.00001	0.57	0.00001
10	0.49	0.00001	0.33	0.00006	0.23	0.01490	0.50	0.00001
11	0.55	0.00001	0.36	0.00002	0.25	0.00637	0.50	0.00001
12	0.34	0.00003	0.23	0.01383	0.35	0.00002	0.35	0.00003
13	0.23	0.01382	0.08	0.94649	0.24	0.00838	0.28	0.00114
14	0.46	0.00001	0.23	0.01935	0.29	0.00065	0.46	0.00001
15	0.62	0.00001	0.34	0.00003	0.45	0.00001	0.66	0.00001
16	0.33	0.00004	0.21	0.04475	0.29	0.00079	0.22	0.03155
17	0.55	0.00001	0.20	0.05121	0.47	0.00001	0.46	0.00001
18	0.37	0.00002	0.34	0.00003	0.36	0.00002	0.32	0.00012
19	0.49	0.00001	0.30	0.00034	0.27	0.00233	0.44	0.00001
20	0.40	0.00001	0.29	0.00065	0.40	0.00001	0.40	0.00001
21	0.18	0.15084	0.20	0.06332	0.23	0.01656	0.18	0.12459
22	0.24	0.00959	0.31	0.00015	0.30	0.00046	0.24	0.00905
23	0.34	0.00004	0.20	0.05471	0.40	0.00001	0.32	0.00012
24	0.18	0.11930	0.27	0.00202	0.29	0.00069	0.20	0.05490
25	0.25	0.00783	0.21	0.05035	0.12	0.63479	0.16	0.25274
26	0.27	0.00271	0.20	0.05547	0.16	0.27298	0.23	0.01712
27	0.32	0.00011	0.40	0.00001	0.36	0.00002	0.36	0.00002
28	0.21	0.04428	0.38	0.00002	0.22	0.02292	0.30	0.00027
29	0.18	0.11624	0.31	0.00018	0.26	0.00298	0.27	0.00254
30	0.17	0.15177	0.21	0.04532	0.21	0.04081	0.18	0.15029
31	0.18	0.12356	0.11	0.74220	0.28	0.00152	0.20	0.05512

Appendix B Table 45 Rhythmic analysis of *per*^{01} behaviour in DD conditions

The table is pertinent to Figure 4.5.5B. Each row indicates an individual *per*^{01} male fly's rhythmic analysis of all four Trumelan behaviours via eJTK_Cycle. See Chapter 2.10 for more information.

	LO		SA		SSB		SSL	
Fly	**Tau**	**emp p**	**Tau**	**emp p**	**Tau**	**emp p**	**Tau**	**emp p**
1	0.20	0.05868	0.12	0.60201	0.14	0.37991	0.17	0.16245
2	0.16	0.25247	0.10	0.77883	0.15	0.32767	0.21	0.04252
3	0.09	0.85204	0.10	0.79983	0.15	0.28421	0.15	0.31202
4	0.16	0.24491	0.11	0.72316	0.11	0.71730	0.13	0.46519
5	0.13	0.47654	0.08	0.93018	0.11	0.73992	0.11	0.65087
6	0.14	0.40494	0.16	0.21731	0.24	0.00885	0.06	0.98810
7	0.24	0.01345	0.17	0.15539	0.23	0.01962	0.22	0.02920
8	0.12	0.56985	0.23	0.02124	0.24	0.01084	0.12	0.62471
9	0.16	0.24284	0.10	0.78322	0.19	0.09061	0.17	0.15825
10	0.13	0.45795	0.05	0.99883	0.13	0.49701	0.19	0.09297
11	0.12	0.59528	0.24	0.00932	0.15	0.31546	0.16	0.22617
12	0.27	0.00202	0.16	0.23933	0.29	0.00054	0.28	0.00138
13	0.36	0.00002	0.23	0.02004	0.33	0.00006	0.27	0.00240
14	0.25	0.00619	0.13	0.53530	0.18	0.11600	0.27	0.00237
15	0.30	0.00034	0.15	0.31522	0.30	0.00046	0.21	0.03952
16	0.30	0.00038	0.17	0.18680	0.25	0.00753	0.27	0.00170
17	0.16	0.25376	0.06	0.99192	0.10	0.78413	0.18	0.15033
18	0.29	0.00058	0.27	0.00179	0.20	0.06595	0.24	0.01142
19	0.27	0.00173	0.20	0.05847	0.23	0.01558	0.25	0.00616
20	0.23	0.01656	0.21	0.04081	0.28	0.00122	0.14	0.43113
21	0.23	0.01577	0.11	0.67882	0.15	0.35123	0.15	0.30450
22	0.08	0.93344	0.12	0.64309	0.18	0.13724	0.13	0.45218

Appendix B Table 46 Rhythmic analysis of *cyc*^{01} behaviour in DD conditions

The table is pertinent to Figure 4.5.5B. Each row indicates an individual *cyc*^{01} male fly's rhythmic analysis of all four Trumelan behaviours via eJTK_Cycle. See Chapter 2.10 for more information.

	LO		SA		SSB		SSL	
Fly	**Tau**	**emp p**	**Tau**	**emp p**	**Tau**	**emp p**	**Tau**	**emp p**
1	0.25	0.00791	0.09	0.89647	0.13	0.51077	0.28	0.00139
2	0.11	0.72286	0.10	0.77883	0.22	0.02795	0.15	0.35267
3	0.26	0.00431	0.14	0.44534	0.24	0.01336	0.31	0.00015
4	0.29	0.00084	0.19	0.08607	0.29	0.00079	0.34	0.00003
5	0.13	0.49063	0.20	0.07083	0.10	0.78469	0.10	0.81905
6	0.22	0.02904	0.14	0.40921	0.28	0.00141	0.20	0.07251
7	0.28	0.00141	0.16	0.26354	0.25	0.00808	0.17	0.16616
8	0.12	0.64107	0.08	0.95559	0.16	0.23850	0.11	0.71601
9	0.18	0.12013	0.16	0.24686	0.25	0.00741	0.09	0.86446
10	0.22	0.02264	0.09	0.87099	0.19	0.10038	0.20	0.06070
11	0.10	0.82393	0.09	0.89040	0.07	0.97292	0.08	0.94771
12	0.08	0.95369	0.10	0.77338	0.10	0.77004	0.09	0.87278
13	0.11	0.74660	0.13	0.53216	0.10	0.75588	0.10	0.80507
14	0.12	0.59073	0.18	0.11831	0.12	0.59963	0.13	0.49170
15	0.12	0.59218	0.16	0.23929	0.13	0.52394	0.07	0.96539
16	0.15	0.34928	0.06	0.98763	0.14	0.41730	0.11	0.72939
17	0.19	0.10723	0.17	0.17044	0.13	0.50979	0.13	0.50261
18	0.07	0.97220	0.14	0.38978	0.22	0.03170	0.07	0.96397
19	0.19	0.08156	0.09	0.86945	0.17	0.16044	0.17	0.16342
20	0.09	0.87077	0.16	0.26657	0.11	0.70498	0.15	0.32965

Appendix B Table 47 Rhythmic analysis of ceiling occupancy for BK, *per*^{01}, and *cyc*^{01} male flies in DD conditions

The table is pertinent to Figure 4.5.6B. The tau and associated empirical p-value via eJTK_Cycle for analysis of LO and Roost ceiling occupancy rhythms for BK, *per*^{01} and *cyc*^{01} males in DD conditions. See Chapter 2.10 for more information.

	BK DD				***per*^{01} DD**				***cyc*^{01} DD**			
	LO		**Roost**		**LO**		**Roost**		**LO**		**Roost**	
Fly	**Tau**	**emp p**	**Tau**	**emp p**	**Tau**	**emp p**	**Tau**	**emp p**	**Tau**	**emp p**	**Tau**	**emp p**
1	0.22	0.04853	0.08	0.96342	0.14	0.42996	0.20	0.07138	0.15	0.48745	0.18	0.26763
2	0.26	0.11917	0.16	0.70314	0.31	0.00040	0.23	0.01926	0.17	0.19462	0.26	0.00562
3	0.28	0.03714	0.22	0.19413	0.08	0.96095	0.11	0.71144	0.18	0.18668	0.20	0.11082
4	0.16	0.56936	0.39	0.00059	0.21	0.05175	0.28	0.00281	0.22	0.08819	0.17	0.31942
5	0.24	0.05484	0.38	0.00006	0.25	0.00979	0.18	0.14742	0.15	0.36270	0.13	0.54063
6	0.37	0.00080	0.39	0.00029	0.25	0.01254	0.40	0.00001	0.14	0.50859	0.11	0.78554
7	0.40	0.00028	0.52	0.00001	0.22	0.05827	0.27	0.00842	0.21	0.08499	0.17	0.26158
8	0.26	0.03494	0.27	0.02568	0.25	0.00946	0.28	0.00272	0.12	0.76581	0.19	0.18399
9	0.19	0.45706	0.35	0.00437	0.20	0.12073	0.21	0.09102	0.05	0.99913	0.23	0.02548
10	0.27	0.10437	0.15	0.75001	0.19	0.08891	0.21	0.04337	0.09	0.92925	0.22	0.07934
11	0.37	0.00241	0.37	0.00283	0.19	0.21585	0.19	0.23748	0.20	0.19032	0.19	0.25526
12	0.36	0.00004	0.36	0.00002	0.17	0.18896	0.23	0.01982	0.14	0.59877	0.20	0.20025
13	0.18	0.29206	0.60	0.00001	0.16	0.31498	0.26	0.00662	0.22	0.21429	0.17	0.48213
14	0.21	0.07056	0.39	0.00002	0.24	0.02304	0.24	0.02195	0.17	0.24901	0.10	0.81131
15	0.37	0.00007	0.32	0.00072	0.07	0.98021	0.15	0.34283	0.23	0.10571	0.15	0.59988
16	0.32	0.00346	0.48	0.00001	0.14	0.38836	0.15	0.34340	0.13	0.67495	0.22	0.09066
17	0.47	0.00001	0.48	0.00001	0.23	0.07749	0.13	0.72118	0.10	0.87463	0.18	0.17136
18	0.20	0.13412	0.53	0.00001	0.17	0.36388	0.23	0.06246	0.13	0.85166	0.20	0.29843
19	0.43	0.00001	0.48	0.00001	0.26	0.00555	0.34	0.00002	0.19	0.29938	0.23	0.10566
20	0.32	0.00117	0.44	0.00001	0.19	0.08943	0.24	0.01505	0.16	0.59624	0.32	0.00928
21	0.29	0.00296	0.21	0.10047	0.30	0.00030	0.24	0.00950	NA	NA	NA	NA
22	0.31	0.00158	0.18	0.25939	0.13	0.48538	0.25	0.00613	NA	NA	NA	NA
23	0.43	0.00001	0.20	0.12506	NA	NA	NA	NA	NA	NA	NA	NA
24	0.28	0.00493	0.27	0.00676	NA	NA	NA	NA	NA	NA	NA	NA
25	0.23	0.03411	0.26	0.01126	NA	NA	NA	NA	NA	NA	NA	NA

	BK DD				*per*^{01} DD				*cyc*^{01} DD			
26	0.37	0.00003	0.31	0.00039	NA	NA	NA	NA	NA	NA	NA	NA
27	0.17	0.29925	0.09	0.94551	NA	NA	NA	NA	NA	NA	NA	NA
28	0.27	0.00671	0.25	0.01562	NA	NA	NA	NA	NA	NA	NA	NA
29	0.30	0.00110	0.14	0.48772	NA	NA	NA	NA	NA	NA	NA	NA
30	0.32	0.00132	0.14	0.56570	NA	NA	NA	NA	NA	NA	NA	NA
31	0.29	0.00133	0.53	0.00001	NA	NA	NA	NA	NA	NA	NA	NA

Appendix B Table 48 Rhythmic amplitude of ceiling occupancy for *per*^{01} and *cyc*^{01} males vs. BK males in DD conditions

The table is pertinent to Figure 4.5.6C. Each row is a DABEST comparison of the rhythmic amplitude (Tau) of either LO or Roost ceiling occupancy in circadian mutant males vs. BK males. See Chapter 2.6 for more information about DABEST plots.

State	Ctr / Test	Sample Size Ctr (n)	Sample Size Test (n)	Ctr Mean±CI (Tau)	Test Mean±CI (Tau)	Delta (Tau)	Delta-CI (Tau)	Delta+CI (Tau)	p-value
LO	BK / *per*^{01}	31	22	0.29±0.03	0.20±0.03	-0.10	-0.14	-0.06	0.0000
LO	BK / *cyc*^{01}	31	20	0.29±0.03	0.16±0.02	-0.14	-0.17	-0.11	0.0000
Roost	BK / *per*^{01}	31	22	0.32±0.05	0.23±0.03	-0.09	-0.15	-0.03	0.0062
Roost	BK / *cyc*^{01}	31	20	0.32±0.05	0.19±0.02	-0.13	-0.18	-0.08	0.0006

Appendix B Table 49 Light has no effect on magnitude of daily ceiling occupancy shift

The table is pertinent to Figure 4.5.7. The first level of analysis computes the difference between night and day for ceiling occupancy of Roost data in LD and DD conditions. The delta-delta computes the difference between the LD and DD experimental deltas. See Chapter 2.6 for more information about DABEST plots.

Genotype	Sex	Light Cycle	Ctr / Test	Sample Size (n)	Ctr Mean±CI (mm)	Test Mean±CI (mm)	Delta (mm)	Delta-CI (mm)	Delta+CI (mm)	p-value
BK	M	LD	Day / Night	60	16.58±3.25	43.70±6.58	25.84	16.53	35.04	0.0000
BK	M	DD	Day / Night	31	20.86±6.38	46.69±9.09	27.12	21.52	33.04	0.0000
BK	M	DD - LD	Day / Night	N/A	N/A	N/A	1.29	-9.75	12.26	0.8740
*per*01	M	LD	Day / Night	40	26.02±5.80	29.51±7.43	1.93	-2.12	5.69	0.3340
per01	M	DD	Day / Night	22	23.40±7.67	25.32±9.11	3.48	-2.22	9.92	0.2638
per01	M	DD - LD	Day / Night	N/A	N/A	N/A	1.56	-5.32	8.97	0.6698
*cyc*01	M	LD	Day / Night	30	23.81±6.95	28.77±8.53	0.59	-3.31	8.08	0.8698
*cyc*01	M	DD	Day / Night	20	13.27±3.47	13.85±6.55	4.96	-4.84	15.11	0.3444
*cyc*01	M	DD - LD	Day / Night	N/A	N/A	N/A	4.37	-7.03	15.68	0.4518

Appendix C Chapter 5

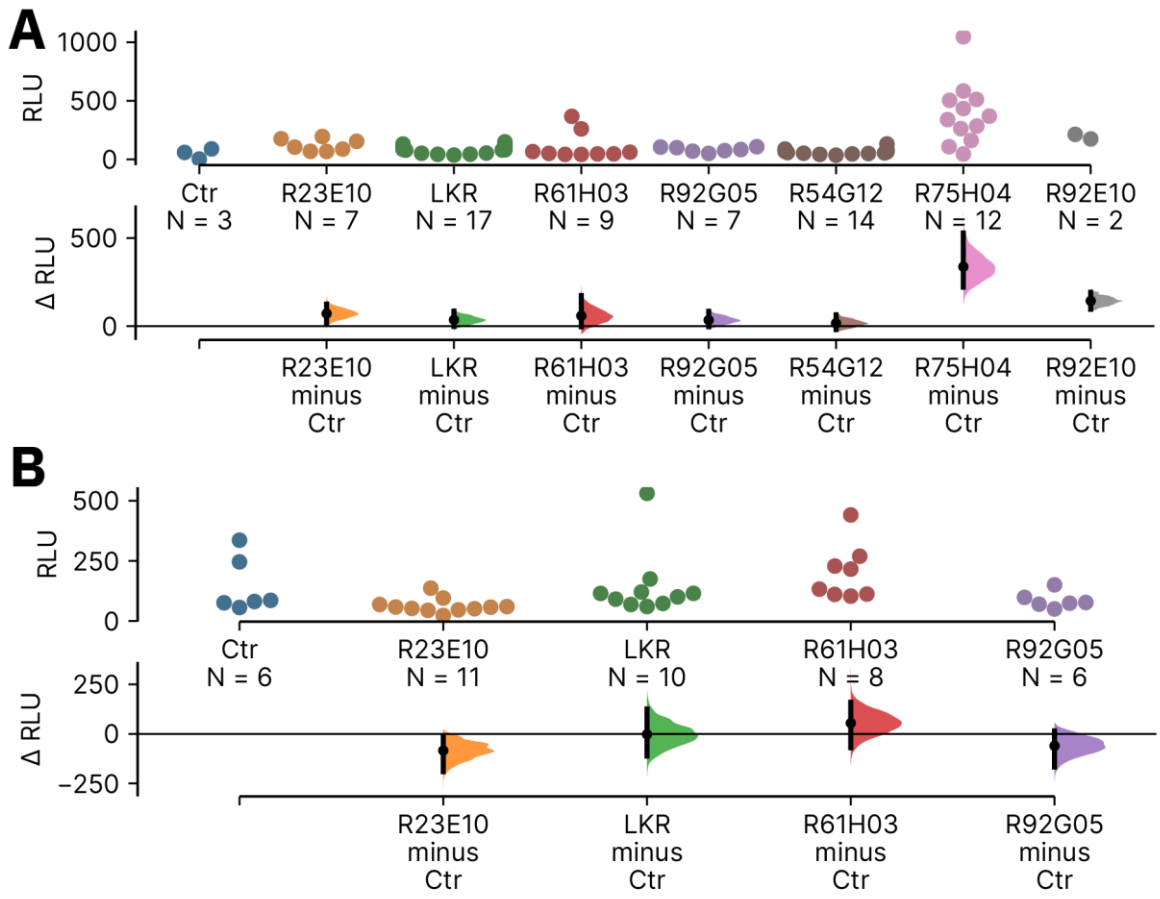

Appendix C Figure 1 Bioluminescence of driver>TRIC-LUC lines vs. a driverless control

DABEST plot comparing the mean bioluminescence (RLU) for driver>TRIC-LUC flies vs. Ctr>TRIC-LUC for males **(A)** and females **(B)**. See Chapter 2.6 for more information about the structure of DABEST plots.

Appendix C Table 1 Bioluminescence of driver>TRIC-LUC lines vs. a driverless control

The table is pertinent to Appendix C Figure 1. Each row is a DABEST comparison of the mean bioluminescence from detrended raw data between a driver>TRIC-LUC genotype vs. Control>TRIC-LUC flies of the same sex. See Chapter 2.6 for more information about DABEST plots.

Ctr	Test	Sex	Ctr (n)	Test (n)	Ctr Mean±CI (RLU)	Test Mean±CI (RLU)	Delta (RLU)	Delta-CI (RLU)	Delta+CI (RLU)	p-value
Ctr	R23E10	M	3	7	50.48±49.60	121.81±38.92	71.33	18.49	124.94	0.0762
Ctr	LKR	M	3	17	50.48±49.60	85.74±15.56	35.26	-1.98	85.11	0.1264
Ctr	R61H03	M	3	9	50.48±49.60	109.21±77.85	58.73	-4.06	173.44	0.4774
Ctr	R92G05	M	3	7	50.48±49.60	84.46±15.53	33.98	-2.77	83.80	0.1102
Ctr	R54G12	M	3	14	50.48±49.60	66.72±12.97	16.24	-20.02	63.62	0.3478
Ctr	R75H04	M	3	12	50.48±49.60	387.50±150.52	337.02	221.34	528.98	0.0506
Ctr	R92E10	M	3	2	50.48±49.60	193.81±38.27	143.33	95.02	191.64	0.0000
Ctr	R23E10	F	6	11	146.86±92.54	63.09±17.81	-83.77	-190.59	-12.81	0.0268
Ctr	LKR	F	6	10	146.86±92.54	144.93±86.52	-1.93	-111.34	126.22	0.9868
Ctr	R61H03	F	6	8	146.86±92.54	201.68±80.09	54.82	-69.64	159.58	0.4084
Ctr	R92G05	F	6	6	146.86±92.54	86.69±27.83	-60.17	-167.09	15.16	0.3086

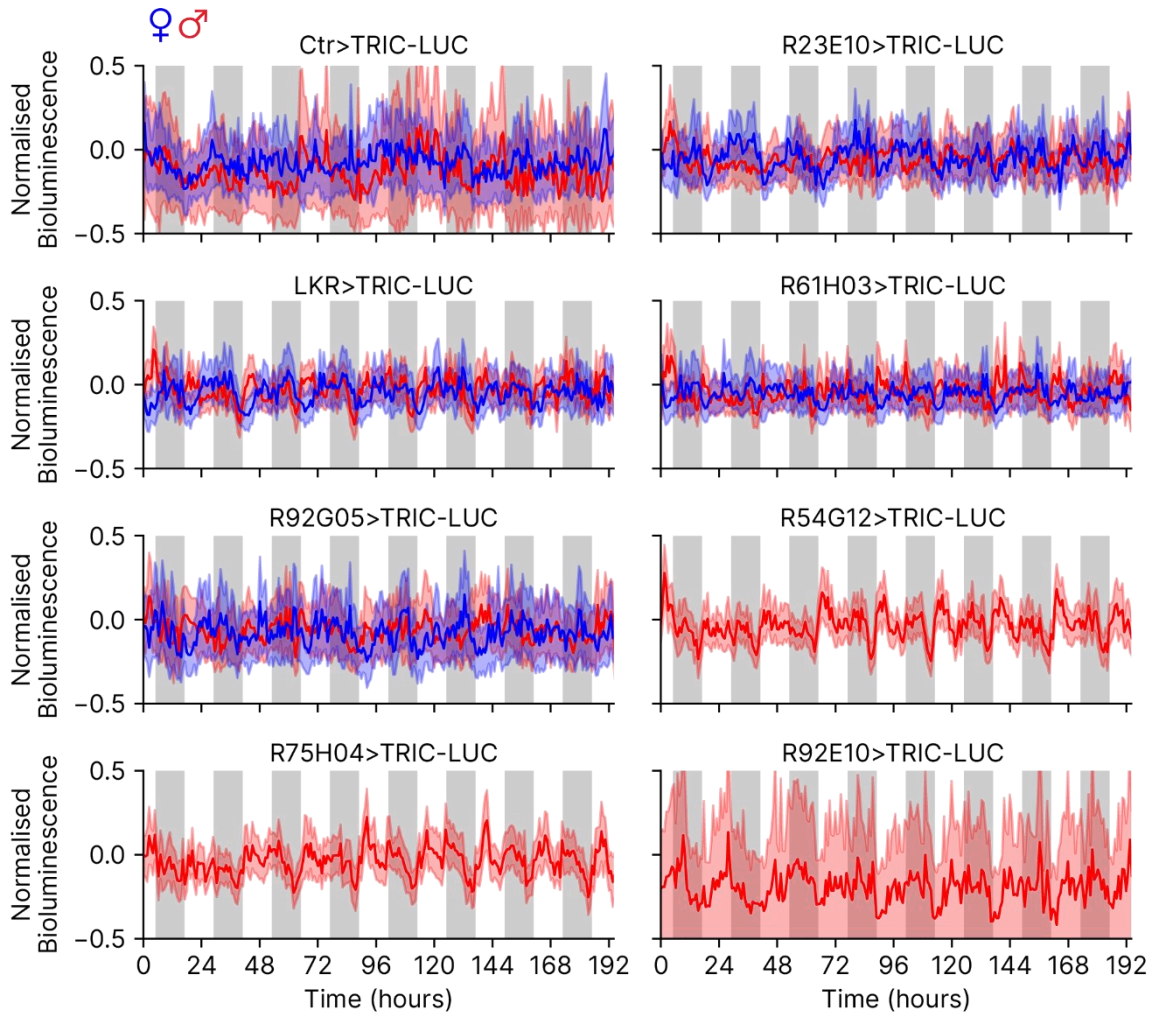

Appendix C Figure 2 Time series plots of driver>TRIC-LUC flies

Average normalised and detrended bioluminescence signal over the course of the experiment from TRIC-LUC males and females with various driver lines. The solid line indicates the mean, the shaded area indicates the 95%CI.

Appendix C

Appendix C Table 2 Control>CaLexA-LUC flies have relatively low bioluminescence

The table is pertinent to Figure 5.1.1B. DABEST comparison of the driverless CaLexA-LUC control females vs. males for their mean bioluminescence from the detrended data. See Chapter 2.6 for more information about DABEST plots.

Genotype	Ctr	Test	Ctr (n)	Test (n)	Ctr Mean±CI (RLU)	Test Mean±CI (RLU)	Delta (RLU)	Delta-CI (RLU)	Delta+CI (RLU)	p-value
Ctr>CaLexA-LUC	Males	Females	13	13	73.58±14.27	99.80±13.39	26.22	9.22	47.57	0.0094

Appendix C Table 3 elav>CaLexA-LUC has strong bioluminescence signal

The table is pertinent to Figure 5.1.2B. DABEST comparison of the mean bioluminescence from the detrended data for pan-neuronal elav>CaLexA-LUC females vs. the driverless CaLexA control females. See Chapter 2.6 for more information about DABEST plots.

Ctr	Test	Sex	Ctr (n)	Test (n)	Ctr Mean±CI (RLU)	Test Mean±CI (RLU)	Delta (RLU)	Delta-CI (RLU)	Delta+CI (RLU)	p-value
Ctr>CaLexA-LUC	elav>CaLexA-LUC	F	13	17	99.80±13.39	826.36±158.17	726.56	587.42	896.97	0.0000

Appendix C Table 4 MB504B>CaLexA-LUC has extremely low bioluminescence signal

The table is pertinent to Figure 5.1.6B. DABEST comparison of the mean bioluminescence from the detrended data for MB504B>CaLexA-LUC vs. the driverless CaLexA control of the same sex. See Chapter 2.6 for more information about DABEST plots.

Ctr	Test	Sex	Ctr (n)	Test (n)	Ctr Mean±CI (RLU)	Test Mean±CI (RLU)	Delta (RLU)	Delta-CI (RLU)	Delta+CI (RLU)	p-value
Ctr>CaLexA-LUC	MB504B>CaLexA-LUC	M	13	15	73.58±14.27	54.08±14.50	-19.50	-38.04	1.75	0.0794
Ctr>CaLexA-LUC	MB504B>CaLexA-LUC	F	13	15	99.80±13.39	67.74±11.30	-32.06	-49.72	-15.44	0.0014

Appendix C Table 5 GeNL signal begins far greater than FLuc levels

The table is pertinent to Figure 5.2.3A. Each row is a DABEST comparison of the mean raw bioluminescence during the first ten hours of recording for nsyb>GeNL with varying concentrations of FFz vs. nsyb>CaLexA-LUC. See Chapter 2.6 for more information about DABEST plots.

Ctr	Test	Sex	Ctr (n)	Test (n)	Ctr Mean±CI (Log10 RLU)	Test Mean±CI (Log10 RLU)	Delta (Log10 RLU)	Delta-CI (Log10 RLU)	Delta+CI (Log10 RLU)	p-value
CaLexA	GeNL with 0.05mM	M	24	5	2.04±0.18	3.18±0.48	1.14	0.48	1.47	0.0000
CaLexA	GeNL with 0.1mM	M	24	15	2.04±0.18	4.52±0.70	2.47	1.87	3.26	0.0000
CaLexA	GeNL with 0.67mM	M	24	5	2.04±0.18	4.89±0.92	2.84	2.08	3.77	0.0000
CaLexA	GeNL with 0.05mM	F	24	4	1.75±0.19	3.83±1.36	2.08	1.02	3.37	0.0000
CaLexA	GeNL with 0.1mM	F	24	24	1.75±0.19	4.11±0.62	2.36	1.78	3.05	0.0000
CaLexA	GeNL with 0.67mM	F	24	4	1.75±0.19	4.71±1.28	2.96	1.80	4.01	0.0000

Appendix C Table 6 GeNL signal rapidly decays to FLuc levels

The table is pertinent to Figure 5.2.3B. Each row is a DABEST comparison of the mean raw bioluminescence during the period of 100-110 hours from the start of recording for nsyb>GeNL with varying concentrations of FFz vs. nsyb>CaLexA-LUC. See Chapter 2.6 for more information about DABEST plots.

Ctr	Test	Sex	Ctr (n)	Test (n)	Ctr Mean±CI (Log10 RLU)	Test Mean±CI (Log10 RLU)	Delta (Log10 RLU)	Delta-CI (Log10 RLU)	Delta+CI (Log10 RLU)	p-value
CaLexA	GeNL with 0.05mM	M	24	5	1.26±0.11	1.48±0.51	0.22	-0.19	0.77	0.1838
CaLexA	GeNL with 0.1mM	M	24	15	1.26±0.11	1.69±0.40	0.43	0.09	0.90	0.0176
CaLexA	GeNL with 0.67mM	M	24	5	1.26±0.11	2.72±0.76	1.46	0.98	2.52	0.0000
CaLexA	GeNL with 0.05mM	F	24	4	1.42±0.20	1.24±0.16	-0.18	-0.43	0.03	0.4844
CaLexA	GeNL with 0.1mM	F	24	24	1.42±0.20	1.54±0.23	0.12	-0.15	0.43	0.4348
CaLexA	GeNL with 0.67mM	F	24	4	1.42±0.20	2.97±1.24	1.55	0.44	2.53	0.0010

Appendix C

Appendix C Table 7 GeNLCa signal begins far greater than FLuc levels

The table is pertinent to Figure 5.2.5A. Each row is a DABEST comparison of the mean raw bioluminescence during the first ten hours of recording for nsyb>GeNLCa with varying concentrations of FFz vs. nsyb>CaLexA-LUC. See Chapter 2.6 for more information about DABEST plots.

Ctr	Test	Sex	Ctr (n)	Test (n)	Ctr Mean±CI (Log10 RLU)	Test Mean±CI (Log10 RLU)	Delta (Log10 RLU)	Delta-CI (Log10 RLU)	Delta+CI (Log10 RLU)	p-value
CaLexA	GeNLCa with 0.05mM	M	24	5	2.04±0.18	3.18±0.48	1.14	0.48	1.47	0.0000
CaLexA	GeNLCa with 0.1mM	M	24	15	2.04±0.18	4.52±0.70	2.47	1.87	3.26	0.0000
CaLexA	GeNLCa with 0.67mM	M	24	5	2.04±0.18	4.89±0.92	2.84	2.08	3.77	0.0000
CaLexA	GeNLCa with 0.05mM	F	24	4	1.75±0.19	3.83±1.36	2.08	1.02	3.37	0.0000
CaLexA	GeNLCa with 0.1mM	F	24	24	1.75±0.19	4.11±0.62	2.36	1.78	3.05	0.0000
CaLexA	GeNLCa with 0.67mM	F	24	4	1.75±0.19	4.71±1.28	2.96	1.80	4.01	0.0000

Appendix C Table 8 GeNLCa signal rapidly decays to FLuc levels

The table is pertinent to Figure 5.2.5B. Each row is a DABEST comparison of the mean raw bioluminescence during the period of 100-110 hours from the start of recording for nsyb>GeNLCa with varying concentrations of FFz vs. nsyb>CaLexA-LUC. See Chapter 2.6 for more information about DABEST plots.

Ctr	Test	Sex	Ctr (n)	Test (n)	Ctr Mean±CI (Log10 RLU)	Test Mean±CI (Log10 RLU)	Delta (Log10 RLU)	Delta-CI (Log10 RLU)	Delta+CI (Log10 RLU)	p-value
CaLexA	GeNLCa with 0.05mM	M	24	5	1.26±0.11	1.48±0.51	0.22	-0.19	0.77	0.1838
CaLexA	GeNLCa with 0.1mM	M	24	15	1.26±0.11	1.69±0.40	0.43	0.09	0.90	0.0176
CaLexA	GeNLCa with 0.67mM	M	24	5	1.26±0.11	2.72±0.76	1.46	0.98	2.52	0.0000
CaLexA	GeNLCa with 0.05mM	F	24	4	1.42±0.20	1.24±0.16	-0.18	-0.43	0.03	0.4844
CaLexA	GeNLCa with 0.1mM	F	24	24	1.42±0.20	1.54±0.23	0.12	-0.15	0.43	0.4348

CaLexA	GeNLCa with 0.67mM	F	24	4	1.42±0.20	2.97±1.24	1.55	0.44	2.53	0.0010

Appendix C Table 9 TMP has a minor impact on bioluminescence levels in Ctr>*tim*-LUC flies

The table is pertinent to Figure 5.3.1C. Each row is a DABEST comparison of the mean raw bioluminescence for driverless controls with added TMP vs. without, for a given sex. See Chapter 2.6 for more information about DABEST plots.

Ctr	Test	Sex	Ctr (n)	Test (n)	Ctr Mean±CI (RLU)	Test Mean±CI (RLU)	Delta (RLU)	Delta-CI (RLU)	Delta+CI (RLU)	p-value
Ctr>*tim*-LUC -TMP	Ctr>*tim*-LUC +TMP	M	24	24	44.17±11.84	92.82±44.04	48.64	12.01	104.65	0.0392
Ctr>*tim*-LUC -TMP	Ctr>*tim*-LUC +TMP	F	24	24	45.32±22.14	98.72±61.84	53.40	10.85	168.13	0.0698

Appendix C Table 10 Addition of a driver greatly increases *tim*-LUC activity, while TMP addition has a mild effect on increasing bioluminescence

The table is pertinent to Figure 5.3.2C. Each row is a DABEST comparison of the mean raw bioluminescence for circadian neuron (tim(uas)-GAL4) driver>*tim*-LUC flies with or without TMP addition to the food vs. a driverless control (Ctr>*tim*-LUC) of the same sex without TMP addition. See Chapter 2.6 for more information about DABEST plots.

Ctr	Test	Sex	Ctr (n)	Test (n)	Ctr Mean±CI (Log10 RLU)	Test Mean±CI (Log10 RLU)	Delta (Log10 RLU)	Delta-CI (Log10 RLU)	Delta+CI (Log10 RLU)	p-value
Ctr>*tim*-LUC -TMP	tim>*tim*-LUC -TMP	M	24	12	1.54±0.10	3.51±0.18	1.97	1.78	2.18	0.0000
Ctr>*tim*-LUC -TMP	tim>*tim*-LUC +TMP	M	24	12	1.54±0.10	3.83±0.11	2.29	2.12	2.41	0.0000
Ctr>*tim*-LUC -TMP	tim>*tim*-LUC -TMP	F	24	24	1.49±0.14	2.70±0.13	1.21	1.00	1.37	0.0000
Ctr>*tim*-LUC -TMP	tim>*tim*-LUC +TMP	F	24	24	1.49±0.14	3.14±0.05	1.65	1.49	1.79	0.0000

Appendix C Table 11 OK371>CRE-LUC has very low bioluminescence regardless of TMP addition

The table is pertinent to Figure 5.3.3C. Each row is a DABEST comparison of the mean raw bioluminescence for a dopaminergic (OK371-GAL4) driver>CRE-LUC flies with or without TMP addition to the food vs. a driverless control (Ctr>CRE-LUC) of the same sex without TMP addition. See Chapter 2.6 for more information about DABEST plots.

Ctr	Test	Sex	Ctr (n)	Test (n)	Ctr Mean±CI (RLU)	Test Mean±CI (RLU)	Delta (RLU)	Delta-CI (RLU)	Delta+CI (RLU)	p-value
Ctr>CRE-LUC -TMP	OK371>CRE-LUC -TMP	M	23	8	21.91±2.52	47.25±5.20	25.34	19.76	30.85	0.0000
Ctr>CRE-LUC -TMP	OK371>CRE-LUC +TMP	M	23	12	21.91±2.52	52.95±16.44	31.04	18.58	52.70	0.0000
Ctr>CRE-LUC -TMP	OK371>CRE-LUC -TMP	F	24	4	22.63±4.64	56.07±31.99	33.44	14.08	69.27	0.0040
Ctr>CRE-LUC -TMP	OK371>CRE-LUC +TMP	F	24	11	22.63±4.64	82.81±36.66	60.18	31.16	101.83	0.0000

Appendix C Table 12 kurs58>CRE-LUC has very low bioluminescence regardless of TMP addition

The table is pertinent to Figure 5.3.4C. Each row is a DABEST comparison of the mean raw bioluminescence for a pars intercerebralis (kurs58-GAL4) driver>CRE-LUC flies with or without TMP addition to the food vs. a driverless control (Ctr>CRE-LUC) of the same sex without TMP addition. See Chapter 2.6 for more information about DABEST plots.

Ctr	Test	Sex	Ctr (n)	Test (n)	Ctr Mean±CI (RLU)	Test Mean±CI (RLU)	Delta (RLU)	Delta-CI (RLU)	Delta+CI (RLU)	p-value
Ctr>CRE-LUC -TMP	kurs58>CRE-LUC -TMP	M	23	12	21.91±2.52	28.29±4.47	6.38	2.02	11.73	0.0118
Ctr>CRE-LUC -TMP	kurs58>CRE-LUC +TMP	M	23	13	21.91±2.52	48.99±27.51	27.08	10.84	83.29	0.0000
Ctr>CRE-LUC -TMP	kurs58>CRE-LUC -TMP	F	24	16	22.63±4.64	39.40±9.12	16.77	8.33	29.40	0.0004
Ctr>CRE-LUC -TMP	kurs58>CRE-LUC +TMP	F	24	12	22.63±4.64	45.33±17.46	22.70	8.44	45.46	0.0046

Appendix C Table 13 Developmental TMP addition has no effect on OK371>CRE-LUC signal

The table is pertinent to Figure 5.3.5C. Each row is a DABEST comparison of the mean raw bioluminescence when adding TMP during development and/or the experimental food media vs. neither in OK371>CRE-LUC flies. See Chapter 2.6 for more information about DABEST plots.

Ctr	Test	Sex	Ctr (n)	Test (n)	Ctr Mean±CI (RLU)	Test Mean±CI (RLU)	Delta (RLU)	Delta-CI (RLU)	Delta+CI (RLU)	p-value
-deTMP	-dTMP +eTMP	M	8	16	18.87±4.87	18.46±3.14	-0.40	-7.05	4.24	0.8858
-deTMP	+dTMP -eTMP	M	8	18	18.87±4.87	27.03±13.15	8.17	-2.39	25.22	0.5808
-deTMP	+dTMP +eTMP	M	8	12	18.87±4.87	22.96±6.64	4.09	-2.47	13.64	0.4698

List of References

Achermann, P. *et al.* (1993) “A model of human sleep homeostasis based on EEG slow-wave activity: quantitative comparison of data and simulations,” *Brain research bulletin*, 31(1–2), pp. 97–113.

Afonso, D. J. S. *et al.* (2015) “TARANIS Functions with Cyclin A and Cdk1 in a Novel Arousal Center to Control Sleep in Drosophila,” *Current biology: CB*, 25(13), pp. 1717–1726.

Agostini, C. (1898) *Sui disturbi psichici e sulle alterazioni del sistema nervoso centrale per insonnia assoluta*. Tipografia di Stefano Calderini e figlio.

Agosto, J. *et al.* (2008) “Modulation of GABAA receptor desensitization uncouples sleep onset and maintenance in Drosophila,” *Nature neuroscience*, 11(3), pp. 354–359.

Ajayi, O. M. *et al.* (2022) “Behavioral and postural analyses establish sleep-like states for mosquitoes that can impact host landing and blood feeding,” *The journal of experimental biology*. The Company of Biologists, 225(11). doi: 10.1242/jeb.244032.

Alam, M. A. *et al.* (2014) “Neuronal activity in the preoptic hypothalamus during sleep deprivation and recovery sleep,” *Journal of neurophysiology*, 111(2), pp. 287–299.

Al-Anzi, B. *et al.* (2010) “The leucokinin pathway and its neurons regulate meal size in Drosophila,” *Current biology: CB*, 20(11), pp. 969–978.

Allada, R. *et al.* (1998) “A mutant Drosophila homolog of mammalian Clock disrupts circadian rhythms and transcription of period and timeless,” *Cell*, 93(5), pp. 791–804.

Allada, R. and Chung, B. Y. (2010) “Circadian organization of behavior and physiology in Drosophila,” *Annual review of physiology*, 72, pp. 605–624.

van Alphen, B. *et al.* (2013) “A dynamic deep sleep stage in Drosophila,” *The Journal of neuroscience: the official journal of the Society for Neuroscience*, 33(16), pp. 6917–6927.

Altman, D. G. and Bland, J. M. (1983) “Measurement in Medicine: The Analysis of Method Comparison Studies,” *Journal of the Royal Statistical Society. Series D (The Statistician)*. [Royal Statistical Society, Wiley], 32(3), pp. 307–317.

Andretic, R. and Shaw, P. J. (2005) “Essentials of sleep recordings in Drosophila: moving beyond sleep time,” *Methods in enzymology*, 393, pp. 759–772.

Andretic, R., van Swinderen, B. and Greenspan, R. J. (2005) “Dopaminergic modulation of arousal in Drosophila,” *Current biology: CB*, 15(13), pp. 1165–1175.

Arnulf, I., Groos, E. and Dodet, P. (2018) “Kleine–Levin syndrome: A neuropsychiatric disorder,” *Revue neurologique*, 174(4), pp. 216–227.

Artiushin, G. *et al.* (2018) “Endocytosis at the Drosophila blood-brain barrier as a function for sleep,” *eLife*, 7. doi: 10.7554/eLife.43326.

Asahina, K. (2018) “Sex differences in Drosophila behavior: qualitative and quantitative dimorphism,” *Current opinion in physiology*. Elsevier BV, 6, pp. 35–45.

Aso, Y., Sitaraman, D., *et al.* (2014) “Mushroom body output neurons encode valence and guide memory-based action selection in Drosophila,” *eLife*, 3, p. e04580.

Aso, Y., Hattori, D., *et al.* (2014) “The neuronal architecture of the mushroom body provides a logic for associative learning,” *eLife*, 3, p. e04577.

Aston-Jones, G. and Bloom, F. E. (1981) “Activity of norepinephrine-containing locus coeruleus neurons in behaving rats anticipates fluctuations in the sleep-waking cycle,” *The Journal of neuroscience: the official journal of the Society for Neuroscience*, 1(8), pp. 876–886.

Attwell, D. and Gibb, A. (2005) “Neuroenergetics and the kinetic design of excitatory synapses,” *Nature reviews. Neuroscience*, 6(11), pp. 841–849.

Awasaki, T. *et al.* (2008) “Organization and postembryonic development of glial cells in the adult central brain of Drosophila,” *The Journal of neuroscience: the official journal of the Society for Neuroscience*, 28(51), pp. 13742–13753.

Axelrod, S., Saez, L. and Young, M. W. (2015) “Studying circadian rhythm and sleep using genetic screens in Drosophila,” *Methods in enzymology*, 551, pp. 3–27.

Ayas, N. T. *et al.* (2003) “A prospective study of sleep duration and coronary heart disease in women,” *Archives of internal medicine*, 163(2), pp. 205–209.

Baker, P. F., Hodgkin, A. L. and Ridgway, E. B. (1971) “Depolarization and calcium entry in squid giant axons,” *The Journal of physiology*, 218(3), pp. 709–755.

Balduzzi, D. and Tononi, G. (2013) “What can neurons do for their brain? Communicate selectivity with bursts,” *Theory in biosciences = Theorie in den Biowissenschaften*, 132(1), pp. 27–39.

Baldwin, C. M. *et al.* (2001) “The association of sleep-disordered breathing and sleep symptoms with quality of life in the Sleep Heart Health Study,” *Sleep*, 24(1), pp. 96–105.

Barber, A. F. *et al.* (2016) “Circadian and feeding cues integrate to drive rhythms of physiology in Drosophila insulin-producing cells,” *Genes & development*, 30(23), pp. 2596–2606.

Barlow, H. B. (1985) “The twelfth Bartlett memorial lecture: the role of single neurons in the psychology of perception,” *The Quarterly journal of experimental psychology. A, Human experimental psychology*, 37(2), pp. 121–145.

Barth, A. L. and Poulet, J. F. A. (2012) “Experimental evidence for sparse firing in the neocortex,” *Trends in neurosciences*, 35(6), pp. 345–355.

Basner, M., Müller, U. and Griefahn, B. (2010) “Practical guidance for risk assessment of traffic noise effects on sleep,” *Applied Acoustics*, 71(6), pp. 518–522.

Basta, M. *et al.* (2007) “CHRONIC INSOMNIA AND STRESS SYSTEM,” *Sleep medicine clinics*, 2(2), pp. 279–291.

Bates, A. S. *et al.* (2020) “Complete Connectomic Reconstruction of Olfactory Projection Neurons in the Fly Brain,” *Current biology: CB*, 30(16), pp. 3183-3199.e6.

Beckwith, E. J. and French, A. S. (2019) “Sleep in Drosophila and Its Context,” *Frontiers in physiology*, 10, p. 1167.

Belenky, G. *et al.* (2003) “Patterns of performance degradation and restoration during sleep restriction and subsequent recovery: a sleep dose-response study,” *Journal of sleep research*. Wiley, 12(1), pp. 1–12.

Belvin, M. P., Zhou, H. and Yin, J. C. (1999) “The Drosophila dCREB2 gene affects the circadian clock,” *Neuron*, 22(4), pp. 777–787.

Benedetto, L., Chase, M. H. and Torterolo, P. (2012) “GABAergic processes within the median preoptic nucleus promote NREM sleep,” *Behavioural brain research*, 232(1), pp. 60–65.

Bentivoglio, M. and Grassi-Zucconi, G. (1997) “The pioneering experimental studies on sleep deprivation,” *Sleep*, 20(7), pp. 570–576.

Bland, J. M. and Altman, D. G. (1986) “Statistical methods for assessing agreement between two methods of clinical measurement,” *The Lancet*, 1(8476), pp. 307–310.

Blau, J. and Young, M. W. (1999) “Cycling vrille expression is required for a functional Drosophila clock,” *Cell*, 99(6), pp. 661–671.

Boivin, D. B. and Boudreau, P. (2014) “Impacts of shift work on sleep and circadian rhythms,” *Pathologie-biologie*, 62(5), pp. 292–301.

Borbély, A. A. (1982) “A two process model of sleep regulation,” *Human neurobiology*, 1(3), pp. 195–204.

Borbély, A. A. *et al.* (2016) “The two-process model of sleep regulation: a reappraisal,” *Journal of sleep research*. Wiley, 25(2), pp. 131–143.

Brainard, J. *et al.* (2015) “Health implications of disrupted circadian rhythms and the potential for daylight as therapy,” *Anesthesiology*. Ovid Technologies (Wolters Kluwer Health), 122(5), pp. 1170–1175.

Brand, A. H. and Dormand, E. L. (1995) “The GAL4 system as a tool for unravelling the mysteries of the Drosophila nervous system,” *Current opinion in neurobiology*, 5(5), pp. 572–578.

Brand, A. H. and Perrimon, N. (1993) “Targeted gene expression as a means of altering cell fates and generating dominant phenotypes,” *Development* , 118(2), pp. 401–415.

Brandes, C. *et al.* (1996) “Novel features of drosophila period Transcription revealed by real-time luciferase reporting,” *Neuron*, 16(4), pp. 687–692.

Branson, K. *et al.* (2009) “High-throughput ethomics in large groups of Drosophila,” *Nature methods*, 6(6), pp. 451–457.

Brown, R. E. *et al.* (2012) “Control of sleep and wakefulness,” *Physiological reviews*, 92(3), pp. 1087–1187.

Burg, J. P. (1972) “The relationship between maximum entropy spectra and maximum likelihood spectra,” *Geophysics*. Society of Exploration Geophysicists, 37(2), pp. 375–376.

Bushey, D., Tononi, G. and Cirelli, C. (2009) “The Drosophila fragile X mental retardation gene regulates sleep need,” *The Journal of neuroscience: the official journal of the Society for Neuroscience*, 29(7), pp. 1948–1961.

Bushey, D., Tononi, G. and Cirelli, C. (2011) “Sleep and synaptic homeostasis: structural evidence in Drosophila,” *Science*, 332(6037), pp. 1576–1581.

Bushey, D., Tononi, G. and Cirelli, C. (2015) “Sleep- and wake-dependent changes in neuronal activity and reactivity demonstrated in fly neurons using in vivo calcium imaging,” *Proceedings of the National Academy of Sciences of the United States of America*, 112(15), pp. 4785–4790.

Buzsaki, G. *et al.* (1988) “Nucleus basalis and thalamic control of neocortical activity in the freely moving rat,” *The Journal of neuroscience: the official journal of the Society for Neuroscience*, 8(11), pp. 4007–4026.

Campbell, S. S. and Tobler, I. (1984) “Animal sleep: a review of sleep duration across phylogeny,” *Neuroscience and biobehavioral reviews*, 8(3), pp. 269–300.

Carskadon, M. A., Dement, W. C. and Others (2005) “Normal human sleep: an overview,” *Principles and practice of sleep medicine*. Elsevier Saunders Philadelphia, 4(1), pp. 13–23.

Carskadon, M. A. and Rechtschaffen, A. (2005) “Chapter 116 - Monitoring and Staging Human Sleep,” in Kryger, M. H., Roth, T., and Dement, W. C. (eds.) *Principles and Practice of Sleep Medicine (Fourth Edition)*. Philadelphia: W.B. Saunders, pp. 1359–1377.

Carskadon, M. A. and Rechtschaffen, A. (2011) “Monitoring and staging human sleep,” *Principles and practice of sleep medicine*, 5, pp. 16–26.

Cassill, D. L. *et al.* (2009) “Polyphasic wake/sleep episodes in the fire ant, Solenopsis invicta,” *Journal of insect behavior*. Springer Science and Business Media LLC, 22(4), pp. 313–323.

Cavanaugh, D. J. *et al.* (2014) “Identification of a circadian output circuit for rest:activity rhythms in Drosophila,” *Cell*, 157(3), pp. 689–701.

Cavey, M. *et al.* (2016) “Circadian rhythms in neuronal activity propagate through output circuits,” *Nature neuroscience*, 19(4), pp. 587–595.

Ceriani, M. F. *et al.* (1999) “Light-dependent sequestration of TIMELESS by CRYPTOCHROME,” *Science*, 285(5427), pp. 553–556.

Chattu, V. K. *et al.* (2018) “The Global Problem of Insufficient Sleep and Its Serious Public Health Implications,” *Healthcare (Basel, Switzerland)*, 7(1). doi: 10.3390/healthcare7010001.

Chen, W. *et al.* (2014) “Regulation of Drosophila circadian rhythms by miRNA let-7 is mediated by a regulatory cycle,” *Nature communications*, 5, p. 5549.

Chen, W.-F. *et al.* (2015) “A neuron-glia interaction involving GABA transaminase contributes to sleep loss in sleepless mutants,” *Molecular psychiatry*, 20(2), pp. 240–251.

Chihara, T. *et al.* (2023) “Akaluc/AkaLumine bioluminescence system enables highly sensitive, non-invasive and temporal monitoring of gene expression in Drosophila,” *Research Square*. doi: 10.21203/rs.3.rs-2858186/v1.

Chiu, J. C. *et al.* (2008) “The phospho-occupancy of an atypical SLIMB-binding site on PERIOD that is phosphorylated by DOUBLETIME controls the pace of the clock,” *Genes & development*, 22(13), pp. 1758–1772.

Chokroverty, S. (2010) “Overview of sleep & sleep disorders,” *The Indian journal of medical research*, 131, pp. 126–140.

Chou, T. C. *et al.* (2002) “Afferents to the ventrolateral preoptic nucleus,” *The Journal of neuroscience: the official journal of the Society for Neuroscience*, 22(3), pp. 977–990.

Chowdhury, S. *et al.* (2006) “Arc/Arg3.1 interacts with the endocytic machinery to regulate AMPA receptor trafficking,” *Neuron*, 52(3), pp. 445–459.

Chu, J. *et al.* (2016) “A bright cyan-excitable orange fluorescent protein facilitates dual-emission microscopy and enhances bioluminescence imaging in vivo,” *Nature biotechnology*, 34(7), pp. 760–767.

Chung, B. Y. *et al.* (2009) “The GABA(A) receptor RDL acts in peptidergic PDF neurons to promote sleep in Drosophila,” *Current biology: CB*, 19(5), pp. 386–390.

Cingi, C., Emre, I. E. and Muluk, N. B. (2018) “Jetlag related sleep problems and their management: A review,” *Travel medicine and infectious disease*, 24, pp. 59–64.

Cirelli, C. and Bushey, D. (2008) “Sleep and wakefulness in Drosophila melanogaster,” *Annals of the New York Academy of Sciences*, 1129, pp. 323–329.

Cirelli, C., Gutierrez, C. M. and Tononi, G. (2004) “Extensive and divergent effects of sleep and wakefulness on brain gene expression,” *Neuron*, 41(1), pp. 35–43.

Cirelli, C. and Tononi, G. (2000a) “Differential expression of plasticity-related genes in waking and sleep and their regulation by the noradrenergic system,” *The Journal of neuroscience: the official journal of the Society for Neuroscience*, 20(24), pp. 9187–9194.

Cirelli, C. and Tononi, G. (2000b) “Gene expression in the brain across the sleep-waking cycle,” *Brain research*, 885(2), pp. 303–321.

Cirelli, C. and Tononi, G. (2008) “Is sleep essential?,” *PLoS biology*, 6(8), p. e216.

Cirrito, J. R. *et al.* (2005) “Synaptic activity regulates interstitial fluid amyloid-beta levels in vivo,” *Neuron*, 48(6), pp. 913–922.

Clark, I. and Landolt, H. P. (2017) “Coffee, caffeine, and sleep: A systematic review of epidemiological studies and randomized controlled trials,” *Sleep medicine reviews*, 31, pp. 70–78.

Cognigni, P., Felsenberg, J. and Waddell, S. (2018) “Do the right thing: neural network mechanisms of memory formation, expression and update in Drosophila,” *Current opinion in neurobiology*, 49, pp. 51–58.

Compte, A. *et al.* (2003) “Cellular and network mechanisms of slow oscillatory activity (<1 Hz) and wave propagations in a cortical network model,” *Journal of neurophysiology*. American Physiological Society, 89(5), pp. 2707–2725.

Connor, J. *et al.* (2002) “Driver sleepiness and risk of serious injury to car occupants: population based case control study,” *BMJ* , 324(7346), p. 1125.

Costa, G. (2015) “Sleep deprivation due to shift work,” *Handbook of clinical neurology*, 131, pp. 437–446.

Coutant, E. P. *et al.* (2020) “Bioluminescence profiling of NanoKAZ/NanoLuc Luciferase using a chemical library of coelenterazine analogues,” *Chemistry (Weinheim an der Bergstrasse, Germany)*. Wiley, 26(4), pp. 948–958.

Crocker, A. *et al.* (2010) “Identification of a neural circuit that underlies the effects of octopamine on sleep:wake behavior,” *Neuron*, 65(5), pp. 670–681.

Crocker, A. and Sehgal, A. (2008) “Octopamine regulates sleep in drosophila through protein kinase A-dependent mechanisms,” *The Journal of neuroscience: the official journal of the Society for Neuroscience*, 28(38), pp. 9377–9385.

Cumming, G. (2014) “The new statistics: why and how,” *Psychological science*, 25(1), pp. 7–29.

Curtis, A. M. and Fitzgerald, G. A. (2006) “Central and peripheral clocks in cardiovascular and metabolic function,” *Annals of medicine*, 38(8), pp. 552–559.

Cyran, S. A. *et al.* (2003) “vrille, Pdp1, and dClock form a second feedback loop in the Drosophila circadian clock,” *Cell*, pp. 329–341.

Daan, S., Beersma, D. G. and Borbély, A. A. (1984) “Timing of human sleep: recovery process gated by a circadian pacemaker,” *The American journal of physiology*, 246(2 Pt 2), pp. R161-83.

Darlington, T. K. *et al.* (1998) “Closing the circadian loop: CLOCK-induced transcription of its own inhibitors per and tim,” *Science*, 280(5369), pp. 1599–1603.

De, J. *et al.* (2023) “Re-examining the role of the dorsal fan-shaped body in promoting sleep in Drosophila,” *Current biology: CB*. Elsevier BV, 33(17), pp. 3660-3668.e4.

Dean, T. *et al.* (2011) “Drosophila QVR/SSS modulates the activation and C-type inactivation kinetics of Shaker K(+) channels,” *The Journal of neuroscience: the official journal of the Society for Neuroscience*, 31(31), pp. 11387–11395.

Dement, W. and Kleitman, N. (1957) “Cyclic variations in EEG during sleep and their relation to eye movements, body motility, and dreaming,” *Electroencephalography and clinical neurophysiology*, 9(4), pp. 673–690.

Depetris-Chauvin, A. *et al.* (2011) “Adult-specific electrical silencing of pacemaker neurons uncouples molecular clock from circadian outputs,” *Current biology: CB*, 21(21), pp. 1783–1793.

Dijk, D. J. *et al.* (1987) “Reduction of human sleep duration after bright light exposure in the morning,” *Neuroscience letters*, 73(2), pp. 181–186.

Dijk, D. J. and Beersma, D. G. (1989) “Effects of SWS deprivation on subsequent EEG power density and spontaneous sleep duration,” *Electroencephalography and clinical neurophysiology*, 72(4), pp. 312–320.

Dissel, S. *et al.* (2015) “Sleep restores behavioral plasticity to Drosophila mutants,” *Current biology: CB*, 25(10), pp. 1270–1281.

Dobens, L. *et al.* (2005) “Bunched sets a boundary for Notch signaling to pattern anterior eggshell structures during Drosophila oogenesis,” *Developmental biology*, 287(2), pp. 425–437.

Dolmetsch, R. E. *et al.* (1997) “Differential activation of transcription factors induced by Ca2+ response amplitude and duration,” *Nature*, 386(6627), pp. 855–858.

Donelson, N. C. *et al.* (2012) “High-resolution positional tracking for long-term analysis of Drosophila sleep and locomotion using the ‘tracker’ program,” *PloS one*, 7(5), p. e37250.

Donlea, J. M. *et al.* (2011) “Inducing sleep by remote control facilitates memory consolidation in Drosophila,” *Science*, 332(6037), pp. 1571–1576.

Donlea, J. M. *et al.* (2018) “Recurrent Circuitry for Balancing Sleep Need and Sleep,” *Neuron*, 97(2), pp. 378-389.e4.

Donlea, J. M., Pimentel, D. and Miesenböck, G. (2014) “Neuronal Machinery of Sleep Homeostasis in Drosophila,” *Neuron*, 81(6), p. 1442.

Driscoll, M. E., Hyland, C. and Sitaraman, D. (2019) “Measurement of Sleep and Arousal in Drosophila,” *Bio-protocol*, 9(12). doi: 10.21769/bioprotoc.3268.

Dubowy, C. and Sehgal, A. (2017) “Circadian Rhythms and Sleep in Drosophila melanogaster,” *Genetics*, 205(4), pp. 1373–1397.

Durmer, J. S. and Dinges, D. F. (2005) “Neurocognitive consequences of sleep deprivation,” *Seminars in neurology*, 25(1), pp. 117–129.

Dworak, M. *et al.* (2010) “Sleep and brain energy levels: ATP changes during sleep,” *The Journal of neuroscience: the official journal of the Society for Neuroscience*, 30(26), pp. 9007–9016.

England, C. G., Ehlerding, E. B. and Cai, W. (2016) “NanoLuc: A Small Luciferase Is Brightening Up the Field of Bioluminescence,” *Bioconjugate chemistry*, 27(5), pp. 1175–1187.

Erbsloh, F., Bernsmeier, A. and Hillesheim, H. (1958) “[The glucose consumption of the brain & its dependence on the liver],” *Archiv fur Psychiatrie und Nervenkrankheiten, vereinigt mit Zeitschrift fur die gesamte Neurologie und Psychiatrie*, 196(6), pp. 611–626.

Esser, S. K., Hill, S. L. and Tononi, G. (2007) “Sleep homeostasis and cortical synchronization: I. Modeling the effects of synaptic strength on sleep slow waves,” *Sleep*, 30(12), pp. 1617–1630.

Farca Luna, A. J., Perier, M. and Seugnet, L. (2017) “Amyloid Precursor Protein in Drosophila Glia Regulates Sleep and Genes Involved in Glutamate Recycling,” *The Journal of neuroscience: the official journal of the Society for Neuroscience*, 37(16), pp. 4289–4300.

Faville, R. *et al.* (2015) “How deeply does your mutant sleep? Probing arousal to better understand sleep defects in Drosophila,” *Scientific reports*, 5, p. 8454.

Feng, K.-L. *et al.* (2021) “Neuropeptide F inhibits dopamine neuron interference of long-term memory consolidation in Drosophila,” *iScience*, 24(12), p. 103506.

Ferrari, S. F. and Ferrari, M. A. L. (1990) “Predator avoidance behaviour in the buffy-headed marmoset,Callithrix flaviceps,” *Primates; journal of primatology*. Springer Science and Business Media LLC, 31(3), pp. 323–338.

Ferre, S. *et al.* (2008) “Adenosine A1-A2A receptor heteromers: new targets for caffeine in the brain,” *Frontiers in bioscience: a journal and virtual library*, 13, pp. 2391–2399.

Ferreiro, M. J. *et al.* (2018) “Drosophila melanogaster White Mutant w1118 Undergo Retinal Degeneration,” *Frontiers in neuroscience*. Frontiers Media SA, 11. doi: 10.3389/fnins.2017.00732.

Flanigan, W. F., Jr (1973) “Sleep and wakefulness in iguanid lizards, Ctenosaura pectinata and Iguana iguana,” *Brain, behavior and evolution*, 8(6), pp. 401–436.

Flanigan, W. F., Jr, Wilcox, R. H. and Rechtschaffen, A. (1973) “The EEG and behavioral continuum of the crocodilian, Caiman sclerops,” *Electroencephalography and clinical neurophysiology*, 34(5), pp. 521–538.

Foltenyi, K., Greenspan, R. J. and Newport, J. W. (2007) “Activation of EGFR and ERK by rhomboid signaling regulates the consolidation and maintenance of sleep in Drosophila,” *Nature neuroscience*, 10(9), pp. 1160–1167.

Ford, D. E. and Kamerow, D. B. (1989) “Epidemiologic study of sleep disturbances and psychiatric disorders. An opportunity for prevention?,” *JAMA: the journal of the American Medical Association*, 262(11), pp. 1479–1484.

Franco, D. L., Frenkel, L. and Ceriani, M. F. (2018) “The Underlying Genetics of Drosophila Circadian Behaviors,” *Physiology* , 33(1), pp. 50–62.

Frank, D. D. *et al.* (2015) “Temperature representation in the Drosophila brain,” *Nature*, 519(7543), pp. 358–361.

Franken, P., Chollet, D. and Tafti, M. (2001) “The homeostatic regulation of sleep need is under genetic control,” *The Journal of neuroscience: the official journal of the Society for Neuroscience*, 21(8), pp. 2610–2621.

Fredriksen, K. *et al.* (2004) “Sleepless in Chicago: tracking the effects of adolescent sleep loss during the middle school years,” *Child development*, 75(1), pp. 84–95.

Fuller, P. M. *et al.* (2011) “Reassessment of the structural basis of the ascending arousal system,” *The Journal of comparative neurology*, 519(5), pp. 933–956.

Gais, S. *et al.* (2002) “Learning-dependent increases in sleep spindle density,” *The Journal of neuroscience: the official journal of the Society for Neuroscience*, 22(15), pp. 6830–6834.

Gallopin, T. *et al.* (2000) “Identification of sleep-promoting neurons in vitro,” *Nature*, 404(6781), pp. 992–995.

Gallopin, T. *et al.* (2004) “Effect of the wake-promoting agent modafinil on sleep-promoting neurons from the ventrolateral preoptic nucleus: an in vitro pharmacologic study,” *Sleep*, 27(1), pp. 19–25.

Gao, X. J. *et al.* (2015) “A transcriptional reporter of intracellular Ca(2+) in Drosophila,” *Nature neuroscience*, 18(6), pp. 917–925.

Garbe, D. S. *et al.* (2015) “Context-specific comparison of sleep acquisition systems in Drosophila,” *Biology open*, 4(11), pp. 1558–1568.

Gardiner, C. *et al.* (2023) “The effect of caffeine on subsequent sleep: A systematic review and meta-analysis,” *Sleep medicine reviews*, 69, p. 101764.

Gaspar, N. *et al.* (2021) “Evaluation of NanoLuc substrates for bioluminescence imaging of transferred cells in mice,” *Journal of photochemistry and photobiology. B, Biology*. Elsevier BV, 216(112128), p. 112128.

Gaus, S. E. *et al.* (2002) “Ventrolateral preoptic nucleus contains sleep-active, galaninergic neurons in multiple mammalian species,” *Neuroscience*, 115(1), pp. 285–294.

Geissmann, Q. *et al.* (2017) “Ethoscopes: An open platform for high-throughput ethomics,” *PLoS biology*, 15(10), p. e2003026.

Geissmann, Q., Beckwith, E. J. and Gilestro, G. F. (2019) “Most sleep does not serve a vital function: Evidence from Drosophila melanogaster,” *Science advances*, 5(2), p. eaau9253.

Giebultowicz, J. M. *et al.* (2000) “Transplanted Drosophila excretory tubules maintain circadian clock cycling out of phase with the host,” *Current biology: CB*, 10(2), pp. 107–110.

Giebultowicz, J. M. and Hege, D. M. (1997) “Circadian clock in Malpighian tubules,” *Nature*, 386(6626), p. 664.

Gilestro, G. F. (2012) “Video tracking and analysis of sleep in Drosophila melanogaster,” *Nature protocols*, 7(5), pp. 995–1007.

Golic, K. G. and Lindquist, S. (1989) “The FLP recombinase of yeast catalyzes site-specific recombination in the Drosophila genome,” *Cell*, 59(3), pp. 499–509.

Gong, H. *et al.* (2004) “Activation of c-fos in GABAergic neurones in the preoptic area during sleep and in response to sleep deprivation,” *The Journal of physiology*, 556(Pt 3), pp. 935–946.

Gottlieb, D. J. *et al.* (2005) “Association of sleep time with diabetes mellitus and impaired glucose tolerance,” *Archives of internal medicine*, 165(8), pp. 863–867.

Gouet, C. *et al.* (2012) “On the mechanism of synaptic depression induced by CaMKIIN, an endogenous inhibitor of CaMKII,” *PloS one*, 7(11), p. e49293.

Graef, I. A. *et al.* (1999) “L-type calcium channels and GSK-3 regulate the activity of NF-ATc4 in hippocampal neurons,” *Nature*, 401(6754), pp. 703–708.

Grandison, R. C. *et al.* (2009) “Effect of a standardised dietary restriction protocol on multiple laboratory strains of Drosophila melanogaster,” *PloS one*. Public Library of Science (PLoS), 4(1), p. e4067.

Gratz, S. J. *et al.* (2015) “CRISPR-Cas9 genome editing in *Drosophila*,” *et al [Current protocols in molecular biology]*. Wiley, 111(1). doi: 10.1002/0471142727.mb3102s111.

Grima, B. *et al.* (2002) “The F-box protein slimb controls the levels of clock proteins period and timeless,” *Nature*, 420(6912), pp. 178–182.

Grima, B. *et al.* (2004) “Morning and evening peaks of activity rely on different clock neurons of the Drosophila brain,” *Nature*, 431(7010), pp. 869–873.

Groen, C. M. *et al.* (2018) “Drosophila strain specific response to cisplatin neurotoxicity,” *Fly*. Informa UK Limited, 12(3–4), pp. 174–182.

Gross, B. A. *et al.* (2015) “Stress-free automatic sleep deprivation using air puffs,” *Journal of neuroscience methods*, 251, pp. 83–91.

Gruntman, E. and Turner, G. C. (2013) “Integration of the olfactory code across dendritic claws of single mushroom body neurons,” *Nature neuroscience*, 16(12), pp. 1821–1829.

Guo, F. *et al.* (2014) “PDF neuron firing phase-shifts key circadian activity neurons in Drosophila,” *eLife*, 3. doi: 10.7554/eLife.02780.

Guo, F. *et al.* (2016) “Circadian neuron feedback controls the Drosophila sleep--activity profile,” *Nature*, 536(7616), pp. 292–297.

Guo, F. *et al.* (2018) “A Circadian Output Circuit Controls Sleep-Wake Arousal in Drosophila,” *Neuron*, 100(3), pp. 624-635.e4.

Guo, F., Chen, X. and Rosbash, M. (2017) “Temporal calcium profiling of specific circadian neurons in freely moving flies,” *Proceedings of the National Academy of Sciences of the United States of America*, 114(41), pp. E8780–E8787.

Gwack, Y. *et al.* (2006) “A genome-wide Drosophila RNAi screen identifies DYRK-family kinases as regulators of NFAT,” *Nature*, 441(7093), pp. 646–650.

Haider, B., Häusser, M. and Carandini, M. (2013) “Inhibition dominates sensory responses in the awake cortex,” *Nature*, 493(7430), pp. 97–100.

Halassa, M. M. *et al.* (2009) “Astrocytic modulation of sleep homeostasis and cognitive consequences of sleep loss,” *Neuron*, 61(2), pp. 213–219.

Hall, M. P. *et al.* (2012) “Engineered luciferase reporter from a deep sea shrimp utilizing a novel imidazopyrazinone substrate,” *ACS chemical biology*, 7(11), pp. 1848–1857.

Hanafusa, S. *et al.* (2013) “Sexual interactions influence the molecular oscillations in DN1 pacemaker neurons in Drosophila melanogaster,” *PloS one*. Public Library of Science (PLoS), 8(12), p. e84495.

Hao, H., Allen, D. L. and Hardin, P. E. (1997) “A circadian enhancer mediates PER-dependent mRNA cycling in Drosophila melanogaster,” *Molecular and cellular biology*, 17(7), pp. 3687–3693.

Harris, C. R. *et al.* (2020) “Array programming with NumPy,” *Nature*, 585(7825), pp. 357–362.

Hashmi, A., Nere, A. and Tononi, G. (2013) “Sleep-Dependent Synaptic Down-Selection (II): Single-Neuron Level Benefits for Matching, Selectivity, and Specificity,” *Frontiers in neurology*, 4, p. 148.

Hasler, G. *et al.* (2004) “The association between short sleep duration and obesity in young adults: a 13-year prospective study,” *Sleep*, 27(4), pp. 661–666.

Hasler, G. *et al.* (2005) “Excessive daytime sleepiness in young adults: a 20-year prospective community study,” *The Journal of clinical psychiatry*, 66(4), pp. 521–529.

Haynes, P. R., Christmann, B. L. and Griffith, L. C. (2015) “A single pair of neurons links sleep to memory consolidation in Drosophila melanogaster,” *eLife*, 4. doi: 10.7554/eLife.03868.

Hediger, H. (1980) “The biology of natural sleep in animals,” *Experientia*, 36(1), pp. 13–16.

Hege, D. M. *et al.* (1997) “Rhythmic expression of a PER-reporter in the Malpighian tubules of decapitated Drosophila: evidence for a brain-independent circadian clock,” *Journal of biological rhythms*, 12(4), pp. 300–308.

Heisenberg, M. (2003) “Mushroom body memoir: from maps to models,” *Nature reviews. Neuroscience*, 4(4), pp. 266–275.

Helfrich-Förster, C. (1995) “The period clock gene is expressed in central nervous system neurons which also produce a neuropeptide that reveals the projections of circadian pacemaker cells within the brain of Drosophila melanogaster,” *Proceedings of the National Academy of Sciences of the United States of America*, 92(2), pp. 612–616.

Helfrich-Förster, C. *et al.* (2007) “The lateral and dorsal neurons of Drosophila melanogaster: new insights about their morphology and function,” *Cold Spring Harbor symposia on quantitative biology*, 72, pp. 517–525.

Helfrich-Förster, C. (2018) “Sleep in Insects,” *Annual review of entomology*, 63, pp. 69–86.

Hendricks, J. C. *et al.* (2000) “Rest in Drosophila is a sleep-like state,” *Neuron*, 25(1), pp. 129–138.

Hendricks, J. C. *et al.* (2003) “Gender dimorphism in the role of cycle (BMAL1) in rest, rest regulation, and longevity in Drosophila melanogaster,” *Journal of biological rhythms*, 18(1), pp. 12–25.

Hendricks, J. C., Sehgal, A. and Pack, A. I. (2000) “The need for a simple animal model to understand sleep,” *Progress in neurobiology*, 61(4), pp. 339–351.

Hill, S., Tononi, G. and Ghilardi, M. F. (2008) “Sleep improves the variability of motor performance,” *Brain research bulletin*, 76(6), pp. 605–611.

Ho, J. *et al.* (2019) “Moving beyond P values: data analysis with estimation graphics,” *Nature methods*, 16(7), pp. 565–566.

Hori, T. *et al.* (2001) “Proposed supplements and amendments to ‘A Manual of Standardized Terminology, Techniques and Scoring System for Sleep Stages of Human Subjects’, the Rechtschaffen & Kales (1968) standard,” *Psychiatry and clinical neurosciences*, 55(3), pp. 305–310.

Houl, J. H. *et al.* (2006) “Drosophila CLOCK is constitutively expressed in circadian oscillator and non-oscillator cells,” *Journal of biological rhythms*, 21(2), pp. 93–103.

Huber, R., Ghilardi, M. F., *et al.* (2004) “Local sleep and learning,” *Nature*, 430(6995), pp. 78–81.

Huber, R., Hill, S. L., *et al.* (2004) “Sleep homeostasis in Drosophila melanogaster,” *Sleep*, 27(4), pp. 628–639.

Hughes, M. E., Hogenesch, J. B. and Kornacker, K. (2010) “JTK_CYCLE: an efficient nonparametric algorithm for detecting rhythmic components in genome-scale data sets,” *Journal of biological rhythms*, 25(5), pp. 372–380.

Huguenard, J. R. and McCormick, D. A. (2007) “Thalamic synchrony and dynamic regulation of global forebrain oscillations,” *Trends in neurosciences*, 30(7), pp. 350–356.

Hulse, B. K. *et al.* (2021) “A connectome of the Drosophila central complex reveals network motifs suitable for flexible navigation and context-dependent action selection,” *eLife*, 10. doi: 10.7554/eLife.66039.

Hunter (2007) “Matplotlib: A 2D Graphics Environment,” 9, pp. 90–95.

Hutchison, A. L. *et al.* (2015) “Improved statistical methods enable greater sensitivity in rhythm detection for genome-wide data,” *PLoS computational biology*, 11(3), p. e1004094.

Iliff, J. J. *et al.* (2012) “A paravascular pathway facilitates CSF flow through the brain parenchyma and the clearance of interstitial solutes, including amyloid β,” *Science translational medicine*, 4(147), p. 147ra111.

Iliff, J. J., Lee, H., *et al.* (2013) “Brain-wide pathway for waste clearance captured by contrast-enhanced MRI,” *The Journal of clinical investigation*, 123(3), pp. 1299–1309.

Iliff, J. J., Wang, M., *et al.* (2013) “Cerebral arterial pulsation drives paravascular CSF-interstitial fluid exchange in the murine brain,” *The Journal of neuroscience: the official journal of the Society for Neuroscience*, 33(46), pp. 18190–18199.

Im, S. H. and Taghert, P. H. (2010) “PDF receptor expression reveals direct interactions between circadian oscillators in Drosophila,” *The Journal of comparative neurology*, 518(11), pp. 1925–1945.

Imeri, L. and Opp, M. R. (2009) “How (and why) the immune system makes us sleep,” *Nature reviews. Neuroscience*, 10(3), pp. 199–210.

Institute of Medicine, Board on Health Sciences Policy and Committee on Sleep Medicine and Research (2006) *Sleep Disorders and Sleep Deprivation: An Unmet Public Health Problem*. National Academies Press.

Isaac, R. E. *et al.* (2010) “*Drosophila* male sex peptide inhibits siesta sleep and promotes locomotor activity in the post-mated female,” *Proceedings. Biological sciences*. The Royal Society, 277(1678), pp. 65–70.

Jang, A. R. *et al.* (2015) “Drosophila TIM binds importin α1, and acts as an adapter to transport PER to the nucleus,” *PLoS genetics*, 11(2), p. e1004974.

Jing, J. and Prekeris, R. (2009) “Polarized endocytic transport: the roles of Rab11 and Rab11-FIPs in regulating cell polarity,” *Histology and histopathology*, 24(9), pp. 1171–1180.

John, J. and Kumar, V. M. (1998) “Effect of NMDA lesion of the medial preoptic neurons on sleep and other functions,” *Sleep*, 21(6), pp. 587–598.

Jones, J. D. *et al.* (2023) “Regulation of sleep by cholinergic neurons located outside the central brain in Drosophila,” *PLoS biology*, 21(3), p. e3002012.

Kadener, S. *et al.* (2007) “Clockwork Orange is a transcriptional repressor and a new Drosophila circadian pacemaker component,” *Genes & development*, 21(13), pp. 1675–1686.

Kaihara, A., Umezawa, Y. and Furukawa, T. (2008) “Bioluminescent indicators for Ca2+ based on split Renilla luciferase complementation in living cells,” *Analytical sciences: the international journal of the Japan Society for Analytical Chemistry*, 24(11), pp. 1405–1408.

Kaiser, W. (1988) “Busy bees need rest, too,” *Journal of Comparative Physiology A*, 163(5), pp. 565–584.

Kaiser, W. (1995) “Rest at night in some solitary bees - a comparison with the sleep-like state of honey bees,” *Apidologie*. EDP Sciences, 26(3), pp. 213–230.

Kalmbach, D. A., Anderson, J. R. and Drake, C. L. (2018) “The impact of stress on sleep: Pathogenic sleep reactivity as a vulnerability to insomnia and circadian disorders,” *Journal of sleep research*, 27(6), p. e12710.

Kaneko, M. and Hall, J. C. (2000) “Neuroanatomy of cells expressing clock genes in Drosophila: transgenic manipulation of the period and timeless genes to mark the perikarya of circadian pacemaker neurons and their projections,” *The Journal of comparative neurology*, 422(1), pp. 66–94.

Kang, J.-E. *et al.* (2009) “Amyloid-beta dynamics are regulated by orexin and the sleep-wake cycle,” *Science*, 326(5955), pp. 1005–1007.

Kapur, V. K. *et al.* (2002) “The relationship between chronically disrupted sleep and healthcare use,” *Sleep*, 25(3), pp. 289–296.

Kattler, H., Dijk, D. J. and Borbély, A. A. (1994) “Effect of unilateral somatosensory stimulation prior to sleep on the sleep EEG in humans,” *Journal of sleep research*, 3(3), pp. 159–164.

Kaun, K. R., Devineni, A. V. and Heberlein, U. (2012) “Drosophila melanogaster as a model to study drug addiction,” *Human genetics*, 131(6), pp. 959–975.

Keene, A. C. and Duboue, E. R. (2018) “The origins and evolution of sleep,” *The Journal of experimental biology*, 221(Pt 11). doi: 10.1242/jeb.159533.

Kerr, R. *et al.* (2000) “Optical imaging of calcium transients in neurons and pharyngeal muscle of C. elegans,” *Neuron*, 26(3), pp. 583–594.

Kidd, P. B., Young, M. W. and Siggia, E. D. (2015) “Temperature compensation and temperature sensation in the circadian clock,” *Proceedings of the National Academy of Sciences of the United States of America*, 112(46), pp. E6284-92.

Kim, E. Y. *et al.* (2002) “Drosophila CLOCK protein is under posttranscriptional control and influences light-induced activity,” *Neuron*, 34(1), pp. 69–81.

Kim, E. Y. *et al.* (2007) “A DOUBLETIME kinase binding domain on the Drosophila PERIOD protein is essential for its hyperphosphorylation, transcriptional repression, and circadian clock function,” *Molecular and cellular biology*, 27(13), pp. 5014–5028.

Kim, E. Y. and Edery, I. (2006) “Balance between DBT/CKIepsilon kinase and protein phosphatase activities regulate phosphorylation and stability of Drosophila CLOCK protein,” *Proceedings of the National Academy of Sciences of the United States of America*. Proceedings of the National Academy of Sciences, 103(16), pp. 6178–6183.

Kim, M. D., Kolodziej, P. and Chiba, A. (2002) “Growth cone pathfinding and filopodial dynamics are mediated separately by Cdc42 activation,” *The Journal of neuroscience: the official journal of the Society for Neuroscience*, 22(5), pp. 1794–1806.

King, A. N. *et al.* (2017) “A Peptidergic Circuit Links the Circadian Clock to Locomotor Activity,” *Current biology: CB*, 27(13), pp. 1915-1927.e5.

Ko, H. W., Jiang, J. and Edery, I. (2002) “Role for Slimb in the degradation of Drosophila Period protein phosphorylated by Doubletime,” *Nature*, 420(6916), pp. 673–678.

Koh, K. *et al.* (2008) “Identification of SLEEPLESS, a sleep-promoting factor,” *Science*, 321(5887), pp. 372–376.

Koh, K., Zheng, X. and Sehgal, A. (2006) “JETLAG resets the Drosophila circadian clock by promoting light-induced degradation of TIMELESS,” *Science*, 312(5781), pp. 1809–1812.

Koksharov, M. (2022) “Monitoring fly feeding behavior and timingby beetle luciferase reporters v2.” doi: 10.17504/protocols.io.b34uqqww.

Konopka, R. J. and Benzer, S. (1971) “Clock mutants of Drosophila melanogaster,” *Proceedings of the National Academy of Sciences of the United States of America*, 68(9), pp. 2112–2116.

Krishnan, S. *et al.* (2014) “The Right Dorsal Habenula Limits Attraction to an Odor in Zebrafish,” *Current biology: CB*, 24(11), pp. 1167–1175.

Kroeger, D. *et al.* (2018) “Galanin neurons in the ventrolateral preoptic area promote sleep and heat loss in mice,” *Nature communications*, 9(1), p. 4129.

Krueger, J. M. *et al.* (2011) “Involvement of cytokines in slow wave sleep,” *Progress in brain research*, 193, pp. 39–47.

Krueger, J. M. *et al.* (2016) “Sleep function: Toward elucidating an enigma,” *Sleep medicine reviews*, 28, pp. 46–54.

Krueger, J. M. and Tononi, G. (2011) “Local use-dependent sleep; synthesis of the new paradigm,” *Current topics in medicinal chemistry*, 11(19), pp. 2490–2492.

Kume, K. *et al.* (2005) “Dopamine is a regulator of arousal in the fruit fly,” *The Journal of neuroscience: the official journal of the Society for Neuroscience*, 25(32), pp. 7377–7384.

Kunst, M. *et al.* (2014) “Calcitonin gene-related peptide neurons mediate sleep-specific circadian output in Drosophila,” *Current biology: CB*, 24(22), pp. 2652–2664.

Kuppermann, M. *et al.* (1995) “Sleep problems and their correlates in a working population,” *Journal of general internal medicine*, 10(1), pp. 25–32.

Lai, S.-L. and Lee, T. (2006) “Genetic mosaic with dual binary transcriptional systems in Drosophila,” *Nature neuroscience*. Springer Science and Business Media LLC, 9(5), pp. 703–709.

Lamaze, A. *et al.* (2018) “A Wake-Promoting Circadian Output Circuit in Drosophila,” *Current biology: CB*, 28(19), pp. 3098-3105.e3.

Landmann, N. *et al.* (2015) “REM sleep and memory reorganization: Potential relevance for psychiatry and psychotherapy,” *Neurobiology of learning and memory*, 122, pp. 28–40.

Landrigan, C. P. *et al.* (2004) “Effect of reducing interns’ work hours on serious medical errors in intensive care units,” *The New England journal of medicine*, 351(18), pp. 1838–1848.

Larson, M. E. *et al.* (2012) “Soluble α-synuclein is a novel modulator of Alzheimer’s disease pathophysiology,” *The Journal of neuroscience: the official journal of the Society for Neuroscience*, 32(30), pp. 10253–10266.

Lee, C., Bae, K. and Edery, I. (1999) “PER and TIM inhibit the DNA binding activity of a Drosophila CLOCK-CYC/dBMAL1 heterodimer without disrupting formation of the heterodimer: a basis for circadian transcription,” *Molecular and cellular biology*, 19(8), pp. 5316–5325.

Lee, G. *et al.* (2013) “Dopamine D2 receptor as a cellular component controlling nocturnal hyperactivities in Drosophila melanogaster,” *Chronobiology international*, 30(4), pp. 443–459.

Lee, M. G., Hassani, O. K. and Jones, B. E. (2005) “Discharge of identified orexin/hypocretin neurons across the sleep-waking cycle,” *The Journal of neuroscience: the official journal of the Society for Neuroscience*, 25(28), pp. 6716–6720.

Léger, D. *et al.* (2002) “Medical and socio-professional impact of insomnia,” *Sleep*, 25(6), pp. 625–629.

Leonelli, S. and Ankeny, R. A. (2013) “What makes a model organism?,” *Endeavour*, 37(4), pp. 209–212.

Levi, F. and Schibler, U. (2007) “Circadian rhythms: mechanisms and therapeutic implications,” *Annual review of pharmacology and toxicology*, 47, pp. 593–628.

Levine, J. D. *et al.* (2002) “Signal analysis of behavioral and molecular cycles,” *BMC neuroscience*, 3, p. 1.

Li, F. *et al.* (2020) “The connectome of the adult Drosophila mushroom body provides insights into function,” *eLife*, 9. doi: 10.7554/eLife.62576.

Liang, X. *et al.* (2019) “Morning and Evening Circadian Pacemakers Independently Drive Premotor Centers via a Specific Dopamine Relay,” *Neuron*, 102(4), pp. 843-857.e4.

Liang, X., Holy, T. E. and Taghert, P. H. (2016) “Synchronous Drosophila circadian pacemakers display nonsynchronous Ca^{2+} rhythms in vivo,” *Science*, 351(6276), pp. 976–981.

Lim, C. *et al.* (2007) “Clockwork orange encodes a transcriptional repressor important for circadian-clock amplitude in Drosophila,” *Current biology: CB*, 17(12), pp. 1082–1089.

Lin, D. M. and Goodman, C. S. (1994) “Ectopic and increased expression of Fasciclin II alters motoneuron growth cone guidance,” *Neuron*, 13(3), pp. 507–523.

Lin, F. J. *et al.* (2010) “Effect of taurine and caffeine on sleep-wake activity in Drosophila melanogaster,” *Nature and science of sleep*, 2, pp. 221–231.

Lin, Y., Stormo, G. D. and Taghert, P. H. (2004) “The neuropeptide pigment-dispersing factor coordinates pacemaker interactions in the Drosophila circadian system,” *The Journal of neuroscience: the official journal of the Society for Neuroscience*, 24(36), pp. 7951–7957.

Link, W. *et al.* (1995) “Somatodendritic expression of an immediate early gene is regulated by synaptic activity,” *Proceedings of the National Academy of Sciences of the United States of America*, 92(12), pp. 5734–5738.

Lisman, J., Yasuda, R. and Raghavachari, S. (2012) “Mechanisms of CaMKII action in long-term potentiation,” *Nature reviews. Neuroscience*, 13(3), pp. 169–182.

Liu, Q. *et al.* (2012) “Two dopaminergic neurons signal to the dorsal fan-shaped body to promote wakefulness in Drosophila,” *Current biology: CB*, 22(22), pp. 2114–2123.

Liu, S. *et al.* (2014) “WIDE AWAKE mediates the circadian timing of sleep onset,” *Neuron*, 82(1), pp. 151–166.

Liu, S. *et al.* (2016) “Sleep Drive Is Encoded by Neural Plastic Changes in a Dedicated Circuit,” *Cell*, 165(6), pp. 1347–1360.

Liu, S. *et al.* (2021) “Brightening up biology: Advances in Luciferase systems for *in vivo* imaging,” *ACS chemical biology*. American Chemical Society (ACS), 16(12), pp. 2707–2718.

Liu, W. W., Mazor, O. and Wilson, R. I. (2015) “Thermosensory processing in the Drosophila brain,” *Nature*, 519(7543), pp. 353–357.

Liu, X. (2004) “Sleep and adolescent suicidal behavior,” *Sleep*, 27(7), pp. 1351–1358.

Liu, Y. *et al.* (2014) “Relationships between housing and food insecurity, frequent mental distress, and insufficient sleep among adults in 12 US States, 2009,” *Preventing chronic disease*, 11, p. E37.

Loomis, A. L., Harvey, E. N. and Hobart, G. A. (1937) “Cerebral states during sleep, as studied by human brain potentials,” *Journal of experimental psychology*, 21(2), pp. 127–144.

Lu, J. *et al.* (2000) “Effect of lesions of the ventrolateral preoptic nucleus on NREM and REM sleep,” *The Journal of neuroscience: the official journal of the Society for Neuroscience*, 20(10), pp. 3830–3842.

Ly, S., Pack, A. I. and Naidoo, N. (2018) “The neurobiological basis of sleep: Insights from Drosophila,” *Neuroscience and biobehavioral reviews*, 87, pp. 67–86.

Lyford, G. L. *et al.* (1995) “Arc, a growth factor and activity-regulated gene, encodes a novel cytoskeleton-associated protein that is enriched in neuronal dendrites,” *Neuron*, 14(2), pp. 433–445.

MacDonald, J. M. *et al.* (2006) “The Drosophila cell corpse engulfment receptor Draper mediates glial clearance of severed axons,” *Neuron*, 50(6), pp. 869–881.

Machado, D. R. *et al.* (2017) “Identification of octopaminergic neurons that modulate sleep suppression by male sex drive,” *eLife*. eLife Sciences Publications, Ltd, 6. doi: 10.7554/elife.23130.

Madsen, P. L. *et al.* (1991) “Cerebral O2 metabolism and cerebral blood flow in humans during deep and rapid-eye-movement sleep,” *Journal of applied physiology*, 70(6), pp. 2597–2601.

Mahr, A. and Aberle, H. (2006) “The expression pattern of the Drosophila vesicular glutamate transporter: a marker protein for motoneurons and glutamatergic centers in the brain,” *Gene expression patterns: GEP*, 6(3), pp. 299–309.

de Manaceine, M. (1894) “Quelques observations experimentales sur l’influence de l’insomnie absolue,” *Archives italiennes de biologie*. cir.nii.ac.jp, 21, pp. 322–325.

Manoli, D. S. *et al.* (2013) “Neural control of sexually dimorphic behaviors,” *Current opinion in neurobiology*. Elsevier BV, 23(3), pp. 330–338.

Maquet, P. (1995) “Sleep function(s) and cerebral metabolism,” *Behavioural brain research*, 69(1–2), pp. 75–83.

Maret, S. *et al.* (2007) “Homer1a is a core brain molecular correlate of sleep loss,” *Proceedings of the National Academy of Sciences of the United States of America*, 104(50), pp. 20090–20095.

Marin, E. C. *et al.* (2020) “Connectomics Analysis Reveals First-, Second-, and Third-Order Thermosensory and Hygrosensory Neurons in the Adult Drosophila Brain,” *Current biology: CB*, 30(16), pp. 3167-3182.e4.

Masuyama, K. *et al.* (2012) “Mapping neural circuits with activity-dependent nuclear import of a transcription factor,” *Journal of neurogenetics*, 26(1), pp. 89–102.

Mathis, A. *et al.* (2018) “DeepLabCut: markerless pose estimation of user-defined body parts with deep learning,” *Nature neuroscience*. Springer Science and Business Media LLC, 21(9), pp. 1281–1289.

Matsuo, N., Reijmers, L. and Mayford, M. (2008) “Spine-type-specific recruitment of newly synthesized AMPA receptors with learning,” *Science*, 319(5866), pp. 1104–1107.

McKinney, W. (2010) “Data Structures for Statistical Computing in Python,” in *Proceedings of the 9th Python in Science Conference*. *Python in Science Conference*, SciPy. doi: 10.25080/majora-92bf1922-00a.

Medic, G., Wille, M. and Hemels, M. E. (2017) “Short- and long-term health consequences of sleep disruption,” *Nature and science of sleep*, 9, pp. 151–161.

Mergenthaler, P. *et al.* (2013) “Sugar for the brain: the role of glucose in physiological and pathological brain function,” *Trends in neurosciences*, 36(10), pp. 587–597.

Mitler, M. M. *et al.* (1988) “Catastrophes, sleep, and public policy: consensus report,” *Sleep*, 11(1), pp. 100–109.

Mittag, M. and Wagner, V. (2003) “The circadian clock of the unicellular eukaryotic model organism Chlamydomonas reinhardtii,” *Biological chemistry*, 384(5), pp. 689–695.

Miyasako, Y., Umezaki, Y. and Tomioka, K. (2007) “Separate sets of cerebral clock neurons are responsible for light and temperature entrainment of Drosophila circadian locomotor rhythms,” *Journal of biological rhythms*, 22(2), pp. 115–126.

Miyazaki, S., Liu, C.-Y. and Hayashi, Y. (2017) “Sleep in vertebrate and invertebrate animals, and insights into the function and evolution of sleep,” *Neuroscience research*, 118, pp. 3–12.

Moga, D. E. *et al.* (2004) “Activity-regulated cytoskeletal-associated protein is localized to recently activated excitatory synapses,” *Neuroscience*, 125(1), pp. 7–11.

Mohawk, J. A., Green, C. B. and Takahashi, J. S. (2012) “Central and peripheral circadian clocks in mammals,” *Annual review of neuroscience*, 35, pp. 445–462.

Monastirioti, M. (1999) “Biogenic amine systems in the fruit flyDrosophila melanogaster,” *Microscopy research and technique*. Wiley, 45(2), pp. 106–121.

Morales-Curiel, L. F. *et al.* (2022) “Volumetric imaging of fast cellular dynamics with deep learning enhanced bioluminescence microscopy,” *Communications biology*. Springer Science and Business Media LLC, 5(1). doi: 10.1038/s42003-022-04292-x.

Myers, E. M., Yu, J. and Sehgal, A. (2003) “Circadian control of eclosion: interaction between a central and peripheral clock in Drosophila melanogaster,” *Current biology: CB*, 13(6), pp. 526–533.

Naidoo, N. *et al.* (1999) “A role for the proteasome in the light response of the timeless clock protein,” *Science*, 285(5434), pp. 1737–1741.

Nall, A. H. *et al.* (2016) “Caffeine promotes wakefulness via dopamine signaling in Drosophila,” *Scientific reports*, 6, p. 20938.

Nall, A. and Sehgal, A. (2014) “Monoamines and sleep in Drosophila,” *Behavioral neuroscience*. American Psychological Association (APA), 128(3), pp. 264–272.

Narasimamurthy, R. and Virshup, D. M. (2017) “Molecular Mechanisms Regulating Temperature Compensation of the Circadian Clock,” *Frontiers in neurology*, 8, p. 161.

Nawathean, P., Stoleru, D. and Rosbash, M. (2007) “A small conserved domain of Drosophila PERIOD is important for circadian phosphorylation, nuclear localization, and transcriptional repressor activity,” *Molecular and cellular biology*, 27(13), pp. 5002–5013.

Nere, A. *et al.* (2013) “Sleep-dependent synaptic down-selection (I): modeling the benefits of sleep on memory consolidation and integration,” *Frontiers in neurology*, 4, p. 143.

Newman, A. B. *et al.* (2000) “Daytime sleepiness predicts mortality and cardiovascular disease in older adults,” *Journal of the American Geriatrics Society*. Wiley, 48(2), pp. 115–123.

Newman, S. M. *et al.* (2008) “Sleep deprivation in the pigeon using the Disk-Over-Water method,” *Physiology & behavior*, 93(1–2), pp. 50–58.

Nitabach, M. N., Blau, J. and Holmes, T. C. (2002) “Electrical silencing of Drosophila pacemaker neurons stops the free-running circadian clock,” *Cell*, 109(4), pp. 485–495.

Nitz, D. A. *et al.* (2002) “Electrophysiological correlates of rest and activity in Drosophila melanogaster,” *Current biology: CB*, 12(22), pp. 1934–1940.

Oh, Y. *et al.* (2013) “Histamine-HisCl1 receptor axis regulates wake-promoting signals in Drosophila melanogaster,” *PloS one*. Public Library of Science (PLoS), 8(7), p. e68269.

Oh, Y. *et al.* (2019) “An orange calcium-modulated bioluminescent indicator for non-invasive activity imaging,” *Nature chemical biology*, 15(5), pp. 433–436.

Okuno, H. *et al.* (2012) “Inverse synaptic tagging of inactive synapses via dynamic interaction of Arc/Arg3.1 with CaMKIIβ,” *Cell*, 149(4), pp. 886–898.

Olcese, U., Esser, S. K. and Tononi, G. (2010) “Sleep and synaptic renormalization: a computational study,” *Journal of neurophysiology*, 104(6), pp. 3476–3493.

Olesen, J. *et al.* (2012) “The economic cost of brain disorders in Europe,” *European journal of neurology: the official journal of the European Federation of Neurological Societies*, 19(1), pp. 155–162.

Packard Topcount NXT scintillation counter: GMI - Trusted Laboratory Solutions (2022). Available at: https://www.gmi-inc.com/product/packard-topcount-nxt-scintillation-counter/ (Accessed: September 26, 2023).

Parisky, K. M. *et al.* (2008) “PDF cells are a GABA-responsive wake-promoting component of the Drosophila sleep circuit,” *Neuron*, 60(4), pp. 672–682.

Park, S. *et al.* (2014) “SIFamide and SIFamide receptor defines a novel neuropeptide signaling to promote sleep in Drosophila,” *Molecules and cells*, 37(4), pp. 295–301.

Parmentier, R. *et al.* (2002) “Anatomical, physiological, and pharmacological characteristics of histidine decarboxylase knock-out mice: evidence for the role of brain histamine in behavioral and sleep-wake control,” *The Journal of neuroscience: the official journal of the Society for Neuroscience*. Society for Neuroscience, 22(17), pp. 7695–7711.

Patel, S. R. *et al.* (2004) “A Prospective Study of Sleep Duration and Mortality Risk in Women,” *Sleep*. Oxford Academic, 27(3), pp. 440–444.

Patke, A., Young, M. W. and Axelrod, S. (2020) “Molecular mechanisms and physiological importance of circadian rhythms,” *Nature reviews. Molecular cell biology*, 21(2), pp. 67–84.

Patrick, G. T. W. and Gilbert, J. A. (1896) “Studies from the psychological laboratory of the University of Iowa: On the effects of loss of sleep,” *Psychological review*. American Psychological Association (APA), 3(5), pp. 469–483.

Pavlou, H. J. and Goodwin, S. F. (2013) “Courtship behavior in Drosophila melanogaster: towards a ‘courtship connectome,’” *Current opinion in neurobiology*, 23(1), pp. 76–83.

Pawlak, V. *et al.* (2010) “Timing is not Everything: Neuromodulation Opens the STDP Gate,” *Frontiers in synaptic neuroscience*, 2, p. 146.

Pedregosa, F. *et al.* (2012) “Scikit-learn: Machine Learning in Python,” *arXiv [cs.LG]*. Available at: https://www.jmlr.org/papers/volume12/pedregosa11a/pedregosa11a.pdf?ref=https:/ (Accessed: March 2, 2023).

Peschel, N. *et al.* (2009) “Light-dependent interactions between the Drosophila circadian clock factors cryptochrome, jetlag, and timeless,” *Current biology: CB*, 19(3), pp. 241–247.

Pimentel, D. *et al.* (2016) “Operation of a homeostatic sleep switch,” *Nature*, 536(7616), pp. 333–337.

Pitman, J. L. *et al.* (2006) “A dynamic role for the mushroom bodies in promoting sleep in Drosophila,” *Nature*, 441(7094), pp. 753–756.

Plautz, J. D. *et al.* (1997) “Quantitative analysis of Drosophila period gene transcription in living animals,” *Journal of biological rhythms*, 12(3), pp. 204–217.

Potdar, S. and Sheeba, V. (2018) “Wakefulness Is Promoted during Day Time by PDFR Signalling to Dopaminergic Neurons in Drosophila melanogaster,” *eNeuro*, 5(4). doi: 10.1523/ENEURO.0129-18.2018.

Qian, Y. *et al.* (2017) “Sleep homeostasis regulated by 5HT2b receptor in a small subset of neurons in the dorsal fan-shaped body of drosophila,” *eLife*. eLife Sciences Publications, Ltd, 6. doi: 10.7554/elife.26519.

Qiao, B. *et al.* (2018) “Automated analysis of long-term grooming behavior in Drosophila using a k-nearest neighbors classifier,” *eLife*, 7. doi: 10.7554/eLife.34497.

Qiao, H.-H. *et al.* (2018) “An efficient and multiple target transgenic RNAi technique with low toxicity in Drosophila,” *Nature communications*. Springer Science and Business Media LLC, 9(1). doi: 10.1038/s41467-018-06537-y.

Qureshi, A. I. *et al.* (1997) “Habitual sleep patterns and risk for stroke and coronary heart disease: a 10-year follow-up from NHANES I,” *Neurology*. Ovid Technologies (Wolters Kluwer Health), 48(4), pp. 904–911.

Raccuglia, D. *et al.* (2019) “Network-Specific Synchronization of Electrical Slow-Wave Oscillations Regulates Sleep Drive in Drosophila,” *Current biology: CB*, 29(21), pp. 3611-3621.e3.

Rau, P. (1938) “Additional observations on the sleep of insects,” *Annals of the Entomological Society of America*. Oxford University Press (OUP), 31(4), pp. 540–556.

Rau, P. and Rau, N. (1916) “The Sleep of Insects; an Ecological Study,” *Annals of the Entomological Society of America*. Oxford Academic, 9(3), pp. 227–274.

Rechtschaffen, A. *et al.* (1983) “Physiological correlates of prolonged sleep deprivation in rats,” *Science*, 221(4606), pp. 182–184.

Rechtschaffen, A. (1998) “Current perspectives on the function of sleep,” *Perspectives in biology and medicine*, 41(3), pp. 359–390.

Rechtschaffen, A. and Bergmann, B. M. (1995) “Sleep deprivation in the rat by the disk-over-water method,” *Behavioural brain research*, 69(1–2), pp. 55–63.

Rechtschaffen, A. and Bergmann, B. M. (2002) “Sleep deprivation in the rat: an update of the 1989 paper,” *Sleep*, 25(1), pp. 18–24.

Reimer, M. A. and Flemons, W. W. (2003) “Quality of life in sleep disorders,” *Sleep medicine reviews*, 7(4), pp. 335–349.

Renn, S. C. *et al.* (1999) “A pdf neuropeptide gene mutation and ablation of PDF neurons each cause severe abnormalities of behavioral circadian rhythms in Drosophila,” *Cell*, 99(7), pp. 791–802.

Rideout, E. J. *et al.* (2010) “Control of sexual differentiation and behavior by the doublesex gene in Drosophila melanogaster,” *Nature neuroscience*. Springer Science and Business Media LLC, 13(4), pp. 458–466.

Riedner, B. A. *et al.* (2007) “Sleep homeostasis and cortical synchronization: III. A high-density EEG study of sleep slow waves in humans,” *Sleep*, 30(12), pp. 1643–1657.

Rieger, D. *et al.* (2006) “Functional analysis of circadian pacemaker neurons in Drosophila melanogaster,” *The Journal of neuroscience: the official journal of the Society for Neuroscience*, 26(9), pp. 2531–2543.

Rieger, D. *et al.* (2009) “Period gene expression in four neurons is sufficient for rhythmic activity of Drosophila melanogaster under dim light conditions,” *Journal of biological rhythms*, 24(4), pp. 271–282.

Riemensperger, T. *et al.* (2011) “Behavioral consequences of dopamine deficiency in the Drosophila central nervous system,” *Proceedings of the National Academy of Sciences of the United States of America*, 108(2), pp. 834–839.

Roberts, L. *et al.* (2015) “Light evokes rapid circadian network oscillator desynchrony followed by gradual phase retuning of synchrony,” *Current biology: CB*, 25(7), pp. 858–867.

Robinow, S. and White, K. (1988) “The locus elav of Drosophila melanogaster is expressed in neurons at all developmental stages,” *Developmental biology*, 126(2), pp. 294–303.

Robinow, S. and White, K. (1991) “Characterization and spatial distribution of the ELAV protein during Drosophila melanogaster development,” *Journal of neurobiology*, 22(5), pp. 443–461.

Roenneberg, T., Daan, S. and Merrow, M. (2003) “The art of entrainment,” *Journal of biological rhythms*, 18(3), pp. 183–194.

Rogulja, D. and Young, M. W. (2012) “Control of sleep by cyclin A and its regulator,” *Science*, 335(6076), pp. 1617–1621.

Rutila, J. E. *et al.* (1998) “CYCLE is a second bHLH-PAS clock protein essential for circadian rhythmicity and transcription of Drosophila period and timeless,” *Cell*, 93(5), pp. 805–814.

Sabatini, B. L., Oertner, T. G. and Svoboda, K. (2002) “The life cycle of Ca(2+) ions in dendritic spines,” *Neuron*, 33(3), pp. 439–452.

Sack, R. L. *et al.* (2007) “Circadian rhythm sleep disorders: part I, basic principles, shift work and jet lag disorders. An American Academy of Sleep Medicine review,” *Sleep*, 30(11), pp. 1460–1483.

Saito, Y. C. *et al.* (2013) “GABAergic neurons in the preoptic area send direct inhibitory projections to orexin neurons,” *Frontiers in neural circuits*, 7, p. 192.

Sanhueza, M. and Lisman, J. (2013) “The CaMKII/NMDAR complex as a molecular memory,” *Molecular brain*, 6, p. 10.

Saper, C. B. *et al.* (2010) “Sleep state switching,” *Neuron*, 68(6), pp. 1023–1042.

Sassani, A. *et al.* (2004) “Reducing motor-vehicle collisions, costs, and fatalities by treating obstructive sleep apnea syndrome,” *Sleep*, 27(3), pp. 453–458.

Scammell, T. E. (2015) “Narcolepsy,” *The New England journal of medicine*, 373(27), pp. 2654–2662.

Scammell, T. E., Arrigoni, E. and Lipton, J. O. (2017) “Neural Circuitry of Wakefulness and Sleep,” *Neuron*, 93(4), pp. 747–765.

Scheffer, L. K. *et al.* (2020) “A connectome and analysis of the adult Drosophila central brain,” *eLife*, 9. doi: 10.7554/eLife.57443.

Schmitt, L. I. *et al.* (2012) “Wakefulness affects synaptic and network activity by increasing extracellular astrocyte-derived adenosine,” *The Journal of neuroscience: the official journal of the Society for Neuroscience*, 32(13), pp. 4417–4425.

Schwarz, J. E. *et al.* (2021) “Hugin+ neurons provide a link between sleep homeostat and circadian clock neurons,” *Proceedings of the National Academy of Sciences of the United States of America*, 118(47). doi: 10.1073/pnas.2111183118.

Sehgal, A. *et al.* (1994) “Loss of circadian behavioral rhythms and per RNA oscillations in the Drosophila mutant timeless,” *Science*, 263(5153), pp. 1603–1606.

Seidner, G. *et al.* (2015) “Identification of Neurons with a Privileged Role in Sleep Homeostasis in Drosophila melanogaster,” *Current biology: CB*, 25(22), pp. 2928–2938.

Seluzicki, A. *et al.* (2014) “Dual PDF signaling pathways reset clocks via TIMELESS and acutely excite target neurons to control circadian behavior,” *PLoS biology*, 12(3), p. e1001810.

Senthilan, P. R. *et al.* (2019) “Role of Rhodopsins as Circadian Photoreceptors in the Drosophila melanogaster,” *Biology*. MDPI AG, 8(1), p. 6.

Sethi, S. and Wang, J. W. (2017) “A versatile genetic tool for post-translational control of gene expression in Drosophila melanogaster,” *eLife*, 6. doi: 10.7554/eLife.30327.

Seugnet, L. *et al.* (2011) “Notch signaling modulates sleep homeostasis and learning after sleep deprivation in Drosophila,” *Current biology: CB*, 21(10), pp. 835–840.

Shafer, O. T. and Keene, A. C. (2021) “The Regulation of Drosophila Sleep,” *Current biology: CB*, 31(1), pp. R38–R49.

Shaner, N. C. *et al.* (2004) “Improved monomeric red, orange and yellow fluorescent proteins derived from Discosoma sp. red fluorescent protein,” *Nature biotechnology*, 22(12), pp. 1567–1572.

Shaner, N. C. *et al.* (2013) “A bright monomeric green fluorescent protein derived from Branchiostoma lanceolatum,” *Nature methods*, 10(5), pp. 407–409.

Shang, Y. *et al.* (2013) “Short neuropeptide F is a sleep-promoting inhibitory modulator,” *Neuron*, 80(1), pp. 171–183.

Shang, Y., Griffith, L. C. and Rosbash, M. (2008) “Light-arousal and circadian photoreception circuits intersect at the large PDF cells of the Drosophila brain,” *Proceedings of the National Academy of Sciences of the United States of America*, 105(50), pp. 19587–19594.

Shaw, P. J. *et al.* (2000) “Correlates of sleep and waking in Drosophila melanogaster,” *Science*, 287(5459), pp. 1834–1837.

Shaw, P. J. *et al.* (2002) “Stress response genes protect against lethal effects of sleep deprivation in Drosophila,” *Nature*, 417(6886), pp. 287–291.

Sheeba, V., Gu, H., *et al.* (2008) “Circadian- and light-dependent regulation of resting membrane potential and spontaneous action potential firing of Drosophila circadian pacemaker neurons,” *Journal of neurophysiology*, 99(2), pp. 976–988.

Sheeba, V., Fogle, K. J., *et al.* (2008) “Large ventral lateral neurons modulate arousal and sleep in Drosophila,” *Current biology: CB*, 18(20), pp. 1537–1545.

Sherin, J. E. *et al.* (1996) “Activation of ventrolateral preoptic neurons during sleep,” *Science*, 271(5246), pp. 216–219.

Sherin, J. E. *et al.* (1998) “Innervation of histaminergic tuberomammillary neurons by GABAergic and galaninergic neurons in the ventrolateral preoptic nucleus of the rat,” *The Journal of neuroscience: the official journal of the Society for Neuroscience*, 18(12), pp. 4705–4721.

Shi, M. *et al.* (2014) “Identification of Redeye, a new sleep-regulating protein whose expression is modulated by sleep amount,” *eLife*, 3, p. e01473.

Shukla, I., Kilpatrick, A. M. and Beltran, R. S. (2021) “Variation in resting strategies across trophic levels and habitats in mammals,” *Ecology and evolution*. Wiley, 11(21), pp. 14405–14415.

Silicheva, M. *et al.* (2010) “Drosophila mini-white model system: new insights into positive position effects and the role of transcriptional terminators and gypsy insulator in transgene shielding,” *Nucleic acids research*, 38(1), pp. 39–47.

Simon, G. E. and VonKorff, M. (1997) “Prevalence, burden, and treatment of insomnia in primary care,” *The American journal of psychiatry*, 154(10), pp. 1417–1423.

Sitaraman, D., Aso, Y., Rubin, G. M., *et al.* (2015) “Control of Sleep by Dopaminergic Inputs to the Drosophila Mushroom Body,” *Frontiers in neural circuits*, 9, p. 73.

Sitaraman, D., Aso, Y., Jin, X., *et al.* (2015) “Propagation of Homeostatic Sleep Signals by Segregated Synaptic Microcircuits of the Drosophila Mushroom Body,” *Current biology: CB*, 25(22), pp. 2915–2927.

Skarpsno, E. S. *et al.* (2017) “Sleep positions and nocturnal body movements based on free-living accelerometer recordings: association with demographics, lifestyle, and insomnia symptoms,” *Nature and science of sleep*, 9, pp. 267–275.

Slawson, J. B. *et al.* (2011) “Central regulation of locomotor behavior of Drosophila melanogaster depends on a CASK isoform containing CaMK-like and L27 domains,” *Genetics*. Oxford University Press (OUP), 187(1), pp. 171–184.

Smith, C. and Lapp, L. (1991) “Increases in number of REMS and REM density in humans following an intensive learning period,” *Sleep*, 14(4), pp. 325–330.

Smolensky, M. H., Sackett-Lundeen, L. L. and Portaluppi, F. (2015) “Nocturnal light pollution and underexposure to daytime sunlight: Complementary mechanisms of circadian disruption and related diseases,” *Chronobiology international*, 32(8), pp. 1029–1048.

Soto-Yéber, L. *et al.* (2018) “The behavior of adult Drosophila in the wild,” *PloS one*. Public Library of Science (PLoS), 13(12), p. e0209917.

Spörrle, M. and Stich, J. (2010) “Sleeping in safe places: an experimental investigation of human sleeping place preferences from an evolutionary perspective,” *Evolutionary psychology: an international journal of evolutionary approaches to psychology and behavior*, 8(3), pp. 405–419.

Stahl, B. A. *et al.* (2018) “The Taurine Transporter Eaat2 Functions in Ensheathing Glia to Modulate Sleep and Metabolic Rate,” *Current biology: CB*, 28(22), pp. 3700-3708.e4.

Stanewsky, R. *et al.* (1997) “Multiple circadian-regulated elements contribute to cycling period gene expression in Drosophila,” *The EMBO journal*, 16(16), pp. 5006–5018.

Stanewsky, Ralf *et al.* (1997) “Temporal and Spatial Expression Patterns of Transgenes Containing Increasing Amounts of the Drosophila Clock Geneperiod and a lacZ Reporter: Mapping Elements of the PER Protein Involved in Circadian Cycling,” *The Journal of neuroscience: the official journal of the Society for Neuroscience*. Society for Neuroscience, 17(2), pp. 676–696.

Stanewsky, R. *et al.* (1998) “The cryb mutation identifies cryptochrome as a circadian photoreceptor in Drosophila,” *Cell*, 95(5), pp. 681–692.

Stephenson, R., Chu, K. M. and Lee, J. (2007) “Prolonged deprivation of sleep-like rest raises metabolic rate in the Pacific beetle cockroach, Diploptera punctata (Eschscholtz),” *The Journal of experimental biology*, 210(Pt 14), pp. 2540–2547.

Steriade, M., Nuñez, A. and Amzica, F. (1993) “A novel slow (< 1 Hz) oscillation of neocortical neurons in vivo: depolarizing and hyperpolarizing components,” *The Journal of neuroscience: the official journal of the Society for Neuroscience*, 13(8), pp. 3252–3265.

Stoleru, D. *et al.* (2004) “Coupled oscillators control morning and evening locomotor behaviour of Drosophila,” *Nature*, 431(7010), pp. 862–868.

Stoleru, D. *et al.* (2005) “A resetting signal between Drosophila pacemakers synchronizes morning and evening activity,” *Nature*, 438(7065), pp. 238–242.

Strawbridge, W. J., Shema, S. J. and Roberts, R. E. (2004) “Impact of spouses’ sleep problems on partners,” *Sleep*, 27(3), pp. 527–531.

Strine, T. W. and Chapman, D. P. (2005) “Associations of frequent sleep insufficiency with health-related quality of life and health behaviors,” *Sleep medicine*, 6(1), pp. 23–27.

Su, T.-S. *et al.* (2017) “Coupled symmetric and asymmetric circuits underlying spatial orientation in fruit flies,” *Nature communications*, 8(1), p. 139.

Su, Y. *et al.* (2020) “Novel NanoLuc substrates enable bright two-population bioluminescence imaging in animals,” *Nature methods*. Springer Science and Business Media LLC, 17(8), pp. 852–860.

Sutters, K. A. and Miaskowski, C. (1997) “Inadequate pain management and associated morbidity in children at home after tonsillectomy,” *Journal of pediatric nursing*, 12(3), pp. 178–185.

Suzuki, K. *et al.* (2016) “Five colour variants of bright luminescent protein for real-time multicolour bioimaging,” *Nature communications*, 7, p. 13718.

Szymusiak, R., Gvilia, I. and McGinty, D. (2007) “Hypothalamic control of sleep,” *Sleep medicine*, 8(4), pp. 291–301.

Taheri, S. *et al.* (2004) “Short sleep duration is associated with reduced leptin, elevated ghrelin, and increased body mass index,” *PLoS medicine*, 1(3), p. e62.

Tainton-Heap, L. A. L. *et al.* (2021) “A Paradoxical Kind of Sleep in Drosophila melanogaster,” *Current biology: CB*, 31(3), pp. 578-590.e6.

Takemura, S.-Y. *et al.* (2017) “A connectome of a learning and memory center in the adult Drosophila brain,” *eLife*, 6. doi: 10.7554/eLife.26975.

Tamakoshi, A., Ohno, Y. and JACC Study Group (2004) “Self-reported sleep duration as a predictor of all-cause mortality: results from the JACC study, Japan,” *Sleep*, 27(1), pp. 51–54.

Tanaka, N. K., Tanimoto, H. and Ito, K. (2008) “Neuronal assemblies of the Drosophila mushroom body,” *The Journal of comparative neurology*, 508(5), pp. 711–755.

Tanenhaus, A. K., Zhang, J. and Yin, J. C. P. (2012) “In vivo circadian oscillation of dCREB2 and NF-κB activity in the Drosophila nervous system,” *PloS one*, 7(10), p. e45130.

Tank, D. W. *et al.* (1988) “Spatially resolved calcium dynamics of mammalian Purkinje cells in cerebellar slice,” *Science*, 242(4879), pp. 773–777.

Tataroglu, O. and Emery, P. (2014) “Studying circadian rhythms in Drosophila melanogaster,” *Methods* , 68(1), pp. 140–150.

Tenaza, R. *et al.* (1969) “Individual behaviour and activity rhythms of captive slow lorises (Nycticebus coucang),” *Animal behaviour*, 17(4), pp. 664–669.

Thakkar, M. M. (2011) “Histamine in the regulation of wakefulness,” *Sleep medicine reviews*, 15(1), pp. 65–74.

Thakkar, M. M., Sharma, R. and Sahota, P. (2015) “Alcohol disrupts sleep homeostasis,” *Alcohol* , 49(4), pp. 299–310.

Thompson, J. F., Hayes, L. S. and Lloyd, D. B. (1991) “Modulation of firefly luciferase stability and impact on studies of gene regulation,” *Gene*, 103(2), pp. 171–177.

Tisdale, R. K. *et al.* (2018) “The low-down on sleeping down low: pigeons shift to lighter forms of sleep when sleeping near the ground,” *The journal of experimental biology*. The Company of Biologists, 221(Pt 19), p. jeb182634.

Tobler, I., I. and Neuner-Jehle, M. (1992) “24-h variation of vigilance in the cockroach Blaberus giganteus,” *Journal of sleep research*, 1(4), pp. 231–239.

Tononi, G. and Cirelli, C. (2003) “Sleep and synaptic homeostasis: a hypothesis,” *Brain research bulletin*, 62(2), pp. 143–150.

Tononi, G. and Cirelli, C. (2006) “Sleep function and synaptic homeostasis,” *Sleep medicine reviews*, 10(1), pp. 49–62.

Tononi, G. and Cirelli, C. (2012) “Time to be SHY? Some comments on sleep and synaptic homeostasis,” *Neural plasticity*, p. 415250.

Tononi, G. and Cirelli, C. (2014) “Sleep and the price of plasticity: from synaptic and cellular homeostasis to memory consolidation and integration,” *Neuron*, 81(1), pp. 12–34.

Touitou, Y. (2015) “Light at night pollution of the internal clock, a public health issue,” *Bulletin de l’Academie nationale de medecine*, 199(7), pp. 1081–1098.

Touitou, Y., Reinberg, A. and Touitou, D. (2017) “Association between light at night, melatonin secretion, sleep deprivation, and the internal clock: Health impacts and mechanisms of circadian disruption,” *Life sciences*, 173, pp. 94–106.

Tubon, T. C., Jr *et al.* (2013) “dCREB2-mediated enhancement of memory formation,” *The Journal of neuroscience: the official journal of the Society for Neuroscience*, 33(17), pp. 7475–7487.

Tye, K. M. *et al.* (2008) “Rapid strengthening of thalamo-amygdala synapses mediates cue-reward learning,” *Nature*, 453(7199), pp. 1253–1257.

Ueno, T. *et al.* (2012) “Identification of a dopamine pathway that regulates sleep and arousal in Drosophila,” *Nature neuroscience*, 15(11), pp. 1516–1523.

Ursin, R. (2002) “Serotonin and sleep,” *Sleep medicine reviews*, 6(1), pp. 55–69.

Uschakov, A. *et al.* (2007) “Efferent projections from the median preoptic nucleus to sleep- and arousal-regulatory nuclei in the rat brain,” *Neuroscience*, 150(1), pp. 104–120.

Vaccaro, A. *et al.* (2020) “Sleep Loss Can Cause Death through Accumulation of Reactive Oxygen Species in the Gut,” *Cell*, 181(6), pp. 1307-1328.e15.

Van Dongen, H. P. A. *et al.* (2003) “The cumulative cost of additional wakefulness: dose-response effects on neurobehavioral functions and sleep physiology from chronic sleep restriction and total sleep deprivation,” *Sleep*, 26(2), pp. 117–126.

Vanderheyden, W. M. *et al.* (2018) “Astrocyte expression of the Drosophila TNF-alpha homologue, Eiger, regulates sleep in flies,” *PLoS genetics*, 14(10), p. e1007724.

de Velasco, B. *et al.* (2007) “Specification and development of the pars intercerebralis and pars lateralis, neuroendocrine command centers in the Drosophila brain,” *Developmental biology*, 302(1), pp. 309–323.

Vetrivelan, R. *et al.* (2012) “Metabolic effects of chronic sleep restriction in rats,” *Sleep*, 35(11), pp. 1511–1520.

Vetrivelan, R., Saper, C. B. and Fuller, P. M. (2014) “Armodafinil-induced wakefulness in animals with ventrolateral preoptic lesions,” *Nature and science of sleep*, 6, pp. 57–63.

Vrontou, E. *et al.* (2006) “fruitless regulates aggression and dominance in Drosophila,” *Nature neuroscience*, 9(12), pp. 1469–1471.

Vyazovskiy, V. V., Achermann, P. and Tobler, I. (2007) “Sleep homeostasis in the rat in the light and dark period,” *Brain research bulletin*, 74(1–3), pp. 37–44.

Walsh, J. K. and Engelhardt, C. L. (1999) “The direct economic costs of insomnia in the United States for 1995,” *Sleep*, 22 Suppl 2, pp. S386-93.

Waskom, M. (2021) “seaborn: statistical data visualization,” *Journal of open source software*. The Open Journal, 6(60), p. 3021.

Webb, W. B. and Agnew, H. W. (1975) “Are we chronically sleep deprived?,” *Bulletin of the Psychonomic Society*, 6(1), pp. 47–48.

Weber, E. (1961) “Über ruhelagen von fischen,” *Zeitschrift fur Tierpsychologie*. Wiley, 18(5), pp. 517–533.

Weissman, M. M. *et al.* (1997) “The morbidity of insomnia uncomplicated by psychiatric disorders,” *General hospital psychiatry*, 19(4), pp. 245–250.

White, K. E., Humphrey, D. M. and Hirth, F. (2010) “The dopaminergic system in the aging brain of Drosophila,” *Frontiers in neuroscience*, 4, p. 205.

Williams, R. H. *et al.* (2014) “Optogenetic-mediated release of histamine reveals distal and autoregulatory mechanisms for controlling arousal,” *The Journal of neuroscience: the official journal of the Society for Neuroscience*, 34(17), pp. 6023–6029.

Wong, R. *et al.* (2009) “Quantification of food intake in Drosophila,” *PloS one*, 4(6), p. e6063.

Wu, M. N. *et al.* (2010) “SLEEPLESS, a Ly-6/neurotoxin family member, regulates the levels, localization and activity of Shaker,” *Nature neuroscience*, 13(1), pp. 69–75.

Xie, L. *et al.* (2013) “Sleep drives metabolite clearance from the adult brain,” *Science*, 342(6156), pp. 373–377.

Yamamoto, D. and Koganezawa, M. (2013) “Genes and circuits of courtship behaviour in Drosophila males,” *Nature reviews. Neuroscience*, 14(10), pp. 681–692.

Yao, Z. and Shafer, O. T. (2014) “The Drosophila circadian clock is a variably coupled network of multiple peptidergic units,” *Science*, 343(6178), pp. 1516–1520.

Yap, M. H. W. *et al.* (2017) “Oscillatory brain activity in spontaneous and induced sleep stages in flies,” *Nature communications*, 8(1), p. 1815.

Yoshii, T. *et al.* (2005) “Temperature cycles drive Drosophila circadian oscillation in constant light that otherwise induces behavioural arrhythmicity,” *The European journal of neuroscience*, 22(5), pp. 1176–1184.

Yoshii, T. *et al.* (2008) “Cryptochrome is present in the compound eyes and a subset of Drosophila’s clock neurons,” *The Journal of comparative neurology*, 508(6), pp. 952–966.

Yoshii, T., Vanin, S., *et al.* (2009) “Synergic entrainment of Drosophila’s circadian clock by light and temperature,” *Journal of biological rhythms*, 24(6), pp. 452–464.

Yoshii, T., Wülbeck, C., *et al.* (2009) “The neuropeptide pigment-dispersing factor adjusts period and phase of Drosophila’s clock,” *The Journal of neuroscience: the official journal of the Society for Neuroscience*, 29(8), pp. 2597–2610.

Young, J. M. and Armstrong, J. D. (2010) “Structure of the adult central complex in Drosophila: organization of distinct neuronal subsets,” *The Journal of comparative neurology*, 518(9), pp. 1500–1524.

Young, M. W. and Kay, S. A. (2001) “Time zones: a comparative genetics of circadian clocks,” *Nature reviews. Genetics*, 2(9), pp. 702–715.

Yuan, Q., Joiner, W. J. and Sehgal, A. (2006) “A sleep-promoting role for the Drosophila serotonin receptor 1A,” *Current biology: CB*, 16(11), pp. 1051–1062.

Zepelin, H. and Rechtschaffen, A. (1974) “Mammalian Sleep, Longevity, and Energy Metabolism; pp. 447–470,” *Brain, behavior and evolution*. S. Karger AG, 10(6), pp. 447–470.

Zhang, L. *et al.* (2010) “DN1(p) circadian neurons coordinate acute light and PDF inputs to produce robust daily behavior in Drosophila,” *Current biology: CB*, 20(7), pp. 591–599.

Zhang, Y. *et al.* (2010) “Light and temperature control the contribution of specific DN1 neurons to Drosophila circadian behavior,” *Current biology: CB*, 20(7), pp. 600–605.

Zhao, H. *et al.* (2005) “Emission spectra of bioluminescent reporters and interaction with mammalian tissue determine the sensitivity of detection in vivo,” *Journal of biomedical optics*, 10(4), p. 41210.

Zheng, X. and Sehgal, A. (2012) “Speed control: cogs and gears that drive the circadian clock,” *Trends in neurosciences*, 35(9), pp. 574–585.

Zielinski, M. R., McKenna, J. T. and McCarley, R. W. (2016) “Functions and Mechanisms of Sleep,” *AIMS neuroscience*, 3(1), pp. 67–104.

Zielinski, T. *et al.* (2014) “Strengths and limitations of period estimation methods for circadian data,” *PloS one*, 9(5), p. e96462.

Zimmerman, J. E. *et al.* (2008) “A video method to study Drosophila sleep,” *Sleep*, 31(11), pp. 1587–1598.